AD_____

Award Number: W81XWH-04-1-0316

TITLE: Prevention of the Angiogenic Switch in Human Breast Cancer

PRINCIPAL INVESTIGATOR: Donald Ingber, M.D., Ph.D.

CONTRACTING ORGANIZATION: Children's Hospital
Boston, MA 02115

REPORT DATE: March 2009

TYPE OF REPORT: Final

PREPARED FOR: U.S. Army Medical Research and Materiel Command
Fort Detrick, Maryland 21702-5012

DISTRIBUTION STATEMENT: Approved for Public Release;
Distribution Unlimited

The views, opinions and/or findings contained in this report are those of the author(s) and should not be construed as an official Department of the Army position, policy or decision unless so designated by other documentation.

REPORT DOCUMENTATION PAGE

Form Approved
OMB No. 0704-0188

1. REPORT DATE *(DD-MM-YYYY)*	**2. REPORT TYPE**	**3. DATES COVERED** *(From - To)*
01-03-2009	Final	15 FEB 2004 - 14 FEB 2009

4. TITLE AND SUBTITLE

Prevention of the Angiogenic Switch in Human Breast Cancer

5a. CONTRACT NUMBER

5b. GRANT NUMBER
W81XWH-04-1-0316

5c. PROGRAM ELEMENT NUMBER

6. AUTHOR(S)
Donald Ingber, M.D., Ph.D.

E-Mail: alexandra.grady@childrens.harvard.edu

5d. PROJECT NUMBER

5e. TASK NUMBER

5f. WORK UNIT NUMBER

7. PERFORMING ORGANIZATION NAME(S) AND ADDRESS(ES)

Children's Hospital
Boston, MA 02115

8. PERFORMING ORGANIZATION REPORT NUMBER

9. SPONSORING / MONITORING AGENCY NAME(S) AND ADDRESS(ES)
U.S. Army Medical Research and Materiel Command
Fort Detrick, Maryland 21702-5012

10. SPONSOR/MONITOR'S ACRONYM(S)

11. SPONSOR/MONITOR'S REPORT NUMBER(S)

12. DISTRIBUTION / AVAILABILITY STATEMENT
Approved for Public Release; Distribution Unlimited

13. SUPPLEMENTARY NOTES

14. ABSTRACT Our studies over the past 5 years have focused on investigating the mechanisms that regulate the angiogenic switch in primary breast cancers and progression towards metastasis, as well as development of novel therapies that target these processes. While it is well accepted that initiation of cancer requires activation of an oncogene and/or loss of tumor suppressors, tumor progression to neoplasia and subsequent tumor mass expansion require activation of the angiogenic switch (1). To determine the mechanisms that regulate the angiogenic switch, we utilized multiple approaches including screens to identify genes that may be causal in triggering this switch, investigation of the role of the breast cancer susceptibility gene (BRCA1) in regulating angiogenic proteins, and identifying soluble factors produced by non-metastatic breast cancer cells that are critical in suppressing the growth of metastatic lesions. To examine the efficacy of novel therapies for breast cancer with anti-angiogenic activity, we focused on two specific anti-angiogenic therapies, a novel oral formulation of the fumagillin analogue TNP-470 called Lodamin and a recombinant peptide consisting of the first 27 amino acids in the endogenous angiogenesis inhibitor endostatin. We evaluated the efficacy of these two novel anti-angiogenic agents on the growth of human breast cancer in immunocompromised mice and confirmed their primary mechanism of action. The results from these studies have advanced our understanding of how the angiogenic switch may be regulated in breast cancer and provide insight into novel targets and signaling pathways for both primary breast tumorigenesis and more advanced metastatic disease.

15. SUBJECT TERMS
Tumor angiogenesis, switch to the angiogenic phenotype, thrombospondin-1, VEGF, platelet angiogenesis proteome, dormant, non-angiogenic human breast cancer, BRCA1, reversal of the angiogenic phenotype, stroma.

16. SECURITY CLASSIFICATION OF:			**17. LIMITATION OF ABSTRACT**	**18. NUMBER OF PAGES**	**19a. NAME OF RESPONSIBLE PERSON**
					USAMRMC
a. REPORT	**b. ABSTRACT**	**c. THIS PAGE**			**19b. TELEPHONE NUMBER** *(include area code)*
U	U	U	UU	174	

Standard Form 298 (Rev. 8-98)
Prescribed by ANSI Std. Z39.18

Table of Contents

DOD Breast Cancer Innovator Award Final Report
PI: Donald Ingber, M.D., Ph.D. *(originally, Judah Folkman, M.D.)*
"Prevention of the Angiogenic Switch in Human Breast Cancer"
February 2004 – February 2009

INTRODUCTION:

To identify genes that may be important in regulating the angiogenic switch in breast cancer, we developed an animal model of human tumor dormancy (*2*). These studies allowed us to isolate microscopic, dormant breast cancer cells before they underwent an angiogenic switch, as well as large macroscopic rapidly growing angiogenic tumors after the switch. Using these two different breast cancer cells, we performed cDNA arrays to determine which genes might be differentially expressed and identified heat shock protein 27 (HSP27) as being significantly upregulated after breast cancer cells have undergone an angiogenic switch. Our studies have focused on validating the role of HSP27 in promoting the angiogenic switch and examining the mechanisms by which downregulation of HSP27 may suppress the switch to the angiogenic phenotype.

Families at high risk for developing breast or ovarian cancer have one mutant copy of *Brca1* in the germ line predisposing an individual to cancer. The second allele is consistently lost in tumors thereby leaving no functional copy of BRCA1 (*3*). Despite the identification of these genes, their roles in breast tumorigenesis are still not clearly defined. Our studies have been focused on determining what role BRCA1 may play in restraining the angiogenic switch and specifically whether BRCA1 regulates expression of endogenous angiogenesis inhibitors. Control of the angiogenic switch is thought to be critically dependent on the balance between pro- and anti-angiogenic factors. While there has been much attention focused on the upregulation of the pro-angiogenic protein VEGF, less is known about the regulation of negative regulators of angiogenesis. Our studies have examined whether BRCA1 may normally function to maintain expression of the potent endogenous angiogenesis inhibitor, thrombospondin-1 (TSP-1) (*4)*. Understanding the mechanisms of BRCA1-mediated breast tumorigenesis may allow the identification of novel targets for both BRCA-1 and non-BRCA-1 mediated breast cancers.

The progression of human cancer to the metastatic stage is a major contributing factor to its lethality. In order for a tumor to form metastases, it must gain access to the vasculature or lymphatic system (intravasation), survive during transit, exit the vascular or lymphatic channels (extravasation), and proliferate at the metastatic site (*5)*. Upon colonization of a distant tissue, tumor cells must induce neovascularization in order to grow beyond a microscopic size. In this process, heterotypic tumor-stromal signaling can affect tumor growth by regulating the production and secretion of growth-

promoting and growth-inhibitory proteins by the surrounding stromal fibroblasts and endothelial cells. Similar to studies examining primary tumor growth, there has been extensive work examining stimulation of the pro-angiogenic protein VEGF in the surrounding stroma (*6)*. However, much less is understood about the role of the angiogenesis inhibitor TSP-1 in regulating metastasis and regulation of its expression in the tumor-associated stroma (*4)*. One aim of this proposal has been to investigate breast cancer metastasis and how TSP-1 may contribute to this process. Our studies have identified a novel mechanism by which tumor cell secretion of a protein called Prosaposin inhibits the metastatic process by its regulation, in part, of TSP-1. These studies indicate that tumor cells at the primary site secrete prosaposin, which acts at distant sites to create a non-permissive environment with respect to colonization by tumor cells.

Another major focus of this proposal has been the exploration of novel therapies that target the angiogenic switch in breast cancer. Regulation of the angiogenic switch is thought to be critically dependent on the balance of pro and anti-angiogenic proteins. Therefore we have been investigating whether treatment with recombinant angiogenesis inhibitors may prevent the switch from a dormant, microscopic tumor to a rapidly growing angiogenic tumor. Specifically we have been examining the efficacy of 3 different angiogenesis inhibitors as anti-angiogenic therapies for breast cancer prevention and treatment. Endostatin and angiostatin are soluble proteolytic fragments of collagen XVIII and plasminogen respectively, and were originally discovered in the Folkman lab (*7)*. Our work has focused on generating these soluble recombinant proteins and utilizing them to treat human breast cancer xenografts in immunocompromised nude mice. We have also generated a novel formulation of the angiogenesis inhibitor TNP-470. TNP-470 is an analogue of fumagillin which was isolated from the fungus *Aspergillus fumigatus fresenius* (*8)* and has been demonstrated to be one of the most potent and generic inhibitors of angiogenesis. It has been shown to bind methionine aminopeptidase (MetAP-2) and affect the cell cycle through p53 activation, or preventing Rac1 activation (*9-12)*. TNP-470 was one of the first antiangiogenic drug to undergo clinical trials (*13)*. However, the poor oral availability of TNP-470 coupled with its extremely short plasma half-life imposed a strict regime of prolonged parenteral administration using continuous intravenous infusions in clinical trials (*14,15)*. Neural side-effects, which were responsible for dose-limiting toxicity, contributed to the termination of the clinical trials (*16)*. Our work has addressed these clinical obstacles and we have now developed an oral formulation of TNP-470 that we renamed Lodamin. This new formulation, which can be administered orally instead of intravenously, has shown to reduced neurological side effects compared to the original TNP-470 (*17)*. The data generated from these studies suggest that both endostatin and our new formulation of TNP-470 have potent anti-tumor activities, and suggest that they might offer a novel therapeutic approach to breast cancer treatment.

BODY:

Mechanisms that regulate the angiogenic switch in breast cancer

As a result of our initial cDNA screen of dormant and angiogenic breast cancer cells, we identified a number of candidates that were differentially expressed in dormant versus angiogenic tumor cells. More recently, we focused on validating the significant upregulation of the heat shock 27 protein (HSP27) that we identified in angiogenic tumor cells. Further, we have been exploring the mechanisms by which down-regulation of HSP27 suppresses the angiogenic switch in human breast cancer. Our studies have shown that conditioned medium from breast cancer cells containing high HSP27 levels stimulates endothelial cell migration *in vitro*, whereas conditioned media from cells with suppressed HSP27 has no effect. Examination of endothelial cell proliferation in tumors expressing low HSP27 levels demonstrate a 3-fold lower rate of growth as compared to tumors with high HSP27. Suppression of HSP27 did not alter proliferation or apoptosis of the breast cancer cells themselves but did lead to reduced secretion of the pro-angiogenic regulators VEGF and bFGF and increased expression of the angiogenesis inhibitor thrombospondin-1 (TSP-1). Moreover, this alteration of VEGF production was transcriptionally regulated. Further, our data show that suppression of HSP27 led to accumulation of intracellular bFGF protein, ultimately leading to reduced secretion of this pro-angiogenic protein. We are currently elucidating the interaction between bFGF and HSP27.

Our studies examining the function of the Breast cancer susceptibility gene, BRCA1 suggested that it might regulate the expression of the endogenous angiogenesis inhibitor, TSP-1. We have generated and characterized a human breast cancer cell line containing either no functional copies of BRCA1 or many wild-type copies of BRCA1. Unexpectedly, our studies found that both of these cell lines form tumors upon orthotopic injection in the mammary fat pad of immunocompromised SCID mice. Further studies have shown that the ratio of TSP-1 production to VEGF correlates with tumor growth, and that both breast cancer cell lines with either no functional BRCA1 or with high levels of BRCA1 over-expression have low levels of TSP-1. We next explored the reasons why restoration of wild-type BRCA1 was not able to rescue TSP-1 expression in our breast cancer cell lines, and found that BRCA1 regulation of TSP-1 may be indirect and mediated through the tumor suppressor p53. Previous studies have implicated p53 in the regulation of TSP-1 expression and we confirmed and extended these observations by demonstrating that p53 binds to the TSP-1 promoter and directly transactivates TSP-1 expression. Since greater than 50% of BRCA1-mediated breast cancers contain secondary mutations in p53, we hypothesized that this decrease in TSP-1 was a consequence of p53 inactivation. On-going studies include activation of BRCA1 in normal breast epithelial cells by specific DNA damaging agents and examining activation of p53 as a consequence of BRCA1 activation. Other

studies are examining whether p53 restoration in breast cancer cells with *Brca1* mutations will be sufficient to increase levels of TSP1.

Finally to determine whether *Brca1* mutations alone were sufficient to promote tumorigenesis, we have been attempting to stably knock-down *Brca1* expression with lentiviral hairpins in normal breast epithelial cells. While we have been successful in significantly reducing BRCA1 expression, we have been unsuccessful in expanding these cell lines. We have also been attempting to re-express *Tsp-1* into our breast cancer cell lines with either BRCA1 mutations or over-expression of BRCA1 to determine whether restoration of high levels of TSP-1 would be sufficient to block tumorigenesis. These studies have also been unsuccessful due to the inability of these cells to expand with high levels of TSP1 expression.

Understanding breast cancer metastasis

Our work investigating the role of TSP-1 in regulating breast cancer metastasis led to the identification of a novel mechanism of metastatic suppression by which tumor cell secretion of Prosaposin (Psap) inhibits this process. Our findings indicate that tumor cells at the primary site secrete prosaposin, which acts at distant sites to create a non-permissive, or refractory, environment with respect to colonization by tumor cells. By comparing cell lines with different metastatic potential, we identified this novel tumor-secreted inhibitor of metastasis, Psap. Psap functions in both a paracrine and endocrine manner by stimulating the expression of TSP-1 in fibroblasts present in both primary tumors and distant organs in a p53-dependent manner. Introduction of Psap into highly metastatic cells significantly reduced the occurrence of metastases, whereas inhibition of Psap production by tumor cells was associated with increased metastatic frequency. These findings suggest that prosaposin, or other agents that stimulate p53 activity in the tumor stroma, may be an effective therapy for inhibiting cancer metastasis.

Anti-angiogenic therapy for breast cancer treatment

During the first years of this grant, there were many challenges in the production of soluble large-scale quantities of the recombinant endogenous angiogenesis inhibitors endostatin and angiostatin for therapeutic use. To circumvent these issues, we utilized a strategy initially described by scientists at Genentech whereby we added the Fc domain of immunoglobulin (IgG) to the ends of these recombinant proteins and in doing so constructed Fc-endostatin and Fc-angiostatin (*18)* peptides. This approach enabled us to not only produce large amounts of these two proteins on the scale of 50 mg/liter in fermentors, but to increase the half-life of the proteins in the circulation to weeks instead of hours as observed for the same proteins without Fc (*19)*. Anti-tumor properties of Fc-endostatin and Fc-angiostatin have been investigated in mice demonstrating efficacy in treatment;

however, the production of Fc-endostatin was time consuming and costly. Further analysis of endostatin demonstrated that a 27 amino acid peptide corresponding to the N-terminus of the protein was equivalent to full-length endostatin in terms of activity and required the zinc binding property of endostatin for its full activity. Our initial studies assessing the anti-angiogenic efficacy of Fc-endostatin peptide utilized the Miles permeability assay in reponse to VEGF and demonstrated that Fc-endostatin peptide inhibited VEGF-induced permeability comparable to full-length Fc-endostatin. These studies indicate that a 27 amino acid peptide from the N-terminal domain of endostatin conjugated to the Fc domain of IgG may be an effective therapy for treatment of breast cancer.

Our studies modifying TNP-470 led to the production of the first oral formulation of TNP-470, which we renamed Lodamin^{TM}: a nanoparticle composed of a conjugate of TNP-470 to poly(ethylene-glycol)-poly(lactic)acid (PEG-PLA). This pegylated version of TNP-470 (or Lodamin) demonstrated significant anti-tumor activity in mice bearing melanoma and lung tumors with little or no toxicity. Our studies demonstrate that Lodamin selectively accumulates in the tumor site, decreased vessel growth and induced apoptosis. We have also examined the consequences of long-term therapy with Lodamin on subcutaneously implanted human breast cancer cells in immunocompromised mice. These studies demonstrated significant inhibition of the growth of human breast MDA-MB-231 tumors when implanted subcutaneously in mice. We are currently investigating the ability of Lodamin to inhibit orthotopic breast cancer in addition to the subcutaneous model.

Our results indicate that Lodamin, administered orally, is effectively absorbed in the intestine and accumulates in tumor tissue. The drug significantly inhibits angiogenesis, as demonstrated by inhibition of endothelial cell proliferation, as well as suppression of angiogenesis in the corneal micropocket assay and in mouse tumor models. Lodamin significantly inhibited primary tumor growth as demonstrated in models of melanoma and lung cancer and successfully prevented liver metastasis of melanoma tumor cells without causing liver-toxicity or other side-effects, and this treatment led to prolonged mouse survival. Importantly, we also demonstrated anti-cancer effect of Lodamin in breast-tumor bearing mice. Lodamin significantly inhibited subcutaneous MDA-MB-231 breast tumor growth by 62% after 47 days (Lodamin 245 mm^3 ± 145, control: 653 mm^3 ± 411) when given in a dose of 30mg/kg q.o.d TNP-470 equivalent. No significant weight loss or other signs of toxicity were found. We are currently evaluating the effects of Lodamin treatment in an orthotopic breast cancer model in mice. These studies suggest that Lodamin may be a novel anti-cancer therapy for use not only in breast cancer but in many different cancer types.

KEY RESEARCH ACCOMPLISHMENTS:

- Identified heat shock protein 27 (HSP27) as a regulator of the angiogenic switch
- Validated the significant upregulation of HSP27 after tumor cells switch to the angiogenic phenotype.
- In a cohort of 120 human breast cancers consisting of size-matched pairs of breast tumors we found that low expression of HSP27 protein is associated with a less aggressive phenotype and improved survival in human breast cancer patients.
- We found that low HSP27 protein expression was also significantly associated with improved patient survival among 97 melanoma patients.
- Established and characterized two different cell lines (with collaborators) with either over-expression of wild-type BRCA1 or with mutant (i.e. no functional copies) BRCA1.
- Determined the *in vitro* production of the angiogenic regulators VEGF, thrombospondin-1 (TSP-1) and bFGF in human breast cancer cell lines with *Brca1* mutations or *Brca1* over-expression and compared it to normal breast epithelial cells with two functional copies of *Brca1*.
- Established the presence of non-angiogenic and angiogenic subpopulations human breast cancer cells with *Brca1* mutations or *Brca1* over-expression in immunocompromised mice and determined the time until each cell line underwent an angiogenic switch.
- Demonstrated that the ratio of TSP-1 to VEGF produced by breast cancer cells with deregulation of BRCA1 correlated with their time of progression to the angiogenic switch (i.e., the lower the ratio, the sooner the cells undergo the switch) in SCID mice.
- Validated decreased TSP-1 expression in patient samples by immunohistochemical analysis of ovarian tumors with *Brca1* mutations.
- Determined that non-metastatic tumors secrete factors that act both locally and systemically to stimulate the expression of Tsp-1 and p53.
- Identified prosaposin as a protein responsible for the stimulation of Tsp-1 and p53.
- Demonstrated that stimulation of Tsp-1by prosaposin inhibits the metastatic spread of tumors.
- Demonstrated that expression of endostatin and angiostatin as fusion proteins containing an Fc domain, the dose requirement for anti-tumor activity is reduced by 40- fold.
- Demonstrated that the anti-tumor activity of endostatin exhibits a U-shaped curve.
- Demonstrated that the N-terminus of endostatin mimicked by a 25-27 amino acids containing the zinc binding domain of the protein, is equivalent to total endostatin in suppressing tumor growth in transplantable tumor models in mice.
- Developed and characterized Lodamin as an oral formulation for TNP-470 and validated the activity of Lodamin following oral administration.
- Directly demonstrated the anti-angiogenic properties of Lodamin as a novel oral formulation of TNP-470.
- Demonstrated anti-tumor effectiveness of Lodamin treatment of breast cancer-bearing mice.

REPORTABLE OUTCOMES:

Presentations:

1/25/07	Harvard Medical School Honorary Event Dr. Folkman- lecturer **"How is it helpful for a medical student to understand why the process of angiogenesis may be an organizing principle in biomedicine?"**
2/14/07	University of California San Diego Moores UCSD Cancer Center Director's Seminar Series Dr. Folkman- Lecture **"Angiogenesis: An Organizing Principle in Medicine and Biology"**
3/23- 3/24/07	Symposium honoring Dr. Josh Fidler Dr. Folkman- presentation **"Angiogenesis Regulatory Molecules that Mediate Preferential Tumor Growth in Orthotopic Sites"** Houston, TX
5/12- 5/15/07	Actar Meeting and Nobel Forum lecture Dr. Folkman- minisymposium lecturer **"Anti-angiogenic therapy in treatment of cancer"** Stockholm, Sweden
8/15- 8/16/07	8th World Congress for Microcirculation Dr. Folkman- Keynote Lecturer **"Endogenous Angiogenesis Inhibitors"** Milwaukee, WI
9/14- 9/15/07	Aultman Cancer Center Aultman Cancer Research Institute **"Antiangiogenic Therapy for Cancer: Principles and New Directions"** Northeastern Ohio University
10/13/07	2007 International Conference on Glioma Research and Therapy Dr. Folkman- Speaking **"Clinical Applications of Antiangiogenic Therapy: New Insights"** Boston, MA
10/20/07	Dr. Folkman- speaker **"Blocked Angiogenesis as a General Mechanism of Tumor Dormancy"** San Diego, CA
10/24- 10/26/07	Emory University School of Medicine's Winship Cancer Institute Dr. Folkman- keynote address **"Angiogenesis: A Paradigm for translating from the laboratory to the clinic and back."** Atlanta, GA

1. Oddbjorn Straume, Takeshi Shimamura, Anne Oyan, Michael Lampa, Christa L. Borgman, Sarah Short, Soo-Young Kang, Randolph Watnick, Liang Chen, Karin Collet, Kwok-Kin Wong, , Geoffrey I. Shapiro, Karl H. Kalland, Judah Folkman, Lars A. Akslen and George N. Naumov. Suppression of Heat Shock Protein 27 induces long-term dormancy in human breast cancer. American Association for Cancer Research, Denver, Co. – April 2009.

2. Lynch R, DelloRusso C, King MC, Folkman J, Ryeom S. “Does the Breast Cancer Susceptibility gene, BRCA1 regulate angiogenesis?” Presentation at Smith Family Foundation Annual Symposium, Boston, MA (2007).

3. AACR Special Conference, San Diego, CA 1/2009 Regulation of Metastasis via Paracrine and Endocrine Signaling

Patents:

1. Provisional patent entitled “HSP27 is a Prognostic Factor in Melanoma", CMCC1693, 61/061,000, June 12, 2008.

2. "Methods for Inhibition of Tumor Angiogenic Switch", CMCC1683, 61/031,078 filed 2/25/08.

3. "HSP27 is a Prognostic Factor in Melanoma", CMCC1693, 61/061,000, June 12, 2008

4. “Methods and Uses Thereof Prosaposin, CMCC1579.

Funding applied for:

1. NIH R01 “Molecular mechanisms of tumor-initiated premetastatic niche formation in lung stroma”. The goal of this project is to identify tumor-secreted proteins and bone marrow-derived cells that localize to sites in the lung that will become colonized by tumor cells. Randy Watnick (co-PI).

2. Investigator Initiated Research Grant: Susan G. Komen Breast Cancer Foundation

“Regulation of breast cancer metastasis via tumor-stromal interactions”. The goal of this project is to identify tumor-secreted proteins that regulate the metastasis of breast cancer to specific organs. Randy Watnick (PI)

3. NIH R01 “Mechanism of Prosaposin-mediated inhibition of lymphangiogenesis”.

The goal of this project is to determine the mechanism of prosaposin-mediated inhibition of lymphangiogenesis and lymph node metastasis via the stimulation of p53 in the primary tumor stroma as well as in distal organs. Randy Watnick (PI)

4. NIH R01 “Tumor-stromal interactions in Metastasis”

The goal of this project is to determine the mechanism of prosaposin-mediated inhibition of metastasis via its ability to stimulate both p53 and thrombospondin-1 in the primary tumor stroma as well as in distal organs. Randy Watnick (PI)

Manuscripts:

Abstract: The "platelet angiogenic profile" was published in November 2004, and presented in December 2004 as a platform presentation to the American Society of Hematology.

Almog N, Henke V, Flores L, Hlatky L, Kung AL, Wright RD, Berger R, Hutchinson L, Naumov GN, Bender E, Akslen LA, Achilles EG, Folkman J. Prolonged dormancy of human liposarcoma is associated with impaired tumor angiogenesis. ***FASEB J*** 2006; 20(7):947-9

Naumov GN, Bender E, Zurakowski D, Kang SY, Sampson D, Flynn E, Watnick RS, Straume O, Akslen LA, Folkman J, Almog N. A model of human tumor dormancy: an angiogenic switch from the nonangiogenic phenotype. ***J Natl Cancer Inst.*** 2006; 98:316-25

Naumov GN, Akslen LA, Folkman J. Role of angiogenesis in human tumor dormancy: animal models of the angiogenic switch. ***Cell Cycle*** 2006; 5:1779-87.

Folkman, J. Angiogenesis: an organizing principle for drug discovery? **Nature Reviews Drug Discovery** (2007), 6:273-286.

Kaipainen A, Kieran MW, Huang S, Butterfield C, Bielenberg D, Mostoslavsky G, Mulligan R, Folkman J, Panigrahy D. PPARα deficiency in inflammatory cells suppresses tumor growth. **PLoS ONE** 2007; 2:e260.

Naumov GN, Folkman J. Strategies to prolong the nonangiogenic dormant state of human cancer. In: Davis DW, Herbst RS, Abbruzzese JL, eds. **Antiangiogenic Cancer Therapy**. CRC Press, Boca Raton, FL, 2007; pp 3-21.

Folkman, J. Endostatin finds a new partner: nucleolin. **Blood** 2007; 110(8): 2786-2787.

Panigrahy D, Kaipainen A, Huang S, Butterfield CE, Barnes CM, Fannon M, Laforme AM, Chaponis DM, Folkman J, Kieran MW. The PPARalpha agonist fenofibrate suppresses tumor growth through direct and indirect angiogenesis inhibition. **Proc Natl Acad Sci USA**; 2008; 105(3):985-990.

Naumov GN, Folkman J, Straume O. Tumor dormancy and the microenvironment. ***Clin & Exp Metastasis***. 2009. 26:51-60. (2008 - online DOI: 10.1007/s10585-008-9176-0)

Naumov GN, Folkman J, Straume O, Akslen LA. Tumor-vascular interactions and tumor dormancy. ***APMIS*** 2008;116:569-585.

Cervi D, Yip T-T, Bhattacharya N, Podust VN, Peterson J, Abou-slaybi A, Naumov GN, Bender E, Almog N, Italiano JE Jr., Folkman J, Klement GL. Platelet-associated PF-4 as a biomarker of early tumor detection. **Blood**; 2008 Feb 1;111(3):1201-7.

Italiano JE, Richardson JL, Patel-Hett S, Battinelli E, Zaslavsky A, Short S, Ryeom S, Folkman J, Klement GL. Angiogenesis is regulated by a novel mechanism: Pro- and anti-angiogenic proteins are organized into separate platelet granules and differentially released. **Blood**, 2008 Feb 1;111(3):1227-33.

Kang, S.Y., Halvorsen, O.J., Lee, J.M., Liu, N.W., Johnston, B.T., Johnston, A.B., Akslen, L.A., and Watnick, R.S. Prosaposin inhibits tumor metastasis via paracrine and endocrine stimulation of stromal p53 and Tsp-1. In Press, Proc Natl Acad Sci USA 2009.

Manuscripts in preparation

Straume O, Shimamura T, Short S, Kalland KH, Folkman J, Akslen LA, Naumov GN. Reversal of the angiogenic phenotype of human breast cancer to a non-lethal dormant microscopic disease by targeting Heat Shock Protein 27. 2008 (*Manuscript in preparation, March 2009)*

Grillo J, DelloRusso C, Zaslavsky A, Folkman J, Ryeom S. Regulation of angiogenesis inhibitors by the breast cancer susceptibility gene (BRCA-1). (*Manuscript in preparation, March 2009).*

LIST OF PERSONNEL WHO WORKED ON THE PROJECT *(over the course of the project)*:

Personnel:	**Role**:	**Period**:
Judah Folkman, M.D.	Principal Investigator	03/01/04 – 01/14/08
Donald Ingber., M.D., Ph.D.	Principal Investigator	03/01/08 – 02/14/09
Kristie Aamodt	Research Technician	07/01/07 – 07/21/08
Bissan Ahmed, M.D., Ph.D.	Research Fellow	07/01/06 – 11/30/06
Nava Almog, Ph.D.	Research Fellow	03/01/04 – 06/30/04
Kwan-Hyuck Baek, Ph.D.	Research Fellow	05/06-09/06 & 11/07-02/08
Ofra Benny-Ratsaby, Ph.D.	Research Fellow	03/01/08 – 02/14/09
Nandita Bhattacharya, Ph.D.	Research Associate	07/05-01/07; 08/01/08-02/14/09
Amy Birsner	Veterniary Assistant	02/22/04 – 02/14/09
Catherine Butterfield	Research Technologist	08/06/06 – 02/14/09
Flavia Cassiola, Ph.D.	Research Fellow	07/01/06 – 01/31/07
David Cervi, Ph.D.	Research Fellow	02/01/05 – 08/31/06
Christiana DelloRusso, Ph.D.	Research Fellow	07/01/07 – 02/14/09
Ofer Fainaru, M.D., Ph.D.	Research Fellow	03/01/08 – 12/03/08
Wendy Foss	Administrative Associate	02/22/04 – 02/29/08
Deborah Freedman, Ph.D.	Research Fellow	03/01/04 – 08/12/05
Alexandra Grady	Program Administrator	02/01/05 – 02/14/09
Jenny Grillo	Research Technician	09/12/05 – 03/01/08
Kashayar Javaherian, Ph.D.	Research Associate	03/01/08 – 02/14/09
Brian Johnston	Research Technician	08/06/06 – 01/31/07
Soo-Young Kang, Ph.D.	Research Fellow	01/01/06 – 02/29/08
Lena Kikuchi	Research Technician	06/24/04 – 09/16/05
Giannoula Klement, M.D.	Research Associate	07/01/04 – 01/31/07
Michael Lampa	Research Technician	10/15/07 – 02/14/09
Jung Lee	Research Technician	05/29/05 – 07/23/07
Tong-Young Lee, Ph.D.	Research Fellow	07/01/07 – 02/29/08
Gang Liang, Ph.D.	Research Fellow	05/10/04 – 02/29/08
Eugene Lifshits, M.D.	Research Fellow	04/01/06 – 09/30/07
Meghan Lorina	Purchasing Coordinator	02/22/04 – 08/24/05
Ryan Lynch	Research Technician	01/08/06 – 08/21/06
George Naumov, Ph.D.	Research Associate	03/01/04 – 02/14/09
Daniela Prox, M.D.	Research Fellow	07/01/04 – 07/31/05
Matthew Rioth	Research Technician	05/31/05 – 06/28/06
Frank Rossi	Laboratory Assistant	08/22/04 – 08/19/06
Sandra Ryeom, Ph.D.	Research Associate	12/15/04 – 02/14/09
Sarah Schmidt	Admin. Assoc.; Purch. Coor.	09/05/04 – 03/01/08
Yuen Shing, Ph.D.	Research Associate	03/01/04 – 02/14/09
Sarah Short, Ph.D.	Research Fellow	11/01/04 – 05/31/05
Dessie Stewart	Laboratory Assistant	08/22/04 – 09/01/07
Randy Watnick, Ph.D.	Research Associate	03/01/04 – 02/14/09
Caitlin Welsh	Administrative Associate	07/30/07 – 03/01/08
Sun Yoo	Research Technician	09/10/07 – 06/28/08
Alexander Zaslavsky, Ph.D.	Research Fellow	07/01/06 – 02/29/08

CONCLUSION:

Our studies have identified HSP27 as a gene that may be important in regulating the angiogenic switch and have identified a novel function of the normal activity of the breast cancer susceptibility gene (BRCA1) as maintaining the expression of the endogenous angiogenesis inhibitor thrombospondin-1. We also have identified a novel protein, Prosaposin which contributes to the suppression of metastatic disease by regulation of TSP-1. These studies identify novel targets for the treatment and prevention of primary breast cancer and metastatic disease. The role of TSP-1 is a repeating theme throughout our studies and suggests that controlling the expression of this endogenous angiogenesis inhibitor through upstream regulators may be an important and novel anti-tumor therapy. In addition, our studies have optimized production of two potent anti-angiogenic therapies, endostatin and Lodamin (pegylated-TNP-470). Our work in identifying the optimal domain with increased stability of endostatin as well as modification of TNP470 for its use as an orally delivered drug paves the way for the preclinical testing of these therapies in breast as well as other cancers.

REFERENCES:

1. Hanahan D and Folkman J., 1996. *Cell* 86, 353-364.
2. Naumov GN, Bender E, Zurakowski D, Kang SY, Sampson D, Flynn E, Watnick RS, Straume O, Akslen LA, Folkman J, Almog N., 2006. *J Natl Cancer Inst*. 2006 98, 316-25
3. Venkitaraman AR. 2002. *Cell* 108, 171-182.
4. Kazerounian S, Yee KO, Lawler J. 2008. *Cell Mol Life Sci*. 65, 700-12.
5. Gupta PB, Mani S, Yang J, Hartwell K, Weinberg RA. 2005. *Cold Spring Harb Symp. Quant Biol*. 70, 291-7.
6. Nagy JA, Dvorak AM, Dvorak HF. 2007. *Annu Rev Pathol*. 2, 251-75.
7. Folkman J. 2004. *APMIS*. 112, 496-507.
8. Ingber, D. et al. 1990. *Nature* 348, 555-557.
9. Nahari, D. et al. 2007. *Mol Cancer Ther* 6, 1329-1337.
10. Sin, N., Meng, L., Wang, MQ., Wen, JJ., Bornmann, WG., Crews, CM. 1997. *Proc Natl Acad Sci U S A* 94, 6099-6103.
11. Zhang, Y., Griffith, E., Sage, J., Jacks, T. & Liu, J. 2000. *Proc Natl Acad Sci U S A* 97, 6427-6432.
12. Mauriz, J. et al. 2007. *Transl Res* 149, 46-53.
13. Kruger, E., Figg, WD. 2000. *Expert Opin Investig Drugs* 9, 1383-1396.
14. Cretton-Scott, E., Placidi, L., McClure, H., Anderson, D. & Sommadossi, 1996. *Cancer Chemother Pharmacol* 38, 117-122.
15. Bhargava, P. et al. 1999. *Clin Cancer Res* 5, 1989-1995.

16. Kudelka, A. et al. 1997. *Clin Cancer Res* 3, 1501-1505.
17. Benny, O. et al. 2008. *Nat Biotechnol* 26, 799-807.
18. Capon D.J., et al., 1989. *Nature* 337, 525.
19. Lee T-Y., et al., 2008. *Clin Cancer Res* 14, 1487.

Blood, 104: 239a, Abstract #839, 2004.

Abstract# 839

Early Tumor Detection Using Platelet Uptake of Angiogenesis Regulators.

Giannoula Klement,[1,2] Lena Kikuchi*,[1] Mark Kieran*,[2] Nava Almog*,[1] Tai-Tung Yip*,[3] Judah Folkman*.[2] *[1]Vascular Biology Program and Department of Surgery, Childrens Hospital and Harvard Medical School, Boston, MA, USA; [2]Pediatric Oncology, Dana-Farber Cancer Institute and Harvard Medical School, Boston, MA, USA; [3]Ciphergen Biosystems Inc., Freemont, CA, USA.*

We report a new function for platelets: selective sequestration of tumor-derived angiogenesis regulatory proteins above the concentration of these molecules in plasma.

Iodinated VEGF in a Matrigel pellet (from 100 to 600 ng/ 100 microl), implanted subcutaneously in mice, accumulates almost exclusively in platelets in a dose-dependent manner over a period as long as 2-3 weeks, without raising plasma levels of VEGF. Similarly, platelet VEGF increases in the presence of a single microscopic VEGF-secreting human tumor of up to only 1 mm^3 in SCID mice without any increase of VEGF in plasma. In addition to VEGF, other factors such as bFGF, PDGF, BDNF, endostatin and other regulators of angiogenesis are taken up by platelets in a selective and quantifiable manner which is dependent on tumor generation of these molecules. Our data show that these proteins are not simply associated with the platelet surface, but are internalized. Furthermore, they are protected from degradation within the platelet, and are not released by classical degranulating agents, such as thrombin, ADP or epinephrine. Incubation of human platelets with endostatin at above physiological levels results in decrease of the majority of platelet-associated VEGF and bFGF in a concentration-dependent manner.

Using SELDI-ToF mass spectroscopy of platelet extracts, we have found that this novel property of platelets enables the detection of microscopic tumors that undetectable by any presently available diagnostic method. The platelet angiogenic profile is more inclusive than a single biomarker because it can detect a wide range of tumor types and tumor sizes. Relative changes in the platelet angiogenic profile permit the tracking of a tumor throughout its development, beginning from an early *in situ* cancer.

Conclusions: (i) While the half-life of mouse platelets is approximately 3 days, the platelet angiogenic profile persists for as long as the tumor (or Matrigel pellet) is present. This indicates that platelets may continuously scavenge proteins which regulate angiogenesis. (ii) The fact that the presence of a human tumor can now be detected at microscopic size, suggests that it may not be necessary to know the type and location of a tumor before initiating treatment, especially since it is feasible to use anti-cancer therapies of little or no toxicity.

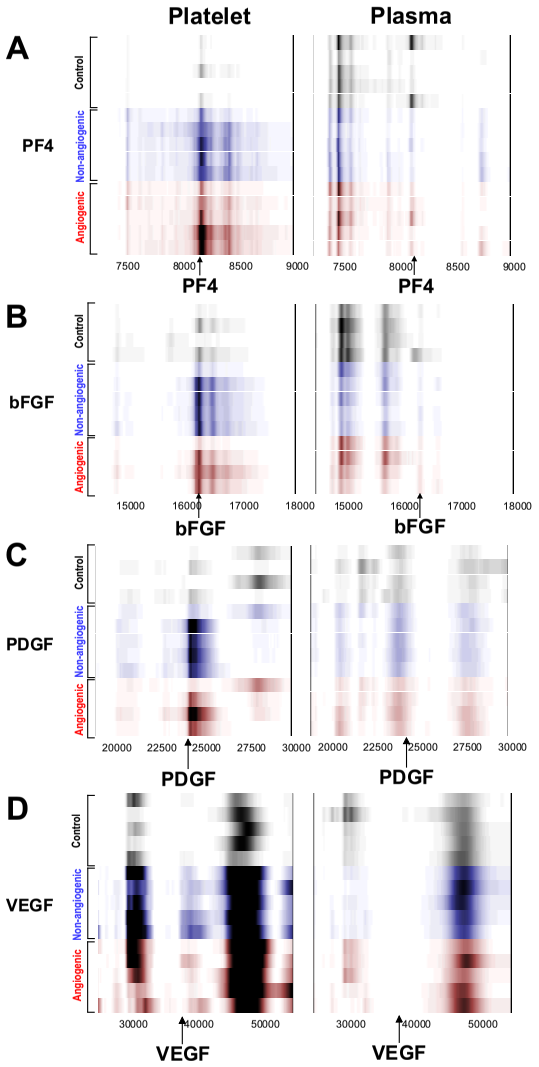

Protein expression maps of platelets and plasma extracts showing differential up-regulation of proteins within the platelets but not in plasma. X-axis is molecular weight of the proteins. Y-axis identifies groups: red are platelet protein extracts collected from mice bearing an angiogenic liposarcoma clone, blue are platelet protein extracts from mice bearing a non-angiogenic liposarcoma clone and grey are platelet protein extracts from control mice without tumors. All platelets samples were collected on day 30 post-tumor implantation. Non-angiogenic tumors are on average 1 mm^3 in size, whereas angiogenic average 1 - 2 cm^3.

Prolonged dormancy of human liposarcoma is associated with impaired tumor angiogenesis

Nava Almog,* Vanessa Henke,* Ludmila Flores,†, Lynn Hlatky,† Andrew L. Kung,‡ Renee D. Wright,‡ Raanan Berger,§ Lloyd Hutchinson,* George N. Naumov,* Elise Bender,* Lars A. Akslen,* Eike-Gert Achilles,‖ Judah Folkman*,[1]

*Vascular Biology Program and Department of Surgery, Children's Hospital Boston, Harvard Medical School, Boston, Massachusetts, USA; †Department of Radiation Oncology, ‡Department of Pediatric Oncology, §Department of Medical Oncology, Dana-Farber Cancer Institute, Harvard Medical School, Boston, Massachusetts, USA; and ‖Clinic for Hepatobiliary Surgery and Visceral Transplantation, University Hospital Hamburg, Germany

To read the full text of this article, go to http://www.fasebj.org/cgi/doi/10.1096/fj.05-3946fje

SPECIFIC AIMS

The aims of the study are: *1)* to characterize an experimental model that recapitulates the clinical dormancy of nonangiogenic human tumors in mice; and *2)* to study the physiological, cellular, and molecular mechanisms that underlie tumor dormancy that result from blocked angiogenesis.

PRINCIPAL FINDINGS

1. We show that while angiogenic liposarcomas expand rapidly after injection, dormant liposarcomas remain microscopic (Fig. 1) up to one-third of the normal SCID mouse life span, although they contain a significant percentage of proliferating tumor cells

At a predictable time, these tumors complete the sequential steps to achieve the angiogenic phenotype, initiate growth, and expand in size. Once dormant tumors undergo the angiogenic switch and initiate growth and expansion of mass, the tumor growth kinetics are similar to those of the angiogenic fast-growing tumors.

2. This tumor growth pattern is similar both in subcutaneous (s.c.) and orthotopic environments

3. The growth and expansion of the tumor mass appears to be blocked because of impaired angiogenesis

This dormant phenotype is characterized by minimal or significantly reduced intratumoral microvessel density, which increases abruptly following the angiogenic switch (**Fig. 2**) and leads to subsequent tumor growth. The scant microvessels that are observed in the microscopic dormant liposarcomas consist mainly of short clusters of endothelial cells that lack lumens.

4. Both tumor types cultured *in vitro* contain fully transformed cells, but only cells from the dormant human liposarcoma secrete relatively high levels of the angiogenesis inhibitors thrombospondin-1 and TIMP-1

5. This paper establishes the utility of using bioluminescence imaging to noninvasively monitor microscopic tumors over prolonged periods of time and to follow the kinetics of tumor dormancy and growth

CONCLUSIONS AND SIGNIFICANCE

The dormant human tumor, which contains fully transformed, proliferating neoplastic cells, is rendered harmless to the host by virtue of impaired angiogenesis (**Fig. 3**). This strengthens the concept that microscopic nonangiogenic dormant tumors may be a potential target for nontoxic antiangiogenic prophylactic cancer therapy. The ability to detect and treat cancer while it is still microscopic in size and years before it is symptomatic, would potentially revolutionize the management of cancer patients. Therefore, this work provides a scientific rational for the treatment of cancer with nontoxic angiogenesis inhibitors guided by biomarkers, years before the tumor can be anatomically located and before it is symptomatic. FJ

[1] Correspondence: Vascular Biology Program, Children's Hospital Boston, Harvard Medical School, Boston, MA 02115, USA. E-mail: judah.folkman@childrens.harvard.edu

doi: 10.1096/fj.05-3946fje

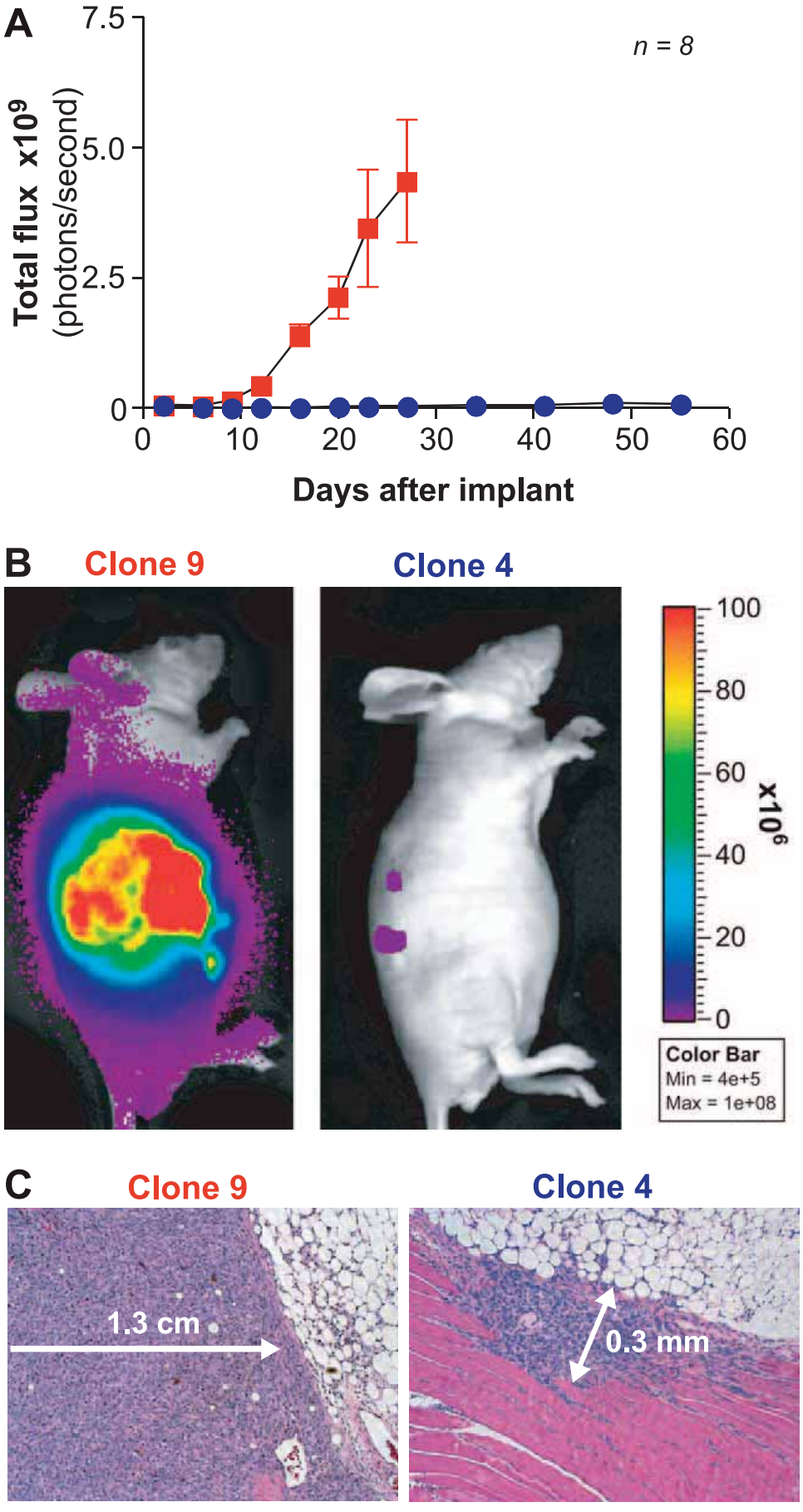

Figure 1. *In vivo* detection of orthotopically injected human tumor cells labeled with the luciferase reporter gene. *A*) Tumor growth of liposarcoma orthotopically injected into the retroperitoneal fat pad was monitored and quantified according to bioluminescence from labeled cells. The red line represents photon emission from mice injected with cells of the angiogenic clone 9, whereas the blue line represents that of mice injected with cells of the nonangiogenic dormant clone 4. Data are presented as mean ± SE. Eight mice were used per group (total of 16 mice per experiment) *B*) Representative mice that were orthotopically injected with cells from clone 9 (*left*) or clone 4 (*right*) at day 27 after injection. The gray photographic images of the mice and bioluminescence color images were superimposed. *C*) The presence of tumors was confirmed by histological analysis according to H&E staining (original magnification ×100).

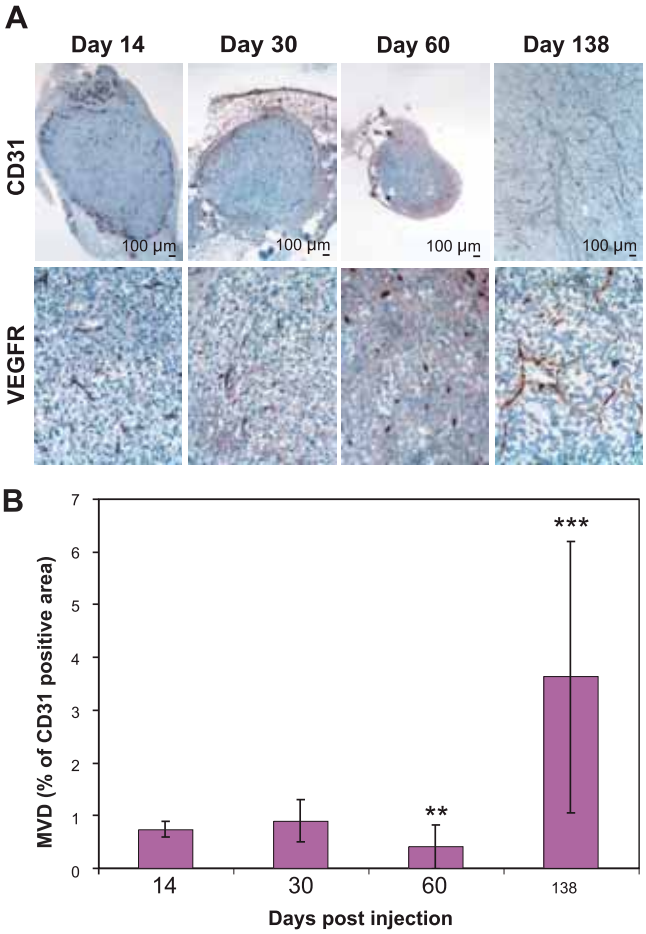

Figure 2. Vasculature in tumors generated from clone 4. *A)* Histological analysis of tumor vasculature was performed by immunostaining for CD31 and VEGF receptor. *Top)* CD31 staining (original magnification ×40). *Bottom)* immunohistochemistry of VEGFR (original magnification ×200). *B)* Quantification of CD31-positive area from tumors described in *A*. $n = 5$ for number of tumors collected at each time point. Compared to tumors collected at day 14 postinjection, there is a statistically significant decrease in microvessel density (MVD) compared to tumors collected at day 60 (P=0.00199). There is statistically significant (P<0.01) increase in MVD in tumors collected after the angiogenic switch (day 138 on average).

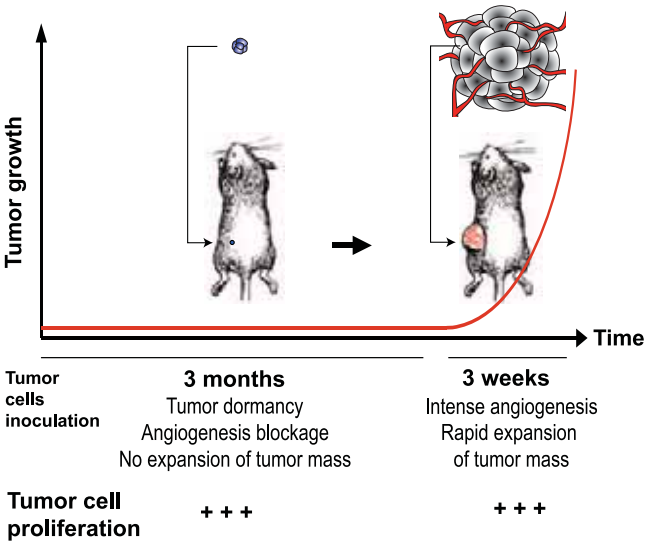

Figure 3. Schematic diagram.

Prolonged dormancy of human liposarcoma is associated with impaired tumor angiogenesis

Nava Almog,* Vanessa Henke,* Ludmila Flores,† Lynn Hlatky,† Andrew L. Kung,‡ Renee D. Wright,‡ Raanan Berger,§ Lloyd Hutchinson,* George N. Naumov,* Elise Bender,* Lars A. Akslen,* Eike-Gert Achilles,‖ and Judah Folkman*,[1]

*Vascular Biology Program and Department of Surgery, Children's Hospital Boston, Harvard Medical School, Boston, Massachusetts, USA; †Department of Radiation Oncology, ‡Department of Pediatric Oncology, §Department of Medical Oncology, Dana-Farber Cancer Institute, Harvard Medical School, Boston, Massachusetts, USA; and ‖Clinic for Hepatobiliary Surgery and Visceral Transplantation, University Hospital, Hamburg, Germany

ABSTRACT **The disease state of cancer appears late in tumor development. Before being diagnosed, a tumor can remain for prolonged periods of time in a dormant state. Dormant human cancer is commonly defined as a microscopic tumor that does not expand in size and remains asymptomatic. Dormant tumors represent an early stage in tumor development and may therefore be a potential target for nontoxic, antiangiogenic therapy that could prevent tumor recurrence. Here, we characterize an experimental model that recapitulates the clinical dormancy of human tumors in mice. We demonstrate that these microscopic dormant cancers switch to the angiogenic phenotype at a predictable time. We further show that while angiogenic liposarcomas expand rapidly after inoculation of tumor cells in mice, nonangiogenic dormant liposarcomas remain microscopic up to one-third of the normal severe combined immune deficiency (SCID) mouse life span, although they contain proliferating tumor cells. Nonangiogenic dormant tumors follow a similar growth pattern in subcutaneous (s.c.) and orthotopic environments. Throughout the dormancy period, development of intratumoral vessels is impaired. In nonangogenic dormant tumors, small clusters of endothelial cells without lumens are observed early after tumor cell inoculation, but the nonangiogenic tumor cannot sustain these vessels, and they disappear within weeks. There is a concomitant decrease in microvessel density, and the nonangiogenic dormant tumor remains harmless to the host. In contrast, microvessel density in tumors increases rapidly after the angiogenic switch and correlates with rapid expansion of tumor mass. Both tumor types cultured *in vitro* contain fully transformed cells, but only cells from the nonangiogenic human liposarcoma secrete relatively high levels of the angiogenesis inhibitors thrombospondin-1 and TIMP-1. This model suggests that as improved blood or urine molecular biomarkers are developed, the microscopic, nonangiogenic, dormant phase of human cancer may be vulnerable to antiangiogenic therapy years before symptoms, or before anatomical location of a tumor can be detected, by conventional methods.—Almog, N., Henke, V., Flores, L., Hlatky, L., Kung, A. L., Wright, R. D., Berger, R., Hutchinson, L., Naumov, G., Bender, E., Akslen, L., Achilles, E.-G., Folkman, J. Prolonged dormancy of human liposarcoma is associated with impaired tumor angiogenesis. *FASEB J.* 20, E1–E10 (2006)**

THE DISEASE STATE of cancer appears late in tumor development (1). Dormant tumors remain microscopic and do not expand in size over prolonged periods of time. These microscopic dormant tumors represent one of the earliest stages of human neoplasia. They are commonly found as occult lesions at autopsies of individuals who died of trauma, but who did not have clinically detectable cancer during life (1–4). Such dormant tumors also include *in situ* carcinomas, residual cancer cells following removal of primary tumors, and micrometastases that can remain clinically asymptomatic and undetectable for years (5,6). While some types of tumor dormancy may be due to a preponderance of noncycling tumor cells, most dormant tumors consist of fully transformed, viable, proliferating tumor cells. Once these tumor cells undergo the switch to the angiogenic phenotype (7), an event often preceded by decreased expression of one or more endogenous angiogenesis inhibitors (8), these angiogenic tumors expand rapidly and kill their hosts.

Without neovascularization, even fully transformed cells, which have the capacity for uncontrolled proliferation, cannot form tumors of a clinically relevant size (7, 8). Blocking various stages of tumor angiogenesis has therefore become a promising strategy for treating cancer (9).

Despite the high prevalence of dormant tumors, their biology is poorly understood (10). This is mainly because of their microscopic size, which renders them invisible to conventional imaging technology and be-

[1] Correspondence: Vascular Biology Program, Children's Hospital Boston, Harvard Medical School, Boston, MA 02115, USA. E-mail: judah.folkman@childrens.harvard.edu

doi: 10.1096/fj.05-3946fje

cause of the lack of suitable experimental models. We previously developed an *in vivo* experimental system of human liposarcoma subclones, which after inoculation into immunodeficient mice, form either nonangiogenic, dormant tumors, or angiogenic, rapidly growing tumors (11). This system was based on the human liposarcoma cell line (SW872) that forms rapidly growing angiogenic tumors when inoculated into mice.

In this report we have selected two of these subclones. One clone generates angiogenic tumors that grow rapidly, reach a size of approximately 1500 mm^3 in 30–35 days, at which time they are also lethal to their host mice. The other clone forms dormant tumors that remain microscopic for 3–4 mo.

We have defined "nonangiogenic" tumor cells as unable to induce or to sustain the induction of new microvessels from the host. Nonangiogenic tumor cells achieve a maximum tumor diameter of ~1 millimeter. The tumor cells themselves maintain a high proliferation rate balanced by a high apoptotic rate *in vivo*. Therefore, dormant microscopic tumors do not expand further until a median of ~3 mo, when tumors switch to the angiogenic phenotype and undergo rapid growth. We have isolated nonangiogenic tumor cells from other human tumors, not shown here. They also switch to the angiogenic phenotype, but at different times and at different percentages than the liposarcoma (11). We chose liposarcoma for this study because it has a higher rate of switching to the angiogenic phenotype than other human tumors.

We also demonstrate that the switch to the angiogenic phenotype from the nonangiogenic microscopic dormant state, can be accurately quantified by bioluminescence of tumors that are less than 1 mm in diameter. We further show that dormant tumors contain fully transformed cells that continuously proliferate and undergo apoptosis. This dormant phenotype is characterized by minimal or significantly reduced intratumoral microvessel density which continues to decrease to virtually no microvasculature by a few weeks after tumor cell inoculation. The scant microvessels that are observed in the early stage of microscopic dormant liposarcomas, consist mainly of short clusters of endothelial cells that lack lumens. These cannot be sustained, and gradually disappear with time. Tumor cells from nonangiogenic dormant tumors secrete high levels of the angiogenesis inhibitors thrombospondin-1 (TSP-1), and tissue inhibitor of metalloproteinases (TIMP-1).

MATERIALS AND METHODS

Cell lines and culture

All cell lines were cultured in Dulbecco's modified Eagle's medium (DMEM) containing 5% inactivated FBS (Life Technologies, Gaithersburg, MD), 1% antibiotics (penicillin, streptomycin) and 0.29 mg/ml L-glutamine in a humidified 5% CO_2 incubator at 37°C. For *in vivo* imaging of luciferase-labeled cells, tumor cells from each of the clones were infected with a virus containing the firefly luciferase (FL) gene as described previously (12). For the proliferation assay, 2500 cells per well were seeded in 24-well plates. Every 24 h, three wells per clone were trypsinized and the number of cells was determined using a cell counter (Coulter).

Animals and tumor cell inoculation

For analysis of s.c. growth of tumors, 6-wk-old male severe combined immune deficiency (SCID) mice from the Massachusetts General Hospital (MGH), Boston, MA. were used. All of these experiments were conducted in compliance with Boston Children's Hospital guidelines. Protocols were approved by the Institutional Animal Care and Use Committee. For monitoring growth of tumors generated by luciferase infected cells, male nude mice were used (Taconic Farms, Germantown, NY). For inoculations of tumor cells into mice, confluent tumor cells were rinsed in PBS (PBS) (Sigma, St. Louis, MO), briefly trypsinized and suspended in DMEM (without serum). The cells were washed in DMEM twice and then adjusted to a final concentration, according to type of analysis. For monitoring s.c. growth of tumors, 25×10^6 viable cells/ml were used. Each mouse was injected s.c. on the dorsal surface with 5×10^6 cells (in 0.2 ml of DMEM without serum) from a single cell line. Each mouse received only one injection of tumor cells. Tumor volumes were recorded every 3–4 days. Tumor volume was calculated using the standard formula: length $\times$ width$^2 \times$ 0.52. For orthotopic injections, an incision of 5 mm was made in the right flank of anesthetized nude mice. The peritoneum was exposed and 0.5×10^6 luciferase infected cells in 0.1 ml of DMEM, which were inoculated into the renal fat pad. For histological analysis of s.c. tumors, each mouse was inoculated at 4 sites on the dorsal surface with $3.8–5 \times 10^6$ viable cells/inoculation.

Immunohistochemistry

Tumor tissues from a mouse were fixed in 10% neutral buffered formalin at room temperature overnight. Tissues were embedded in paraffin, and sections (5 μm thick) were stained with hematoxylin and eosin (H&E). For immunohistochemical staining for CD31 (Pharmingen, San Diego, CA) and vascular endothelial growth factor receptor (Pharmingen), slides were treated with proteinase K at 37°C after deparaffinization, then blocked with TNT buffer for 30 min at room temperature. The slides were incubated with primary antibody (Ab) overnight at 4°C. Slides were then incubated in SA-HRB for 30 min at room temperature, biotinyl tyramide for 7 min at room temperature (PerkinElmer Life Science, Norwalk, CT), and alkaline phosphatase conjugated to avidin (Vector Laboratories, Burlingame, CA), for 30 min. The slides were then developed with the substrate Nova Red (Vector), according to the manufacturer's instructions. Slides were counterstained for 2–4 min in Gill's hematoxylin and mounted with a coverslip.

Apoptosis was assessed by terminal deoxynucleotidyltransferase-mediated dUTP nick end labeling (TUNEL) with ApopTag Apoptosis Detection System (Intergen, Purchase, NY) according to the manufacturer's instruction. Tumor cell proliferation was analyzed by PCNA staining with the monoclonal anti-PCNA Ab PC10 (DAKO, Glostrup, Denmark). After deparaffinization, slides were treated with citrate buffer 0.1 M (Sigma) in a microwave oven to near boiling for 10 min and blocked with 10% goat serum in PBS with 0.3% triton-X (PBS-TX) for 30 min. The slides were then incubated with the primary Ab diluted 1:100 for 1 h. Slides were then incubated in biotinylated goat antimouse IgG (Vector) for 30 min (1:400). The slides were incubated with alkaline phosphatase

conjugated to avidin (Vector), for 30 min. The slides were then incubated with substrate Nova Red (Vector), according to the manufacturer's instructions. Slides were counterstained for 2–4 min in Gill's hematoxylin, and mounted with a coverslip.

Imaging and determination of microvessel density

For imaging we used a Polyvar microscope (Leica Cambridge), a 3-CCD camera, and slides with high color contrast. Each slide was measured by individual frames of standard size. We measured the area (the total number of detected pixels within the field), as well as other features, including length, width, roundness, and bifurcation, using Quantimet 570 software in color detection mode (22).

The intensity of immunohistochemical staining of CD31 was quantified through evaluation of the Nova Red endpoint. The tumor area sampled was within the central area of the tumor. Peripheral areas of the tumor were excluded from analysis. The size of the sampled area, which varied with the size of the tumor, was divided into a grid of from 3 to 20 frames. Within each frame, quantification of the positively stained areas was achieved by operator-controlled threshholding, which summed all areas within the selected wavelengths. Five tumors from the nonangiogenic clone 4 were collected at each of the following time points: day 14, 30, and 60 after tumor cell inoculation. From these five tumors, 46, 12, and 25 frames, respectively, were imaged and quantified. Five large (over 1000 mm^3) angiogenic tumors (originally from nonangiogenic clone 4) were collected following the angiogenic switch at 105–168 days (on average 138 days) after tumor cell inoculation. For quantification of microvessel density (MVD), a total of 134 frames from these tumors from clone 4 were imaged and quantified. Five large tumors (over 1000 mm^3) from the angiogenic clone 9 were collected on days 31–37 after injection (day 34 on average). A total of 173 frames from tumors from clone 9 were imaged and quantified. For quantification of the percentage of proliferating cells (PCNA positively stained cells), a total of 80 frames (from 4 tumors) of clone 4 tumors were imaged and quantified. A total of 97 frames (from 5 tumors) of clone 9 tumors were imaged and quantified. For quantifying the branching sites, the incidence of two vessels arising from the same site on a vessel were automatically counted per a defined area of tumor. A total of 1138 frames from tumors on day 14 and 625 frames from tumors on day 138 (on average) were automatically counted.

In vivo detection of luciferase-labeled cells

Mice anesthetized by intraperitoneal (i.p.) injection of 155 mg/kg of ketamine and 2 mg/kg xylazine, were imaged using the in vivo imaging system (IVIS, Xenogen, Alameda, CA), as described previously (14). Bioluminescence was not normalized to bioluminescence at the initiation of experiment.

ELISA and Western blot for angiogenic factors from conditioned media

0.5×10^6 cells from each cell line were seeded in each well of a 6-well plate. The next day the medium was changed to DMEM without serum for ELISA analysis of TIMP-1 and TSP-1, and with 1% serum for ELISA analysis of vascular endothelial growth factor (VEGF) and basic fibroblast growth factor (bFGF), and the cells were incubated for 24 h. Conditioned medium was then collected and centrifuged to eliminate cell debris. VEGF, bFGF, and TIMP-1 levels were determined using the Quantikine ELISA kits for human VEGF and TIMP-1, and the Quantikine high-sensitivity ELISA kit for human bFGF (R&D System, Minneapolis, MN).

Soft agar assay

Assays to determine anchorage independence of tumor cells were performed as described previously (15).

Statistical methods

In vivo data were expressed as mean ± SE. *In vitro* data were expressed as mean ± SD Statistical significance was assessed using Student's t test. $P < 0.05$ was considered statistically significant. All statistical tests were two-sided.

RESULTS

Analysis of s.c. tumor growth in immunodeficient mice

We previously developed an *in vivo* experimental system of human liposarcoma single cell-derived subclones, which form either nonangiogenic, dormant tumors or angiogenic rapidly growing tumors in immunodeficient mice (12). These subclones, which were not artificially genetically modified, generated tumors with distinctly different vasculature. For this study of a detailed analysis of the angiogenic potential and cellular characteristics of the tumor cells, clone 9, which forms angiogenic rapidly growing tumors, and clone 4, which most consistently forms dormant tumors, were chosen.

The angiogenic human liposarcoma clone 9 generated large, lethal tumors 30–40 days after the injection of the cells, while microscopic-sized tumors of up to 1 mm in diameter, generated from the nonangiogenic clone 4, remained undetectable by gross examination at these time points (**Fig. 1*A***). Cells from nonangiogenic clone 4 generated detectable tumors only after the angiogenic switch (which occurred at a range of ~87–120 days after tumor cell inoculation, i.e., approximately one-third of the SCID mouse life span).

All of the nonangiogenic dormant tumors switched to the angiogenic phenotype and began rapid growth. These newly emerging angiogenic tumors grew as rapidly as tumors from clone 9 that were angiogenic when they were initially inoculated. In fact, angiogenic tumor cells from clone 9, grew to large sizes of approximately over 1500 mm^3 diameter by 4–5 wk after tumor cell inoculation.

The most pronounced difference between sizes of tumors from the clones was seen 4–5 wk after injection. At that time, large and highly vascularized tumors developed from clone 9, while in mice injected with clone 4, tumors could be seen only on the inner side of the skin, sometimes requiring a hand-lens (Fig. 1*B*). The presence of these microscopic tumors was confirmed by histochemical analysis (Fig. 1*C*). Indeed, throughout the dormancy periods of tumors from clone 4, H&E staining revealed that all tumors were less than 1.5 mm diameter.

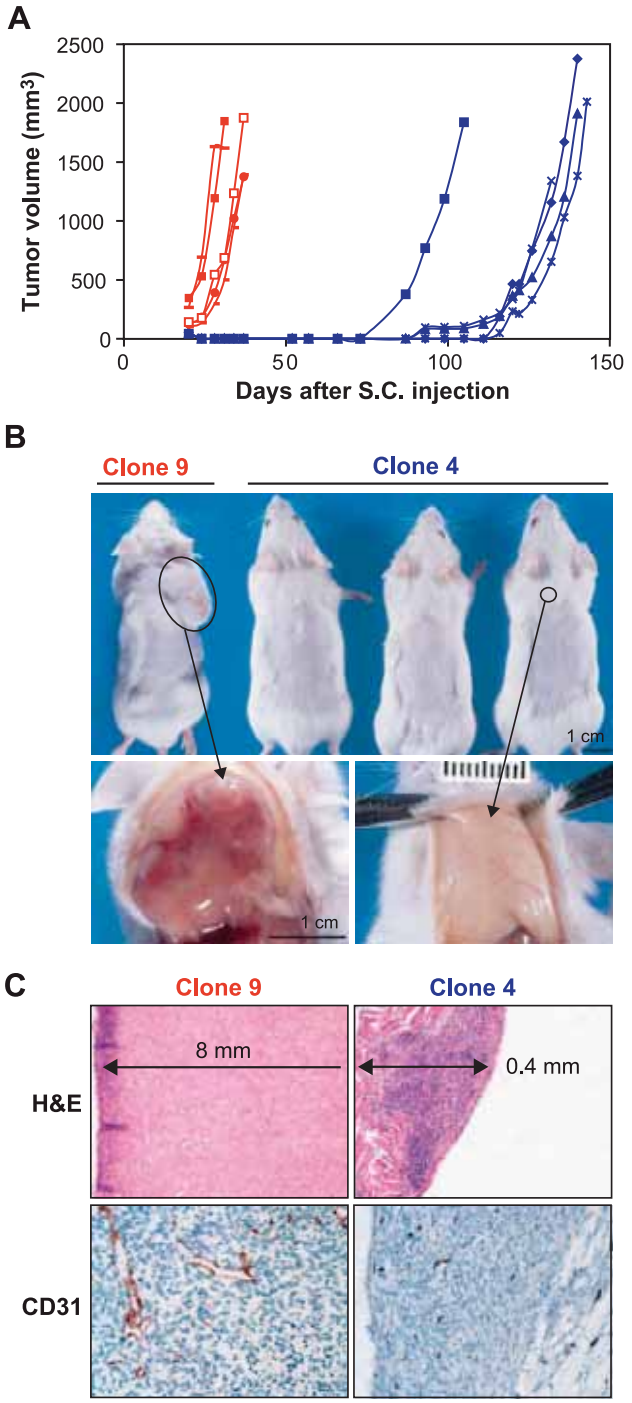

Figure 1. Characterization of human liposarcomas growth s.c. in SCID mice. *A)* Growth kinetics of tumors generated from clone 9 (red lines) or from clone 4 (blue lines). Each line represents one tumor. Five mice were used per group (total of 10 mice per experiment) *B)* Representative tumor-bearing mice that were injected with cells from clone 9 or clone 4 at 31 and 42 days after injection, respectively (*top*). *Bottom)* tumors from clone 9 (*bottom, left*) and from clone 4 (*bottom, right*). *C)* Histological analysis of representative tumors derived from clone 9 and clone 4 shown in *B*. Tissue sections were stained with hematoxylin and eosin (H&E; original magnification ×100) or with antibodies directed against CD31 (original magnification ×200).

Four to five weeks after tumor cell inoculation, new functional blood vessels were abundant in angiogenic, rapidly growing tumors from clone 9. These vessels had large lumens that contained red blood cells. In contrast, these vessels were not found in the nonangiogenic dormant tumors. The only structures resembling microvasculature in the nonangiogenic dormant tumors were short clusters of endothelial cells, the majority of which had no lumens and contained no red blood cells (Fig. 1*C*). Even these could not be sustained and gradually disappeared by 40–60 days (see below).

Characterization of orthotopic tumor growth

To determine whether the differences in tumor growth are influenced by the host's s.c. microenvironment, we also studied orthotopic tumor growth. Tumor cells were labeled with firefly luciferase (FL), a cellular bioluminescence marker that allows convenient detection *in vivo*. These tumor cells were inoculated into the renal fat pad of nude mice. The fate of labeled cells was followed *in vivo* with a highly sensitive cooled charge-coupled camera (Xenogen). This method enabled us to pinpoint the location of the microscope-sized dormant tumors and to monitor the viability of the tumor cells and the precise time of the angiogenic switch in a quantitative, real time and noninvasive manner. (**Fig. 2**).

The patterns of tumor growth in the renal fat pad were similar to those in the s.c. location (Fig. 2*A*). While cells from the angiogenic clone 9 generated rapidly growing tumors, cells from the nonangiogenic clone 4 generated microscopic sized, dormant tumors that remained at the initial size of ~1 mm diameter or less, for a prolonged period of 62–106 days after tumor cell inoculation. Nonangiogenic tumors from clone 4 could not be detected by gross examination of the mice, except by luciferase bioluminescence.

Angiogenic tumors from clone 9 generated large tumors (diameter of over 1 cm) by ~27 days (Fig. 2*B*). In contrast, nonangiogenic tumor cells from clone 4 formed dormant tumors (as quantified by luminescence). On examination of the peritoneum, large, vascularized tumors were evident in the peritoneal cavity of mice that were injected with angiogenic tumor cells from clone 9, whereas no tumors were detected following gross examination of the peritoneum of mice that received inoculations of nonangiogenic tumor cells from clone 4. The presence of microscopic, dormant tumors from clone 4 was revealed only after histological analysis of the renal fat pad (Fig. 2*C*). The size of the orthotopic dormant tumors was very similar to those of dormant tumors formed in the s.c. space.

Tumor cell proliferation is not inhibited during tumor dormancy

To rule out that tumor dormancy of nonangiogenic tumors did not simply result from low or no tumor cell proliferation, we analyzed tumor cell viability and pro-

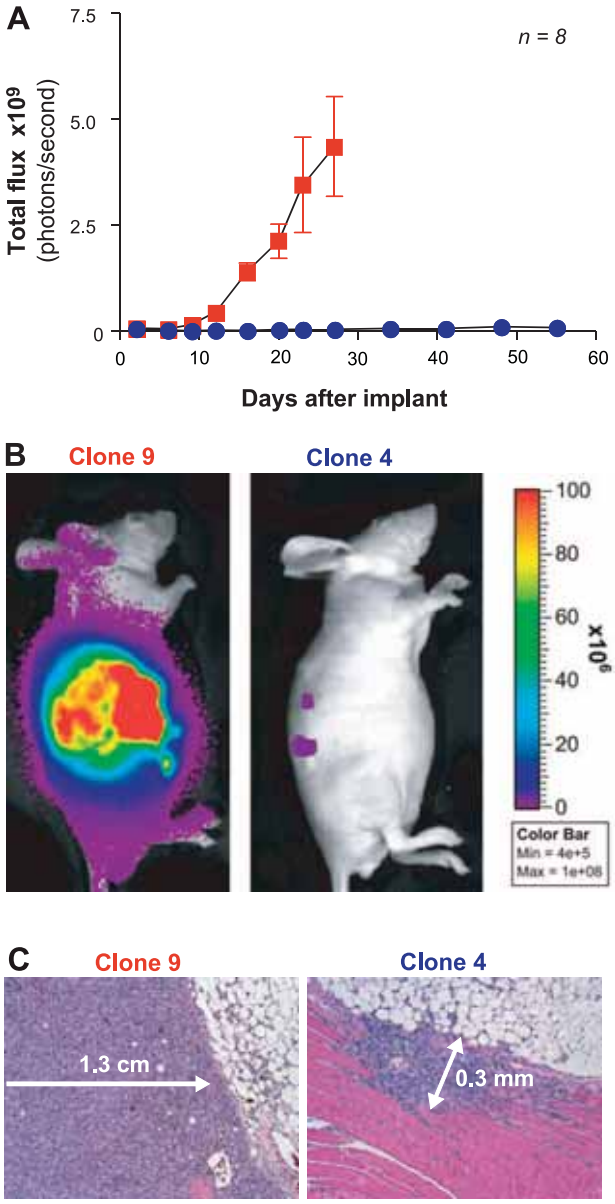

Figure 2. *In vivo* detection of orthotopically injected human tumor cells labeled with the luciferase reporter gene. *A)* Tumor growth of liposarcoma orthotopically injected into the retroperitoneal fat pad was monitored and quantified according to bioluminescence from labeled cells. The red line represents photon emission from mice injected with cells of clone 9, whereas the blue line represents that of mice injected with cells of clone 4. Data are presented as mean ± SE. Eight mice were used per group (total of 16 mice per experiment) *B)* Representative mice that were orthotopically injected with cells from clone 9 (*left*) or clone 4 (*right*) at day 27 after injection. The gray photographic images of the mice and bioluminescence color images were superimposed. *C)* The presence of tumors was confirmed by histological analysis according to H&E staining (original magnification ×100).

liferation *in vivo* throughout the dormancy period. We collected tumors that were generated from nonangiogenic tumors at different time points following tumor cell inoculation, before and after the angiogenic switch and the subsequent tumor growth (**Fig. 3*A***). Tumors were harvested during the initial 2 mo after tumor cell inoculation, and also from 105 to 168 days postinoculation (the average day is 138), when after the angiogenic switch, tumor diameter had reached or exceeded 10 mm.

Throughout the dormancy period, tumors maintained a diameter of less than 1.5 mm (Fig. 3*A*, *top*, H&E staining). However, in all tumors collected, numerous tumor cells staining positively for PCNA were evident (Fig. 3*A*, *bottom*). Apoptotic cells were evident in all of the dormant tumors analyzed (data not shown). This result suggests that tumor cell proliferation is balanced by cell death. We further quantified and compared the percentage of proliferating cells in nonangiogenic tumors generated from clone 4 and angiogenic tumors from clone 9. Large tumors with a diameter >10 mm were collected 105–168 or 31–37 days post-tumor cell inoculation, respectively. 46.88% (±24.5%) of cells in nonangiogenic clone 4 tumors were positively stained for PCNA, compared to 81.3% (±18.12%) tumor cells positively stained for PCNA in angiogenic tumors from clone 9.

We confirmed the existence, location, and viability of tumor cells by following the fate of tumor cells from clone 4 that were labeled with luciferase (FL) and injected s.c. in nude mice and by monitoring the bioluminescence from the tumor cells (Fig. 3*B*). The enzymatic activity of luciferase is rapid and transient and can be detected only following injection of the substrate. Throughout the dormant period (up to 120 days), tumor cells could be detected by the luciferase enzymatic activity, although no tumor was visible by gross examination on the dorsal surface of the mice. This implies that viable and metabolically active tumor cells persist and survive at the site of injection. Moreover, luminescence intensity increased ~2 to 3-fold before any tumor growth could be detected by gross examination. An increase of luminescence was followed by growth of the tumor. Therefore, tumor dormancy in this model does not result from eradication, or from cell cycle arrest of the tumor cells.

Vascular structure in microscopic tumors

To examine the angiogenic potential of the nonangiogenic dormant tumors, we analyzed the presence, size, and structure of vessels in tumors by immunohistochemical staining for CD31 and VEGF receptor (VEGFR).

At least until 60 days after inoculation, the majority of the vessels inside of tumors appear as small clusters of endothelial cells that lack open lumens (**Fig. 4*A***). At the periphery of the dormant tumors at an early stage (day 14), abundant vessels with open lumens that contain red blood cells are observed (Fig. 4*A*). This type of vessel is rare inside the dormant tumor. After the angiogenic switch, when tumors enlarge and expand in mass, many large vessels are evident. Only then, intratumoral ves-

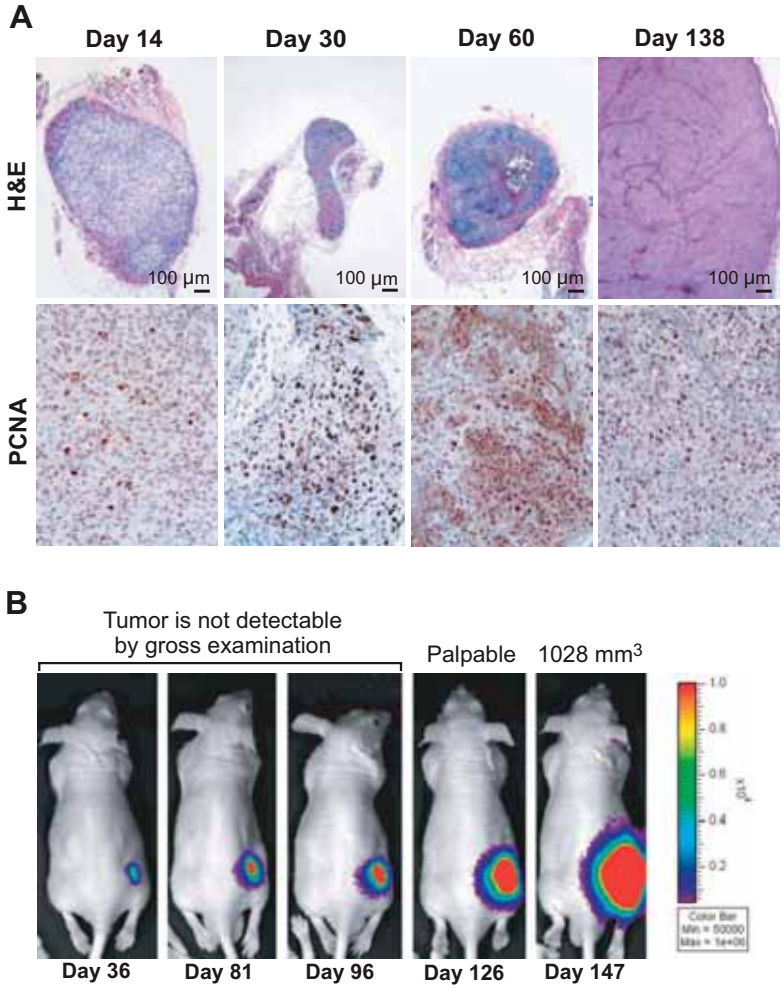

Figure 3. Analysis of tumor cell viability and proliferation in tumors generated from clone 4. *A)* Histology of tumors generated from clone 4 that were collected at different time points. Dormant tumors, undetectable by gross examination, were collected at days 14, 30, and 60 postinjection. Large tumors with diameter greater than 10 mm were collected on days 105–168 postinjection (averaged day of collection is 138). $n = 5$ for tumors collected at day 14, 30, and 60 and for large tumors at day 105–168. H&E images were taken at original magnification of ×40 (scale bars represent size of 100 μm) and of PCNA at ×200. *B)* Luciferase-labeled cells from clone 4 were injected s.c., and tumor growth was monitored both by gross examination and by luminescence detection. Tumor size measured by palpation is indicated.

sels often reveal large lumens and contain red blood cells. In addition, these vessels have more branching sites (number of branching sites in tumors on day 14 was 0.3±0.85 while in tumors on day 138 there were 0.55±1.61). This pattern of vasculature is similar to that found in large tumors generated from the angiogenic clone 9 (Fig. 1*C*).

We analyzed the microvessel density (MVD), as well as the average length of intratumoral vessels throughout the dormancy period. Interestingly, in tumors generated from nonangiogenic clone 4, the microvessel density, as well as the average length of intratumoral vessels, decreased between day 14 to 60 post inoculation (Fig. 4*B*, as well as data not shown). The decrease is most pronounced in the second month post inoculation (from day 30 to day 60). The microvessel density and average intratumoral vessel length, perimeter, and area increase after the angiogenic switch (Fig. 4*B* as well as data not shown). This suggests that tumor dormancy is associated with inhibition of angiogenesis. The inhibition is relieved following the angiogenic switch.

MVD was measured also in large tumors (with diameters over 10 mm). The MVD in large tumors from clone 4 (collected after the angiogenic switch at 105–168 days postinoculation) was significantly higher (3.63±2.6, $P<0.01$) than that in similar sizes of clone 9 angiogenic tumors at (1.98±1.51).

Comparison of angiogenic potential

We further analyzed the relative expression and secretion of angiogenic factors that are known to affect tumor angiogenesis, focusing on VEGF and bFGF.

Expression of these factors was higher in the tumor cells that formed nonangiogenic dormant tumors (**Fig. 5*A*** and ***B***). However, these tumor cells also released significant quantities of thrombospondin-1 (TSP-1) into their conditioned medium (Fig. 5*D*). The thrombospondin-1 levels in cells that form nonangiogenic dormant tumors were consistently higher than in cells that generated angiogenic tumors (Fig. 5*D*). High levels of TSP-1 were previously reported to result from elevated levels of phosphorylated Myc (15). Consistent with these observations, significantly higher levels of Myc protein and its phosphorylated form were found in the nonangiogenic tumor cells (clone 4) than in angiogenic tumor cells (clone 9) (Watnick, R., personal communication).

In the search for markers of nonangiogenic dormant tumors, we compared the protein profiles in the conditioned medium of the cell lines that generate the

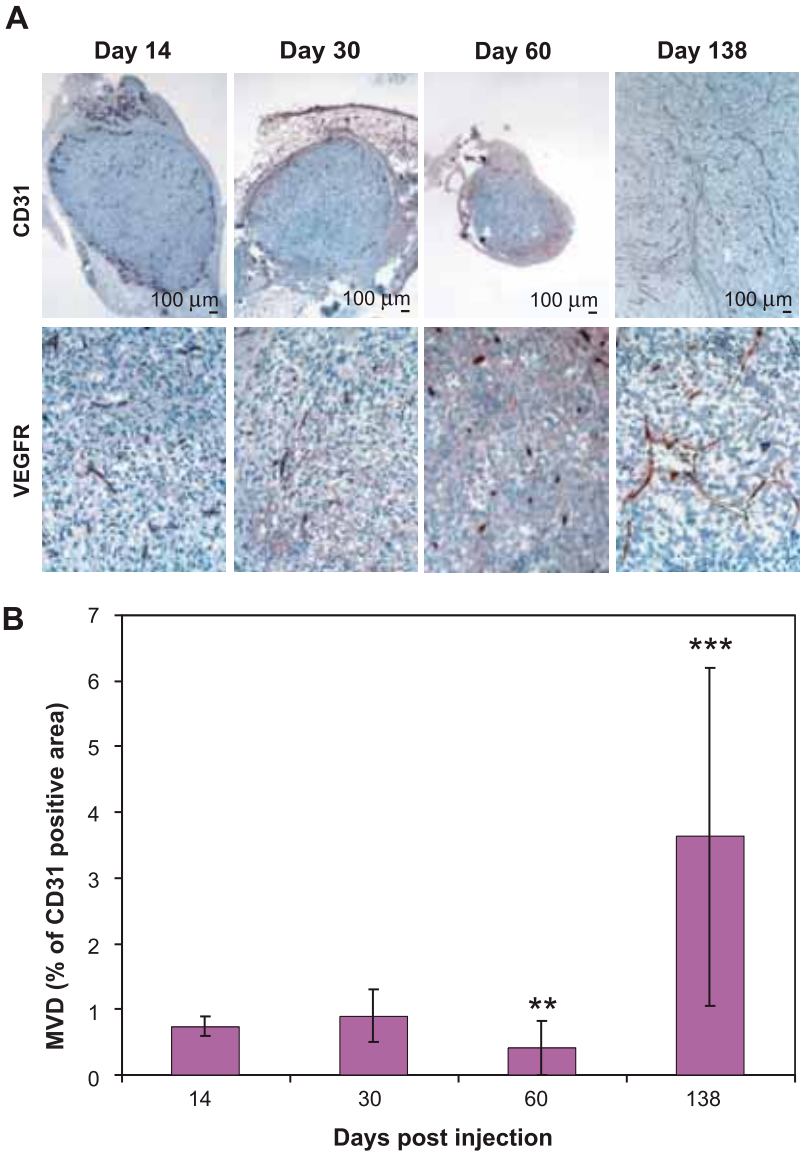

Figure 4. Vasculature in tumors generated from clone 4. *A)* Histological analysis of tumor vasculature was performed by immunostaining for CD31 and VEGF receptor. *Top)* CD31 staining (original magnification ×40). *Bottom)* immunohistochemistry of VEGFR (original magnification ×200). *B)* Quantification of CD31-positive area from tumors described in *A*. $n = 5$ for number of tumors collected at each time point. Compared to tumors collected at day 14 postinjection, there is a statistically significant decrease in microvessel density (MVD) compared to tumors collected at day 60 (P=0.00199). There is statistically significant (P<0.01) increase in MVD in tumors collected after the angiogenic switch (day 138 on average).

different tumor types. We used two-dimensional gel electrophoresis to separate proteins and bioinformatic analysis to isolate proteins that are highly expressed in the dormant tumors and not in the angiogenic rapidly growing tumors (data not shown). Using this approach, we found that the dormant nonangiogenic liposarcoma cells secrete a relatively high concentration of tissue inhibitor of metalloproteinase (TIMP-1). This result was further confirmed by ELISA for TIMP-1 (Fig. 5*C*) and by a radiometric MMP/TIMP activity assay (personal communication by M. Moses and G. Louis).

Human liposarcoma cells from both nonangiogenic and angiogenic clones are fully transformed

To analyze the tumorigenicity of cells, we compared their ability to grow in an anchorage-independent manner. Tumor cells from both nonangiogenic and angiogenic clones were seeded in soft agar and the presence of colonies was recorded 34 days later. Both clones consist of fully transformed cells that are able to grow and form colonies in soft agar (**Fig. 6*A***).

Although both clones were anchorage independent, colonies generated from angiogenic tumor cells (clone 9) appeared larger and more abundant than colonies generated from nonangiogenic tumor cells (clone 4). *In vitro*, the proliferation of the angiogenic tumor cells from clone 9 was slightly increased compared to nonangiogenic tumor cells from clone 4 (Fig. 6*B*). This is consistent with the differences of the percentage of proliferating cells *in vivo* and may explain, in part, the ability of angiogenic clone 9 tumor cells to form somewhat larger colonies in soft agar.

DISCUSSION

We show here that dormant, nonangiogenic human liposarcoma contains fully transformed, proliferating, neoplastic cells throughout the dormancy period (of approximately one-third of the life span of a SCID

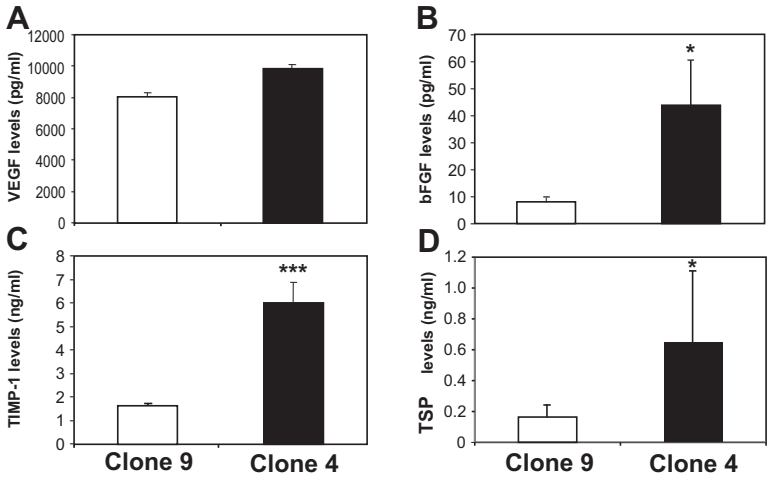

Figure 5. Measurements of secreted angiogenic and antiangiogenic factors in the conditioned medium of tumor cells grown *in vitro*. Solid bars represent results from conditioned medium collected from clone 4, whereas open bars represent those from clone 9. *A)* VEGF levels as determined by ELISA and normalized per 10^6 cells. There is no statistically significant difference between VEGF levels generated by the two clones (P=0.231). *B)* bFGF levels as determined by ELISA and normalized per 10^6 cells. There is a statistically significant difference between bFGF levels generated by the two clones (P=0.024). *C)* TIMP-1 levels as determined by ELISA and normalized per 10^6 cells. There is a statistically significant difference between TIMP-1 levels generated by the two clones (P=0.0006). *D)* TSP-1 levels as determined by ELISA and normalized per 10^4 cells. There is a statistically significant difference between TSP-1 levels generated by the two clones (P=0.03).

mouse) but is harmless to the host because of impaired angiogenesis. In this model, tumor dormancy is associated with the inability of tumor cells to sustain the induction of new capillary blood vessels. Proliferating tumor cells in the dormant tumor appear to be balanced by tumor cells undergoing apoptosis. Importantly, in contrast to rapidly growing tumors, which induce angiogenesis and quickly expand in size, the process of tumor angiogenesis in dormant tumors appears to be impaired. In dormant liposarcomas presented here, vessels rarely have lumens or contain red blood cells. This suggests that these dormant tumors are unable to successfully complete the process of developing functional vessels.

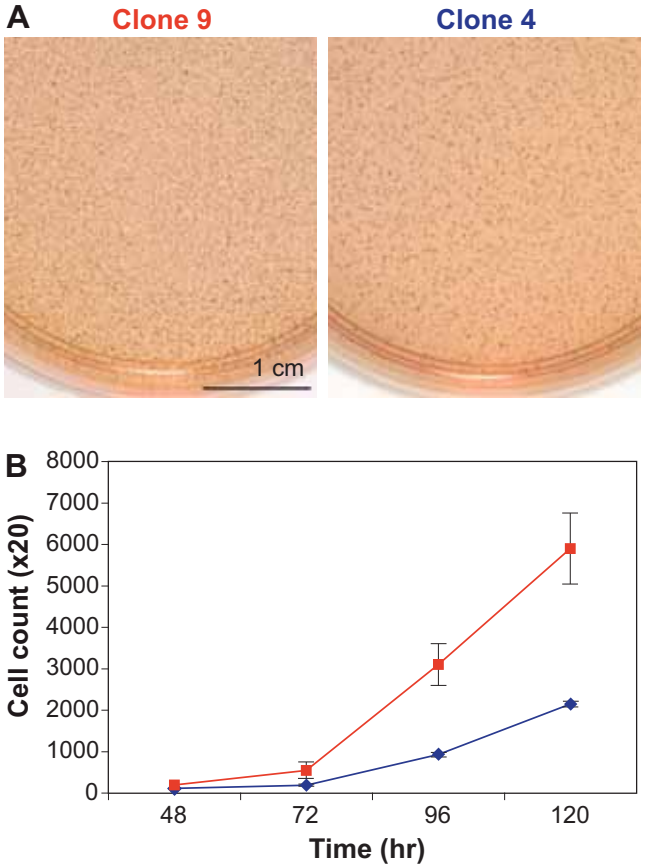

Figure 6. Characterization of growth of the liposarcoma clones *in vitro*. *A)* Photographs of soft agar plates (original magnification ×10). 50,000 cells from each clone were seeded in soft agar. After 34 days, cells were stained using MTT and the plates were photographed. *B)* Proliferation assay of cells from clone 9 (red line) and from clone 4 (blue line) grown *in vitro*.

Throughout this study we inoculated mice s.c. with 5×10^6 tumor cells to obtain viable tumor take for both nonangiogenic and angiogenic tumors. The temporary induction of a few scant microvessels without lumens, as well as the inward migration of scattered endothelial cells into the nonangiogenic, microscopic, dormant (clone 4) tumors was at first puzzling. At the completion of the study, we realized that the initial temporary burst of impaired neovascular sprouts in the nonangiogenic tumors was possibly due to an excess of inoculated tumor cells. We now know that the excess of tumor cells in an inoculum of 5 million tumor cells contributed a temporary excess of pro-angiogenic proteins. For future experiments with this human liposarcoma we will use an inoculation size of between 500,000 and 1 million tumor cells, and we would recommend this to other investigators.

Nevertheless, the artificially high tumor cell inoculum of 5 million cells used in the present study demonstrated that even with this robust proangiogenic challenge, the nonangiogenic tumors could not sustain the temporary neovascularization contributed to them by the excess of proangiogenic factors carried with tumor cells in the inoculum. In fact, microvessel density steadily decreased after inoculation of nonangiogenic tumor cells. In other words, even given an artificial burst of proangiogenic proteins that likely accompanied the inoculation of 5 million nonangiogenic tumor cells, these cells could not sustain the neovascularization. This effect was at least, in part, due to high levels of thrombospondin-1 produced by the nonangiogenic

tumor cells and by their stromal fibroblasts and other stromal cells.

At a predictable time, nonangiogenic, dormant tumors switch to the angiogenic phenotype. The molecular events that initiate the switch are not yet known but are being studied in our laboratory. Once dormant tumors undergo the angiogenic switch and initiate growth and expansion of mass, the tumor growth kinetics are similar to those of the rapidly growing angiogenic tumors. This further supports the concept that inhibition of angiogenesis, rather than slower proliferation rate of the dormant tumor cells, is the mainstay of tumor dormancy in this model. Additional mechanisms that contribute to tumor growth, other than angiogenesis, could still play a role in tumor dormancy, including interactions with stromal cells (17).

The angiogenic switch is regulated by several angiogenic stimulators and inhibitors produced by the tumor and host cells. *In vitro* the dormant liposarcoma cells secrete relatively high levels of the angiogenic proteins VEGF and bFGF, but also high levels of the endogenous inhibitors of angiogenesis thrombospondin-1 and tissue inhibitor of metalloproteinases 1 (TIMP-1). The inhibition of angiogenesis by thrombospondin and TIMP-1 is further enhanced by indirect effects. Thrombospondin-1 reduces the bioavailability and function of bFGF (18) and VEGF (19). Both thrombospondin-1 and TIMP-1, whose expression is elevated in dormant tumors, interfere with MMP-9 activity (20, 21), which has been reported to help mediate the angiogenic switch (22, 23).

The nonangiogenic dormant tumors as well as the angiogenic rapidly growing tumors investigated here were generated from clones that were derived from the same human liposarcoma cell line, without any directed genetic modification. The patterns of tumor growth were similar at both s.c. and orthotopic sites. To our knowledge, this is the first time that dormant tumors have been monitored *in vivo* in a noninvasive method for such prolonged periods of time. We wish to emphasize that in addition to liposarcoma, other tumor types are likely to generate a spectrum of dormant phenotypes that differ in the sequential morphological steps during the angiogenic switch. In other words, progression toward the angiogenic switch in a dormant tumor appears to proceed at different rates for different tumor types.

This experimental system is a reproducible animal model of dormant human cancer, which recapitulates clinical dormant tumors found in humans. The dormant phase of a nonangiogenic tumor may be a potential target for antiangiogenic therapy aimed at preventing tumor recurrence, for example after initial treatment of breast cancer or colon cancer. The ongoing development, in many laboratories, of molecular biomarkers (24) sufficiently sensitive and specific to detect the presence of microscopic dormant tumors, before or just after the angiogenic switch, without necessarily having to know anatomical location, will be an important step for the clinical application of preventive antiangiogenic cancer therapy. FJ

This work was supported by a grant from the Breast Cancer Research Foundation to J.F. by the Department of Defense Innovator Award W81XWH-04-1-0316, by a postdoctoral training fellowship from the Institute of Cancer Research/Oliver R. Grace, Jr. Fellowship and by NIH Grant CA-78496 (for L.H.), and by NIH Grant CA-64481 to J.F. We thank Dr. Vania Nose from the department of Pathology at the Brigham and Women's Hospital, Boston, for reviewing the histological slides and for very helpful comments. We are very grateful to Kristin Gullage for photography and to David Zurakowski for reviewing the statistical calculations. We thank Carolyn Cooney for excellent technical assistance with imaging, Dr. Gil Blander, for providing iRNA constructs and generating stable infected clones, and Dr. Dipak Panigrahy for helping with orthotopic injections of tumor cells.

REFERENCES

1. Folkman, J., and Kalluri, R. (2004) Cancer without disease. *Nature* **427,** 787
2. Black, W. C., and Welch, H. G. (1993) Advances in diagnostic imaging and overestimations of disease prevalence and the benefits of therapy. N. *Engl. J. Med.* **328,** 1237–1243
3. Henson, D. E., and Albores-Saavedra, J. (2001) *Pathology of Incipient Neoplasia* (3rd ed.). Oxford University Press, New York, pp. 1–5
4. Harach, H. R., Franssila, K. O., and Wasenius, V. M. (1985) Occult papillary carcinoma of the thyroid. A "normal" finding in Finland. A systematic autopsy study. *Cancer* **56,** 531–538
5. Demicheli, R. (2001) Tumour dormancy: findings and hypotheses from clinical research on breast cancer. *Semin. Cancer Biol.* **11,** 297–306
6. Uhr, J. W., Scheuermann, R. H., Street, N. E., and Vitetta, E. S. (1997) Cancer dormancy: Opportunities for new therapeutic approaches. *Nature Med.* **3,** 505–509
7. Folkman, J. (2000) Tumor angiogenesis. In: *Cancer Medicine* (5th ed.), edited by J. F. Holland, E. Frei III, R. C. Bast Jr., D. W. Kufe, R. E. Pollock, and R. R. Weichselbaum. B.C. Decker, Ontario, Canada 2000; pp. 132–152.
8. Hanahan, D., and Weinberg, R. A. (2000) The hallmarks of cancer. *Cell* **100,** 57–70
9. Kerbel, R., and Folkman, J. (2002) Clinical translation of angiogenesis inhibitors. *Nat. Rev. Cancer* **2,** 727–739
10. Hart, I. R. (1999) Perspective: tumor spread—the problems of latency. *J. Pathol.* **187,** 91–94
11. Naumov, G. N., Bender, E., Zurowski, D., Kang, S. Y., Sampson, D., Flynn, E., Watnick, R. S., Straume, O., Akslen, L. A., Folkman, J., and Almog, N. (2006) A model of human tumor dormancy: an angiogenic switch from the nonangiogenic phenotype. *J. Natl. Cancer Inst.* **98,** 316–325
12. Achilles, E. G., Fernandez, A., Allred, E. N., Kisker, O., Udagawa, T., Beecken, W. D., Flynn, E., and Folkman, J. (2001) Heterogeneity of angiogenic activity in a human liposarcoma: a proposed mechanism for "no take" of human tumors in mice. *J. Natl. Cancer Inst.* **93,** 1075–1081
13. Armstrong, S. A., Kung, A. L., Mabon, M. E., Silverman, L. B., Stam, R. W., Den Boer, M. L., Pieters, R., Kersey, J. H., Sallan, S. E., Fletcher, J. A., Golub, T. R., Griffin, J. D., and Korsmeyer, S. J. (2003) Inhibition of FLT3 in MLL. Validation of a therapeutic target identified by gene expression based classification. *Cancer Cell* **3,** 173–183
14. Rubin, J. B., Kung, A. L., Klein, R. S., Chan, J. A., Sun, Y., Schmidt, K., Kieran, M. W., Luster, A. D., and Segal, R. A. (2003) A small-molecule antagonist of CXCR4 inhibits intracranial growth of primary brain tumors. *Proc. Natl. Acad. Sci. U. S. A.* **100,** 13,513–13,518
15. Cifone, M. A., and Fidler, I. J. (1980) Correlation of patterns of anchorage-independent growth with in vivo behavior of cells

from a murine fibrosarcoma. *Proc. Natl. Acad. Sci. U. S. A.* **77,** 1039–1043
16. Watnick, R. S., Cheng, Y. N., Rangarajan, A., Ince, T. A., and Weinberg, R. A. (2003) Ras modulates Myc activity to repress thrombospondin-1 expression and increase tumor angiogenesis. *Cancer Cell* **3,** 219–231
17. Govindarajan, B., Shah, A., Cohen, C., Arnold, R. S., Schechner, J., Chung, J., Mercurio, A. M., Alani, R., Ryu, B., Fan, C. Y., Cuezva, J. M., Martinez, M., and Arbiser, J. L. (2005) Malignant transformation of human cells by constitutive expression of platelet-derived growth factor-BB. *J. Biol. Chem.* **280,** 13,936–13,943
18. Margosio, B., Marchetti, D., Vergani, V., Giavazzi, R., Rusnati, M., Presta, M., and Taraboletti, G. (2003) Thrombospondin 1 as a scavenger for matrix-associated fibroblast growth factor 2. *Blood* **102,** 4399–4406
19. Gupta, K., Gupta, P., Wild, R., Ramakrishnan, S., and Hebbel, R. P. (1999) Binding and displacement of VEGF by thrombospondin: effect on human microvascular endothelial cell proliferation and angiogenesis. *Angiogenesis* **3,** 147–158
20. Bode, W., Fernandez-Catalan, C., Grams, F., Gomis-Ruth, F. X., Nagase, H., Tschesche, H., and Maskos, K. (1999) Insights into MMP-TIMP interactions. *Ann. N. Y. Acad. Sci.* **878,** 73–91
21. Rodriguez-Manzaneque, J. C., Lane, T. F., Ortega, M. A., Hynes, R. O., Lawler, J., and Iruela-Arispe, M. L. (2001) Thrombospondin-1 suppresses spontaneous tumor growth and inhibits activation of matrix metalloproteinase-9 and mobilization of VEGF. *Proc. Natl. Acad. Sci. U. S. A.* **98,** 12,485–12,490
22. Bergers, G., Brekken, R., McMahon, G., Vu, T. H., Itoh, T., Tamaki, K., Tanzawa, K., Thorpe, P., Itohara, S., Werb, Z., and Hanahan, D. (2000) Matrix metalloproteinase-9 triggers the angiogenic switch during carcinogenesis. *Nat Cell Biol.* **2,** 737–744
23. Arbiser, J. L., Moses, M. A., Fernandez, C. A., Ghiso, N., Cao, Y., Klauber, N., Frank, D., Brownlee, M., Flynn, E., Parangi, S., Byers, H. R., and Folkman, J. (1997) Oncogenic H-ras stimulates tumor angiogenesis by two distinct pathways. *Proc. Natl. Acad. Sci. U. S. A.* **94,** 861–866
24. Roy, R., Wewer, U. M., Zurakowski, D., Pories, S. E., and Moses, M. A. (2004) ADAM 12 cleaves extracellular matrix proteins and correlates with cancer status and stage. *J. Biol. Chem.* **279,** 51,323–51,330

Received for publication June 3, 2005.
Accepted for publication December 23, 2005.

A Model of Human Tumor Dormancy: An Angiogenic Switch From the Nonangiogenic Phenotype

George N. Naumov, Elise Bender, David Zurakowski, Soo-Young Kang, David Sampson, Evelyn Flynn, Randolph S. Watnick, Oddbjorn Straume, Lars A. Akslen, Judah Folkman, Nava Almog

Background: **Microscopic human cancers can remain dormant for life. Tumor progression depends on sequential events, including a switch to the angiogenic phenotype, i.e., initial recruitment of new vessels. We previously demonstrated that human tumors contain tumor cell populations that are heterogeneous in angiogenic activity. Here, we separated angiogenic from nonangiogenic human tumor cell populations and compared their growth.** ***Methods:*** **Severe combined immunodeficient (SCID) mice were inoculated with nonangiogenic human MDA-MB-436 breast adenocarcinoma, KHOS-24OS osteosarcoma, or T98G glioblastoma cells. Most of the resulting tumors remained microscopic (<1 mm diameter), but some eventually became angiogenic and enlarged and were used to isolate angiogenic tumor cells. Angiogenic and nonangiogenic tumor cells were inoculated into SCID mice, and time to the development of palpable tumors was determined. Cell proliferation was assayed in vitro by growth curves and in vivo by staining for proliferating cell nuclear antigen or Ki67. Microscopic tumors from both tumor cell populations were examined for histologic evidence of vascular development 14 days after inoculation in mice. Expression of the angiogenesis inhibitor thrombospondin-1 was examined by immunoblotting.** ***Results:*** **Nonangiogenic tumors of each tumor type developed palpable tumors after means of 119 days (range: 53–185 days) for breast cancer, 238 days (184–291 days) for osteosarcoma, and 226 days (150–301 days) for glioblastoma. Angiogenic cells developed palpable tumors within 20 days after inoculation. However, nonangiogenic and angiogenic cells of each tumor type had similar proliferation rates. Fourteen days after tumor cell inoculation, tumors from angiogenic cells showed evidence of functional vasculature. In contrast, nonangiogenic tumors remained microscopic in size with absent or nonfunctional vasculature. Thrombospondin-1 expression was statistically significantly lower (by five- to 23-fold, depending on tumor type) in angiogenic than nonangiogenic cells.** ***Conclusions:*** **This model provides a conceptual framework and a reproducible in vivo system to study unresolved central questions in cancer biology regarding the initiation, reversibility, and molecular regulation of the timing of the angiogenic switch. [J Natl Cancer Inst 2006;98:316–25]**

Multiple events are involved in cancer progression. One such event is angiogenesis; it is well established that tumor growth beyond the size of 1–2 mm is angiogenesis dependent *(1–4)*. Autopsy studies in individuals who died of trauma without having had cancer diagnosed in their lifetime have shown a high frequency of microscopic cancers in various organs, e.g., breast, prostate, and thyroid *(5,6)*. Only a small proportion (<0.5%) of such lesions will eventually present as clinical cancers *(2,6,7)*. One possible explanation for these observations is that most human tumors arise in the absence of angiogenic activity and exist in a microscopic dormant state for months to years without neovascularization. We have proposed *(2,4)* that diagnosed tumors are those that have switched to the angiogenic phenotype, i.e., that have initiated recruitment of new vessels. Once a tumor has undergone surgical treatment or other forms of therapy, local or metastatic recurrences may also be attributed to the switch to the angiogenic phenotype in otherwise microscopic dormant tumors *(8–13)*. Despite the clinical importance of this phenomenon, the biology of tumor dormancy is poorly understood.

Several animal models have been developed to study tumor dormancy. Hanahan et al. *(14)* described a spontaneous tumor model (RIP1-Tag2) in transgenic mice, in which autochthonous tumors arise in the pancreatic islets as a result of the expression of the simian virus 40 T antigen (Tag) oncogene. In this model, only 4% of tumors are angiogenic, i.e., contain evidence of neovascularization, after 13 weeks, whereas the remaining 96% remain microscopic and nonangiogenic *(15,16)*. The spontaneous progression of nonangiogenic lesions to the angiogenic phenotype in these tumor-bearing mice was termed the "angiogenic switch."

The angiogenic switch has also been documented in human tumors. For example, we have shown that human cancers contain subpopulations of tumor cells that differ in their angiogenic potential *(17)*. Transfection of nonangiogenic human tumor cells with an activated Ras oncogene resulted in their switch to the angiogenic phenotype in a mouse model of human osteosarcoma dormancy *(18)*. In these previous animal models of human tumor dormancy, the angiogenic and nonangiogenic tumor cell populations were derived from either single-cell clones or from

Affiliations of authors: Departments of Surgery (GNN, EB, DZ, S-YK, DS, EF, RSW, LAA, JF, NA) and Biostatistics (DZ), Vascular Biology Program (GNN, EB, S-YK, DS, RSW, LAA, JF, NA), Children's Hospital, and Harvard Medical School, Boston, MA; The Gade Institute, Section for Pathology, University of Bergen, Bergen, Norway (OS, LAA).

Correspondence to: Judah Folkman, MD, Karp Family Research Laboratories 12.128, 300 Longwood Ave., Boston, MA 02115 (e-mail: judah.folkman@childrens.harvard.edu).

See "Notes" following "References."

DOI: 10.1093/jnci/djj068

genetically modified tumor cells [i.e., Ras-transfected dormant cells *(17–19)*].

To better understand the pathogenesis and timing of the angiogenic switch in human tumors, we developed a novel approach in which we created separate populations of nonangiogenic and angiogenic tumor cells in vivo without using molecular alterations. We used this approach to study three different human cancer types in severe combined immunodeficient (SCID) mice: breast cancer, osteosarcoma, and glioblastoma. For angiogenic and nonangiogenic populations of each tumor type, we compared proliferation rates in vitro and in vivo and determined ratios of proliferation to apoptosis. The angiogenic switch in vivo was characterized by examining changes in the vasculature.

Methods

Establishment of Nonangiogenic and Angiogenic Human Cancer Cell Lines

Human breast adenocarcinoma (MDA-MB-436), osteosarcoma (KHOS-24OS), glioblastoma (T98G), and human embryonic kidney (293T) cell lines were obtained from the American Type Culture Collection (ATCC, Manassas,VA) and confirmed to be free of mycoplasma. The breast carcinoma, osteosarcoma, and glioblastoma cell lines were defined as nonangiogenic based on: 1) the absence of angiogenic activity, as evidenced by repulsion of existing blood vessels and/or absence of microvessels within the tumor; 2) their growth to only approximately 1 mm in diameter or less in vivo, at which time further expansion stopped; 3) the apparent absence of "tumor take" for at least 130–238 days, until the emergence of the angiogenic phenotype; and 4) the fact that the tumors remained harmless to the host until they switched to the angiogenic phenotype.

In mice injected with nonangiogenic human tumor cells (i.e., the cell lines as originally obtained from ATCC), occasional tumors grew for each of the three cancer types following a prolonged dormancy period. These vascularized tumors were removed under sterile conditions, and tumor cell lines were established from them using standard tissue culture techniques. The cell lines derived from the nonangiogenic (i.e., dormant) tumors that had switched to the angiogenic phenotype were called "angiogenic" because they produced large angiogenic tumors (up to 2000 mm^3) within 1 month of their subsequent inoculation into mice. For breast cancer, a single cell–derived clone, designated clone A1, was also isolated from the angiogenic subpopulation. This clone formed occasional angiogenic tumors following a prolonged dormancy period.

All cell lines were maintained in tissue culture (37 °C, 5% CO_2, humidified atmosphere). Breast cancer MDA-MB-436 cells were maintained in Dulbecco's modified Eagle medium (DMEM; Invitrogen, Carlsbad, CA) supplemented with 10% fetal bovine serum (FBS; Invitrogen). Osteosarcoma KHOS-24OS cells were maintained in Minimum Essential Medium (MEM; Invitrogen) supplemented with 10% FBS and 0.1 mM nonessential amino acids. Brain tumor T98G cells were maintained in MEM supplemented with 10% FBS, 0.1 mM nonessential amino acids, and 1 mM sodium pyruvate. For in vivo experiments, subconfluent monolayers of tumor cells were harvested by trypsinization and resuspended in DMEM to a final concentration of 2.5×10^7 cells/mL.

In Vitro Tumor Cell Proliferation

In vitro growth curves were generated by plating 5×10^4 cells in 60-mm dishes in triplicate. The cells were counted daily over a 7-day period. In an additional experiment, cells were collected during the exponential growth phase for subsequent histologic characterization (staining for Ki67).

Anchorage-Independent Growth In Vitro

For all three cancer types, the ability of nonangiogenic and angiogenic cells to undergo anchorage-independent growth was compared. In brief, 10^4 cells were suspended in 5 mL of 0.4% agar and plated in triplicate on 10-cm plates that had been precoated with 4 mL of 0.6% agar. An immortalized and transformed human kidney cell line (293T) was used as a positive control. Plates were monitored every other day, and when colonies became evident (after 3 weeks), plates were incubated for 8 hours with 2 mL of thiazolyl blue tetrazolium bromide (MTT) (Sigma, St. Louis, MO) to visualize viable cell colonies. The number of colonies was then counted from 10 digital images of random high-power fields for each plate.

Subcutaneous Tumor Growth

SCID male mice aged 6–8 weeks (Massachusetts General Hospital, Boston) were used for in vivo studies and were cared for in accordance with the standards of the Institutional Animal Care and Use Committee (IACUC) under a protocol approved by the Animal Care and Use Committee of the Children's Hospital Boston. Mice were anesthetized using a 2% isoflurane (Baxter, Deerfield, IL) inhalation oxygen mixture. Suspensions of 5×10^6 human breast cancer (MDA-MB-436), osteosarcoma (KHOS-24OS), or glioblastoma (T98G) cells in 0.2 mL of DMEM were then inoculated subcutaneously into the lower-right quadrant of the flank of each mouse. For in vivo characterization of the dormancy period, we inoculated mice as follows: 21 mice were inoculated with nonangiogenic breast cancer cells, 11 mice with angiogenic breast cancer cells, and 12 mice with nonangiogenic clone A1 tumor cells; 18 mice with nonangiogenic osteosarcoma cells and 11 mice with angiogenic osteosarcoma cells; five mice with nonangiogenic glioblastoma cells and five mice with angiogenic glioblastoma cells. Mice were monitored every other day for palpable tumors at the site of tumor cell inoculation. Tumors could be detected by palpation in these shaved SCID mice once the tumors reached approximately 50 mm^3. Once tumors became palpable, tumor size was measured twice a week. Mice were killed by cervical dislocation when the tumor size reached approximately 1200 mm^3. To assess tumor growth kinetics, tumors were measured from the time that they were first palpable until they reached 500 mm^3. Mice that did not form palpable tumors were monitored for tumor growth for up to 350 days after tumor cell inoculation. The number and proportion of angiogenic tumors that had switched from dormancy was compared between all three cancer types at day 160 after tumor cell inoculation. Representative mice were killed at various time points for histology of microscopic and macroscopic tumors (for example, at 14, 47, and 77 days after tumor cell inoculation).

Additional mice were inoculated with 5×10^6 MDA-MB-436 breast cancer cells for morphologic and histologic analysis as follows: 25 mice were inoculated with angiogenic, 30 mice with

nonangiogenic, and 30 mice with nonangiogenic clone A1 breast cancer cells. Tumor cell proliferation and apoptosis were analyzed at the following intervals: 4–7 days (10 mice) and 29–40 days (10 mice) after inoculation with angiogenic tumor cells; 4–14 days (15 mice) and 40–70 days (10 mice) after inoculation with nonangiogenic tumor cells, and 4–15 days (15 mice) and 40–70 days (10 mice) after inoculation with nonangiogenic clone A1 breast cancer cells.

Histology and Immunohistochemistry

Tumor tissue was excised from mice killed by cervical dislocation, rinsed in ice-cold phosphate-buffered saline (PBS), fixed in 4% paraformaldehyde, and embedded in paraffin. Representative 4-μm tumor cross-sections were cut from paraffin-embedded tissue, and sets of four adjacent sections were stained as follows: 1) To identify proliferating cells, section 1 was stained with a 1 : 150 dilution of PC10 monoclonal antibody (DAKO, Carpinteria, CA) against proliferating cell nuclear antigen or with a 1 : 50 dilution of the monoclonal antibody against Ki-67 (M7240, clone MIB-1; DakoCytomation, Copenhagen, Denmark) after antigen retrieval for 20 minutes in citrate buffer in a microwave at 500 W; 2) To evaluate tissue quality and tumor morphology, section 2 was stained with hematoxylin and eosin; 3) To assess fragmented DNA, section 3 was labeled by the terminal deoxynucleotidyl transferase biotin–dUTP nick-end labeling (TUNEL) technique (ApopTag kit, Intergen, Purchase, NY) according to the method of Gavrielli et al. *(20)*; 4) To identify endothelial cells, section 4 was stained with a 1 : 250 dilution of anti-CD31 antibody (Pecam; BD Biosciences, San Diego, CA) after antigen retrieval by Proteinase K treatment. Necrotic areas were avoided for all histologic analyses.

In Vivo Permeability Assay

A modified Miles assay *(21)* was performed to investigate differences in vascular permeability in size-matched nonangiogenic and angiogenic tumors. Five mice per group were inoculated with 5×10^6 angiogenic, nonangiogenic, or nonangiogenic clone A1 human breast cancer cells. The modified Miles assay was performed at day 14 after tumor cell inoculation. Mice were anesthetized by intraperitoneal injection of Avertin (150 mg/kg of body weight) and were then inoculated intravenously with filtered Evans blue solution (100 μL of 1% in PBS per mouse), which was allowed to circulate systemically for 30 minutes while the mice were maintained at 30 °C. All mice were then perfused systemically with PBS (pH 7.4) for 3 minutes at a pressure of 120 mm Hg from an 18-gauge cannula that was inserted into the aorta via an incision in the left ventricle. The right atrium was then incised to create a route for the saline to escape. Patches of the dorsal skin of each mouse were harvested to permit visualization of dye leakage from blood vessels to subcutaneous tumor tissues, to the skin overlying the tumor, and to control skin from the contralateral flank (this perfusion ensured that no dye remained in the vascular lumen). For each mouse, three types of tissues (tumor, overlying and control skin) were excised, weighed, and placed in 1 mL of formamide (Sigma) for 5 days at room temperature to extract all dye from the tissues. The extracted dye was quantified by measuring optical density at 620 nm of the formamide at the end of the 5-day incubation. All optical densitometry values were normalized to tumor (or skin) tissue weight.

ELISA Quantification of Secreted $VEGF_{165}$, bFGF, and Thrombospondin-1

Nonangiogenic and angiogenic tumor cells from each of the three cancer types were plated in triplicate (5×10^6 cells/15 cm plate) in 15 mL of DMEM supplemented with 10% FBS. After 24 hours, the medium was replaced with 15 mL of serum-free medium. The medium was then collected, and enzyme-linked immunosorbent assay (ELISA) kits were used to determine concentrations of human vascular endothelial growth factor ($VEGF_{165}$; R&D, Minneapolis, MN), basic fibroblast growth factor (bFGF; R&D), and thrombospondin-1 (CYT Immune Science, College Park, MD) according to the manufacturers' protocols. For each sample, blank values (i.e., those for serum-free media) were subtracted, and mean results were normalized per 10^4 cells. This assay was performed in triplicate.

Protein Extraction and Immunoblot Analysis

Angiogenic and nonangiogenic breast cancer cells (MDA-MB-436) were grown in 10-cm tissue culture plates in DMEM supplemented with 10% FBS. When cells reached 80% confluence, half the plates were treated with the phosphoinositide 3-kinase (PI3K) inhibitor LY294002 (Calbiochem, San Diego, CA) at a final concentration of 10 μM in DMEM with 0.1% FBS for 12 hours. The remaining plates were untreated. For immunoblotting, cells were harvested by mechanical scraping into 4 °C PBS. Cell pellets were then lysed in 50 mM Tris–HCl (pH 7.4), 150 mM NaCl, 1% NP40, 1 mM sodium orthovanadate, 5 mM NaF, 20 mM β-glycerophosphate, and complete protease inhibitor (Roche, Indianapolis, IN). Fifty micrograms of protein was loaded in the wells of a 4%–12% precast Bis–Tris gel (Bio-Rad, Hercules, CA). Membranes were blocked with 5% nonfat milk and incubated with primary antibodies to c-Myc (Abcam, Cambridge, UK), phospho-Myc (Cell Signaling Technology, Beverly, MA), thrombospondin-1 (LabVision, Fremont, CA), and β-actin (Abcam, Cambridge, MA). Antibody binding was detected by incubating blots with horseradish peroxidase–conjugated secondary antibodies, either goat anti–mouse (c-Myc, thrombospondin-1, and β-actin) or goat anti–rabbit (p-Myc) (Jackson Immunoresearch Labs, West Grove, PA). Bands were visualized with enhanced chemiluminescence reagent (Pierce, Rockford, IL).

Statistical Analysis

The time to development of a palpable tumor (i.e., after tumor cell inoculation) was used as the endpoint of the dormancy period in survival analyses. For each of the three tumor types, times to palpable tumor for the angiogenic, nonangiogenic, and nonangiogenic clone A1 (breast cancer) cells were compared using the Kaplan–Meier product limit method *(22)*. Confidence intervals around estimated survival curves were calculated using Greenwood's formula *(22)*. In a subgroup analysis, we compared time to palpation for angiogenic breast carcinoma, osteosarcoma, and glioblastoma tumor cell populations. The log-rank test was used to compare the statistical significance of differences between survival curves *(23)*. For tumors that switched to the angiogenic phenotype, we compared the median times from initial tumor palpation (i.e., from a size of approximately 50 mm^3) until the tumor reached a size of 500 mm^3 using the nonparametric

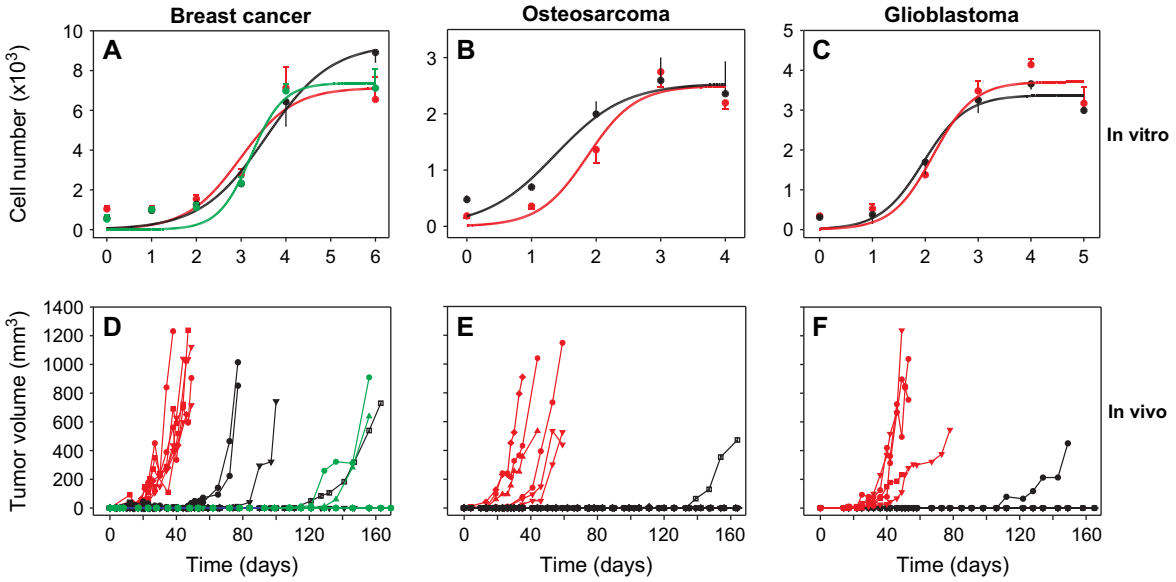

Fig. 1. In vitro and in vivo growth of nonangiogenic and angiogenic tumor cells of three cancer types. In vitro growth (panels **A–C**) and in vivo subcutaneous tumor growth (**D–F**) of angiogenic (**red**), nonangiogenic (**black**), and nonangiogenic clone A1 (**green**) human MDA-MB-436 breast cancer (**A, D**), KHOS-24OS osteosarcoma (**B, E**), and T98G glioblastoma (**C, F**) cell lines. For in vitro growth curves, each line represents a mean number of cells from three independent replicate assays with **error bars** denoting 95% confidence intervals. For growth of subcutaneous tumors, each line represents a single mouse. Numbers of mice were as follows: angiogenic breast cancer, n = 7; nonangiogenic breast cancer, n = 5; nonangiogenic breast cancer clone A1, n = 5; angiogenic osteosarcoma, n = 6; nonangiogenic osteosarcoma, n = 8; angiogenic glioblastoma, n = 5; nonangiogenic gliobastoma, n = 5. Day of tumor cell inoculation was designated as day 0. Mice inoculated with nonangiogenic cells that did not develop palpable tumors by 160 days were monitored for up to 350 days.

Mann–Whitney *U* test. The Student's *t* test was used to compare angiogenic and nonangiogenic tumor cell lines with respect to continuous data including in vitro tumor cell doubling times, anchorage-independent growth, vascular permeability, and ELISA. Two-tailed *P* values less than .05 were considered statistically significant. Statistical analyses were performed with the SPSS package (version 13.0 SPSS, Chicago, IL).

Results

In Vitro Growth of Nonangiogenic and Angiogenic Tumor Cells

In vitro assessment of doubling times of all three cancer types showed no statistically significant difference between the nonangiogenic and angiogenic cell lines (Fig. 1, A–C). During the exponential tumor cell proliferation phase, approximately 90% of both nonangiogenic and angiogenic breast cancer cells expressed comparable levels of Ki-67 protein (data not shown).

We then analyzed the differences in anchorage-independent growth between nonangiogenic and angiogenic tumor cells for all three tumor types (Fig. 2). Both nonangiogenic and angiogenic subpopulations of the breast carcinoma, osteosarcoma, and glioblastoma formed colonies 3 weeks after plating in soft agar with no statistically significant differences (all $P>.05$) in the number of colonies formed.

Subcutaneous Tumor Growth

To investigate in vivo tumor growth, we inoculated mice with either angiogenic or nonangiogenic cells from each cancer type and monitored them for as long as 350 days. Additional mice were inoculated with the nonangiogenic clone A1 breast cancer cells. The number and proportion of angiogenic tumors that had switched from dormancy within a period of 160 days after tumor cell inoculation was determined for all mice. For breast carcinoma, palpable tumors developed in all seven mice inoculated with angiogenic cells, in four of the five mice inoculated with nonangiogenic cells, and in three of the eight mice inoculated with nonangiogenic clone A1 cells. For osteosarcoma, angiogenic tumors developed in all six mice inoculated with angiogenic cells and in one of the eight mice inoculated with nonangiogenic cells. For glioblastoma, angiogenic tumors developed in all five mice inoculated with angiogenic

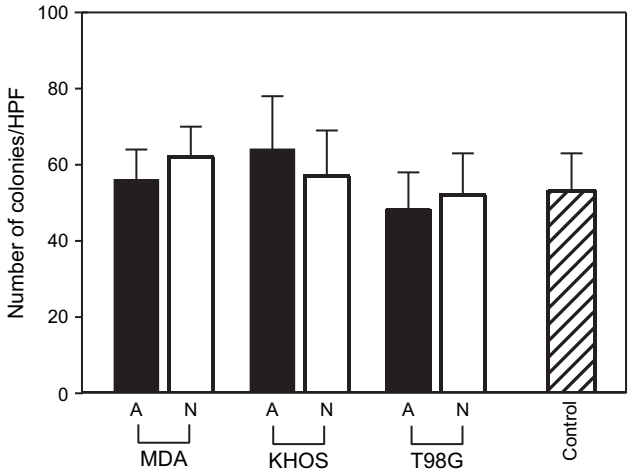

Fig. 2. Anchorage-independent in vitro growth of nonangiogenic and angiogenic cells of three cancer types. Colony formation was assessed by a standard soft agar assay. Number of colonies (in soft agar) per high power field of view (HPF) is shown for both angiogenic (**A; black bars**) and nonangiogenic (**N; white bars**) cells of MDA-MB-436 (MDA; breast cancer), KHOS-24OS (KHOS; osteosarcoma), and T98G (glioblastoma). For a control, 293T cells were used. Data represent mean values with **error bars** denoting the upper limit of the 95% confidence intervals.

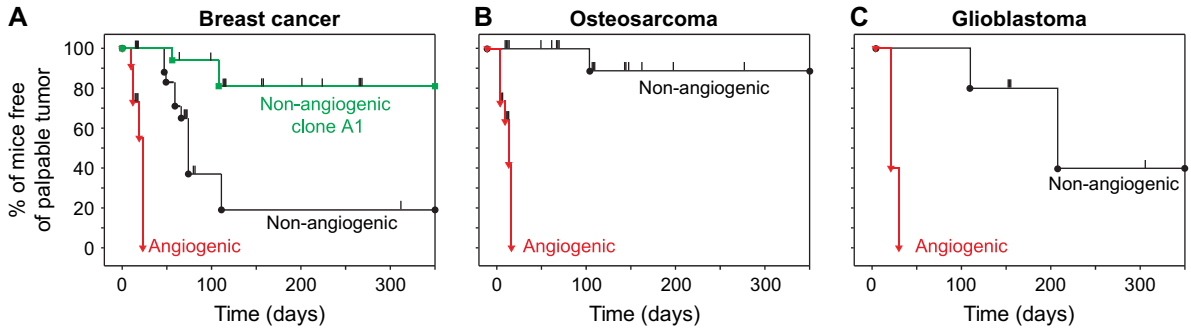

Fig. 3. Kaplan–Meier analysis of time from tumor cell inoculation to palpable tumor detection. The persistence of mice free of palpable tumors was represented using the Kaplan–Meier analysis. Mice were inoculated with either angiogenic or nonangiogenic tumor cell lines: (**A**) Breast cancer MDA-MB-436 (angiogenic, n = 11 mice; nonangiogenic, n = 21; nonangiogenic clone A1, n = 12). (**B**) Osteosarcoma KHOS-24OS (angiogenic, n = 11; nonangiogenic, n = 18). (**C**) T98G glioblastoma (angiogenic, n = 5; nonangiogenic, n = 5). A drop in the curve indicates the occurrence of a palpable tumor at the corresponding time since tumor cell inoculation. **Tick marks** denote mice euthanized for histologic analysis that had not developed a palpable tumor at that time (i.e., censored data). Log-rank tests for differences between angiogenic and nonangiogenic cell populations yielded $P<.001$ for breast cancer and osteosarcoma and $P = .002$ for glioblastoma.

cells and in one of the five mice inoculated with nonangiogenic cells (Fig. 1, D–F).

Kaplan–Meier analysis was used to compare the time between inoculation of tumor cells and detection of palpable tumors for nonangiogenic and angiogenic cell populations of all three cancer cell lines (Fig. 3). This analysis accounted for those mice in which tumor cells switched to the angiogenic phenotype and formed tumors as well as those mice that remained free of palpable tumor for a prolonged time and were censored at various time points during the dormancy period for histological analysis (as denoted by tick marks along the Kaplan–Meier curves in Fig. 3). The mean times between tumor cell inoculation and the development of palpable tumors (i.e., tumors of approximately 50 mm^3) were 19 days (95% confidence interval [CI] = 16 to 22 days) in mice (n = 11) inoculated with angiogenic breast cancer cells, 119 days (95% CI = 53 to 185 days) in mice (n = 21) inoculated with nonangiogenic cells (log-rank $P<.001$), and 234 days (95% CI = 199 to 269 days) in mice (n = 12) inoculated with nonangiogenic clone A1 breast cancer cells (log-rank $P<.001$ for comparison with angiogenic cells). Mean times to develop palpable tumors were 21 days (95% CI = 18 to 25 days) in mice (n = 11) inoculated with angiogenic osteosarcoma cells and 238 days (95% CI = 184 to 291 days) for mice (n = 18) inoculated with nonangiogenic osteosarcoma cells (log-rank $P<.001$). Finally, mean times to palpable tumor were 20 days (95% CI = 16 to 24 days) for mice (n = 5) inoculated with angiogenic glioblastoma cells and 226 days (95% CI = 150 to 301 days) for mice (n = 5) inoculated with nonangiogenic glioblastoma cells (log-rank $P = .002$). By contrast, comparison of time to develop a palpable tumor for angiogenic tumor cell populations of the three cancer types showed no differences ($P = .15$). Similar dormancy times were observed for the breast and glioblastoma tumors when inoculated orthotopically in the mammary fat pad or brain (George Naumov, unpublished data).

To determine whether tumors from nonangiogenic cells, once they emerge from dormancy, have growth kinetics similar to those of tumors from angiogenic cells, we assessed the kinetics of tumor growth in mice that developed palpable tumors from both angiogenic and nonangiogenic cell lines of each cancer type (including for breast cancer, clone A1). For this analysis, we determined the time from the detection of a palpable tumor to the time tumors reached 500 mm^3. For breast cancer, the median times to reach 500 mm^3 were 22 days (range = 11–36 days, n = 7) for angiogenic cell populations and 38 days (range = 25–51 days, n = 4) for nonangiogenic cell subpopulations. For osteosarcoma, median times to reach this size were 30 days (range = 17–33 days, n = 6) and 25 days (n = 1) for angiogenic and nonangiogenic cell subpopulations, respectively. For glioblastoma, median times were 26 days (range = 21–61 days, n = 5) and 39 days (range = 25–43 days, n = 2) for angiogenic and nonangiogenic cell subpopulations, respectively. There were no differences in the time to reach 500 mm^3 between nonangiogenic and angiogenic subpopulations for any of the three cancer cell types, indicating that, after a tumor emerged from dormancy (i.e., in mice inoculated with the nonangiogenic tumor cells), its growth rate was comparable to that of angiogenic tumors regardless of the length of the dormancy period.

Histologic Differences Between Nonangiogenic and Angiogenic Tumors

We analyzed tumors for evidence of blood vessels on day 14 after tumor cell inoculation, when mice inoculated with either the angiogenic or nonangiogenic tumor cells had only microscopic tumors (Fig. 4, A, C, D), and when tumors reached 1000–2000 mm^3 (Fig. 4, B, E). Fig. 4 shows results for breast cancer cells; results for osteosarcoma and glioblastoma were similar (data not shown). At day 14 after inoculation, angiogenic tumors (i.e., derived from angiogenic cell lines), although still less than 1 mm in diameter, contained functional blood microvessels that were CD31 positive (Fig. 4, K) and were filled with red blood cells (Fig. 4, F). By contrast, at the same time point nonangiogenic tumors either lacked vasculature (CD31 negative, Fig. 4, H, M) or contained sparse microvessels that lacked red blood cells (Fig. 4, I, N). At this early time point, nonangiogenic tumors either appeared white or contained microvessels mainly at the periphery of the lesion by gross examination (Fig. 4, C, D). By contrast, all angiogenic tumors appeared red and vascularized by gross examination (Fig. 4, A). Histologic examination of the nonangiogenic tumors at day 14 after inoculation showed that a minority of tumors (<10%) were completely avascular with no evidence of intratumoral endothelial cells, as demonstrated by absence of CD31 staining (Fig. 4, M); most tumors showed histologic evidence of undeveloped (CD31 positive) microvasculature that lacked lumens, had no red blood cells (Fig. 4, I), and possibly contained a few blind vascular sprouts that were CD31 positive (Fig. 4, N). Macroscopic tumors that had spontaneously switched

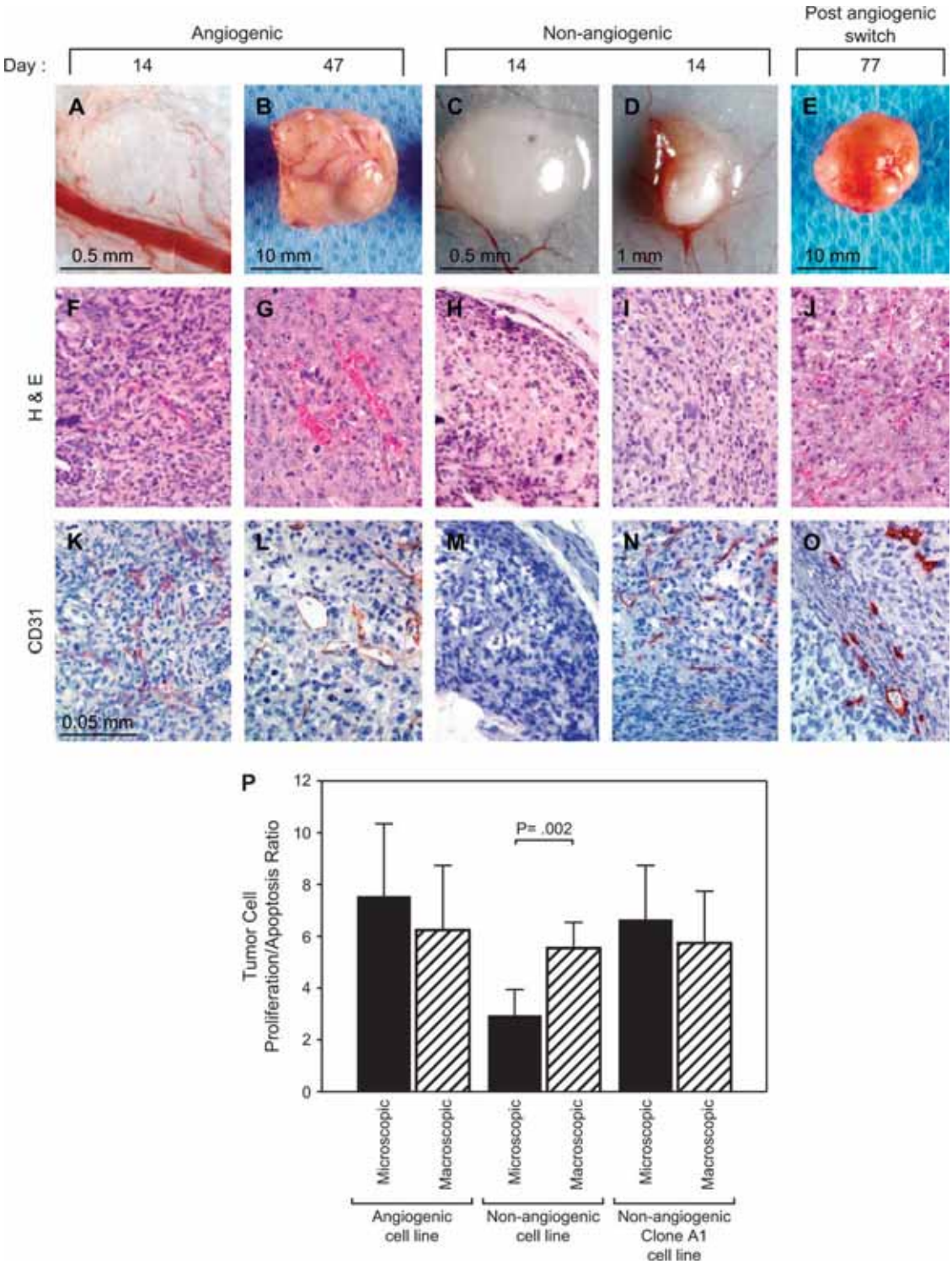

Fig. 4. Histologic analysis of tumors from nonangiogenic and angiogenic human MDA-MB-436 breast cancer cells. Photomicrographs of representative tumors are shown at day 14 (**panels A, C, D**) and day 47 or 77 (**panels B, E**) after inoculation for both nonangiogenic and angiogenic tumor variants (human breast cancer). **Panels A** and **B** represent microscopic and macroscopic tumors generated from angiogenic tumor cell lines, respectively. **Panels C** and **D** represent microscopic tumors, generated from a nonangiogenic tumor cell line, that differ in morphologic appearance. **Panel E** represents a macroscopic tumor, generated from a nonangiogenic cell line, that has spontaneously switched to the angiogenic phenotype from tumor dormancy. For each tumor, representative hematoxylin and eosin–stained sections (**F–J**) and CD31-stained sections (**K–O**) in high power field of views (×400) are shown. At day 14 after inoculation, angiogenic tumors (although still less than 1 mm in diameter) contained functional blood microvessels that were CD31 positive (**K**) and were filled with red blood cells (**F**). At the same time point, size-matched nonangiogenic tumors either lacked vasculature (absence of CD31 stain [**M**] and red blood cells [**H**]) or contained microvessels (**N**) that were not filled with red blood cells (**I**). Ratios of tumor cell proliferation to apoptosis were determined by immunohistochemical staining for Ki67 and terminal deoxynucleotidyl transferase biotin–dUTP nick-end labeling (TUNEL). These ratios were statistically significantly lower for microscopic than macroscopic tumors from the nonangiogenic cell line (P = .002) but not for the angiogenic line or nonangiogenic clone A1. **Bars** represent means based on at least 10 independent mice, with upper 95% confidence intervals.

to the angiogenic phenotype in mice inoculated with nonangiogenic tumor cells showed histologic evidence of vessels with open lumens (Fig. 4, O) that were filled with red blood cells (Fig. 4, J), similar to the microvasculature of tumors derived from angiogenic cell lines (Fig. 4, G, L).

Next, we analyzed breast tumor cell proliferation and apoptosis to determine whether tumor dormancy resulted from tumor cell quiescence. Histologic studies of tumors generated from the angiogenic cell line revealed similar ratios of tumor cell proliferation to apoptosis in tumors generated up to 14 days after inoculation and in tumors that had reached a size of more than 1000 mm^3 (around day 40). For tumors generated from the angiogenic breast cancer cell line, the mean ratios of Ki-67 stain to TUNEL assay results, in arbitrary units, were 7.6 (95% CI = 4.8 to 10.4) for 14-day microscopic tumors and 6.3 (95% CI = 3.8 to 8.8) for 40-day macroscopic tumors (not statistically significantly different, P = .43) (Fig. 4, P). Similar ratios were observed in tumors derived from the nonangiogenic clone A1 cells, both during early dormancy (4–14 days after inoculation) and after the switch to the angiogenic phenotype, i.e., past day 70 of inoculation (early dormancy, 6.8 [95% CI = 4.6 to 8.9]; angiogenic, 5.8 [95% CI = 3.8 to 7.8]; P = .53). However, the ratios in nonangiogenic tumors during early dormancy were statistically significantly lower than those in tumors that had switched to the angiogenic phenotype (early dormancy, 3.1 [95% CI = 2.1 to 4.1], angiogenic, 5.6 [95% CI = 4.5 to 6.6]; P = .002). More than 50% of tumor cells were proliferative and more than 10% underwent apoptosis in all microscopic and macroscopic tumors analyzed. These findings indicate that nonangiogenic tumors, even before they have switched from dormancy to the angiogenic phenotype, have high proliferation rates and therefore are not quiescent (i.e. are not in a G_0 state). These results are consistent with those of previous reports *(13,17,24)*. Moreover, establishment of angiogenic and expanding tumors appeared to be independent of the tumor cell proliferation/apoptosis ratio.

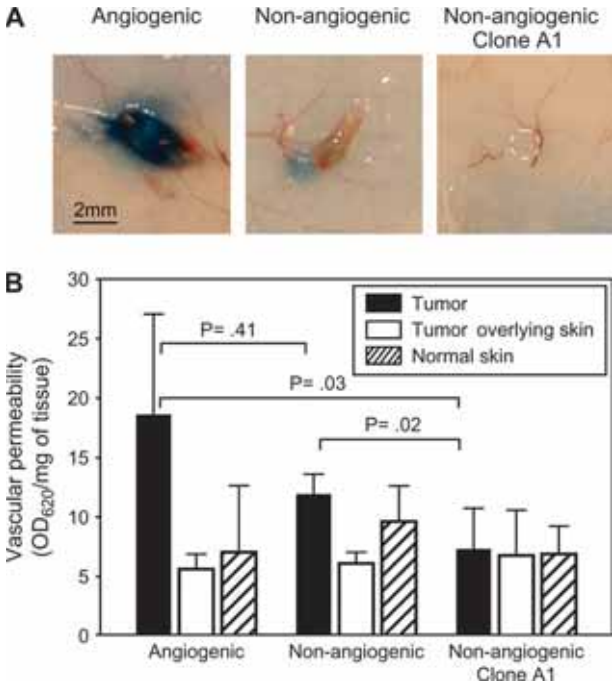

Fig. 5. In vivo Miles assay comparing vascular permeability between tumors generated from nonangiogenic and angiogenic cell lines. Mice were inoculated with either nonangiogenic or angiogenic tumor cells. A modified Miles assay was performed in mice bearing size-matched tumors (from nonangiogenic or angiogenic tumor cells) at day 14 after inoculation. (**A**) Gross morphology of dye-containing angiogenic and dye-excluding nonangiogenic tumors. **Dashed circle** indicates the location of a tumor generated from the nonangiogenic clone A1. (**B**) Quantification of tissue retention of the Evans blue dye (normalized to weight of the tissue samples) showed 1.5- to 2.5-fold higher vascular permeability of the dye in angiogenic tumors than in nonangiogenic tumors (at least seven mice per group). Nonangiogenic tumors and mouse skin samples (tumor-overlying or normal control) had similar permeability. Data represent mean values with **error bars** denoting the upper limit of the 95% confidence intervals. Vascular permeability between tumors from nonangiogenic and angiogenic cell lines was compared using analysis of variance (ANOVA).

Vascular Integrity and Functionality

To compare vascular integrity and functionality between angiogenic and nonangiogenic tumors, we performed a modified Miles assay. Vascular permeability was assessed within size-matched nonangiogenic and angiogenic tumors, as well as in the skin overlying the tumor and in control skin from the contralateral flank of the mouse (Fig. 5). We assessed permeability by measuring Evans blue dye that had leaked from the vasculature after removing intravascular dye by systemic perfusion of the mice with PBS (Fig. 5, B). Both macroscopic analysis (Fig. 5, A) and quantification of extracted dye indicated that angiogenic tumors retained the dye, and nonangiogenic tumors remained dye free. Vascular permeability within the skin that remained in contact with the tumor was comparable to that of skin obtained from the contralateral flank of the mouse. Thus, the observed differences in vascular permeability between angiogenic and nonangiogenic tumors appeared to be localized to the neoplastic tissue and did not affect the permeability of adjacent nonneoplastic tissue (i.e., skin).

Differences in Expression of Pro- and Antiangiogenic Proteins Between Nonangiogenic and Angiogenic Tumor Cells

Levels of bFGF and $VEGF_{165}$ (both of which are proangiogenic) and thrombospondin-1 (which is an angiogenesis inhibitor) secreted by tumor cells were quantified in the media of cells grown in vitro (Fig. 6). In all three cancer types, angiogenic tumor cells secreted much higher levels of bFGF than nonangiogenic cells (13-fold difference for breast cancer cells, 79-fold for osteosarcoma, and fourfold for glioblastoma; P<.001 for all three cancer types, Student's t test). All tumor cells secreted substantial levels of $VEGF_{165}$. However, whereas angiogenic osteosarcoma cells secreted 66-fold higher levels of $VEGF_{165}$ than nonangiogenic tumor cells (P<.001), levels of $VEGF_{165}$ secreted by nonangiogenic and angiogenic tumor cells were similar for both breast carcinoma and glioblastoma. In all three cancer types, nonangiogenic subpopulations secreted statistically significantly higher levels of thrombospondin-1 than angiogenic cells (23-fold difference for breast cancer cells, sixfold for osteosarcoma, and fivefold for glioblastoma and breast carcinoma; P = .011, osteosarcoma and glioblastoma; P<.001).

Repression of Thrombospondin-1 Activity via the PI3K–c-Myc Pathway Correlates With the Switch From Dormancy to the Angiogenic Phenotype

Because nonangiogenic cells secreted higher levels of thrombospondin-1 than angiogenic cells, we hypothesized that thrombospondin-1 expression plays a role during tumor dormancy.

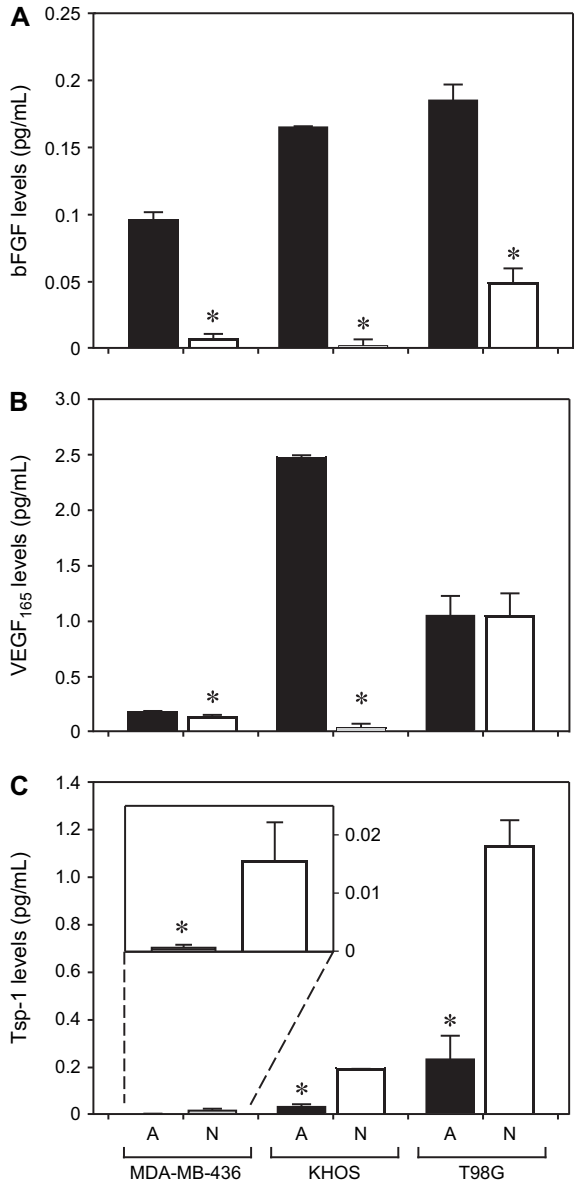

Fig. 6. Secretion of basic fibroblast growth factor (bFGF), vascular endothelial growth factor ($VEGF_{165}$), and thrombospondin-1 by nonangiogenic and angiogenic tumor cells in vitro. Tissue culture medium from angiogenic (**A, black bars**) and nonangiogenic (**N, white bars**) cells was analyzed for levels of bFGF (**panel A**), $VEGF_{165}$ (**panel B**), and thrombospondin-1 (**panel C**) using enzyme-linked immunosorbent assay, for all three human tumor cell lines: MDA-MB-436 (breast cancer), KHOS-24OS (osteosarcoma), and T98G (glioblastoma). All results were standardized per number of viable tumor cells at the time of the assay. Data represent mean values with **error bars** denoting the upper limit of the 95% confidence intervals. Statistically significantly different results between the nonangiogenic and angiogenic pairs are shown with an asterisk (*) above the bar (angiogenic versus nonangiogenic cell comparisons for bFGF, all $P<.001$; for VEGF levels, MDA-436, $P = .005$; KHOS, $P<.001$; for Tsp-1 levels, MDA-MB-436, $P = .011$; KHOS-24OS and T98G, $P<.001$).

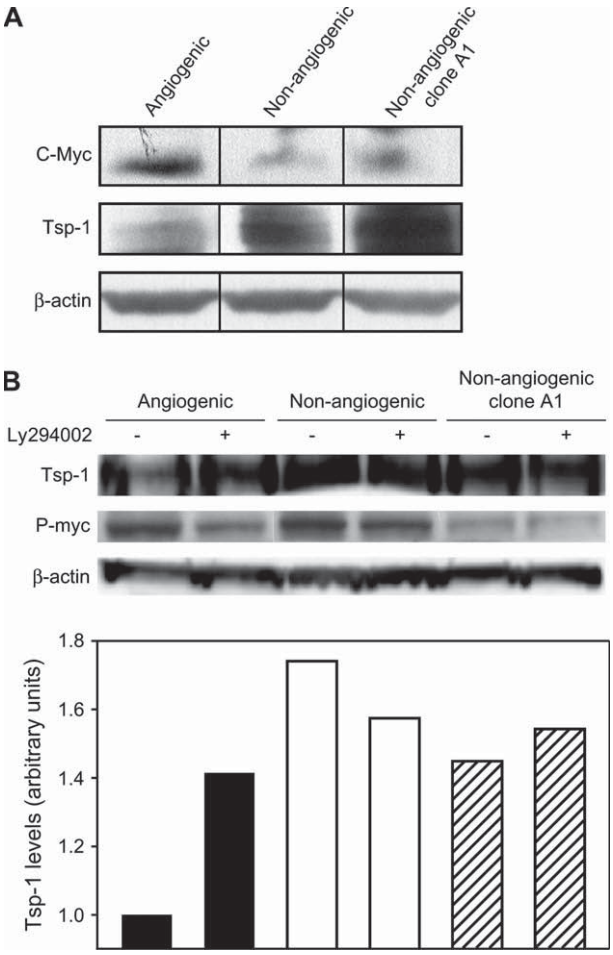

Fig. 7. Thrombospondin-1 expression in nonangiogenic and angiogenic MDA-MB-436 human breast cancer cells. (**A**) Western blot analysis of c-Myc, thrombospondin-1 (Tsp-1), and β-actin (loading control) in angiogenic, nonangiogenic, and nonangiogenic clone A1 variants of MDA-MB-436 cells. (**B**) Upper panel is a representative immunoblot analysis of thrombospondin-1 and phosphorylated c-Myc (p-Myc) in cells treated with the phosphoinositide 3-kinase inhibitor LY294002 (+) or left untreated (−). Lower panel shows thrombospondin-1 expression levels, normalized to total protein gel loading as quantified by staining for β-actin.

Previous work *(19)* in a different breast cancer cell line (MDA-MB-435) demonstrated that thrombospondin-1 expression is governed by the PI3K–c-Myc signaling pathway. Therefore, we compared the expression levels of c-Myc, phosphorylated-Myc (p-Myc), and thrombospondin-1 in cell lysates of nonangiogenic and angiogenic tumor cells. Western blot analysis showed 2.5-fold higher levels of c-Myc and p-Myc in angiogenic cells than in their nonangiogenic counterparts (Fig. 7, A, B). By contrast, angiogenic tumor cells contained lower levels of thrombospondin-1 than nonangiogenic cells. This finding confirmed the results obtained by measuring secreted thrombospondin-1. PI3K has previously been demonstrated to induce a signal transduction cascade leading to the phosphorylation of c-Myc and subsequent repression of thrombospondin-1 *(19)*. Therefore, we sought to determine whether this pathway was active in the angiogenic cell line. We treated both angiogenic and nonangiogenic tumor cells with the PI3K inhibitor LY294002. Treatment with this compound caused thrombospondin-1 levels within angiogenic cells to increase but had no effect on the levels in nonangiogenic cells (or those in nonangiogenic clone A1 cells) (Fig. 7, B). Therefore, we conclude that the PI3K signaling pathway is responsible for the repression of thrombospondin-1 and is differently regulated in angiogenic and nonangiogenic tumor cells.

Discussion

The results presented here show that the switch to the angiogenic phenotype in human cancer cells is highly reproducible in frequency and proportion of otherwise microscopic and dormant

tumors. The model for human tumor dormancy that we have developed here is novel because the angiogenic tumor cell lines had spontaneously switched from the nonangiogenic cell lines without the use of in vitro selection (by a particular tumor cell marker) or artificial genetic alterations *(15,17–19)*. Our results suggest that the onset and extent of angiogenesis are critical determinants of tumor progression and growth. Also, our results indicate that the establishment of angiogenic and expanding tumors in vivo (i.e., the angiogenic switch) is independent of the ratio of tumor cell proliferation to apoptosis.

Histologic examination of microscopic nonangiogenic breast cancers revealed two categories of such tumors: 1) completely avascular tumors and 2) tumors containing empty lumens, without red blood cells, which we assume represent blind sprouts. Neither category of nonangiogenic tumors showed evidence of vascular permeability, most likely because of the absence of vasculature or presumably inefficient vascular sprouting. These categories are likely to represent early stages leading to the angiogenic switch. The gross difference between the nonangiogenic tumors and angiogenic tumors (i.e., white versus red tumors) is most likely due to the reactive hyperemia that accompanies the onset of blood flow after the angiogenic switch is completed in a previously hypoxic tumor.

In the experiments reported here, we used 5×10^6 tumor cells in each inoculation. We observed sparse microvessels in the nonangiogenic tumors up to 40 days after inoculation. These structures did not appear to be functional microvessels, as evidenced by lack of vascular lumens and absence of red blood cells. After 40 days, these microvascular structures could not be sustained, and they disappeared until the angiogenic switch. After the completion of this study, further work (data not shown) indicated that these sparse microvessels could be induced by excessive VEGF or other proangiogenic proteins carried over in the original tumor cell inoculum. Therefore, we decreased the inoculum by decrements from 5×10^6 to 500 tumor cells. We found the optimum inoculum to be 10^6 tumor cells; this inoculum produced nonangiogenic, microscopic, dormant tumors that were completely avascular until the time of the angiogenic switch. Therefore, in future studies, we suggest that the model we now report could be optimized by using approximately 10^6 tumor cells as the initial inoculum.

Although our findings indicate that the lack of angiogenesis is a rate-limiting step for tumor expansion in the dormant state, there may also be other processes involved in human tumor dormancy, such as differentiation programs, tumor cell survival, or immune response of the host. Although the precise mechanism and timing of tumor dormancy have not yet been completely elucidated, our novel approach provides a means to determine the molecular events and sequential steps of the angiogenic switch. The kinetics of individual stages might be of substantial practical importance for identifying an optimal therapeutic window in the treatment of early cancer.

In other animal models, the growth of angiogenic tumors has been associated with reduced expression of endogenous angiogenesis inhibitors, such as angiostatin *(24)*, endostatin *(25)*, tumstatin *(26)*, pigment epithelium–derived factor *(27)*, and thrombospondin-1 *(28)*. Although it is likely that other endogenous angiogenesis inhibitors play a role in the switch to the angiogenic phenotype for other cancer types, in these experiments we focused on the differences in thrombospondin-1 expression between nonangiogenic and angiogenic tumor cells. In our experiments, thrombospondin-1 appeared to be a major negative regulator of angiogenesis. That is, thrombospondin-1 expression had to be reduced in the angiogenic tumor cells for the angiogenic switch to take place. This finding further strengthens Noël Bouck's hypothesis that the onset of tumor angiogenesis is associated with a substantial decrease in thrombospondin-1 levels *(29)*. Previous reports have shown that transfection of thrombospondin-1 into human breast cancer cell lines decreased angiogenesis, tumor growth, and metastasis in immunocompromised mice *(19,30)*. Immunohistochemical analysis of human breast cancer tissue has shown marked increases in levels of thrombospondin-1 mRNA in stromal cells immediately adjacent to ductal carcinomas in situ compared with normal breast tissue *(31)*. These findings raise the possibility that increased expression of thrombospondin-1 in stromal cells and cancer cells may inhibit angiogenesis induced by VEGF and bFGF.

Our dormancy model of breast cancer shows that thrombospondin-1 expression is regulated by the PI3K–c-Myc signaling pathway. This finding is consistent with those of previous reports *(19,32–34)*. Western blot analysis demonstrated that the angiogenic MDA-MB-436 breast cancer cells expressed higher levels of c-Myc and lower levels of thrombospondin-1 than the nonangiogenic cell line or the nonangiogenic single cell–derived clone A1. Furthermore, when the activity of PI3 kinase was inhibited in the angiogenic cells, levels of p-Myc decreased and levels of thrombospondin-1 increased compared with levels in the nonangiogenic cells. We conclude that the PI3K–c-Myc pathway plays a key role in the regulation of thrombospondin-1 and may contribute to the observed differences in growth in vivo.

In our study, most of the nonangiogenic glioblastoma and osteosarcoma tumors never switched to an angiogenic phenotype during the lifetimes of the mice. By contrast, most of the nonangiogenic breast tumors did undergo the angiogenic switch. Therefore, the amount of time until the angiogenic switch appears to be distinct for a given tumor type and to differ among tumor types. We speculate that most human microscopic cancers can survive for prolonged periods by keeping the balance of pro- and antiangiogenic proteins in a steady state that favors dormancy.

The human tumor dormancy model has a few limitations. One limiting factor is that experiments characterizing the timing of the angiogenic switch can be time-consuming, lasting up to 1 year or longer. Consequently, up to this point, the mechanism of the angiogenic switch is still unclear and under investigation. Nonangiogenic tumors are invisible until the angiogenic switch, unless they are imaged using luciferase or green fluorescent protein.

Our results provide the basis for further analysis of dormant nonangiogenic tumors. Among the questions that it can be used to address are the following: 1) What are the determinants and mechanism for the "clock" that governs the angiogenic switch? Why is the timing of the switch to the angiogenic phenotype so predictable for a given tumor type? For example, why do 100% of angiogenic breast cancers become palpable at a median of 19 days, when less than 20% of nonangiogenic (clone A1) breast cancers switch to the angiogenic phenotype after approximately 1 year? In vivo growth of these single-cell clones demonstrates heterogeneity in the dormancy clock and will be used for subsequent molecular studies of this process. 2) What is the sequence of the different stages of the angiogenic switch, i.e., lumen formation, initiation of flow, and hyperemia? 3) Is the angiogenic switch reversible? Can angiogenic tumor cells revert to nonangiogenic cells? If not, why is it possible to isolate nonangiogenic

tumor cells from angiogenic tumors, such as the nonangiogenic clone A1 of breast cancer?

During the dormancy period, nonangiogenic tumors had high proliferation rates and were therefore not quiescent (i.e. were not in a G_0 state). Moreover, the angiogenic switch appeared to be independent of the tumor cell proliferation/apoptosis ratio. Therefore, angiogenesis and proliferation/apoptosis represent different programs in tumor progression. These models can permit further studies of the angiogenic switch, especially the different stages and timing of the process. Also, this approach may be suitable for the study of sensitive angiogenesis-based biomarker assays and novel treatment strategies. We, along with others, are currently developing an angiogenesis-based panel of blood and urine biomarkers that can be quantified and used to detect microscopic tumors before or during the angiogenic switch. If this approach is feasible, microscopic tumors could possibly be treated years before they become symptomatic or their anatomical site is detectable. The use of this animal model has taught us that in the future, it may be possible to liberate the management of cancer from dependency on anatomical site.

References

(1) Folkman J, Cole P, Zimmerman S. Tumor behavior in isolated perfused organs: in vitro growth and metastases of biopsy material in rabbit thyroid and canine intestinal segment. Ann Surg 1966;164:491.

(2) Folkman J, Kalluri R. Cancer without disease. Nature 2004;427:787.

(3) Gimbrone MA Jr, Leapman SB, Cotran RS, Folkman J. Tumor dormancy in vivo by prevention of neovascularization. J Exp Med 1972;136:261–76.

(4) Folkman J. Antiangiogenesis agents. In Cancer: Principles and Practice of Oncology, 7th ed. VT DeVita Jr, S Hellman, and SA Rosenberg, editors. Philadelphia (PA): Lippincott Williams & Wilkins; 2004. pp. 2865–82.

(5) Nielsen M, Thomsen JL, Primdahl S, Dyreborg U, Andersen JA. Breast cancer and atypia among young and middle-aged women: a study of 110 medicolegal autopsies. Br J Cancer 1987;56:814–9.

(6) Black WC, Welch HG. Advances in diagnostic imaging and overestimators of disease prevalence and the benefits of therapy. N Engl J Med 1993;328:1237–43.

(7) Feldman AR, Kessler L, Myers MH, Naughton MD. The prevalence of cancer. Estimates based on the Connecticut Tumor Registry. N Engl J Med 1986;315:1394–7.

(8) Demicheli R, Terenziani M, Valagussa P, Moliterni A, Zambetti M, Bonadonna G. Local recurrences following mastectomy: support for the concept of tumor dormancy. J Natl Cancer Inst 1994;86:45–8.

(9) Meng S, Tripathy D, Frenkel EP, Shete S, Naftalis EZ, Huth JF, et al. Circulating tumor cells in patients with breast cancer dormancy. Clin Cancer Res 2004;10:8152–62.

(10) Mizuno I, Izeki O, Nakahara S, Kawamoto K, Onga T, Matsuoka H, et al. Disseminated carcinomatosis of the bone marrow occurring 11 years after subtotal gastrectomy for gastric cancer. Rinsho Ketsueki 1998;39:670–5.

(11) Crowley NJ, Seigler HF. Relationship between disease-free interval and survival in patients with recurrent melanoma. Arch Surg 1992;127:1303–8.

(12) Badgley CE, Batts M. Osteogenic sarcoma: an analysis of eighty cases. Arch Surg 1941;43:541–50.

(13) Holmgren L, O'Reilly MS, Folkman J. Dormancy of micrometastases: balanced proliferation and apoptosis in the presence of angiogenesis suppression. Nat Med 1995;1:149–53.

(14) Folkman J, Watson K, Ingber D, Hanahan D. Induction of angiogenesis during the transition from hyperplasia to neoplasia. Nature 1989;339:58–61.

(15) Hanahan D, Folkman J. Patterns and emerging mechanisms of the angiogenic switch during tumorigenesis. Cell 1996;86:353–64.

(16) Hanahan D, Christofori G, Naik P, Arbeit J. Transgenic mouse models of tumor angiogenesis: the angiogenic switch, its molecular controls, and prospects for preclinical therapeutic models. Eur J Cancer 1996;14:2386–93.

(17) Achilles EG, Fernandez A, Allred EN, Kisher O, Udagawa T, Beecken WD, et al. Heterogeneity of angiogenic activity in a human liposarcoma: a proposed mechanism for "no take" of human tumors in mice. J Natl Cancer Inst 2001;93:1075–81.

(18) Udagawa T, Fernandez A, Achilles E, Folkman J, D'Amato RJ. Persistence of microscopic human cancers in mice: alterations in the angiogenic balance accompanies loss of tumor dormancy. FASEB J 2002;16:1361–70.

(19) Watnick RS, Cheng Y, Rangarajan A, Ince TA, Weinberg RA. Ras modulates Myc activity to repress thrombospondin-1 expression and increase tumor angiogenesis. Cancer Cell 2003;3:219–31.

(20) Gavrieli Y, Sherman Y, Ben-Sasson SA. Identification of programmed cell death in situ via specific labeling of nuclear DNA fragmentation. J Cell Biol 1992;119:493–501.

(21) Miles A, Miles E. Vascular reactions to histamine, histamine-liberator and leukotaxine in the skin of guinea pigs. J Physiol 1952;118:228–57.

(22) Kaplan EL, Meier P. Nonparametric estimation from incomplete observations. J Am Stat Assoc 1958;53:457–81.

(23) Mantel N. Evaluation of survival data and two new rank order statistics arising in its consideration. Cancer Chemother Rep 1966;50:163–70.

(24) O'Reilly MS, Holmgren L, Chen C, Folkman J. Angiostatin induces and sustains dormancy of human primary tumors in mice. Nat Med 1996;2:689–92.

(25) O'Reilly MS, Boehm T, Shing Y, Fukai N, Vasios G, Lane WS, et al. Endostatin: an endogenous inhibitor of angiogenesis and tumor growth. Cell 1997;88:277–85.

(26) Maeshima Y, Sudhakar A, Lively JC, Ueki K, Kharbanda S, Kahn CR, et al. Tumstatin, an endothelial cell-specific inhibitor of protein synthesis. Science 2002;295:140–3.

(27) Dawson DW, Volpert OV, Gillis P, Crawford SE, Xu H, Benedict W, et al. Pigment epithelium-derived factor: a potent inhibitor of angiogenesis. Science 1999;285:245–8.

(28) Good DJ, Polverini PJ, Rastinejad F, Le-Beau MM, Lemons RS, Frazier WA, et al. A tumor suppressor-dependent inhibitor of angiogenesis is immunologically and functionally indistinguishable from a fragment of thrombospondin. Proc Natl Acad Sci U S A 1990;87:6624–8.

(29) Rastinejad F, Polverini PJ, Bouck NP. Regulation of the activity of a new inhibitor of angiogenesis by a cancer suppressor gene. Cell 1989;56: 345–55.

(30) Weinstat-Saslow DL, Zabrenetzky VS, VanHoutte K, Frazier WA, Roberts DD, Steeg PS. Transfection of thrombospondin 1 complementary DNA into a human breast carcinoma cell line reduces primary tumor growth, metastatic potential, and angiogenesis. Cancer Res 1994;54:6504–11.

(31) Brown LF, Guidi AJ, Schnitt SJ, Van De Water L, Iruela-Arispe ML, Yeo TK, et al. Vascular stroma formation in carcinoma in situ, invasive carcinoma, and metastatic carcinoma of the breast. Clin Cancer Res 1999;5: 1041–56.

(32) Aguirre-Ghiso JA, Kovalski K, Ossowski L. Tumor dormancy induced by downregulation of urokinase receptor in human carcinoma involves integrin and MAPK signaling. J Cell Biol 1999;147:89–104.

(33) Aguirre-Ghiso JA, Liu D, Mignatti A, Kovalski K, Ossowski L. Urokinase receptor and fibronectin regulate the ERK(MAPK) to p38(MAPK) activity ratios that determine carcinoma cell proliferation or dormancy in vivo. Mol Biol Cell 2001;12:863–79.

(34) Aguirre-Ghiso JA, Estrada Y, Liu D, Ossowski L. ERK(MAPK) activity as a determinant of tumor growth and dormancy; regulation by p38(SAPK). Cancer Res 2003;63:1684–95.

Notes

We thank Amy Birsner, Nathan Liu, and Gerd Lillian Hallseth for excellent technical assistance; Dr. Raanan Berger (Dana-Farber Cancer Institute) for technical help with the in vitro anchorage-independent growth assay; Drs. Giannoula Klement and Sandra Ryeom for valuable comments; and Kristin Gullage for photography.

Supported by the Breast Cancer Research Foundation, an Innovator Award (W81XWH-04-1-0316) from the Department of Defense, and Institute of Cancer Research/Oliver R. Grace fellowship to Dr. Nava Almog. The funding agencies did not have a role in the design, conduct, and reporting of this study.

Funding to pay the Open Access publication charges for this article was provided by the Breast Cancer Research Foundation.

Manuscript received June 20, 2005; revised December 19, 2005; accepted January 11, 2006.

[Cell Cycle 5:16, 1779-1787, 15 August 2006]; ©2006 Landes Bioscience

Spotlight on Cancer Cell Dormancy

Role of Angiogenesis in Human Tumor Dormancy

Animal models of the Angiogenic Switch

George N. Naumov[1,2]
Lars A. Akslen[3]
Judah Folkman[1,2]*

[1]Department of Surgery; Harvard Medical School; [2]Vascular Biology Program; Children's Hospital Boston; Boston, Massachusetts USA

[3]Section for Pathology; The Gade Institute; University of Bergen; Bergen, Norway

*Correspondence to: Judah Folkman; Karp Family Research Laboratories 12.128; 300 Longwood Avenue; Boston, Massachusetts 02115; USA; Tel.: 617.919.2346; Fax: 617.739.5891; Email: judah.folkman@childrens.harvard.edu

Previously published online as a *Cell Cycle* E-publication:
http://www.landesbioscience.com/journals/cc/abstract.php?id=3018

KEY WORDS

dormancy, human tumors, metastasis, angiogenesis

ACKNOWLEDGEMENTS

We thank Professor Leif Andersson (University of Helsinki, Finland) for kindly providing clinical samples of human thyroid cancer. The authors are grateful to Dr. T. Udagawa, Dr. D. Zurakowski, Katherine Novak, and Robert Bolcome for critical reading of this manuscript. We also thank Kristin Johnson for help with graphics.

ABSTRACT

Tumor progression depends on sequential events, including a switch to the angiogenic phenotype (i.e., initial recruitment of blood vessels). Failure of a microscopic tumor to complete one or more early steps in this process may lead to delayed clinical manifestation of the cancer. Microscopic human cancers can remain in an asymptomatic, non-detectable, and occult state for the life of a person. Clinical and experimental evidence suggest that human tumors can persist for long periods of time as microscopic lesions that are in a state of dormancy (i.e., not expanding in tumor mass). Because it is well established that tumor growth beyond the size of 1–2 mm is angiogenesis-dependent, we hypothesized that presentation of large tumors is attributed to a switch to the angiogenic phenotype in otherwise microscopic, dormant tumors. Although clinically important, the biology of human tumor dormancy is poorly understood. The development of animal models which recapitulate the clinically observed timing and proportion of dormant tumors which switch to the angiogenic phenotype are reviewed here. The contributing molecular mechanisms involved in the angiogenic switch and different strategies for isolation of both angiogenic and non-angiogenic tumor cell populations from otherwise heterogeneous human tumor cell lines or surgical specimens are also summarized. Several imaging techniques have been utilized for the qualitative and quantitative detection of microscopic tumors in mice and their strengths and limitations are discussed. The animal models employed here permitted further studies of the angiogenic switch. These models also allowed development of an angiogenesis-based panel of blood and urine biomarkers that can be quantified and used to detect microscopic tumors before or during the angiogenic switch. If the information obtained from these animal models is translatable to the clinic, it may be possible in the future to liberate the management of cancer from a dependency on anatomical site years before it becomes symptomatic and detectable.

BACKGROUND

Consider a cancer cell that has progressed through a series of mutations and has become: (1) self-sufficient in growth signaling, by activation of certain oncogenes and by the loss of specific suppressor genes, (2) insensitive to antigrowth signals, (3) unresponsive to apoptotic signals, (4) capable of limitless cell replications and (5) tumorigenic.[1] Current evidence indicates that these neoplastic properties may be necessary, but not sufficient for a cancer cell to expand into a population of tumor cells that becomes clinically detectable, metastatic, and lethal. For a tumor to develop such a highly malignant and deadly phenotype, it must first recruit and sustain its own blood supply, a process called tumor angiogenesis.[2,3]

Cancer becomes clinically detectable only after a tumor mass undergoes continuous expansion. However, expansion of a tumor mass beyond the initial microscopic size of a non-angiogenic tumor is dependent on the recruitment of its own vascular supply, by angiogenesis and/or blood vessel cooption.[3-6] The ability of a tumor to progress from a non-angiogenic to angiogenic phenotype is central to the progression of cancer and is termed the "angiogenic switch".[7] Failure of a tumor to recruit new microvascular endothelial cells or to reorganize the existing surrounding vasculature results in a non-angiogenic tumor that is microscopic in size. Because of their non-functional or non-existent vasculature, non-angiogenic tumors are highly dependent on their microenvironment for oxygen and the supply of nutrients. The diffusion limit of oxygen is approximately 100 μm requiring that all mammalian cells be located within 100–200 μm of blood vessels.[8] Because non-angiogenic tumors fail to recruit new blood vessels, but require oxygen and nutrients for their long-term survival, they remain limited in size to less than 1 mm in diameter. As

some non-angiogenic tumors expand in mass, some tumor cells will be outside the oxygen diffusion limit and become hypoxic. Hypoxia increases cellular hypoxia inducible factor (HIF) transcription, leading to upregulation of proangiogenic proteins, such as VEGF, PDGF and NOS.[9] It is presumed that these relatively short-lived pro-angiogenic proteins exceed the local concentration of anti-angiogenic proteins, ultimately allowing angiogenesis to occur and permitting the tumor to expand in mass.

CLINICAL EVIDENCE FOR HUMAN TUMOR DORMANCY: CANCER WITHOUT DISEASE

Clinically, tumor dormancy has been observed in patients who have been treated for primary cancer and have relapsed after a disease-free period of several months to many years.[10,11] Also, pathologists performing autopsies on individuals who have died in automobile accidents or other trauma have documented the presence of in situ or small invasive (microscopic) carcinomas. These findings, summarized by Black and Welch,[12] reveal that carcinoma in situ is found in the breast of 39% of women age 40 to 50 years who die of trauma, but only 1% are ever diagnosed with cancer during life in the same age range. Carcinoma in situ of the prostate is diagnosed in 46% of men age 60 to 70 years who die of trauma,[13] but only 1–1.5% are diagnosed with cancer during their lives.[14,15] Most strikingly, microscopic carcinoma (many of them less than 1 mm in diameter) is found in the thyroid of more than 98%[12] of individuals age 50 to 70 years who die of trauma, but is diagnosed in only 0.1% during life, in individuals in this age range.

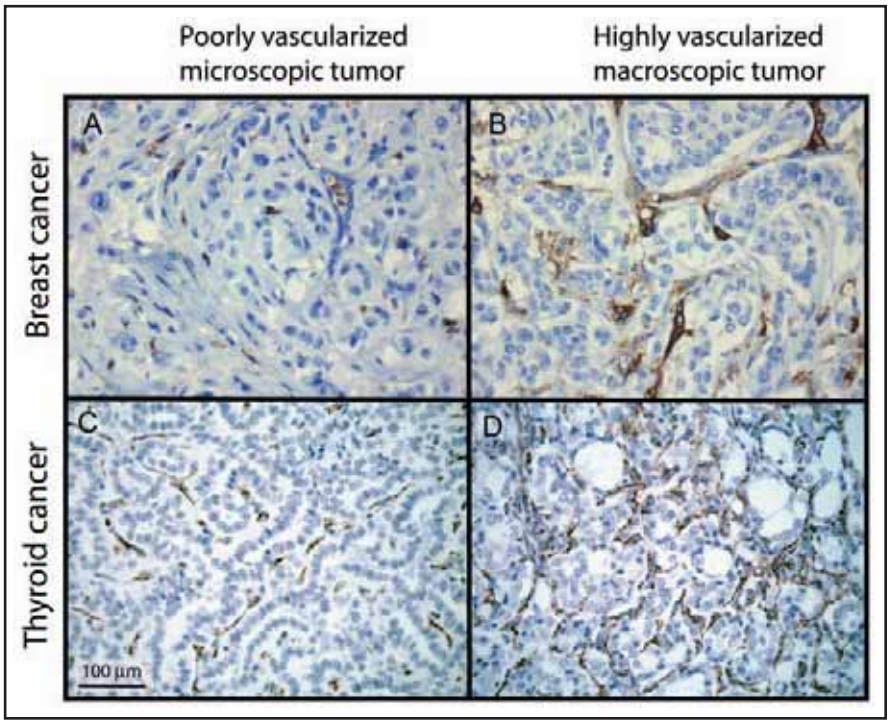

Figure 1. Representative micrographs of human breast (A and B) and thyroid (C and D) tumors stained with endothelial cell marker (CD-31). Microscopic human tumors (A and C; less than 2 mm in size) are poorly vascularized, as demonstrated by minimal CD-31 intratumoral staining. However, large tumors (B and D; tumor diameter larger than 10 cm) are well vascularized. Human thyroid tumors are a contribution from Professor Leif Andersson. Size bar represents 100 µm.

This evidence for the presence of microscopic and clinically occult cancer comes from two types of studies: (1) autopsy performed on individuals who have not been diagnosed with cancer at the time of death or (2) careful histologic examination of the normal tissue in patients diagnosed with cancer (i.e., from examination of the contralateral breast in women diagnosed with breast cancer).

These studies are associated with an inherent variability depending on the methodology used. For example, tissue sampling in some of these studies involved only one to five small tissue blocks per organ. Other factors include selection of the study population, age groups, histological classification, and grading. However, despite methodological limitations, all of these studies suggest that as a person ages, there is higher incidence of occult disease, but only a small fraction of these microscopic tumors become clinically detectable. This model assumes that all invasive and clinically detectable cancers evolve from an in situ or small invasive (microscopic) carcinomas and that do not undergo complete spontaneous regression. Although there are anecdotal clinical cases of spontaneous tumor regression, they are rare events and are not expected to significantly change this working model of cancer progression.

What keeps these microscopic carcinomas in check? Several hypotheses have been proposed over the past few years in attempts to explain the phenomenon of human tumor dormancy. Some have assumed that tumor cells enter a prolonged state of G_0 during dormancy.[16] Others hypothesized that tumor size is controlled by the immune system or depletion of hormones in hormone-dependent tumors.[17-22] Another explanation for these observations is that most human tumors arise without angiogenic activity and exist in a microscopic dormant state for months to years without neovascularization. Such protection may be attributed to the host-derived factors that prevent microscopic carcinomas from switching to the angiogenic phenotype.[23]

To address whether blocked or impaired angiogenesis can be one cause of human tumor dormancy, representative microscopic and macroscopic human tumors were stained with an endothelial cell marker (CD-31). Examples of breast and thyroid cancers are shown in Figure 1 Microscopic (approximately 1–2 mm in diameter) human tumors were characterized by minimal CD-31 intratumoral staining, representing isolated endothelial cells or a few small vessels (Fig. 1A and C). However, CD-31 staining of large (~10 cm in diameter) macroscopic tumors revealed well organized vascular structures filled with red blood cells, suggesting the presence of a functional vasculature (Fig. 1B and D). These observations support the hypothesis that human tumors are dependent on angiogenesis for progressive growth beyond an occult (in situ) microscopic lesion to a large clinically detectable tumor.

These findings suggest that tumors remain harmless to the host during the non-angiogenic dormant state. The "disease" of cancer is not manifested until after a tumor mass continuously expands beyond the microscopic size of non-angiogenic tumors[23] (Fig. 2). This tumor mass expansion is associated with the recruitment of endothelial cells, which occurs after the tumor cells (and stroma) undergo a switch from a non-angiogenic dormant phenotype to the angiogenic phenotype.[24] The switch to the angiogenic phenotype is

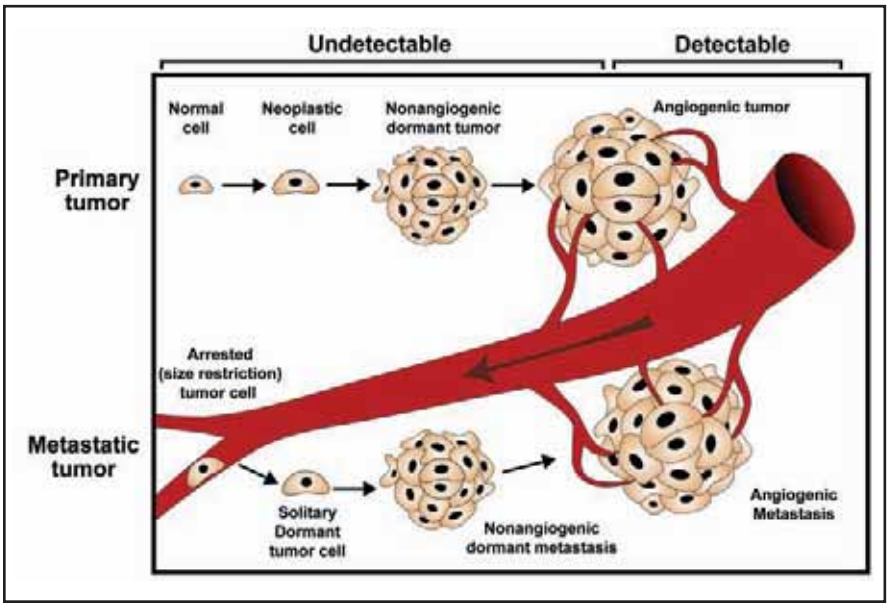

Figure 2. Steps in tumor progression at a primary and metastatic site. Human cancers can remain dormant (tumor cells actively proliferating and undergoing apoptosis) at a microscopic size due to a lack of angiogenesis both as a primary tumor and a metastasis. Moreover, solitary dormant cells can persist at a metastatic site in G_0 growth arrest. Only angiogenic macroscopic primary tumors and metastases are clinically detectable. Microscopic dormant tumors and solitary cancer cells can remain occult for long time periods.

driven by: (1) increased expression by tumor cells of angiogenic proteins, such as vascular endothelial growth factor (VEGF) and basic fibroblast growth factor (bFGF); (2) increased expression of angiogenic proteins by stromal cells (i.e., stromal fibroblasts), a process induced by the tumor itself; (3) decreased expression of endogenous angiogenesis inhibitors (i.e., thrombospondin-1, TSP1) by tumor cells and by stromal fibroblasts; and (4) in some tumors recruitment of bone marrow-derived endothelial precursors. The expansion of tumor mass accompanying the switch to the angiogenic phenotype inevitably produces symptomatic, clinically detectable, and potentially lethal cancers either from a local mass that mechanically interferes with organ function (e.g., a brain tumor or intestinal obstruction from ovarian cancer), from a systemically dispersed mass (i.e., multiple metastases), or from the release of molecules that affect normal physiologic functions (e.g., cytokines that interfere with hemostasis and result in abnormal clotting or bleeding, the two most common causes of death in cancer patients). In summary, the absence of tumor angiogenesis precludes tumor mass expansion beyond a microscopic size, resulting in an asymptomatic and non-metastatic state. This dormancy state is not potentially lethal in most individuals, i.e., "cancer without disease".[23] However, once they have become angiogenic, tumors may rapidly expand in mass and become lethal.

ANIMAL MODELS OF TUMOR DORMANCY

One of the earliest in vivo demonstrations that tumor dormancy can result from blocked angiogenesis was in the rabbit eye.[25] A 1 mm^3 implant of V2 carcinoma was allowed to float in the aqueous humor of the anterior chamber, or was adhered to the posterior surface of the cornea. These avascular tumor implants remained viable, with proliferation tumor cells throughout the experiment (>6 weeks). Neovascularization appeared in the iris vessels, indication that the tumor was releasing a diffusible angiogenic factor(s). However, the new capillary blood vessels could not grow through the aqueous humor to reach the tumor implants. When the implants were manipulated so that they were directly apposed to the iris vessels, the tumor implants became neovascularized within five days and tumor mass expanded exponentially, by 16,000 times the original volume in 14 days.

Hanahan et al.[26] described a tumor model (RIP1-Tag2) in transgenic mice, in which autochthonous tumors arise in the pancreatic islets as a result of the expression of simian virus 40 T antigen (Tag) oncogene. In this model, only 4% of tumors are angiogenic after 13 weeks, whereas the remaining 96% remain microscopic and non-angiogenic.[26,27] The spontaneous progression of non-angiogenic lesions to the angiogenic phenotype in these transgenic tumor-bearing mice led to the development of the "angiogenic switch" concept.[24]

Subsequently, we showed that human cancers contain subpopulations of tumor cells that differ in their angiogenic potential.[28] This heterogeneity of angiogenic activity among human tumor cells allowed for the development of new animal dormancy models using various human cancer types.

The isolation of angiogenic and non-angiogenic human tumor cells in these new animal models was based on the ability of otherwise "non-tumorigenic" or "no take" tumor cells to spontaneously switch to the angiogenic phenotype in immunocompromised mice (Fig. 3). To date, we have obtained more than 15 human tumor cell lines from the American Type Culture Collection (ATCC, Manassas, VA), based on their "no take" phenotype in immunocompromised mice. Following tumor cell expansion under tissue culture conditions their in vivo ability to form tumors in SCID mice was assessed. In this in vivo assay, SCID mice were inoculated subcutaneously with a suspension of 5 x 10^6 tumor cells in 0.2 ml of PBS or serum-free media. Mice were monitored for palpable tumors at the site of tumor cell inoculation for more than one year and, sometimes, for the life of the animal. Seven of the tested human tumor cell lines did not form palpable tumors for more than 500 days after cancer cell inoculation. There was no presence of a microscopic tumor, as evidenced by microscopic examination of the site of tumor cell inoculation after animals were killed so that the inner side of the skin could be examined. Based on this long-term in vivo assay, such cell lines were considered truly non-tumorigenic. However, half of the tested human tumor cell lines spontaneously formed palpable tumors after a dormancy period that varied from months to more than a year, depending on the cancer type (Fig. 3). Once palpable, these tumors expanded in mass, becoming angiogenic and lethal within approximately 50 days.

Table 1 summarizes the dormancy periods and proportion of tumors that switch to the angiogenic phenotype of some of these cell lines. Each cancer type has a characteristic and predictable dormancy period (i.e., a dormancy "clock"), and a consistent proportion of tumors that switch to the angiogenic phenotype. However, once non-angiogenic tumors switched to the angiogenic phenotype, they always rapidly expanded in mass, independent of the cancer type.

Stable cell lines were established from representative angiogenic tumors and their growth in vivo was assessed.[29] When inoculated into SCID mice, the angiogenic variants always formed large (>1 cm in diameter) tumors within a month (i.e., without a dormancy period), regardless of the cancer type. In contrast to the harmless microscopic dormant tumors, these angiogenic tumors were always lethal to the animals. These findings suggest that once human tumors become angiogenic, they lose their dormancy "clock". These animal models recapitulate the human tumor dormancy period and the proportion of tumors that eventually become angiogenic as observed in the clinical setting. Therefore, mechanisms of the angiogenic switch in human dormant tumors can be further explored using these animal models.

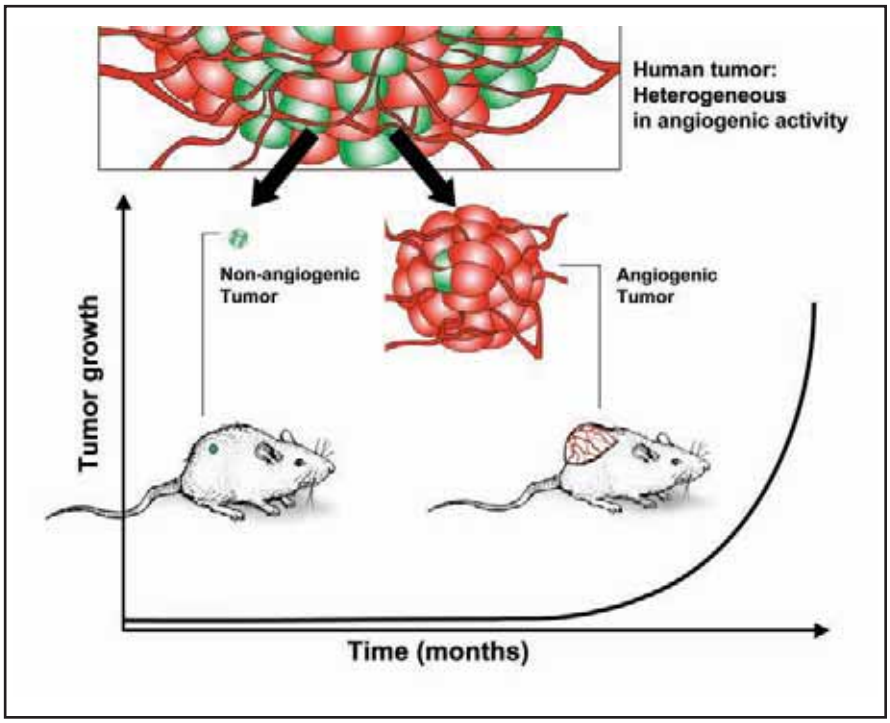

Figure 3. Schematic representation of in vivo isolation of the angiogenic and the non-angiogenic human tumor cell populations from an otherwise heterogeneous (in angiogenic activity) human tumor. Non-angiogenic cells are inoculated into immunocompromised mice and allowed to spontaneously switch to the angiogenic phenotype. Once angiogenic, human cancer cells form large tumors in mice within a month.

HUMAN DORMANT TUMOR CELLS ACTIVELY PROLIFERATE AND DIE

During the non-angiogenic phase, when angiogenic activity is absent or insufficient, growth and doubling times for the whole tumor may be years. However, this does not mean that tumor cells are proliferating slowly or that they are in G_0 phase, as demonstrated in other tumor dormancy models.[30-32] In our human tumor dormancy models, the tumor cell proliferation index can be as high as that of large vascularized tumors. In a breast cancer (MDA-MB-436 cells) animal model, more than 50% of tumor cells were proliferating and more than 10% underwent apoptosis in all microscopic and macroscopic tumors when analyzed at various time points.[29] In a human osteosarcoma (MG-63 and SAOS-2 cells) and gastric cancer (ST-2 cells) dormancy model, microscopic tumors were not able to grow beyond a threshold size due to a balance between proliferating cells and cells undergoing apoptosis.[33] Tumor cell proliferation in these tumors was approximately 12% and tumor cell apoptosis varied between 4 and 7.5%.

DEFINITION OF A HUMAN DORMANT TUMOR AS OBSERVED IN MICE

In its simplest terms, a "dormant" tumor can be defined as microscopic in size and non-expanding in mass. A "stable" tumor is macroscopic and expanding in mass. In more detail, human dormant tumors are defined as:

(1) unable to induce angiogenic activity, as evidenced by repulsion of existing blood vessels in the local stroma and/or relative absence of microvessels within the tumor;

Table 1 **Human tumor cell lines that spontaneously switch to the angiogenic phenotype after a prolonged dormancy period in immunocompromised mice**

Human cell line	Cancer type	Dormancy period	Spontaneous angiogenic switch (% of tumors that switch to the angiogenic phenotype)	Reference
MDA-MB-436	Breast	4 months	~80%	Naumov et al., JNCI 2006
KHOS-24OS	Osteosarcoma	8 months	~20%	Naumov et al., JNCI 2006
T98G	Brain	8 months	~60%	Naumov et al., JNCI 2006
SAOS-2	Osteosarcoma	12 months	~10–15%	Udagawa et al., FASEB 2002 and unpublished results
ST-2	Gastric	>8 months	<3%	Udagawa et al., FASEB 2002
MG-63	Osteosarcoma	12 months	~5%	Udagawa et al., FASEB 2002 and unpublished results
MDA-MB-436-A1*	Breast	8 months	~20%	Naumov et al., JNCI 2006
SW 872*	Liposarcoma	4 months	>95%	Almog et al., FASEB 2006

*Single cell clone-derived tumor cell populations.

(2) remain harmless to the host until they switch to the angiogenic phenotype (i.e., may be harmless for 1 year or more, which is half the life-span of a mouse);

(3) express equal or more antiangiogenic (i.e., thrombospondin-1) compared to angiogenic (i.e., VEGF, bFGF) proteins;

(4) grow to approximately 1 mm in diameter or less in vivo, at which time further expansion ceases;

(5) are only visible by a hand lens or a dissecting microscope (5–10 X magnification);

(6) are white or transparent by gross examination;

(7) never metastasize spontaneously from the microscopic dormant state;

(8) show active tumor cell proliferation in mice, and remain metabolically active during the dormancy period;

(9) can be cloned from a human angiogenic tumor, because human tumors are heterogeneous and contain a mixture of non-angiogenic and angiogenic tumor cells.

VISUALIZATION OF HUMAN DORMANT TUMORS

Dormant tumors are by definition microscopic in size, therefore, in most instances, undetectable by palpation (limited to tumor sizes smaller than 50 mm^3) when located in the subcutaneous space or mammary fat pad. This detection challenge is even more evident when microscopic tumors appear in internal organs either as primary tumors or metastases. In the originally published dormancy models, the presence of dormant osteosarcomas (MG-63) was revealed by hair growth overlying the original tumor inoculation site.[33] Careful examination under the area of hair growth revealed a small white lesion, which was found to contain tumor cells only by histology. Although phenomenologically interesting this detection method does not provide quantitative information about the size of the tumor.

FLUORESCENT PROTEIN LABELING OF TUMOR CELLS

Three techniques can be employed to reliably detect microscopic tumors, such as stable infection of tumor cells with green fluorescent protein (GFP), red fluorescent protein (RFP), or luciferase. GFP-expressing tumor cells can be visualized non-invasively from the skin surface by blue light (488 nm) epi-illumination. When mice are killed and the skin opened, GFP-expressing tumors can be easily localized even if they contain only a few tumor cells. Moreover, vessel cooption or new blood vessels appear dark on the background of a fluorescent tumor, allowing for tumor-associated vascular visualization and quantification. The utility of fluorescence visualization has been reported by Udagawa et al., using osteosarcoma (MG-63 and SAOS-2) and gastric (ST-2) dormancy models.[33] More recently, this labeling technique was used to determine the minimum number of human tumor cells necessary to form a non-angiogenic microscopic tumor in mice (Naumov et al., unpublished). Fluorescence-labeled human tumor cells can be easily observed non-invasively in superficial organs (such as the skin and mammary fat pad). However, if tumor growth occurs in internal organs, such observations are difficult and in most cases impossible to detect. The only way to visualize internal GFP-labeled tumors (especially at the microscopic size) is to kill and dissect the animal. The tissue depth limitation of this technique becomes even more evident during visualization of microscopic brain tumors. In the brain, excitation/emission of fluorescently labeled tumor cells is not only limited by tissue depth, but also by light penetration through the skull. Other tumor cell visualization techniques can be employed to circumvent this limitation of fluorescence labeling.

LUCIFERASE LABELING OF TUMOR CELLS

Internal organ and brain tumors can be reliably detected in vivo using a luciferase reporter gene. This imaging modality can be used for non-invasive and sequential detection of human microscopic tumors in mice. This technique has been used for the detection of dormant human liposarcoma tumors in the renal fat pad of mice[34] and for monitoring the growth of human glioblastoma tumors stereotactically inoculated in the brain of mice (Naumov et al., unpublished work). The luciferase reporter allows for the reliable detection of a signal from tumors that are less than 1 mm in diameter, as verified by histology. The sensitivity of this method makes it useful for the detection of microscopic tumors in organs that are otherwise challenging for real-time imaging, such as the brain. This technique has been used to follow the growth of human glioblastomas implanted in the brain of SCID mice, during a 2–3 month dormancy period as well as after these tumors have switched to the angiogenic phenotype. There are limitations, however. Although luciferase signal intensity is directly correlated with the size of a tumor, this imaging modality does not provide a clear tumor boundary or a definite anatomical location of the tumor. Small animal MRI imaging provides clear definition of the geometry of a microscopic tumor, and can be used in combination with luciferase imaging (Naumov et al., unpublished).

The enzymatic activity of luciferase is rapid and transient, and can be detected only following intravenous injection of the substrate (Luciferine). Only viable and metabolically active tumor cells (expressing the luciferase construct gene) can be detected. Therefore, this method allows for real-time monitoring of tumor cell presence and viability during the dormancy period as well as throughout the angiogenic switch. The presence of a luciferase signal during the dormancy period of microscopic human tumors confirms the previous conclusion (based on histology) that dormancy does not result from tumor cell cycle arrest or eradication. In all cases, an increase in luminescence intensity was followed by the growth of tumors. Therefore, this imaging modality is a sensitive method for the detection of microscopic human tumors during the dormancy phase and throughout the switch to the angiogenic phenotype. Although this imaging modality has great potential for aiding our understanding of the biology of the angiogenic switch, it cannot be employed clinically for the detection of microscopic tumors.

Other imaging methods have been recently reported for non-invasive longitudinal detection of small micrometastases and single cancer cells in a mouse brain. Graham et al.[35] demonstrated that three-dimensional high-frequency ultrasound can be used to quantitatively monitor the growth of liver metastases as small at 0.5 mm in diameter. Heyn et al.[36] have demonstrated that single cancer cells can be detected in a mouse brain using magnetic resonance imaging (MRI). Individual cancer cells trapped within the brain microcirculation were detected using MRI and validated using high-resolution confocal microscopy. These recent advances in imaging sensitivity enable non-invasive, real-time, longitudinal observations of single cancer cell trafficking and non-angiogenic tumor growth.

STRATEGIES FOR SEPARATION OF ANGIOGENIC AND NON-ANGIOGENIC TUMOR CELLS

We have previously shown that human cancers are heterogeneous, containing both non-angiogenic and angiogenic tumor cell populations[28] (Fig. 3). At least two different approaches can be utilized to separate these two tumor cell populations in vitro or in vivo. Previous studies used established human tumor cell lines (obtained from ATCC) which were described by the literature as "non-tumorigenic" or as having a "no take" phenotype. Achilles et al., investigated whether heterogeneity of angiogenic activity could be responsible for the well-known "no take" phenomenon of human tumors transplanted into immunodeficient mice. These studies demonstrated that mice inoculated with human liposarcoma cells developed three kinds of tumors: (1) highly angiogenic tumors, (2) weakly angiogenic or slow growing tumors, and (3) non-angiogenic tumors. Because non-angiogenic tumors were neither grossly visible nor palpable, they have previously been called "no take" or "non-tumorigenic". Moreover, the spontaneous switch of dormant tumors to the angiogenic phenotype would have been missed if the length of the study was less than a year. Therefore, some of the existing human tumor cells lines have been wrongfully termed "non-tumorigenic" when indeed they can form tumors, but only after existing for months as microscopic tumors. However, after testing more than 15 of the "non-tumorigenic" human tumor cell lines available from ATCC, we identified half of them as truly dormant (i.e., remained at a microscopic size for long periods of time and then spontaneously switched to the angiogenic phenotype). Approximately half of the human tumor cell lines tested did not form microscopic tumors and the tumor cells apparently died sometime after inoculation in immunodeficient mice. Therefore, approximately half of the "no take" human tumor cell lines available through ATCC are truly "non-tumorigenic", and half undergo a dormancy period before they spontaneously switch to the angiogenic phenotype.

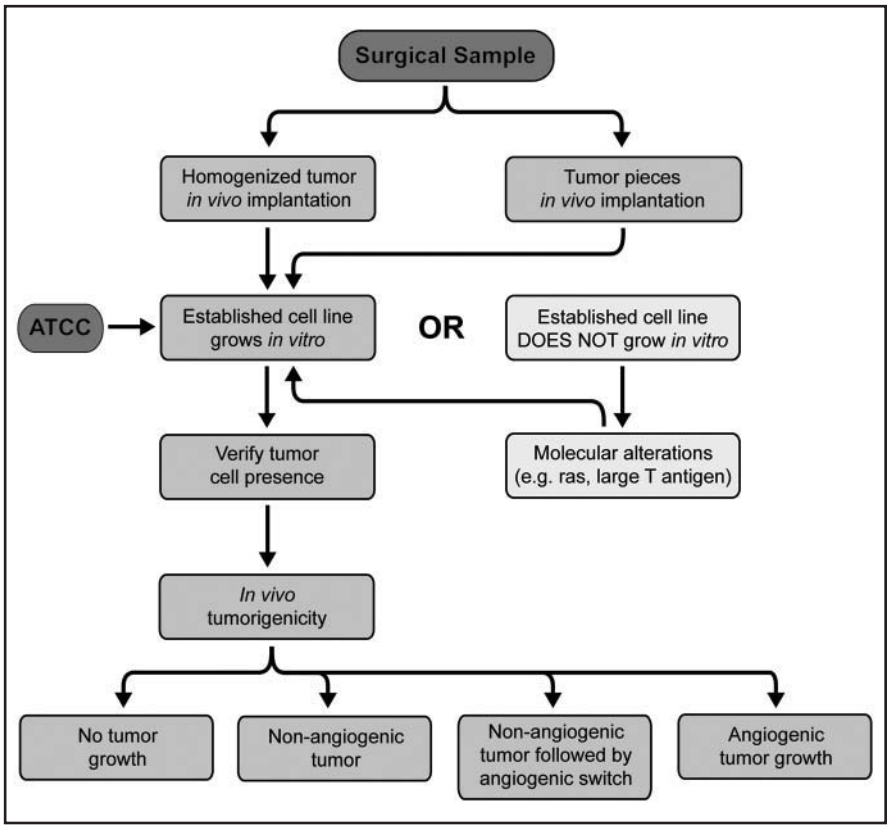

Figure 4. Strategies for isolation of non-angiogenic and angiogenic human tumor cell populations.

In this human tumor dormancy model, Achilles et al., developed single cell clones from the original human liposarcoma cell line (SW-872). These clones were than expanded in vitro and the resulting cell populations were then tested for tumor cell proliferation in vitro. The single cell clones with the highest and lowest proliferation rates were selected and tested in vivo for their angiogenic potential. Achilles et al.[28] found that the single cell-derived clone with the highest proliferation rate was very angiogenic in vivo and formed large tumors within a month of tumor cell inoculation. In contrast, the clone with the lowest in vitro proliferation remained microscopic in size for approximately 130 days. After this dormancy period, spontaneous tumors formed and became angiogenic. These initial studies raised the following questions: (1) is tumor cell proliferation associated with tumor angiogenesis, and (2) can the angiogenic and non-angiogenic phenotypes observed in vivo using the single cell clones be reproduced with heterogeneous populations of human tumor cells?

Subsequent studies by Udagawa et al., addressed these questions by transfecting dormant human tumor cell lines with either $VEGF_{165}$ or activated *c-Ha-ras*.[33] Stable transfection of these cell lines induced loss of dormancy and provided supporting evidence that escape from the angiogenic phenotype is controlled, in part, by a switch to the angiogenic phenotype. In this animal model, the angiogenic tumor cells were produced by genetic manipulation of otherwise dormant human tumor cells.

More recently, Naumov et al., isolated non-angiogenic and angiogenic human tumor cell populations that did not differ in proliferation rates, were derived from heterogeneous tumor cell populations (rather than a single cell clone), and were not molecularly or genetically modified.[29] Human tumor cell lines were selected from ATCC based on their "non-tumorigenic in immunocompromised mice" phenotype. These were expanded in vitro, and their in vivo tumorigenic potential was assessed through the duration of the life of SCID mice. Spontaneous tumors began to form at the site of inoculation after a dormancy period which varied in length (from 3 months to more than a year) depending on cancer type (Fig. 3 and Table 1). Stable cell lines were established from representative spontaneous tumors. When reinoculated into animals, these cell lines formed large (more than 1 cm in diameter) angiogenic tumors within a month in 100% of the animals. This result was confirmed in all cancer types tested to date (breast cancer, glioblastoma, osteosarcoma and liposarcoma). Using this approach, angiogenic and non-angiogenic tumor cell populations were isolated from various human cancer types. Most importantly, the non-angiogenic and angiogenic tumor cell populations did not differ significantly in proliferation rates[29] or cytogenetically (unpublished results).

In the future, non-angiogenic and angiogenic tumor cell populations from human cancers might be separable in vitro using a panel of tumor cell features. For example, a subpopulation of tumor cells that overexpress thrombospondin-1, but secrete low levels of VEGF and bFGF would be expected to exhibit the dormant phenotype in vivo. The development of in vitro assays which can segregate the non-angiogenic and angiogenic tumor cell populations is currently under investigation.

In summary, in vivo separation of non-angiogenic and angiogenic human tumor cell populations can be achieved by inoculating a large number of tumor cells (5 x 10^6 cells) into immunocompromised mice. The origin of these human tumor cells can be either a surgical specimen or an established cell line from ATCC (Fig. 4). If a surgical specimen is used, part of the tissue can be homogenized and the other portion can be cut into tumor tissue cubes of known size (e.g., 1–2 mm^3) and implanted into the subcutaneous space in mice. Tumor tissue implantation is preferred because the original stromal architecture of the tumor is preserved as much as possible without the mechanical or enzymatic damage introduced by the homogenization process. When tumors are well established, a stable cell line can be created under tissue culture conditions. In some instances tumor cells that had grown in vivo would not proliferate in vitro but remained sub0confluent for months. Genetic manipulation of these cells is an option, but is not advisable as it is not known how this step in the process would alter their in vivo behavior. It is imperative that the established cell line is confirmed to consist of the desired tumor cells, rather than stromal contaminants. A panel of antibodies specific to the cancer type can be used to identify the proportion of tumor cells in culture using flow cytometry, fixed cells grown on cover slips, or histology on cell pellets. Once the identity of the established cell line is established, the angiogenic potential of this tumor cell population can be assessed in vivo.

In order to palpate and to compare the in vivo growth of different cancer types, tumor cells should be inoculated subcutaneously in a consistent manner (i.e., same anatomical location, same volume of tumor cell suspension, same gauge of needle, under the same environmental conditions, i.e., room temperature). Four outcomes are possible from this assay: (1) no tumors are evident either by palpation from the outside of the skin or by microscopic examination of the inner side of the skin at the site of tumor cell inoculation, (2) no angiogenic tumors develop for the duration of the animal's life, but there are microscopic tumors on the inner side of the skin (seen only by microscope 10 X magnification), (3) microscopic non-angiogenic tumors are present for months followed by spontaneous switch to the angiogenic phenotype, or (4) angiogenic tumor grows within a month of tumor cell inoculation. If a cell line confirms to outcomes 2 or 3, it can be used for the development of a human tumor dormancy animal model (i.e., inoculation of tumor cells results in the development of microscopic non-angiogenic tumor that never switches to the angiogenic phenotype or does so after prolonged period of dormancy). If no tumor cells are observed microscopically and no tumor ever forms at the site of inoculation, then the cell line is truly "non-tumorigenic".

When characterizing a new human tumor cell line for the first time, it may be problematic to label the tumor cells with fluorescence markers or luciferase, because this could potentially affect the in vivo behavior of the cells. Palpation and histological assessment of the inoculation area are the preferred methods for detection of tumor growth. Once the true angiogenic potential of a cell line is established and characterized, these cells can be labeled with green fluorescence protein, luciferase, or other methods for orthotopic growth assessment may be used.

ANGIOGENIC SWITCH-RELATED BIOMARKERS FOR DETECTION OF DORMANT TUMORS

Even with recent advances in clinical detection of human cancer, a tumor that is microscopic in size (~1 mm in diameter) remains undetectable. A panel of angiogenic switch-related biomarkers has been developed using the human tumor animal models. These biomarkers include circulating endothelial progenitor cells and platelets in the blood, as well as matrix metalloproteinases (MMPs) in the urine. The detection of a single microscopic human tumor in existing animal models can be achieved using each one of these biomarkers alone or as a panel.[37-39]

We compared the in vivo ability of angiogenic and non-angiogenic breast tumors (MDA-MB-436 cells) to mobilize mature circulating endothelial cells (CECs) ($CD45^-$, Flk^+, $CD31^+$, $CD117^-$) and circulating endothelial progenitor cells (CEPs) ($CD45^-$, Flk^+, $CD31^+$, $CD117^+$).[37] The number of blood-borne CECs and CEPs was quantified using a flow cytometer. The percent of mature CECs in the blood of mice inoculated with angiogenic and non-angiogenic cells did not differ significantly. However, mice inoculated with non-angiogenic cells had ~4-fold decrease in CEPs when compared to control mice. Mice inoculated with angiogenic cells had comparable levels of CEPs to control mice. Previous reports[29] have shown that these non-angiogenic breast cancer cells (MDA-MB-436 cells) secrete at least 20-fold higher levels of thrombospondin-1 (Tsp-1) as compared to their angiogenic counterparts. Other studies have suggested that endogenous inhibitors of angiogenesis such as Tsp-1 and endostatin may inhibit the mobilization of CEPs.[40] These observations suggest that microscopic dormant (non-angiogenic) tumors may suppress the mobilization of CEPs from the bone marrow via Tsp-1.

Klement et al., recently reported that blood platelets can sequester both pro- and anti-angiogenic factors. Therefore, platelets could act as blood biomarker amplifiers by accumulating angiogenesis-based proteins.[39] Using a novel "platelet angiogenic proteome", as quantitatively assessed using SELDI-ToF technology (Ciphergen, Freemont, CA), the presence of microscopic human tumors in mice can be detected.[39] Using this technology, the accumulation and reduction in angiogenesis-related proteins sequestered in platelets can be quantitatively followed throughout the angiogenic switch. The identification of proteins that are associated with the angiogenic switch and that may be used as angiogenesis-based biomarkers is currently under investigation.

In summary, the dormancy animal models permit further clarification of the role of CEC/CEPs, platelets and MMPs as participants in the "angiogenic switch". Moreover, this angiogenesis-related biomarker panel may prove to be a useful diagnostic method for the presence of microscopic cancers at primary and metastatic sites long before detection by conventional methods. It may be feasible to develop a panel of angiogenesis-based biomarkers that can identify the presence of a microscopic human tumor, predict its switch to the angiogenic phenotype, and possibly guide antiangiogenic therapy. In the future it may be possible for a patient who is at risk for cancer recurrence to take an oral drug that can elevate endogenous anti-angiogenic proteins in platelets and delay, if not prevent the formation of recurrent tumors.

DORMANCY IN METASTASIS

Metastasis, the spread of cancer from a primary tumor to secondary organs, is the major cause of cancer related deaths. Although lethal, it has been shown that the metastatic process is highly inefficient, whereby only a few cancer cells that leave a primary tumor can successfully form a large tumor at a secondary site.[41-43] However, for a macrometastasis to become clinically relevant, all steps in the process must be completed successfully. Two steps have been identified to contribute to the inefficiency of the metastatic process due to two different types of tumor dormancy.

Previous studies by Holmgren et al.,[4,44] have identified preangiogenic micrometastases as a potential contributor to metastatic dormancy. These studies have shown that dormant mirometastases did not grow in size beyond 200 μm, but remained metabolically active. This size limitation was associated with a steady-state balance between rates of tumor cell proliferation and apoptosis, and no net growth of the metastases. Changes in the intrinsic properties of these "dormant" micrometastases, or their microenvironment at a later time, triggered metastatic growth associated with a disturbance of the proliferation/apoptosis balance. Progressive growth in such micrometastases was restricted due to the failure of the tumors to become vascularized.

Previous reports by Naumov et al., have identified another possible source of metastatic dormancy: viable solitary tumor cells that are neither proliferating nor undergoing apoptosis once in a metastatic organ.[45] These studies have shown that a large percentage (~50–80%) of breast cancer cells, distributed to mouse liver via the circulation, can remain in the tissue for extended periods of time (up to 77 days) as solitary non-proliferating dormant cells. This surprising phenomenon was observed for a population of breast cancer cells of both high and low metastatic ability. In the case of the highly metastatic cell line (D2A1 cells), lethal macrometastases grew from a very small subset of cells (~0.006%), with the majority (~80% cell loss) of injected cells undergoing apoptosis or being destroyed by leukocytes. However, a fraction (~20%) of the injected cells persisted as dormant non-proliferating cells.

In contrast, approximately 80% of poorly metastatic breast cancer cells remained as dormant solitary cells in the mouse liver. A subset of these cells could be recovered and grown under in vitro culture conditions 11 weeks after injection into mice. Moreover, these cells retained their ability to form primary tumors in the mammary fat pad. These solitary dormant tumor cells may be a potential source of an occasional non-angiogenic tumor and even more rare, but lethal, angiogenic metastasis.

Taken together, these studies have shown that metastasis is a dynamic process, where solitary dormant cancer cells, non-angiogenic micrometastases and angiogenic macrometastases can co-exist at each step of the process. While non-angiogenic micrometastases might be vulnerable to anti-angiogenic and cytotoxic chemotherapeutic agents (administered in a metronomic, low dose regimen as described by Browder et al.[46] and Kerbel et al.[47,48]), solitary non-proliferating dormant cells might remain unaffected.

Naumov et al., has shown that non-proliferating solitary dormant breast cancer cells remained unaffected by doxorubicin treatment.[49] However, the same treatment successfully inhibited actively growing macrometastases in the same mice. Therefore, doxorubicin chemotherapy that successfully reduced the metastatic burden failed to affect the number of solitary non-proliferating dormant cells. These findings have important clinical implications for patients undergoing adjuvant chemotherapy. It is possible that dormant tumor cells can remain unaffected by standard chemotherapy and may retain the potential to initiate growth at a later date. Both solitary non-proliferating cancer cells and non-angiogenic metastases can remain dormant and occult for months or years, leading to uncertainty in the prognosis for patients already treated for primary cancer.

CANCER WITHOUT DISEASE

Early primary and metastatic tumor detection and treatment is thought to be a determinant of cancer survival. If the majority of humans harbor microscopic cancer and the switch of these tumors to the angiogenic phenotype is so infrequent, then this "Achilles' heel" of cancer progression could be exploited and the growth of many harmless early lesions to the few lethal tumors, currently detectable and treatable, could be prevented. This goal may be achieved by elevating endogenous anti-angiogenic proteins with the administration of low dose, non-toxic compounds.[23]

An understanding of the mechanisms underlying the angiogenic switch and the use of angiogenic switch-related biomarkers to detect microscopic human tumors, although not necessarily their anatomical location, suggest the possibility of intervening early in cancer progression and preventing the disease of cancer.

References

1. Folkman J, Heymach J and Kalluri R. Tumor Angiogenesis. Edited by Kufe DW, Bast RC Jr., Hite WH, Hong WK, Pollack RE, Weichselbaum RR, Holland JF, Frei E III. Hamilton, Ontario, B.C. Decker, 2006.
2. Folkman J. Tumor angiogenesis: therapeutic implications. N Engl J Med 1971; 285:1182-6.
3. Folkman J. What is the evidence that tumors are angiogenesis dependent? J Natl Cancer Inst 1990; 82:4-6.
4. Holmgren L, O'Reilly MS, Folkman J. Dormancy of micrometastases: balanced proliferation and apoptosis in the presence of angiogenesis suppression. Nat Med 1995; 1:149-53.
5. Wesseling P, Ruiter DJ, Burger PC. Angiogenesis in brain tumors; pathobiological and clinical aspects. J Neurooncol 1997; 32:253-65.
6. Pezzella F, Pastorino U, Tagliabue E, Andreola S, Sozzi G, Gasparini G, Menard S, Gatter KC, Harris AL, Fox S, Buyse M, Pilotti S, Pierotti M, Rilke F. Non-small-cell lung carcinoma tumor growth without morphological evidence of neo-angiogenesis. Am J Pathol 1997; 151:1417-23.
7. Folkman J, Watson K, Ingber D, Hanahan D. Induction of angiogenesis during the transition from hyperplasia to neoplasia. Nature 1989; 339:58-61.
8. Torres Filho IP, Leunig M, Yuan F, Intaglietta M, Jain RK. Non-invasive measurement of microvascular and interstitial oxygen profiles in a human tumor in SCID mice. Proc Natl Acad Sci USA 1994; 91:2081-5.
9. North S, Moenner M, Bikfalvi A. Recent developments in the regulation of the angiogenic switch by cellular stress factors in tumors. Cancer Lett 2005; 218:1-14.
10. Demicheli R, Terenziani M, Valagussa P, Moliterni A, Zambetti M, Bonadonna G. Local recurrences following mastectomy: support for the concept of tumor dormancy. J Natl Cancer Inst 1994; 86:45-8.
11. Uhr JW, Scheuermann RH, Street NE, Vitetta ES. Cancer dormancy: opportunities for new therapeutic approaches. Nat Med 1997; 3:505-9.
12. Black WC, Welch HG. Advances in diagnostic imaging and overestimations of disease prevalence and the benefits of therapy. N Engl J Med 1993; 328:1237-43.
13. Montie JE, Wood DP, Jr., Pontes JE, Boyett JM, Levin HS. Adenocarcinoma of the prostate in cystoprostatectomy specimens removed for bladder cancer. Cancer 1989; 63:381-5.
14. Feldman AR, Kessler L, Myers MH, Naughton MD. The prevalence of cancer. Estimates based on the Connecticut Tumor Registry. N Engl J Med 1986; 315:1394-7.
15. 1975-2002. NCISCSR: http://seer.cancer.gov/csr/1975_2002/results_merged/sect_23_prostate.pdf. 2002.
16. Rastinejad F, Polverini PJ, Bouck NP. Regulation of the activity of a new inhibitor of angiogenesis by a cancer suppressor gene. Cell 1989; 56:345-55.
17. Saudemont A, Jouy N, Hetuin D, Quesnel B. NK cells that are activated by CXCL10 can kill dormant tumor cells that resist CTL-mediated lysis and can express B7-H1 that stimulates T cells. Blood 2005; 105:2428-35.
18. Dameron KM, Volpert OV, Tainsky MA, Bouck N. Control of angiogenesis in fibroblasts by p53 regulation of thrombospondin-1. Science 1994; 265:1582-4.
19. Van Meir EG, Polverini PJ, Chazin VR, Su Huang HJ, de Tribolet N, Cavenee WK. Release of an inhibitor of angiogenesis upon induction of wild type p53 expression in glioblastoma cells. Nat Genet 1994; 8:171-6.

20. O'Reilly MS, Holmgren L, Shing Y, Chen C, Rosenthal RA, Cao Y, Moses M, Lane WS, Sage EH, Folkman J. Angiostatin: a circulating endothelial cell inhibitor that suppresses angiogenesis and tumor growth. Cold Spring Harb Symp Quant Biol 1994; 59:471-82.
21. Saudemont A, Quesnel B. In a model of tumor dormancy, long-term persistent leukemic cells have increased B7-H1 and B7.1 expression and resist CTL-mediated lysis. Blood 2004; 104:2124-33.
22. Stewart TH. Immune mechanisms and tumor dormancy. Medicina (B Aires) 1996; 56(Suppl 1):74-82.
23. Folkman J, Kalluri R. Cancer without disease. Nature 2004; 427:787.
24. Hanahan D, Folkman J. Patterns and emerging mechanisms of the angiogenic switch during tumorigenesis. Cell 1996; 86:353-64.
25. Gimbrone MA, Jr., Leapman SB, Cotran RS, Folkman J. Tumor dormancy in vivo by prevention of neovascularization. J Exp Med 1972; 136:261-76.
26. Hanahan D, Folkman J. Patterns and emerging mechanisms of the angiogenic switch during tumorigenesis. Cell 1996; 86:353-64.
27. Hanahan D, Christofori G, Naik P, Arbeit J. Transgenic mouse models of tumour angiogenesis: the angiogenic switch, its molecular controls, and prospects for preclinical therapeutic models. Eur J Cancer 1996; 32A:2386-93.
28. Achilles EG, Fernandez A, Allred EN, Kisker O, Udagawa T, Beecken WD, Flynn E, Folkman J. Heterogeneity of angiogenic activity in a human liposarcoma: a proposed mechanism for "no take" of human tumors in mice. J Natl Cancer Inst 2001; 93:1075-81.
29. Naumov GN, Bender E, Zurakowski D, Kang SY, Sampson D, Flynn E, Watnick RS, Straume O, Akslen LA, Folkman J, Almog N. A model of human tumor dormancy: an angiogenic switch from the nonangiogenic phenotype. J Natl Cancer Inst 2006; 98:316-25.
30. Aguirre Ghiso JA, Kovalski K, Ossowski L. Tumor dormancy induced by downregulation of urokinase receptor in human carcinoma involves integrin and MAPK signaling. J Cell Biol 1999; 147:89-104.
31. Aguirre-Ghiso JA, Liu D, Mignatti A, Kovalski K, Ossowski L. Urokinase receptor and fibronectin regulate the ERK(MAPK) to p38(MAPK) activity ratios that determine carcinoma cell proliferation or dormancy in vivo. Mol Biol Cell 2001; 12:863-79.
32. Aguirre-Ghiso JA, Estrada Y, Liu D, Ossowski L. ERK(MAPK) activity as a determinant of tumor growth and dormancy: regulation by p38(SAPK). Cancer Res 2003; 63:1684-95.
33. Udagawa T, Fernandez A, Achilles EG, Folkman J, D'Amato RJ. Persistence of microscopic human cancers in mice: alterations in the angiogenic balance accompanies loss of tumor dormancy. Faseb J 2002; 16:1361-70.
34. Almog N, Henke V, Flores L, Hlatky L, Kung AL, Wright RD, Berger R, Hutchinson L, Naumov GN, Bender E, Akslen LA, Achilles EG, Folkman J. Prolonged dormancy of human liposarcoma is associated with impaired tumor angiogenesis. Faseb J 2006; 20:947-9.
35. Graham KC, Wirtzfeld LA, MacKenzie LT, Postenka CO, Groom AC, MacDonald IC, Fenster A, Lacefield JC, Chambers AF. Three-dimensional high-frequency ultrasound imaging for longitudinal evaluation of liver metastases in preclinical models. Cancer Res 2005; 65:5231-7.
36. Heyn C, Ronald JA, Mackenzie LT, MacDonald IC, Chambers AF, Rutt BK, Foster PJ. In vivo magnetic resonance imaging of single cells in mouse brain with optical validation. Magn Reson Med 2006; 55:23-9.
37. Naumov GN, Beaudry P, Bender ER, Zurakowski D, Watnick R, Almog N, Heymach J, Folkman J. Clinical and Experimental Metastasis. Edited by Springer, 2004; p. 636.
38. Jay Harper GNN, Alexis Exarhopoulos, Elise Bender, Gwendolyn Louis, Judah Folkman, and Marsha A. Moses. Predicting the switch to the angiogenic phenotype in a human tumor model. 2006; p. 837.
39. Klement G, Kikuchi L, Kieran M, Almog N, Yip T, Folkman J. Early tumor detection using platelet uptake of angiogenesis regulators. 2004; p. 239a.
40. Schuch G, Heymach JV, Nomi M, Machluf M, Force J, Atala A, Eder JP, Jr., Folkman J, Soker S. Endostatin inhibits the vascular endothelial growth factor-induced mobilization of endothelial progenitor cells. Cancer Res 2003; 63:8345-50.
41. Chambers AF, Groom AC, MacDonald IC. Dissemination and growth of cancer cells in metastatic sites. Nat Rev Cancer 2002; 2:563-72.
42. Chambers AF, Naumov GN, Vantyghem SA, Tuck AB. Molecular biology of breast cancer metastasis. Clinical implications of experimental studies on metastatic inefficiency. Breast Cancer Res 2000; 2:400-7.
43. Weiss L. Metastatic inefficiency. Adv Cancer Res 1990; 54:159-211.
44. Murray C. Tumor dormancy: not so sleepy after all. Nat Med 1995; 1:117-8.
45. Naumov GN, MacDonald IC, Weinmeister PM, Kerkvliet N, Nadkarni KV, Wilson SM, Morris VL, Groom AC, Chambers AF. Persistence of solitary mammary carcinoma cells in a secondary site: a possible contributor to dormancy. Cancer Res 2002; 62:2162-8.
46. Browder T, Butterfield CE, Kraling BM, Shi B, Marshall B, O'Reilly MS, Folkman J. Antiangiogenic scheduling of chemotherapy improves efficacy against experimental drug-resistant cancer. Cancer Res 2000; 60:1878-86.
47. Kerbel RS, Viloria-Petit A, Klement G, Rak J. 'Accidental' anti-angiogenic drugs. anti-oncogene directed signal transduction inhibitors and conventional chemotherapeutic agents as examples. Eur J Cancer 2000; 36:1248-57.
48. Klement G, Baruchel S, Rak J, Man S, Clark K, Hicklin DJ, Bohlen P, Kerbel RS. Continuous low-dose therapy with vinblastine and VEGF receptor-2 antibody induces sustained tumor regression without overt toxicity. J Clin Invest 2000; 105:R15-24.
49. Naumov GN, Townson JL, MacDonald IC, Wilson SM, Bramwell VH, Groom AC, Chambers AF. Ineffectiveness of doxorubicin treatment on solitary dormant mammary carcinoma cells or late-developing metastases. Breast Cancer Res Treat 2003; 82:199-206.

OPINION

Angiogenesis: an organizing principle for drug discovery?

Judah Folkman

Abstract | Angiogenesis — the process of new blood-vessel growth — has an essential role in development, reproduction and repair. However, pathological angiogenesis occurs not only in tumour formation, but also in a range of non-neoplastic diseases that could be classed together as 'angiogenesis-dependent diseases'. By viewing the process of angiogenesis as an 'organizing principle' in biology, intriguing insights into the molecular mechanisms of seemingly unrelated phenomena might be gained. This has important consequences for the clinical use of angiogenesis inhibitors and for drug discovery, not only for optimizing the treatment of cancer, but possibly also for developing therapeutic approaches for various diseases that are otherwise unrelated to each other.

The term angiogenesis is generally applied to the growth of microvessel sprouts the size of capillary blood vessels, a process that is orchestrated by a range of angiogenic factors and inhibitors (FIG. 1). Although proliferating endothelial cells undergoing DNA synthesis are a common hallmark of angiogenic microvascular sprouts, extensive sprouts can grow for periods of time, mainly by the migration of endothelial cells[1]. Physiological angiogenesis is distinct from arteriogenesis and lymphangiogenesis and occurs in reproduction, development and wound repair. It is usually focal, such as in blood coagulation in a wound, and self-limited in time, taking days (ovulation), weeks (wound healing) or months (placentation). By contrast, pathological angiogenesis can persist for years. Pathological angiogenesis is necessary for tumours and their metastases to grow beyond a microscopic size and it can give rise to bleeding, vascular leakage and tissue destruction. These consequences of pathological angiogenesis can be responsible, directly or indirectly, for the symptoms, incapacitation or death associated with a broad range of 'angiogenesis-dependent diseases'[2]. Examples of such diseases include cancer, autoimmune diseases, age-related macular degeneration and atherosclerosis (TABLE 1).

The concept of angiogenesis-dependent diseases originated in 1972 with the recognition that certain non-neoplastic diseases, such as the chronic inflammatory disease psoriasis, depend on chronic neovascularization to provide a conduit for the continual delivery of inflammatory cells to the inflammatory site[3–5]. Subsequently, other non-neoplastic diseases were recognized to be in part angiogenesis dependent, for example, infantile haemangiomas[6], peptic ulcers[7], ocular neovascularization[8], rheumatoid arthritis[9] and atherosclerosis[3,10,11]. This led to a more general understanding that the process of angiogenesis itself could be considered as an 'organizing principle'. Organizing principles are common in the physical sciences, and are now starting to be recognized in biology — other examples might be inflammation or apoptosis, which are also aspects of many otherwise unrelated diseases. The heuristic value of such a principle is that it permits connections between seemingly unrelated phenomena. For example, the discovery of a molecular mechanism for one phenomenon might be more rapidly demonstrated for a second phenomenon if one understands *a priori* that the two are connected. Furthermore, when the mechanisms underlying different diseases can be related in this way, the development of therapeutics for one disease could aid the development of therapeutics for others. Although it remains to be determined to what extent treating pathological angiogenesis in different angiogenesis-dependent diseases will be successful, the recent approval of ranibizumab (Lucentis; Genentech) — an antibody fragment based on the anti-angiogenic cancer drug bevacizumab (Avastin; Genentech) — for age-related macular degeneration suggests that such strategies merit investigation.

Here, I provide an overview of the current state of drug development of angiogenesis inhibitors, as well as certain drugs that have varying degrees of anti-angiogenic activity in addition to their other functions, and highlight examples of anti-angiogenic strategies in unrelated diseases. Furthermore, I discuss burgeoning new directions in angiogenic research, the optimization of anti-angiogenic strategies and how viewing angiogenesis as an organizing principle might uncover fruitful connections for future drug discovery.

A brief history of angiogenesis inhibitors

The attempt to discover angiogenesis inhibitors became possible after my group and others had developed bioassays for angiogenesis during the 1970s. These included the long-term culture of vascular endothelial cells[12], the development of the chick-embryo chorioallantoic-membrane bioassay[13], the development of sustained-release polymers[14] and the implantation of these polymers as pellets in the rabbit[15] and murine[16] cornea to quantify the angiogenic activity of tumour-derived proteins.

The first angiogenesis inhibitors were reported in the 1980s from the Folkman laboratory, during a study that continued over 25 years[17,18] (TIMELINE). No angiogenesis inhibitors existed before 1980, and few scientists thought at that time that such molecules would ever be found. However, the effort to isolate and purify them was driven by preliminary data that led to the 1971 hypothesis that tumour growth is dependent on angiogenesis[19]. This effort was also informed by preliminary data that the removal of an angiogenic sustained-release pellet from the rabbit cornea led to a rapid regression (weeks) of neovascularization that was induced by the pellet[20].

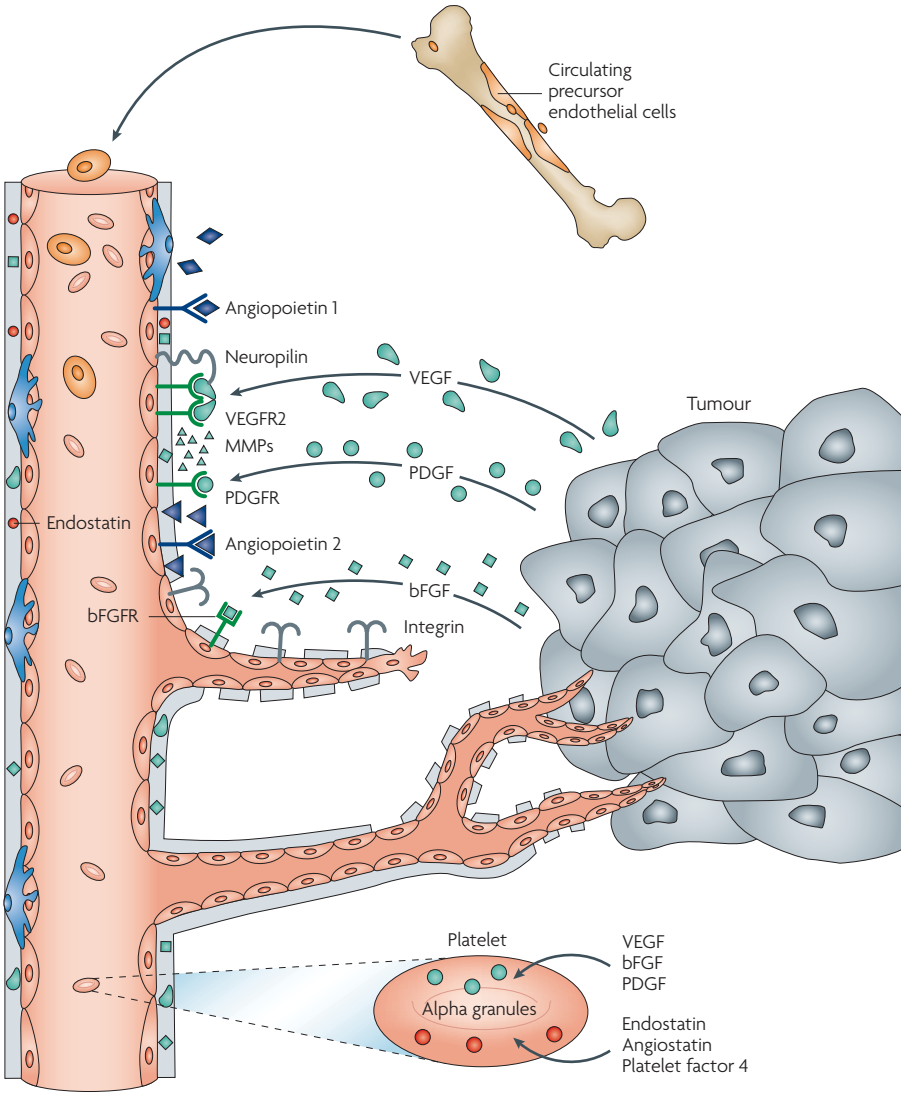

Figure 1 | **Key steps in tumour angiogenesis.** Angiopoietin 1 (ANGPT1), expressed by many cells, binds to the endothelial TIE2 (also known as TEK) receptor and helps maintain a normalized state in blood vessels. Vascular endothelial growth factor (VEGF) is secreted by tumour cells and binds to its receptor (VEGFR2) and to neuropilin on endothelial cells. It is the most common of at least six other pro-angiogenic proteins from tumours. Matrix metalloproteinases (MMPs) are released from tumour cells, but also by VEGF-stimulated endothelial cells. MMPs mobilize pro-angiogenic proteins from stroma, but can also cleave endostatin from collagen 18 in the vessel wall and participate in the cleavage of angiostatin from circulating plasminogen. Tumour cells secrete angiopoietin 2 (ANGPT2), which competes with ANGPT1 for binding to the endothelial TIE2 receptor. ANGPT2 increases the degradation of vascular basement membrane and migration of endothelial cells, therefore facilitating sprout formation. Platelet-derived growth factor (PDGF), an angiogenic protein secreted by some tumours, can upregulate its own receptor (PDGFR) on endothelial cells. Basic fibroblast growth factor (bFGF; also known as FGF2) is secreted by other tumours. Integrins on endothelial cells carry signals in both directions. Integrins facilitate endothelial cell binding to extracellular membranes, a requirement for the cells to maintain viability and responsiveness to growth regulatory proteins. Endothelial cells are among the most anchorage-dependent cells. Certain pro-angiogenic proteins upregulate endothelial integrins and are thought to sustain endothelial cell viability during the intermittant detachments that are required to migrate towards a tumour and to simultaneously increase their sensitivity to growth regulators — both mitogenic (VEGF or bFGF) and anti-mitogenic (endostatin). New endothelial cells do not all originate from neighbouring vessels. A few arrive as precursor bone-marrow-derived endothelial cells. Endothelial growth factors are not all delivered to the local endothelium directly from tumour cells. Some angiogenic regulatory proteins (both pro- and anti-angiogenic) are scavenged by platelets, stored in alpha granules and seem to be released within the tumour vasculature. It was recently discovered that pro- and anti-angiogenic proteins are stored in different sets of alpha granules (depicted in green and red respectively)[63].

After the mid-1980s, we and others began to discover additional angiogenesis inhibitors[21–29] (TIMELINE). By the mid-1990s, new drugs with anti-angiogenic activity entered clinical trials. These drugs began to receive Food and Drug Administration (FDA) approval in the United States by 2003. Bevacizumab, which received FDA approval for colorectal cancer in 2004, was the first drug developed solely as an angiogenesis inhibitor[30]. However, certain non-endothelial cells (haematopoietic-derived cells that colonize tumour stroma and some cancer cells, such as those in pancreatic cancer) can also express receptors for vascular endothelial growth factor (VEGF; also known as VEGFA), raising the possibility that this drug might also have direct antitumour effects[31,32]. At the time of writing this article, 10 new drugs — in which anti-angiogenic activity is considered to be central to their therapeutic effects — have been approved by the FDA in the United States, and by equivalent agencies in 30 other countries, for the treatment of cancer and age-related macular degeneration (TABLE 2). At least 43 other drugs that have varying degrees of anti-angiogenic activity are currently in clinical trials in the United States for different types of cancer, ten of which are in Phase III (TABLE 3). Other FDA-approved drugs revealed anti-angiogenic activity in addition to anticancer activity directed against tumour cells. For example, bortezomib (Velcade; Millennium Pharmaceuticals), approved as a proteasome inhibitor for the treatment of multiple myeloma, was subsequently demonstrated to also have potent anti-angiogenic activity[33].

As the treatment range of angiogenesis inhibitors covers not only many types of cancer, but also unrelated diseases such as age-related macular degeneration and possibly others, angiogenesis inhibitors, or drugs that have varying degrees of anti-angiogenic activity, might be defined as a class of drugs that specifically target an organizing principle in biomedicine.

Angiogenesis as an organizing principle

Clinical advantages to understanding angiogenesis as an organizing principle. There are important clinical advantages to viewing angiogenesis as an organizing principle. For example, if a clinician recognizes that a patient's disease might be partly angiogenesis-dependent, it is conceivable that an angiogenesis inhibitor approved for one type of tumour could be used for a different type of tumour, or even used off-label for a different disease.

Table 1 | **Angiogenesis-dependent diseases**

Disease	Symptoms
Diabetic retinopathy	Loss of vision
Rheumatoid arthritis[2]	Pain and immobility from destroyed cartilage
Atherosclerotic plaques[3]	Chest pain, dyspnoea
Endometriosis[4,5]	Abdominal pain from intraperitoneal bleeding
Crohn's disease[6]	Intestinal bleeding
Psoriasis[7]	Persistent severe itching
Uterine fibroids	Vaginal bleeding, abdominal pain
Benign prostatic hypertrophy	Urinary retention
Cancer	Bleeding, thrombosis, anaemia, abdominal ascites, bone pain, seizures from cerebral oedema around a tumour and others

An example of the former is the use of bevacizumab in colorectal cancer and also in non-small-cell lung cancer, and an example of off-label use is its use for age-related macular degeneration. Oncologists might also benefit from knowing that certain anticancer drugs (for example, cyclophosphamide) that were originally developed to target cancer cells also have anti-angiogenic activity.

A connection between colorectal cancer and macular degeneration. Bevacizumab is an antibody that neutralizes VEGF and was approved by the FDA for colorectal cancer in 2004 (REFS 30,34). Ranibizumab is a fragment of bevacizumab. In randomized clinical trials, ranibizumab injected into the eye at monthly intervals showed dramatic success in patients with age-related macular degeneration. In patients who were legally blind, with an average visual acuity of ~20/300, approximately 40% recovered their sight and improved to a visual acuity of 20/40 (sufficient for some to drive a car). In ~90–95% of patients, the disease was arrested, and there was no further loss of sight. By contrast, patients who were treated with a placebo continually lost visual acuity over a 12-month period, as was expected[35–40] (FIG. 3a). Pegaptanib (Macugen; OSI Pharmaceuticals), an anti-VEGF aptamer, was the first anti-VEGF drug to be approved by the FDA (2004) for the treatment of age-related macular degeneration. More than 75,000 patients with age-related macular degeneration have been treated with pegaptanib since its approval, and in the past year more than 50,000 patients have been treated with either intravitreal ranibizumab or off-label bevacizumab.

This might be the first time that a relatively non-toxic anticancer drug has been injected into the eye to treat ocular neovascularization. It is rare to treat diseases as diverse as colorectal cancer and age-related macular degeneration with the same agent — with the exception that the target for each was known to be VEGF[41–44].

Discovery of dual roles for cancer drugs. The cancer drugs erlotinib (Tarceva; Genentech, OSI Pharmaceuticals, Roche), cetuximab (Erbitux; Bristol–Myers Squibb, Merck) and vandetanib were originally developed as inhibitors of the epidermal growth factor receptor (EGFR) tyrosine kinase. For this reason, they are also known as anti-oncoprotein signal-transduction inhibitors[45]. However, they were subsequently found to also inhibit tumour angiogenesis by blocking the VEGF receptor. Cetuximab, an anti-EGFR agent, produces an antitumour effect *in vivo* that is due to the direct blockade of the EGFR-dependent mitogenic pathway and in part to the inhibition of secretion of various pro-angiogenic proteins such as VEGF, basic fibroblast growth factor (bFGF; also known as FGF2) and transforming growth factor-α (TGFα)[46].

Timeline | **Discovery of angiogenesis inhibitors**

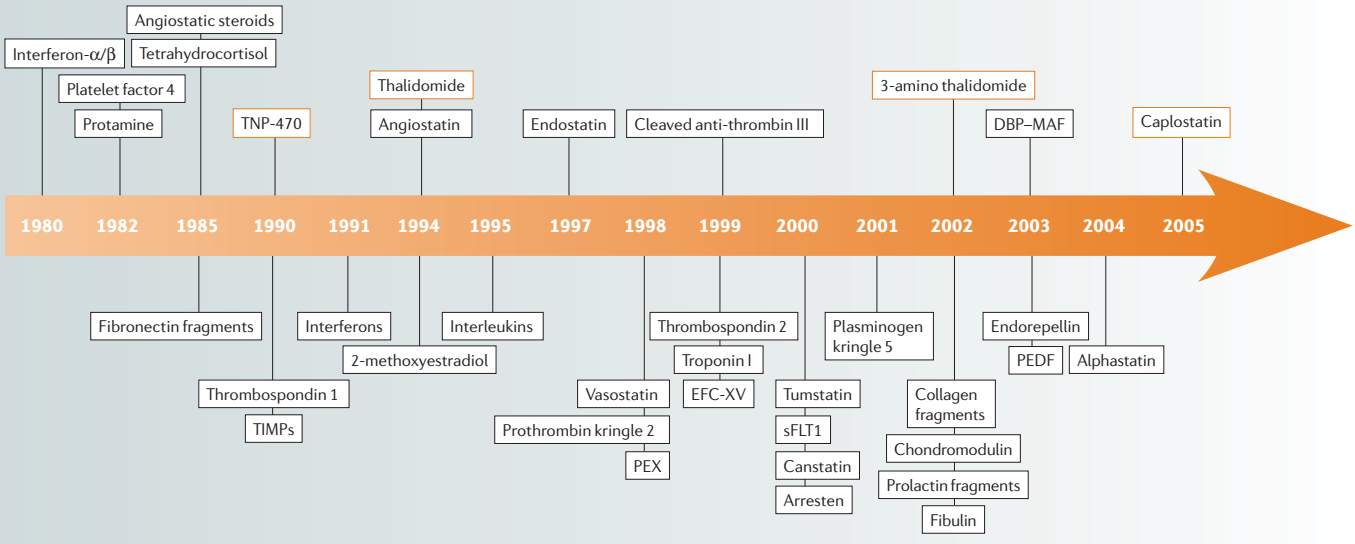

Synthetic angiogenesis inhibitors (orange keyline) and endogenous angiogenesis inhibitors that were identified in the Folkman laboratory are depicted above the timeline. Examples of additional endogenous angiogenesis inhibitors discovered in other laboratories are depicted below the timeline. The first drugs with anti-angiogenic activity were approved in 2003 (TABLE 2). DBP–MAF, vitamin-D-binding protein–macrophage-activating factor; EFC-XV, endostatin-like fragment from type XV collagen; PEDF, pigment epithelium-derived factor (also known as SERPINF1); PEX, haemopexin C domain autolytic fragment of matrix metalloproteinase 2; sFLT1, soluble fms-related tyrosine kinase 1; TIMP, tissue inhibitors of matrix metalloproteinase.

With this knowledge of their dual role[45], these drugs might be used more effectively by oncologists who could follow guidelines for dose-efficacy of angiogenesis inhibitors, which differ from conventional cytotoxic chemotherapies (see below).

Emerging research directions

The usefulness of recognizing an underlying organizing principle during angiogenesis research is illustrated by several fascinating insights into diverse biological processes. Some examples of these are new insights into platelet biology[47], metastases[22], endothelial control of tissue mass[48,49,72], the concept of oncogene dependence[50] and the surprising discovery that some of the ligand–receptor pairs that mediate axon-pathway finding also mediate

Table 2 | **Anti-angiogenic drugs approved for clinical use and phase of clinical trials for other indications**

Drug (Trade name; company)	Approved*	Phase III	Phase II	Phase I
Bortezomib (Velcade; Millennium Pharmaceuticals)	Multiple myeloma (2003)	NSCLC, multiple myeloma, NHL	Multiple myeloma, NHL, NSCLC, lymphoma, gliomas, melanoma, Waldenstrom's macroglobinaemia, prostate, head and neck, breast, liver, nasopharyngeal, gastric, pancreatic, colorectal, cervical/vaginal cancer, and others	Lymphoma, myelodysplasia, multiple myeloma, NHL, solid tumours, head and neck, cervical, colorectal, ovarian, prostate cancer, and others
Thalidomide (Thalomid; Celgene Corporation)	Multiple myeloma (2003‡)	Multiple myeloma, brain metastases, SCLC, NSCLC, prostate, kidney, ovarian, hepatocellular cancer	Soft tissue sarcoma, multiple myeloma, ALS, melanoma, neuroendocrine tumours, leukaemia, glioma, glioblastomas, paediatric neuroblastoma, NSCLC, NHL, paediatric solid tumours, myelofibrosis, myelodysplastic syndrome, AML, CLL, SCLC, Hodgkin's disease, paediatric brain stem, liver, colorectal, kidney, neuroendocrine, endometrial, thyroid, uterine, ovarian cancer, and others	Solid tumours, glioma
Bevacizumab (Avastin; Genentech)	Colorectal cancer (2004), lung cancer (2006)	NSCLC, GIST, diabetic retinopathy, vascular occlusions, retinopathy of prematurity, colorectal, breast, ovarian, peritoneal, pancreatic, prostate, kidney cancer	Glioblastoma, glioma, mesothelioma, NSCLC, AML, CLL, CML, lymphoma, angiosarcoma, melanoma, billary tumours, SCLC, Kaposi's sarcoma, sarcomas, NHL, carcinoid, oesophagogastric, gastric, renal cell, head and neck, rectal, hepatocellular, bladder, pancreatic, gall bladder, breast, neuroendocrine, cervical, ovarian, endometrial cancer, and others	NSCLC, pancreatic, solid tumours, head and neck tumours, VHL, retinal tumours
Erlotinib (Tarceva; Genentech, OSI Pharmaceuticals, Roche)	Lung cancer (2004)	NSCLC, colorectal, pancreatic, ovarian, head and neck, oral cancer	NSCLC, mesothelioma, glioblastoma, glioma, gall bladder, GIST, biliary tumours, bladder cancer prevention, malignant peripheral nerve sheath tumours, endometrial, colorectal, pancreatic, breast, renal cell, prostate, ovarian, head and neck, gastric/oesophageal, liver cancer, and others	NSCLC, glioblastoma, solid tumours, colorectal, pancreatic, head and neck cancer
Pegaptanib (Macugen; OSI Pharmaceuticals)	Age-related macular degeneration (2004)			
Endostatin (Endostar)	Lung cancer (2005§)			
Sorafenib (Nexavar; Onyx Pharmaceuticals)	Kidney cancer (2005)	Kidney, melanoma, hepatocellular cancer	Melanoma, glioblastoma, GIST, SCLC, thyroid, neuroendocrine, mesothelioma, soft tissue sarcoma, NSCLC, CLL, multiple myeloma, cholangiocarcinoma, NHL, kidney, colorectal, prostate, ovarian, peritoneal, pancreatic, breast, gastric, head and neck, uterine, gall bladder, bladder cancer, and others	Solid tumours, melanoma, glioblastoma, NHL, glioma, multiple myeloma, Kaposi's sarcoma, ALL, CML, MDS
Lenalidomide (Revlimid; Celgene Corporation)	Myelodysplastic syndrome (2005)	Multiple myeloma, myelodysplastic syndrome	NSCLC, NHL, multiple myeloma, CLL, myelofibrosis, myelodysplastic syndrome, glioblastoma, ocular melanoma, AML, mantle-cell lymphoma, Waldenstrom's macroglobinaemia, ovarian/peritoneal, thyroid, prostate cancer	Multiple myeloma, prostate cancer, melanoma, myelodysplastic syndrome, solid tumours, paediatric CNS tumours
Sunitinib (Sutent; Pfizer)	GIST, kidney cancer (2006)	Renal cell cancer, GIST	Melanoma, VHL/solid tumour, NSCLC, GIST, hepatocellular, colorectal, prostate, breast, renal cell, gastric, neuroendocrine cancer, and others	Melanoma, solid tumours, colorectal, breast cancer
Ranibizumab (Lucentis; Genentech)	Age-related macular degeneration (2006)			

*Year of first approval by the US Food and Drug Administration, unless stated otherwise. ‡Australia, approved by US Food and Drug Administration in 2006. §China State Food and Drug Administration. ALS, amyotrophic lateral sclerosis (or Lou Gehrig's disease); ALL, acute lymphoblastic leukaemia; AML, acute myeloid leukaemia; CLL, chronic lymphocytic leukaemia; CML, chronic myeloid leukaemia; CNS, central nervous system; GIST, gastrointestinal stromal tumour; MDS, myelodysplastic syndromes; NSCLC, non-small-cell lung cancer; NHL, non-Hodgkin's lymphoma; SCLC, small-cell lung cancer; VHL, von Hippel Lindau.

angiogenesis[51]. Furthermore, genetic variations in the expression of angiogenic proteins between different groups of individuals[52] provide further clues about the role of these angiogenesis-regulatory proteins in different diseases.

Endothelium and neurons share regulatory proteins. In 1998, Klagsbrun and colleagues reported that neuropilin, a cell-surface protein originally identified as a receptor for a signal that guides growing nerves, is also a receptor for VEGF[53,54]. This marked the beginning of a merger between the fields of neural guidance and angiogenesis. It was discovered that various ligand–receptor pairs that mediate axon-pathway finding also mediate angiogenesis[51].

Also, during development, sensory nerves determine the pattern of arterial differentiation in blood-vessel branching in the skin[55]. It was found that in the highly vascular dorsal root ganglia, neuronal VEGF interacts with endothelial cell VEGF receptor 2 (VEGFR2; also known as KDR)[56], which is necessary for endothelial survival. As the interactions of growth and motility proteins for neurons and endothelial cells are gradually uncovered, they might have important roles in drug discovery, for example, for drugs that can repair spinal-cord injuries, reverse Alzheimer's disease or broaden the efficacy of currently approved angiogenesis inhibitors.

New platelet biology. In a review in 2001, my colleagues and I assembled the reports that showed that most of the endogenous angiogenesis-regulatory proteins known at that time were contained in platelets or were on the platelet surface[57]. Several studies subsequently reported that circulating platelets in mice take up and sequester angiogenesis regulatory proteins, such as VEGF, bFGF and connective-tissue-activating peptide, when a microscopic human tumour is present in a mouse[58–60].

The angiogenisis-regulatory proteins are sequestered in alpha granules of platelets at a significantly higher concentration than in plasma. In fact, when radiolabelled VEGF is implanted subcutaneously in a Matrigel pellet in mice, platelet lysates take up virtually all of the radiolabelled VEGF and none is found in plasma[58]. Mouse platelets live for ~3–4 days. Nevertheless, platelets seem to recycle the angiogenesis-regulatory proteins they have scavenged, because the concentration of these proteins increases in the platelets over time (weeks to months), as long as the source of an angiogenesis-regulatory protein is present. Also, a single intravenous injection of thrombospondin 1 (THBS1) (2 μg) into *THBS1*-null mice continues to appear in platelet lysates for weeks (S. Ryeom, personal communication). Furthermore, it was recently reported that in patients with cancer who were receiving bevacizumab, the antibody was taken up by platelets where it was bound to VEGF[61].

This new platelet property, quantifiable by mass spectroscopy of platelet lysates, might permit the development of a biomarker for early detection of tumour recurrence. In tumour-bearing mice, the platelet-angiogenesis proteome detects microscopic tumours at a millimetre size, before they have become angiogenic, but when they are generating angiogenic proteins (VEGF, bFGF and platelet-derived growth factor; PDGF) and anti-angiogenic proteins (endostatin or THBS1)[58,62].

Italiano *et al*. have recently discovered that angiogenesis-regulatory proteins are in fact segregated among two sets of alpha granules in platelets: positive regulators of angiogenesis in one set of alpha granules and negative regulators in the other set[63]. This previously unknown function of platelets links them with the process of angiogenesis. A new opportunity lies ahead to determine whether and how platelets release pro-angiogenic proteins at a wound site and then later release anti-angiogenic proteins. Furthermore, the putative role of platelet release of angiogenesis-regulatory molecules in tumours remains to be elucidated. It might also be possible to develop drugs that selectively release anti-angiogenic proteins from platelets trapped in haemangiomas or in cancer. It is likely that in the future novel angiogenesis-regulatory molecules that could be developed into drugs will be discovered in platelets.

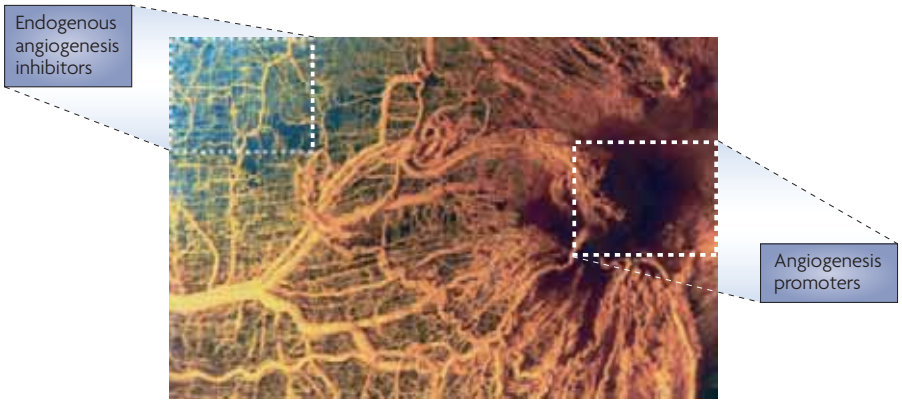

Figure 2 | **Angiogenesis in rat sarcoma.** In this micrograph, blood vessels grow towards a sarcoma (dark area at right) in rat muscle. This contrasts with the normal grid-like pattern of blood vessels that appears at the upper left. (Courtesy of L. Heuser and R. Ackland, University of Louisville, USA)[141].

A new mechanism for site specificity of metastasis. It is known that THBS1 is a potent angiogenesis inhibitor[64] that is expressed by fibroblasts and other stromal cells in many tissues. It is also clear that reduction of THBS1 expression in a tumour bed is a necessary prerequisite for induction of neovascularization and for a microscopic tumour to become neovascularized and to grow[65,66]. Watnick and colleagues recently found that certain human tumours produce a novel protein that specifically represses THBS1 in the stromal tissue to which the tumour is subsequently able to metastasize[67]. Suppression of anti-angiogenic activity at the future metastatic site facilitates the initiation of angiogenesis by metastatic tumour cells. If this discovery can be generalized to other tumours, it could be the basis for the development of drugs such as antibodies that could neutralize the THBS1 suppressor protein produced by the primary tumour.

When a new angiogenesis-based metastatic mechanism is uncovered, it is prudent to ask whether the new cancer mechanism could have a physiological counterpart. As in normal tissues, THBS1 is highly expressed under normal conditions in the endometrium[68]. It is not known whether THBS1 is suppressed before the implantation of a fertilized ovum or of a blastocyst, and if so, by what mechanism. This is a topic of current investigation, and there are potential clinical implications. More than 10% of all pregnancies miscarry early in the first trimester. Some women have repeated early miscarriages and are unable to carry a baby to term. *In vitro* fertilization often requires multiple cycles of ovum implantation. Could these problems be the result of insufficient suppression of endometrial THBS1, or of some other endogenous angiogenesis

Table 3a | **Clinical trials of drugs that have shown anti-angiogenic activity in preclinical models**

Inhibitor (Company)	Target/mechanism	Clinical development
2-methoxyestradiol-EntreMed (EntreMed)	Inhibits HIF1α and tubulin polymerization	• Phase I: Breast cancer and solid tumours • Phase II: Glioblastoma, multiple myeloma, neuroendocrine, renal cell, prostate, ovarian cancer
A6 (Angstrom Pharmaceuticals)	Binds to uPA cell-surface receptor	• Phase II: History of ovarian cancer with rising CA125
Abergrin (MedImmune)	Anti αvβ3 antibody	• Phase I: Melanoma, solid tumours, colorectal cancer • Phase II: Melanoma, prostate cancer, psoriasis, arthritis
ABT-510 (Abbott Laboratories)	Thrombospondin 1 receptor CD36	• Phase I: Head and neck cancer, solid tumours • Phase II: Lymphoma, renal cell, head and neck, NSCLC, soft tissue sarcoma
Actimid (Celgene Corporation)	Downregulates TNF	• Phase II: Prostate cancer (completed)
AG-013736 (Pfizer)	VEGFR, PDGFR	• Phase I: Breast cancer • Phase II: NSCLC, melanoma, thyroid, breast, pancreatic, renal cell cancer
AMG706 (Amgen)	VEGFR, PDGFR, KITR, RETR	• Phase I: Lymphoma, solid tumours, NSCLC, breast, colorectal cancer • Phase II: Solid tumours, NSCLC, gastrointestinal stromal tumours (GIST), breast, thyroid cancer
AP23573 (Ariad Pharmaceuticals)	mTOR, VEGF	• Phase I: Glioma, sarcoma, solid tumours, multiple myeloma • Phase II: Endometrial cancer, prostate cancer, haem malignancies
AS1404 (Antisoma)	Vascular disrupting agent, releases TNF and vWF	• Phase II: Prostate cancer
ATN-161 (Attenuon)	α5β1 antagonist	• Phase II: Renal cell cancer, malignant glioma
AZD2171 (AstraZeneca)	VEGFR1, VEGFR2, VEGFR3, PDGFR	• Phase I: NSCLC, AML, colorectal, head and neck cancer, CNS tumours (child) • Phase II: Solid tumours, NSCLC, glioblastoma, melanoma, mesothelioma, neurofibromatosis, ovarian, CLL, colorectal, breast, kidney, liver, SCLC • Phase III: NSCLC
BMS-275291 (Bristol–Myers Squibb)	MMP inhibitor	• Phase I: Kaposi's sarcoma • Phase II: Kaposi's sarcoma, prostate cancer, NSCLC • Phase III: NSCLC
CCI-779 (Wyeth)	mTOR, VEGFR	• Phase I: Solid tumours, prostate cancer, CML, and others • Phase II: CLL, melanoma, glioblastoma, multiple myeloma, GIST, SCLC, NHL, NSCLC, neuroendocrine tumours, breast, pancreatic, endometrial cancer, and others
CDP-791 (Imclone Systems)	VEGFR2, KDR	• Phase II: NSCLC
Celecoxib (Pfizer)	Increases endostatin	• Phase I: NSCLC, pancreatic, prostate cancer, solid tumours • Phase II: Head and neck cancer prevention, breast cancer prevention, lung cancer prevention, NSCLC, paediatric solid tumours, Ewing's sarcoma, glioma, skin cancer prevention, basal cell nevus syndrome, Barrett's oesophagus, hepatocellular, oesophogael, prostate, cervical, colorectal, head and neck, breast, thyroid, nasopharyngeal cancer, and others • Phase III: Colon, prostate, bladder cancer, NSCLC, and others
Cilengitide (EMD Pharmaceuticals)	αvβ3 and 5 antagonist	• Phase I: Solid tumours, lymphomas, paediatric brain tumours • Phase II: Glioblastoma, gliomas
Combretastatin (Oxigene)	VE-cadherin	• Phase I: Solid tumours • Phase II: Solid tumours, anaplastic thyroid cancer
E7820 (Eisia Medical Research Inc.)	Inhibits integrin α2 subunit on endothelium	• Phase I: Lymphoma • Phase II: Colorectal cancer
Everolimus (Novartis)	VEGFR, mTOR	• Phase I: Breast cancer, solid tumours, lymphoma • Phase II: NSCLC, melanoma, AML, ALL, CML, lymphoma, glioblastoma, prostate, colorectal, neuroendocrine, breast, endometrial, kidney cancer, paediatric tumours, solid tumours • Phase III: Islet cell pancreas II/III, and others
Genistein (National Cancer Institute (NCI), USA)	Suppresses VEGF and neuropilin and MMP9 in tumour cells, upregulates CTAP	• Phase I: Melanoma, kidney, prostate, bladder, breast cancer
Homoharringtonine (ChenGenex Therapeutics)	Downregulates VEGF in leukaemic cells	• Phase II: CML, APML • Phase III: CML
IMC-1121b (Imclone Systems)	VEGFR2, KDR	• Phase I: Solid tumours
INGN 241 (Introgen Therapeutics)	MDA7, VEGF	• Phase II: Melanoma

Table 3b | **Clinical trials of drugs that have shown anti-angiogenic activity in preclinical models**

Inhibitor (Company)	Target/mechanism	Clinical development
Interleukin-12 (NCI)	Upregulates IP10	• Phase I: Solid tumours, melanoma, paediatric neuroblastoma, kidney, breast cancer • Phase II: Melanoma, NHL, multiple myeloma, breast, ovarian, peritoneal, prostate cancer
Enzastaurin (Eli Lilly and Company)	VEGF	• Phase I: Solid tumours, gliomas • Phase II: Gliomas, lymphoma, brain tumours, NSCLC, pancreatic, colorectal cancer • Phase III: Lymphoma prevention, glioblastoma
Neovastat (Aeterna Zentaris)	MMP inhibitor	• Phase II: Multiple myeloma • Phase III: Kidney, NSCLC
NM-3 (Genzyme Corporation)	Inhibits VEGF expression by tumour cells, inhibits endothelial proliferation	• Phase I: Solid tumours
NPI-2358 (Nereus Pharmaceuticals)	β-tubulin	• Phase I: Solid tumours
Phosphomannopentaose sulphate (Progen Industries, Medigen Biotechnology)	bFGF, stimulates release of TFP1	• Phase II: Melanoma, NSCLC, prostate, hepatocellular cancer
PKC412 (Novartis)	VEGFR2	• Phase I: AML • Phase II: Mast-cell leukaemia
PPI-2458 (Praecis)	METAP2	• Phase I: Solid tumours, NHL
Prinomastat (Agouron Pharmaceuticals)	MMP inhibitor	• Phase II: Glioblastoma
PXD101 (CuraGen Corporation)	HDAC inhibitor	• Phase I: Solid tumours, haem malignancies • Phase II: Multiple myeloma, myelodysplastic syndrome, lymphoma, AML, NHL, ovarian/peritoneal, liver cancer
Suramin (NCI)	IGF1, EGFR, PDGFR, TGFβ, inhibits VEGF and bFGF	• Phase I: Bladder, breast, kidney cancer • Phase II: Glioblastoma, breast, kidney, adrenocortical cancer • Phase III: Prostate cancer
Tempostatin (Collard Biopharmaceuticals)	Extracellular matrix proteins	• Phase I: Solid tumours • Phase II: Kaposi's sarcoma
Tetrathiomolybdate (Sigma–Aldrich)	Copper chelator	• Phase II: Prostate, oesophageal, breast, colorectal cancer • Phase III: Psoriasis
TKI-258 (Novartis, Chiron Corporation)	FGFR3, VEGFR	• Phase I: Multiple myeloma, AML, melanoma
Vatalanib (Novartis)	VEGFR1,2, PDGFR	• Phase I: Solid tumours, NSCLC, gynaelogic tumours • Phase II: GIST, AML, CML, solid tumours, NSCLC, VHL, haemangioblastoma, mesothelioma, breast, prostate, pancreatic, neuroendocrine cancer, glioblastoma, meningioma, myelodysplastic syndrome, multiple myeloma, age-related macular degeneration • Phase III: Colorectal cancer
VEGF Trap (Regeneron Pharmaceuticals)	VEGF	• Phase I: NHL, age-related macular degeneration, diabetic macular oedema • Phase II: Kidney, ovarian cancer, NSCLC, age-related macular degeneration • Phase III: Ovarian cancer
XL184 (Exelixis)	MMET, VEGFR, RTK, FLT3, TIE2	• Phase I: Solid tumours
XL880 (Exelixis)	C-met, RTK	• Phase I: Solid tumours • Phase II: Papillary renal cell carcinoma
XL999 (Exelixis)	VEGFR, PDGFR, EGFR, FLT3, Src	• Phase I: Solid tumours • Phase II: Multiple myeloma, colorectal, ovarian, renal cell cancer, AML, NSCLC
ZD6474 (AstraZeneca)	VEGFR2, EGFR	• Phase I: Glioma • Phase II: Breast cancer, NSCLC, SCLC, thyroid, gliomas, multiple myeloma • Phase III: NSCLC

AML, acute myeloid leukaemia; APML, acute promyelocytic leukaemia; bFGF, basic fibroblast growth factor; CML, chronic myeloid leukaemia; CLL, chronic lymphocytic leukaemia; CNS, central nervous system; CTAP, connective tissue activation peptide; EGFR, epidermal growth factor receptor; FGFR3, fibroblast growth factor receptor 3; FLT3, fms-related tyrosine kinase 3; HDAC, histone deacetylase; HIF1, hypoxia-inducible factor 1; IGF1, insulin-like growth factor 1; IP10, inducible protein 10; KDR, kinase insert domain receptor; MDA7, interleukin-24; METAP2, methionyl aminopeptidase 2; MMP, matrix metalloproteinase; mTOR, mammalian target of rapamycin; NHL, non-Hodgkin's lymphoma; NSCLC, non-small-cell lung cancer; PDGFR, platelet-derived growth factor receptor; RETR, ret proto-oncogene (multiple endocrine neoplasia and medullary thyroid carcinoma 1, Hirschsprung disease) receptor; SCLC, small-cell lung cancer; TFP1, transferrin pseudogene 1; TGFβ, transforming growth factor-β; TNF, tumour-necrosis factor; uPA, urokinase-type plasminogen activator; VE-cadherin, vascular/endothelial-cadherin; VEGF(R), vascular endothelial growth factor (receptor); vWF, von Willebrand factor.

inhibitor in the endometrium? If so, could this condition be diagnosed by the measurement of THBS1 in the vaginal fluid? Could endometrial THBS1 then be suppressed, for example, by a vaginal suppository containing a putative short-acting THBS1-suppressor protein? Another intriguing finding is that haemangiomas, benign tumours of infancy, have the gene signature of cells of the fetal placental endothelium, implying that they might originate from the fetal placenta[69,70] (BOX 1). As haemangiomas usually regress spontaneously, they might reveal important clues about the molecular mechanisms of spontaneous regression of new blood vessels.

Endothelial cell control of tissue mass. When approximately 70% of the liver is removed in a rat (hepatectomy), the original mass regenerates completely in approximately 10 days[71]. Hepatocyte proliferation and endothelial cell proliferation are initiated the day after surgery. At approximately day 8, there is a wave of endothelial cell apoptosis, following which hepatocyte proliferation ceases[48]. The liver stops growing at ~10 days. However, if an angiogenic protein, such as VEGF or bFGF, is administered systemically, endothelial cells continue to proliferate and the liver continues to grow beyond its normal size. By contrast, if a specific inhibitor of endothelial proliferation is administered, liver regeneration is prevented and the liver remains at 30% of its normal size. Discontinuation of the endothelial inhibitor is followed immediately by liver regeneration that is complete by 10 days[48]. These experiments indicate that normal tissue and organ regeneration are controlled in part by the microvascular endothelium.

Growth and regression of fat is controlled by endothelial proliferation or apoptosis, respectively[49]. Leptin-deficient mice gain up to approximately 1 gram per day, mainly in fat. Adipocyte enlargement and proliferation is accompanied by endothelial proliferation that is restricted to fat. Systemic administration of an angiogenesis inhibitor (TNP-470 or endostatin) specifically induces endothelial apoptosis and a decrease in fat accompanied by rapid weight loss. When the normal weight for age is reached, weight loss stops. A similar result is obtained when endothelial cells in fat are specifically targeted by a genetically regulated inhibitor of proliferation[72]. Growth of normal prostate is also under endothelial control[73], and so is bone growth[74]. Therefore, it seems that microvascular endothelial cells can control tissue mass, regardless of whether the cells in this mass have a normal genome or a cancer genome[75]. This raises a provocative question: Is there some type of set-point or feedback mechanism in endothelial cells that tells them when a normal organ, such as liver, has reached its normal mass? If so, do tumour cells override this mechanism, and how?

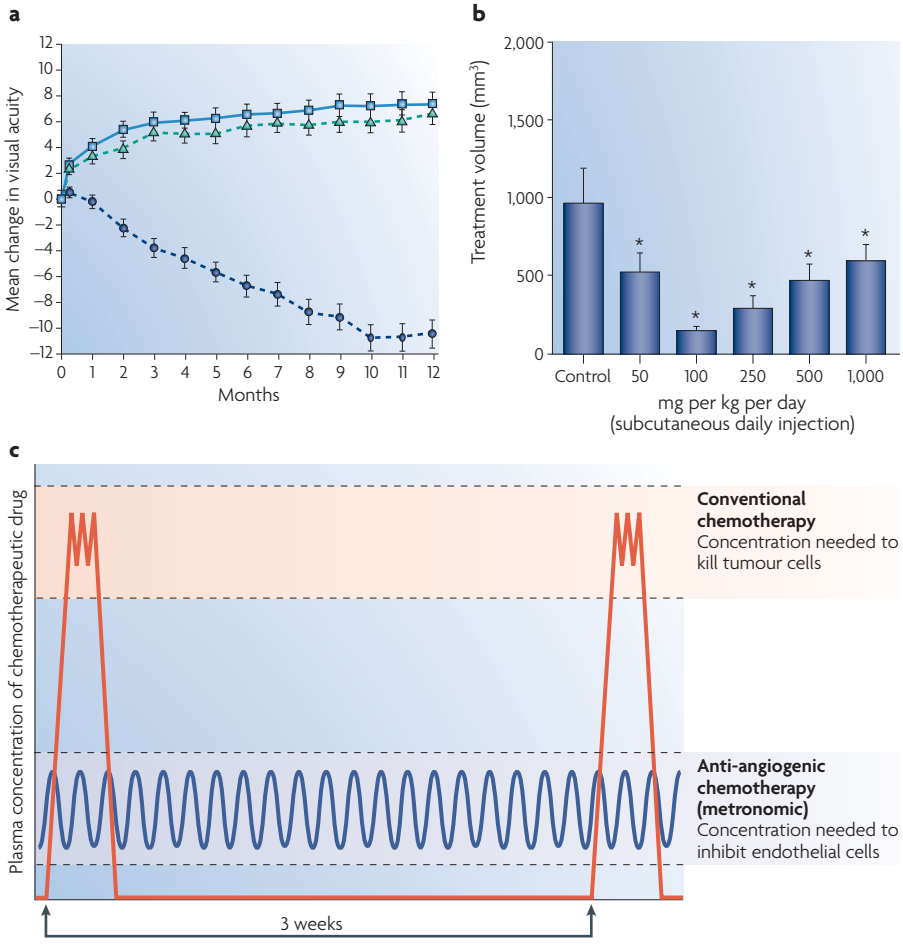

Figure 3 | **Examples of anti-angiogenic therapy. a** | Phase III clinical trial of Lucentis (ranibizumab; Genentech), a fragment of Avastin, an antibody to vascular endothelial growth factor (VEGF). Lucentis is used for intra-ocular injection in patients with age-related macular degeneration[37]. **b** | A biphasic (U-shaped) dose-efficacy curve for human pancreatic cancer in immunodeficient mice treated with endostatin. The tumour cells are also deficient in p53 (adapted from REF. 119). **c** | Dosing schedule differences between conventional chemotherapy (red) and anti-angiogenic (metronomic) chemotherapy (blue) (adapted from REF. 131 and from discussions with R. Kerbel).

What are the implications of this general principle for drug discovery? There is the possibility that specific endothelial inhibitors might be used to control obesity[72], as well as overgrowth of other tissues, such as uterine fibroids, overgrowth of bone caused by lymphangiogenesis and ectopic bone growth (fibrodysplasia ossificans progressiva)[76]. Specific endothelial inhibitors might also be used to control vascular malformations that grow rapidly after puberty or after attempts at surgical excision, and for which there are currently no drugs. The endocrine-specific angiogenesis-regulatory proteins, such as *Bombina variegata* peptide 8 kDa protein[77] (Bv8; also known as PROK2; testicular-cancer-specific), are of particular interest.

Is oncogene dependence angiogenesis dependent? The recognition that endothelial cells control tumour mass is crucial for a more complete understanding of how oncogenes initiate tumour growth. The conventional wisdom is that oncogene activation in a cell leads directly to the formation of large lethal tumours in mice. This concept is reinforced by experiments in which *Ras* or *Myc* oncogenes, under the control of the doxycycline promoter, induce rapid tumour growth when the oncogene is activated, leading to rapid tumour regression when the oncogene is inactivated[78–83]. This phenomenon is called oncogene dependence or oncogene addiction[84].

However, my group has found that during oncogene-induced tumour growth there is intense tumour angiogenesis associated with suppression of THBS1 in the tumour bed. When an oncogene is inactivated, the expression of THBS1, a potent angiogenesis inhibitor, is increased in the tumour bed, leading us to propose that oncogene addiction is angiogenesis dependent[83]. This hypothesis has now been supported by the deletion of THBS1 in the tumour and the host. In these mouse models, an activated oncogene induces more rapid tumour growth than in wild-type mice, but tumours do not regress after the inactivation of the oncogene[82]. Restoration of THBS1 expression in the tumour results in tumour regression upon oncogene inactivation[50].

How could this change in thinking about oncogene addiction provide new opportunities in drug discovery? Conventional wisdom (FIG. 4) suggests that the development of drugs targeted against oncogenes should be sufficient to control cancer. Imatinib (Gleevec; Novartis), which targets the product of the *BCR–ABL* oncogene, has demonstrated proof-of-concept by its success in the treatment of chronic myeloid leukaemia. Furthermore, imatinib targets the product of the oncogene *cKIT*, and has also proved successful in treating gastrointestinal stromal tumours in which this protein has a key role[85,86]. However, many patients eventually develop drug resistance[87], and there are numerous other oncogenes that could be responsible for inducing expression of redundant growth factors in these tumours. The imatinib experience also suggests that drugs will need to be developed against combinations of many oncogenes. A single angiogenesis inhibitor, especially a broad-spectrum angiogenesis inhibitor such as endostatin[28] or caplostatin, or a combination of angiogenesis inhibitors might block the effect of a large family of oncogenes, as the blockade of angiogenesis can prevent tumour growth downstream of oncogene activation. Analysis of 15 of the most studied oncogenes revealed that the majority of them increase the expression of VEGF (and/or bFGF) and decrease the expression of THBS1 in tumour cells[88,89].

Genetic regulation of angiogenesis. Although we all carry endogenous angiogenesis inhibitors in our blood and tissues (at least 29 at the time of writing)[24,25,90], different individuals reveal distinct genetic differences in their angiogenic response to a given stimulus. For example, individuals with Down syndrome are protected against diabetic retinopathy, although they have a similar incidence of diabetes as individuals without Down syndrome[52,91]. They also have higher levels of circulating endostatin (~1.6-fold) than normal individuals because of an extra copy of the gene for the endostatin precursor (collagen XVIII) on chromosome 21 (REFS 91,92). Interestingly, they seem to be among the most protected of all humans against cancer. Although testicular cancer and a megakaryocytic leukaemia have been reported for individuals with Down syndrome, they have the lowest incidence of the other ~200 human cancers compared with age-matched controls[52,91]. Conversely, individuals with a polymorphism in endostatin (specifically arginine substituted for alanine at N104) have a significantly higher risk of breast cancer[93]. The correlation between endostatin levels and cancer susceptibility was demonstrated in mice. Mice that were engineered to genetically overexpress endostatin to mimic individuals with Down syndrome have tumours that grow 300% slower[94], and in mice that had THBS1 deleted, tumours grow approximately 300% more rapidly, and more quickly still if two angiogenesis inhibitors are knocked out (tumstatin and THBS1)[94].

Another interesting finding is that African Americans rarely develop the 'wet' form of age-related macular degeneration. They usually do not have intravitreal haemorrhages and do not go blind from the 'dry' form of this disease[95]. By contrast, African Americans have a similar incidence of diabetic retinopathy. In age-related macular degeneration, neovascularization is in the choroidal layer that is surrounded by melanocytes containing melanin. In diabetic retinopathy, neovascularization arises from the retina. The retinal pigmented epithelial cells contain a lighter form of oxidized melanin, which differs from melanin in the choroid or in the skin. Also, African American infants rarely develop cutaneous haemangiomas compared with white infants.

These correlations suggest that factors linked to pigmentation and melanin are producing an inhibitory influence on the angiogenic balance in the melanin-rich tissues. However, there is no melanin in prostate or breast tissue, and African Americans are not protected from cancer of these organs.

This hypothesis was examined in animal experiments. When the gene for tyrosinase (in the melanin pathway) was deleted from mice, the albino relatives C57Bl/6J-Tyr$^{c\text{-}2J}$ showed intense iris neovascularization and haemorrhage (hyphaema) compared with weak neovascularization and no haemorrhage in the pigmented iris of wild-type mice. The amount of corneal neovascularization was not significantly different between these two strains because the cornea is not a pigmented tissue[96,97].

Genetic variations of angiogenic factors have important consequences for the clinical treatment of angiogenesis-dependent

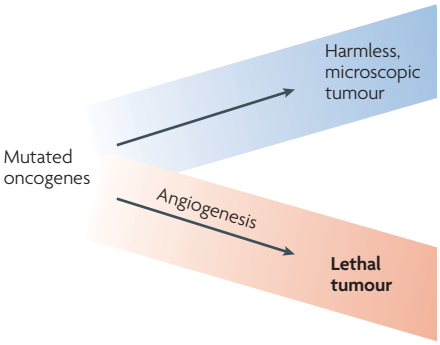

Figure 4 | **Oncogene addiction is angiogenesis dependent.** An oncogene-induced tumour that cannot recruit new blood vessels will remain as a harmless microscopic tumour in experimental animals[50,83].

Box 1 | Are infantile haemangiomas metastases from the placenta?

Haemangiomas are benign tumours made of capillary blood vessels that appear in 1 out of 100 newborns and usually begin to undergo spontaneous regression at approximately the end of the first year[6]. Some haemangiomas can be life threatening if they occur in the brain, airway or liver. The mechanism of haemangioma regression is unclear. Haemangiomas provide the possibility that they might reveal a clue about molecular mechanisms of spontaneous regression of new blood vessels. It was recently reported that all infantile haemangiomas express the glucose receptor GLUT1 (also known as SLC2A1), and that this receptor is also found on the endothelium of the placenta[69]. This observation led to a gene array analysis of endothelial cells from haemangioma and other tissues, which revealed that gene expression of haemangioma endothelium is identical to gene expression of fetal placental endothelium, but not to any other tissue analyzed[70]. The implication is that haemangiomas might be metastases from the fetal placenta. A further implication is that putative endogenous angiogenesis inhibitors that control the regression of placental vasculature at term might also be involved in the regression of haemangiomas. This speculation remains to be tested, but it illustrates how viewing a given process as part of an organizing principle can be useful.

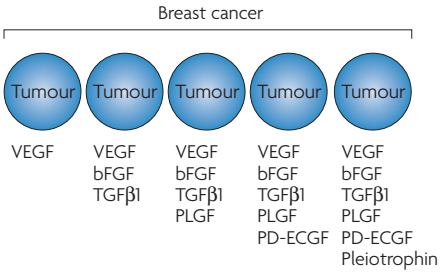

Figure 5 | **Angiogenic proteins in breast cancer.** Human breast cancer can cause the expression of at least six different angiogenic proteins (adapted from REF. 142). bFGF, basic fibroblast growth factor (also known as FGF2); PD-ECGF, platelet-derived endothelial cell growth factor (also known as ECGF1); PLGF, placental growth factor (also known as PGF); TGFβ1, transforming growth factor-β1; VEGF, vascular endothelial growth factor.

diseases. For example, some tumours that seem poorly vascularized and have a low microvessel density will be inhibited by a significantly lower dose of an angiogenesis inhibitor than is required for a highly vascularized tumour with a significantly higher microvessel density[98]. This may be counter-intuitive to clinicians who might inform a patient that their tumour is not very vascular and therefore will not respond to anti-angiogenic therapy. In fact, these tumours might be expressing their own angiogenesis inhibitors[99,100] and might respond to a lower therapeutic dose of angiogenesis inhibitor than would be required for a highly vascularized tumour.

The genetic heterogeneity of the angiogenic response is another reason for the pressing need to develop blood or urine biomarkers[101] to optimize the dosing of anti-angiogenic therapy. Furthermore, when mice are used for preclinical studies of angiogenesis inhibitors, it is crucial to know the genetic background of the mice in regards to their angiogenic responsiveness.

Optimizing anti-angiogenic therapy

Insights into the molecular mechanisms and significance of angiogenesis in different biological contexts are creating exciting new opportunities for drug discovery. However, as in some cases including cancer, anti-angiogenic therapies can also be used in combination with existing drugs. It is important to understand the difference between anti-angiogenic and cytotoxic drugs to optimize efficacy.

Anti-angiogenic therapy and cytotoxic chemotherapy. In February 2004, when the FDA approved bevacizumab for colorectal cancer, M. McClellan, then FDA Commissioner, said: "Anti-angiogenic therapy can now be considered the fourth modality for cancer treatment."[102]. It is a different modality because there are certain notable differences about chemotherapy that do not always readily transfer to anti-angiogenic therapy.

Importantly, anti-angiogenic therapy primarily targets the activated microvascular endothelial cells in a tumour bed rather than the tumour itself. It can accomplish this directly by preventing endothelial cells from responding to angiogenic proteins, as endostatin[28] and caplostatin[103,104] do. Anti-angiogenic therapy can also inhibit endothelial cell proliferation and motility indirectly by suppressing a tumour's production of angiogenic proteins, as erlotinib does[105], or by neutralizing one of these proteins, as bevacizumab does.

Also, although chemotherapy is usually more effective on rapidly growing tumours than on slowly growing tumours, the opposite is often true of anti-angiogenic therapy. More rapidly growing tumours can require higher doses of anti-angiogenic therapy[98]. Furthermore, chemotherapy is optimally given at a maximum tolerated dose, with off-therapy intervals of 1–3 weeks to rescue bone marrow and intestine. Anti-angiogenic therapy might optimally require that endothelial cells be exposed to steady blood levels of the inhibitor[100]. Therefore, daily dosing is optimal for those angiogenesis inhibitors with a short half-life. However, certain antibodies such as bevacizumab can be administered every 2 weeks because of long-lasting antibody levels in plasma, and perhaps because of neutralization of VEGF in platelets by bevacizumab that enters the platelets and binds with VEGF[61]. Zoledronate (Zometa; Novartis) is an amino-bisphosphonate that has been shown to inhibit angiogenesis[106] by targeting matrix metalloproteinase 9 (MMP9)[107], by reducing circulating levels of pro-angiogenic proteins in the circulation[108] or by suppressing multiple circulating pro-angiogenic factors in patients with cancer[109]. It accumulates in bone and can therefore be administered every month. However, after prolonged use, zoledronate may need to be administered less frequently to avoid osteonecrosis of the jaw.

Another important difference concerns the side effects of anti-angiogenic therapy compared with chemotherapy. Bone-marrow suppression, hair loss, severe vomiting and diarrhoea, and weakness are less common with anti-angiogenic therapy, and endostatin has shown minimal or no side effects in animals[110] and in humans[111]. It has to be noted though, that certain angiogenesis inhibitors increase the incidence of thrombotic complications, such as thalidomide (Thalomid; Celgene)[112] and bevacizumab. The risk of thrombosis is increased when these angiogenesis inhibitors are administered together with conventional chemotherapy[113]. Other side effects of inhibitors of VEGF include hypertension, intratumoural bleeding and bowel

Table 4 | **Three types of angiogenesis inhibitors**

Mechanism	Drug	Action
Type I		
Blocks one main angiogenic protein	Avastin (Avastin; Genentech)	Blocks VEGF
	VEGF Trap (Regeneron Pharmaceuticals)	Blocks VEGF
Type II		
Blocks two or three main angiogenic proteins	Sutent (Sutent; Pfizer)	Downregulates VEGF receptor 2, PDGF receptor, cKIT receptor
	Tarceva (Tarceva; Genentech, OSI Pharmaceuticals, Roche)	Downregulates VEGF production, bFGF production, TGFα by tumour cell
Type III		
Blocks a broad range of angiogenic regulators	Endostatin	Downregulates VEGF, bFGF, bFGF receptor, HIF1α, EGF receptor, ID1, neuropilin Upregulates thrombospondin 1, maspin, HIF1α, TIMP2
	Caplostatin	Broad anti-angiogenic and anticancer spectrum

bFGF, basic fibroblast growth factor; EGF, epidermal growth factor; HIF1α, hypoxia-inducible factor 1α; ID1, inhibitor of DNA binding 1, dominant negative helix–loop–helix protein; PDGF, platelet-derived growth factor; TIMP2, tissue inhibitor of metalloproteinase 2; TGFα, transforming growth factor-α; VEGF, vascular endothelial growth factor.

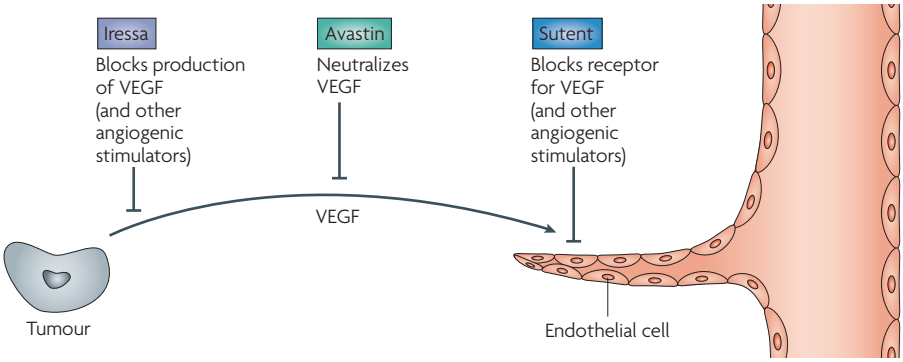

Figure 6 | **Three general mechanisms of angiogenesis inhibitors currently approved by the FDA.** Iressa blocks tumour expression of an angiogenic factor. Avastin blocks an angiogenic factor after its secretion from a tumour. Sutent blocks an endothelial cell receptor. VEGF, vascular endothelial growth factor.

perforation, especially in cases in which the intestine contains a tumour. Thalidomide has a slightly higher incidence of thromboembolic complications, as well as constipation and peripheral neuropathy — these are usually reversible upon discontinuation of thalidomide. Lenalidomide (Revlimid; Celgene), an FDA-approved derivative of thalidomide, has significantly reduced side effects. Side effects need to be carefully considered, especially when anti-angiogenic and cytotoxic medications are combined. So far, there are almost no data that allow a direct comparison of clotting risk for anti-angiogenic therapy alone, compared with cytotoxic therapy or combination therapy.

However, there can also be unexpected benefits from combining angiogenesis inhibitors, or drugs that have varying degrees of anti-angiogenic activity, with conventional chemotherapy. For example, Jain has shown that bevacizumab, by decreasing vascular leakage in a tumour, can lower intratumoral-tissue pressure and increase delivery of chemotherapy to a tumour[114]. In other words, anti-angiogenic therapy might 'normalize' tumour vessels[115]. Teicher *et al*. showed that anti-angiogenic therapy could decrease intratumoural pressure, which resulted temporarily in increased oxygenation to a tumour with subsequent increased sensitivity to ionizing radiation[116].

Biphasic dose efficacy of anti-angiogenic therapy. Dose efficacy is generally a linear function for chemotherapy. By contrast, several angiogenesis inhibitors have been reported to follow a biphasic, U-shaped dose-efficacy curve (known as hormesis[117]). For example, interferon-α (IFNα) is anti-angiogenic at low doses, but not at higher doses[118]. Similarly, rosiglitazone (Avandia; GlaxoSmithKline), a peroxisome proliferator-activated receptor-γ (PPARγ) ligand, as well as endostatin protein therapy[119] (FIG. 3b) and endostatin gene therapy[120] inhibit angiogenesis with a U-shaped dose-efficacy curve[121]. Before the U-shaped dose-efficacy response was recognized for anti-angiogenic gene therapy, my group had observed that gene therapy of endostatin could produce such high blood levels that all anti-angiogenic activity was lost[122]. It is now clear that blood levels of certain angiogenesis inhibitors (such as endostatin) that are too high or too low will be ineffective, and that the biphasic dose-efficacy curve offers the best explanation for why endostatin gene therapy of murine leukaemia failed[123,124].

Even the effect of endostatin on the gene expression (for example, hypoxia-inducible factor 1α; HIF1α) of fresh human endothelial cells *in vitro* reveals a U-shaped dose-efficacy pattern[28]. This is important information for drug discovery. For example, in the ranibizumab trial for age-related macular degeneration, a higher dose did not increase efficacy over a lower dose.

Anti-angiogenic therapy and drug resistance. Tumours might become refractory to anti-angiogenic therapy, especially if a mono-anti-angiogenic therapy targets only one angiogenic protein (for example, VEGF)[124]. Endothelial cells seem to have a lower probability for developing resistance to anti-angiogenic therapy, even though mouse endothelial cells in a tumour bed can become genetically unstable[80,125]. Although VEGF is expressed by up to 60% of human tumours, most tumours can also express five to eight other angiogenic proteins — for example, human breast cancers can express up to six angiogenic proteins (FIG. 5). High-grade brain tumours might express more angiogenic proteins than other tumours. When the expression of one angiogenic protein is suppressed for a long period, the expression of other angiogenic proteins might emerge[126]. The mechanism of this 'compensatory' response is unclear. Some angiogenesis inhibitors target up to three angiogenic proteins, whereas others target a broad range of angiogenic proteins (TABLE 4). Certain tumours, such as high-grade giant-cell tumours and angioblastomas, produce bFGF as their predominant angiogenic protein and do not seem to deviate from this. For this reason, low-dose daily IFNα therapy for 1–3 years is sufficient to return abnormally high levels of bFGF in the urine of these patients to normal. IFNα has been reported to suppress the production of bFGF by human cancer cells[118]. This treatment regimen has produced long term complete remissions (up to 10 years) without drug resistance (at the time of writing; see REFS 127–129 and L. Kaban, personal communication).

Currently, the majority of FDA-approved angiogenesis inhibitors, as well as those in Phase III clinical trials, neutralize VEGF, target its receptor or suppress its expression by tumour cells (FIG. 6). When drug resistance develops to some of these inhibitors, they are often perceived to represent the whole class of angiogenesis inhibitors. It remains to be seen if broad-spectrum angiogenesis inhibitors will develop less drug resistance than angiogenesis inhibitors that target against a single angiogenic protein. In experimental tumours, TNP-470, a synthetic analogue of fumagillin and caplostatin, its derivative[103,130], did not induce drug resistance when administered to mice for prolonged periods of time[104].

Anti-angiogenic chemotherapy (metronomic therapy). Browder *et al*. first reported that when murine tumours were made drug resistant to cyclophosphamide and then cyclophosphamide was administered on a conventional chemotherapy maximum-tolerated dose schedule, all mice died of large tumours[131]. However, if cyclophosphamide was administered more frequently at a lower dose, the tumours were potently inhibited because of endothelial apoptosis. If an angiogenesis inhibitor (TNP-470)[104] was added, which by itself could only inhibit the tumours by 50%, the drug-resistant tumours were eradicated[131]. This experiment demonstrated a new principle: a cytotoxic chemotherapeutic agent could be redirected to an endothelial target by changing its dose and frequency of

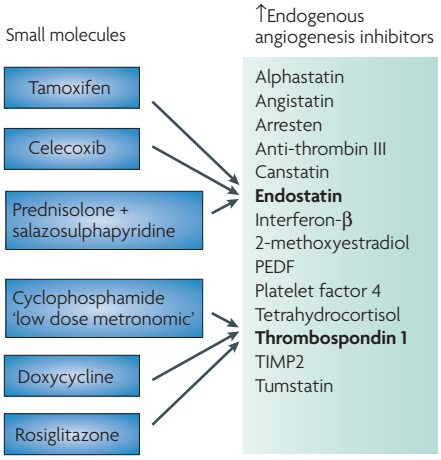

Figure 7| **Small molecules to increase endogenous angiogenesis inhibitors.** Examples of small molecules that are orally available and might induce increased levels of endogenous angiogenesis inhibitors in the blood or joint fluid. PEDF, pigment epithelium-derived factor; TIMP2, tissue inhibitor of matrix metalloproteinase 2 (REF. 124).

administration. Browder *et al.* called this regimen anti-angiogenic chemotherapy. Klement *et al.* confirmed this approach with a different chemotherapeutic agent[132]. Bocci *et al.*[133] further showed that anti-angiogenic chemotherapy increased circulating THBS1, and that deletion of the *THBS1* gene in mice completely abrogated the antitumour effect of this anti-angiogenic therapy. These results suggested that THBS1 acts as a mediator of anti-angiogenic chemotherapy[133]. The optimization of chemotherapy to treat vascular endothelium in the tumour bed is also called 'metronomic' therapy[134] (FIG. 3c) and has entered clinical trials for brain tumours and other tumours that were refractory to conventional chemotherapy. Kieran *et al.* recently studied 20 children with different types of brain tumours refractory to surgery, radiotherapy and chemotherapy, who were treated for 6 months with daily oral thalidomide and celecoxib (Celebrex; Pfizer), plus daily low-dose oral cyclophosphamide alternated every 21 days with daily low-dose oral etoposide[135]. Twenty-five percent of the patients were progression free more than 2.5 years from starting therapy. Forty percent of patients completed the 6 months of therapy, resulting in prolonged or persistent disease-free status. Sixteen percent of patients showed a radiographic partial response. Only elevated THBS1 levels in the blood correlated with prolonged response. This is consistent with the elevated circulating THBS1 levels observed in tumour-bearing mice treated with anti-angiogenic (metronomic) cyclophosphamide[133]. It is possible that angiogenesis inhibitors, such as bevacizumab, might be augmented by low dose anti-angiogenic (metronomic) chemotherapy with fewer side effects than conventional dosing of chemotherapy.

New pharmacology: oral drugs that increase endogenous angiogenesis inhibitors. The clinical finding that individuals with Down syndrome have an elevated circulating level of endostatin approximately 1.6-fold higher than normal individuals[91] is provocative. It suggests that small elevations of one or more endogenous angiogenesis inhibitors in the blood might protect against recurrent cancer, or might prevent the switch to the angiogenic phenotype in women at high risk for breast cancer. It is also possible that other genes on chromosome 21 have anti-angiogenic activity.

It has been found that certain orally available small molecules can upregulate expression of specific endogenous anti-angiogenic proteins, opening the way for a new field of pharmacology (FIG. 7). Endostatin is increased by tamoxifen[136], celecoxib[137] and (in joint fluid) by prednisolone plus salazosulphapyridine[138]. THBS1 is upregulated by low dose cyclophosphamide[133], doxycycline[139] and rosiglitazone[121]. This unifying concept points to future drug discovery in which the known endogenous angiogenesis inhibitors could be screened for small-molecule inducers that would increase the circulating level of one or more of them.

Outlook

Angiogenesis inhibitors are now being approved and introduced into medical practice throughout the world. At the same time, a need for molecular biomarkers is being met by an expanding worldwide research effort to develop gene-based and protein-based molecular signatures in blood, platelets and urine for very early diagnosis of recurrent cancer. One can speculate that if these two fields intersect, it might someday be possible to diagnose microscopic tumours at a millimetre size, at about the time of the angiogenic switch but perhaps years before they are symptomatic, or before they can be visualized by any conventional methods.

For example, today most individuals with the diagnosis of colon cancer are operated on. At least 50–60% of these patients are cured by the surgery. In the other patients, cancer will recur in approximately 4–6 years. Physicians are helpless to do anything until symptoms (such as pain and jaundice) occur, or until the recurrent cancer can be located by ultrasound, magnetic resonance imaging or CAT (computed axial tomography) scan. However, sensitive and specific molecular biomarkers that are being developed today could be used in the future to diagnose the presence of a microscopic recurrent tumour even before it could be anatomically located. Once these biomarkers are validated in clinical trials, then physicians could 'treat the rising biomarker' with non-toxic angiogenesis inhibitors until the biomarker returns to normal. A paradigm shift would be that recurrent cancer would be treated without waiting to see it, when it is still relatively harmless with low or no metastatic potential (that is, before the switch to the angiogenic phenotype). It might also be possible to use angiogenesis-based biomarkers to monitor the progression or regression of certain angiogenesis-dependent diseases that are non-neoplastic. These could include atherosclerosis, endometriosis, Crohn's disease and rheumatoid arthritis, among others.

There might be an analogy in the history of the treatment of infection. Before 1930, there were virtually no drugs for any infection, and most infections progressed to abscesses. Surgeons had to wait until the abscess was large enough to be located by X-rays so that the abscess could be surgically drained. The surgical textbooks of that era instructed surgeons how to locate an abscess: above the liver, behind the liver, in the mastoid, and so on. The term 'laudable' pus was commonly used to mean that if a surgeon could successfully drain an abscess the patient might live. After 1941, when antibiotics were introduced, it was no longer necessary to precisely locate an infection. Today the treatment of most infections is simply guided by blood tests (white-blood-cell count or blood cultures). As we continue to gain insight into angiogenesis and the role of angiogenic factors in seemingly unrelated diseases, the consequent potential of angiogenic modulators could see P. Carmeliet's prediction in the December 2005 issue of *Nature*[140] becoming prophetic: "Angiogenesis research will probably change the face of medicine in the next decades, with more than 500 million people worldwide predicted to benefit from pro- or anti-angiogenesis treatments"[140].

Judah Folkman is at the Children's Hospital and Harvard Medical School Boston, Massachusetts, USA.
e-mail: judah.folkman@childrens.harvard.edu
doi:10.1038/nrd2115

1. Sholley, M. M., Ferguson, G. P., Seibel, H. R., Montour, J. L., & Wilson, J. D. Mechanisms of neovascularization. Vascular sprouting can occur without proliferation of endothelial cells. *Lab. Invest.* **51**, 624–634 (1984).
2. Folkman, J. Angiogenesis. in *Harrison's Textbook of Internal Medicine* (eds Braunwald, E. *et al.*) (McGraw–Hill, New York, 2001).
3. Moulton, K. S. *et al.* Inhibition of plaque neovascularization reduces macrophage accumulation and progression of advanced atherosclerosis. *Proc. Natl Acad. Sci. USA* **100**, 4736–4741 (2003).
4. Folkman, J. Angiogenesis in psoriasis: therapeutic implications. *J. Invest. Dermatol.* **59**, 40–43 (1972).
5. Zeng, X., Chen, J., Miller, Y. I., Javaherian, K. & Moulton, K. S. Endostatin binds biglycan and LDL and interferes with LDL retention to the subendothelial matrix during atherosclerosis. *J. Lipid Res.* **46**, 1849–1859 (2005).
6. Ezekowitz, A., Mulliken, J. & Folkman, J. Interferon-α therapy of haemangiomas in newborns and infants. *Br. J. Haematol.* **79** (Suppl. 1), 67–68 (1991).
7. Szabo, S. *et al.* Accelerated healing of duodenal ulcers by oral administration of a mutein of basic fibroblast growth factor in rats. *Gastroenterology* **106**, 1106–1111 (1994).
8. Miller, J. W. *et al.* Vascular endothelial growth factor/vascular permeability factor is temporally and spatially correlated with ocular angiogenesis in a primate model. *Am. J. Pathol.* **145**, 574–584 (1994).
9. Folkman J. in *Targeted Therapies in Rheumatology* (eds Smolen, J. S. & Lipsky P. E.) 111–131 (Martin Dunitz, London, 2003).
10. Moulton, K. S. *et al.* Angiogenesis inhibitors endostatin or TNP-470 reduce intimal neovascularization and plaque growth in apolipoprotein E-deficient mice. *Circulation* **99**, 1726–1732 (1999).
11. Moulton, K. S. Angiogenesis in atherosclerosis: gathering evidence beyond speculation. *Curr. Opin. Lipidol.* **17**, 548–555 (2006).
12. Gimbrone, M. A., Jr., Cotran, R. S. & Folkman, J. Human vascular endothelial cells in culture. Growth and DNA synthesis. *J. Cell Biol.* **60**, 673–684 (1974).
13. Ausprunk, D. H., Knighton, D. R. & Folkman, J. Vascularization of normal and neoplastic tissues grafted to the chick chorioallantois. Role of host and preexisting graft blood vessels. *Am. J. Pathol.* **79**, 597–628 (1975).
14. Langer, R. & Folkman, J. Polymers for the sustained release of proteins and other macromolecules. *Nature* **263**, 797–800 (1976).
15. Gimbrone, M. A. Jr., Cotran, R. S., Leapman, S. B. & Folkman, J. Tumor growth and neovascularization: an experimental model using the rabbit cornea. *J. Natl Cancer Inst.* **52**, 413–427 (1974).
16. Auerbach, R., Arensman, R., Kubai, L. & Folkman, J. Tumor-induced angiogenesis: lack of inhibition by irradiation. *Int. J. Cancer* **15**, 241–245 (1975).
17. Taylor, S. & Folkman, J. Protamine is an inhibitor of angiogenesis. *Nature* **297**, 307–312 (1982).
18. Crum, R., Szabo, S. & Folkman, J. A new class of steroids inhibits angiogenesis in the presence of heparin or a heparin fragment. *Science* **230**, 1375–1378 (1985).
19. Folkman, J. Tumor angiogenesis: therapeutic implications. *N. Engl. J. Med.* **285**, 1182–1186 (1971).
20. Ausprunk, D. H., Falterman, K. & Folkman, J. The sequence of events in the regression of corneal capillaries. *Lab. Invest.* **38**, 284–294 (1978).
21. Maeshima, Y. *et al.* Tumstatin, an endothelial cell-specific inhibitor of protein synthesis. *Science* **295**, 140–143 (2002).
22. O'Reilly, M. S. *et al.* Angiostatin: a novel angiogenesis inhibitor that mediates the suppression of metastases by a Lewis lung carcinoma. *Cell* **79**, 315–328 (1994).
23. Frater-Schroder, M., Risau, W., Hallmann, R., Gautschi, P. & Bohlen, P. Tumor necrosis factor type α, a potent inhibitor of endothelial cell growth *in vitro*, is angiogenic *in vivo*. *Proc. Natl Acad. Sci. USA* **84**, 5277–5281 (1987).
24. Folkman, J. Endogenous angiogenesis inhibitors. *Acta Pathol. Microbiol. Immunol. Scand.* **112**, 496–507 (2004).
25. Nyberg, P., Xie, L. & Kalluri, R. Endogenous inhibitors of angiogenesis. *Cancer Res.* **65**, 3967–3979 (2005).
26. Folkman, J. in *Cancer Medicine* 7th Edn (eds Kufe, D. W. *et al*) (B.C. Decker, Hamilton, Ontario, 2006).
27. O'Reilly, M. S. *et al.* Endostatin: an endogenous inhibitor of angiogenesis and tumor growth. *Cell* **88**, 277–285 (1997).
28. Abdollahi, A. *et al.* Endostatin's antiangiogenic signaling network. *Mol. Cell* **13**, 649–663 (2004).
29. Inoue, K., Korenaga, H., Tanaka, N. G., Sakamoto, N. & Kadoya, S. The sulfated polysaccharide — peptidoglycan complex potently inhibits embryonic angiogenesis and tumor growth in the presence of cortisone acetate. *Carbohydr. Res.* **181**, 135–142 (1988).
30. Hurwitz, H. *et al.* Bevacizumab plus irinotecan, fluorouracil, and leucovorin for metastatic colorectal cancer. *N. Engl. J. Med.* **350**, 2335–2342 (2004).
31. Udagawa, T. *et al.* Analysis of tumor-associated stromal cells using SCID GFP transgenic mice: contribution of local and bone marrow-derived host cells. *FASEB J.* **20**, 95–102 (2006).
32. Higgins, K.J., Abdelrahim, M., Liu, S., Yoon, K. & Safe, S. Regulation of vascular endothelial growth factor receptor-2 expression in pancreatic cancer cells by Sp proteins. *Biochem. Biophys. Res. Commun.* **345**, 292–301 (2006).
33. Yasui, H., Hideshima, T., Richardson, P. G. & Anderson, K. C. Recent advances in the treatment of multiple myeloma. *Curr. Pharm. Biotechnol.* **7**, 381–393 (2006).
34. Ranieri, G. *et al.* Vascular endothelial growth factor (VEGF) as a target of bevacizumab in cancer: from the biology to the clinic. *Curr. Med. Chem.* **13**, 1845–1857 (2006).
35. Rosenfeld, P. J. Intravitreal bevacizumab: the low cost alternative to lucentis? *Am. J. Ophthalmol.* **142**, 141–143 (2006).
36. Rosenfeld, P. J., Heier, J. S., Hantsbarger, G. & Shams, N. Tolerability and efficacy of multiple escalating doses of ranibizumab (lucentis) for neovascular age-related macular degeneration. *Ophthalmology* **113**, 623–632 (2006).
37. Kim, I. K. *et al.* Effect of intravitreal injection of ranibizumab in combination with verteporfin PDT on normal primate retina and choroid. *Invest. Ophthalmol. Vis. Sci.* **47**, 357–363 (2006).
38. Husain, D. *et al.* Safety and efficacy of intravitreal injection of ranibizumab in combination with verteporfin PDT on experimental choroidal neovascularization in the monkey. *Arch. Ophthalmol.* **123**, 509–516 (2005).
39. Michels, S. & Rosenfeld, P. J. [Treatment of neovascular age-related macular degeneration with ranibizumab/lucentis]. *Klin. Monatsbl. Augenheilkd.* **222**, 480–484 (2005) (in German).
40. Pieramici, D. J. & Avery, R. L. Ranibizumab: treatment in patients with neovascular age-related macular degeneration. *Expert Opin. Biol. Ther.* **6**, 1237–1245 (2006).
41. Shima, D. T. *et al.* Hypoxic induction of endothelial cell growth factors in retinal cells: identification and characterization of vascular endothelial growth factor (VEGF) as the mitogen. *Mol. Med.* **1**, 182–193 (1995).
42. Ng, E. W. & Adamis, A. P. Targeting angiogenesis, the underlying disorder in neovascular age-related macular degeneration. *Can. J. Ophthalmol.* **40**, 352–368 (2005).
43. Lim, M. S. Re: Correlational of oral tongue cancer inversion with matrix metalloproteinases (MMPs) and vascular endothelial growth factor (VEGF) expression, by Kim S-H, Cho NH, Kim K, *et al. J. Surg. Oncol.* **93**, 253–254 (2006).
44. Des Guetz, G. *et al.* Microvessel density and VEGF expression are prognostic factors in colorectal cancer. Meta-analysis of the literature. *Br. J. Cancer* **94**, 1823–1832 (2006).
45. Kerbel, R. S., Viloria-Petit, A., Klement, G. & Rak, J. "Accidental" anti-angiogenic drugs. Anti-oncogene directed signal transduction inhibitors and conventional chemotherapeutic agents as examples. *Eur. J. Cancer* **36**, 1248–1257 (2000).
46. Morelli, M.P. *et al.* Anti-tumor activity of the combination of cetuximab, and anti-EGFR blocking monoclonal antibody and ZD6474, an inhibitor of BEGFR and EGFR tyrosine kinases. *J. Cell Physiol.* **208**, 344–353 (2006).
47. Pinedo, H.M. *et al.* Involvement of platelets in tumour angiogenesis? *Lancet* **352**, 1775–1777 (1998).
48. Greene, A. K. *et al.* Urinary matrix metalloproteinases and their endogenous inhibitors predict hepatic regeneration after murine partial hepatectomy. *Transplantation* **78**, 1139–1144 (2004).
49. Rupnick, M. A. *et al.* Adipose tissue mass can be regulated through the vasculature. *Proc. Natl Acad. Sci. USA* **99**, 10730–10735 (2002).
50. Giuriato, S. *et al.* Sustained regression of tumors upon MYC inactivation requires p53 or thrombospondin-1 to reverse the angiogenic switch. *Proc. Natl Acad. Sci. USA* **103**, 16266–16271 (2006).
51. Klagsbrun, M. & Eichmann, A. A role for axon guidance receptors and ligands in blood vessel development and tumor angiogenesis. *Cytokine Growth Factor Rev.* **16**, 535–548 (2005).
52. Yang, Q., Rasmussen, S. A. & Friedman, J. M. Mortality associated with Down's syndrome in the USA from 1983 to 1997: a population-based study. *Lancet* **359**, 1019–1025 (2002).
53. Soker, S., Takashima, S., Miao, H. Q., Neufeld, G. & Klagsbrun, M. Neuropilin-1 is expressed by endothelial and tumor cells as an isoform-specific receptor for vascular endothelial growth factor. *Cell* **92**, 735–745 (1998).
54. Vogel, G. Developmental biology. The unexpected brains behind blood vessel growth. *Science* **307**, 665–667 (2005).
55. Mukouyama, Y. S., Shin, D., Britsch, S., Taniguchi, M. & Anderson, D. J. Sensory nerves determine the pattern of arterial differentiation and blood vessel branching in the skin. *Cell* **109**, 693–705 (2002).
56. Kutcher, M. E., Klagsbrun, M. & Mamluk, R. VEGF is required for the maintenance of dorsal root ganglia blood vessels but not neurons during development. *FASEB J.* **18**, 1952–1954 (2004).
57. Folkman, J., Browder, T. & Palmblad, J. Angiogenesis research: guidelines for translation to clinical application. *Thromb. Haemost.* **86**, 23–33 (2001).
58. Klement, G. *et al.* Early tumor detection using platelet uptake of angiogenesis regulators. *Blood* **104** (ASH Annual Meeting Abstracts), 839 (2004).
59. Naumov, G. N. *et al.* A model of human tumor dormancy: an angiogenic switch from the nonangiogenic phenotype. *J. Natl Cancer Inst.* **98**, 316–325 (2006).
60. Almog, N. *et al.* Prolonged dormancy of human liposarcoma is associated with impaired tumor angiogenesis. *FASEB J.* **20**, 947–949 (2006).
61. Verheul, H. M. *et al.* Uptake of bevacizumab by platelets blocks the biological activity of platelet-derived vascular endothelial growth factor (VEGF). *Proc. Amer. Assoc. Cancer Res.* **47**, Abstract #5708 (2006).
62. Klement, G., Cervi, D., Yip, T. T., Folkman, J. & Italiano, J. Platelet PF-4 is an early marker of tumor angiogenesis. *Blood* **108** (ASH Annual Meeting Abstract), 1476 (2006).
63. Italiano, J., Richardson, J. L., Folkman, J. & Klement, G. Blood platelets organize pro- and anti-angiogenic factors into separate, distinct alpha granules: implications for the regulation of angiogenesis. *Blood* **108** (ASH Annual Meeting Abstracts), 393 (2006).
64. Volpert, O. V., Lawler, J. & Bouck, N. P. A human fibrosarcoma inhibits systemic angiogenesis and the growth of experimental metastases via thrombospondin-1. *Proc. Natl Acad. Sci USA* **95**, 6343–6348 (1998).
65. Rastinejad, F., Polverini, P. J. & Bouck, N. P. Regulation of the activity of a new inhibitor of angiogenesis by a cancer suppressor gene. *Cell* **56**, 345–355 (1989).
66. Dameron, K. M., Volpert, O. V., Tainsky, M. A. & Bouck, N. Control of angiogenesis in fibroblasts by p53 regulation of thrombospondin-1. *Science* **265**, 1582–1584 (1994).
67. Kang, S. -Y. *et al.* Repression of stromal thrombospondin-1 is a determinant for metastatic tissue specificity. *Proc. Amer. Assoc. Cancer Res.* **47**, Abstract #2798 (2006).
68. Iruela-Arispe, M. L., Porter, P., Bornstein, P. & Sage, E. H. Thrombospondin-1, an inhibitor of angiogenesis, is regulated by progesterone in the human endometrium. *J. Clin. Invest.* **97**, 403–412 (1996).
69. North, P. E. *et al.* A unique microvascular phenotype shared by juvenile hemangiomas and human placenta. *Arch. Dermatol.* **137**, 559–570 (2001).
70. Barnes, C. M. *et al.* Evidence by molecular profiling for a placental origin of infantile hemangioma. *Proc. Natl Acad. Sci USA* **102**, 19097–19102 (2005).
71. Greene, A. K. *et al.* Endothelial-directed hepatic regeneration after partial hepatectomy. *Ann. Surg.* **237**, 530–535 (2003).
72. Kolonin, M. G., Saha, P. K., Chan, L., Pasqualini, R. & Arap, W. Reversal of obesity by targeted ablation of adipose tissue. *Nature Med.* **10**, 625–632 (2004).

73. Folkman, J. Is tissue mass regulated by vascular endothelial cells? Prostate as the first evidence. *Endocrinology* **139**, 441–442 (1998).
74. Street, J. *et al*. Vascular endothelial growth factor stimulates bone repair by promoting angiogenesis and bone turnover. *Proc. Natl Acad. Sci. USA* **99**, 9656–9661 (2002).
75. Gerber, H. P., & Ferrara, N. The role of VEGF in normal and neoplastic hematopoiesis. *J. Mol. Med.* **81**, 20–31 (2003).
76. Kaplan, F. *et al*. Urinary basic fibroblast growth factor. A biochemical marker for preosseous fibroproliferative lesions in patients with fibrodysplasia ossificans progressiva. *Clin. Orthop.* **346**, 59–65 (1998).
77. Ferrara, N., LeCouter, J., Lin, R., & Peale, F. EG-VEGF and Bv8: a novel family of tissue-restricted angiogenic factors. *Biochim. Biophys. Acta* **1654**, 69–78 (2004).
78. Chin, L. & DePinho, R. A. Flipping the oncogene switch: illumination of tumor maintenance and regression. *Trends Genet.* **16**, 147–150 (2000).
79. Felsher, D. W. & Bishop, J. M. Reversible tumorigenesis by MYC in hematopoietic lineages. *Mol. Cell.* **4**, 199–207 (1999).
80. Felsher, D. W. & Bishop, J. M. Transient excess of MYC activity can elicit genomic instability and tumorigenesis. *Proc. Natl Acad. Sci. USA* **96**, 3940–3944 (1999).
81. Shachaf, C. M. *et al*. MYC inactivation uncovers pluripotent differentiation and tumour dormancy in hepatocellular cancer. *Nature* **431**, 1112–1117 (2004).
82. Jang, J. W., Boxer, R. B. & Chodosh, L. A. Isoform-specific ras activation and oncogene dependence during MYC- and Wnt-induced mammary tumorigenesis. *Mol. Cell. Biol.* **26**, 8109–8121 (2006).
83. Folkman, J. & Ryeom, S. Is oncogene addiction angiogenesis-dependent? *Cold Spring Harb. Symp. Quant. Biol.* **70**, 389–397 (2005).
84. Weinstein, I. B. & Joe, A. K. Mechanisms of disease: oncogene addiction — a rationale for molecular targeting in cancer therapy. *Nat. Clin. Pract. Oncol.* **3**, 448–457 (2006).
85. Demetri, G. D. Targeting *c-kit* mutations in solid tumors: scientific rationale and novel therapeutic options. *Semin. Oncol.* **28**, 19–26 (2001).
86. Duensing, A. *et al*. Mechanisms of oncogenic KIT signal transduction in primary gastrointestinal stromal tumors (GISTs). *Oncogene* **23**, 3999–4006 (2004).
87. Ritchie, E. & Nichols, G. Mechanisms of resistance to imatinib in CML patients: a paradigm for the advantages and pitfalls of molecularly targeted therapy. *Curr. Cancer Drug Targets* **6**, 645–657 (2006).
88. Rak, J. *et al*. Oncogenes and tumor angiogenesis: differential modes of vascular endothelial growth factor up-regulation in ras-transformed epithelial cells and fibroblasts. *Cancer Res.* **60**, 490–498 (2000).
89. Rak, J., Yu, J. L., Klement, G. & Kerbel, R. S. Oncogenes and angiogenesis: signaling three-dimensional tumor growth. *J. Investig. Dermatol. Symp. Proc.* **5**, 24–33 (2000).
90. Yoshioka, M. *et al*. Chondromodulin-1 maintains cardiac valvular function by preventing angiogenesis. *Nature Med.* **12**, 1151–1159 (2006).
91. Zorick, T. S. *et al*. High serum endostatin levels in Down syndrome: implications for improved treatment and prevention of solid tumours. *Eur. J. Hum. Genet.* **9**, 811–814 (2001).
92. Hesser, B. A. *et al*. Down syndrome critical region protein 1 (DSCR1), a novel VEGF target gene that regulates expression of inflammatory markers on activated endothelial cells. *Blood* **104**, 149–158 (2004).
93. Lourenco, G. J. *et al*. A high risk of occurrence of sporadic breast cancer in individuals with the 104NN polymorphism of the *COL18A1* gene. *Breast Cancer Res. Treat.* **100**, 335–338 (2006).
94. Sund, M. *et al*. Function of endogenous inhibitors of angiogenesis as endothelium-specific tumor suppressors. *Proc. Natl Acad. Sci. USA* **102**, 2934–2939 (2005).
95. Sommer, A. *et al*. Racial differences in the cause-specific prevalence of blindness in east Baltimore. *N. Engl. J. Med.* **325**, 1412–1417 (1991).
96. Rohan, R. M., Fernandez, A., Udagawa, T., Yuan, J. & D'Amato, R. J. Genetic heterogeneity of angiogenesis in mice. *FASEB J.* **14**, 871–876 (2000).
97. Rogers, M. S., Rohan, R. M., Birsner, A. E. & D'Amato, R. J. Genetic loci that control vascular endothelial growth factor-induced angiogenesis. *FASEB J.* **17**, 2112–2114 (2003).
98. Beecken, W. D. *et al*. Effect of antiangiogenic therapy on slowly growing, poorly vascularized tumors in mice. *J. Natl Cancer Inst.* **93**, 382–387 (2001).
99. Schuch, G., Kisker, O., Atala, A. & Soker, S. Pancreatic tumor growth is regulated by the balance between positive and negative modulators of angiogenesis. *Angiogenesis* **5**, 181–190 (2002).
100. Kisker, O. *et al*. Continuous administration of endostatin by intraperitoneally implanted osmotic pump improves the efficacy and potency of therapy in a mouse xenograft tumor model. *Cancer Res.* **61**, 7669–7674 (2001).
101. Roy, R., Wewer, U. M., Zurakowski, D., Pories, S. E. & Moses, M. A. ADAM 12 cleaves extracellular matrix proteins and correlates with cancer status and stage. *J. Biol. Chem.* **279**, 51323–51330 (2004).
102. In "Washington Post". (February 28, 2004).
103. Satchi-Fainaro, R. *et al*. Inhibition of vessel permeability by TNP-470 and its polymer conjugate, caplostatin. *Cancer Cell*. **7**, 251–261 (2005).
104. Satchi-Fainaro, R. *et al*. Targeting angiogenesis with a conjugate of HPMA copolymer and TNP-470. *Nature Med.* **10**, 255–261 (2004).
105. Pore, N. *et al*. EGFR tyrosine kinase inhibitors decrease VEGF expression by both hypoxia-inducible factor (HIF)-1-independent and HIF-1-dependent mechanisms. *Cancer Res.* **15**, 3197–3204 (2006).
106. Wood, J. *et al*. Novel antiangiogenic effects of the bisphosphonate compound zoledronic acid. *J. Pharmacol. Exp. Ther.* **302**, 1055–1061 (2002).
107. Giraudo, E., Inoue, M., and Hanahan, D. An amino-bisphosphonate targets MMP-9-expressing macrophages and angiogenesis to impair cervical carcinogenesis. *J. Clin. Invest.* **114**, 623–633 (2004).
108. Ferretti, G. *et al*. Zoledronic-acid-induced circulating level modifications of angiogenic factors, metalloproteinases and proinflammatory cytokines in metastatic breast cancer patients. *Oncology* **69**, 35–43 (2005).
109. Santini, D. *et al*. Zoledronic acid induces significant and long-lasting modifications of circulating angiogenic factors in cancer patients. *Clin. Cancer Res.* **9**, 2893–2897 (2003).
110. Boehm, T. *et al*. Antiangiogenic therapy of experimental cancer does not induce acquired drug resistance. *Nature* **390**, 404–407 (1997).
111. Kulke, M.H. *et al*. Phase II study of recombinant human endostatin in patients with advanced neuroendocrine tumors. *J. Clin. Oncol.* **24**, 3555–3561 (2006).
112. Mehta, P. Thalidomide and thrombosis. *Clin. Adv. Hematol. Oncol.* **1**, 464–465 (2003).
113. Fernandez, P. M. & Rickles, F. R. Tissue factor and angiogenesis in cancer. *Curr. Opin. Hematol.* **9**, 401–406 (2002).
114. Jain, R.K. Antiangiogenic therapy for cancer: current and emerging concepts. *Oncology* **9**, 7–16 (2005).
115. Jain, R.K. Normalization of tumor vasculature: an emerging concept in antiangiogenic therapy. *Science* **307**, 58–62 (2006).
116. Teicher, B.A. *et al*. Antiangiogenic agents can increase tumor oxygenation and response to radiation therapy. *Radiat. Oncol. Investig.* **2**, 269–176 (1995).
117. Calabrese, E. J., Staudenmayer, J. W. & Stanek, E. J. Drug development and hormesis: changing conceptual understanding of the dose response creates new challenges and opportunities for more effective drugs. *Curr. Opin. Drug Discov. Devel.* **9**, 117–123 (2006).
118. Slaton, J. W., Perrotte, P., Inoue, K., Dinney, C. P. & Fidler, I. J. Interferon-α-mediated down-regulation of angiogenesis-related genes and therapy of bladder cancer are dependent on optimization of biological dose and schedule. *Clin. Cancer Res.* **5**, 2726–2734 (1999).
119. Celik, I. *et al*. Therapeutic efficacy of endostatin exhibits a biphasic dose-response curve. *Cancer Res.* **65**, 11044–11050 (2005).
120. Tjin Tham Sjin, R. M. *et al*. Endostatin therapy reveals a U-shaped curve for antitumor activity. *Cancer Gene Ther.* (2006).
121. Panigrahy, D. *et al*. PPARγ ligands inhibit primary tumor growth and metastasis by inhibiting angiogenesis. *J. Clin. Invest.* **110**, 923–932 (2002).
122. Kuo, C. J. *et al*. Comparative evaluation of the antitumor activity of antiangiogenic proteins delivered by gene transfer. *Proc. Natl Acad. Sci USA* **98**, 4605–4610 (2001).
123. Marshall, E. Cancer therapy. Setbacks for endostatin. *Science* **295**, 2198–2199 (2002).
124. Folkman, J. Antiangiogenesis in cancer therapy — endostatin and its mechanisms of action. *Exp. Cell Res.* **312**, 594–607 (2006).
125. Hida, K. *et al*. Tumor-associated endothelial cells with cytogenetic abnormalities. *Cancer Res.* **64**, 8249–8255 (2004).
126. Dorrell, M.I., Aguilar, E., Scheppke, L. Barnett, F. H. & Friedlander, M. Combination angiostatic therapy completely inhibits ocular and tumor angiogenesis. *Proc. Natl Acad. Sci. USA* 8 Jan 2007 (doi:10.1073/pnas.0607542104).
127. Kaban, L. B. *et al*. Antiangiogenic therapy of a recurrent giant cell tumor of the mandible with interferon α-2a. *Pediatrics* **103**, 1145–1149 (1999).
128. Marler, J. J. *et al*. Successful antiangiogenic therapy of giant cell angioblastoma with interferon α 2b: report of 2 cases. *Pediatrics* **109**, e37 (2002).
129. Kaban, L. B. *et al*. Antiangiogenic therapy with interferon α for giant cell lesions of the jaws. *J. Oral Maxillofac. Surg.* **60**, 1103–1111 (2002).
130. Folkman, J. *The Harvey Lectures, Series 92, 1996–1997*. 65–82 (John Wiley & Sons, New York, 1998).
131. Browder, T. *et al*. Antiangiogenic scheduling of chemotherapy improves efficacy against experimental drug-resistant cancer. *Cancer Res.* **60**, 1878–1886 (2000).
132. Klement, G. *et al*. Continuous low-dose therapy with vinblastine and VEGF receptor-2 antibody induces sustained tumor regression without overt toxicity. *J. Clin. Invest.* **105**, R15–R24 (2000).
133. Bocci, G., Francia, G., Man, S., Lawler, J. & Kerbel, R. S. Thrombospondin 1, a mediator of the antiangiogenic effects of low-dose metronomic chemotherapy. *Proc. Natl Acad. Sci. USA* **100**, 12917–12922 (2003).
134. Hanahan, D., Bergers, G. & Bergsland, E. Less is more, regularly: metronomic dosing of cytotoxic drugs can target tumor angiogenesis in mice. *J. Clin. Invest.* **105**, 1045–1047 (2000).
135. Kieran, M. W. *et al*. A feasibility trial of antiangiogenic (metronomic) chemotherapy in pediatric patients with recurrent or progressive cancer. *J. Pediatr. Hematol. Oncol.* **27**, 573–581 (2005).
136. Nilsson, U. W. & Dabrosin, C. Estradiol and tamoxifen regulate endostatin generation via matrix metalloproteinase activity in breast cancer *in vivo*. *Cancer Res.* **66**, 4789–4794 (2006).
137. Ma, L., del Soldato, P. & Wallace, J. L. Divergent effects of new cyclooxygenase inhibitors on gastric ulcer healing: shifting the angiogenic balance. *Proc. Natl Acad. Sci. USA* **99**, 13243–13247 (2002).
138. Nagashima, M., Asano, G. & Yoshino, S. Imbalance in production between vascular endothelial growth factor and endostatin in patients with rheumatoid arthritis. *J. Rheumatol.* **27**, 2339–2342 (2000).
139. Kalas, W. *et al*. Restoration of thrombospondin 1 expression in tumor cells harbouring mutant *ras* oncogene by treatment with low doses of doxycycline. *Biochem. Biophys. Res. Commun.* **310**, 109–114 (2003).
140. Carmeliet, P. Angiogenesis in life, disease and medicine. *Nature* **438**, 932–936 (2005).
141. Marx, J. Angiogenesis. A boost for tumor starvation. *Science* **301**, 452–454 (2003).
142. Relf, M. *et al*. Expression of the angiogenic factors vascular endothelial cell growth factor, acidic and basic fibroblast growth factor, tumor growth factor β1 platelet-derived endothelail cell growth factor, placenta growth factor, and pleiotrophin in human primary breast cancer and its relation to angiogenesis. *Cancer Res.* **57(5)**, 963–969 (1997).

Acknowledgements

This work is supported in part by the Breast Cancer Research Foundation, a Department of Defense Innovator Award and a Department of Defense Congressional Award. I thank S. Connors and J. Grillo for help with the manuscript.

Competing interests statement

The author declares no competing financial interests.

DATABASES

The following terms in this article are linked online to:

Entrez Gene:
http://www.ncbi.nlm.nih.gov/entrez/query.fcgi?db=gene
EGFR | FGF2 | KDR | PF4 | PPRγ | PROK2 | TGFα | THBS1 | VEGFA

OMIM:
http://www.ncbi.nlm.nih.gov/entrez/query.fcgi?db=OMIM
Age-related macular degeneration | Alzheimer's disease | chronic myeloid leukaemia | colorectal cancer | Down syndrome | infantile haemangiomas | multiple myeloma | non-small-cell lung cancer | rheumatoid arthritis | testicular cancer

FURTHER INFORMATION

Judah Folkman's homepage: http://www.childrenshospital.org/cfapps/research/data_admin/Site105/mainpageS105P0.html

Access to this links box is available online.

Folkman online
Author biography
Judah Folkman is the Andrus Professor of Pediatric Surgery at Harvard Medical School, USA, and Surgeon-in-Chief, Emeritus, at Children's Hospital, Boston, USA. He is currently Director of the Vascular Biology Program at the Children's Hospital. He founded the field of angiogenesis research. He has received more than 130 awards and honors, including memberships in the National Academy of Sciences, the American Academy of Arts and Sciences, the American Philosophical Society, the Institute of Medicine of the National Academy of Sciences. He is the recipient of 17 honorary degrees.

Online links
Entrez: http://www.ncbi.nlm.nih.gov/entrez/query.fcgi?db=gene
EGFR
http://www.ncbi.nlm.nih.gov/entrez/query.fcgi?db=gene&cmd=Retrieve&dopt=full_report&list_uids=1956

FGF2
http://www.ncbi.nlm.nih.gov/entrez/query.fcgi?db=gene&cmd=Retrieve&dopt=full_report&list_uids=2247

KDR
http://www.ncbi.nlm.nih.gov/entrez/query.fcgi?db=gene&cmd=Retrieve&dopt=full_report&list_uids=3791

PPRγ
http://www.ncbi.nlm.nih.gov/entrez/query.fcgi?db=gene&cmd=Retrieve&dopt=full_report&list_uids=5468

PROK2
http://www.ncbi.nlm.nih.gov/entrez/query.fcgi?db=gene&cmd=Retrieve&dopt=full_report&list_uids=60675

TGFα
http://www.ncbi.nlm.nih.gov/entrez/query.fcgi?db=gene&cmd=Retrieve&dopt=full_report&list_uids=7039

THBS1
http://www.ncbi.nlm.nih.gov/entrez/query.fcgi?db=gene&cmd=Retrieve&dopt=full_report&list_uids=7057

VEGFA
http://www.ncbi.nlm.nih.gov/entrez/query.fcgi?db=gene&cmd=Retrieve&dopt=full_report&list_uids=7422

OMIM: http://www.ncbi.nlm.nih.gov/entrez/query.fcgi?db=OMIM
Age-related macular degeneration
http://www.ncbi.nlm.nih.gov/entrez/dispomim.cgi?id=603075

Alzheimer's disease
http://www.ncbi.nlm.nih.gov/entrez/dispomim.cgi?id=104300

Chronic myeloid leukaemia
http://www.ncbi.nlm.nih.gov/entrez/dispomim.cgi?id=608232

Colorectal cancer
http://www.ncbi.nlm.nih.gov/entrez/dispomim.cgi?id=114500

Down syndrome
http://www.ncbi.nlm.nih.gov/entrez/dispomim.cgi?id=190685

Infantile haemangiomas
http://www.ncbi.nlm.nih.gov/entrez/dispomim.cgi?id=602089

Multiple myeloma
http://www.ncbi.nlm.nih.gov/entrez/dispomim.cgi?id=254500

Non-small-cell lung cancer
http://www.ncbi.nlm.nih.gov/entrez/dispomim.cgi?id=211980

Rheumatoid arthritis
http://www.ncbi.nlm.nih.gov/entrez/dispomim.cgi?id=180300

Testicular cancer
http://www.ncbi.nlm.nih.gov/entrez/dispomim.cgi?id=273300

Further Information
Judah Folkman's homepage: http://www.childrenshospital.org/cfapps/research/data_admin/Site105/mainpageS105P0.html

TOC Blurb
Pathological angiogenesis plays a role in a wide range of diseases. Folkman argues that viewing angiogenesis as an 'organizing principle' in biology can lead to novel insights into the molecular mechanisms of seemingly unrelated phenomena, and facilitate the development of new therapeutic approaches.

OPEN ACCESS Freely available online

PLoS one

PPARα Deficiency in Inflammatory Cells Suppresses Tumor Growth

Arja Kaipainen[1], Mark W. Kieran[1,2], Sui Huang[1], Catherine Butterfield[1], Diane Bielenberg[1], Gustavo Mostoslavsky[3], Richard Mulligan[3], Judah Folkman[1], Dipak Panigrahy[1]*

1 Vascular Biology Program, Department of Surgery, Children's Hospital, Harvard Medical School, Boston, Massachusetts, United States of America, 2 Department of Pediatric Oncology, Dana-Farber Cancer Institute, Harvard Medical School, Boston, Massachusetts, United States of America, 3 Department of Genetics, Harvard Medical School, Boston, Massachusetts, United States of America

Inflammation in the tumor bed can either promote or inhibit tumor growth. Peroxisome proliferator-activated receptor (PPAR)α is a central transcriptional suppressor of inflammation, and may therefore modulate tumor growth. Here we show that PPARα deficiency in the host leads to overt inflammation that suppresses angiogenesis via excess production of the endogenous angiogenesis inhibitor thrombospondin-1 and prevents tumor growth. Bone marrow transplantation and granulocyte depletion show that PPARα expressing granulocytes are necessary for tumor growth. Neutralization of thrombospondin-1 restores tumor growth in PPARα-deficient mice. These findings suggest that the absence of PPARα activity renders inflammatory infiltrates tumor suppressive and, thus, may provide a target for inhibiting tumor growth by modulating stromal processes, such as angiogenesis.

Citation: Kaipainen A, Kieran MW, Huang S, Butterfield C, Bielenberg D, et al (2007) PPARα Deficiency in Inflammatory Cells Suppresses Tumor Growth. PLoS ONE 2(2): e260. doi:10.1371/journal.pone.0000260

INTRODUCTION

Non-neoplastic "host" cells, such as endothelial, stromal and inflammatory cells, play a critical role in tumor growth; and genes prognostic for cancer outcome may be expressed in the non-neoplastic tissue compartment [1]. While tumor angiogenesis has been intensely studied for more than two decades and has become an accepted target in cancer therapy, it is only in the last few years that inflammation has entered center stage of investigations into non-cell autonomous processes in cancer.

Chronic inflammation in the tumor stroma has long been known to contribute to tumor progression. Increased infiltration of innate immune cells to the tumor, such as macrophages, mast cells and neutrophils, correlates with increased angiogenesis and poor prognosis [2,3]. In contrast, lymphocytic/monocytic inflammatory infiltrates are sometimes associated with tumor inhibition and a more favorable prognosis [3–5]. Recently, NF-κB, a central positive regulator of inflammation, has emerged as a molecular link between inflammation and cancer growth. NF-κB promotes tumor growth not only in a cancer cell-autonomous manner by transactivating anti-apoptotic genes, but it also stimulates inflammatory processes in the microenvironment that lead to the production of tumor-promoting cytokines [6].

Conversely, PPARα, a ligand-activated nuclear receptor/transcription factor, is a key negative regulator of inflammation. Activation of PPARα by ligands inhibits inflammation [7] whereas PPARα deficient mice exhibit enhanced inflammation [8]. Despite PPARα's role in suppressing inflammation, it appears to be necessary and sufficient for rodent tumorigenesis [9]. In fact, prolonged PPARα activation by peroxisome proliferators induces hepatocarcinogenesis in rodents; conversely PPARα KO mice are resistant to tumorigenesis induced by PPARα agonists [10,11]. This may be due in part to cell-autonomous effect of PPARα, because it is expressed in many tumor cell lines [12,13]. Another possibility is that in PPARα deficient mice, stromal processes, such as inflammation, inhibit tumor growth, which results in microscopic-sized tumors that remain dormant. The role of PPARα in inflammation has been extensively studied in normal physiological processes (wound healing) and cardiovascular diseases (atherosclerosis) [14,15]; but the effect of PPARα mediated suppression of inflammation on tumors has not been characterized. Here we show that overt inflammation in the absence of PPARα in the host tissue prevents tumor growth. This indicates that in contrast to the emerging notion that inflammatory infiltrates promote tumors, the specific nature of the inflammatory process must be considered when linking inflammation to tumorigenesis.

RESULTS

Deletion of PPARα in Host Tissue inhibits Tumor Growth and Metastasis

We used several murine models to determine how the increased inflammatory response observed in the absence of PPARα affects tumor growth and metastasis. Fi rst, we stably transformed mouse embryonic fibroblasts (MEF) with SV40 large T antigen and H-ras [16] to obtain isogeneic tumorigenic cell lines that were either wild type (PPARα(+/+)MEF/RS) or lacked PPARα (PPARα(−/−) MEF/RS). These two tumorigenic cell lines allowed us to distinguish between the tumor cell- autonomous role and the host tissue role of PPARα. We found that the growth of these isogeneic tumors derived from both cell lines was almost completely suppressed in KO host mice that lacked PPARα, but not in WT

Academic Editor: Mikhail Blagosklonny, Ordway Research Institute, Inc., United States of America

Received October 16, 2006; **Accepted** February 2, 2007; **Published** February 28, 2007

Funding: This study was supported by the Stop & Shop Pediatric Brain Tumor Fund and the C.J. Buckley Pediatric Brain Tumor Research Fund (M.K.) and Department of Defense Innovator Award #W81XWH-04-1-0316 and private philanthropic funds (J.F.).

Competing Interests: The authors have declared that no competing interests exist.

* **To whom correspondence should be addressed.** E-mail: dipak.panigrahy@childrens.harvard.edu

animals, $p<0.0001$ (Figures 1A and 1B). Although tumors derived from MEFs deficient of PPARα were partially suppressed in WT animals (by 41%), indicating a cell-autonomous role of PPAR in tumor growth, a drastic effect in tumor suppression was observed when the host was PPARα deficient both in the case of PPARα(+/+) tumors (87% suppression) as well as PPARα(−/−) tumors (97% suppression) (Figure 1C). These results suggest that the presence of PPARα gene in the host animals is essential for tumor growth.

To examine the role of established tumor murine models we first used WT and KO mice derived from WT (S1)×KO (S4) crossmating. The growth of B16-BL6 tumor was almost completely inhibited in the PPARα KO (S1/S4) host, but was not affected in PPARα WT (S1/S4) animals, $p<0.0001$ (Figure 1D). This result suggests that presence of the PPARα gene in the host tissue is essential to support tumor growth.

Given that the above results clearly suggest that the status of the PPARα locus in the host affects tumor growth, we next evaluated the growth of three PPARα-positive murine tumor models in PPARα KO (S4) animals, including Lewis lung carcinoma (LLC), metastatic B16-F10/GFP melanoma, and B16-BL6 melanoma, $p<0.001$ (Figure 1E–G). LLC tumors have been reported to grow aggressively at similar rates in the Sv129, C57BL/6 and Sv129/C57BL/6 strains without evidence of transplantation immunity. This suggests that disparity in either minor or major immunohistocompatibility genes does not affect tumor growth in these models [17] (Figure S1). Macroscopic growth of LLC and B16-F10/GFP tumors was completely suppressed in PPARα KO mice, even when mice were monitored for more than 100 days post implantation (Figure 1E–G). Similarly, tumor metastasis was also suppressed in PPARα KO mice. When B16-F10/GFP melanoma

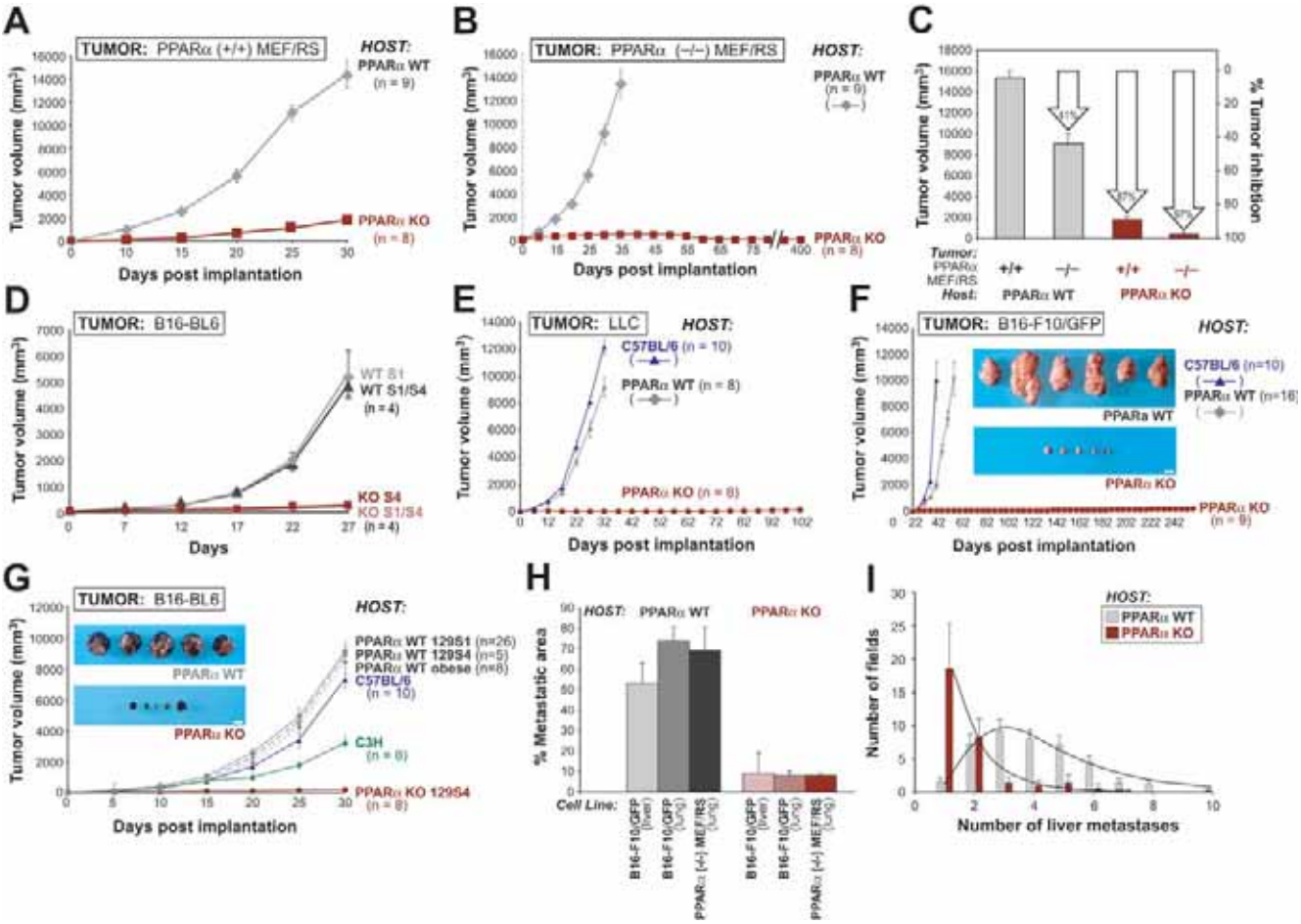

Figure 1. Tumor growth and metastasis are inhibited in PPARα knockout (KO) mice. PPARα wild type (WT) and PPARα KO mice were injected subcutaneously or intravenously with various tumor cell lines; (n) = number of mice/group. **(A–C)** The growth of engineered PPARα(+/+) MEF/RS and PPARα(−/−) MEF/RS tumors in PPARα WT and KO mice. **(A)** PPARα(+/+)MEF/RS tumor growth in PPARα WT (◆ gray) and KO (■ brown) mice. **(B)** The growth curves of PPARα(−/−)MEF/RS in PPARα WT (◆ gray) and KO (■ brown) mice.**(C)** Columns summarize the inhibitory effect of PPARα (−/−) tumor and host cells at day 30 post implantation (average±standard error of the mean). **(D–F)** The growth of different murine tumors in different mouse strains. **(D)** The growth of B16-BL6 melanoma was compared in WTS1 (◆ gray), WTS1/S4 (▲gray), KOS4 (■ brown) and KO S1/S4 (◆ pink) strains. WT S1/S4, PPARα WT second generation littermates from PPARα WT 129/S1 and KO 129/S4; KO S1/S4, PPARα KO second generation littermates from PPARα KO 129/S4. **(E)** Lewis lung carcinoma growth in PPARα WT (◆ gray), PPARα KO (■ brown) and C57BL/6 (▲ blue) mice. **(F)** B16-F10/GFP tumor growth in PPARα WT, PPARα KO and C57BL/6 mice, blue insets demonstrate representative B16-F10/GFP tumors in PPARα WT and KO mice on day 30 post implantation. Scale bar, 1 cm. **(G)** B16-BL6 melanoma was implanted in mice of indicated genetic backgrounds. Representative B16-BL6 tumors in PPARα WT (◆ gray) and PPARα KO (■ brown) mice on day 30 post implantation are shown (blue insets). Scale bar, 1 cm. **(H–I)** Metastasis in PPARα WT and KO mice. **H:** Metastatic areas of B16-F10/GFP and PPARα(−/−)MEF/RS tumor cells at day 21 post-injection in lung and liver of PPARα WT (◆ gray) and KO mice (■ brown). **I:** Number of liver metastases in PPARα WT (■ gray) and KO (■ brown) mice injected with B16-F10/GFP tumor cells (average±standard deviation).
doi:10.1371/journal.pone.0000260.g001

cells and engineered PPARα deficient tumor cells, PPARα (−/−) MEF/RS (see below) were injected via tail vein, 21 out of 21 PPARα wild-type (WT) mice died of lung and/or liver metastasis by day 21. In contrast, the PPARα KO hosts suppressed metastatic growth in lung and liver, reducing the infiltration of the tumor cells from 50–70% of normal organ tissue area in the WT hosts to less than 10% tissue area in PPARα KO animals (Figure 1H). Furthermore, the incidence of metastasis, as measured by the number of histologically identified metastatic foci, was strongly suppressed in PPARα KO mice. The majority of microscopic fields of liver sections in PPARα KO mice revealed only one or two metastases compared to 4–5 foci in livers of WT hosts (Figure 1I). Together these findings support the importance of PPARα expression in host cells for tumor development.

The non-growing PPARα(−/−)MEF/RS tumors in PPARα KO mice prompted us to investigate whether these tumors were just a mass of connective tissue or viable dormant microtumors, a state in which tumor cell proliferation is balanced by cell death [18,19]. Analysis of the small (<2 mm), non-growing lesions at the injection site identified viable PPARα(−/−) MEF/RS large T antigen expressing and proliferating tumor cells (Figure 2A). When re-transplanted to PPARα WT mice, these tumors grew rapidly to over 10,000 mm^3 (Figure 2A) indicating that PPARα in the host can rescue PPARα −/− tumor cells. Although these findings suggest that the presence of PPARα both in the tumor cells as well as in the host is necessary for unabated tumor growth, they also demonstrate that PPARα in tumor cells is not necessary for tumor cell viability. Conversely, the results underscore the importance of PPARα in the host tissue to sustain tumor growth.

Histological examination revealed a pronounced leukocyte infiltration (based on CD45-positive staining) in the non-necrotic stroma of all tumors grown in PPARα KO mice (Figure 2B). In contrast, PPARα WT animals exhibited the usual leukocytic infiltrate that was limited to necrotic areas (Figure 2B). Moreover, PECAM-1 staining performed to visualize blood capillaries revealed a decreased microvessel density in tumors from PPARα KO hosts when compared to tumors from WT hosts of the same size at day 7 (data not shown), as well as at day 30 post

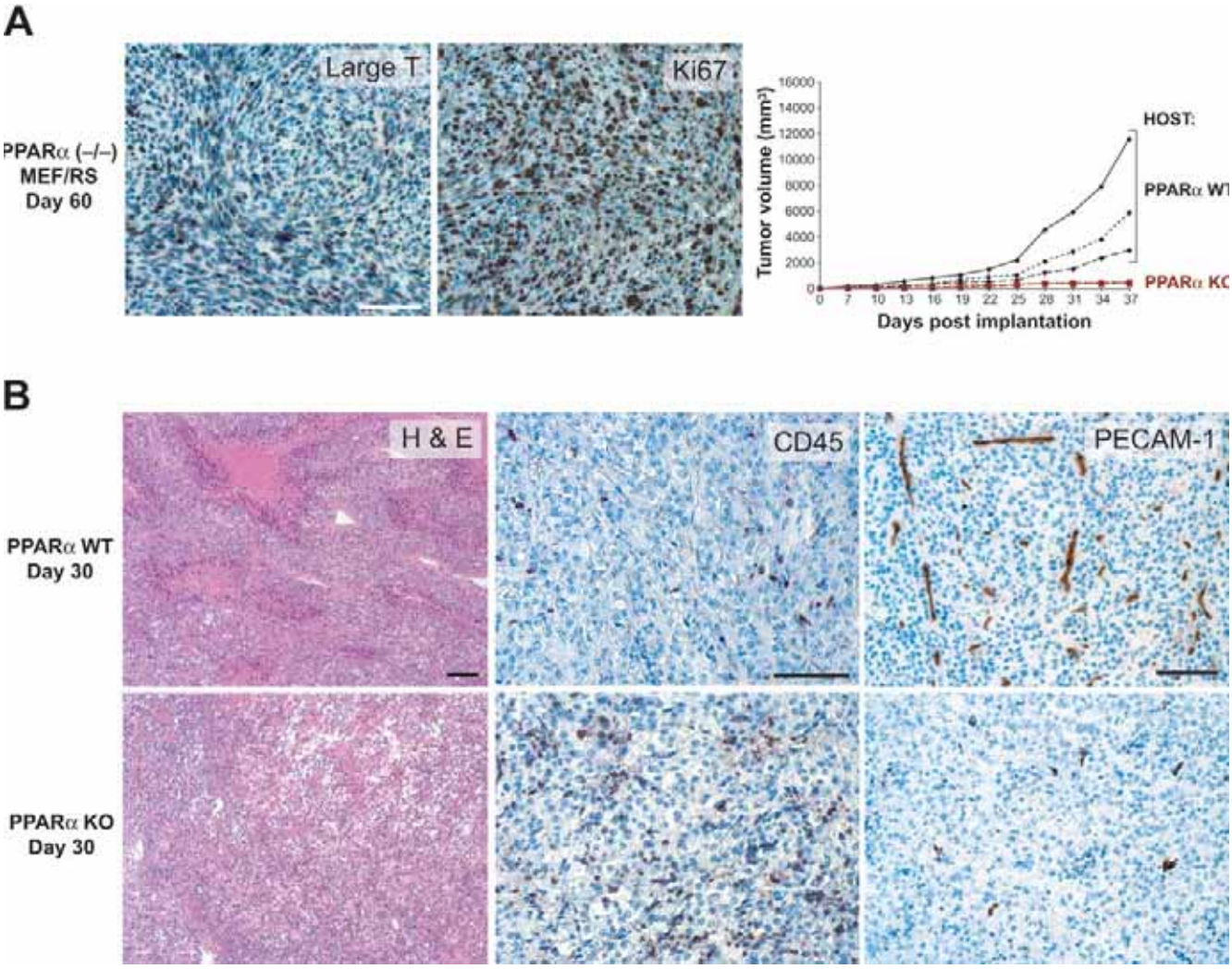

Figure 2. Immunohistological analysis of dormant tumors in PPARα KO mice. The dormant tumors contain viable and proliferating cells, and show decreased microvessel (PECAM1) and increased leukocyte (CD45) staining. **(A)** Dormant PPARα(−/−)MEF/RS tumors in PPARα KO mice from day 60 post-tumor implantation revealed abundant SV40 large T-antigen staining and proliferation (Ki-67). Dormant PPARα(−/−)MEF/RS tumors on day 60 were implanted as pieces (1 mm^3) into PPARα WT and KO mice (3 mice in each group). **(B)** Immunohistochemical analysis of subcutaneous B16-F10/GFP tumors (H&E, CD45/brown color, PECAM-1/brown color) from day 30 post-implantation in PPARα WT mice and KO mice. Scale bars, 100 μm.
doi:10.1371/journal.pone.0000260.g002

implantation (Figure 2B). Therefore, the absence of PPARα in the stromal tissue of the host appears to have two major consequences: an increase in inflammation and a decrease in tumor angiogenesis.

Loss of Host PPARα Inhibits Corneal Neovascularization and Permeability

Decreased microvessel density may reflect direct or indirect antiangiogenic effects caused by the lack of PPARα activity. Because all tumors used here are known to produce the angiogenic cytokine VEGF, we first investigated whether PPARα plays a role in VEGF signaling in the host cells. We employed two different *in vivo* VEGF-activity assays: VEGF-mediated, FGF2-induced corneal neovascularization, and VEGF-induced vascular permeability. Implantation of pellets containing 20 ng of FGF2 into the corneas of mice promotes the extravasation of leukocytes and stimulates VEGF-dependent corneal neovascularization [20,21]. PPARα KO mice exhibited >50% inhibition of vessel length when compared to WT animals, while the initial sprouting (reflected in clock hours of the neovascularized area) was not affected (Figure 3A). Complete abrogation of angiogenesis in the WT mice in the presence of soluble VEGF-receptor-1 (VEGFR1) confirmed that angiogenesis in these WT animals was mediated by VEGF (Figure 3A), consistent with previous studies [20]. In our second approach, we evaluated whether host PPARα affected VEGF-induced vascular permeability, a standard test of *in vivo* VEGF activity [22,23]. In response to VEGF, WT mice displayed Evans blue extravasation into the subcutaneous skin and ears (Figure 3B) that was 300–400% greater than that of PPARα KO mice (Figure 3B). Together, these results indicate that host PPARα is indispensable for VEGF-dependent signaling.

PPARα Deficiency in Bone Marrow Cells Inhibits Tumor Growth

Given the observation that the tumor bed of PPARα KO mice exhibited an increased inflammatory response, we performed reciprocal bone marrow transplantations between WT and KO mice to determine whether the hematopoietic compartment of PPARα deficient mice plays a role in the inhibition of tumor growth. Bone marrow cells from WT mice were capable of restoring the "wild-type" tumor growth pattern of B16-BL6 tumors in PPARα deficient hosts (Figure 4A). Conversely, PPARα-deficient bone marrow cells, when transplanted into WT hosts, conferred the tumor-suppressing phenotype of PPARα KO mice, $p<0.0001$ (Figure 4A). It is important to note that in the bone marrow transplantation protocol used, >90% of the hematopoietic system of the recipient was derived from the donor marrow (Figure S2A); this argues against the possibility that PPARα KO bone marrow cells have a direct, "dominant-negative" effect that overrides a tumor promoting effect of WT bone marrow cells. Instead, the result strongly suggests that the influence of host PPARα on tumor growth is conveyed solely by PPARα activity in bone marrow derived cells, because in these reciprocal trans-

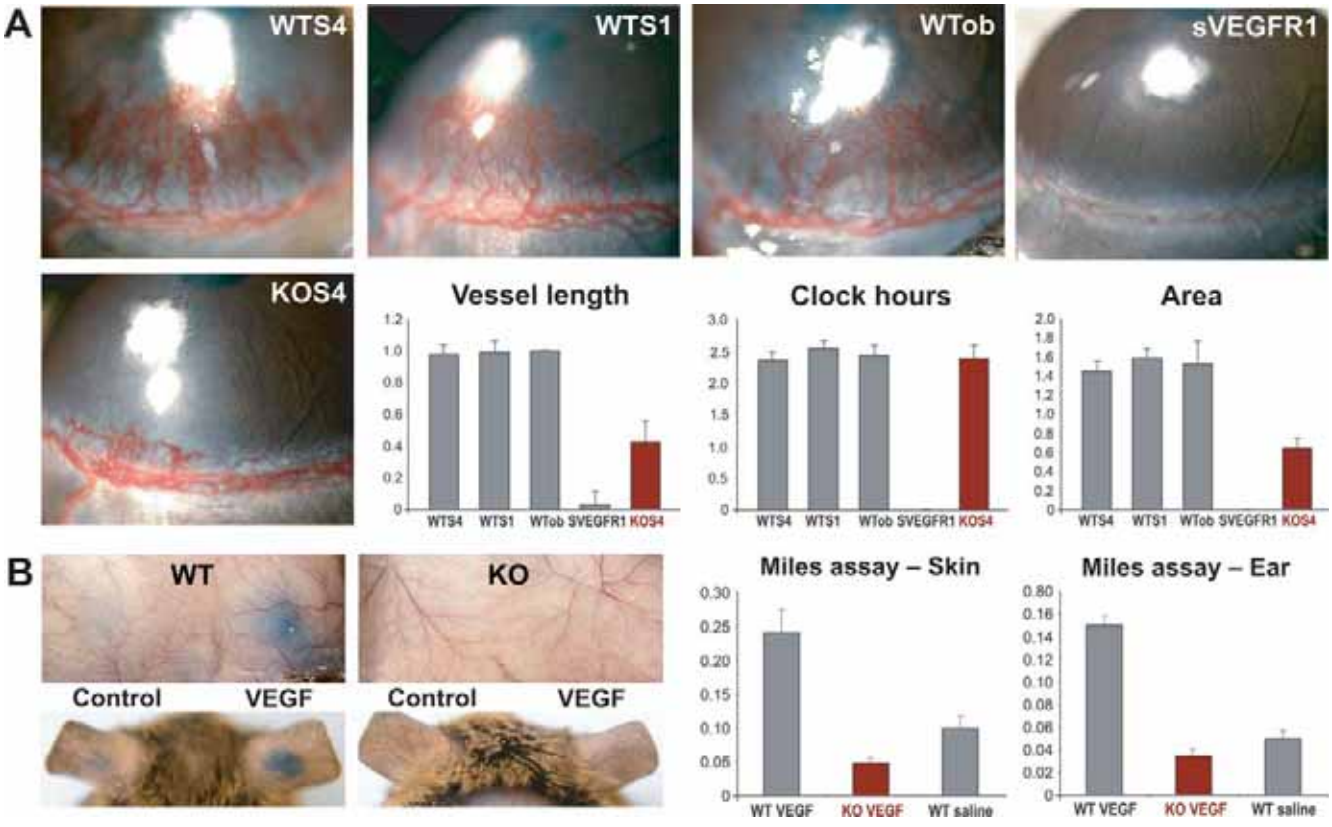

Figure 3. FGF2-induced corneal neovascularization and VEGF-induced vascular permeability are inhibited in PPARα KO mice. **(A)** FGF-2 (20 ng) stimulates corneal neovascularization in WT 129S4/SvJae strain, WT 129S1/SvIMJ strain and obese WT (129S1/SvJae) mice. Soluble murine VEGFR1 completely inhibits FGF2-induced angiogenesis in WT mouse (sVEGFR1). FGF2-induced corneal neovascularization is potently suppressed in PPARα KO mouse (KOS4). Vessel length, clock hours, and area of neovascularization in PPARα WT and KO mice are represented in bar graphs (average±standard deviation). **(B)** Evans blue dye leakage in dorsal skin and ears after injection with VEGF or saline in PPARα WT and KO mice (n = 6 mice/group). Spectrophotometric analysis of extravasated Evans blue of skin and ear is represented in bar graph (average±standard deviation).
doi:10.1371/journal.pone.0000260.g003

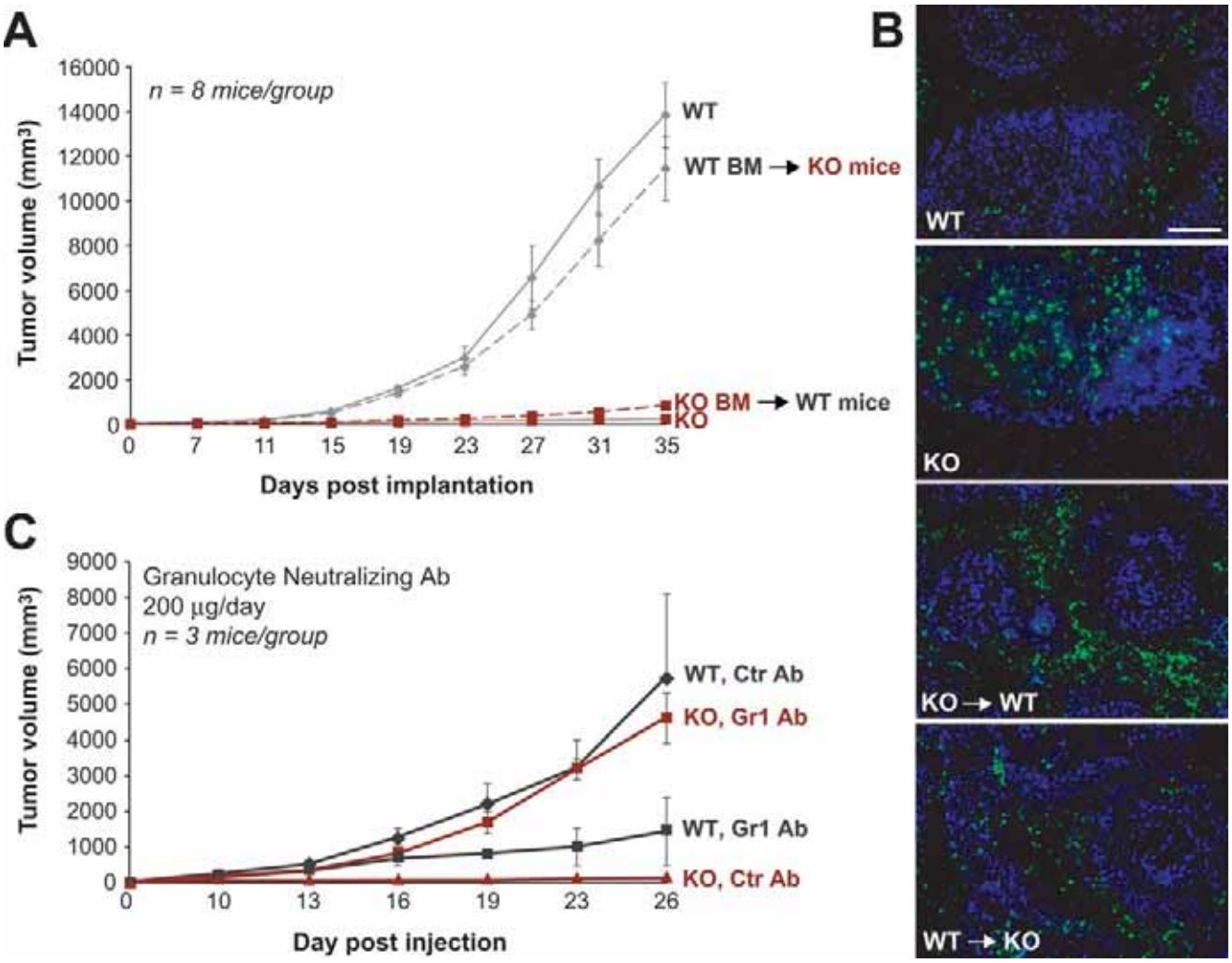

Figure 4. The inhibitory effect of PPARα resides in the hematopoietic compartment. **(A)** B16-BL6 melanoma growth in WT mice receiving KO bone marrow (KO BM →WT mice) compared to PPARα KO mice receiving WT bone marrow (WT BM →KO mice). WT bone marrow "rescues" tumor growth in PPARα KO mice. **(B)** Subcutaneous B16-BL6 tumors on day 28 post-implantation show abundant CD45 staining in PPARα WT mice receiving KO bone marrow (KO →WT). In B16-BL6 tumors in KO mice receiving WT bone marrow (WT→KO) CD45 staining (shown in green) was markedly reduced. Hoechst staining of nuclei is blue. Scale bar, 100 µM. **(C)** Effect of granulocyte depletion using Gr-1 antibody or control antibody (Ctr Ab, IgG2b) on B16-BL6 melanoma growth rate in PPARα KO and WT mice.
doi:10.1371/journal.pone.0000260.g004

plantation experiments the PPARα status of the transplanted bone marrow cells recapitulates the tumor phenotype of the host. However, it cannot be excluded that the suppressor activity carried by PPARα-deficient bone marrow cells overrides a potential tumor stimulatory contribution of PPARα in other, non-bone marrow derived host cells, such as from the local stroma.

Depletion of Granulocytes in the PPARα KO Mice Restores Tumor Growth

Immunohistological analysis of B16-BL6 tumors in WT mice transplanted with PPARα-deficient bone marrow cells showed an intense increase in leukocyte staining, mimicking the intratumoral leukocyte profile of tumors grown in PPARα KO mice (Figure 4B). This pronounced leukocyte infiltration in WT mice transplanted with PPARα-deficient bone marrow cells suggests that the presence of PPARα within the inflammatory cells prevents an overt inflammatory response to tumors. Histological and immunohistological analysis of the dormant tumors in PPARα knockout mice revealed that the leukocyte population was predominantly composed of granulocytes, mainly neutrophils (Figure S2B). To corroborate an active role of these PPARα-deficient granulocytes in tumor suppression, we depleted them in the host animals. Flow cytometry analysis confirmed that the granulocyte-specific neutralizing antibody GR1 completely depleted neutrophils (Figure S2C). The anti-granulocyte antibody GR1 restored tumor growth rate in the PPARα KO mice almost completely by day 26 (Figure 4C). In PPARα KO mice that received the control antibody (IgG2b), tumor growth remained inhibited. Conversely, in WT mice the GR1 antibody suppressed tumor growth (Figure 4C vs. 4A), confirming the previous reports that neutrophils are necessary for tumor growth [2,3]. However, tumor inhibition was even stronger in WT animals whose bone marrow had been replaced with that of PPARα KO mice (Figure 4A) as well as in PPARα deficient hosts (Figure 4A and 4C), again suggesting that not only is PPARα necessary for tumor growth, but that its absence confers a tumor suppressor activity on neutrophils.

The Inhibitory Role of TSP-1 on Tumor Growth

We next asked why are tumor growth and angiogenesis inhibited by PPARα-deficient leukocytes? Activated inflammatory cells promote angiogenesis, tumor cell proliferation and metastasis through the production of angiogenic mediators, growth factors, chemokines and proteases [2,24–26]. A connection between the positive and negative mediators of the inflammatory response, NF-κB and PPARα, has recently been suggested, because PPARα has been shown to repress NF-κB activity/expression [27]. However, this model disagrees with our result that PPARα-mediated suppression of inflammation is permissive for tumor growth rather than inhibitory. Therefore, our finding suggests that PPARα regulates an aspect of inflammation that is different from that controlled by NF-κB and hence, PPARα modulation of inflammation affects tumor growth independently of NF-κB. While NF-κB exerts its tumor-promoting effect by induction of cytokines, we investigated whether PPARα deficiency suppresses tumor growth by increasing the expression of the matrix protein thrombospondin-1 (TSP-1) which inhibits angiogenesis and stimulates granulocyte migration [28].

In fact, TSP-1 was elevated in the plasma and tumor tissue of PPARα KO mice (Figure 5A and Figure S2D). Because TSP-1 can be expressed in several cell types, including tumor cells, endothelial cells and fibroblasts, we next determined the cellular origin for TSP-1 in the tumors of PPARα deficient mice. B16-BL6 and B16-F10/GFP melanomas in PPARα KO mice contained high levels of TSP-1 protein (Figure 5A), despite that these tumor cells do not express TSP-1 [29]. TSP-1 was found in tumors in PPARα WT mice only when the mice received bone marrow from PPARα KO animals. In contrast, little or no TSP-1 was detected in the tumors in PPARα KO mice whose bone marrow cells had been replaced by those from PPARα WT animals (Figure 5B). Moreover, in B16-BL6 tumors from PPARα KO mice treated with GR1 antibody, little or no TSP-1 was detected (Figure 5C). Purified peripheral blood leukocytes from tumor- bearing PPARα deficient mice expressed high levels of TSP-1 while WT leukocytes express very little if any TSP-1 (Figure 5D). Taken together, these findings suggest that in this model system, TSP-1 was produced predominantly by the inflammatory cells, and not by resident stromal cells.

To corroborate the role of TSP-1 in angiogenesis in PPARα deficient animals, we performed the corneal neovascularization assay in the presence of neutralizing anti-TSP-1 antibody. Suppression of vessel length (endothelial cell migration and invasion) in PPARα KO mice was partially reversed by inactivation of TSP-1 function (Figure 5E). There was no effect on the contiguous circumferential zone of the limbal vessel sprouting as measured by clock hours (Figure 5E). In contrast, in the WT mice, corneal neovascularization was not affected by the TSP-1 antibody (Figure 5E).

Provided that neovascularization is a valid marker for tumor angiogenesis, these results are in agreement with the established role of TSP-1 in tumor inhibition [30]. However, we found that the neutralizing TSP-1 antibody did not completely restore tumor growth in PPARα KO mice to the level of that in WT mice, $p<0.02$ (Figure 5F). This may be either due to the limited access of TSP-1 antibody to the tumor bed or suggests that other endogenous inhibitors of angiogenesis may be involved. In fact, endostatin and IL-12 levels were significantly higher in PPARα KO mice (data not shown). Unexpectedly, we found that in WT animals neutralization of TSP-1 also had an inhibitory (rather than promoting) effect on the tumor, suppressing tumor growth by approximately 71% when compared to control antibody-treated mice, $p<0.02$ (Figure 5F). This suggests a complex, dualistic role of TSP-1 as a regulator of tumor growth.

DISCUSSION

In this study we identified the cellular basis for the tumor suppressing phenotype of PPARα deficient mice. Thus, PPARα pathway represents a new link between inflammation, angiogenesis, and tumorigenesis. Absence of PPARα in host granulocytes leads to inhibition of tumor growth, as demonstrated by: (1) transplantation of bone marrow cells from PPARα KO mice to PPARα WT mice and (2) by depletion of granulocytes by the neutralizing antibody, Gr1. Interestingly, PPARα deficient granulocytes carried TSP-1, a protein that inhibits angiogenesis, leukocyte migration and tumor growth. When TSP-1 was depleted by neutralizing antibody in PPARα KO mice, tumor growth was partially reversed.

PPARα is best known as a critical regulator of lipid metabolism and inflammation [31], and is expressed in tissues that catabolize fatty acids such as the liver, as well as in various cell types including smooth muscle cells, monocyte/macrophages, lymphocytes, and endothelial cells [31]. PPARα is the molecular target of the fibrate class of lipid-lowering drugs, which have been widely used for decades in the treatment of dyslipidaemia. Upon activation by PPARα ligands, PPARα heterodimerizes with retinoic acid receptor (RXR) regulating target gene expressions. PPARα ligands act as PPARα agonists. In addition to controlling lipid levels, they also function as potent anti-inflammatory agents in diseases such as atherosclerosis, colitis, and dermatitis [32–35]. Accordingly, PPARα KO mice exhibit significant reduction of atherosclerotic lesions, delayed wound healing, and delayed liver regeneration [14,15,36], due to overt inflammatory processes. PPARα deficiency also results in a prolonged inflammatory response to lipid mediators [8]. These findings collectively suggest that PPARα has a physiological role in suppressing inflammation [7].

PPARα agonists have been reported to induce liver tumors in rodents, but not in humans [10,37,38]. The mechanism for this species difference is still unclear. Accordingly, PPARα KO mice are totally resistant to liver tumors induced by PPARα ligands such as WY-14643 and clofibrate. This indicates that PPARα is required for ligand-induced peroxisome proliferation and hepatocarcinogenesis in rodents in a cell-autonomous manner [9]. It is unclear to what extent this requirement of PPARα for tumor growth is due to tumor cell-autonomous effects or its role in the host compartment of tumors, as shown by our current findings. In our experimental model the suppression of tumor growth in PPARα KO mice is mediated by leukocytes, mainly neutrophils. PPARα deletion is a second example for suppression of tumor growth by ablation of a gene in inflammatory cells; deletion of IKKβ in myeloid cells inhibits epithelial cell tumor growth [26]. However, our model does not exclude a contribution by cell-autonomous tumor promoting effects of PPARα. In fact, we found that deletion of PPARα in the tumor cell itself potentiated the tumor suppressing effect of PPARα-deficiency in the host tissue (Figure 1G and H), in agreement with the earlier reports of the requirement for PPARα in PPARα agonist induced liver tumors [9]. Therefore, PPARα, in addition to NF-κB, may represent another example of an oncogenic protein with a dual role in cancer by controlling essential functions both in cancer cell-autonomous processes as well as processes in the tumor bed, such as inflammation and angiogenesis. Oncogenes and NF-κB have been shown to stimulate tumor cell proliferation and angiogenesis by modifying cytokine expression profiles [25]. Therefore, PPARα does not simply suppress inflammation, acting in opposition to NF-κB, but it does so in a qualitatively different manner in that

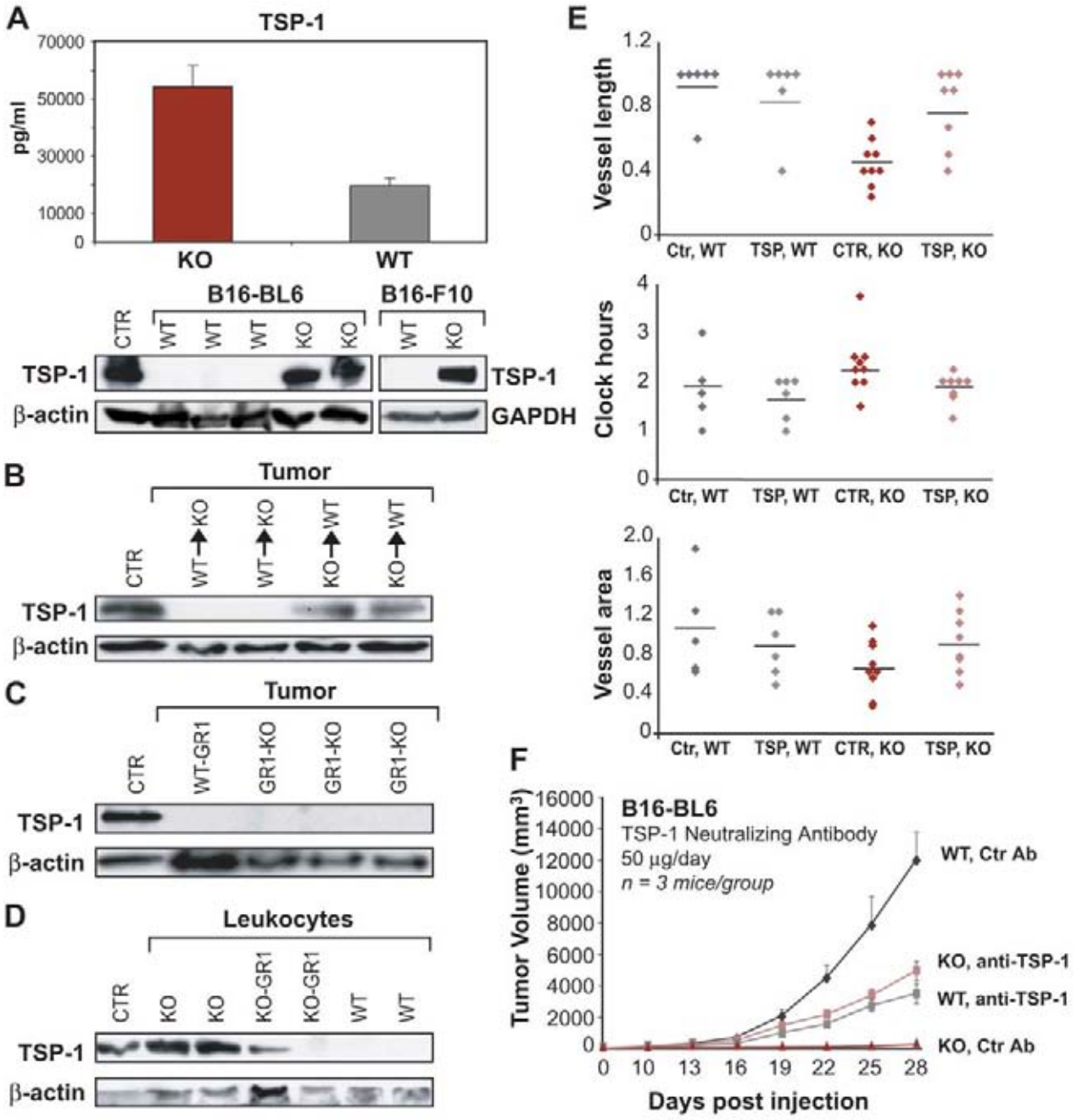

Figure 5. Effects of thrombospondin-1 (TSP-1) on angiogenesis and tumor growth in the PPARα-deficient state. **(A)** First panel demonstrates TSP-1 levels in plasma of PPARα KO and WT mice (ELISA); second panel shows TSP-1 levels in B16-BL6 and B16-F10/GFP tumor lysates at day 30 grown in PPARα WT and KO mice (western blotting); positive CTR for TSP-1, proliferating HUVECs. **(B)** Western blot analysis of TSP-1 protein in B16-BL6 tumor lysates from PPARα KO mice receiving WT bone marrow (WT BM→KO), and PPARα WT mice receiving KO bone marrow (KO BM→WT); positive CTR for TSP-1, proliferating HUVECs. **(C)** TSP-1 protein expression is lost in B16-BL6 tumor lysates from PPARα KO mice depleted of granulocytes (GR-1 antibody); positive CTR for TSP-1, proliferating HUVECs. **(D)** Western blot analysis of TSP-1 expression from isolated leukocytes from tumor-bearing PPARα KO mice; positive CTR, proliferating HUVECs. Levels of β-actin demonstrate protein loading. **(E)** Effect of TSP-1 neutralizing antibody and control antibody (IgM) on vessel length (n = 6–9 eyes), clock hours (n = 5–9 eyes) and vessel area (n = 5–9 eyes) in the corneal neovascularization assay. **(F)** B16-BL6 melanoma growth in KO and WT mice treated with TSP-1 neutralizing or control antibody (IgM).
doi:10.1371/journal.pone.0000260.g005

cellular infiltrates that do not express PPARα, actively suppress rather than stimulate tumor growth.

PPARα-deficient leukocytes produce TSP-1, a potent inducer of leukocyte migration and inhibitor of angiogenesis. Thrombospondin-1 (TSP-1) is a trimeric glycoprotein (450kD) that has several functional domains with different binding affinities. It binds to several cell surface receptors (CD36, integrins αVβ3, α3β1, α4β1, α5β1, heparan sulfate proteoglycans) and also binds calcium and extracellular proteins, such as plasminogen, fibrinogen, fibronectin and urokinase [30,39]. This multitude of binding partners may explain the diversity of TSP-1 functions: TSP-1 modulates cell adhesion, migration, proliferation and differentiation regulating

processes such as inhibition of angiogenesis (through CD36 and β1- integrin) and stimulation of neutrophil migration [28,40,41]. TSP-1 is expressed in several cell types in the host: platelets, neutrophils, monocytes, fibroblasts, pericytes, endothelial cells, and tumor cells [42]. Through its role as an activator of TGF-β, it also modulates inflammatory reactions which may contribute to the lethality of TSP-1 KO mice [43]. TSP-1 inhibits tumor growth in mice when overexpressed, putatively via suppression of angiogenesis [40,44,45]. However, TSP-1 may also act as a promoter of tumor growth, because anti-TSP-1 receptor antibody inhibited breast tumor growth [46]. Moreover, in vitro TSP-1 has been shown to promote tumor cell invasion and chemotaxis [47–49]. In addition, further complicating the picture, in human plasma and tumor stroma the levels of TSP-1 have been correlated with both good and poor cancer prognosis [50–56]. This conflicting influence of TSP-1 is recapitulated in our animal model: TSP-1 delivered by leukocytes inhibited tumor growth. However, in the WT animals neutralization of TSP-1 also strongly inhibited tumor growth (Figure 5C). A possible explanation for this apparent paradox is that TSP-1 may have a biphasic effect on angiogenesis and leukocyte migration so that low doses (as found physiologically in WT animals) stimulate and high doses (present in PPARα KO mice) inhibit these processes [57]. Such a "U-shape" dose-effect curve has been reported for many cytokines and bioactive molecules, such as interferon-α, PPARγ ligands and endostatin which all exhibit a biphasic effect on angiogenesis [58–62]. Therefore, in WT mice, TSP-1 may operate in the dose-effective window of promoting inflammation which in turn stimulates angiogenesis and tumor growth. In contrast, in PPARα KO mice where TSP-1 is constitutively high, it would act as an inhibitor of tumor growth, perhaps through its antiangiogenic effects. Another possibility, technical rather than biological, is that the activity of TSP-1 is always inhibitory under the conditions studied, but the TSP-1 antibody itself generates the biphasic effect. High levels of TSP-1 in KO mice in the presence of TSP-1 antibodies may promote formation of large antigen - antibody complexes that facilitate TSP-1 clearance, while at low levels, as in WT mice, TSP-1 may be stabilized by the antibody [63].

Given the accumulating findings pointing to the importance for tumor growth of processes in non-cancer host tissues, such as angiogenesis, inflammation and other functions mediated by residual stroma and infiltrating bone marrow cells, our results add a new element to the emerging paradigm that tumor formation is not only a cell-autonomous process. Hence, the action of genes involved in tumor formation must be seen in the broader context of host and tumor [64]. While several pro-inflammatory factors stimulate tumor growth, we report a new molecular link between inflammation and cancer, in that abnormal inflammatory processes can inhibit tumor growth and angiogenesis - thus broadening the spectrum for anticancer therapies that aim at interfering with stromal processes.

MATERIALS AND METHODS

Tumor Xenograft Studies

All the animal studies were reviewed and approved by the animal care and use committee of Children's Hospital Boston. Three to six-month old male PPARα knockout mice (129S4/SvJae), corresponding age-matched WT mice (129S1/SvIMJ, C57BL/6), obese WT mice (129S1/SvIMJ-retired breeders), C3H/HeJ and Balb/cJ mice were obtained from Jackson laboratories (Bar Harbor, ME). Retired WT breeders (35–40 gram) were used to control for weight as PPARα KO mice become obese with age [65]. WT mice (129S4/SvJae) were provided by Dr. John Heymach, Children's Hospital, Boston. PPARα WT and KO littermates were F2 generation. For tumor studies, PPARα negative (−/−) and PPARα positive (+/+) tumors were developed by transforming mouse embryonic fibroblasts (embryonic day 11) isolated from PPARα KO and WT mice, respectively, with SV40 large T-antigen and H-ras (generous gift from Dr. William Hahn). Tumor cells were injected subcutaneously (1×10^6 cells in 0.1 ml PBS). B16-BL6 melanoma cells were implanted directly from tissue culture; the growth of LLC and B16-F10/GFP tumors was achieved in 129 strains as follows: LLC and B16-F10/GFP cells were first grown in C57BL/6 mice and transplanted as pieces (1 mm^3) subcutaneously into PPARα WT mice. When tumors were 1000–2000 mm^3, they were serially passaged from mouse to mouse as 1 mm^3 pieces and then grown in culture [59]. For experiments, LLC and B16-F10/GFP tumor cells were injected subcutaneously into the 129S PPARα WT and PPARα KO mice either from culture or from mouse to mouse as a cell suspension as described [59]. Tumors were measured every 3–5 days, and the volume was calculated as $\text{width}^2\times\text{length}\times0.52$. For metastasis studies, 500,000 cells in 0.1 ml PBS were injected via tail vein (n = 15 mice/group). On day 21, when the PPARα WT mice died, all remaining mice were euthanized. Histological sections of livers were quantified for liver metastasis (n = 34–53 fields). For corneal tumor studies, tumor pieces (1 mm^3) were implanted into the cornea, and the angiogenic response was recorded; photos were taken weekly using a slit-lamp microscope. For granulocyte depletion studies, GR-1 or control antibody (IgG2b) at 300 μg/mouse (Biolegend, San Diego, CA) was administered intraperitoneally two days prior to B16-BL6 melanoma implantation in PPARα WT and PPARα KO mice, and every 3 days post-implantation. Granulocyte depletion was confirmed by flow cytometry using phycoerythrin conjugated Ly-6G (GR-1) antibody (Biolegend, San Diego, CA).

For neutralizing antibody experiments the A4.1 anti-TSP-1 monoclonal antibody (Lab Vision, Fremont, CA) (CSVTCG/CD36) or control antibody (IgM) at 50 μg/mouse were administered intraperitoneally daily to PPARα WT and KO mice in the corneal neovascularization and B16-BL6 melanoma experiments.

Immunohistochemistry

Tumor samples were processed and immunohistochemical stainings were performed according to standard protocols [59]. For rat anti-mouse PECAM1 (BD Biosciences, San Jose, CA) staining, sections were treated with 40 μg/ml proteinase K (Roche Diagnostics Corp.) for 25 minutes at 37°C. Detection of PECAM1 staining was completed using the tyramide amplification system according to the manufacturer's instructions (PerkinElmer, Boston, MA). For mouse monoclonal thrombospondin-1 (clone A6.1, Lab Vision, Fremont, CA) staining, sections were pretreated with pepsin for 15 minutes at 37°C (Biomeda, Foster City, CA). For rat anti-mouse CD45 (BD Biosciences, San Jose, CA), and mouse monoclonal NP57 neutrophil elastase (Lab Vision, Fremont, CA) stainings no pretreatments were needed, and stainings were performed using Innogenex IHC kit (San Ramon, CA).

Angiogenesis Assays

Corneal neovascularization assays were performed. Vessel length was the length of the vessels from the limbal vessel to the pellet. Vessel sprouting was measured as clock hours, the contiguous circumferential zone of the neovascularization, using a 360° reticule (where 30° of arc equals one clock hour). Vessel area was determined using the formula $0.2\pi\times$vessel length$\times$clock hours of vessels [66].

For *in vivo* Miles permeability assay, PPARα WT and KO mice received an intravenous injection with 0.5% Evans blue dye (100 μl) retro-orbitally. After ten minutes, the mice were given intradermal injections (50 μl) into the dorsal skin or ear at 2 different sites, consisting of vehicle control or VEGF (50 ng; R&D Systems Inc., Minneapolis, MN). Twenty minutes later the dorsal skin and/or ears were harvested for densitometric analysis to quantify dye leakage. Columns represent mean±standard deviation (n = 6 mice per group; experiments were performed three times).

Transplantation of Bone Marrow Stem Cells

PPARα WT and KO recipient mice were lethally irradiated with 14 Gy (in a split dose, 4 hours apart) 24 hours before bone marrow transplantation (BMT). Bone marrow cells (1×10^6) were injected retro-orbitally into recipient mice under isoflurane anesthesia. Neomycin sulfate antibiotic (2 mg/ml) was administered for two weeks post BMT in the drinking water. Mice recovered for a minimum of 2–3 months prior to tumor implantation.

Western Blot Analysis

For preparation of tumor lysates from PPARα WT and KO mice, B16BL6 tumors were homogenized with protease inhibitor (Roche, Germany). Total protein extracts (50 μg) were analyzed on blots incubated with primary mouse monoclonal TSP-1 (Ab-11, Lab Vision, Fremont, CA) and HRP-conjugated secondary antibodies (Amersham Biosciences Corp. Piscataway, NJ). A positive control for TSP-1 was obtained from exponentially growing HUVECs. For isolation of leukocytes, peripheral blood of PPARα WT and KO mice was obtained by retro-orbital bleeding under isoflurane anesthesia, red cells were cleared by incubating samples for 30 minutes on ice in red blood cell lysis buffer (Sigma-Aldrich, St. Louis, MO). Leukocytes were lysed in 100 μl of a solution consisting of 20 mmol/L imidazole hydrochloride, 100 mmol/L KCl, 1 mmol/L MgCl, 1 mmol/L EGTA, 1% Triton X-100, 10 mmol/L NaF, 1 mmol/L sodium molybdenate, 1 mmol/L EDTA and protease inhibitor cocktail [67].

TSP-1 ELISA

TSP-1 was measured by ELISA (Cytimmune, Rockville, MD) in blood plasma collected from non-tumor bearing PPARα WT and KO mice. Blood was collected via retro-orbital puncture.

Statistical Analyses

Statistical ananlyses were performed by Student's *t* test. The results were considered statistically significant for $p<0.05$.

SUPPORTING INFORMATION

Figure S1 Tumor angiogenesis is inhibited in the cornea of PPARα KO mice. PPARα WT and KO host mice were implanted with tumor pieces (1 mm3) as indicated. (A) Comparison of PPARα(+/+)MEF/RS and PPARα(−/−)MEF/RS in WT mice day 9 and day 16. (B) PPARα(+/+)MEF/RS and PPARα(−/−)MEF/RS in PPARα KO day 9 and day 16. The angiogenic response of PPARα(−/−)MEF/RS in PPARα KO mice regressed by day 16. (C) Lewis Lung Carcinoma (LLC) in PPARα WT and KO, C3H/HeJ and Balb/cJ on day 12. LLC tumors induced tumor angiogenesis independent of host haplotype. Therefore, major histo-incompatibility (MHC) does not prevent tumor-induced neovascularization and tumor growth. In contrast, LLC tumors failed to trigger any angiogenic response in PPARα KO host. (D) B16-BL6 melanoma in PPARα WT and KO on day 16. (E) Histology of B16-BL6 melanoma in the cornea of PPARα WT and KO mice. Scale bars, 500 μm (left) and 100 μm (right) (F) Leukocyte (CD45, brown) staining of LLC tumors in the cornea of PPARα WT and KO mice. Scale bar, 100 μm.
Found at: doi:10.1371/journal.pone.0000260.s001 (8.59 MB AI)

Figure S2 (A) FACS analysis demonstrates % of CD45.1 host cells. In our bone marrow transplantation protocol, >90% of the hematopoietic system of the host was derived from the donor marrow (as proved by using CD45.1 mice as recipients and PPARα KO mice that are CD45.2 as donors). (B) Panleukocyte (CD45, brown) and neutrophil elastase (red) staining in PPARα(−/−)MEF/RS tumors in PPARα WT (day 25) and PPARα KO mice (day 55). Scale bar, 500 μm. (C) FACS analysis demonstrates granulocyte depletion in PPARα KO mice. (D) TSP-1 expression (brown) in B16-F10 (day 30) and PPARα(−/−)MEF/RS (day 60) tumors in PPARα KO and WT mice as determined by immunohistochemical staining. Scale bars, 100μm and 500 μm, respectively.
Found at: doi:10.1371/journal.pone.0000260.s002 (5.12 MB TIF)

Text S1 Genetic Background and Transplantation Immunity.
Found at: doi:10.1371/journal.pone.0000260.s003 (0.05 MB DOC)

ACKNOWLEDGMENTS

We thank Deborah Freedman, Carmen Barnes, Michel Aguet, Thomas Boehm and Walter Wahli for helpful discussions in preparing the manuscript. We thank William Hahn for Large T- antigen and H-ras constructs. The excellent technical assistance of Andrea Laforme and Ricky Sanchez is acknowledged. We thank Kristin Johnson for photography.

Author Contributions

Conceived and designed the experiments: SH DP AK. Performed the experiments: SH DP AK. Analyzed the data: SH DP AK. Contributed reagents/materials/analysis tools: SH. Wrote the paper: SH DP AK. Other: Participated in designing the studies and data analysis and participated in the intellectual input and discussions with AK and DP, and contributed to the writing of the paper: JF. Participated in designing the studies and data analysis and participated in the intellectual input and discussions with AK and DP and contributed to the writing of the paper: SH. Participated in designing all bone marrow transplantation and antibody depletion studies and performed the and contributed to the writing of the paper: GM. Participated in data analysis and the intellectual input and discussions with AK and DP: MK. Participated in designing the corneal assays and performed them: CB. Participated in designing all the metastasis assays and performed them: DB. Participated in designing the bone marrow transplantation experiments and the intellectual input and discussions with GM: RM.

REFERENCES

1. Bhowmick NA, Neilson EG, Moses HL (2004) Stromal fibroblasts in cancer initiation and progression. Nature 432: 332–337.
2. Lin EY, Pollard JW (2004) Role of infiltrated leucocytes in tumour growth and spread. Br J Cancer 90: 2053–2058.
3. de Visser KE, Eichten A, Coussens LM (2006) Paradoxical roles of the immune system during cancer development. Nat Rev Cancer 6: 24–37.
4. Kammertoens T, Schuler T, Blankenstein T (2005) Immunotherapy: target the stroma to hit the tumor. Trends Mol Med 11: 225–231.

5. Zhang L, Conejo-Garcia JR, Katsaros D, Gimotty PA, Massobrio M, et al. (2003) Intratumoral T cells, recurrence, and survival in epithelial ovarian cancer. N Engl J Med 348: 203–213.
6. Pikarsky E, Porat RM, Stein I, Abramovitch R, Amit S, et al. (2004) NF-kappaB functions as a tumour promoter in inflammation-associated cancer. Nature 431: 461–466.
7. Staels B, Koenig W, Habib A, Merval R, Lebret M, et al. (1998) Activation of human aortic smooth-muscle cells is inhibited by PPARalpha but not by PPARgamma activators. Nature 393: 790–793.
8. Devchand PR, Keller H, Peters JM, Vazquez M, Gonzalez FJ, et al. (1996) The PPARalpha-leukotriene B4 pathway to inflammation control. Nature 384: 39–43.
9. Gonzalez FJ (2002) The peroxisome proliferator-activated receptor alpha (PPARalpha): role in hepatocarcinogenesis. Mol Cell Endocrinol 193: 71–79.
10. Peters JM, Cattley RC, Gonzalez FJ (1997) Role of PPAR alpha in the mechanism of action of the nongenotoxic carcinogen and peroxisome proliferator Wy-14,643. Carcinogenesis 18: 2029–2033.
11. Hays T, Rusyn I, Burns AM, Kennett MJ, Ward JM, et al. (2005) Role of peroxisome proliferator-activated receptor-alpha (PPARalpha) in bezafibrate-induced hepatocarcinogenesis and cholestasis. Carcinogenesis 26: 219–227.
12. Collett GP, Betts AM, Johnson MI, Pulimood AB, Cook S, et al. (2000) Peroxisome proliferator-activated receptor α is an androgen-responsive gene in human prostate and is highly expressed in prostatic adenocarcinoma. Clin Canc Res 6: 3241–3248.
13. Thuillier P, Anchiraico GJ, Nickel KP, Maldve RE, Gimenez-Conti I, et al. (2000) Activators of peroxisome proliferator-activated-α partially inhibit mouse skin tumor promotion. Mol Carcinog 29: 134–142.
14. Michalik L, Desvergne B, Tan NS, Basu-Modak S, Escher P, et al. (2001) Impaired skin wound healing in peroxisome proliferator-activated receptor (PPAR)alpha and PPARbeta mutant mice. J Cell Biol 154: 799–814.
15. Tordjman K, Bernal-Mizrachi C, Zemany L, Weng S, Feng C, et al. (2001) PPARalpha deficiency reduces insulin resistance and atherosclerosis in apoE-null mice. J Clin Invest 107: 1025–1034.
16. Serrano M, Lin AW, McCurrach ME, Beach D, Lowe SW (1997) Oncogenic ras provokes premature cell senescence associated with accumulation of p53 and p16INK4a. Cell 88: 593–602.
17. Lyden D, Young AZ, Zagzag D, Yan W, Gerald W, et al. (1999) Id1 and Id3 are required for neurogenesis, angiogenesis and vascularization of tumour xenografts. Nature 401: 670–677.
18. Achilles EG, Fernandez A, Allred EN, Kisker O, Udagawa T, et al. (2001) Heterogeneity of angiogenic activity in a human liposarcoma: a proposed mechanism for "no take" of human tumors in mice. J Natl Cancer Inst 93: 1075–1081.
19. Udagawa T, Fernandez A, Achilles EG, Folkman J, D'Amato RJ (2002) Persistence of microscopic human cancers in mice: alterations in the angiogenic balance accompanies loss of tumor dormancy. Faseb J 16: 1361–1370.
20. Chang LK, Garcia-Cardeña G, Farnebo F, Fannon M, Chen EJ, et al. (2004) Dose-dependent response of FGF-2 for lymphangiogenesis. Proc Natl Acad Sci U S A 101: 11658–11663.
21. Seghezzi G, Patel S, Ren CJ, Gualandris A, Pintucci G, et al. (1998) Fibroblast growth factor-2 (FGF-2) induces vascular endothelial growth factor (VEGF) expression in the endothelial cells of forming capillaries: an autocrine mechanism contributing to angiogenesis. J Cell Biol 141: 1659–1673.
22. Miles AA, Miles EM (1952) Vascular reactions to histamine, histamine-liberator and leukotaxine in the skin of guinea-pigs. J Physiol 118: 228–257.
23. Dvorak HF (2002) Vascular permeability factor/vascular endothelial growth factor: a critical cytokine in tumor angiogenesis and a potential target for diagnosis and therapy. J Clin Oncol 20: 4368–4380.
24. Coussens LM, Werb Z (2002) Inflammation and cancer. Nature 420: 860–867.
25. Sparmann A, Bar-Sagi D (2004) Ras-induced interleukin-8 expression plays a critical role in tumor growth and angiogenesis. Cancer Cell 6: 447–458.
26. Greten FR, Eckmann L, Greten TF, Park JM, Li ZW, et al. (2004) IKKbeta links inflammation and tumorigenesis in a mouse model of colitis-associated cancer. Cell 118: 285–296.
27. Delerive P, De Bosscher K, Besnard S, Vanden Berghe W, Peters JM, et al. (1999) Peroxisome proliferator-activated receptor alpha negatively regulates the vascular inflammatory gene response by negative cross-talk with transcription factors NF-kappaB and AP-1. J Biol Chem 274: 32048–32054.
28. Mansfield PJ, Boxer LA, Suchard SJ (1990) Thrombospondin stimulates motility of human neutrophils. J Cell Biol 111: 3077–3086.
29. Hamano Y, Sugimoto H, Soubasakos MA, Kieran M, Olsen BR, et al. (2004) Thrombospondin-1 associated with tumor microenvironment contributes to low-dose cyclophosphamide-mediated endothelial cell apoptosis and tumor growth suppression. Cancer Res 64: 1570–1574.
30. Lawler J, Detmar M (2004) Tumor progression: the effects of thrombospondin-1 and -2. Int J Biochem Cell Biol 36: 1038–1045.
31. Berger J, Moller DE (2002) Mechanism of action of PPARs. Ann Rev Med 53: 409–435.
32. Tanaka T, Kohno H, Yoshitani S, Takashima S, Okumuru A, et al. (2001) Ligands for peroxisome proliferator-activated receptors α and γ inhibit chemically induced colitis and formation of aberrant crypt foci in rats. Cancer Res 61: 2424–2428.
33. Neve BP, Fruchart JC, Staels B (2000) Role of the peroxisome proliferator-activated receptors (PPAR) in atherosclerosis. Biochem Pharmacol 60: 1245–1250.
34. Li AC, Brown KK, Silvestre MJ, Wilson TM, Palinski W, et al. (2000) Peroxisome proliferator-activated receptor γ ligands inhibit development of atherosclerosis in LDL receptor-deficient mice. J Clin Invest 106: 523–531.
35. Komuves LG, Hanley K, Lefebvre AM, Man MQ, Ng DC, et al. (2000) Stimulation of PPARalpha promotes epidermal keratinocyte differentiation in vivo. J Invest Dermatol 115: 353–360.
36. Anderson SP, Yoon L, Richard EB, Dunn CS, Cattley RC, et al. (2002) Delayed liver regeneration in peroxisome proliferator-activated receptor-alpha-null mice. Hepatology 36: 544–554.
37. Lee SS, Pineau T, Drago J, Lee EJ, Owens JW, et al. (1995) Targeted disruption of the alpha isoform of the peroxisome proliferator-activated receptor gene in mice results in abolishment of the pleiotropic effects of peroxisome proliferators. Mol Cell Biol 15: 3012–3022.
38. Cattley RC, DeLuca J, Elcombe C, Fenner-Crisp P, Lake BG, et al. (1998) Do peroxisome proliferating compounds pose a hepatocarcinogenic hazard to humans? Regul Toxicol Pharmacol 27: 47–60.
39. Bornstein P (2001) Thrombospondins as matricellular modulators of cell function. J Clin Invest 107: 929–934.
40. de Fraipont F, Nicholson AC, Feige JJ, Van Meir EG (2001) Thrombospondins and tumor angiogenesis. Trends Mol Med 7: 401–407.
41. Short SM, Derrien A, Narsimhan RP, Lawler J, Ingber DE, et al. (2005) Inhibition of endothelial cell migration by thrombospondin-1 type-1 repeats is mediated by beta1 integrins. J Cell Biol 168: 643–653.
42. Esemuede N, Lee T, Pierre-Paul D, Sumpio BE, Gahtan V (2004) The role of thrombospondin-1 in human disease. J Surg Res 122: 135–142.
43. Lawler J, Weinstein R, Hynes RO (1988) Cell attachment to thrombospondin: the role of ARG-GLY-ASP, calcium, and integrin receptors. J Cell Biol 107: 2351–2361.
44. Streit M, Velasco P, Brown LF, Skobe M, Richard L, et al. (1999) Overexpression of thrombospondin-1 decreases angiogenesis and inhibits the growth of human cutaneous squamous cell carcinomas. Am J Pathol 155: 441–452.
45. Weinstat-Saslow DL, Zabrenetzky VS, VanHoutte K, Frazier WA, Roberts DD, et al. (1994) Transfection of thrombospondin 1 complementary DNA into a human breast carcinoma cell line reduces primary tumor growth, metastatic potential, and angiogenesis. Cancer Res 54: 6504–6511.
46. Wang TN, Qian XH, Granick MS, Solomon MP, Rothman VL, et al. (1996) Inhibition of breast cancer progression by an antibody to a thrombospondin-1 receptor. Surgery 120: 449–454.
47. Crawford SE, Flores-Stadler EM, Huang L, Tan XD, Ranalli M, et al. (1998) Rapid growth of cutaneous metastases after surgical resection of thrombospondin-secreting small blue round cell tumor of childhood. Hum Pathol 29: 1039–1044.
48. Wang TN, Qian X, Granick MS, Solomon MP, Rothman VL, et al. (1996) Thrombospondin-1 (TSP-1) promotes the invasive properties of human breast cancer. J Surg Res 63: 39–43.
49. Albo D, Berger DH, Tuszynski GP (1998) The effect of thrombospondin-1 and TGF-beta 1 on pancreatic cancer cell invasion. J Surg Res 76: 86–90.
50. Tuszynski GP, Smith M, Rothman VL, Capuzzi DM, Joseph RR, et al. (1992) Thrombospondin levels in patients with malignancy. Thromb Haemost 67: 607–611.
51. Nathan FE, Hernandez E, Dunton CJ, Treat J, Switalska HI, et al. (1994) Plasma thrombospondin levels in patients with gynecologic malignancies. Cancer 73: 2853–3858.
52. Yamashita Y, Kurohiji T, Tuszynski GP, Sakai T, Shirakusa T (1998) Plasma thrombospondin levels in patients with colorectal carcinoma. Cancer 82: 632–638.
53. Grossfeld GD, Ginsberg DA, Stein JP, Bochner BH, Esrig D, et al. (1997) Thrombospondin-1 expression in bladder cancer: association with p53 alterations, tumor angiogenesis, and tumor progression. J Natl Cancer Inst 89: 219–227.
54. Ohta Y, Shridhar V, Kalemkerian GP, Bright RK, Watanabe Y, et al. (1999) Thrombospondin-1 expression and clinical implications in malignant pleural mesothelioma. Cancer 85: 2570–2576.
55. Mehta R, Kyshtoobayeva A, Kurosaki T, Small EJ, Kim H, et al. (2001) Independent association of angiogenesis index with outcome in prostate cancer. Clin Cancer Res 7: 81–88.
56. Oshiba G, Kijima H, Himeno S, Kenmochi T, Kise Y, et al. (1999) Stromal thrombospondin-1 expression is correlated with progression of esophageal squamous cell carcinomas. Anticancer Res 19: 4375–4378.
57. Motegi K, Harada K, Pazouki S, Baillie R, Schor AM (2002) Evidence of a biphasic effect of thrombospondin-1 on angiogenesis. Histochem J 34: 411–421.
58. Slaton JW, Perrotte P, Inoue K, Dinney C, Fidler IJ (1999) Interferon-α-mediated down-regulation of angiogenesis-related genes and therapy of bladder cancer are dependent on optimization of biological dose and schedule. Clin Cancer Res 5: 2726–2734.
59. Panigrahy D, Singer S, Shen LQ, Butterfield CE, Freedman DA, et al. (2002) PPARγ ligands inhibit primary tumor growth and metastasis by inhibiting angiogenesis. J Clin Invest 110: 923–932.

60. Celik I, Surucu O, Dietz C, Heymach JV, Force J, et al. (2005) Therapeutic efficacy of endostatin exhibits a biphasic dose-response curve. Cancer Res 65: 11044–11050.
61. Hadley C (2003) What doesn't kill you makes you stronger. A new model for risk assessment may not only revolutionize the field of toxicology, but also have vast implications for risk assessment. EMBO Rep 4: 924–926.
62. Tjin Tham Sjin RM, Naspinski J, Birsner AE, Li C, Chan R, et al. (2006) Endostatin therapy reveals a U-shaped curve for antitumor activity. Cancer Gene Ther..
63. Crommelin DJA, Sindelar RD (2002) Immunogenicity. In: Crommelin DJA, Sindelar RD, eds. Pharmaceutical biotechnology : an introduction for pharmacists and pharmaceutical scientists. 2nd ed. ed. New York: Routledge. pp. 125–127.
64. Dave SS, Wright G, Tan B, Rosenwald A, Gascoyne RD, et al. (2004) Prediction of survival in follicular lymphoma based on molecular features of tumor-infiltrating immune cells. N Engl J Med 351: 2159–2169.
65. Costet P, Legendre C, More J, Edgar A, Galtier P, et al. (1998) Peroxisome proliferator-activated receptor alpha-isoform deficiency leads to progressive dyslipidemia with sexually dimorphic obesity and steatosis. J Biol Chem 273: 29577–29585.
66. Kenyon BM, Voest EE, Chen CC, Flynn E, Folkman J, et al. (1996) A model of angiogenesis in the mouse cornea. Invest Ophthalmol Vis Sci 37: 1625–1632.
67. Joussen AM, Poulaki V, Qin W, Kirchhof B, Mitsiades N, et al. (2002) Retinal vascular endothelial growth factor induces intercellular adhesion molecule-1 and endothelial nitric oxide synthase expression and initiates early diabetic retinal leukocyte adhesion in vivo. Am J Pathol 160: 501–509.

Naumov GN, Folkman J. Strategies to prolong the nonangiogenic dormant state of human cancer. In: Davis DW, Herbst RS, Abbruzzese JL, eds.
Antiangiogenic Cancer Therapy, CRC Press, Boca Raton, FL, 2008; pp 3-21

1 Strategies to Prolong the Nonangiogenic Dormant State of Human Cancer

George N. Naumov and Judah Folkman

CONTENTS

1.1 CLINICAL "LATENCY" IN CANCER RECURRENCE FOLLOWING A PRIMARY TUMOR TREATMENT

Cancer recurrence after treatment of the primary tumor is a major cause of mortality among cancer patients. It may take years to decades before local or distant (i.e., metastatic) recurrence becomes clinically detectable as cancer. This "disease-free" period is a time of uncertainty for patients who appear "cured." For example, Demicheli et al.[1] have demonstrated two hazardous peaks of breast cancer recurrence in patients undergoing mastectomy alone without adjuvant therapy. In a group of 1173 patients, the first peak of cancer recurrence occurred at ~18 months after surgery. A second peak in cancer recurrence developed at ~5 years after surgery and was associated with a plateau-like tail extending up to 15 years.[1] Patients experiencing cancer recurrences within 5 years following surgery have a shorter overall survival than those with recurrences occurring at a later time point.[2]

Similar "latency periods" in cancer recurrence have been documented since the beginning of the twentieth century. Rupert A. Willis has summarized the "time elapsing between the excision of a human malignant tumor and the appearance of a clinically recognizable recurrence" for a variety of human cancers. For example, the latency period in breast cancer patients can be from 6 to 20 years; cutaneous and ocular melanoma, 14 to 32 years; kidney carcinoma,

6 to 8 years; and stomach and colon carcinoma, 5 to 6 years.[3] Moreover, Willis was the first to realize that these latency periods do not correspond with the natural progression of cancer, and he introduced the concept of a "dormant cancer cell" as a possible explanation.

Over the past few years, several hypotheses have been proposed in an attempt to explain the phenomenon of human tumor dormancy. Initially, it was proposed that tumor cells enter a prolonged state of mitotic arrest.[4,5] Others hypothesized that tumor size is controlled by the immune system[6–11] or hormonal deprivation in hormone-dependent tumors.[11–13] In 1972, Folkman and Gimbrone demonstrated that dormancy in human tumors could be due to blocked angiogenesis. In the following years, Folkman and colleagues have presented evidence supporting the concept that most human tumors arise without angiogenic activity and exist in a microscopic dormant state for months to years without neovascularization.[14] Such protection may be attributed in part to host-derived factors, which prevent microscopic tumors from switching to the angiogenic phenotype.

1.2 ANGIOGENESIS DEPENDENCE OF TUMOR GROWTH

Cancer progression is a multistep process (Figure 1.1). With each step, the genetic and epigenetic events in the process become increasingly complex and may be more difficult to

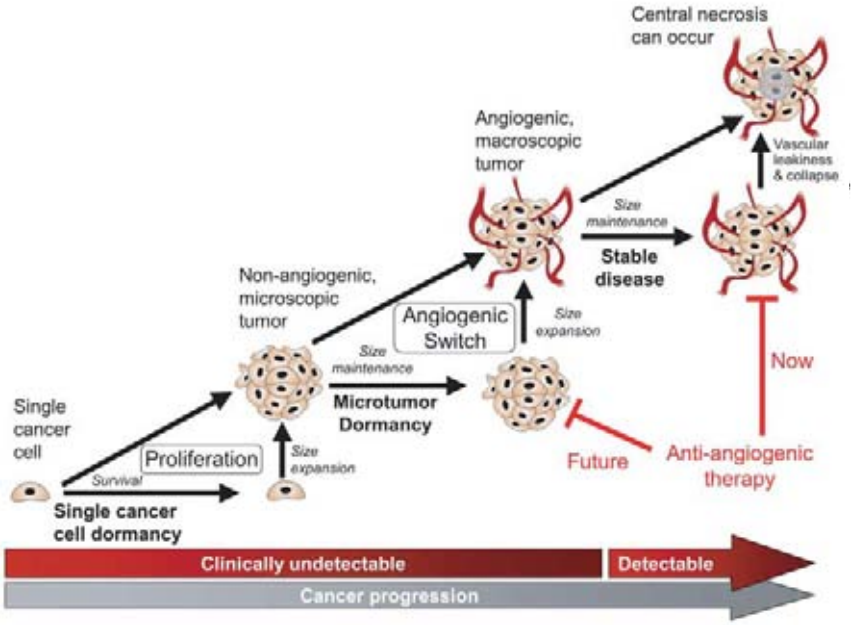

FIGURE 1.1 (See color insert following page 558.) Rate-limiting steps in the tumor progression. Solitary nonproliferating, dormant cancer cells can persist for long periods of time, until they come out of G_0 arrest and start to proliferate. Tumor mass can expand only to a microscopic mass without the recruitment of new blood vessels. Human cancers can remain nonangiogenic and dormant for long periods of time, delaying the tumor progression process. During this microscopic dormant state, nonangiogenic tumors are actively proliferating and undergoing apoptosis. Nonangiogenic tumors can expand in mass after undergoing the angiogenic switch and recruitment of new blood vessels. Angiogenic macroscopic tumors that do not expand in mass are known as "stable disease," although angiogenic tumors can remain at a constant size for prolonged periods of time. Current antiangiogenic therapy targets angiogenic microscopic and macroscopic tumors. However, future antiangiogenic therapy will target nonangiogenic microscopic tumors with the aim of keeping them in a dormant state by preventing the angiogenic switch.

treat. As the cancer progresses from a single neoplastic cell to a large, lethal tumor, it acquires a series of mutations, becoming: (1) self-sufficient in growth signaling, by oncogene activation and loss of tumor suppressor genes, (2) insensitive to antigrowth signaling, (3) unresponsive to apoptotic signaling, (4) capable of limitless cell replications, and (5) tumorigenic and metastatic.[15] Current experimental and clinical evidence indicates that these neoplastic properties may be necessary, but not sufficient, for a cancer cell to progress into a population of tumor cells, which becomes clinically detectable, metastatic, and lethal. For a tumor to develop a highly malignant and deadly phenotype, it must first recruit and sustain its own blood supply, a process known as tumor angiogenesis.[16,17]

For more than a century, it has been observed that surgically removed tumors are hyperemic compared to normal tissues.[18,19] Generally, this phenomenon was explained as simple dilation of existing blood vessels induced by tumor factors. However, Ide et al.[20] demonstrated that tumor-associated hyperemia could be related to new blood vessel growth, and vasodilation may not be the sole explanation for this phenomenon. They showed that when a wound induced in a transparent rabbit ear chamber completely regressed, the implantation of a tumor in the chamber resulted in the growth of new capillary blood vessels.[20] These initial observations were later confirmed by Algire et al.,[21,22] demonstrating that new vessels in the periphery of a tumor implant arose from preexisting host vessels, and not from the tumor implant itself. At the time, this novel concept of tumor-induced neovascularization was generally attributed to an inflammatory reaction, thought to be a side effect of tumor growth, and it was not perceived as a requirement for tumor growth.[23]

In the early 1960s, Folkman and Becker observed that tumor growth in isolated perfused organs was severely restricted in the absence of tumor vascularization.[24–28] In 1971, Folkman proposed the hypothesis that tumor growth is angiogenesis-dependent.[16] This hypothesis suggested that tumor cells and vascular endothelial cells within a neoplasm may constitute a highly integrated, two-compartment system, which dictates tumor growth. This concept indicated that endothelial cells may switch from a resting state to a rapid growth phase because of "diffusible" signals secreted from the tumor cells. Moreover, Folkman proposed that angiogenesis could be a relevant target for tumor therapy (i.e., antiangiogenic therapy).

We now know that angiogenesis plays an important role in numerous physiologic and pathologic processes. The hallmark of pathologic angiogenesis is the persistent growth of blood vessels. Sustained neovascularization can continue for months or years during the progression of many neoplastic and nonneoplastic diseases.[29,30] However, tumor angiogenesis is rarely, if ever, downregulated spontaneously. The fundamental objective of antiangiogenic therapy is to inhibit the progression of pathologic angiogenesis. In contrast, the goal of antivascular therapy is to rapidly occlude new blood vessels so that the blood flow stops. Both therapeutic approaches target the ability of tumors to progress from the nonangiogenic to the angiogenic phenotype, a process termed the "angiogenic switch."[31,40]

Cancer usually becomes clinically detectable only after tumors have become angiogenic and have expanded in mass. Failure of a tumor to recruit new vasculature or to reorganize the existing surrounding vasculature results in a nonangiogenic tumor, which is microscopic in size and unable to increase in mass (Figure 1.1). Without new blood supply, microscopic tumors are usually restricted to a size of <1–2 mm in diameter and are highly dependent on surrounding blood vessels for oxygen and nutrient supply. At sea level, the diffusion limit of oxygen is ~100 μm.[32] Therefore, all mammalian cells, including neoplastic cells, are required to be within 100–200 μm of a blood vessel. As nonangiogenic tumors attempt to expand in mass, attributed to uncontrolled cancer cell proliferation, some tumor cells fall outside the oxygen diffusion limit and become hypoxic. It is well known that hypoxic conditions induce a set of compensatory responses within cancer cells, such as increased transcription of the

hypoxia-inducible factor (HIF). Subsequently, this hypoxic signaling leads to upregulation of proangiogenic proteins, such as vascular endothelial growth factor (VEGF), platelet-derived growth factor (PDGF), and nitric oxide synthase (NOS).[33] The angiogenic switch in tumors is presumed to be closely regulated by the presence of pro- and antiangiogenic proteins in the tumor microenvironment. An increase in the local concentration of proangiogenic proteins allows angiogenesis to occur and ultimately permits a tumor to expand in mass. Antiangiogenic therapy offers a fourth anti-cancer modality, in addition to conventional therapeutic approaches, which target well-established and genetically unstable tumors.

1.3 EXPERIMENTAL MODELS OF HUMAN TUMOR DORMANCY

As early as the 1940s, experimental systems involving the transplantation of tumor pieces in isolated perfused organs and in the anterior chamber of the eyes of various species of animals have demonstrated the effects of neovascularization on tumor growth. Greene et al.,[34] observed that H-31 rabbit carcinoma tumor implanted into the eyes of guinea pigs did not vascularize and failed to grow for 16–26 months. During this period, the transplants measured ~2.5 mm in diameter. However, when the same tumors were reimplanted into their original host (i.e., rabbit eyes), they vascularized and grew to fill the anterior chamber within 50 days. Similarly, Folkman et al.[25] showed that in isolated perfused thyroid and intestinal segment tumors, implants grew and arrested at a small size (2–3 mm diameter). This inability of neoplasms to evoke a new blood supply was later attributed to endothelial cell degeneration in the perfused organs that are perfused with platelet-free hemoglobin solution.[35] In 1972, Gimbrone et al.[36] provided in vivo evidence that the progressive growth of a homologous solid tumor can be deliberately arrested at a microscopic size when neovascularization is prevented. In these experiments, two comparable tumor pieces were implanted in each eye of the same animal: one directly on the iris (i.e., angiogenic milieu) and the other suspended in the anterior chamber (i.e., avascular milieu) in the opposing eye. The vascularized tumor implanted on the iris grew to a size 15,000 times the initial volume and filled the anterior chamber of the rabbit eye within 14 days. In contrast, the tumor implant in the avascular anterior chamber remained avascular, and by day 14 after implantation, had only increased by 4 times its initial volume. These "dormant" tumors remained at a size of ~1 mm in diameter for up to 44 days. During this period, the tumors developed a central necrotic core surrounded by a layer of viable tumor cells, in which mitotic figures were observed. Overall, these microscopic tumors remained avascular, as demonstrated through microscopic and histological analyses and fluorescein tests. The malignant growth potential of these microscopic tumors was demonstrated in vivo by reimplanting the tumors directly on the irises of fresh animals. In the irises, the dormant tumors became vascularized and grew rapidly until the anterior chambers of the eyes were filled with tumor, in a manner similar to the control iris implants. These fundamental observations established the relationship between tumor growth and angiogenesis. Moreover, they provided an in vivo experimental model for further investigations of tumor dormancy.

One of the most pressing questions at that time was whether tumor-induced angiogenesis could be inhibited, preventing dormant tumors from progressing to the angiogenic phenotype. Using a V2 rabbit carcinoma in the corneal implant animal model, Brem et al.,[37] demonstrated that tumor angiogenesis could be blocked by diffusible proteins from the cartilage of newborn rabbits. The coimplants of tumor and cartilage pieces completely prevented vascularization in 28% of tumors and significantly delayed the vascularization in the remaining tumors, which eventually became vascularized. In addition, cartilage pieces inhibited vessel formation around a tumor implant in the chorioallantoic membrane (CAM) of chick embryos. The inhibitory proteins found in cartilage were later identified, isolated, and characterized as tissue inhibitors of metalloproteinases (TIMPs).[37a] Subsequently, other

angiogenesis inhibitors were identified. Endostatin and angiostatin were discovered as internal peptide fragments of plasminogen and 20 kDa C-terminal fragments of collagen XVIII, respectively.[38,39]

A spontaneous tumor dormancy model in transgenic mice was described by Hanahan and Folkman,[40] in which autochthonous tumors arise in the pancreatic islets as a result of simian virus 40 T antigen (Tag) oncogene expression. In this experimental model, only 4% of tumors become angiogenic after 13 weeks. In contrast, the remaining 96% of pancreatic islet tumors remain microscopic and nonangiogenic.[40,41] The spontaneous progression of non-angiogenic lesions to the angiogenic phenotype in these transgenic tumor-bearing mice led to the development of the "angiogenic switch" concept.[40]

More recently, Achilles et al.[42] reported that human cancers contain subpopulations that differ in their angiogenic potential. These findings suggested that the angiogenic phenotype of a human tumor cell may be controlled by genetic and epigenetic mechanisms. Therefore, human tumors can contain both angiogenic and nonangiogenic tumor cell populations, characterized by their in vivo ability to recruit new blood vessels to a tumor. However, the factors involved in the proportional regulation of these two tumor cell populations are still unknown. The observed heterogeneity of angiogenic activity among human tumor cells allowed for the isolation of these two populations of cancer cells and the development of new and fruitful human tumor dormancy experimental models.

Single-cell cloning of a human tumor cell line was employed as a strategy for the isolation of angiogenic and nonangiogenic tumor cell populations.[42] Achilles et al. established and selected subclones from a human liposarcoma cell line (SW-872) based on high, intermediate, or low proliferation rates in vitro. These clones were expanded in vitro into a population of tumor cells and were then inoculated into immunodeficient (SCID) mice. Three different growth patterns were observed: (1) highly angiogenic and rapidly growing tumors, (2) weakly angiogenic and slowly growing tumors, and (3) nonangiogenic and dormant tumors. In a subsequent experiment, Almog et al.[43] demonstrated that the nonangiogenic tumors spontaneously switch to the angiogenic phenotype and initiate exponential growth ~130 days after subcutaneous inoculation.[43] During the 130 day dormancy period, microscopic (~1–2 mm in diameter) tumors remain avascular and are virtually undetectable by palpation. Because this animal dormancy model was based on the in vitro tumor cell proliferation differences between the angiogenic and nonangiogenic liposarcoma clones, it raised two fundamental questions: (1) Is there a correlation between tumor cell proliferation and angiogenic potential? (2) Can the observed differences in tumor growth be recapitulated using populations of human tumor cells that have not been cloned?

To address these questions, human tumor cell lines were obtained from the American Type Culture Collection (ATCC, Manassas, VA) based on their "no take" phenotype in immunodeficient mice. These cell lines were assessed for in vivo tumor growth over extended time periods. Following a subcutaneous inoculation of a tumor cell suspension, mice were monitored for palpable tumors at the site of inoculation for more than a year (i.e., about half the normal life span of a mouse) and, sometimes, for the life of the animal. Some of the mice inoculated with the "no take" tumor cells spontaneously formed palpable tumors after a dormancy period, which varied from months to more than a year, depending on cancer type (Figure 1.2). With time, tumors became angiogenic, and palpable, expanded in mass exponentially, and within ~50 days of first detection, killed the host animal. Stable cell lines were established from representative angiogenic tumors. When reinoculated into SCID mice, these angiogenic tumor cells formed large (>1 cm in diameter) tumors within a month following inoculation (i.e., without a dormancy period), in 100% of the inoculated mice. It was found that each cancer type had a characteristic and predictable dormancy period and generated a consistent proportion of tumors that switched to the angiogenic phenotype. However, once nonangiogenic tumors switched to the angiogenic phenotype, they escaped

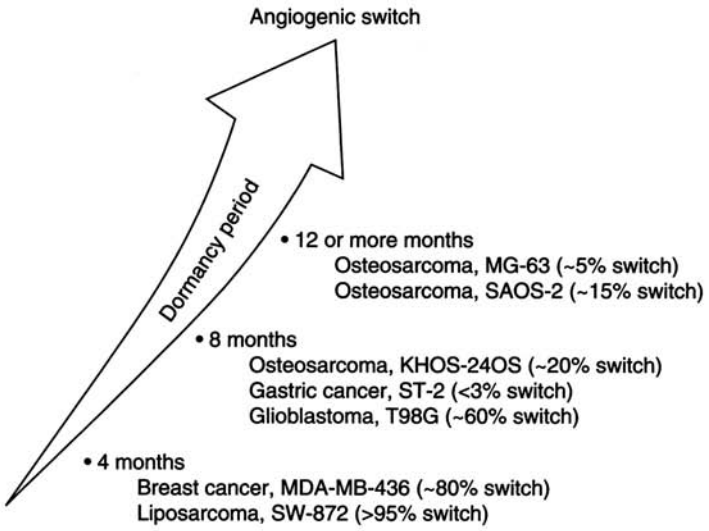

FIGURE 1.2 Human tumor cell lines that spontaneously switch to the angiogenic phenotype after a prolonged dormancy period in immunodeficient mice. The percent of mice that switch to the angiogenic phenotype is shown in brackets and varies between human tumor types.

from the dormancy state and formed lethal tumors in 100% of the mice, regardless of cancer type. At this time, tumor cell population–based animal dormancy models have been developed and characterized for breast cancer, osteosarcoma, and glioblastoma (Figure 1.2).[44] In contrast to the single-cell-derived human liposarcoma animal model, the angiogenic and the nonangiogenic tumor cell populations of the rest of the animal models were derived by in vivo selection for the angiogenic and nonangiogenic phenotypes. These in vivo models of nonangiogenic human tumors permit analysis of the switch to the angiogenic phenotype, and make it possible to address the question of whether the switch can be bi-directional.

1.4 DORMANT TUMORS HAVE BALANCED PROLIFERATION AND APOPTOSIS

After inoculation in animals, human tumor cells can remain dormant for more than a year. However, this does not mean that the tumor cells are in G_0 arrest. Although some tumor cells might be in mitotic arrest, as demonstrated in some tumor dormancy models,[45–47] we reported that the majority of tumor cells are proliferating or undergoing apoptosis. The tumor cell proliferation index in nonangiogenic tumors can be as high as that of large, vascularized tumors. In a human breast cancer (MDA-MB-436) animal model, more than 50% of tumor cells were proliferating and more than 10% were undergoing apoptosis in all microscopic tumors analyzed at various time points during dormancy, as well as in all macroscopic angiogenic tumors.[44] In a different human osteosarcoma (MG-63 and SAOS-2) and gastric (ST-2) cancer dormancy models, microscopic tumors were unable to grow beyond a threshold size of ~1–2 mm in diameter. Within these nonangiogenic tumors, there appears to be a balance between proliferating cells and cells undergoing apoptosis.[48] Tumor cell proliferation in these tumors was ~12%, and tumor cell apoptosis ranged from 4% to 7.5%.

1.5 DEFINITION OF A HUMAN DORMANT TUMOR BASED ON EXPERIMENTAL ANIMAL MODELS

Based on xenograft models of various human tumors inoculated or surgically implanted into immunodeficient animals, a "dormant" tumor can be defined by its microscopic size and nonexpanding mass. In contrast, a "stable" tumor is macroscopic and expanding in mass. In more detail, we define human nonangiogenic tumors as:

1. Unable to induce angiogenic activity, by repulsion of existing blood vessels in the local stroma and/or relative absence of intratumoral microvessels.
2. Remain harmless to the host until they switch to the angiogenic phenotype (i.e., may remain harmless for 1 year or more, which is half the life span of a mouse).
3. Express equal or more antiangiogenic (i.e., thrombospondin-1) than angiogenic (i.e., VEGF, bFGF) proteins.
4. Grow in vivo to ~1 mm in diameter or less, at which time further expansion ceases.
5. Only visible with a hand lens or a dissecting microscope (5–10 × magnification).
6. White or transparent by gross examination.
7. Unable to spontaneously metastasize from the microscopic dormant state.
8. Show active tumor cell proliferation and apoptosis in mice and remain metabolically active during the dormancy period.
9. Can be cloned from a human angiogenic tumor, because human tumors are heterogeneous and contain a mixture of nonangiogenic and angiogenic tumor cells.

In contrast, angiogenic human tumors (as observed in our animal models) are defined as:

1. Able to induce angiogenic activity, by recruiting blood vessels form the surrounding stroma and/or forming new blood vessels within the tumor tissue.
2. Lethal to the host in only few weeks.
3. Express significantly more angiogenic than antiangiogenic proteins.
4. Grow along an exponential curve until they kill the host.
5. Visible and easily detectable based on their macroscopic size.
6. Red by gross examination.
7. Can spontaneously metastasize to various organs.
8. Can be cloned from a human angiogenic tumor, because human tumors are heterogeneous and contain a mixture of nonangiogenic and angiogenic tumor cells.

1.6 IN VIVO IMAGING OF HUMAN DORMANT TUMORS

Traditionally, various in vivo imaging techniques have been used for the detection and quantification of tumors implanted orthotopically or ectopically (i.e., outside their orthotopic site). However, some of these techniques can be employed for the in vivo detection of microscopic dormant tumors. By definition, nonangiogenic, dormant tumors are microscopic in size. Therefore, they are usually undetectable by palpation (limited to tumor sizes 50 mm^3 and smaller) when located in the subcutaneous space or mammary fat pad. It is an even greater challenge to detect microscopic tumors located in internal organs. In the originally published dormancy model of osteosarcoma (MG-63), the presence of dormant tumors in a fraction of the inoculated mice was revealed through careful examination of the hair growth overlying the original tumor inoculation site.[48] The inner side of the skin in the area associated with hair growth contained a microscopic white lesion, from which a histology section showed a viable tumor. Although this detection method clearly reveals this interesting phenomenon, it is terminal (i.e., the animal has to be euthanized) and does not provide longitudinal quantitative information about the tumor size.

Stable infection of tumor cells with fluorescent proteins (such as green fluorescent protein [GFP] and red fluorescent protein [RFP]) or luciferase allows for in vivo longitudinal detection of tumors even at a microscopic size. GFP-expressing tumor cells can be visualized noninvasively from the skin surface by directed blue light (488 nm) epi-illumination. Submillimeter tumors can be localized using this method. The utility of fluorescence visualization of dormant tumors has been reported by Udagawa et al.,[48] using osteosarcoma (MG-63 and SAOS-2) and gastric cancer (ST-2) dormancy models. Tumor-associated blood vessels appear dark against the background of a fluorescent tumor tissue, allowing for morphological (e.g., vessel diameters, tortuousity, branching) and even functional (e.g., red blood cell velocity) quantification of angiogenesis.[49] More recently, this labeling technique was used to determine the minimum number of human tumor cells necessary to form a nonangiogenic, dormant microscopic tumor in mice (Naumov et al., unpublished). However, detecting fluorescently labeled tumors has its limitations. Microscopic tumors in internal organs can only be visualized ex vivo. Certain procedures, such as in vivo videomicroscopy, can be used for visualization of liver and lung metastases.[50,51] However, in the brain, excitation or emission of fluorescently labeled tumor cells is not only limited by tissue depth, but also by light penetration through the skull.

Infection of tumor cells with the luciferase reporter gene allows for the reliable detection in mice of a signal from tumors that are <1 mm in diameter (as verified by histology) in all internal organs, including the brain. Almog et al.[43] has used the luciferase method for the detection of dormant human liposarcoma tumors in the renal fat pad of mice. The method can also be used to monitor the growth of microscopic human glioblastomas stereotactically after tumor cells are inoculated in the brains of mice (Naumov et al., unpublished work). Following intravenous injection of the luciferine substrate, the enzymatic activity of luciferase is rapid and transient. Only viable and metabolically active tumor cells can be detected by luminescence. The transient effect of the enzymatic reaction allows for real-time detection of tumor cells and for monitoring their viability during the dormancy period, as well as at times throughout the angiogenic switch. The persistent luciferase signal during the dormancy period of microscopic human tumors confirms the previous conclusion (based on histology) that dormancy does not result from tumor cell cycle arrest or eradication. Although the intensity of the luciferase signal directly correlates with the size of tumor, this imaging modality does not provide a clear tumor boundary or an anatomical outline of the tumor. However, small animal magnetic resonance imaging (MRI) provides a clear anatomical definition of a microscopic tumor, and it can be effectively used in combination with luciferase imaging (Naumov et al., unpublished work). Recent reports have demonstrated that single cancer cells can be detected in a mouse brain using MRI.[52] Individual tumor cells trapped within the brain microcirculation were detected using MRI and validated using high-resolution confocal microscopy. Graham et al.[53] demonstrated that three-dimensional, high-frequency ultrasound can quantitatively monitor the growth of liver micrometastases as small as 0.5 mm in diameter.

Collectively, these recent advances in animal imaging modalities enable, in most cases, noninvasive, real-time, longitudinal observations of single cancer cell trafficking and detection of nonangiogenic microscopic tumors in vivo during the dormancy period and as they switch to the angiogenic phenotype. Quantitative imaging of tumors throughout their progression to the angiogenic phenotype can be used for evaluating the efficacy of antiangiogenic therapy in primary and metastatic tumors.

1.7 MOLECULAR MECHANISMS OF THE HUMAN ANGIOGENIC SWITCH

Transfection of human osteosarcoma (MG-63 and SAOS-2) and gastric cancer (ST-2) cells with activated c-*Ha-ras* oncogene induces loss of dormancy in otherwise nonangiogenic human cell lines.[48] When inoculated in immunosuppressed mice, wild-type (or control

vector-transfected) tumor cells did not form palpable tumors for more than 8 months. White tumor foci, which were avascular or contained sparse vessels, were found throughout the dormancy period at the site of inoculation. However, *ras*-transfected human osteosarcoma (MG-63 and SAOS-2) and gastric cancer (ST-2) cells formed vascularized large tumors within 1 month. The in vivo growth of *ras*-transfected tumor cells was associated with significantly increased angiogenic response, increased proliferation, and decreased apoptosis when compared with wild-type tumor cells. Loss of the dormant phenotype induced by activated *ras* correlated with increased levels (1.5 to 2.5-fold) of $VEGF_{165}$, as assessed in the conditioned media relative to the control tumor cells.[48] Overexpression of $VEGF_{165}$ in the tumor cells also resulted in a loss of dormancy and induced a robust angiogenic response in 30% of animals inoculated with gastric cancer and 40% of animals inoculated with osteosarcoma. In contrast to *ras*-transfected tumor cells, loss of dormancy in $VEGF_{165}$-transfected tumor cells was not associated with an increase in tumor cell proliferation, but was associated with reduced apoptosis. Therefore, the angiogenic response induced by $VEGF_{165}$ was found to be sufficient for the induction of a loss of dormancy by reducing apoptosis. Activation of *ras* can directly induce tumor cell proliferation and confer resistance to apoptosis.[54,55] In addition, *ras* activation can indirectly stimulate an angiogenic response in tumors by inducing proangiogenic proteins, such as VEGF,[56] and by downregulating angiogenesis inhibitors, such as thrombospondin.[57–60] Similar to *ras*, other oncogenes and tumor suppressor genes can indirectly affect tumor growth via an angiogenic mechanism. For example, *p53*, *PTEN*, and *Smad 4* have been shown to increase thrombospondin-1 expression by upregulation of *Tsp-1* gene or by increased mRNA expression.[12,61–63] Thrombospondin-1 expression can be decreased by *Myc*, *Ras*, *Id1*, *WT1*, c-*jun*, and v-*stc* via transcriptional repression, myc phosphorylation, or regulation of mRNA turnover and stability.[59,60,64–69] The inherently low toxicity of natural angiogenesis inhibitors, in addition to their selective effect on pathological neovascularization without harm to normal vasculature, makes them attractive therapeutic agents.

In addition to thrombospondin-1 regulation, the *p53* tumor suppressor gene regulates other currently unidentified inhibitors of angiogenesis.[70] Teodoro et al.[71] recently reported that wild-type *p53* mobilizes endostatin through a specific α(II) collagen prolyl-4-hydroxylase (α(II)PH gene product), which binds to *p53*. *p53* is inactivated in over 50% of all human tumors. Reintroduction of wild-type *p53* into mouse fibrosarcoma (T241) cells correlates with increased thrombospondin-1 expression and induces angiogenesis-restricted dormancy.[72] Inoculation of parental T241 fibrosarcoma cells into a mouse ear resulted in vascularized, visible tumors within 2 weeks. In contrast, when wild-type *p53* was introduced in the same cells, only 12% of the tumors became angiogenic 2 months after inoculation. Therefore, expression of wild-type *p53* resulted in the loss of an angiogenic phenotype. Loss of the angiogenic phenotype was also correlated with the upregulation of the mRNA-encoding thrombospondin-1. This experimental model demonstrated that *p53* can act as a tumor suppressor, independent of its direct effects on cell proliferation and survival. Moreover, *p53* had an indirect antitumor effect by inhibiting angiogenesis and increasing the rate of apoptosis.

In a recent report, Naumov et al.[44] compared the tumor cell secretion and intracellular levels of thrombospondin-1 in nonangiogenic and angiogenic tumor cell populations isolated from a human breast cancer cell line (MDA-MB-436). Angiogenic cells contain 2.5-fold higher levels of c-Myc and p-Myc than their nonangiogenic counterparts, as assessed by Western blot. In contrast, angiogenic tumor cells contain significantly lower levels of thrombospondin-1 than nonangiogenic tumor cells. Moreover, nonangiogenic human breast cancer cells secrete at least 20-fold higher levels of thrombospondin-1 than angiogenic cells. Similar findings were reported using a different human breast cancer cell line (MDA-MB-435).[60] Watnick et al.[60] reported that phosphoinositide 3-kinase (PI3K) can induce a signal transduction cascade leading to the phosphorylation of c-Myc and the subsequent repression of

thrombospondin-1. Treatment with LY294002 (a PI3K inhibitor) caused thrombospondin-1 levels within angiogenic cells to increase but had no effect on levels in nonangiogenic cells.[44] Therefore, the PI3K signaling pathway is responsible for the repression of thrombospondin-1, and it is regulated differently in angiogenic and nonangiogenic human tumor cells.

1.8 INDUCTION OF TUMOR DORMANCY USING ANTIANGIOGENIC THERAPY

Tumor progression is highly dependent on the surrounding stroma, including the endothelial cells, fibroblasts, local basement membrane factors, macrophages, platelets, T cells, and other cellular compartments. Antiangiogenic therapy can target the endothelial cell compartment in atleast two distinct ways: directly or indirectly (Figure 1.3).[73]

Direct angiogenesis inhibitors block vascular endothelial cells from proliferating, migrating, or increasing their survival. For example, SU 11248 directly blocks VEGF receptors (among other receptors involved with angiogenic signaling) on endothelial cells (Figure 1.3). Direct angiogenesis inhibitors include: (1) synthetic inhibitors or peptides designed to interfere with specific steps in the angiogenic process (e.g., inhibitors of metalloproteinases, antagonists of the $\alpha_V\beta_3$ or $\alpha_5\beta_1$ integrins), (2) low molecular weight molecules (e.g., TNP-470, caplostatin, thalidomide, 2-methoxyestradiol), and (3) endogenous (i.e., natural) angiogenesis inhibitors (e.g., TSP-1, platelet factor 4, interferon-α, IL-12, angiostatin, endostatin, arrestin, canstatin, tumstatin).[5,39,74–92]

Bouck et al.[93] were the first to demonstrate that a tumor can generate angiogenesis inhibitor (i.e., thrombospondin-1). They subsequently suggested that the angiogenic phenotype was a result of a net imbalance of endogenous angiogenesis stimulators and inhibitors.

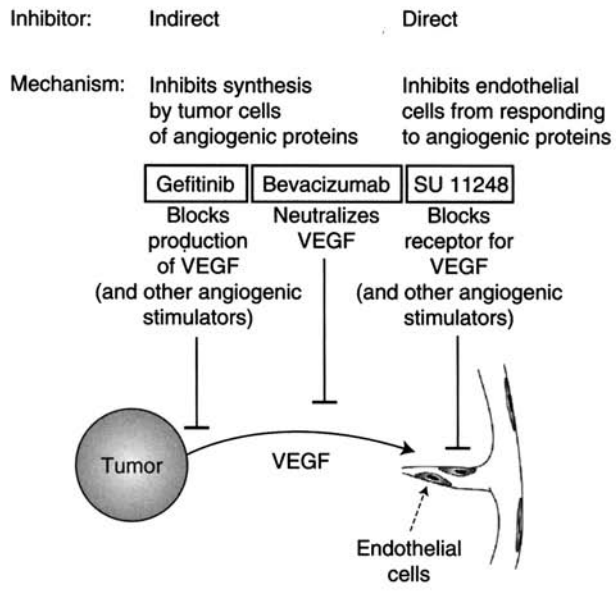

FIGURE 1.3 Examples of direct and indirect angiogenesis inhibitors that can block production of a tumor cell angiogenic protein (Gefitinib), or neutralize a systemic proangiogenic protein (Bevacizumab), or block a receptor for a tumor cell produced angiogenic protein (SU 11248). (Adapted from Folkman, J. et al., *Cancer Medicine*, 7th edn., 2006. With permission.)

In a series of experiments, Folkman and colleagues reported that the surgical removal of a primary Lewis lung carcinoma tumor in mice results in the exponential growth of lung metastases.[94,95] In these experimental animal models, the presence of a primary tumor generated increased circulating angiostatin levels. Angiostatin is a potent antiangiogenic plasminogen fragment,[96] which inhibits the in vivo growth of Lewis lung metastases by preventing neovascularization.[77] However, gene transfer of a cDNA coding for mouse angiostatin into murine T241 fibrosarcoma cells successfully suppressed lung metastatic tumor growth after the removal of the primary tumor.[97] Cao et al.[97] demonstrated that pulmonary micrometastases, expressing angiostatin, remain in a dormant and avascular state for 2–5 months after removal of primary tumors. These dormant micrometastases were characterized as having a high rate of apoptosis counterbalanced by a high proliferation rate.

Holmgren et al.[95] investigated whether treatment with an exogenous angiogenesis inhibitor could replace the endogenous angiogenesis suppressive ability of a primary tumor. In animals with surgically removed primary Lewis lung carcinoma, or T241 mouse sarcomas, treatment with TNP-470 resulted in the suppression of metastases comparable to that observed in the presence of the primary tumor. Therefore, exogenous treatment can be used to replace the endogenous angiogenesis inhibition of a primary tumor. Moreover, it can be used for the systemic suppression of angiogenesis-maintained micrometastases of both Lewis lung cancer and T241 fibrosarcoma in a dormant state. These dormant micrometastases were characterized as having high tumor cell proliferation counterbalanced by high cell death rate (i.e., apoptosis), indicating that inhibition of angiogenesis limits tumor growth by elevating tumor cell apoptosis. Exogenous angiogenesis inhibitors, such as TNP-470, mimic the primary tumor suppression by maintaining high apoptosis in the lung micrometastases, but without having an effect on tumor cell proliferation. A similar mechanism of sustained micrometastatic dormant state has been demonstrated using angiostatin, which maintains a high apoptotic index in lung metastases after the removal of a primary tumor without affecting tumor cell proliferation.[38]

Indirect angiogenesis inhibitors target tumor cell proteins created by oncogenes that drive the angiogenic switch. In general, their mechanism of action is by decreasing or blocking the expression of other tumor cell products, neutralizing the tumor cell product itself, or by blocking receptors on endothelial cells. The impact of oncogenes on tumor angiogenesis has been reviewed by Rak and Kerbel.[59,98,99] For example, gefitinib (Iressa) blocks VEGF production from tumor cells. However, even systemically available VEGF can be neutralized by bevacizumab (Avastin) before it binds to VEGF receptors on endothelial cells (Figure 1.3). There is an emerging group (e.g., thyrosine kinase inhibitors) of anticancer drugs originally developed to target oncogenes, which also have "indirect" antiangiogenic activity. For example, the *ras* farnesyl transferase inhibitors block oncogene signaling pathways, which upregulate tumor cell production of VEGF and downregulate production of Tsp-1.[100] Trastuzumab, an antibody that blocks *HER2/neu* receptor tyrosine kinase signaling, suppresses tumor cell production of angiogenic proteins, such as TGF-α, angiopoietin 1, plasminogen activator inhibitor-1 (PAI-1), and VEGF.[101,102] At the same time, trastuzumab has been shown to upregulate the expression of Tsp-1 (endogenous angiogenesis inhibitor), which may be an important mechanism of its antiangiogenic activity.[102] Upregulation of endogenous antiangiogenic proteins, using direct or indirect angiogenesis inhibitors, can be a useful approach for preventing the angiogenic switch and keeping human tumors in a microscopic dormant state (Figure 1.4).

Acquired drug resistance is a major obstacle in the treatment of cancer. Genetic instability, heterogeneity, and high mutational rates of tumor cells are the major causes of drug resistance.[103] In contrast, antiangiogenic therapy targets endothelial cells, which are genetically stable and have a low mutational rate. In an experimental animal model,

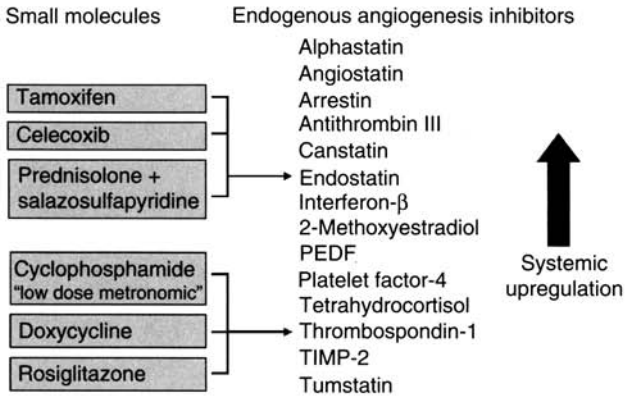

FIGURE 1.4 Summary of a few small molecules and the corresponding increase in endogenous angiogenesis inhibitors. Examples of small molecules that are orally available and may induce increased systemic levels of endogenous angiogenesis inhibitors. Chronic systemic increase of antiangiogenic proteins can prevent the angiogenic switch and delay the progression of cancer. (Adapted from Folkman, J., *Exp. Cell Res.*, 312(5), 594, 2006. With permission.)

Boehm et al.[104] reported that antiangiogenic therapy targeted against tumor-associated endothelial cells does not result in drug resistance. In this study, Lewis lung cancer, T241 fibrosarcoma, and B16F10 melanoma were repeatedly treated with endostatin. When tumors reached the size of ~350–400 mm^3, endostatin treatment was initiated until the tumor became undetectable. Endostatin therapy was then stopped, and the tumor was allowed to regrow. Endostatin therapy was resumed when tumors reached a mean volume of 350–400 mm^3. After the second (for melanoma), fourth (for fibrosarcoma), and sixth (for Lewis lung carcinoma) cycles of endostatin treatment, all tumors remained as barely visible subcutaneous nodules (size 5–50 mm^3) for up to 360 days. In contrast, endostatin resistance developed rapidly when Lewis lung carcinomas were treated with conventional cytotoxic chemotherapy. These studies demonstrated that repeated cycles of endostatin therapy induced tumor dormancy, which persisted indefinitely after therapy.

1.9 METASTATIC DORMANCY

Metastasis, the spread of cancer from a primary tumor to secondary organs, is the major cause of cancer-related deaths. Hematogenous or lymphatic spread of only a few cancer cells from a primary tumor can successfully form a macroscopic tumor at a secondary site.[50,105,106] However, for a macrometastasis to become lethal, it must successfully complete a number of steps (Figure 1.1).[107] Two different types of tumor dormancy have been identified in the metastatic process: (1) solitary dormant cancer cells, which are in G_0 cell cycle arrest and (2) dormant nonangiogenic tumors, in which tumor cells are actively proliferating and dying, but the tumor fails to recruit blood vessels. Both of these steps can contribute to a latency period associated with metastatic growth of human cancer (Figure 1.1).[108]

Previous studies by Holmgren and colleagues[95,109] have identified nonangiogenic micrometastases as a potential contributor to metastatic dormancy. These studies showed that dormant micrometastases did not grow in size beyond 200 μm, but they remained metabolically active. This size limitation was associated with a steady-state balance between the rates of tumor cell proliferation and apoptosis, with no net growth of the metastases. Changes in the intrinsic properties of these dormant micrometastases, or their microenvironment at a later time, triggered metastatic growth associated with a disturbance of the proliferation and apoptosis balance. Progressive growth in such micrometastases was restricted due to suppression of tumor angiogenesis.

Naumov et al.[110] have identified another possible source of metastatic dormancy: viable, solitary dormant tumor cells that are neither proliferating nor undergoing apoptosis after arriving at a metastatic site. These studies showed that more than 50%–80% of breast cancer cells, distributed to mouse liver via the circulation, can remain in the tissue for extended periods of time (up to 77 days) as solitary nonproliferating dormant cells. This surprising phenomenon was observed in populations of breast cancer cells of high and low metastatic ability. In the case of the highly metastatic cell line (D2A1 cells), lethal macrometastases grew from a very small subset of cells (~0.006%), with the majority (~80% cell loss) of injected cells undergoing apoptosis or destroyed by leukocytes. However, ~20% of the injected cells persisted as nonproliferating dormant cells. In contrast, ~80% of poorly metastatic breast cancer cells remained as nonproliferating dormant solitary cells in the mouse liver. A subset of these cells could be recovered and grown under in vitro culture conditions 11 weeks after injection into mice. The recovered tumor cells retained their ability to form primary tumors in the mammary fat pad of mice. These solitary dormant tumor cells may be a potential source of an occasional nonangiogenic metastasis, and of an even rarer, but lethal, angiogenic metastasis.

Taken together, these studies demonstrated that metastasis is a dynamic process, where solitary, nonproliferating dormant cancer cells, nonangiogenic micrometastases, and angiogenic macrometastases can coexist at each stage of the metastatic process. While nonangiogenic micrometastases could be vulnerable to antiangiogenic and cytotoxic chemotherapeutic agents (administered in a metronomic, low-dose regimen, as described by Browder et al.[111] and Kerbel and colleagues[112,113]), solitary dormant cells could remain unaffected because of their inability to proliferate.

Naumov et al.[114] showed that nonproliferating solitary dormant breast cancer cells remained unaffected by doxorubicin treatment. However, the same treatment successfully inhibited actively growing macrometastases in the same mice. Therefore, doxorubicin chemotherapy, which successfully reduced the metastatic burden, failed to affect the number of solitary dormant cells. These findings have important clinical implications for patients undergoing adjuvant chemotherapy. It is possible that dormant nonproliferating tumor cells can remain unaffected by standard chemotherapy and may retain their potential to initiate growth at a later date. Both solitary cancer cells and nonangiogenic metastases can remain dormant and undetectable for months or years, leading to an uncertainty in the prognosis for patients who have already been treated for the primary cancer.

1.10 ANGIOGENIC SWITCH-RELATED BIOMARKERS FOR DETECTION OF DORMANT TUMORS

Even with recent advances in the clinical detection of human cancer, a tumor that is microscopic in size (~1 mm in diameter) remains undetectable. A panel of angiogenic switch-related biomarkers is under development using the human tumor dormancy models. These biomarkers include circulating endothelial progenitor cells (CEPs) and platelets in the blood, as well as matrix metalloproteinases (MMPs) in the urine. The detection of a single microscopic human tumor in existing animal models can be achieved using each one of these biomarkers alone or in combination.[115–117]

We compared the in vivo ability of angiogenic and nonangiogenic human breast tumors (MDA-MB-436 cells) to mobilize mature circulating endothelial cells (CECs) (CD45−, Flk+, CD31+, CD117−) and CEPs (CD45−, Flk+, CD31+, CD117+).[115] The number of blood-borne CECs and CEPs was quantified using a flow cytometer. There was little difference in the percent of mature CECs in the blood of mice inoculated with angiogenic and nonangiogenic cells. However, mice inoculated with nonangiogenic cells had approximately fourfold decrease in CEPs when compared with control mice. Mice inoculated with angiogenic cells

had levels of CEPs comparable to those in the control mice. Previous reports[44] have shown that these nonangiogenic breast cancer cells (MDA-MB-436 cells) secrete at least 20-fold higher levels of thrombospondin-1 (Tsp-1) than their angiogenic counterparts. Other studies have suggested that endogenous inhibitors of angiogenesis, such as Tsp-1 and endostatin, may inhibit the mobilization of CEPs.[118] These observations suggest that microscopic dormant (nonangiogenic) tumors may suppress the mobilization of CEPs from the bone marrow via systemic thrombospondin-1.

Klement et al.[117] recently reported that blood platelets can sequester both pro- and antiangiogenic proteins. It is estimated that at least 100 billion platelets are produced per day by megakaryocytes in the bone marrow of an average 70 kg person.[119,120] With a life span of 7–8 days in humans, it is estimated that there are approximately a trillion platelets in constant circulation.[119,121] Folkman and colleagues proposed that the platelet compartment of the blood stream can potentially accumulate angiogenesis-related proteins and possibly release them at a later time.[117] Using a novel "platelet angiogenic proteome," as quantitatively assessed by SELDI-ToF technology (Ciphergen, Freemont, CA), the presence of microscopic human tumors in mice can be detected.[117] Using this technology, the accumulation and reduction in angiogenesis-related proteins sequestered in platelets can be quantitatively followed throughout the angiogenic switch. The identification of proteins that are associated with the angiogenic switch and that may be used as angiogenic switch-related biomarkers is currently under investigation.

In summary, the tumor dormancy animal models presented here permit further clarification of the role of CEC/CEPs, platelets, and MMPs as participants in the "angiogenic switch." Moreover, this angiogenic switch-related biomarker panel may prove to be a useful diagnostic method for the presence of microscopic cancers at primary and metastatic sites long before detection by conventional methods. It may be feasible to develop a panel of angiogenesis-associated biomarkers that can identify the presence of a microscopic human tumor, predict its switch to the angiogenic phenotype, and possibly serve as a guide for antiangiogenic therapy. In the future, it may be possible for a patient who is at risk for cancer recurrence to take an oral drug that can elevate endogenous platelet-associated antiangiogenic proteins and delay, if not prevent, the formation of recurrent tumors.

1.11 CONCLUSION

We speculate that the development of more specific and sensitive biomarkers may permit the very early detection of recurrent cancer, possibly years before symptoms or anatomical location. If this concept can be validated, then relatively nontoxic angiogenesis inhibitors may be used to "treat the biomarkers" without ever seeing the recurrent tumor (i.e., cancer without disease).[14]

ACKNOWLEDGMENTS

The authors thank Ms. Jenny Grillo for critical reading and editing of this chapter. We also thank Kristin Johnson for help with graphics. This work was supported by the Breast Cancer Research Foundation, NIH Program Project (grant #P01CA45548), and an Innovator Award from the Department of Defense.

REFERENCES

1. Demicheli R, Abbattista A, Miceli R, Valagussa P, Bonadonna G. Time distribution of the recurrence risk for breast cancer patients undergoing mastectomy: further support about the concept of tumor dormancy. *Breast Cancer Res Treat* 1996;41(2):177–185.

2. Karrison TG, Ferguson DJ, Meier P. Dormancy of mammary carcinoma after mastectomy. *J Natl Cancer Inst* 1999;91(1):80–85.
3. Willis RA. *Pathology of tumours*. London: Butterworth; 1948.
4. Hadfield G. The dormant cancer cell. *Br Med J* 1954;4888:607–610.
5. Rastinejad F, Polverini PJ, Bouck NP. Regulation of the activity of a new inhibitor of angiogenesis by a cancer suppressor gene. *Cell* 1989;56(3):345–355.
6. Wheelock EF, Weinhold KJ, Levich J. The tumor dormant state. *Adv Cancer Res* 1981;34:107–140.
7. Saudemont A, Jouy N, Hetuin D, Quesnel B. NK cells that are activated by CXCL10 can kill dormant tumor cells that resist CTL-mediated lysis and can express B7-H1 that stimulates T cells. *Blood* 2005;105(6):2428–2435.
8. Stewart TH. Immune mechanisms and tumor dormancy. *Medicina (B Aires)* 1996;56(Suppl 1): 74–82.
9. Saudemont A, Quesnel B. In a model of tumor dormancy, long-term persistent leukemic cells have increased B7-H1 and B7.1 expression and resist CTL-mediated lysis. *Blood* 2004;104(7):2124–2133.
10. Marches R, Scheuermann R, Uhr J. Cancer dormancy: from mice to man. *Cell Cycle* 2006;5(16): 1772–1778.
11. Jain RK, Safabakhsh N, Sckell A et al. Endothelial cell death, angiogenesis, and microvascular function after castration in an androgen-dependent tumor: role of vascular endothelial growth factor. *Proc Natl Acad Sci USA* 1998;95(18):10820–10825.
12. Dameron KM, Volpert OV, Tainsky MA, Bouck N. Control of angiogenesis in fibroblasts by p53 regulation of thrombospondin-1. *Science* 1994;265(5178):1582–1584.
13. O'Reilly MS, Holmgren L, Shing Y et al. Angiostatin: a circulating endothelial cell inhibitor that suppresses angiogenesis and tumor growth. *Cold Spring Harb Symp Quant Biol* 1994;59:471–482.
14. Folkman J, Kalluri R. Cancer without disease. *Nature* 2004;427(6977):787.
15. Folkman J, Heymach J, Kalluri R. *Tumor angiogenesis*. 7th edn. Hamilton, Ontario: B.C. Decker; 2006.
16. Folkman J. Tumor angiogenesis: therapeutic implications. *N Engl J Med* 1971;285(21):1182–1186.
17. Folkman J. What is the evidence that tumors are angiogenesis dependent? *J Natl Cancer Inst* 1990;82(1):4–6.
18. Coman D, Sheldon WF. The significance of hyperemia around tumor implants. *Am J Pathol* 1946;22:821–831.
19. Warren B. The vascular morphology of tumors. In: Peterson H-I, ed. *Tumor blood circulation: angiogenesis, vascular morphology and blood flow of experimental human tumors*. Florida: CRC Press; 1979:1–47.
20. Ide A, Baker NH, Warren SL. Vascularization of the Brown–Pearce rabbit epithelioma transplant as seen in the transparent ear chamber. *Am J Roentgenol* 1939;42:891–899.
21. Algire G, Legallais, FY. Growth rate of transplanted tumors in relation to latent period and host vascular reaction. *Cancer Res* 1947;7:724.
22. Algire G, Chalkely HW, Legallais FY, Park H. Vascular reactions of normal and malignant tumors in vivo: I. Vascular reactions of mice to wounds and to normal and neoplastic transplants. *J Natl Cancer Inst* 1945;6:73–85.
23. Folkman J. Toward an understanding of angiogenesis: search and discovery. *Perspect Biol Med* 1985;29(1):10–36.
24. Folkman J, Long DM, Jr., Becker FF. Growth and metastasis of tumor in organ culture. *Cancer* 1963;16:453–467.
25. Folkman J, Cole P, Zimmerman S. Tumor behavior in isolated perfused organs: in vitro growth and metastases of biopsy material in rabbit thyroid and canine intestinal segment. *Ann Surg* 1966;164(3):491–502.
26. Folkman J. Anti-angiogenesis: new concept for therapy of solid tumors. *Ann Surg* 1972;175(3):409–416.
27. Folkman J. The vascularization of tumors. *Sci Am* 1976;234(5):58–64, 70–73.
28. Folkman J. The intestine as an organ culture. In: Burdette W, ed. *Carcinoma of the colon and antecedent epithelium*. Springfield (IL): CC Thomas; 1970:113–127.
29. Folkman J, Brem H. Angiogenesis and inflammation. In: Gallin JI, Goldstein IM, Snyderman R, eds. *Inflammation: basic principles and clinical correlates*. 2nd edn. New York: Raven Press; 1992:821–839.

30. Folkman J. Angiogenesis in arthritis. In: Smolen J, Lipsky P, eds. *Targeted therapies in rheumatology*. London: Martin Dunitz; 2003:111–131.
31. Folkman J, Watson K, Ingber D, Hanahan D. Induction of angiogenesis during the transition from hyperplasia to neoplasia. *Nature* 1989;339(6219):58–61.
32. Torres Filho IP, Leunig M, Yuan F, Intaglietta M, Jain RK. Noninvasive measurement of microvascular and interstitial oxygen profiles in a human tumor in SCID mice. *Proc Natl Acad Sci USA* 1994;91(6):2081–2085.
33. North S, Moenner M, Bikfalvi A. Recent developments in the regulation of the angiogenic switch by cellular stress factors in tumors. *Cancer Lett* 2005;218(1):1–14.
34. Greene HSN. Heterologous transplantation of mammalian tumors. *J Exp Med* 1941;73:461–486.
35. Gimbrone MA, Jr., Aster RH, Cotran RS, Corkery J, Jandl JH, Folkman J. Preservation of vascular integrity in organs perfused in vitro with a platelet-rich medium. *Nature* 1969;222(188):33–36.
36. Gimbrone MA, Jr., Leapman SB, Cotran RS, Folkman J. Tumor dormancy in vivo by prevention of neovascularization. *J Exp Med* 1972;136(2):261–276.
37. Brem H, Folkman J. Inhibition of tumor angiogenesis mediated by cartilage. *J Exp Med* 1975;141(2):427–439.
37a. Moses MA, Sudhalter J, Langer R. Identification of an inhibitor of neovascularization from the cartilage. *Science* 1990;248:1408–1410.
38. O'Reilly MS, Holmgren L, Chen C, Folkman J. Angiostatin induces and sustains dormancy of human primary tumors in mice. *Nat Med* 1996;2(6):689–692.
39. O'Reilly MS, Boehm T, Shing Y et al. Endostatin: an endogenous inhibitor of angiogenesis and tumor growth. *Cell* 1997;88(2):277–285.
40. Hanahan D, Folkman J. Patterns and emerging mechanisms of the angiogenic switch during tumorigenesis. *Cell* 1996;86(3):353–364.
41. Hanahan D, Christofori G, Naik P, Arbeit J. Transgenic mouse models of tumour angiogenesis: the angiogenic switch, its molecular controls, and prospects for preclinical therapeutic models. *Eur J Cancer* 1996;32A(14):2386–2393.
42. Achilles EG, Fernandez A, Allred EN et al. Heterogeneity of angiogenic activity in a human liposarcoma: a proposed mechanism for "no take" of human tumors in mice. *J Natl Cancer Inst* 2001;93(14):1075–1081.
43. Almog N, Henke V, Flores L et al. Prolonged dormancy of human liposarcoma is associated with impaired tumor angiogenesis. *FASEB J* 2006;20(7):947–949.
44. Naumov GN, Bender E, Zurakowski D et al. A model of human tumor dormancy: an angiogenic switch from the nonangiogenic phenotype. *J Natl Cancer Inst* 2006;98(5):316–325.
45. Aguirre Ghiso JA, Kovalski K, Ossowski L. Tumor dormancy induced by downregulation of urokinase receptor in human carcinoma involves integrin and MAPK signaling. *J Cell Biol* 1999;147(1):89–104.
46. Aguirre-Ghiso JA, Liu D, Mignatti A, Kovalski K, Ossowski L. Urokinase receptor and fibronectin regulate the ERK(MAPK) to p38(MAPK) activity ratios that determine carcinoma cell proliferation or dormancy in vivo. *Mol Biol Cell* 2001;12(4):863–879.
47. Aguirre-Ghiso JA, Estrada Y, Liu D, Ossowski L. ERK(MAPK) activity as a determinant of tumor growth and dormancy; regulation by p38(SAPK). *Cancer Res* 2003;63(7):1684–1695.
48. Udagawa T, Fernandez A, Achilles EG, Folkman J, D'Amato RJ. Persistence of microscopic human cancers in mice: alterations in the angiogenic balance accompanies loss of tumor dormancy. *FASEB J* 2002;16(11):1361–1370.
49. Naumov GN, Wilson SM, MacDonald IC et al. Cellular expression of green fluorescent protein, coupled with high-resolution in vivo videomicroscopy, to monitor steps in tumor metastasis. *J Cell Sci* 1999;112(Pt 12):1835–1842.
50. Chambers AF, Groom AC, MacDonald IC. Dissemination and growth of cancer cells in metastatic sites. *Nat Rev Cancer* 2002;2(8):563–572.
51. Naumov GN, MacDonald IC, Chambers AF, Groom AC. Solitary cancer cells as a possible source of tumour dormancy? *Semin Cancer Biol* 2001;11(4):271–276.
52. Heyn C, Ronald JA, Mackenzie LT et al. In vivo magnetic resonance imaging of single cells in mouse brain with optical validation. *Magn Reson Med* 2006;55(1):23–29.

53. Graham KC, Wirtzfeld LA, MacKenzie LT et al. Three-dimensional high-frequency ultrasound imaging for longitudinal evaluation of liver metastases in preclinical models. *Cancer Res* 2005;65(12):5231–5237.
54. Goustin AS, Leof EB, Shipley GD, Moses HL. Growth factors and cancer. *Cancer Res* 1986;46(3):1015–1029.
55. Bonni A, Brunet A, West AE, Datta SR, Takasu MA, Greenberg ME. Cell survival promoted by the Ras-MAPK signaling pathway by transcription-dependent and -independent mechanisms. *Science* 1999;286(5443):1358–1362.
56. Rak J, Mitsuhashi Y, Bayko L et al. Mutant *ras* oncogenes upregulate VEGF/VPF expression: implications for induction and inhibition of tumor angiogenesis. *Cancer Res* 1995; 55(20):4575–4580.
57. Good DJ, Polverini PJ, Rastinejad F et al. A tumor suppressor-dependent inhibitor of angiogenesis is immunologically and functionally indistinguishable from a fragment of thrombospondin. *Proc Natl Acad Sci USA* 1990;87(17):6624–6628.
58. Sheibani N, Frazier WA. Repression of thrombospondin-1 expression, a natural inhibitor of angiogenesis, in polyoma middle T transformed NIH3T3 cells. *Cancer Lett* 1996;107(1):45–52.
59. Rak J, Yu JL, Klement G, Kerbel RS. Oncogenes and angiogenesis: signaling three-dimensional tumor growth. *J Investig Dermatol Symp Proc* 2000;5(1):24–33.
60. Watnick RS, Cheng YN, Rangarajan A, Ince TA, Weinberg RA. Ras modulates Myc activity to repress thrombospondin-1 expression and increase tumor angiogenesis. *Cancer Cell* 2003;3(3):219–231.
61. Volpert OV, Dameron KM, Bouck N. Sequential development of an angiogenic phenotype by human fibroblasts progressing to tumorigenicity. *Oncogene* 1997;14(12):1495–1502.
62. Chandrasekaran L, He CZ, Al-Barazi H, Krutzsch HC, Iruela-Arispe ML, Roberts DD. Cell contact-dependent activation of alpha3beta1 integrin modulates endothelial cell responses to thrombospondin-1. *Mol Biol Cell* 2000;11(9):2885–2900.
63. Lawler J, Sunday M, Thibert V et al. Thrombospondin-1 is required for normal murine pulmonary homeostasis and its absence causes pneumonia. *J Clin Invest* 1998;101(5):982–992.
64. Volpert OV. Modulation of endothelial cell survival by an inhibitor of angiogenesis thrombospondin-1: a dynamic balance. *Cancer Metastasis Rev* 2000;19(1–2):87–92.
65. Mettouchi A, Cabon F, Montreau N et al. SPARC and thrombospondin genes are repressed by the c-*jun* oncogene in rat embryo fibroblasts. *EMBO J* 1994;13(23):5668–5678.
66. Dejong V, Degeorges A, Filleur S et al. The Wilms' tumor gene product represses the transcription of thrombospondin 1 in response to overexpression of c-*Jun*. *Oncogene* 1999;18(20):3143–3151.
67. Slack JL, Bornstein P. Transformation by v-*src* causes transient induction followed by repression of mouse thrombospondin-1. *Cell Growth Differ* 1994;5(12):1373–1380.
68. Tikhonenko AT, Black DJ, Linial ML. Viral Myc oncoproteins in infected fibroblasts down-modulate thrombospondin-1, a possible tumor suppressor gene. *J Biol Chem* 1996; 271(48):30741–30747.
69. Janz A, Sevignani C, Kenyon K, Ngo CV, Thomas-Tikhonenko A. Activation of the myc oncoprotein leads to increased turnover of thrombospondin-1 mRNA. *Nucleic Acids Res* 2000;28(11):2268–2275.
70. Van Meir EG, Kikuchi T, Tada M et al. Analysis of the *p53* gene and its expression in human glioblastoma cells. *Cancer Res* 1994;54(3):649–652.
71. Teodoro JG, Parker AE, Zhu X, Green MR. p53-mediated inhibition of angiogenesis through up-regulation of a collagen prolyl hydroxylase. *Science* 2006;313(5789):968–971.
72. Holmgren L, Jackson G, Arbiser J. p53 induces angiogenesis-restricted dormancy in a mouse fibrosarcoma. *Oncogene* 1998;17(7):819–824.
73. Kerbel R, Folkman J. Clinical translation of angiogenesis inhibitors. *Nat Rev Cancer* 2002;2(10):727–739.
74. Taylor S, Folkman J. Protamine is an inhibitor of angiogenesis. *Nature* 1982;297(5864):307–312.
75. Ingber D, Fujita T, Kishimoto S et al. Synthetic analogues of fumagillin that inhibit angiogenesis and suppress tumour growth. *Nature* 1990;348(6301):555–557.
76. Brooks PC, Montgomery AM, Rosenfeld M et al. Integrin alpha v beta 3 antagonists promote tumor regression by inducing apoptosis of angiogenic blood vessels. *Cell* 1994;79(7):1157–1164.

77. O'Reilly MS, Holmgren L, Shing Y et al. Angiostatin: a novel angiogenesis inhibitor that mediates the suppression of metastases by a Lewis lung carcinoma. *Cell* 1994;79(2):315–328.
78. O'Reilly MS, Pirie-Shepherd S, Lane WS, Folkman J. Antiangiogenic activity of the cleaved conformation of the serpin antithrombin. *Science* 1999;285(5435):1926–1928.
79. Stetler-Stevenson WG, Krutzsch HC, Liotta LA. Tissue inhibitor of metalloproteinase (TIMP-2). A new member of the metalloproteinase inhibitor family. *J Biol Chem* 1989;264(29):17374–17378.
80. Moses MA, Sudhalter J, Langer R. Identification of an inhibitor of neovascularization from cartilage. *Science* 1990;248(4961):1408–1410.
81. Kruger EA, Figg WD. TNP-470: an angiogenesis inhibitor in clinical development for cancer. *Expert Opin Investig Drugs* 2000;9(6):1383–1396.
82. D'Amato RJ, Loughnan MS, Flynn E, Folkman J. Thalidomide is an inhibitor of angiogenesis. *Proc Natl Acad Sci USA* 1994;91(9):4082–4085.
83. Folkman J. Angiogenesis-dependent diseases. *Semin Oncol* 2001;28(6):536–542.
84. Crum R, Szabo S, Folkman J. A new class of steroids inhibits angiogenesis in the presence of heparin or a heparin fragment. *Science* 1985;230(4732):1375–1378.
85. D'Amato RJ, Lin CM, Flynn E, Folkman J, Hamel E. 2-Methoxyestradiol, an endogenous mammalian metabolite, inhibits tubulin polymerization by interacting at the colchicine site. *Proc Natl Acad Sci USA* 1994;91(9):3964–3968.
86. Fotsis T, Zhang Y, Pepper MS et al. The endogenous oestrogen metabolite 2-methoxyoestradiol inhibits angiogenesis and suppresses tumour growth. *Nature* 1994;368(6468):237–239.
87. Voest EE, Kenyon BM, O'Reilly MS, Truitt G, D'Amato RJ, Folkman J. Inhibition of angiogenesis in vivo by interleukin 12. *J Natl Cancer Inst* 1995;87(8):581–586.
88. Maione TE, Gray GS, Petro J et al. Inhibition of angiogenesis by recombinant human platelet factor-4 and related peptides. *Science* 1990;247(4938):77–79.
89. Colorado PC, Torre A, Kamphaus G et al. Anti-angiogenic cues from vascular basement membrane collagen. *Cancer Res* 2000;60(9):2520–2526.
90. Kamphaus GD, Colorado PC, Panka DJ et al. Canstatin, a novel matrix-derived inhibitor of angiogenesis and tumor growth. *J Biol Chem* 2000;275(2):1209–1215.
91. Maeshima Y, Colorado PC, Torre A et al. Distinct antitumor properties of a type IV collagen domain derived from basement membrane. *J Biol Chem* 2000;275(28):21340–21348.
92. Dawson DW, Volpert OV, Gillis P et al. Pigment epithelium-derived factor: a potent inhibitor of angiogenesis. *Science* 1999;285(5425):245–248.
93. Bouck N. Tumor angiogenesis: the role of oncogenes and tumor suppressor genes. *Cancer Cells* 1990;2(6):179–185.
94. O'Reilly M, Rosenthal R, Sage HE, Smith S, Holmgren L, Moses M, Shing Y, Folkman J. The suppression of tumor metastases by a primary tumor. *Surg Forum* 1993;44:474–476.
95. Holmgren L, O'Reilly MS, Folkman J. Dormancy of micrometastases: balanced proliferation and apoptosis in the presence of angiogenesis suppression. *Nat Med* 1995;1(2):149–153.
96. Lay AJ, Jiang XM, Kisker O et al. Phosphoglycerate kinase acts in tumour angiogenesis as a disulphide reductase. *Nature* 2000;408(6814):869–873.
97. Cao Y, O'Reilly MS, Marshall B, Flynn E, Ji RW, Folkman J. Expression of angiostatin cDNA in a murine fibrosarcoma suppresses primary tumor growth and produces long-term dormancy of metastases. *J Clin Invest* 1998;101(5):1055–1063.
97a. Camphausen K, Moses MA, Beecken WD, Khan MK, Folkman J, O'Reilly MS. Radiation therapy to a primary tumor accelerates metastatic growth in mice. 2001;61(5):2207–2211.
98. Kerbel RS, Viloria-Petit A, Okada F, Rak J. Establishing a link between oncogenes and tumor angiogenesis. *Mol Med* 1998;4(5):286–295.
99. Rak J, Yu JL, Kerbel RS, Coomber BL. What do oncogenic mutations have to do with angiogenesis/vascular dependence of tumors? *Cancer Res* 2002;62(7):1931–1934.
100. Okada F, Rak JW, Croix BS et al. Impact of oncogenes in tumor angiogenesis: mutant K-*ras* up-regulation of vascular endothelial growth factor/vascular permeability factor is necessary, but not sufficient for tumorigenicity of human colorectal carcinoma cells. *Proc Natl Acad Sci USA* 1998;95(7):3609–3614.

101. Petit AM, Rak J, Hung MC et al. Neutralizing antibodies against epidermal growth factor and ErbB-2/neu receptor tyrosine kinases down-regulate vascular endothelial growth factor production by tumor cells in vitro and in vivo: angiogenic implications for signal transduction therapy of solid tumors. *Am J Pathol* 1997;151(6):1523–1530.
102. Izumi Y, Xu L, di Tomaso E, Fukumura D, Jain RK. Tumour biology: herceptin acts as an anti-angiogenic cocktail. *Nature* 2002;416(6878):279–280.
103. Moscow J, Schneider E, Sikic BI, Morrow CS, Cowan KH. Drug resistance and its clinical circumvention. In: Kufe DW, Bast RC, Jr., Hite WH, Hong WK, Pollock RE, Weichselbaum RR, Holland JF, Frei E, III, eds. *Cancer medicine*. Hamilton: B.C. Decker Inc.; 2006:630–647.
104. Boehm T, Folkman J, Browder T, O'Reilly MS. Antiangiogenic therapy of experimental cancer does not induce acquired drug resistance. *Nature* 1997;390(6658):404–407.
105. Chambers AF, Naumov GN, Vantyghem SA, Tuck AB. Molecular biology of breast cancer metastasis. Clinical implications of experimental studies on metastatic inefficiency. *Breast Cancer Res* 2000;2(6):400–407.
106. Weiss L. Metastatic inefficiency. *Adv Cancer Res* 1990;54:159–211.
107. Fidler IJ. Antivascular therapy of cancer metastasis. *J Surg Oncol* 2006;94(3):178–180.
108. Naumov GN, Akslen LA, Folkman J. Role of angiogenesis in human tumor dormancy: animal models of the angiogenic switch. *Cell Cycle* 2006;5(16).
109. Murray C. Tumour dormancy: not so sleepy after all. *Nat Med* 1995;1(2):117–118.
110. Naumov GN, MacDonald IC, Weinmeister PM et al. Persistence of solitary mammary carcinoma cells in a secondary site: a possible contributor to dormancy. *Cancer Res* 2002;62(7):2162–2168.
111. Browder T, Butterfield CE, Kraling BM et al. Antiangiogenic scheduling of chemotherapy improves efficacy against experimental drug-resistant cancer. *Cancer Res* 2000;60(7):1878–1886.
112. Kerbel RS, Viloria-Petit A, Klement G, Rak J. 'Accidental' anti-angiogenic drugs. Anti-oncogene directed signal transduction inhibitors and conventional chemotherapeutic agents as examples. *Eur J Cancer* 2000;36(10):1248–1257.
113. Klement G, Baruchel S, Rak J et al. Continuous low-dose therapy with vinblastine and VEGF receptor-2 antibody induces sustained tumor regression without overt toxicity. *J Clin Invest* 2000;105(8):R15–R24.
114. Naumov GN, Townson JL, MacDonald IC et al. Ineffectiveness of doxorubicin treatment on solitary dormant mammary carcinoma cells or late-developing metastases. *Breast Cancer Res Treat* 2003;82(3):199–206.
115. Naumov GN, Beaudry P, Bender ER, Zurakowski D, Watnick R, Almog N, Heymach J, Folkman J. Suppression of circulating endothelial progenitor cells by human dormant breast cancer cells. *Clin Exp Met* 2004;21(7):636.
116. Harper J, Naumov GN, Exarhopoulos A, Bender E, Louis G, Folkman J, Moses MA. Predicting the switch to the angiogenic phenotype in a human tumor model. In: Proceedings of the American Association for *Cancer Res* 2006:837.
117. Klement G, Kikuchi L, Kieran M, Almog N, Yip T, Folkman J. Early tumor detection using platelet uptake of angiogenesis regulators. Blood 2004;104:239a, abstract 839.
118. Schuch G, Heymach JV, Nomi M et al. Endostatin inhibits the vascular endothelial growth factor-induced mobilization of endothelial progenitor cells. *Cancer Res* 2003;63(23):8345–8350.
119. Harker LA, Finch CA. Thrombokinetics in man. *J Clin Invest* 1969;48(6):963–974.
120. Italiano JE, Hartwig JH. Megakaryocyte development and platelet formation. In: Michelson AD, ed. *Platelets*. Boston: Academic Press; 2002:21–36.
121. Kaushansky K. Lineage-specific hematopoietic growth factors. *N Engl J Med* 2006; 354(19):2034–2045.

blood

2007 110: 2786-2787
doi:10.1182/blood-2007-08-102178

Endostatin finds a new partner: nucleolin

Judah Folkman

Blood (print ISSN 0006-4971, online ISSN 1528-0020), is published semimonthly by the American Society of Hematology, 1900 M St, NW, Suite 200, Washington DC 20036.

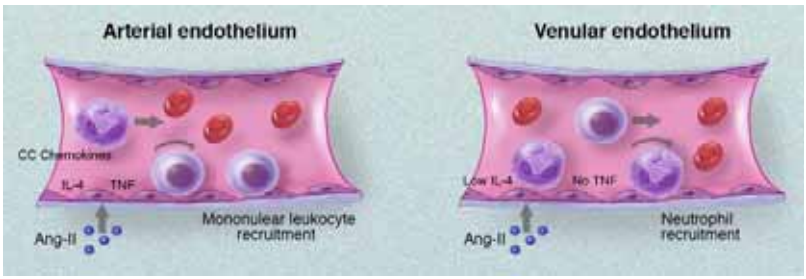

Comparison of angiotensin-II (Ang-II)–mediated leukocyte recruitment in arterioles and venules. In arterioles, high constitutive expression of IL-4 and Ang-II–induced TNF induces expression of CC chemokines such as MCP-1 and RANTES over a time course of several hours. These chemokines mediate selective arrest of mononuclear leukocytes in arterioles. In contrast, in postcapillary venules, Ang-II induces rolling and arrest within 60 minutes, predominantly recruiting neutrophils to the endothelial surface. This process does not require either IL-4 or TNF.

Conflict-of-interest disclosure: The authors declare no competing financial interests. ■

REFERENCES

1. Kunkel EJ, Jung U, Ley K. TNF-alpha induces selectin-mediated leukocyte rolling in mouse cremaster muscle arterioles. Am J Physiol. 1997;272:H1391-H1400.

2. Hickey MJ, Sharkey KA, Sihota EG, et al. Inducible nitric oxide synthase (iNOS)-deficient mice have enhanced leukocyte-endothelium interactions in endotoxemia. FASEB J. 1997;11:955-964.

3. Eriksson EE, Kie X, Werr J, Thoren P, Lindbom L. Direct viewing of atherosclerosis in vivo: plaque invasion by leukocytes is initiated by endothelial selectins. FASEB J. 2001;15:1149-1157.

4. Alvarez A, Cerda-Nicolas M, Naim Abu Nabah Y, et al. Direct evidence of leukocyte adhesion in arterioles by angiotensin II. Blood. 2004;104:402-408.

5. Hickey MJ, Granger DN, Kubes P. Molecular mechanisms underlying IL-4-induced leukocyte recruitment *in vivo*: a critical role for the α_4-integrin. J Immunol. 1999;163:3441-3448.

6. Bernhagen J, Krohn R, Lue H, et al. MIF is a noncognate ligand of CXC chemokine receptors in inflammatory and atherogenic cell recruitment. Nat Med. 2007;13:587-596.

7. Langheinrich AC, Kampschulte M, Buch T, Bohle RM. Vasa vasorum and atherosclerosis - Quid novi? Thromb Haemost. 2007;97:873-879.

8. Mullick AE, Tobias PS, Curtiss LK. Toll-like receptors and atherosclerosis: key contributors in disease and health? Immunol Res. 2006;34:193-209.

HEMOSTASIS

Comment on Shi et al, page 2899

Endostatin finds a new partner: nucleolin

Judah Folkman CHILDREN'S HOSPITAL AT HARVARD MEDICAL SCHOOL

In this issue of *Blood*, Shi and colleagues examine the endostatin binding of nucleolin on angiogenic endothelial cells, as well as the transport of nucleolin to the nucleus, where it prevents proliferation—thus revealing a novel mechanism for endostatin's antiangiogenic activity.

During the past 3 years, 8 new drugs with antiangiogenic activity have received approval from the Food and Drug Administration of the United States for the treatment of cancer and age-related macular degeneration, and have also been approved in more than 30 other countries. These are mainly antibodies, aptamers, or synthetic molecules. They block at least 1 to 3 proangiogenic proteins or their receptors.[1] This new class of drugs has been prescribed for more than 1.2 million patients. More than 50 drugs with antiangiogenic activity are in phase 2 or 3 clinical trials.[2] Since 1980, 28 endogenous angiogenesis inhibitors, including platelet factor 4, angiostatin, endostatin, thrombospondin-1, tumstatin, and canstatin, have been discovered in blood or tissues.[3,4] At this writing, more than 1000 reports on endostatin have been published since its discovery in 1997, and reveal that endostatin has the broadest antitumor spectrum of the endogenous angiogenesis inhibitors. It is also the first endogenous inhibitor to receive approval for anticancer therapy, under the trade name "Endostar" in China.

The integrin $\alpha_5\beta_1$ has been proposed as a receptor for endostatin, and endostatin has been shown to regulate an entire program of antiangiogenic gene expression in human microvascular endothelial cells stimulated by VEGF or bFGF.[5] Nevertheless, certain antiangiogenic actions of endostatin have no molecular explanation and remain as open questions. In this issue of *Blood*, Shi and colleagues address 3 of these questions. Why does endostatin specifically target angiogenic blood vessels, but not quiescent blood vessels? Why does endostatin inhibit tumor angiogenesis with virtually no toxicity in animal studies and clinical trials? Why has the antiangiogenic activity of endostatin appeared to be heparin-dependent in previous studies? These questions are answered by a novel and important finding: that nucleolin is expressed on the surface of proliferating angiogenic human microvascular endothelial cells, but not on the surface of quiescent endothelium. In angiogenic endothelial cells, the cell-surface nucleolin binds endostatin and transports it to the nucleus, where endostatin inhibits phosphorylation of nucleolin. Phosphorylation of nucleolin induced by VEGF or bFGF has been reported to be essential for cell proliferation. Furthermore, endostatin does not inhibit proliferation of many types of tumor cells per se, possibly because while they express nucleolin on their surfaces, they do not internalize it in the presence of endostatin. The heparin binding sites on nucleolin were found to be critical for endostatin. Increasing concentrations of exogenous heparin dissociated the binding of endostatin to nucleolin.

The article by Shi and colleagues is also thought-provoking because the endostatin-nucleolin connection is now fertile soil for future studies. For example, it will be interesting to learn how specific the binding of endostatin is to nucleolin compared with other proteins that also bind to endostatin, as reported by the authors. Furthermore, it will be helpful if the relationship of nucleolin to other cell-surface endostatin-binding proteins can be uncovered, particularly $\alpha_5\beta_1$. Will this endostatin-nucleolin connection lead to the uncovering of a mechanism

for the biphasic, ∪-shaped anticancer dose-response curve recently reported for endostatin,[6] and originally shown for the antiendothelial activity of interferon α?[7] This biphasic dose response is common to other angiogenesis inhibitors. Endostatin increases nucleolin expression in human microvascular endothelial cells in vitro by approximately 20%.[5] Is p53-mediated inhibition of angiogenesis, in part through increased expression of endostatin,[8,9] also regulated by nucleolin? Because the endothelial-cell expression of another endogenous angiogenesis inhibitor, thrombospondin-1, is up-regulated by endostatin, is thrombospondin-1 indirectly nucleolin-dependent? Are any other endogenous angiogenesis inhibitors regulated by binding to nucleolin? Angiogenesis in wound healing and pregnancy is not delayed by high endostatin levels, as for example in individuals with Down syndrome, or in animals receiving endostatin therapy.[10] Is this because proliferating endothelial cells in reproduction and repair do not express nucleolin on their cell surface, or do not internalize it?

The novel role for nucleolin, as a regulator of the antiangiogenic activities of endostatin, has fundamental implications for understanding the biology of endostatin and for its clinical application.

Acknowledgment: I thank Sandra Ryeom and Kashi Javaherian for helpful discussions.

Conflict-of-interest disclosure: The author declares no competing financial interests. ■

REFERENCES

1. Folkman J. Angiogenesis: an organizing principle for drug discovery? Nat Rev Drug Discov. 2007;6:273-286.
2. Davis DW, Herbst RS, Abbruzzese JL, eds. Antiangiogenic Cancer Therapy. Boca Raton, FL: CRC; 2008.
3. Folkman J. Endogenous angiogenesis inhibitors. Acta Pathologica, Microbiologica, et Immunologica Scandinavica. 2004;112:496-507.
4. Nyberg P, Xie L, Kalluri R. Endogenous inhibitors of angiogenesis. Cancer Res. 2005;10:3967-3979.
5. Abdollahi A, Hahnfeldt P, Maercker C, et al. Endostatin's antiangiogenic signaling network. Mol Cell. 2004;13:649-663.
6. Celik I, Surucu O, Dietz C, et al. Therapeutic efficacy of endostatin exhibits a biphasic dose-response curve. Cancer Res. 2005;65:11044-11050.
7. Slaton JW, Perrotte P, Inoue K, Dinney CP, Fidler IJ. Interferon-alpha-mediated down-regulation of angiogenesis-related genes and therapy of bladder cancer are dependent on optimization of biological dose and schedule. Clin Cancer Res. 1999;5:2726-2734.
8. Teodoro JG, Parker AE, Zhu X, Green MR. p53-mediated inhibition of angiogenesis through up-regulation of a collagen prolyl hydroxylase. Science. 2006;313:968-971.
9. Folkman J. Tumor suppression by p53 is mediated in part by the antiangiogenic activity of endostatin and tumstatin. Sci STKE. 2006;354:pe35.
10. Becker CM, Sampson DA, Rupnick MA, et al. Endostatin inhibits the growth of endometriotic lesions but does not affect fertility. Fertil Steril. 2005;84:1144-1155.

HEMATOPOIESIS

Comment on Chen et al, page 2889

Cited2: master regulator of HSC function?

Hal E. Broxmeyer INDIANA UNIVERSITY SCHOOL OF MEDICINE

Defining intracellular molecules involved in hematopoietic stem cell (HSC) function is important for future efforts to enhance transplantation. Toward this aim, Chen and colleagues report that Cited2, a transcriptional modifier, is necessary for mouse fetal liver hematopoiesis.

Understanding intracellular events that mediate functions of hematopoietic stem cells (HSCs) is important for realizing improved efficacy of HSC transplantation. In this issue of *Blood*, Chen and colleagues have advanced this area by demonstrating a new role for Cited2 (cAMP-responsive element–binding protein [CBP]/p300-interacting transactivators with glutamic acid [E] and aspartic acid [D]–rich tail 2)[1] in steady-state embryogenesis.

Gene-expression profiling linked Cited2 expression with long-term marrow HSC activity.[2] However, the current authors had to study Cited2$^{-/-}$ fetal liver hematopoiesis, since functional deletion of Cited2, a member of a new family of transcriptional modulators, results in embryonic lethality.[3] A role for Cited2 in hematopoiesis was shown by the authors in elegant studies demonstrating that Cited2$^{-/-}$ fetal liver was greatly reduced in phenotyped hematopoietic progenitors (HPCs); compromised reconstitution of T- and B-lymphocyte and myeloid cells was apparent after both primary and secondary transplantation of Cited2$^{-/-}$ fetal liver cells, and the competitive repopulating capacity of these HSCs was decreased.

Exactly how Cited2 acts, alone or in combination with other mediators, to regulate normal hematopoiesis is not known. A number of receptor and intracellular signals are reported to modulate HSC and HPC functions.[4] These include Notch and Notch ligands, Wnt signaling, HoxB4/PBX1, Bmi-1, C/EBPα, Gfi-1, p21$^{cip1/waf1}$, p27^{kip1}, PTEN, Nov/CLN3, glycogen synthase kinase-3, ERK1/2- and p38-MAP kinase, ME/ELK4, RAR-γ, Stat3, Stat5, and Mad2. Microarray analysis by Chen and colleagues showed decreased expression of Wnt5a and a panel of myeloid markers in Cited2$^{-/-}$ fetal livers, as well as decreased expression of Bmi-1, Notch, LEF-1, Mcl-1, and GATA-2 in Cited2$^{-/-}$ c-kit^{+} lineage^{-} fetal liver cells. Placing these molecules into correct positions within interacting networks required to properly mediate self-renewal, proliferation, survival, differentiation, and migration of HSCs—and determining where Cited2 fits into this schema—are vital missing pieces of information. For example, which signals are in linear, branching, or completely separate pipelines, and which occupy key regulatory positions in the cascading sequence of events? Do any of these molecules act as a master switch, and is Cited2 a master regulator? What other roles, if any, does Cited2 play in HSC/HPC function and hematopoiesis? The authors propose future studies involving overexpression of genes identified from the current study in Cited2$^{-/-}$ HSCs, and generation of conditional Cited2 knockout mice at specific development stages and in specific hematopoietic lineages. This should bring us closer to knowing what Cited2 does and does not do.

How HSCs renew themselves is still essentially unknown. While investigators continue to dig away, little by little, at this crucial HSC function, it may be that the field needs to be more creative and think out of the box to get a true picture of the renewal of HSCs, which may not occur as we currently envision it. Whatever model or models are eventually identified for renewal of HSCs, it may be that Cited2 will be an important player in these events. We look forward to finding out.

Conflict-of-interest disclosure: The author declares no competing financial interests. ■

PPARα agonist fenofibrate suppresses tumor growth through direct and indirect angiogenesis inhibition

Dipak Panigrahy*†, Arja Kaipainen*, Sui Huang*‡, Catherine E. Butterfield*, Carmen M. Barnés*, Michael Fannon§, Andrea M. Laforme*¶, Deviney M. Chaponis*¶, Judah Folkman*†, and Mark W. Kieran*†¶

*Vascular Biology Program, Children's Hospital, Department of Surgery, Harvard Medical School, Boston, MA 02115; ¶Division of Pediatric Oncology, Dana–Farber Cancer Institute, Harvard Medical School, Boston, MA 02115; and §Department of Ophthalmology and Visual Sciences, University of Kentucky, Lexington, KY 40536

Contributed by Judah Folkman, November 30, 2007 (sent for review September 7, 2007)

Angiogenesis and inflammation are central processes through which the tumor microenvironment influences tumor growth. We have demonstrated recently that peroxisome proliferator-activated receptor (PPAR)α deficiency in the host leads to overt inflammation that suppresses angiogenesis via excess production of thrombospondin (TSP)-1 and prevents tumor growth. Hence, we speculated that pharmacologic activation of PPARα would promote tumor growth. Surprisingly, the PPARα agonist fenofibrate potently suppressed primary tumor growth in mice. This effect was not mediated by cancer-cell-autonomous antiproliferative mechanisms but by the inhibition of angiogenesis and inflammation in the host tissue. Although PPARα-deficient tumors were still susceptible to fenofibrate, absence of PPARα in the host animal abrogated the potent antitumor effect of fenofibrate. In addition, fenofibrate suppressed endothelial cell proliferation and VEGF production, increased TSP-1 and endostatin, and inhibited corneal neovascularization. Thus, both genetic abrogation of PPARα as well as its activation by ligands cause tumor suppression via overlapping antiangiogenic pathways. These findings reveal the potential utility of the well tolerated PPARα agonists beyond their use as lipid-lowering drugs in anticancer therapy. Our results provide a mechanistic rationale for evaluating the clinical benefits of PPARα agonists in cancer treatment, alone and in combination with other therapies.

stroma | inflammation | fibrates | microenvironment

Peroxisome proliferator-activated receptors (PPARs) are a family of nuclear receptors comprising three isoforms, PPARα, PPARδ, and PPARγ, which act as ligand-activated transcriptional factors. PPARs play key roles in energy homeostasis by modulating glucose and lipid metabolism and transport (1). PPARα is also critical in inflammation (2) and is the molecular target of the fibrate class of drugs, such as fenofibrate, which act as agonistic ligands of PPARα.

Long-term administration of certain PPARα agonists (clofibrate and WY14643) induces hepatocarcinogenesis in rodents but not in humans (3). Consequently, PPARα has not been established as a molecular target for cancer therapy by its agonistic ligands. In contrast, PPARγ and PPARδ agonists have been extensively studied to evaluate their anticancer effects because of their antiproliferative, proapoptotic, antiapoptotic, and differentiation-promoting activity (4). However, recent studies have revealed the expression of PPARα in tumor cells (5, 6), and PPARα ligands suppress the growth of several cancer lines, including colon, breast, endometrial and skin, *in vitro* (7–10). PPARα ligands also suppress the metastatic potential of melanoma cells *in vitro* and *in vivo* (11, 12). Furthermore, PPARα ligands decrease tumor development in murine colon carcinogenesis (7). Clofibric acid inhibits the growth of human ovarian cancer in mice (13). Most recently, the PPARα agonist WY14643 suppresses tumorigenesis in a PPARα-dependent manner (14).

Together, these data suggest that PPARα ligands may have an important role as antitumor agents, although the mechanism remains elusive. PPARα is expressed not only in tumor cells but also in endothelial and inflammatory cells (15, 16). Also, PPARα ligands can inhibit endothelial cell proliferation and migration and induce endothelial cell apoptosis *in vitro* (17–19). In addition, fenofibrate reduces adventitial angiogenesis and inflammation in a porcine model (20) and decreases VEGF levels in patients with hyperlipidemia and atherosclerosis (21). However, the relative role of PPARα in tumor angiogenesis and tumor inflammation has not been studied.

Here, we report that PPARα is expressed both in tumor cells and in tumor endothelium. We show that PPARα ligands have potent antitumor and antiangiogenic effects, both *in vitro* and *in vivo*. Our data demonstrate that PPARα expression in the host rather than in the tumor cell is critical for the antitumor, antiangiogenic, and antiinflammatory activity of PPARα ligands. This extends the repertoire of potential targets of PPARα ligands beyond cell-autonomous mechanisms of cancer. Our findings may be of clinical relevance because PPARα ligands such as fenofibrate are orally administered, Food and Drug Administration-approved drugs widely used for the treatment of hyperlipidemia with minimal side effects.

Results

PPARα Is Expressed in Tumor Cells *in Vitro* and in Tumor Endothelium *in Vivo*. We first screened 19 human tumor cell lines for PPARα expression *in vitro*. In Western blot analysis of cell cultures, we found that all tumor cell lines examined expressed the PPARα protein, although at varying levels (Fig. 1*a*). We obtained similar results in murine tumor cell lines, albeit at a lower intensity. The signal could be specifically neutralized with a blocking peptide (Fig. 1*b*). Expression patterns in tumor tissues were assessed by immunofluorescent double staining for PPARα and the endothelial marker CD31. PPARα staining was examined in s.c. implanted human pancreatic cancer cells (BxPC3) grown in mice (Fig. 1*c*), as well as in clinical specimens from human prostate carcinoma (Fig. 1*d*). We found expression of PPARα in the tumor cells as well as in human and murine endothelial cells of microvessels (Fig. 1 *c* and *d*).

Author contributions: D.P. and A.K. contributed equally to this work; D.P., A.K., S.H., J.F., and M.W.K. designed research; D.P., A.K., C.E.B., M.F., A.M.L., and D.M.C. performed research; D.P., A.K., S.H., C.E.B., and C.M.B. analyzed data; and D.P., A.K., and S.H. wrote the paper.

The authors declare no conflict of interest.

Freely available online through the PNAS open access option.

†To whom correspondence may be addressed. E-mail: dipak.panigrahy@childrens.harvard.edu, judah.folkman@childrens.harvard.edu, or mark_kieran@dfci.harvard.edu.

‡Present address: Institute for Biocomplexity and Informatics, University of Calgary, Calgary, Alberta, Canada T2N 1N4.

This article contains supporting information online at www.pnas.org/cgi/content/full/0711281105/DC1.

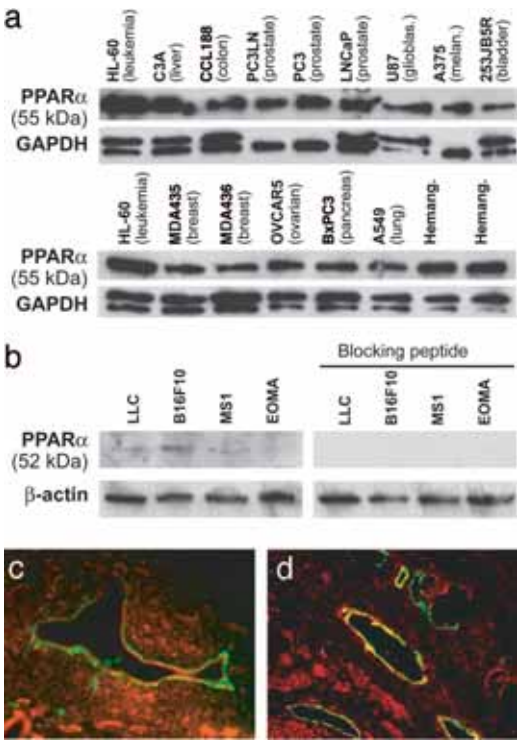

Fig. 1. PPARα is expressed in tumor cells and endothelium of neoplastic tissues. (*a*) Western blot analysis of PPARα expression in cultured human tumor cells and hemangioma specimens. Nuclear extract from leukemia cells (HL-60) was used as a control. (*b*) Western blot analysis of PPARα expression in cultured mouse tumor cells. The specificity of protein expression was confirmed by abrogation by a PPARα-blocking peptide. GAPDH and β-actin levels were measured to demonstrate equal loading of protein in each lane. (*c* and *d*) Immunofluorescent double staining for CD31 and PPARα demonstrates PPARα expression in endothelium of human pancreatic cancer (BxPC3) in SCID mice (*c*) and in patient prostate cancer tissue specimens (*d*). CD31-stained endothelial cells are shown in green, PPARα-positive cells are red, and colocalization of the two colors are yellow. Colocalization of red and green fluorescence (yellow) indicates PPARα expression in blood vessels.

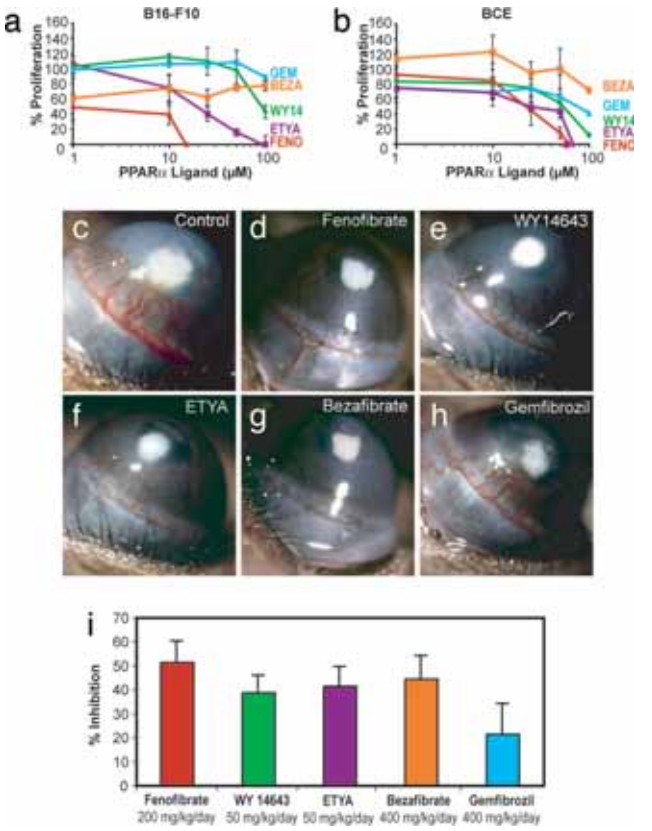

Fig. 2. PPARα ligands have direct antitumor and antiendothelial effects *in vitro* and *in vivo*. (*a*) Percentage of proliferation of tumor cells (B16-F10 melanoma) is determined by comparing cells grown in media plus 10% FBS, and the PPARα ligands, to starved cells. FENO, fenofibrate; WY14, WY14643; BEZA, bezafibrate; GEM, gemfibrozil. (*b*) Percentage of proliferation of BCE cells is determined by comparing cells exposed to an angiogenic stimulus (FGF2) with those exposed to FGF2 and PPARα ligands (fenofibrate, WY14643, gemfibrozil, ETYA, and bezafibrate) relative to unstimulated cells. (*c*) FGF2-induced neovascularization in control cornea on day 6 in a mouse receiving vehicle. (*d–h*) Systemic treatment with fenofibrate at 200 mg/kg per day (*d*), WY14643 at 50 mg/kg per day (*e*), ETYA at 50 mg/kg per day (*f*), bezafibrate at 400 mg/kg per day (*g*), or gemfibrozil at 400 mg/kg per day (*h*). (*i*) Area of inhibition (percentage) by administration of various PPARα ligands: fenofibrate (200 mg/kg per day), 52% inhibition; WY14643 (50 mg/kg per day), 39% inhibition; ETYA (50 mg/kg per day), 42% inhibition; bezafibrate (400 mg/kg per day), 44% inhibition; and gemfibrozil (400 mg/kg per day), 22% inhibition. Inhibition was determined on day 6 by the following formula: pellet distance × 0.2π × neovessel length × clock hours of neovessels. ($n = 6$ eyes per group; the experiment was performed three times.)

PPARα Ligands Have Direct Antitumor and Antiendothelial Effects *in Vitro*. Given the presence of PPARα in multiple cell types, we next compared the effect of PPARα ligands for their ability to inhibit the proliferation of tumor cells, endothelial cells, and fibroblasts. PPARα ligands examined included fenofibrate, gemfibrozil, bezafibrate, WY14643, and 5,8,11,14-eicosatetraynoic acid (ETYA). Fenofibrate was most potent in suppressing the proliferation of all tumor cell lines tested, including melanoma (B16-F10), breast carcinoma (MDA436), and Lewis lung carcinoma (LLC) cells [Fig. 2*a* and supporting information (SI) Fig. 6]. Fenofibrate, WY14643, and ETYA inhibited FGF2-induced proliferation of bovine capillary endothelial cells up to 95% after 3 days (Fig. 2*b*). In addition, fenofibrate inhibited VEGF-stimulated proliferation of human umbilical vein endothelial cells (HUVECs) (data not shown). In contrast to tumor and endothelial cells, PPARα ligands failed to inhibit the proliferation of fibroblasts (foreskin) at doses <50 μM (SI Fig. 7*a*). Moreover, fenofibrate and WY14643 inhibited VEGF-stimulated endothelial cell migration (SI Fig. 7 *b* and *c*). These doses used here are clinically relevant because fibrates in humans readily achieve similar serum levels (22).

To determine whether PPARα ligands could inhibit angiogenesis by down-regulating tumor-secreted growth factors and/or up-regulating endogenous angiogenesis inhibitors, such as thrombospondin (TSP)-1, we measured VEGF, FGF2, and TSP-1 levels in tumor-conditioned media. Fenofibrate and WY14643 at 50 μM inhibited VEGF secretion in glioblastoma (U87) cells by 43–55% and in LLC by 51–58% (SI Fig. 8 *a* and *b*). Both PPARα ligands also inhibited FGF2 secretion in K1000 cells (a tumor cell line that expresses and secretes high levels of FGF2) by up to 70% (SI Fig. 8*c*). In addition, fenofibrate also increased the expression of TSP-1 by 3- to 4-fold in HT-1080 fibrosarcoma and in LLC tumor cells (SI Fig. 8*d* and data not shown). Therefore, in addition to their direct antitumor and antiendothelial effects, PPARα ligands may suppress angiogenesis indirectly by inhibiting tumor cell production of VEGF and FGF2 and by increasing TSP-1.

PPARα Ligands Inhibit FGF2-Induced Corneal Neovascularization. To determine the optimal antiangiogenic doses of PPARα ligands for daily administration in mice, we performed the cornea angiogenesis assay in the presence of five different PPARα ligands (Fig. 2 *c–h*). Systemic oral administration of these

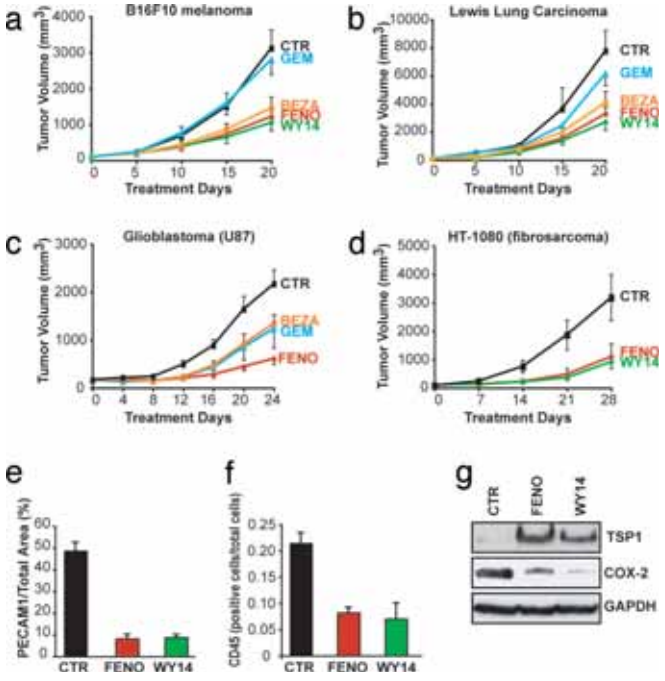

Fig. 3. Systemic therapy with PPARα ligands inhibits primary tumor growth. When tumors reached 100 mm^3 in size, PPARα ligand treatment was initiated (day 0). On the last day of treatment, the statistical difference between control and treated group was determined by Student's *t* test. The most potent antitumor activity was obtained by fenofibrate and WY14643 at the following doses: fenofibrate, 200 mg/kg per day; WY14643, 50 mg/kg per day; bezafibrate, 200 mg/kg per day; and gemfibrozil, 200 mg/kg per day. (*a*) B16-F10 melanoma ($P < 0.001$). (*b*) LLC ($P < 0.001$). (*c*) Glioblastoma (U87) ($P < 0.005$). (*d*) Fibrosarcoma (HT-1080) ($P < 0.0001$). (*e*) Vessel density in fenofibrate-, WY14643-, and vehicle-treated B16-F10 tumors, as defined by the percentage of vessel area = PECAM1-positive area/tumor area in each field. (*f*) Leukocyte counts per total number of cells per field in fenofibrate-treated and WY14643-treated and vehicle-treated B16-F10 tumors, as determined by CD45 staining. (*g*) Western blot analysis of TSP-1 and COX-2 proteins in tumor lysates of fenofibrate-, WY14643-, and vehicle-treated B16-F10 melanomas on day 20.

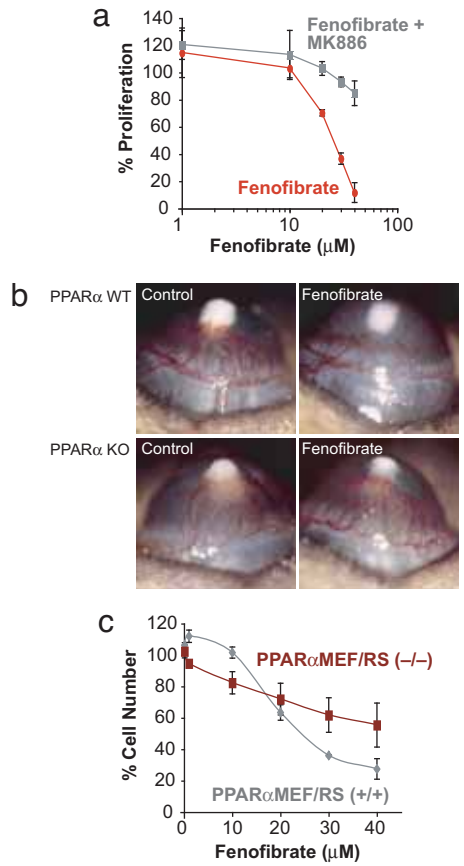

Fig. 4. PPARα ligands have PPARα-dependent and -independent effects. (*a*) Effect of fenofibrate with or without MK886 treatment on the percentage of proliferation on endothelial cells. (*b*) Corneal neovascularization (80 ng of FGF2 pellets) in fenofibrate- and vehicle-treated PPARα WT and PPARα KO mice. (*c*) Effect of fenofibrate treatment on proliferation of PPARα-positive tumor PPARα$^{+/+}$MEF/RS and PPARα-negative tumor PPARα$^{-/-}$MEF/RS on day 3.

PPARα agonists significantly inhibited FGF2-induced corneal angiogenesis by >50% compared with the control (depending on the compound) (Fig. 2*i*).

Systemic Therapy with PPARα Ligands Inhibits Primary Tumor Growth. To determine whether these antiangiogenic effects of PPARα agonists translate to suppression of primary tumors, we treated established s.c. tumors of 100 mm^3 with PPARα agonists. Oral fenofibrate (200 mg/kg per day) inhibited B16-F10 melanoma, LLC, glioblastoma (U87), and fibrosarcoma (HT1080) tumor growth by 61%, 58%, 72%, and 66%, respectively, and was more potent than other fibrates, such as bezafibrate and gemfibrozil (Fig. 3 *a*–*d*). Systemic therapy with WY14643 also inhibited the growth of B16-F10 melanoma, LLC, and fibrosarcoma (HT1080) by 66%, 65%, and 71%, respectively (Fig. 3 *a*, *b*, and *d*). No weight loss or evidence of other drug-related toxicity was observed. Furthermore, no signs of hepatocarcinogenesis were observed in mice treated with PPARα ligands.

Given the *in vitro* evidence for antiangiogenic activity and the known inflammation-modulatory role of PPARα stimulation, we analyzed the tissues of PPARα ligand treated B16-F10 tumors for antiangiogenic and antiinflammatory effects. Fenofibrate and WY14643 treatment reduced vessel density by 83% and 81%, respectively, relative to that in the control tumors (Fig. 3*e* and SI Fig. 9), consistent with the decrease of microvessel density in murine tumor models after treatment with PPARα ligands (13, 14).

In addition, fenofibrate and WY14643 treated tumors exhibited a dramatic reduction in leukocytes by 62% and 67% (CD45) (Fig. 3*f* and SI Fig. 9). Treatment with PPARα ligands also led to an increase of TSP-1 in B16-F10 tumors (Fig. 3*g*). In contrast, the enzyme COX-2, which is an important mediator of inflammation and also regulates endothelial cell activity (23), was suppressed in both fenofibrate- and WY14643-treated B16-F10 tumors (Fig. 3*g*).

Antiangiogenic and Antitumor Effects of PPARα Ligands Are Specific to the Activation of PPARα. To demonstrate the activation of PPARα in endothelial cells, we measured the kinetics of induction of the medium chain acyl-dehydrogenase (MCAD), a target gene of PPARα, in HUVECs. After 12–24 h of fenofibrate treatment (25 μM), MCAD levels increased in a dose-dependent manner, indicating PPARα activation (data not shown). Furthermore, PPARα ligand-mediated inhibition of FGF2-induced proliferation of bovine capillary endothelial cells was reduced by 90% with the PPARα antagonist MK886 (10 μM; $P < 0.001$) (Fig. 4*a*). In addition, PPARα ligands inhibited corneal neovascularization in PPARα WT (52%) but not in PPARα KO mice (Fig. 4*b*). These findings indicate that the antiangiogenic activity of PPARα ligands specifically depends on activation of PPARα.

To confirm that the suppression of tumor cell proliferation by PPARα agonists was specific to PPARα activation, we examined whether fenofibrate could inhibit the proliferation of PPARα-deficient tumor cells. Therefore, we created a PPARα-negative tumor cell line by transforming mouse embryonic fibroblasts

MEDICAL SCIENCES

(MEFs) derived from PPARα KO mice. Embryonic fibroblasts from PPARα KO and WT mice were transformed with SV40 large T antigen and H-ras, giving rise to two tumorigenic cell lines, PPARα$^{-/-}$MEF/RS and PPARα$^{+/+}$MEF/RS, respectively (SI Fig. 10). Although fenofibrate treatment for 3 days showed 44% dose-dependent inhibition of proliferation of the PPARα$^{-/-}$ cells, suggesting off-target effects, the inhibition in the PPARα$^{+/+}$ was significantly higher ($P < 0.02$), with a maximal proliferation inhibition of 73% (Fig. 4*c*). Thus, whereas PPARα ligands may have PPARα-independent antiproliferative effects, pronounced inhibition of cell proliferation requires the presence of the nominal PPARα targets.

The Antitumor Activity of PPARα Ligands Depends on Host PPARα Receptors. Our observations suggest a dual effect of PPARα ligands on both endothelial cells and tumor cells. To evaluate the relative importance of host cells versus tumor cells as targets of PPARα ligands, we treated PPARα-positive tumors (PPARα$^{+/+}$MEF/RS) in PPARα WT and KO mice and PPARα-negative tumors (PPARα$^{-/-}$MEF/RS) in PPARα WT mice. The reason we chose the MEF tumor to test the antitumor activity of fenofibrate was that it has shown sufficient growth in the PPARα KO mouse to reveal inhibition by a drug (24). The MEF tumors grew in the PPARα KO mice mainly because they were transfected with two oncogenes. This gave rise to MEF tumors that were capable of inducing angiogenesis over and above the antiangiogenic state imposed by the PPARα KO mice. In contrast, all other tumors remained viable but dormant and did not grow and therefore were not suitable for testing a drug that inhibits tumor growth.

At the stage when the tumors were 100 mm^3 (corresponding to 9 days postimplantation in PPARα WT mice and 23 days postimplantation in PPARα KO mice), mice were treated with PPARα ligands or vehicle for 16 days. In PPARα WT mice, fenofibrate and WY14643 inhibited the growth of PPARα-positive tumors by 90–95% (Fig. 5*a*) and of PPARα negative tumors by 75–90% by day 25 postimplantation (Fig. 5*b*). The near complete inhibition of tumor growth by PPARα ligands in PPARα-positive and PPARα-negative tumor cells indicates that PPARα in the tumor cell is not the major target of PPARα ligands. Conversely, in PPARα KO mice, fenofibrate and WY14643 failed to significantly inhibit the growth of PPARα$^{+/+}$ tumors (13% and 33%, respectively; Fig. 5*c*) by day 39 postimplantation. Thus, expression of PPARα in the nontumor host tissue is essential for the antitumor activity of PPARα ligands and is sufficient to mediate the antitumor effects of PPARα agonists even if the tumors lack PPARα (Fig. 5*d*).

The suppression of tumor growth in the absence of host PPARα has been associated with increased plasma levels of the antiangiogenic protein TSP-1 (24). TSP-1 was not detected in the plasma of WT mice but was present in PPARα KO mice (Fig. 5*e*). In WT but not PPARα KO mice, fenofibrate induced high levels of TSP-1, consistent with the strong tumor suppression in WT, ligand-treated animals (Fig. 5 *a* and *b*). Fenofibrate also induced high levels of endostatin in the plasma of non-tumor-bearing PPARα WT mice. Fenofibrate did not have an effect in PPARα KO mice, which already exhibited elevated basal levels of both TSP-1 and endostatin (Fig. 5 *e* and *f*), indicating that these antiangiogenic effects of fenofibrate were PPARα-mediated. In summary, PPARα agonists induced an antiangiogenic state characterized by elevated TSP-1 and endostatin, which is qualitatively similar to the effect of PPARα deficiency.

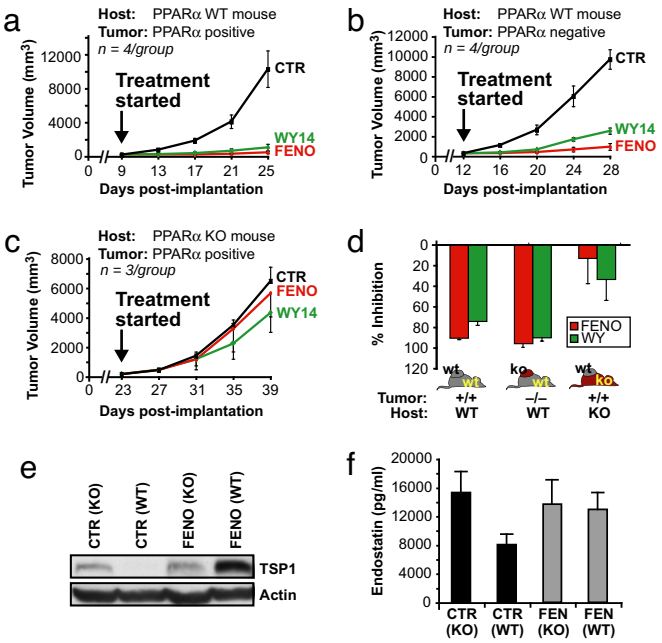

Fig. 5. The antitumor activity of PPARα ligands is host PPARα receptor-dependent. After PPARα-positive (PPARα$^{+/+}$MEF/RS) or PPARα-negative (PPARα$^{-/-}$MEF/RS) tumors were 100 mm^3 in size, PPARα ligand treatment was initiated (day 0). The doses were as follows: fenofibrate, 200 mg/kg per day; and WY14643, 50 mg/kg per day. (*a*) The effect of systemic therapy of PPARα ligands on PPARα-positive tumors (PPARα$^{+/+}$MEF/RS) in PPARα WT mice (90–95% inhibition). (*b*) The effect of systemic therapy on PPARα-negative tumors (PPARα$^{-/-}$MEF/RS) in PPARα WT (75–90% inhibition). (*c*) The effect of systemic therapy of PPARα-positive tumors (PPARα$^{+/+}$MEF/RS) in PPARα (KO) mice (13–33% inhibition). (*d*) The columns summarize the effects of fenofibrate and WY14643 in host or tumor cells. (*e*) Western blot analysis of TSP-1 in plasma from fenofibrate and vehicle treated PPARα WT and PPARα KO mice. (*f*) Endostatin levels in plasma from fenofibrate- and vehicle-treated PPARα WT and PPARα KO mice.

Discussion

The development of cancer is not simply attributable to the loss of growth control of a single cell clone but rather a developmental disease that involves the tumor cell as well as its interaction with the host tissue. This microenvironment includes endothelial cells, inflammatory cells, and other stromal elements. Therefore, targeting the noncancerous host tissue, mainly by antiangiogenesis mechanisms, has emerged as an important opportunity for tumor therapy (25). More recently, modulation of tumor-promoting inflammation in the tumor bed has been proposed as a target for cancer treatment (26).

Here, we report that expression of PPARα in the host tissue is required for PPARα agonists to exert their tumor-suppressing effect. The *in vivo* antitumor effect was not likely mediated by the *in vitro* observed direct antitumor cell activity of PPARα agonists, because in PPARα WT animals, the presence of PPARα in the tumor was not necessary to confer responsiveness to PPARα agonists. In summary, animal studies indicate that expression of PPARα in the nontumor host tissue is necessary and sufficient for the tumor-suppressive effect of PPARα agonists. The host tissue contribution may be local (tumor bed) or systemic. Our analysis suggests that this host-mediated effect of PPARα ligands may be attributable to the inhibition of angiogenesis.

Importantly, the doses of the pharmacological PPARα agonists required for tumor inhibition are in the same range as those used clinically to treat hyperlipidemia (22). PPARα ligands administered at continuous low doses in the diet can suppress tumor and metastatic growth in various experimental tumor models including melanoma, colon, and breast carcinogenesis (11, 27, 28). However, fenofibrate at daily low doses (25 mg/kg or 0.1–0.25%) lacked antitumor activity in primary hamster melanoma (11) and murine endometrial cancer (9). This finding is consistent with our observation that 25 mg/kg of fenofibrate had minimal antitumor and

antiangiogenic effects (data not shown), whereas 200 mg/kg inhibited angiogenesis and tumor growth.

The antitumor activity of PPARα ligands is primarily PPARα-dependent but may also be mediated by PPARα-independent ("off-target") pathways (22). Here we demonstrated specific PPARα-dependent effects of the nominal PPARα ligands: (*i*) direct activation of the target gene, MCAD, in endothelial cells; (*ii*) inhibition of tumor and endothelial cell proliferation at doses that selectively activate PPARα *in vitro* and that were reversed by a PPARα antagonist; and (*iii*) inhibition of corneal neovascularization in WT but not in PPARα KO mice. Conversely, the presence of PPARα-independent activity was evidenced in the moderate inhibition of proliferation of PPARα-negative cells. However, this effect may not contribute to *in vivo* tumor suppression because the antitumor effect of PPARα agonists was mediated by PPARα expressed in the nontumor host tissue.

In addition to the antiproliferative activity, PPARα ligands such as fenofibrate induce a dose-dependent increase in endothelial cell apoptosis and causes arrest in the cell cycle in the G_0/G_1 phase at higher doses (18). However, even higher PPARα concentrations also can activate PPARγ and/or PPARδ (22). Our studies also show that bezafibrate minimally suppressed the proliferation of endothelial cells yet strongly inhibited corneal neovascularization *in vivo*. Bezafibrate is a pan-PPAR agonist that activates all three nuclear receptors, PPARα, PPARγ, and PPARδ (22). We and others have found that ligand-induced activation of PPARγ inhibits endothelial proliferation and corneal angiogenesis (29). In contrast, activation of PPARδ promotes endothelial proliferation (30). Thus, one possibility to explain the weak antiendothelial activity of bezafibrate *in vitro* compared with its robust antiangiogenic activity *in vivo* is by the relative contribution of each activated PPAR to the overall angiogenic response.

Although our *in vitro* data revealed a potent role of PPARα ligands in the inhibition of tumor cells, endothelial cell proliferation, and angiogenesis, PPARα ligands also have antiinflammatory effects. The antiinflammatory effect of PPARα ligands is mediated notably through inhibition of inducible NOS, COX-2, and TNFα (31). Inflammatory cells present in the tumor play an important tumor-promoting role (26) by secretion of trophic cytokines for tumor cells as well as proangiogenic factors. Suppression of inflammation in tumors may correlate with improved prognosis and growth inhibition. In agreement with the role of inflammatory cells in tumors and the antiinflammatory activity of PPARα agonists, we show that tumor growth suppression caused by PPARα ligands significantly decreased leukocyte expression within the tumor. Moreover, expression of an inflammatory mediator, COX-2, was decreased in the PPARα ligand-treated tumors.

Although the role of PPARα in inflammation has been well characterized, the modulating effect of PPARα on inflammatory processes in the context of tumor growth remains unclear. We recently reported that PPARα KO mice exhibited a significant increase in inflammatory infiltrates in tumors (24), consistent with the role of PPARα in the negative modulation of inflammation (2). However, contrary to the recent notion of inflammation as a tumor promoter (26), this overt inflammation in PPARα KO mice not only failed to support tumor growth but also appeared to actively suppress it. Specifically, the lack of PPARα resulted in an increase of TSP-1 and endostatin levels in plasma and/or tumors, which may explain the observed tumor suppression.

It is counterintuitive that PPARα activation by agonists and genetic abrogation of PPARα in the host would both lead to tumor inhibition. Treatment of PPARα WT mice with a PPARα agonist led to an increase in TSP-1 and endostatin in tumors and/or plasma, producing an antiangiogenic state similar to the PPARα KO mice (24). Two perturbations of PPARα activity in opposite directions both inhibit tumor growth and increase TSP-1 and endostatin levels. This underscores the central role of these angiogenesis inhibitors in the control of tumor growth. Endostatin induces TSP-1 expression (32). This raises the possibility that these two angiogenesis inhibitors are coordinated.

An analogous paradox of PPARα effect has been described in atherosclerosis. Plaque growth depends on angiogenesis (33). Atherosclerosis is suppressed not only in PPARα KO mice (34) but also in mice treated with fenofibrate (35). In more general terms, these counterintuitive results suggest a biphasic (U-shaped) dose–response curve of host tissue to PPARα activity, as is also observed with PPARγ agonists (29). In other words, very high concentrations or "very low" concentrations of PPARα in the host yield the same outcome: maximal suppression of tumor angiogenesis.

Of interest, clinical evidence suggests that long-term administration of fibrates may reduce melanoma progression. Gemfibrozil-treated patients had a 9-fold decrease in melanoma compared with placebo-treated controls, whereas statin-treated patients had a 1.9-fold reduced incidence of melanoma compared with placebo treated controls (36). Fenofibrate also increased the response rate to retinoids in a human clinical trial for cutaneous T cell lymphoma (37), suggesting that PPARα ligands may potentiate the effect of other anticancer agents.

In conclusion, we provide a mechanistic rationale for extending the clinical use of the well tolerated PPARα agonists to anticancer therapy, and we show their efficacy in tumor treatment in animal models. The antitumor properties of PPARα ligands appear to be mediated primarily by their direct and indirect antiangiogenic effects and their antiinflammatory activity but also by direct antitumor effects. This provides another example for the paradigm of achieving antitumor efficacy through synergistic attack on multiple targets that encompass cell autonomous and non-cell-autonomous mechanisms of cancer growth. Because of their multifaceted effects and excellent safety and tolerability profile after chronic and prolonged exposure, PPARα ligands may be potential tumor-preventative agents. They may be used for maintenance of long-term angiogenesis suppression. Furthermore, our findings support recent studies (11–14) that suggest that PPARα ligands may be ideally suited to complement conventional modalities for cancer treatment. Specifically, because fenofilerate is commercially available, it could be evaluated as an extension of existing multidrug regimens, notably in metronomic (antiangiogenic) chemotherapy schemes (38, 39). However, further research into the pathophysiological role of PPARα and their pharmacological regulators will be paramount to unravel all mechanisms for the antitumor effects of PPARα agonists.

Materials and Methods

Cells and Reagents. Endothelial cells, fibroblasts, and tumor cells were maintained as described (29) in *SI Methods*. Fenofibrate, bezafibrate, and gemfibrozil were obtained from Sigma; WY14643 and ETYA were from Chem-Syn.

Western Blot Analysis. Western blots were performed by using tumor cell lysates collected from plated cells that were 60% confluent. Total protein extracts (30 μg) were analyzed on PVDF membrane blots incubated overnight with rabbit anti-mouse PPARα (Affinity Bioreagents) or rabbit anti-human PPARα (Active Motif). All blots were incubated for 1 h with their corresponding HRP-conjugated secondary antibodies (Amersham Biosciences) and developed with ECL (Pierce). For immunoblotting of TSP and COX-2 (Labvision), the primary antibody was incubated at room temperature for 2 h.

Immunohistochemistry. Sections of tumors were treated with 40 μg/ml proteinase K (Roche Diagnostics) for 25 min at 37°C for PECAM1. PECAM1 was amplified by using tyramide signal amplification direct and indirect kits (NEN Life Science Products). CD45 (BD Biosicences) was detected by using a rat-on-mouse kit (InnoGenex).

Proliferation Assays. Endothelial, fibroblast, and tumor cell proliferation were assayed as described (29). For PPARα antagonist studies, MK886 (Alexis Biochemicals) was used. For proliferation of PPARα-negative and PPARα-positive cells, percentage cell number = $100 \times (\text{cells}_{\text{ligand}})/(\text{cells}_{\text{stimluated}})$.

Angiogenesis Assays. Corneal neovascularization assays were performed as described (29). After implantation of 80 ng of FGF-2 into C57Bl6, PPARα WT, and PPARα KO mice, PPARα ligands were administered over 6 days by gavage in an aqueous solution of 10% DMSO in 0.5% methylcellulose, whereas control mice received vehicle. Tumor cells were injected s.c. (1×10^6 cells in 0.1 ml of PBS) into C57BL/6, SCID, PPARα WT, or PPARα KO mice (The Jackson Laboratory). Once tumors reached 100 mm^3, PPARα ligands were administered by daily gavage for 20–28 days. Tumor volume was calculated as width squared $\times$ length $\times$ 0.52.

Statistical Analysis. The Student's paired *t* test was used to analyze the difference between the two groups. Values were considered significant at $P < 0.05$.

Note. During the finalization of this article, Pozzi *et al.* (14) published a report in which they showed PPARα-mediated inhibition of angiogenesis and tumor growth. Their findings, although by using a different tumor model and focusing on a single agonist, WY14643, are consistent with ours and confirm the important role of PPARα in tumor suppression.

ACKNOWLEDGMENTS. We thank Lars Akslen for helpful discussions regarding pathology; Deborah Freedman-Cass (Fox Chase Cancer Center, Philadelphia) and Michael Rogers for suggestions in preparing the manuscript; William Hahn (Dana–Farber Cancer Institute) for Large T and ras constructs; Kristin Johnson for photography; and Giorgio Pietramaggiori and Ricky Sanchez for excellent technical assistance. This work was supported by the Stop and Shop Pediatric Brain Tumor Fund, the C. J. Buckley Pediatric Brain Tumor Research Fund (M.W.K., D.P., A.K.), Department of Defense Innovator Award W81XWH-04-1-0316 (to J.F.), the Breast Cancer Research Foundation (J.F.), National Cancer Institute Grant R01CA064481 (to J.F.), and private philanthropic funds.

1. Lefebvre P, Chinetti G, Fruchart JC, Staels B (2006) Sorting out the roles of PPARα in energy metabolism and vascular homeostasis. *J Clin Invest* 116:571–580.
2. Devchand PR, *et al.* (1996) The PPARα-leukotriene B4 pathway to inflammation control. *Nature* 384:39–43.
3. Peters JM, Cattley RC, Gonzalez FJ (1997) Role of PPARα in the mechanism of action of the nongenotoxic carcinogen and peroxisome proliferator Wy 14,643. *Carcinogenesis* 18:2029–2033.
4. Michalik L, Desvergne B, Wahli W (2004) Peroxisome-proliferator-activated receptors and cancers: complex stories. *Nat Rev Cancer* 4:61–70.
5. Collett GP, *et al.* (2000) Peroxisome proliferator-activated receptorα is an androgen-responsive gene in human prostate and is highly expressed in prostatic adenocarcinoma. *Clin Cancer Res* 6:3241–3248.
6. Suchanek KM, *et al.* (2002) Peroxisome proliferator-activated receptorα and the human breast cancer cell lines MCF-7 and MDA-MB-231. *Mol Carcinog* 34:165–171.
7. Tanaka T, *et al.* (2001) Ligands for peroxisome proliferator-activated receptorsα and γ inhibit chemically induced colitis and formation of aberrant crypt foci in rats. *Cancer Res* 61:2424–2428.
8. Maggiora M, *et al.* (2004) An overview of the effect of linoleic and conjugated-linoleic acids on the growth of several human tumor cell lines. *Int J Cancer* 112:909–919.
9. Saidi SA, Holland CM, Charnock-Jones DS, Smith SK (2006) *In vitro* and *in vivo* effects of the PPARα agonists fenofibrate and retinoic acid in endometrial cancer. *Mol Cancer* 5:13.
10. Thuillier P, *et al.* (2000) Activators of peroxisome proliferator-activated-α partially inhibit mouse skin tumor promotion. *Mol Carcinog* 29:134–142.
11. Grabacka M, *et al.* (2004) Inhibition of melanoma metastases by fenofibrate. *Arch Dermatol Res* 296:54–58.
12. Grabacka M, Plonka PM, Urbanska K, Reiss K (2006) Peroxisome proliferator-activated receptorα activation decreases metastatic potential of melanoma cells *in vitro* via down-regulation of Akt. *Clin Cancer Res* 12:3028–3036.
13. Yokoyama Y, *et al.* (2007) Clofibric acid, a peroxisome proliferator-activated receptorα ligand, inhibits growth of human ovarian cancer. *Mol Cancer Ther* 6:1379–1386.
14. Pozzi A, *et al.* (2007) Peroxisomal proliferator-activated receptor-α-dependent inhibition of endothelial cell proliferation and tumorigenesis. *J Biol Chem* 282:17685–17695.
15. Marx N, Sukhova GK, Collins T, Libby P, Plutzky J (1999) PPARα activators inhibit cytokine-induced vascular cell adhesion molecule-1 expression in human endothelial cells. *Circulation* 99:3125–3131.
16. Berger J, Moller DE (2002) Mechanism of action of PPARs. *Annu Rev Med* 53:409–435.
17. Goetze S, *et al.* (2002) PPAR activators inhibit endothelial cell migration by targeting Akt. *Biochem Biophys Res Commun* 293:1431–1437.
18. Varet J, *et al.* (2003) Fenofibrate inhibits angiogenesis *in vitro* and *in vivo*. *Cell Mol Life Sci* 60:810–819.
19. Meissner M, *et al.* (2004) PPARα activators inhibit vascular endothelial growth factor receptor-2 expression by repressing Sp1-dependent DNA binding and transactivation. *Circ Res* 94:324–332.
20. Kasai T, Miyauchi K, Yokoyama T, Aihara K, Daida H (2006) Efficacy of peroxisome proliferative activated receptor (PPAR)-α ligands, fenofibrate, on intimal hyperplasia and constrictive remodeling after coronary angioplasty in porcine models. *Atherosclerosis* 188:274–280.
21. Blann AD, Belgore FM, Constans J, Conri C, Lip GY (2001) Plasma vascular endothelial growth factor and its receptor Flt-1 in patients with hyperlipidemia and atherosclerosis and the effects of fluvastatin or fenofibrate. *Am J Cardiol* 87:1160–1163.
22. Willson TM, Brown PJ, Sternbach DD, Henke BR (2000) The PPARs: From orphan receptors to drug discovery. *J Med Chem* 43:527–550.
23. Grau R, Punzon C, Fresno M, Iniguez MA (2006) Peroxisome-proliferator-activated receptorα agonists inhibit cyclo-oxygenase 2 and vascular endothelial growth factor transcriptional activation in human colorectal carcinoma cells via inhibition of activator protein-1. *Biochem J* 395:81–88.
24. Kaipainen A, *et al.* (2007) PPARα deficiency in inflammatory cells suppresses tumor growth. *PLoS ONE* 2:e260.
25. Folkman J (1971) Tumor angiogenesis: Therapeutic implications. *N Engl J Med* 285:1182–1186.
26. Coussens LM, Werb Z (2002) Inflammation and cancer. *Nature* 420:860–867.
27. Niho N, *et al.* (2003) Concomitant suppression of hyperlipidemia and intestinal polyp formation in Apc-deficient mice by peroxisome proliferator-activated receptor ligands. *Cancer Res* 63:6090–6095.
28. Pighetti GM, *et al.* (2001) Therapeutic treatment of DMBA-induced mammary tumors with PPAR ligands. *Anticancer Res* 21:825–829.
29. Panigrahy D, *et al.* (2002) PPARγ ligands inhibit primary tumor growth and metastasis by inhibiting angiogenesis. *J Clin Invest* 110:923–932.
30. Piqueras L, *et al.* (2007) Activation of PPARβ/δ induces endothelial cell proliferation and angiogenesis. *Arterioscler Thromb Vasc Biol* 27:63–69.
31. Moraes LA, Piqueras L, Bishop-Bailey D (2006) Peroxisome proliferator-activated receptors and inflammation. *Pharmacol Ther* 110:371–385.
32. Abdollahi A, *et al.* (2004) Endostatin's antiangiogenic signaling network. *Mol Cell* 13:649–663.
33. Moulton KS, *et al.* (1999) Angiogenesis inhibitors endostatin or TNP-470 reduce intimal neovascularization and plaque growth in apolipoprotein E-deficient mice. *Circulation* 99:1726–1732.
34. Tordjman K, *et al.* (2001) PPARα deficiency reduces insulin resistance and atherosclerosis in apoE-null mice. *J Clin Invest* 107:1025–1034.
35. Duez H, *et al.* (2002) Reduction of atherosclerosis by the peroxisome proliferator-activated receptorα agonist fenofibrate in mice. *J Biol Chem* 277:48051–48057.
36. Dellavalle RP, Nicholas MK, Schilling LM (2003) Melanoma chemoprevention: A role for statins or fibrates? *Am J Ther* 10:203–210.
37. Talpur R, Ward S, Apisarnthanarax N, Breuer-Mcham J, Duvic M (2002) Optimizing bexarotene therapy for cutaneous T-cell lymphoma. *J Am Acad Dermatol* 47:672–684.
38. Kieran MW, *et al.* (2005) A feasibility trial of antiangiogenic (metronomic) chemotherapy in pediatric patients with recurrent or progressive cancer. *J Pediatr Hematol Oncol* 27:573–581.
39. Kerbel RS, Kamen BA (2004) The anti-angiogenic basis of metronomic chemotherapy. *Nat Rev Cancer* 4:423–436.

Clin Exp Metastasis (2009) 26:51–60
DOI 10.1007/s10585-008-9176-0

RESEARCH PAPER

Tumor dormancy due to failure of angiogenesis: role of the microenvironment

George N. Naumov · Judah Folkman · Oddbjorn Straume

Received: 22 February 2008 / Accepted: 26 April 2008 / Published online: 18 June 2008

Abstract Tumor progression is dependent on a number of sequential steps, including initial recruitment of blood vessels (i.e., angiogenic switch). Failure of a microscopic tumor to complete one or more of these early steps may lead to delayed clinical manifestation of the cancer. In this review we summarize some of the clinical and experimental evidence suggesting that microscopic human cancers can remain in an asymptomatic, non-detectable, and occult state for the life of a person or animal. We present three clinical cases where tumors present shortly after an accidental trauma in otherwise healthy individuals. We also review current experimental human tumor dormancy models with special emphasis on the angiogenic switch which closely recapitulates clinically observed delay in tumor recurrence.

G. N. Naumov · J. Folkman · O. Straume
Vascular Biology Program, Children's Hospital Boston, 300 Longwood Ave., Boston, MA 02115, USA

G. N. Naumov · J. Folkman · O. Straume
Department of Surgery, Harvard Medical School, 300 Longwood Ave., Boston, MA 02115, USA

G. N. Naumov (✉)
Karp Family Research Laboratories 12007C, 300 Longwood Avenue, Boston, MA 02115, USA
e-mail: george.naumov@childrens.harvard.edu

O. Straume
The Gade Institute, Section of Pathology, University of Bergen, Bergen, Norway

O. Straume
Institute of Internal Medicine, Section of Oncology, University of Bergen, Bergen, Norway

Keywords Dormancy · Human tumors · Metastasis · Angiogenesis · Microenvironment · Trauma

Clinical evidence of tumor dormancy

More than a third of US citizens are diagnosed with cancer (in situ or invasive) during their lifetime, and more than 10,000,000 people alive have been previously diagnosed with cancer (~3.5% of the US population) (http://seer.cancer.gov/). Those numbers have been steadily increasing in most industrialized countries due to increased lifetime expectancy, improved diagnostics, and screening programs [1–3]. However, autopsy studies on individuals who died in automobile accidents or other trauma have demonstrated an even higher prevalence of microscopic cancer. These findings indicate that a large proportion of the population can carry microscopic cancers that never progress into clinically detectable disease [3]. These harmless and microscopic in size tumors can remain dormant for life. Nielsen et al. reported that as many as 39% of women (ages 40–49 years) have clinically occult (i.e. undetectable) breast cancer [4]. However, only ~1.8% of women are ever diagnosed with breast cancer in the same age group (Table 1). Similar differences (i.e., 11 to 16-fold) between clinically diagnosed breast cancer and microscopic disease found at autopsy were reported for younger (30–39 years old) and older (50–54 years old) Scandinavian women populations. A high prevalence of microscopic cancer is also reported for other cancer types. For example, carcinoma in situ of the prostate is surreptitiously discovered in as high as 31% of men age 60–70 years who die of trauma, but is clinically diagnosed in only ~8% of men in this age group (Table 1) [5]. Most strikingly, microscopic carcinoma (often less than 1 mm in diameter) is found in

Table 1 Summary of autopsy studies performed on people who have died without clinically diagnosed cancer. This table compares the prevalence of microscopic "occult" cancer found in the breast, prostate or thyroid to the cumulative risk of clinically detectable cancer by age groups

Cancer type	Age group (years)	Prevalence of microscopic cancer (%)	Cumulative risk of this diagnosis for age group (SEER database) (%)	Reference
Breast cancer	30–39	8	~0.5	Nielsen et al. [4, 74]
	40–49	39	~1.8	
	50–54	33	~2.9	
Prostate cancer	20–29	3.6	~0.001	Sanchez-Chapado et al. [5]
	30–39	8.8	~0.009	
	40–49	14.3	~0.29	
	50–59	23.8	~2.4	
	60–69	31.7	~8.1	
	70– 80	33.3	~13.9	
Thyroid carcinoma	21–40	25	~0.2	Harach et al. [6]
	41–60	38.1	~0.5	
	61–80	35.6	~0.7	
	81–100	31.3	~0.7	

the thyroid of more than 38% of individuals age 41 to 60 years who died of trauma, but is diagnosed in only 0.5% during life, in individuals in this age group [6]. This clinical evidence originates from detailed autopsy studies performed by sectioning the organs approximately 2–5 mm apart and systematically examining throughout the whole organ. Due to this resolution limitation, microscopic lesions in the vicinity of 1–2 mm in diameter could be easily overlooked and their total numbers underestimated. Therefore, Black and Welch speculated that after steriological adjustment, microscopic thyroid cancer can be found in as many as 98% of individuals age 50–70 years who die of trauma [3].

Additional clinical evidence in support of tumor dormancy comes from studies focused on recurrence patterns of cancer after primary surgery [7]. Data from the Milan series of more than 1,000 breast cancer patients treated with mastectomy alone show a two peak recurrence pattern that cannot be explained by a continuous tumor growth model, but is in accordance with a model that includes periods of dormant metastasis [8]. The recurrence pattern showed an early peak at about 18 months after surgery, followed by a second peak at approximately 60 months and a tapered plateau-like tail extending up to 15 years [9]. This recurrence pattern has also been recently confirmed in a series of ~956 Asian patients [10], and it has further been hypothesized that the recurrence patterns observed in these series can be in part explained by surgery-driven interruption of dormant micrometastatic breast cancer [9]. The early recurrence peak could best be explained by a triggering, synchronizing event at the time of surgery, and for these patients the surgery itself may have caused a release of different growth factors sufficient to break the dormancy of the micrometastases already present in the body [9, 11].

Influence of trauma on the tumor dormancy period

During 2000 to 2003, we recorded three cases of trauma-induced lymphoma growth at the Department of Oncology, Haukeland University Hospital, Bergen, Norway.

Case 1

Woman, 70 years old. In January 2001, the patient fell off a ladder and hit her forehead on the edge of a table, as she was cleaning the house after Christmas. A bump and a hematoma presented immediately after the accident, but the bump persisted as a painless swelling. During the next 6 months the swelling, interpreted as a post traumatic hematoma, slowly grew in size to include most of her forehead. Finally, in October 2001, malignancy was suspected and an MRI was taken (Fig. 1a), showing an expansive process on the outside of the os frontalis, affecting the bone, but without intracranial growth. Clinically, she presented a hard and fixed tumor including most of the forehead from temple to temple. A distinct and significant vessel growth in the skin covering the tumor was grossly visible. There were multiple delimited and smaller tumors towards the vertex. The patient was diagnosed with diffused large B-cell lymphoma, as assessed by a biopsy (Fig. 1b–c). CT scan showed two small lesions in the spleen, but additional staging examinations were negative, the disease was classified as stage IIIEA.

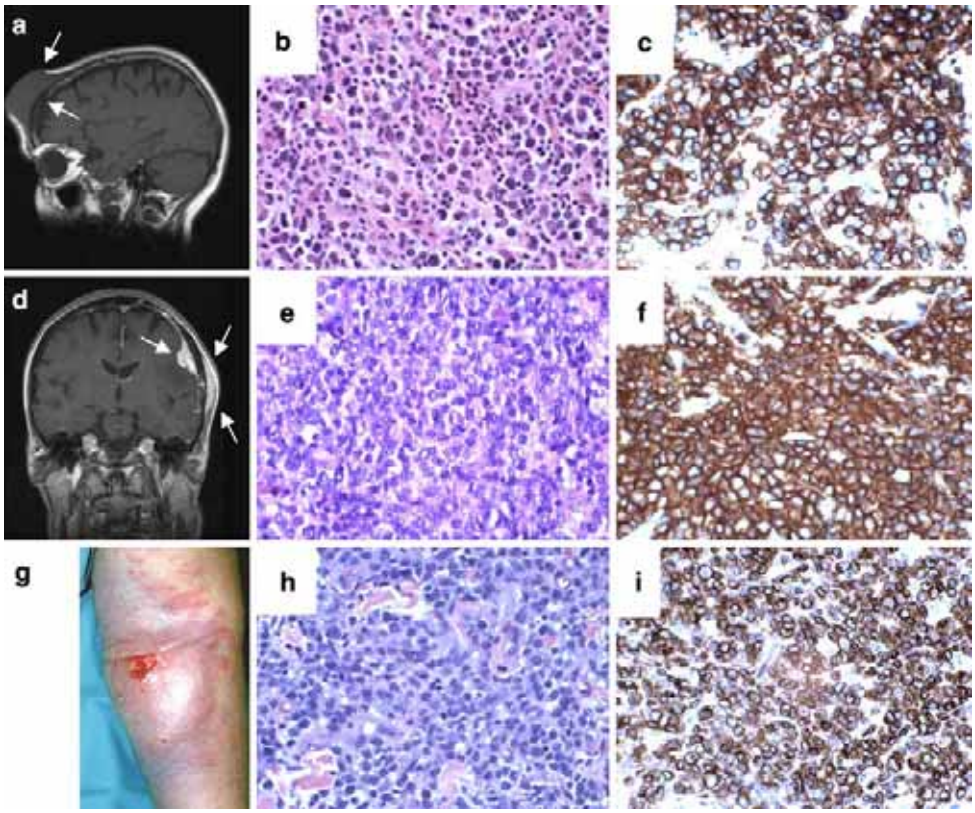

Fig. 1 Three cases of trauma induced lymphomas. Case 1 (**a**-**c**), sagittal MRI section showing a forehead tumor (**a**), large B-cell lymphoma stained by HE (**b**) and CD20 (**c**). Case 2 (**d**–**f**), coronal MRI section showing a soft tissue tumor extending through the left temporal bone and growing along the dura, large B-cell lymphoma stained by HE (**e**) and CD20 (**f**). Case 3 (**g**–**i**), large cutaneous tumor growing in the left fossa cubiti (**g**), large cell T-cell lymphoma stained by HE (**h**) and CD3 (**i**). The histological pictures were kindly provided by Dr Leif Bostad, The Gade Institute, Department Pathology, University of Bergen, Norway

Case 2

Woman, 66 years old. In December 2000, as she was Christmas shopping, the patient hit her left temporal region of her head on the doorframe while entering a car. She presented with a temporary hematoma and swelling. After a few weeks a painless swelling occurred in the region of the initial trauma. At the same time, the patient was feeling dizzy, and after a minor seizure she was hospitalized. MRI showed extra cranial induration of soft tissue in the left temporal region which extended through the bone and showed intracranial growth along the dura (Fig. 1d). The condition was interpreted as intraosseous meningioma, and a craniotomy was performed. Histology showed tumor tissue with lymphoid malignant cells (Fig. 1e), positive for CD45 and CD20 (Fig. 1f) and with more than 80% of the cells being positive for Ki67. The diagnosis was corrected to diffuse large B-cell lymphoma stage IAE, and no other lymphoma manifestations were found.

Case 3

Woman, 72 years old. In 2003 she had a routine venepunction taken from her left fossa cubiti. A hematoma, approximately 5 × 5 cm in size, presented in the area after the procedure, but the discoloration disappeared after a week. Still, during a couple of weeks after the venesection, the skin over the previous hematoma slowly became infiltrated and thickened. The swelling grew larger and formed a painful tumor, and at the end of the month she was hospitalized for suspicion of abscess (Fig. 1g). Bacteriological tests were negative, and when a biopsy was performed, it revieled a tumor infiltrating the skin consisting of large blasts. There were abundant mitoses and >90% of the cells were Ki67 positive, and the tumor was positive for CD3 (Fig. 1h, i). This patient was diagnosed with cutaneous large cell T-cell lymphoma. Except from two enlarged lymph nodes in the left axilla, staging examination were negative, thus the lymphoma was staged as IIEA.

These three cases illustrate a phenomenon where local trauma causes a permissive microenvironmental niche for a tumor to grow. It is very unlikely that the trauma causes the primary transformation of lymphatic cells into malignant lymphoma cells, because of the very short time span between the trauma and the onset of malignant growth. In addition, the trauma sites were extralymphatic, suggesting that a dormant lymphoma was not likely present prior to the injury. In fact, further examination of 2 out of the 3 patients showed signs of asymptomatic (i.e., occult) systemic disease at the time of diagnosis. The fast growth rate of the tumors indicates that a local switch occurred at the time of implantation in the wounded tissue, a possible switch from dormant lymphoma cells present in the

circulation and lymphatic organs, into lymphoma cells capable of proliferation and induction of angiogenesis necessary for tumor growth.

In addition to these three cases presented, other reports have documented similar phenomenon in a number of primary or metastatic cancer types including lymphoma [12], meningioma [13], colon cancer [14] and melanoma [15]. A study by Flook et al. [16] describing the recurrence pattern after melanoma surgery, provides further support of the hypothesis that wounds are able to attract circulating cancer cells, and offer a permissive environment for growth. Traditionally, surgeons are trained not to remove skin grafts (for melanoma defects) from the same limb as the melanoma to avoid in transit lymphatic metastasis in the wound. This practice was questioned by Flook and colleagues who compared the recurrence patterns between patients with ipsilateral and contralateral donor sites, and found no increased metastasis on the ipsilateral sites. In fact, they found metastasis to occur in donor sites outside the lymphatic drainage area of the primary tumor [16], suggesting that the cancer cells were spread by the hematogenous route, and soiled in a permissive area of acute trauma, namely the donor site wound.

The hypothesis that injury influences tumor growth is not new [17, 18]. Marjolin's ulcer is a special form of this phenomenon where tumor growth, almost exclusively squamous cell carcinoma, occurs at the site of chronic ulceration, as well as in fistulas and scars (typically burn scars) [19]. These cancers are more likely to represent malignant transformation on the site of the wound, because of the mutagenic potential of the event causing the trauma (i.e. chemical mutagens, chronic inflammation, thermal or toxic influence, immunodeficiency etc). [19], and might take several years to occur. Bissell and colleagues have demonstrated the importance of the tumor-microenvironment signaling communication [20]. Experimental evidence from this group has shown that tissue wounding can induce inflammation and can promote local epithelial transformation and tumor growth in Rous sarcoma virus (RSV)-infected chickens [21, 22].

In contrast to Marjolin's ulcers, it has been suggested that the acute trauma, hematoma, or wound attracts circulating cancer cells [23]. If the dormancy of cancer cells can be influenced by microenvironmental trauma, this can have significant clinical impact, considering that dormant circulating tumor cells have been detected more than 20 years after mastectomy in women without clinical evidence of cancer recurrence [24].

In a series of studies, Murthy and colleagues showed that injection of TA3Ha transplantable murine mammary carcinoma cells did not cause liver or kidney metastasis in a cohort of 116 mice. However, if hepatic wedge resection was performed immediately before the cancer cell injection, over 50% of the animals had tumor formation at the site of surgery [25]. This tumor-take was significantly reduced if injection of cancer cells was delayed, indicating that the acute and early wound healing supports tumor implantation better. The same authors also reported that the tumor implantation and formation in the wounded liver, was inhibited by plasminogen activators in a dose-dependent matter [26]. Acceleration of secondary tumor growth following excision of a primary tumor has been attributed to the removal of primary tumor-derived inhibitory factors like angiostatin [27]. Others have also shown that the surgical procedure itself induces the growth of both the primary tumor and the metastasis, suggesting the ability of malignant tissue to respond to surgical wounding of normal tissue, and indicates the presence also of a systemic tumor stimulating factor [28].

In an experimental study, Gill and colleagues demonstrated an important role of the bone marrow in wound repair after vascular trauma. Burn injury or surgical manipulation resulted in a rapid mobilization of circulating endothelial precursor (CEP) cells from the bone marrow, which comprised as much as 12% of the total circulation mononuclear cells 24 h after the injury. This was accomplished by an elevation of VEGF in the plasma. This suggests that VEGF released as a result of vascular injury promotes the mobilization of CEPs [29]. Also, the recruitment of CEPs from the bone marrow was found to be dependent on upregulation of Id1 and Id3 [30].

Abramovitch and colleagues studied the impact of wound fluids derived from cutaneous injuries of pigs on the growth of C6 glioma xenografts. They found that angiogenesis was increased and tumor growth was accelerated [31]. The same study concluded that among several growth factors present in the wound fluid, EGF and PDGF were particularly important. Recently, Indraccolo et al. showed that coadministration of proliferation-arrested Kaposi's sarcoma cells or recombinant angiogenic factors interrupts dormancy of poorly angiogenic leukemia cells by providing a brief angiogenic burst [32, 33]. It has also been observed that the transplantation of skin, containing a premalignant skin lesion to cover a skin deficit after a burn injury, might have caused the transformation into a highly malignant melanoma [15].

Presence of systemic growth factors in patients experiencing their first recurrence after a primary treatment is indicated by the fact that, except from local or locoregional recurrences, the growth of recurrent disease seems to be synchronized. The mathematical likelihood of finding only one lung metastasis as the first recurrent lesion 10 years after breast cancer surgery is statistically higher than finding two or more [34], but clinical observations and follow up studies, show that most breast cancer patients present two or more lesions at the time of first recurrence

[34–37]. These findings support the concept that there is a systemic and synchronized process breaking the dormancy of the micrometastatic state of the malignant disease.

If proven to be clinically significant, the short-term angiogenic burst model [33], and the model of surgery driven influence on the dormancy of micrometastatic disease [9] would potentially have dramatic impact on future clinical practice. Would the administration of anti-angiogenic, anti-inflammatory or other anti-growth factor drugs directly before primary surgery and/or immediately after primary surgery lead to a reduction of recurrences during the first peak at about 18 months? Should all women treated for more careful not to get injuries, and if they do get injured, should they then take a short-term treatment of an anti-VEGF drug to keep their micrometastases dormant? Importantly, we also should consider the ethical aspects of this discussion when designing clinical studies and questionnaires to address this question. If we ask a person if she experienced a significant injury within 6 months ahead of her first recurrence, we might introduce a feeling of guilt about the development of the cancer, and the idea that outcome would be different if she had responded differently.

Angiogenesis dependence of tumor growth

Tumor progression from a harmless single neoplastic cell to a lethal distant organ macrometastsis is a multistep process. The genetic and epigenetic events taking place at each step in the process become increasingly complex, introducing new treatment challenges. As the cancer progresses it acquires a series of mutations and gene amplifications, becoming: (1) self-sufficient in growth signaling, by oncogene activation and loss of tumor suppressor genes, (2) insensitive to antigrowth signaling, (3) unresponsive to apoptotic signaling, (4) capable of limitless tumor cell replications, and (5) tumorigenic and metastatic growth [38]. However, current experimental and clinical evidence indicates these hallmark properties may be necessary, but not sufficient, for a cancer cell to progress into a clinically detectable, metastatic, and lethal tumor. For a tumor to develop a highly malignant and deadly phenotype, it must first recruit and sustain its own blood supply, a process known as tumor angiogenesis [39, 40].

Clinical observations that surgically resected tumors are hyperemic compared to normal tissues date back more than a century [41, 42]. At the time, this phenomenon was explained as a general dilation of existing blood vessels induced by tumor-produced factors. However, Ide et al. [43] demonstrated that when a wound induced in a transparent rabbit ear chamber completely regressed, the implantation of a tumor in the chamber resulted in the growth of new capillary blood vessels [43]. These initial observations that tumor-associated hyperemia could be related to new blood vessel growth, i.e. vasodilation may not be the sole mechanism for this phenomenon were later confirmed by Algire et al. [44, 45]. They showed that new vessels in the periphery of a tumor implant arose from preexisting host vessels, and not from the tumor implant itself. At the time, this novel concept of tumor-induced neovascularization was generally attributed to an inflammatory reaction, thought to be a side effect of tumor growth, and it was not perceived as a requirement for tumor growth [46].

In the early 1960s, Folkman and Becker demonstrated that tumor growth in isolated perfused organs was severely restricted in the absence of tumor vascularization [47–51]. In 1971, Folkman proposed the hypothesis that tumor growth is angiogenesis-dependent [39]. This hypothesis suggested that tumor growth is dictated by a two-compartment system of highly integrated tumor cells and vascular endothelial cells. This concept indicated that endothelial cells may switch from a resting state to a rapid growth phase induced by "diffusible" signals secreted from the tumor cells. Moreover, Folkman proposed that angiogenesis could be a relevant target for tumor therapy (i.e., antiangiogenic therapy). Antiangiogenic therapy offers a fourth anti-cancer modality, in addition to conventional therapeutic approaches, which target well-established and genetically unstable tumors. Currently, there are more than 10 (FDA and other international regulating agencies) approved angiogenesis inhibitors for clinical use of a variety of cancers, multiple myeloma, and age-related macular degeneration [52].

We now know that angiogenesis plays an important role in numerous physiologic and pathologic processes. The hallmark of pathologic angiogenesis is the persistent growth of blood vessels. Sustained neovascularization can continue for months or years during the progression of many neoplastic and non-neoplastic diseases [53, 54]. However, tumor angiogenesis is rarely, if ever, downregulated spontaneously. The fundamental objective of antiangiogenic therapy is to inhibit the progression of pathologic angiogenesis. In contrast, the goal of antivascular therapy is to rapidly occlude new blood vessels so the blood flow stops. Both therapeutic approaches target the ability of tumors to progress from the nonangiogenic to the angiogenic phenotype, a process termed the "angiogenic switch" [55, 56].

Cancer usually becomes clinically detectable only after tumors have become angiogenic and have expanded in mass. Failure of a tumor to recruit new vasculature or to reorganize the existing surrounding vasculature results in a nonangiogenic tumor, which is microscopic in size and unable to increase in mass (Fig. 2). In the absence of new

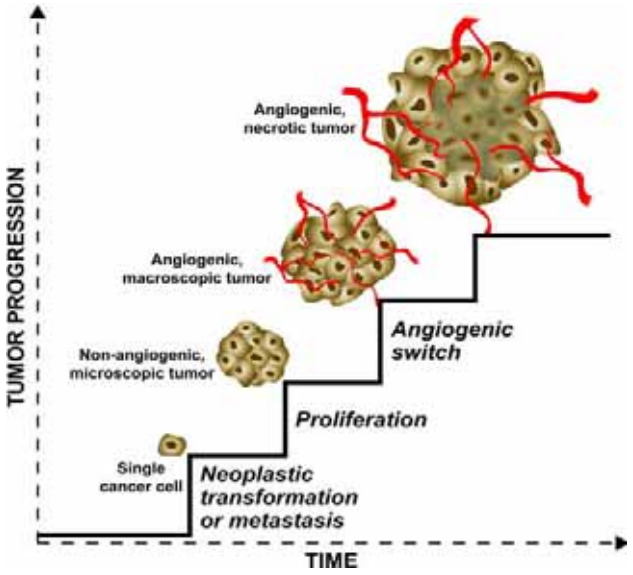

Fig. 2 Summary of rate-limiting steps in the tumor progression

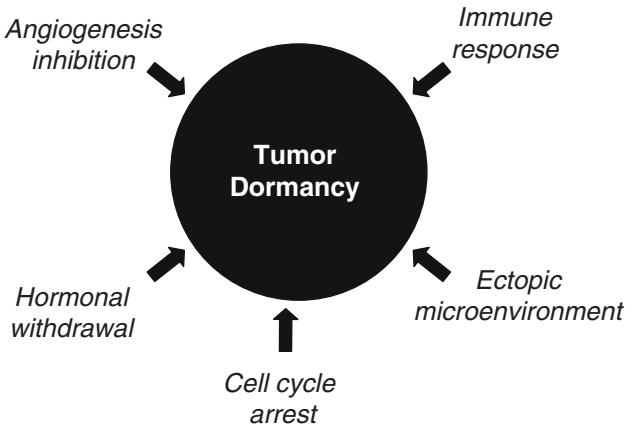

Fig. 3 Summary of various factors affecting human tumor dormancy

blood supply, microscopic tumors are usually restricted to a size of <1–2 mm in diameter. At this harmless size, microscopic tumors are highly dependent on surrounding blood vessels for oxygen and nutrient supply. At sea level, the diffusion limit of oxygen is approximately 100 μm [57]. Therefore, all mammalian cells, including neoplastic cells, are required to be within 100–200 μm of a blood vessel. As nonangiogenic tumors attempt to expand in mass, attributed to uncontrolled cancer cell proliferation, some tumor cells fall outside the oxygen diffusion limit and become hypoxic. These new hypoxic conditions induce a set of compensatory responses within the tumor cell population, such as increased transcription of the hypoxia-inducible factor (HIF). This hypoxia-induced signaling leads to subsequent upregulation of proangiogenic proteins, such as vascular endothelial growth factor (VEGF), platelet-derived growth factor (PDGF), and nitric oxide synthase (NOS) [58]. The angiogenic switch in tumors is presumed to be closely regulated by the presence of pro- and anti-angiogenic proteins in the tumor microenvironment. An increase in the local concentration of proangiogenic proteins allows angiogenesis to occur and ultimately permits a tumor to expand in mass. Therefore, the microenvironment is an important regulator in the fate of a tumor, to expand in mass and become lethal or to remain microscopic in size and harmless to the host (Fig. 3). In the following we will review the current understanding on the role of the failure of the angiogenic switch in inducing tumor dormancy. For a broader overview of other factors involved in human tumor dormancy, we refer to a recent review article by Aguirre-Ghiso [59].

Experimental models of human tumor dormancy

The effects of neovascularization on tumor growth have been demonstrates as early as the 1940s in experimental systems involving the transplantaion of tumor pieces in isolated perfused organs and in the anterior chamber of the eyes of various animal species. Green et al. [60] observed that H-31 rabbit carcinoma tumor implanted into the eyes of guinea pigs did not vascularize and failed to grow for 16–26 months. The transplants remained at a size of approximately 2.5 mm in diameter for the duration of the experiment. However, when the same tumors were reimplanted into the eyes of their original host, they vascularized and expanded in mass, filling the anterior chamber within 50 days. Similarly, Folkman et al. [48] showed that implants in isolated perfused thyroid and intestinal segment tumors grew and arrested at a small size (2–3 mm diameter). This inability of neoplasms to evoke a new blood supply was later attributed to endothelial cell degeneration in the perfused organs that were perfused with platelet-free hemoglobin solution [61]. In 1972, Gimbrone et al. [62] provided in vivo evidence that the progressive growth of a homologous solid tumor can be deliberately arrested at a microscopic size when neovasculature is prevented. In these experiments, two comparably sized tumor pieces were implanted in each eye of the same animal: one directly on the iris (known to be an angiogenic milieu) and the other suspended in the anterior chamber (known to be avascular milieu) in the opposing eye. The tumor implanted on the iris became vascularized and grew to a size 15,000 times the initial volume. The same tumor filled the anterior chamber of the rabbit eye within 14 days. In contrast, the tumor implant in the avascular anterior chamber remained avascular, and had increased only 4 times its initial volume, by day 14 after implantation. These "dormant" tumors remained at a size of ~1 mm in diameter for up to 44 days. During this dormancy period, the tumors developed a central necrotic core surrounded by a

layer of viable tumor cells, in which mitotic figures were observed. Overall, these microscopic tumors remained avascular, as demonstrated by using microscopic and histological analyses and fluorescein tests. The malignant growth potential of these microscopic tumors was evidenced by reimplanting the tumors directly on the irises of fresh animals. In this angiogenic microenvironment (i.e. the irises), the dormant tumors became vascularized and grew rapidly until the anterior chambers of the eyes were filled with tumor, in a manner similar to the control iris implants. These fundamental observations established the relationship between tumor growth and angiogenesis. They also provided one of the first in vivo experimental models for further investigations of tumor dormancy.

More recently, Hanahan and Folkman [56] described a spontaneous tumor dormancy model in transgenic mice. In this experimental model, autochthonous tumors arise in the pancreatic islets as a result of simian virus 40 T antigen (Tag) oncogene expression. Only 4% of these pancreatic islet tumors became angiogenic 13 weeks after birth of the animals. In contrast, the remaining 96% of pancreatic islet tumors remained microscopic and nonangiogenic [56, 63]. The spontaneous progression of nonangiogenic lesions to the angiogenic phenotype in these transgenic tumor-bearing mice led to the development of the "angiogenic switch" concept [56].

In 2001, Achilles et al. [64] reported that human tumors contain subpopulations that differ in their angiogenic potential. These findings suggested that the overall angiogenic phenotype of an individual human tumor cell may be controlled by genetic and epigenetic mechanisms. Therefore, human tumors can contain both angiogenic and nonangiogenic tumor cell populations, characterized by their ability to recruit new blood vessels to a tumor. However, the dynamic interplay of these two tumor cell populations with each other and the surrounding microenvironment are currently not known. Moreover, the key factors involved in the proportional regulation of these two tumor cell populations are still under investigation.

One strategy for the isolation of angiogenic and nonangiogenic tumor cell populations is through single-cell cloning of a human tumor cell line. Achilles et al. [64] established and selected subclones from a human liposarcoma cell line (SW-872) based on high, intermediate, or low proliferation rates in vitro. These clones were subsequently expanded in vitro into distinct populations of tumor cells and were then inoculated into immunodeficient (SCID) mice. Three different in vivo growth patterns were observed: (1) highly angiogenic and rapidly growing tumors, (2) weakly angiogenic and slowly growing tumors, and (3) nonangigoenic and dormant tumors. Further investigation by Almog et al. [65] showed that the nonangiogenic tumors spontaneously switch to the angiogenic phenotype and initiate exponential growth approximately 130 days after inoculation into the subcutaneous space. During the 130 day dormancy period, microscopic tumors remained avascular and were virtually undetectable by palpation (approximate size of 1–2 mm in diameter). Because the angiogenic and nonangiogenic tumor cell populations in these models were segregated based on these in vitro tumor cell proliferation differences, it raised three fundamental questions: (1) Is there a correlation between tumor cell proliferation and angiogenic potential? (2) Can the observed differences in tumor growth be recapitulated using populations of human tumor cells that have not been cloned? and (3) Can nonangiogenic and angiogenic tumor cell populations be segregated for other human cancer types?

To address these questions, human tumor cell lines were obtained from the American Type Culture Collection (ATCC, Manassas, VA) based on their "no take" phenotype in immunodeficient mice. These cell lines were assessed for in vivo tumor growth over extended time periods (over 1 year) after subcutaneous inoculation of a tumor cell suspension. Some of the mice inoculated with the "no take" tumor cells spontaneously formed palpable tumors after a dormancy period, which varied from months to more than a year, depending on cancer type. With time, tumors became angiogenic, palpable, expanded in mass exponentially, and killed the host animal within $\sim$50 days of first detection [66, 67]. Stable cell lines were established from representative tumors which became angiogenic following a dormancy period. When reinoculated into SCID mice, these now angiogenic tumor cells formed large tumors (>1 cm in diameter) within a month following inoculation, however, without a dormancy period. The permanency of the angiogenic switch in human tumors was documented by the fact that 100% of mice inoculated with the angiogenic cells formed tumors, regardless of the cancer type. In contrast, it was found that each cancer type had a characteristic and predictable dormancy period and generated a consistent proportion of tumors that spontaneously switched to the angiogenic phenotype. To date, tumor cell population-based animal dormancy models have been developed and characterized for breast cancer, osteosarcoma, and glioblastoma [66]. In contrast to the single-cell-derived human liposarcoma animal model, the angiogenic and nonangiogenic tumor cell populations of the rest of the animal models were derived by in vivo selection for the angiogenic and nonangigoenic phenotypes. Moreover, in these population-based dormancy models, the angiogenic and nonangiogenic populations did not differ significantly in tumor cell proliferation [66].

As demonstrated by the established dormancy models, certain human tumor cells can remain dormant for more than a year after inoculation in animals. However, this does

not mean that the tumor cells are in G_o growth arrest. Although some tumor cells might be in mitotic arrest, as demonstrated in some tumor dormancy models [59, 68–70], we reported that the majority of tumor cells are metabolically active, proliferating and undergoing apoptosis [65, 66]. In a human breast cancer (MDA-MB-436) animal model, more than 50% of tumor cells were proliferating and more than 10% were undergoing apoptosis in all microscopic tumors analyzed by immunohistochemistry at various time points during dormancy [66]. These rates of proliferation and apoptosis were similar within macroscopic and angiogenic tumors. In a different human osteosarcoma (MG-63 and SAOS-2) and gastric (ST-2) cancer dormancy models, reported by Udagawa et al., [71] microscopic tumors were unable to grow beyond a threshold size of $\sim$1–2 mm in diameter. Tumor cell proliferation in these tumors was $\sim$12% and tumor cell apoptosis ranged from 4 to 7.5%. Therefore, the tumor cell proliferation index within nonangiogenic tumors can be as high as that of large vascularized tumors. Moreover, nonangiogenic tumors appear to have a balance between proliferating cells and cells undergoing apoptosis.

Although the nonangiogenic and angiogenic tumor cell populations did not differ significantly in proliferation, they express and secrete different amounts of pro- and antiangiogenic proteins. Naumov et al. [66] compared the tumor cell secretion and intracellular levels of Thrombospondin-1 (Tsp-1) in nonangiogenic and angiogenic tumor cell populations isolated from a human breast cancer cell line (MDA-MB-436). Angiogenic cells contained 2.5-fold higher levels of c-Myc and p-Myc (phosphorylated) than their nonangiogenic counterparts, as assessed by Western blot. In contrast, angiogenic breast cancer cells contain significantly lower levels of Tsp-1 than nonangiogenic tumor cells. Secretion of Tsp-1 from nonangiogenic tumor cells was 20-fold higher than angiogenic cells. Similar findings were previously reported for a different breast cancer cells line (MDA-MB-435)[72]. Watnick et al. [72] reported that phosphoinositide 3-kinase (PI3K) can induce a signal transduction cascade leading to the phosphorylation of c-Myc and subsequent repression of Tsp-1. Treatment with a PII3K inhibitor (LY294002) caused Tsp-1 levels within angiogenic cells to increase, but had no effect on levels in nonangiogenic cells [66]. Therefore, PI3K signaling pathway is responsible for the repression of Tsp-1, and it is regulated differently in angiogenic and nonangiogenic human tumor cells.

Definition of a dormant human tumor based on experimental animal models

A "dormant" tumor can be defined, based on xenograft dormancy models, by its microscopic size and nonexpanding mass. In contrast, a "stable" tumor is macroscopic and nonexpanding in mass. In more detail, we have previously defined nonangiogenic tumors as [73]:

1. Unable to induce angiogenic activity, by repulsion of existing blood vessels in the local stroma and/or relative absence of intratumoral microvessels.
2. Remain harmless to the host until they switch to the angiogenic phenotype.
3. Express equal or more antiangiogenic (i.e., thrombospondin-1) than angiogenic (i.e., VEGF, bFGF) proteins.
4. Grow in vivo to $\sim$1 mm in diameter or less, at which time further expansion ceases.
5. Only visible with a hand lens or a dissecting microscope (5–10× magnification).
6. White or transparent by gross examination.
7. Unable to spontaneously metastasize from the microscopic dormant state.
8. Show active tumor cell proliferation and apoptosis in vivo and remain metabolically active during the dormancy period.
9. Can be cloned from a human angiogenic tumor, because human tumors are heterogeneous and contain a mixture of nonangiogenic and angiogenic tumor cells.

In contrast, angiogenic human tumors (as observed in our dormancy models) are defined as:

1. Able to induce angiogenic activity, by recruiting blood vessels from the surrounding stroma and/or forming new blood vessels within the tumor tissue.
2. Lethal to the host in only a few weeks.
3. Express significantly more angiogenic than antiangiogenic proteins.
4. Grow along an exponential curve until they kill the host.
5. Visible and easily detectable based on their macroscopic size.
6. Red by gross examination.
7. Can spontaneously metastasize to various organs.
8. Can be cloned from a human angiogenic tumor, because human tumors are heterogeneous and contain a mixture of nonangiogenic and angiogenic tumor cells.

Acknowledgements The authors thank Dr. T. Lokeland MD for clinical data on the clinical cases, Dr. L. Bostad MD for the histological pictures, and Dr. R. Watnick for critical reading and editing of this manuscript. We also thank Kristin Johnson for help with graphics. This work was supported by the Breast Cancer Research Foundation, NIH Program Project (grant #P01CA45548), and an Innovator Award from the Department of Defense, The Norwegian Cancer Society and Helse Vest Norway.

References

1. Larsen I, Smastuen M, Parkin D et al (2007) Cancer in Norway 2006- Cancer incidence, mortality, survival and prevalence in Norway. Cancer Registry of Norway, Oslo
2. Tabar L, Vitak B, Chen HH et al (2000) The Swedish Two-County Trial twenty years later. Updated mortality results and new insights from long-term follow-up. Radiol Clin North Am 38(4):625–651. doi:10.1016/S0033-8389(05)70191-3
3. Black WC, Welch HG (1993) Advances in diagnostic imaging and overestimations of disease prevalence and the benefits of therapy. N Engl J Med 328(17):1237–1243. doi:10.1056/NEJM199304293281706
4. Nielsen M, Thomsen JL, Primdahl S et al (1987) Breast cancer and atypia among young and middle-aged women: a study of 110 medicolegal autopsies. Br J Cancer 56(6):814–819
5. Sanchez-Chapado M, Olmedilla G, Cabeza M et al (2003) Prevalence of prostate cancer and prostatic intraepithelial neoplasia in Caucasian Mediterranean males: an autopsy study. Prostate 54(3):238–247. doi:10.1002/pros.10177
6. Harach HR, Franssila KO, Wasenius VM (1985) Occult papillary carcinoma of the thyroid. A "normal" finding in Finland. A systematic autopsy study. Cancer 56(3):531–538. doi:10.1002/1097-0142(19850801)56:3<531::AID-CNCR2820560321>3.0.CO;2-3
7. Demicheli R, Terenziani M, Valagussa P et al (1994) Local recurrences following mastectomy: support for the concept of tumor dormancy. J Natl Cancer Inst 86(1):45–48. doi:10.1093/jnci/86.1.45
8. Demicheli R, Abbattista A, Miceli R et al (1996) Time distribution of the recurrence risk for breast cancer patients undergoing mastectomy: further support about the concept of tumor dormancy. Breast Cancer Res Treat 41(2):177–185. doi:10.1007/BF01807163
9. Demicheli R, Retsky MW, Hrushesky WJ et al (2007) Tumor dormancy and surgery-driven interruption of dormancy in breast cancer: learning from failures. Nat Clin Pract Oncol 4(12):699–710. doi:10.1038/ncponc0999
10. Gao F, Tan SB, Machin D et al (2007) Confirmation of double-peaked time distribution of mortality among Asian breast cancer patients in a population-based study. Breast Cancer Res 9(2):R21. doi:10.1186/bcr1658
11. Coffey JC, Wang JH, Smith MJ et al (2003) Excisional surgery for cancer cure: therapy at a cost. Lancet Oncol 4(12):760–768. doi:10.1016/S1470-2045(03)01282-8
12. Morihara K, Takenaka H, Morihara T et al (2007) Primary cutaneous anaplastic large cell lymphoma associated with vascular endothelial growth factor arising from a burn scar. J Am Acad Dermatol 57(5 Suppl):S103–S105. doi:10.1016/j.jaad.2006.10.018
13. Kotzen RM, Swanson RM, Milhorat TH et al (1999) Post-traumatic meningioma: case report and historical perspective. J Neurol Neurosurg Psychiatry 66(6):796–798
14. Oosterling SJ, van der Bij GJ, van Egmond M et al (2005) Surgical trauma and peritoneal recurrence of colorectal carcinoma. Eur J Surg Oncol 31(1):29–37. doi:10.1016/j.ejso.2004.10.005
15. Gamatsi IE, McCulloch TA, Bailie FB et al (2000) Malignant melanoma in a skin graft: burn scar neoplasm or a transferred melanoma? Br J Plast Surg 53(4):342–344. doi:10.1054/bjps.2000.3322
16. Flook D, Horgan K, Taylor BA et al (1986) Surgery for malignant melanoma: from which limb should the graft be taken? Br J Surg 73(10):793–795. doi:10.1002/bjs.1800731011
17. Deelman H (1927) The part played by injury and repair in the development of cancer. Br Med J 1:872
18. Alexander J, Altemeier W (1964) Suseptibility of injured tissues to hematogenous metastasis: an experimental study. Ann Surg 159:933–944
19. Hatzis GP, Finn R (2007) Marjolin's ulcer: a review of the literature and report of a unique patient treated with a CO(2) laser. J Oral Maxillofac Surg 65(10):2099–2105. doi:10.1016/j.joms.2006.07.017
20. Bissell MJ, Radisky D (2001) Putting tumours in context. Nat Rev Cancer 1(1):46–54. doi:10.1038/35094059
21. Dolberg DS, Hollingsworth R, Hertle M et al (1985) Wounding and its role in RSV-mediated tumor formation. Science 230(4726):676–678. doi:10.1126/science.2996144
22. Sieweke MH, Thompson NL, Sporn MB et al (1990) Mediation of wound-related Rous sarcoma virus tumorigenesis by TGF-beta. Science 248(4963):1656–1660. doi:10.1126/science.2163544
23. Jewell WR, Romsdahl MM (1965) Recurrent malignant disease in operative wounds not due to surgical implantation from the resected tumor. Surgery 58(5):806–809
24. Meng S, Tripathy D, Frenkel EP et al (2004) Circulating tumor cells in patients with breast cancer dormancy. Clin Cancer Res 10(24):8152–8162. doi:10.1158/1078-0432.CCR-04-1110
25. Murthy SM, Goldschmidt RA, Rao LN et al (1989) The influence of surgical trauma on experimental metastasis. Cancer 64(10):2035–2044. doi:10.1002/1097-0142(19891115)64:10<2035::AID-CNCR2820641012>3.0.CO;2-L
26. Murthy MS, Summaria LJ, Miller RJ et al (1991) Inhibition of tumor implantation at sites of trauma by plasminogen activators. Cancer 68(8):1724–1730. doi:10.1002/1097-0142(19911015)68:8<1724::AID-CNCR2820680813>3.0.CO;2-W
27. O'Reilly MS, Holmgren L, Shing Y et al (1994) Angiostatin: a novel angiogenesis inhibitor that mediates the suppression of metastases by a Lewis lung carcinoma. Cell 79(2):315–328. doi:10.1016/0092-8674(94)90200-3
28. Bogden AE, Moreau JP, Eden PA (1997) Proliferative response of human and animal tumours to surgical wounding of normal tissues: onset, duration and inhibition. Br J Cancer 75(7):1021–1027
29. Gill M, Dias S, Hattori K et al (2001) Vascular trauma induces rapid but transient mobilization of VEGFR2(+)AC133(+) endothelial precursor cells. Circ Res 88(2):167–174
30. Benezra R, Rafii S, Lyden D (2001) The Id proteins and angiogenesis. Oncogene 20(58):8334–8341. doi:10.1038/sj.onc.1205160
31. Abramovitch R, Marikovsky M, Meir G et al (1999) Stimulation of tumour growth by wound-derived growth factors. Br J Cancer 79(9–10):1392–1398. doi:10.1038/sj.bjc.6690223
32. Indraccolo S, Favaro E, Amadori A (2006) Dormant tumors awaken by a short-term angiogenic burst: the spike hypothesis. Cell Cycle 5(16):1751–1755
33. Indraccolo S, Stievano L, Minuzzo S et al (2006) Interruption of tumor dormancy by a transient angiogenic burst within the tumor microenvironment. Proc Natl Acad Sci USA 103(11):4216–4221. doi:10.1073/pnas.0506200103
34. Withers HR, Lee SP (2006) Modeling growth kinetics and statistical distribution of oligometastases. Semin Radiat Oncol 16(2):111–119. doi:10.1016/j.semradonc.2005.12.006
35. Tomiak E, Piccart M, Mignolet F et al (1996) Characterisation of complete responders to combination chemotherapy for advanced breast cancer: a retrospective EORTC Breast Group study. Eur J Cancer 32A(11):1876–1887. doi:10.1016/0959-8049(96)00189-X
36. Swenerton KD, Legha SS, Smith T et al (1979) Prognostic factors in metastatic breast cancer treated with combination chemotherapy. Cancer Res 39(5):1552–1562
37. Greenberg PA, Hortobagyi GN, Smith TL et al (1996) Long-term follow-up of patients with complete remission following combination chemotherapy for metastatic breast cancer. J Clin Oncol 14(8):2197–2205
38. Folkman J, Heymach J, Kalluri R (2006) Tumor angiogenesis. B.C. Decker, Hamilton, Ontario
39. Folkman J (1971) Tumor angiogenesis: therapeutic implications. N Engl J Med 285(21):1182–1186

40. Folkman J (1990) What is the evidence that tumors are angiogenesis dependent?. J Natl Cancer Inst 82(1):4–6. doi:10.1093/jnci/82.1.4
41. Coman D, Sheldon WF (1946) The significance of hyperemia around tumor implants. Am J Pathol 22:821–31
42. Warren B (1979) The vascular morphology of tumors. In: Peterson H-I (ed) Tumor blood circulation: angiogenesis, vascular morphology and blood flow of experimental human tumors. CRC Press, Florida, pp 1–47
43. Ide A, Baker NH, Warren SL (1939) Vascularization of the Brown-Pearce rabbit epithelioma transplant as seen in the transparent ear chamber. Am J Roentgenol 42:891–899
44. Algire G, Legallais FY (1947) Growth rate of transplanted tumors in relation to latent period and host vascular reaction. Cancer Res 7:724
45. Algire G, Chalkely HW, Legallais FY, Park H (1945) Vascular reactions of normal and malignant tumors in vivo: I. Vascular reactions of mice to wounds and to normal and neoplastic transplants. J Natl Cancer Inst 6:73–85
46. Folkman J (1985) Toward an understanding of angiogenesis: search and discovery. Perspect Biol Med 29(1):10–36
47. Folkman J, Long DM Jr, Becker FF (1963) Growth and metastasis of tumor in organ culture. Cancer 16:453–67. doi:10.1002/1097-0142(196304)16:4<453::AID-CNCR2820160407>3.0.CO;2-Y
48. Folkman J, Cole P, Zimmerman S (1966) Tumor behavior in isolated perfused organs: in vitro growth and metastases of biopsy material in rabbit thyroid and canine intestinal segment. Ann Surg 164(3):491–502. doi:10.1097/00000658-196609000-00012
49. Folkman J (1972) Anti-angiogenesis: new concept for therapy of solid tumors. Ann Surg 175(3):409–416. doi:10.1097/00000658-197203000-00014
50. Folkman J (1976) The vascularization of tumors. Sci Am 234(5):58–64, 70–3
51. Folkman J (1970) The intestine as an organ culture. In: Burdette W (ed) Carcinoma of the colon and antecedent epithelium. CC Thomas, Springfield (IL), pp 113–127
52. Folkman J (2007) Angiogenesis: an organizing principle for drug discovery? Nat Rev Drug Discov 6(4):273–286. doi:10.1038/nrd2115
53. Folkman J, Brem H (1992) Angiogenesis and inflamation. In: Gallin JLGI, Snyderman R (eds) Inflamation: basic principles and clinical correlates, 2nd edn. Raven Press, New York, pp 821–839
54. Folkman J (2003) Angiogenesis in arthritis. In: Smolen J, Lipsky P (eds) Targeted therapies in rheumatology. Martin Dunitz, London, pp 111–131
55. Folkman J, Watson K, Ingber D et al (1989) Induction of angiogenesis during the transition from hyperplasia to neoplasia. Nature 339(6219):58–61. doi:10.1038/339058a0
56. Hanahan D, Folkman J (1996) Patterns and emerging mechanisms of the angiogenic switch during tumorigenesis. Cell 86(3):353–364 doi:10.1016/S0092-8674(00)80108-7
57. Torres Filho IP, Leunig M, Yuan F et al (1994) Noninvasive measurement of microvascular and interstitial oxygen profiles in a human tumor in SCID mice. Proc Natl Acad Sci USA 91(6):2081–2085 doi:10.1073/pnas.91.6.2081
58. North S, Moenner M, Bikfalvi A (2005) Recent developments in the regulation of the angiogenic switch by cellular stress factors in tumors. Cancer Lett 218(1):1–14 doi:10.1016/j.canlet.2004.08.007
59. Aguirre-Ghiso JA (2007) Models, mechanisms and clinical evidence for cancer dormancy. Nat Rev Cancer 7(11):834–846 doi:10.1038/nrc2256
60. Greene HSN (1941) Heterolgous transplantation of mammalian tumors. J Exp Med 73:461–486. doi:10.1084/jem.73.4.461
61. Gimbrone MA Jr, Aster RH, Cotran RS et al (1969) Preservation of vascular integrity in organs perfused in vitro with a platelet-rich medium. Nature 222(188):33–36. doi:10.1038/222033a0
62. Gimbrone MA Jr, Leapman SB, Cotran RS et al (1972) Tumor dormancy in vivo by prevention of neovascularization. J Exp Med 136(2):261–276. doi:10.1084/jem.136.2.261
63. Hanahan D, Christofori G, Naik P et al (1996) Transgenic mouse models of tumour angiogenesis: the angiogenic switch, its molecular controls, and prospects for preclinical therapeutic models. Eur J Cancer 32A(14):2386–2393. doi:10.1016/S0959-8049(96)00401-7
64. Achilles EG, Fernandez A, Allred EN et al (2001) Heterogeneity of angiogenic activity in a human liposarcoma: a proposed mechanism for "no take" of human tumors in mice. J Natl Cancer Inst 93(14):1075–1081. doi:10.1093/jnci/93.14.1075
65. Almog N, Henke V, Flores L et al (2006) Prolonged dormancy of human liposarcoma is associated with impaired tumor angiogenesis. Faseb J 20(7):947–949. doi:10.1096/fj.05-3946fje
66. Naumov GN, Bender E, Zurakowski D et al (2006) A model of human tumor dormancy: an angiogenic switch from the nonangiogenic phenotype. J Natl Cancer Inst 98(5):316–325
67. Naumov GN, Akslen LA, Folkman J (2006) Role of angiogenesis in human tumor dormancy: animal models of the angiogenic switch. Cell Cycle 5(16):1779–1787
68. Aguirre Ghiso JA, Kovalski K, Ossowski L (1999) Tumor dormancy induced by downregulation of urokinase receptor in human carcinoma involves integrin and MAPK signaling. J Cell Biol 147(1):89–104. doi:10.1083/jcb.147.1.89
69. Aguirre-Ghiso JA, Liu D, Mignatti A et al (2001) Urokinase receptor and fibronectin regulate the ERK(MAPK) to p38(MAPK) activity ratios that determine carcinoma cell proliferation or dormancy in vivo. Mol Biol Cell 12(4):863–879
70. Aguirre-Ghiso JA, Estrada Y, Liu D et al (2003) ERK(MAPK) activity as a determinant of tumor growth and dormancy; regulation by p38(SAPK). Cancer Res 63(7):1684–1695
71. Udagawa T, Fernandez A, Achilles EG et al (2002) Persistence of microscopic human cancers in mice: alterations in the angiogenic balance accompanies loss of tumor dormancy. Faseb J 16(11):1361–1370. doi:10.1096/fj.01-0813com
72. Watnick RS, Cheng YN, Rangarajan A et al (2003) Ras modulates Myc activity to repress thrombospondin-1 expression and increase tumor angiogenesis. Cancer Cell 3(3):219–231. doi:10.1016/S1535-6108(03)00030-8
73. Naumov GN, Folkman J (2008) Strategies to prolong the non-angiogenic dromant state of human cancer. In: Davis DW, Herbst RS, Abbruzzese JL (eds) Antiangiogenic cancer therapy. CRC Press, Boca Raton, FL, pp 3–21
74. Nielsen M (1989) Autopsy studies of the occurrence of cancerous, atypical and benign epithelial lesions in the female breast. APMIS Suppl 10:1–56

APMIS 116: 569–85, 2008
Printed in Denmark . All rights reserved

ISSN 0903-4641

Tumor-vascular interactions and tumor dormancy

GEORGE N. NAUMOV[1,2], JUDAH FOLKMAN[1,2], ODDBJORN STRAUME[1,2,3,4] and LARS A. AKSLEN[3]

[1]Department of Surgery, Harvard Medical School, [2]Vascular Biology Program, Children's Hospital Boston, Boston, MA, [3]The Gade Institute, Section for Pathology, and [4]Institute of Internal Medicine, Section of Oncology, University of Bergen, Norway

Naumov GN, Folkman J, Straume O, Akslen LA. Tumor-vascular interactions and tumor dormancy. APMIS 1008:116;569–85.

Tumor progression is dependent on a number of sequential steps, including initial tumor-vascular interactions and recruitment of blood vessels (*i.e.,* the angiogenic switch), as well as tumor cells interacting with the surrounding microenvironment and its different components. Failure of a microscopic tumor to complete one or more of these early stages may lead to delayed clinical manifestation of the cancer and a state of stable non-progressing disease (*i.e.*, tumor dormancy). In this review, some of the clinical and experimental evidence is summarized, suggesting that microscopic human cancers, either primary, recurrent or metastatic, can remain in an asymptomatic, non-detectable, and occult state for a long period of time. We also review current experimental human tumor dormancy models which closely recapitulate clinically observed delay in tumor progress.

Key words: Dormancy; human tumors; metastasis; angiogenesis; animal model; trauma; occult cancer.

George N. Naumov, Children's Hospital Boston, Karp Family Research Laboratories, 12007C, 300 Longwood Avenue, Boston, MA 02115, USA. e-mail: george.naumov@childrens.harvard.edu

DEFINITIONS OF TUMOR DORMANCY

There are several possible definitions of *tumor dormancy.* This condition could be regarded as a "steady state" where fully transformed tumor cells do not expand into a clinically detectable cancer. This is possibly due to lack of stimulatory or permissive signals, or due to active inhibitory mechanisms or a combination of these. This might apply to early stages of primary cancers, to remnants of primary tumors which would be "seeds" for disease recurrences, and to "dormant" micrometastases which could, after a latency period, be "reactivated" and evolve into clinically manifest disease.

In the experimental setting, such as in xenograft dormancy models, a "dormant" tumor can be defined by its microscopic size and stable non-expanding mass. In more detail, we have previously defined non-angiogenic and dormant tumors as being characterized by (1):

1. Tumor growth *in vivo* to ~1 mm in diameter or less, at which time further expansion ceases;
2. Inability to induce angiogenic activity, by lack of or relative absence of intra-tumoral microvessels, or by active repulsion of existing blood vessels in the local microenvironment. These tumors are white or transparent on gross examination;
3. Expression of equal or more anti-angiogenic (*i.e.,* thrombospondin-1) than angiogenic (*i.e.,* VEGF, bFGF) proteins;
4. Active tumor cell proliferation and apoptosis *in vivo*, and metabolic activity during the dormancy period;
5. Possibility of cloning from a human angiogenic tumor, because human tumors are heterogeneous and contain a mixture of non-angiogenic and angiogenic tumor cells;
6. Inability to spontaneously metastasize from the microscopic dormant state;
7. Harmlessness to the host until they switch to the angiogenic phenotype.

Invited review.

In contrast, angiogenic and non-dormant human tumors (as observed in our dormancy models) are characterized by:

1. Growth along an exponential curve until they kill the host;
2. Ability to induce angiogenic activity, by recruiting blood vessels from the surrounding stroma and/or forming new blood vessels within the tumor tissue. These tumors are red on gross examination;
3. Expression of significantly more angiogenic than anti-angiogenic proteins;
4. Possibility of cloning from a human angiogenic tumor, because human tumors are heterogeneous and contain a mixture of non-angiogenic and angiogenic tumor cells;
5. Spontaneous metastasis to various organs;
6. Host lethality in only a few weeks.

CLINICALLY UNDETECTED PRIMARY CANCER: EVIDENCE FROM AUTOPSY STUDIES

Early stages of human cancer might be represented by various pre-invasive lesions or by fully developed but small invasive cancers with very slow progression. Some of these latter lesions might appear as clinically "dormant". This "very slow progression" or steady state with a balance between proliferation, apoptosis and no net tumor growth (expansion) might apply to untreated primary tumors, remnants of primary tumors after treatment (residual disease) as seeds for tumor recurrences, and the regulation of micrometastases.

There is a vast difference between the prevalence of clinically presenting cancer and the small malignant tumors found in autopsy studies. The reasons for this discrepancy are not fully known. Thus, more than a third of the US population are diagnosed with either *in situ* or invasive cancer during their lifetime (2). In most industrialized countries numbers have been steadily increasing due to increased lifetime expectancy, improved diagnostics, and population screening programs (3–5). To date, technology has improved immensely, allowing the detection of cancer in its early stages and with higher frequency in the general population (3). It has been speculated that this improved detection might lead to over-diagnosis and over-treatment of early cancers that might never have developed into clinically significant disease (6–8).This raises the question "Do we (the general population, who have never been diagnosed with cancer) live with undetectable cancer for the majority of our lives?" The answer to this question has been addressed by autopsy studies on individuals who died in automobile accidents or by other trauma and were never diagnosed with cancer during their lifetime. These studies demonstrate that a large portion of the population carry microscopic cancers, some of which will never progress into clinically detectable disease (3). Nielsen et al. reported that as many as 39% of women (age 40–49 years) have clinically occult (*i.e.* undetected) breast cancer (9). However, only ~1.8% (22-fold less) of women are diagnosed with breast cancer *in the same age group* (Table 1). Similarly, 11-fold and 16-fold discrepancies between clinically diagnosed breast cancer and microscopic disease found at autopsy were reported for younger (age 30–39 years) and older (age 50–54 years) Scandinavian women. Earlier autopsy studies (10–14) have been less informative due to limited tissue sampling.

A high prevalence of microscopic and clinically occult ("dormant") cancer has also been reported for other cancer types. Most strikingly, microscopic thyroid carcinoma (often less than 1 mm in diameter) is very frequent at autopsy (~36% prevalence for age 61–80 years), in marked contrast to the rare occurrence of clinically presenting thyroid cancer (15–21) (summarized in Table 3). In the prostate, 2–8-fold discrepancies between the prevalence of occult microscopic lesions and lifetime risk of cancer (age 60–69 years) were reported (22) (162 prostates, 33% prevalence of occult lesions *versus* 8.1% expected incidence of clinical cancer; 4-fold difference) (summarized in Table 2). Similar findings have been reported by others (23–29). Some of these studies were conducted before the widespread use of PSA screening. A recent study by Konety et al. shows that there has been a decrease in the prevalence of latent prostate cancer reported in routine hospital autopsy records when comparing the 1955–60 and 1991–2001 time periods (30).

The evidence from autopsy studies of occult breast, thyroid and prostate cancer originates from detailed autopsy studies performed by sec-

TABLE 1. *Summary of autopsy studies performed on persons who have died without clinically diagnosed cancer. Comparison of microscopic "occult" cancer found in breast to the cumulative risk of clinically detectable cancer by age group*

Breast cancer						
Reference	Population	Study type	No. of patients	Age group (years)	Prevalence of microscopic cancer (%)	SEER US lifetime risk of cancer (%)
Nielsen et al., Cancer 1984	Denmark	Autopsy, hospital	77	>20	25.4	12.2
Nielsen et al., Br J Cancer 1987	Denmark	Autopsy, forensic	23 36 33 18	20–29 30–39 40–49 50–54	0 8 39 33	0.06 0.5 1.8 2.9
Kramer et al., Cancer 1973	US	Autopsy, hospital	70	>70	5.7	12.2
Alpers et al., Hum Pathol 1985	US	Autopsy, hospital	101	15–99	8.9	12.2
Bhathal et al., Br J Cancer 1985	Australia	Autopsy, forensic	207	>20	13	12.2
Ryan et al., Can J Surg 1962	Canada	Autopsy, hospital	100	>20	0–12	12.2
Bartow et al., Cancer 1987	US	Autopsy, forensic	519	>14	3.3	12.2

tioning the organs approximately 2–5 mm apart with extensive tissue sampling. Still, microscopic lesions in the vicinity of 1–2 mm in diameter could be easily overlooked and their total numbers underestimated. Therefore, Black & Welch speculated that after adjustment for sub-total sampling, microscopic thyroid cancer can be found in as many as 98% of individuals aged 50 to 70 years (3). Collectively, the available evidence from autopsy studies suggests that past a certain age most of us harbor microscopic tumors which in many instances remain harmless for life.

CLINICALLY RECURRENT CANCER: IS THERE A PHASE OF DORMANCY AND LATE RECURRENCES?

In addition to autopsy findings demonstrating that various organs can harbor clinically undetected (occult) primary tumors, increasing clinical evidence is emerging in support of a cancer latency (*i.e.* dormancy) period following treatment in patients who later present with recurrent disease. Demicheli et al. (31) and other groups have described the recurrence patterns of cancer after primary surgery. Data from more than 1000 breast cancer patients treated with mastectomy demonstrate a two-peak recurrence pattern that cannot be explained by a continuous tumor growth model. These observations are in accordance with a tumor progression model that includes periods of dormant metastases (32). In their study, the recurrence pattern showed an early peak at approximately 18 months after surgery, whereas a second peak of recurrence was documented at approximately 60 months, followed by a plateau-like tail extending up to 15 years (33). This recurrence pattern has recently been confirmed by two independent studies of 956 (34) and 2,213 patients (35). It has been speculated that these patterns can in part be explained by surgery-driven interruption of dormant micrometastatic breast cancer by a surge of growth factors (33, 36). In addition to surgery, physical trauma has been associated with clinical manifestation of cancer, possibly acting by a reactivation of dormant tumor cells (37).

MECHANISMS OF TUMOR DORMANCY

Tumor progression from a harmless single neoplastic cell to lethal metastases in distant organs is a multistep process (Fig. 1). The genetic and epigenetic events taking place at each step in this process have become increasingly complex, but also present novel treatment possibilities (Fig. 2). As the cancer progresses it acquires a series of genetic and molecular alterations, subsequently becoming: 1. self-sufficient in growth signaling,

TABLE 2. *Summary of autopsy studies performed on persons who have died without clinically diagnosed cancer. Comparison of microscopic "occult" cancer found in prostate to the cumulative risk of clinically detectable cancer by age group*

Reference	Tumor type	Population	Study type	No of patients	Age group (years)	Prevalence of microscopic cancer (%)	SEER US lifetime risk of cancer (%)
Guileyardo et al., JNCI 1980	Prostate HgPIN and/or IC	US	Autopsy, hospital and forensic	3	25–29	0	0.001
				9	30–44	33	0.06
				215	45–59	22	2.4
				162	60–69	33	8.1
				111	70+	42	13.9
				Total: 500		30	
Sakr et al., In Vivo 1994	Prostate IC	US	Autopsy, hospital	51	20–29	2	0.001
				83	30–39	29	0.009
				82	40–49	32	0.3
				22	50–59	55	2.4
				11	60–69	63	8.1
				Total: 249		28	
Sakr et al., In Vivo 1994	Prostate HgPIN	US	Autopsy, hospital	51	20–29	0	0.001
				83	30–39	5	0.009
				82	40–49	10	0.3
				22	50–59	41	2.4
				11	60–69	63	8.1
				Total: 249		11	
Shiraishi et al., In Vivo 1994	Prostate IC	Japan	Autopsy, hospital	34	30–39	6	
				94	40–49	17	
Shiraishi et al., In Vivo 1994	Prostate IC	US	Autopsy, hospital	3	30–39	0	0.009
				15	40–49	20	0.3
Soos et al., Eur Urol 2005	Prostate HgPIN and/or IC	Hungary	Autopsy, hospital	9	18–30	0	
				20	31–40	20	
				30	41–50	30	
				28	51–60	39	
				20	61–70	70	
				17	71–80	88	
				15	81–95	100	
				Total: 139		49	
Breslow et al., Int J Cancer 1977	Prostate HgPIN and/or IC	Singapore	Autopsy, hospital and forensic	242	>45	13.2	13.9
		Hong Kong		173		15.8	
		Uganda		150		19.5	
		Israel		143		22	
		Jamaica		168		29.8	
		Germany (BRD)		145		28.4	
		Sweden		306		31.6	
				Total: 1327			
Stamatiou et al., Prostate 2006	Prostate IC	Greece	Autopsy, hospital	18	30–39	0	0.009
				38	40–49	2.6	0.3
				38	50–59	5.2	2.4
				36	60–69	13.8	8.1
				36	70–79	30.5	13.9
				30	80–89	40	16.3
				16	>90	56.2	16.7
				Total: 212		19	
Sanches-Chapado et al., Prostate 2003	Prostate IC	Spain	Autopsy, forensic	162	20–29	3.58	0.001
					30–39	8.82	0.009
					40–49	14.28	0.3
					50–59	23.8	2.4
					60–69	31.7	8.1
					70–80	33.33	13.9
Montie et al., Cancer 1989	Prostate IC	US	Cysto-prostat-ectomy	27	<60	26	2.4
				38	60–74	61	11.3
				7	>74	43	13.9
Konety et al., J Urol 2005	Prostate IC	US	Autopsy, hospital	206	40–49	0	0.3
				231	50–59	0.8	2.4
				249	60–69	2	8.1
				244	70–79	2.5	13.9
				95	80–89	3.2	16.3
				Total: 1025			
Stemmermann et al., CEBP 1992	Prostate IC	Hawaii Japanese origin	Autopsy, hospital	48	<59	19	2.4
				131	60–69	22	8.1
				98	70–79	33	13.9
				16	>80	63	16.3
				Total: 293		27	

TABLE 3. *Summary of autopsy studies performed on persons who have died without clinically diagnosed cancer. Comparison of microscopic "occult" cancer found in thyroid to the cumulative risk of clinically detectable cancer by age group*

Reference	Tumor type	Population	Study type	No of patients	Age group (years)	Prevalence of microscopic cancer (%)	SEER US lifetime risk of cancer (%)
Harach et al., Cancer 1985	Thyroid (OTC)	Finland	Autopsy, hospital	1 4 21 59 16 Total: 101	0–20 21– 40 41–60 61– 80 81– 100	100 25 21/59 36 31 36	0.013 0.18 0.45 0.67 0.73
Solares et al., Am J Otolaryngol 2005	OTC	Guatemala	Autopsy, hospital and forensic	150	20–84	Male 1.7 Female 2.9	Male 0.35 Female 1.0
Ottino et al., Cancer 1989	OTC	Argentina	Autopsy, hospital	100	25–80	Male 13.6 Female 7.3	Male 0.35 Female 1.0
Sampson et al., Cancer 1974	OTC	US	Autopsy, hospital	157	41–60 61–80 80+	M F 15.3 12.5 4.5 3.5 0 0	M F 0.19 0.72 0.35 1.0 0.38 1.1
Mitselou et al., Anticancer Res 2002	OTC	Greece	Autopsy, forensic	36 39 69 17 Total: 160	<40 41–60 61–80 80+	0 8 6 12 5.6	0.18 0.45 0.68 0.7
Bondeson et al., Cancer 1981	OTC	Sweden	Autopsy, hospital	500	>20	8.6	0.67
Mortensen et al., Surg Forum 1955	TC	US	Autopsy, hospital	70 239 432 259 Total: 1000	<20 20–49 50–69 >70	M F 0 0 1 3 4 4 2 4 2 4	M F 0.004 0.02 0.1 0.5 0.3 0.9 0.4 1.1

by oncogene activation and loss of tumor suppressor genes, 2. insensitive to anti-growth signaling, 3. unresponsive to apoptotic signaling, 4. capable of limitless tumor cell replications, 5. sustained angiogenesis, and 6. tissue invasion and metastasis (38).

Tumor-vascular interactions

For a tumor to develop a highly malignant and deadly phenotype, it must recruit and sustain its own blood supply, a process known as tumor angiogenesis (39, 40). Thus, cancer is usually clinically detectable only after it becomes angiogenic and has significantly expanded in mass. Failure of a tumor to recruit new vasculature or to reorganize the existing surrounding vasculature results in a non-angiogenic and non-progressing stable tumor (Fig. 1). Folkman also suggested that tumor growth is dictated by a two-compartment system of highly integrated tumor cells and vascular endothelial cells (39). This concept indicated that endothelial cells may switch from a resting state to a rapid growth phase induced by "diffusible" signals secreted from the tumor cells. Moreover, Folkman proposed that angiogenesis could be a relevant target for tumor therapy (*i.e.,* anti-angiogenic therapy). To date, there are more than 10 (FDA and other international regulating agencies) approved angiogenesis inhibitors for clinical use of a variety of angiogenesis-dependent diseases, such as cancer and age-related macular degeneration (41). The fundamental objective of anti-angiogenic therapy is to inhibit the progression of pathologic angiogenesis, whereas the goal of anti-vascular therapy is to rapidly occlude new blood vessels so that the blood flow stops. Both therapeutic approaches target the ability of tumors to progress from the non-angiogenic to the angiogenic phenotype, a process termed the "angiogenic switch" (42, 43).

At sea level, the diffusion limit of oxygen has been reported to be approximately 100 μm (44). Therefore, in order to survive, all mammalian cells (including neoplastic cells) are required to be within 100–200 μm of a blood vessel. As non-

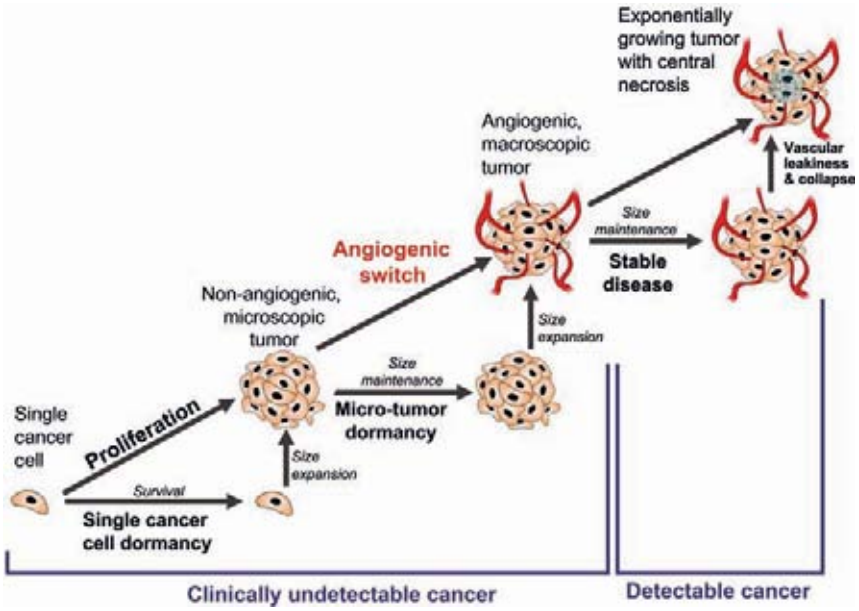

Fig. 1. Summary of rate-limiting steps in the process of tumor progression.

angiogenic tumors attempt to expand in mass, a property attributed to uncontrolled cancer cell proliferation, some tumor cells fall outside the oxygen diffusion limit and become hypoxic. These new hypoxic conditions induce a set of compensatory responses within this tumor cell population, such as activation of the hypoxia-inducible factor (HIF1α). This hypoxia-induced signaling leads to subsequent up-regulation of pro-angiogenic proteins, such as vascular endothelial growth factor (VEGF), platelet-derived growth factor (PDGF), and nitric oxide synthase (NOS) (45). The angiogenic switch in tumors is presumed to be closely regulated by the presence of pro- and anti-angiogenic proteins in the tumor microenvironment. An increase in the local concentration of pro-angiogenic proteins allows angiogenesis to occur and ultimately permits a tumor to expand in mass. Therefore, the microenvironment is an important permissive regulator for a tumor to expand in mass and become lethal, or to remain microscopic in size and harmless to the host (Figs. 1 & 2).

Experimental models of human tumor dormancy

The consequences of tumor angiogenesis, as well as blocked neovascularization, for the growth and expansion of tumors, have been studied for a long time. Thus, the effects of neovascularization on tumor growth were demonstrated as early as in the 1940s in experimental systems involving the transplantation of tumor pieces in isolated perfused organs and in the anterior chamber of the eyes of various species of animals. Green at al. (46) observed that H-31 rabbit carcinoma tumor implanted into the eyes of guinea pigs did not vascularize and failed to grow for 16–26 months. The transplants remained at a size of approximately 2.5 mm in diameter for the duration of the experiment. However, when the same tumors were re-implanted into the eyes of their original host, they vascularized and expanded in mass, filling the anterior chamber within 50 days. Similarly, Folkman et al. (47) showed that as implants in isolated perfused thyroid and intestinal segments, tumors grew and arrested at a small size (2–3 mm diameter).

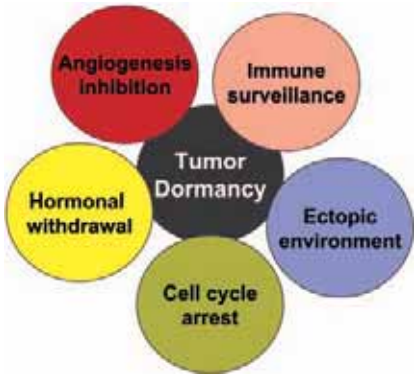

Fig. 2. Summary of various factors affecting the process of human tumor dormancy.

This inability of neoplasms to evoke a new blood supply was later attributed to endothelial cell degeneration in the perfused organs that were perfused with platelet-free hemoglobin solution (48). In 1972, Gimbrone et al. (49) provided *in vivo* evidence that the progressive growth of a homologous solid tumor can be deliberately arrested at a microscopic and stable size when neovasculature is prevented. In these experiments, two comparably sized tumor pieces were implanted in each eye of the same animal: one directly on the iris (known to be an angiogenic milieu) and the other suspended in the anterior chamber (known as an avascular milieu) of the opposing eye. The tumor implanted on the iris became vascularized and grew to a size 15,000 times the initial volume. The same tumor filled the anterior chamber of the rabbit eye within 14 days. In contrast, the tumor implant in the avascular anterior chamber remained avascular and had increased only four times its initial volume by day 14 after implantation. These "dormant" tumors remained at a size of ~1 mm in diameter for up to 44 days. During this dormancy period, the tumors developed a central necrotic core surrounded by a layer of viable tumor cells, in which mitotic figures were observed. Overall, these microscopic tumors remained avascular, as demonstrated by histologic studies. Still, the malignant growth potential of these microscopic tumors was evidenced by re-implantation directly on the irises of fresh animals. In this angiogenic microenvironment (*i.e.* the irises), the dormant tumors became vascularized and grew rapidly until the anterior chambers of the eyes were filled with tumor tissue, in a manner similar to the control iris implants. These fundamental observations established the relationship between tumor growth and angiogenesis. Importantly, they also provided one of the first *in vivo* experimental models for further investigations of tumor dormancy.

More recently, Hanahan & Folkman (43) described a spontaneous tumor dormancy model in transgenic mice. In this experimental model, autochthonous tumors arise in the pancreatic islets as a result of simian virus 40 T antigen (Tag) oncogene expression. Only 4% of these pancreatic islet tumors became angiogenic 13 weeks after birth of the animals. In contrast, the remaining 96% of pancreatic islet tumors remained microscopic and non-angiogenic (43, 50). The spontaneous progression of non-angiogenic lesions to the angiogenic phenotype in these transgenic tumor-bearing mice led to the development of the "angiogenic switch" concept (43).

In 2001, Achilles et al. (51) reported that human tumors contain tumor cell subpopulations that differ in their angiogenic potential. These findings suggested that the overall angiogenic phenotype of an individual human tumor cell may be controlled by genetic or epigenetic mechanisms. Therefore, human tumors can contain both angiogenic and non-angiogenic tumor cell populations, characterized by their ability to recruit new blood vessels to a tumor. However, the dynamic interplay of these two tumor cell populations with each other and the surrounding microenvironment is currently not known. Moreover, the key factors involved in the regulation of these two tumor cell populations are still under investigation.

One strategy for the isolation of angiogenic and non-angiogenic tumor cell populations is through single-cell cloning of a human tumor cell line. Achilles et al. (51) established and selected subclones from a human liposarcoma cell line (SW-872) based on high, intermediate, or low proliferation rates *in vitro*. These clones were subsequently expanded *in vitro* into distinct populations of tumor cells and were then inoculated into immunodeficient (SCID) mice. Three different *in vivo* growth patterns were observed: 1. highly angiogenic and rapidly growing tumors, 2. weakly angiogenic and slowly growing tumors, and 3. non-angigoenic and dormant tumors. Further investigation by Almog et al. (52) showed that the non-angiogenic tumors may spontaneously switch to the angiogenic phenotype and initiate exponential growth approximately 130 days after inoculation into the subcutaneous space. During a dormancy period of 130 days, microscopic tumors remained avascular and were virtually undetectable by palpation (approximate size of 1–2 mm in diameter). Because the angiogenic and non-angiogenic tumor cell populations in these models were segregated based on tumor cell proliferation differences *in vitro*, it raised three fundamental questions: 1. Is there a correlation between tumor cell proliferation and the angiogenic potential? 2. Can the observed differences in tumor growth be recapitulated using populations of human tumor cells that have not been cloned? and 3. Can non-

angiogenic and angiogenic tumor cell populations be segregated for other human cancer types?

To address these questions, human tumor cell lines were obtained from the American Type Culture Collection (ATCC, Manassas, VA) based on their "no take" phenotype in immunodeficient mice. These cell lines were assessed for *in vivo* tumor growth over extended time periods (over one year) after subcutaneous inoculation of a tumor cell suspension. Some of the mice, inoculated with the "no take" tumor cells, spontaneously formed palpable tumors after a dormancy period, which varied from months to more than a year, depending on cancer type. With time, tumors became angiogenic, palpable, expanded exponentially in mass, and killed the host animal within ~50 days of first detection (53, 54). Stable cell lines were established from representative tumors which became angiogenic following a dormancy period. When re-inoculated into SCID mice, these now angiogenic tumor cells formed large tumors (> 1 cm in diameter) within a month following inoculation, however without a dormancy period. The permanency of the angiogenic switch in human tumors was documented by the fact that 100% of mice inoculated with the angiogenic cells formed tumors, regardless of the cancer type. In contrast, it was found that each cancer type had a characteristic and predictable dormancy period and generated a consistent proportion of tumors that spontaneously switched to the angiogenic phenotype. To date, tumor cell population-based animal dormancy models have been developed and characterized for breast cancer, osteosarcoma, and glioblastoma (53). In contrast to the single-cell-derived human liposarcoma animal model, the angiogenic and non-angiogenic tumor cell populations of the rest of the animal models were derived by *in vivo* selection for the angiogenic and non-angiogenic phenotypes. Moreover, in these spontaneous (*not* single-cell-derived) dormancy models, the angiogenic and non-angiogenic populations did not differ significantly in tumor cell proliferation (53).

As demonstrated by the established dormancy models, certain human tumor cells can remain dormant for more than a year after inoculation in animals. However, this does not mean that the tumor cells are in G_o growth arrest. Although some tumor cells might be in mitotic arrest, as demonstrated in some tumor dormancy models (55–58), we reported that the majority of tumor cells are metabolically active, proliferating and undergoing apoptosis (52, 53). In a human breast cancer (MDA-MB-436) animal model, more than 50% of tumor cells were proliferating and more than 10% were undergoing apoptosis in all microscopic tumors analyzed by immunohistochemistry at various time points during dormancy (53). These rates of proliferation and apoptosis were similar within the macroscopically expanding angiogenic tumors. Similarly, in human osteosarcoma (MG-63 and SAOS-2) and gastric (ST-2) cancer dormancy models, reported by Udagawa et al. (59), microscopic tumors were unable to grow beyond a threshold size of ~1–2 mm in diameter. Tumor cell proliferation in these tumors was ~12% and tumor cell apoptosis ranged from 4% to 7.5%. Thus, tumor cell proliferation index within non-angiogenic tumors can be as high as that of large vascularized tumors. Moreover, non-angiogenic tumors appear to have a balance between proliferating cells and cells undergoing apoptosis.

Molecular pathways of human tumor dormancy

Transfection of human osteosarcoma (MG-63 and SAOS-2) and gastric cancer (ST-2) cells with activated *c-Ha-ras* oncogene induces loss of dormancy in otherwise non-angiogenic human cell lines (59). When inoculated in immunosuppressed mice, wild-type (or control vector-transfected) tumor cells did not form palpable tumors for more than 8 months. White tumor foci that were avascular or contained sparse vessels were found throughout the dormancy period at the site of inoculation. However, *ras*-transfected human osteosarcoma (MG-63 and SAOS-2) and gastric cancer (ST-2) cells formed vascularized large tumors within 1 month. The *in vivo* growth of *ras*-transfected tumor cells was associated with significantly increased angiogenic ability, increased tumor cell proliferation, and decreased tumor cell apoptosis when compared to wild-type tumor cells. Loss of the dormant phenotype induced by activated *ras* correlated with increased levels (1.5- to 2.5-fold difference) of $VEGF_{165}$, as assessed in conditioned media relative to the control tumor cells (59). Overexpression of $VEGF_{165}$ in the tumor cells also resulted in a loss of dormancy and induced a robust

angiogenic response in 30% of animals inoculated with gastric cancer and 40% of animals inoculated with osteosarcoma. In contrast to *ras*-transfected tumor cells, loss of dormancy in $VEGF_{165}$-transfected tumor cells was not associated with an increase in tumor cell proliferation, but was associated with reduced apoptosis. Therefore, the angiogenic response induced by $VEGF_{165}$ was found to be sufficient for the loss of dormancy by reducing apoptosis.

It has been demonstrated that *ras* can directly induce tumor cell proliferation and confer resistance to apoptosis (60, 61). In addition, *ras* activation can indirectly stimulate an angiogenic response in tumors by inducing pro-angiogenic proteins, such as VEGF (62), and by down-regulating angiogenesis inhibitors, such as thrombospondin-1 (63–66). Similarly to *ras*, other oncogenes and tumor suppressor genes can indirectly affect tumor growth via angiogenic mechanisms. For example, *p53*, *PTEN* and *Smad 4* have been shown to increase thrombospondin-1 expression transcriptionally or translationally (67–70). Thrombospondin-1 expression can be decreased by *Myc, Ras*, *Id1*, *WT1*, *C-jun* and *v-stc* via transcriptional repression, myc phosphorylation, or regulation of mRNA turnover and stability (65, 66, 71–76). The inherently low toxicity of natural angiogenesis inhibitors, in addition to their selective effect on pathologic neovascularization without harming normal vasculature, makes them an attractive therapeutic target.

In addition to thrombospondin-1 regulation, the *p53* tumor suppressor gene regulates other currently unidentified inhibitors of angiogenesis (77). Teodoro et al. (78) reported that wild-type p53 mobilizes endostatin through a specific alpha(II) collagen prolyl-4-hydroxylase (alpha(II)PH gene product) that binds to p53. *p53* is inactivated in over 50% of all human cancers. Re-introduction of wild-type *p53* into mouse fibrosarcoma (T241) cells correlates with increased thrombospondin-1 expression and induces angiogenesis-restricted dormancy (79). Inoculation of parental T241 fibrosarcoma cells into a mouse ear resulted in vascularized and visible tumors within 2 weeks. In contrast, when wild-type *p53* was introduced in the same cells, only 12% of the tumors became angiogenic 2 months after inoculation. Therefore, expression of wild-type *p53* resulted in the loss of an angiogenic phenotype. Loss of the angiogenic phenotype was also correlated with the up-regulation of the mRNA-encoding thrombospondin-1. This experimental model demonstrated that *p53* can act as a tumor suppressor, independent of its direct effects on cell proliferation and survival. Moreover, *p53* had an indirect anti-tumor effect by inhibiting angiogenesis and increasing the rate of apoptosis.

Although the non-angiogenic and angiogenic tumor cell populations did not differ significantly in tumor cell proliferation, they expressed and secreted different amounts of pro- and anti-angiogenic proteins. Naumov et al. (53) compared the tumor cell secretion and intracellular levels of Thrombospondin-1 (Tsp-1) in non-angiogenic and angiogenic tumor cell populations isolated from a human breast cancer cell line (MDA-MB-436). Angiogenic cells contained 2.5-fold higher levels of c-Myc and p-Myc (phosphorylated) than their nonangiogenic counterparts, as assessed by Western blot. In contrast, angiogenic breast cancer cells contained significantly lower levels of Tsp-1 than non-angiogenic tumor cells. Secretion of Tsp-1 from non-angiogenic tumor cells was 20-fold higher than that from angiogenic cells. Similar findings were previously reported for a different breast cancer cell line (MDA-MB-435) (66). Watnick et al. (66) reported that phosphoinositide 3-kinase (PI3K) can induce a signal transduction cascade leading to the phosphorylation of c-Myc and subsequent repression of Tsp-1. Treatment with a PI3K inhibitor (LY294002) caused Tsp-1 levels within angiogenic cells to increase but had no effect on levels in non-angiogenic cells (53). Therefore, the PI3K signaling pathway is responsible for the repression of Tsp-1, and it is regulated differently in angiogenic and non-angiogenic human tumor cells.

Tumor-stroma interactions

Interactions between tumor cells and their surrounding stroma are important for tumor progression (37). The possible stimulatory effect of trauma on this process might be one example. Bissell and colleagues have elegantly demonstrated the importance of signaling cross-talk between tumor cells and their microenvironment (80). Experimental evidence from this group has demonstrated that tissue wounding can induce inflammation and can

promote local epithelial transformation and tumor growth in Rous sarcoma virus (RSV)-infected chickens (81, 82).

In addition to clinical observations suggesting a relationship between trauma and tumor progression (83–86), Flook et al. (87) provided further support for the hypothesis that wounds are able to attract circulating cancer cells, suggesting that cancer cells are spread by the hematogenous route and soiled in a permissive area of acute trauma, *i.e.* the donor site wound.

In a series of studies, Murthy et al. showed that injection of TA3Ha transplantable murine mammary carcinoma cells did not cause liver or kidney metastasis in a cohort of 116 mice. However, if hepatic wedge resection was performed immediately before the surgery, over 50% of the animals had tumor formation at the site of surgery (88). This tumor take was significantly reduced if injection of cancer cells was delayed, indicating that the acute and early wound healing process supports tumor implantation. The same group had also reported that the tumor implantation and formation in the wounded liver was inhibited by plasminogen activators in a dose-dependent matter (89).

In an experimental study, Gill et al. demonstrated an important role of the bone marrow in wound repair after vascular trauma. Burn injury or surgical manipulation resulted in a rapid mobilization of circulating endothelial precursor (CEP) cells from the bone marrow and systemic elevation of plasma VEGF, suggesting that VEGF can promote CEP mobilization (90). The recruitment of CEPs from the bone marrow was dependent on up-regulation of Id1 and Id3 (91). Also, Abramovitch and colleagues found accelerated C6 glioma xenografts and increased angiogenesis associated with cutaneous injuries of pigs (92). Among several growth factors present in the wound fluid, EGF and PDGF were important for the stimulation of tumor growth. Clinical observations and follow-up studies indicate that most breast cancer patients present two or more lesions at the time of first recurrence (93–96), supporting the concept of a systemic and synchronized process breaking the dormancy of the micrometastatic state.

If proven to be clinically significant, the short-term angiogenic burst model (97) and the model of surgery-driven influence on the dormancy of micrometastatic disease (33) would potentially have a significant impact on future clinical practice. Would the administration of anti-angiogenic, anti-inflammatory or other anti-growth factor drugs directly before or during primary surgery lead to a reduction of recurrences during the first peak at about 18 months?

CLINICAL IMPLICATIONS OF TUMOR DORMANCY

Therapeutic implications of tumor dormancy

Tumor progression is highly dependent on the surrounding stroma, including endothelial cells, fibroblasts, extracellular matrix, macrophages, lymphocytes, platelets, and other cellular components. The communication between tumor cells and other cell types is fundamental. Anti-angiogenic therapy targets the endothelial cell compartment in two distinct ways: directly or indirectly (Fig. 3) (98).

Direct angiogenesis inhibitors block vascular endothelial cells from proliferating, migrating, or increasing their survival by pro-angiogenic proteins such as VEGF, PDGF, bFGF, IL-8, and others. For example, sunitinib directly blocks VEGF receptors (among other receptors involved in angiogenic signaling) on endothelial cells, blocking endothelial sprouting. Such direct angiogenesis inhibitors include: 1. synthetic inhibitors or peptides designed to interfere with specific steps in the angiogenic process (*e.g.*, inhibitors of metalloproteinases, antagonists of the $\alpha_V\beta_3$ or $\alpha_5\beta_1$ integrins); 2. low molecular weight molecules (*e.g.* TNP-470, caplostatin, thalidomide, 2-methoxyestradiol); and 3. natural endogenous angiogenesis inhibitors (*e.g.,* Tsp-1, platelet factor 4, interferon-α, IL-12, angiostatin, endostatin, arrestin, canstatin, tumstatin) (Fig. 3).

Bouck et al. were the first to demonstrate that a tumor can generate angiogenesis inhibitors (*i.e.,* thrombospondin-1) (99). This group subsequently suggested that the angiogenic phenotype was the result of a net imbalance of endogenous angiogenesis stimulators and inhibitors. In a series of experiments, Folkman et al. reported that the surgical removal of a primary Lewis lung carcinoma tumor in mice results in the exponential growth of lung metastases (100,

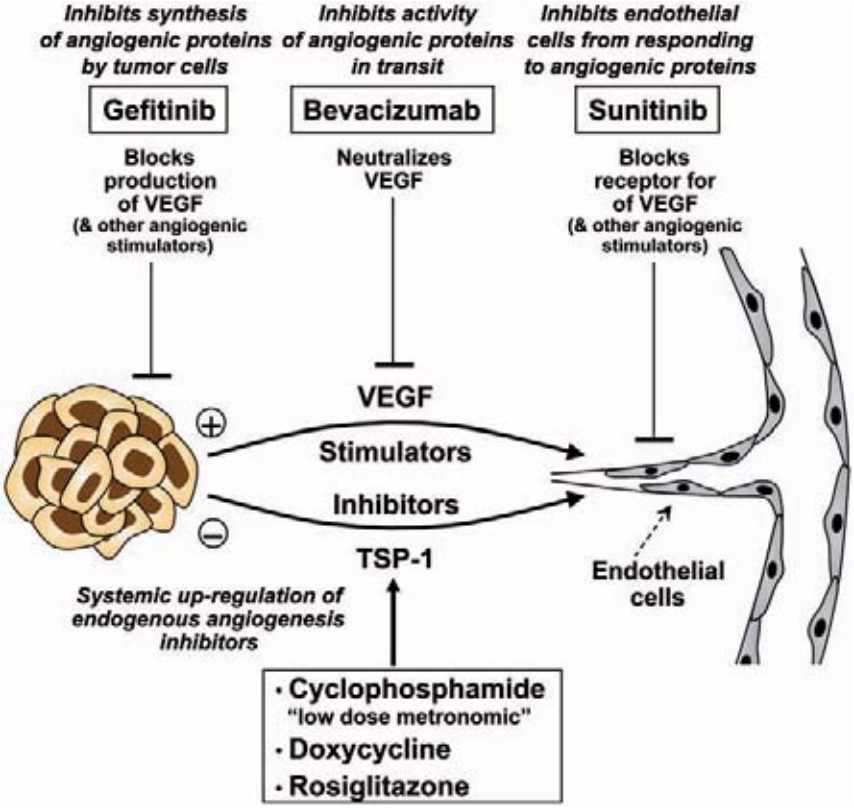

Fig. 3. Examples of various mechanisms of angiogenesis inhibition.

101). In these studies, the presence of a primary tumor generated increased circulating angiostatin levels. Angiostatin is a potent anti-angiogenic plasminogen fragment (102) which inhibits the *in vivo* growth of Lewis lung metastases by preventing neovascularization (103). However, gene transfer of a cDNA coding for mouse angiostatin into murine T241 fibrosarcoma cells successfully suppressed lung metastatic tumor growth after removal of the primary tumor (104). Cao et al. (104) demonstrated that pulmonary micrometastases remain in a dormant and avascular state for 2–5 months after removal of primary tumors. These dormant micrometastases revealed a high tumor cell proliferation rate which was counterbalanced by a high rate of apoptosis.

Holmgren et al. (101) investigated whether treatment with an exogenous angiogenesis inhibitor could replace the endogenous angiogenesis suppressive ability of a primary tumor. In animals with surgically removed primary Lewis lung carcinoma, or T241 mouse sarcomas, treatment with TNP-470 resulted in the suppression of metastases comparable to that observed in the presence of the primary tumor. Therefore, exogenous treatment can be used to replace the endogenous angiogenesis inhibition of a primary tumor. Moreover, it can be used for the systemic suppression of angiogenesis-maintained micrometastases of both Lewis lung cancer and T241 fibrosarcoma in a dormant state. These dormant micrometastases were characterized as having high tumor cell proliferation counterbalanced by high cell death rate (*i.e.* apoptosis), indicating that inhibition of angiogenesis limits tumor growth by elevating tumor cell apoptosis. Thus, exogenous angiogenesis inhibitors, such as TNP-470, mimic the primary tumor suppression by maintaining high apoptosis in the lung micrometastases, but without having an effect on tumor cell proliferation. A similar mechanism of sustained micrometastatic dormant state has been demonstrated using angiostatin (105).

Indirect angiogenesis inhibitors target tumor cell proteins created by oncogenes that drive the angiogenic switch. In general, their mechanism

of action is by decreasing or blocking the expression of other tumor cell products, neutralizing the tumor cell product itself, or by blocking receptors on endothelial cells. The impact of oncogenes on tumor angiogenesis has been reviewed by Rak & Kerbel (65, 106, 107). For example, gefitinib (Iressa) blocks VEGF production from tumor cells. However, even systemically available VEGF can be neutralized by bevacizumab (Avastin) before it binds to VEGF receptors on endothelial cells (Fig. 3). There is an emerging group (*e.g.* tyrosine kinase inhibitors) of anti-cancer drugs originally developed to target oncogenes which also have "indirect" anti-angiogenic activity. For example, the *ras* farnesyl transferase inhibitors block oncogene signaling pathways which up-regulate tumor cell production of VEGF and down-regulate production of Tsp-1 (108). Trastuzumab, an antibody that blocks *HER2/neu* receptor tyrosine kinase signaling, suppresses tumor cell production of angiogenic proteins, such as TGF-α, angiopoietin 1, plasminogen activator inhibitor-1 (PAI-1) and VEGF (109, 110). At the same time, trastuzumab has been shown to up-regulate the expression of Tsp-1 (endogenous angiogenesis inhibitor), which may be an important mechanism of its anti-angiogenic activity (110). Up-regulation of endogenous anti-angiogenic proteins, using direct and/or indirect angiogenesis inhibitors, can be a viable approach for preventing the angiogenic switch and keeping human tumors in a microscopic and dormant state (Fig. 3). This anti-angiogenic therapeutic approach is associated with low toxicity, relatively low drug concentrations, and reduced drug resistance compared to traditional chemotherapy (41).

Acquired drug resistance is a major obstacle in the treatment of cancer, being caused by genetic instability, high mutational rates of tumor cells, and tumor heterogeneity (111). In contrast, anti-angiogenic therapy targets endothelial cells, which are genetically stable and have a low mutational rate. In an experimental animal model, Boehm et al. reported that anti-angiogenic therapy targeted against tumor-associated endothelial cells does not result in drug resistance (112). In this study, Lewis lung cancer, T241 fibrosarcoma and B16F10 melanoma were repeatedly treated with endostatin. When tumors reached an approximate size of 350–400 mm^3 endostatin treatment was initiated until the tumor became undetectable. Endostatin therapy was then stopped, and the tumor was allowed to re-grow. Endostatin therapy was resumed when tumors reached a mean volume of 350–400 mm^3. After two (for melanoma), four (for fibrosarcoma), and six (for Lewis lung carcinoma) cycles of endostatin treatment, all tumors remained as barely visible subcutaneous nodules (size 5–50 mm^3) for up to 360 days. In contrast, endostatin resistance developed rapidly when Lewis lung carcinomas were treated with cytotoxic chemotherapy. These studies demonstrate that repeated cycles of endostatin therapy induced tumor dormancy that persisted after therapy.

Systemic markers of dormant tumors

Even with recent advances in the clinical detection of human cancer, a tumor that is microscopic in size (~1 mm in diameter) remains undetectable. Identification of markers that could detect tumors at a dormant state would provide a basis for early adjuvant treatment (especially related to residual disease and micrometastases). A panel of angiogenic switch-related biomarkers is now under development using the human tumor dormancy models. These biomarkers include circulating endothelial progenitor cells and proteins in blood platelets, as well as matrix metalloproteinases (MMPs) detected in the urine. In animal models, the detection of a single microscopic human tumor can be achieved using each one of these biomarkers alone or in combination (113–116).

We compared the *in vivo* ability of angiogenic and non-angiogenic human breast tumors (MDA-MB-436 cells) to mobilize mature circulating endothelial cells (CECs) (CD45−, Flk+, CD31+, CD117−) and circulating endothelial progenitor cells (CEPs) (CD45−, Flk+, CD31+, CD117+) (113). The number of blood-borne CECs and CEPs was quantified using flow cytometry. There was only a small difference in the percent of mature CECs in the blood of mice inoculated with angiogenic and non-angiogenic cells. However, mice inoculated with non-angiogenic cells had a ~4-fold decrease in CEPs when compared to control mice. Mice inoculated with angiogenic cells had levels of CEPs comparable to those in the control mice. Previous reports (53) have shown that these

non-angiogenic breast cancer cells (MDA-MB-436 cells) secrete at least 20-fold higher levels of thrombospondin-1 (Tsp-1) as compared to their angiogenic counterparts. Other studies have suggested that endogenous inhibitors of angiogenesis, such as Tsp-1 and endostatin, may inhibit the mobilization of CEPs (117). These observations suggest that microscopic dormant (non-angiogenic) tumors may suppress the mobilization of CEPs from the bone marrow via systemic thrombospondin-1.

Italiano et al. (118) recently reported that blood platelets can sequester both pro- and anti-angiogenic proteins. It is estimated that at least 100 billion platelets are produced per day (119, 120), and with a lifespan of 7–8 days in humans, there are approximately a trillion platelets in constant circulation (119, 121). Folkman, Klement & Naumov proposed that the platelet compartment can potentially accumulate angiogenesis-related proteins and possibly release them at a later time (115). Using a novel "platelet angiogenic proteome", as quantitatively assessed by SELDI-ToF technology, the presence of microscopic human tumors in mice can be detected (116).The accumulation and reduction in angiogenesis-related proteins sequestered in platelets can be quantitatively followed throughout the angiogenic switch. The identification of proteins that are associated with the angiogenic switch and that may be used as angiogenic switch-related biomarkers is currently under investigation.

In summary, the tumor dormancy animal models presented here permit further clarification of the role of CEC/CEPs, blood platelets and MMPs as participants in the "angiogenic switch". Moreover, this angiogenic switch-related biomarker panel may prove to be a useful diagnostic platform for detecting microscopic cancers at primary and metastatic sites long before detection by conventional methods. Thus, these angiogenesis-associated biomarkers might identify the presence of microscopic human tumors, predict their switch to the angiogenic phenotype, and possibly serve as a guide for anti-angiogenic therapy. As predicted by Folkman, it may one day be possible for a patient who is at a risk of cancer recurrence to take an oral drug that can elevate endogenous platelet-associated anti-angiogenic proteins and delay, if not prevent, the formation of recurrent tumors (122).

The authors would like to dedicate this article to the memory of Judah Folkman, M.D. (1933–2008), a world-class mentor and colleague. We thank Dr. R. Watnick for critical reading and editing of this manuscript. We also thank Kristin Johnson for help with graphics. This work was supported by the Breast Cancer Research Foundation, NIH Program Project (grant #P01CA45548), an Innovator Award from the Department of Defense, the Norwegian Research Council, the Norwegian Cancer Society, and Helse Vest Norway.

REFERENCES

1. Naumov GN, Folkman J. Strategies to prolong the nonangiogenic dormant state of human cancer. In: Davis DW, Herbst RS, Abbruzzese JL, editors. Antiangiogenic Cancer Therapy. Boca Raton, FL: CRC Press, 2008:3–21.
2. Institute NC. Surveillance Epidemiology and End Results (SEER) database. [Web page] April 15, 2008; Available from: http://seer.cancer.gov/
3. Black WC, Welch HG. Advances in diagnostic imaging and overestimations of disease prevalence and the benefits of therapy. N Engl J Med 1993;328:1237–43.
4. Tabar L, Vitak B, Chen HH, Duffy SW, Yen MF, Chang CF, et al. The Swedish Two-County Trial twenty years later. Updated mortality results and new insights from long-term follow-up. Radiol Clin North Am 2000;38:625–51.
5. Larsen I, Smastuen M, Parkin D, Bray F. Cancer in Norway 2006. Cancer incidence, mortality, survival and prevalence in Norway. Oslo: Cancer Registry of Norway, 2007.
6. Biesheuvel C, Barratt A, Howard K, Houssami N, Irwig L. Effects of study methods and biases on estimates of invasive breast cancer overdetection with mammography screening: a systematic review. Lancet Oncol 2007;8:1129–38.
7. Jonsson H, Johansson R, Lenner P. Increased incidence of invasive breast cancer after the introduction of service screening with mammography in Sweden. Int J Cancer 2005;117:842–7.
8. Zahl PH, Strand BH, Maehlen J. Incidence of breast cancer in Norway and Sweden during introduction of nationwide screening: prospective cohort study. BMJ 2004;328:921–4.
9. Nielsen M, Thomsen JL, Primdahl S, Dyreborg U, Andersen JA. Breast cancer and atypia among young and middle-aged women: a study of 110 medicolegal autopsies. Br J Cancer 1987;56:814–9.
10. Kramer WM, Rush BF Jr. Mammary duct proliferation in the elderly. A histopathologic study. Cancer 1973;31:130–7.
11. Alpers CE, Wellings SR. The prevalence of carci-

noma in situ in normal and cancer-associated breasts. Hum Pathol 1985;16:796–807.
12. Bhathal PS, Brown RW, Lesueur GC, Russell IS. Frequency of benign and malignant breast lesions in 207 consecutive autopsies in Australian women. Br J Cancer 1985;51:271–8.
13. Ryan JA, Coady CJ. Intraductal epithelial proliferation in the human breast—a comparative study. Can J Surg 1962;5:12–9.
14. Bartow SA, Pathak DR, Black WC, Key CR, Teaf SR. Prevalence of benign, atypical, and malignant breast lesions in populations at different risk for breast cancer. A forensic autopsy study. Cancer 1987;60:2751–60.
15. Harach HR, Franssila KO, Wasenius VM. Occult papillary carcinoma of the thyroid. A "normal" finding in Finland. A systematic autopsy study. Cancer 1985;56:531–8.
16. Mortensen JD, Bennett WA, Woolner LB. Incidence of carcinoma in thyroid glands removed at 1000 consecutive routine necropsies. Surg Forum 1955;5:659–63.
17. Solares CA, Penalonzo MA, Xu M, Orellana E. Occult papillary thyroid carcinoma in postmortem species: prevalence at autopsy. Am J Otolaryngol 2005;26:87–90.
18. Ottino A, Pianzola HM, Castelletto RH. Occult papillary thyroid carcinoma at autopsy in La Plata, Argentina. Cancer 1989;64:547–51.
19. Sampson RJ, Woolner LB, Bahn RC, Kurland LT. Occult thyroid carcinoma in Olmsted County, Minnesota: prevalence at autopsy compared with that in Hiroshima and Nagasaki, Japan. Cancer 1974;34:2072–6.
20. Mitselou A, Vougiouklakis TG, Peschos D, Dallas P, Boumba VA, Agnantis NJ. Immunohistochemical study of the expression of S-100 protein, epithelial membrane antigen, cytokeratin and carcinoembryonic antigen in thyroid lesions. Anticancer Res 2002;22:1777–80.
21. Bondeson L, Ljungberg O. Occult thyroid carcinoma at autopsy in Malmo, Sweden. Cancer 1981;47:319–23.
22. Guileyardo JM, Johnson WD, Welsh RA, Akazaki K, Correa P. Prevalence of latent prostate carcinoma in two U.S. populations. J Natl Cancer Inst 1980;65:311–6.
23. Sakr WA, Grignon DJ, Crissman JD, Heilbrun LK, Cassin BJ, Pontes JJ, et al. High grade prostatic intraepithelial neoplasia (HGPIN) and prostatic adenocarcinoma between the ages of 20–69: an autopsy study of 249 cases. In Vivo 1994;8:439–43.
24. Stamatiou K, Alevizos A, Agapitos E, Sofras F. Incidence of impalpable carcinoma of the prostate and of non-malignant and precarcinomatous lesions in Greek male population: an autopsy study. Prostate 2006;66:1319–28.
25. Stemmermann GN, Nomura AM, Chyou PH, Yatani R. A prospective comparison of prostate cancer at autopsy and as a clinical event: the Hawaii Japanese experience. Cancer Epidemiol Biomarkers Prev 1992;1:189–93.
26. Shiraishi T, Watanabe M, Matsuura H, Kusano I, Yatani R, Stemmermann GN. The frequency of latent prostatic carcinoma in young males: the Japanese experience. In Vivo 1994;8:445–7.
27. Soos G, Tsakiris I, Szanto J, Turzo C, Haas PG, Dezso B. The prevalence of prostate carcinoma and its precursor in Hungary: an autopsy study. Eur Urol 2005;48:739–44.
28. Breslow N, Chan CW, Dhom G, Drury RA, Franks LM, Gellei B, et al. Latent carcinoma of prostate at autopsy in seven areas. The International Agency for Research on Cancer, Lyons, France. Int J Cancer 1977;20:680–8.
29. Montie JE, Wood DP Jr, Pontes JE, Boyett JM, Levin HS. Adenocarcinoma of the prostate in cystoprostatectomy specimens removed for bladder cancer. Cancer 1989;63:381–5.
30. Konety BR, Bird VY, Deorah S, Dahmoush L. Comparison of the incidence of latent prostate cancer detected at autopsy before and after the prostate specific antigen era. J Urol 2005;174:1785–8; discussion 1788.
31. Demicheli R, Terenziani M, Valagussa P, Moliterni A, Zambetti M, Bonadonna G. Local recurrences following mastectomy: support for the concept of tumor dormancy. J Natl Cancer Inst 1994;86:45–8.
32. Demicheli R, Abbattista A, Miceli R, Valagussa P, Bonadonna G. Time distribution of the recurrence risk for breast cancer patients undergoing mastectomy: further support about the concept of tumor dormancy. Breast Cancer Res Treat 1996;41:177–85.
33. Demicheli R, Retsky MW, Hrushesky WJ, Baum M. Tumor dormancy and surgery-driven interruption of dormancy in breast cancer: learning from failures. Nat Clin Pract Oncol 2007;4:699–710.
34. Gao F, Tan SB, Machin D, Wong NS. Confirmation of double-peaked time distribution of mortality among Asian breast cancer patients in a population-based study. Breast Cancer Res 2007;9:R21.
35. Yin W, Di G, Zhou L, Lu J, Liu G, Wu J, et al. Time-varying pattern of recurrence risk for Chinese breast cancer patients. Breast Cancer Res Treat 2008 Apr 19 [Epub ahead of print].
36. Coffey JC, Wang JH, Smith MJ, Bouchier-Hayes D, Cotter TG, Redmond HP. Excisional surgery for cancer cure: therapy at a cost. Lancet Oncol 2003;4:760–8.
37. Naumov GN, Folkman J, Straume O. Tumor dormancy due to failure of angiogenesis: role of the microenvironment. Clin Exp Metastasis 2008 Jun 18 [Epub] ahead of print.

38. Hanahan D, Weinberg RA. The hallmarks of cancer. Cell 2000;100:57–70.
39. Folkman J. Tumor angiogenesis: therapeutic implications. N Engl J Med 1971;285:1182–6.
40. Folkman J. What is the evidence that tumors are angiogenesis dependent? J Natl Cancer Inst 1990; 82:4–6.
41. Folkman J. Angiogenesis: an organizing principle for drug discovery? Nat Rev Drug Discov 2007; 6:273–86.
42. Folkman J, Watson K, Ingber D, Hanahan D. Induction of angiogenesis during the transition from hyperplasia to neoplasia. Nature 1989;339: 58–61.
43. Hanahan D, Folkman J. Patterns and emerging mechanisms of the angiogenic switch during tumorigenesis. Cell 1996;86:353–64.
44. Torres Filho IP, Leunig M, Yuan F, Intaglietta M, Jain RK. Noninvasive measurement of microvascular and interstitial oxygen profiles in a human tumor in SCID mice. Proc Natl Acad Sci USA 1994;91:2081–5.
45. North S, Moenner M, Bikfalvi A. Recent developments in the regulation of the angiogenic switch by cellular stress factors in tumors. Cancer Lett 2005;218:1–14.
46. Greene HSN. Heterolgous transplantation of mammalian tumors. J Exp Med 1941;73:461–86.
47. Folkman J, Cole P, Zimmerman S. Tumor behavior in isolated perfused organs: in vitro growth and metastases of biopsy material in rabbit thyroid and canine intestinal segment. Ann Surg 1966;164:491–502.
48. Gimbrone MA Jr, Aster RH, Cotran RS, Corkery J, Jandl JH, Folkman J. Preservation of vascular integrity in organs perfused in vitro with a platelet-rich medium. Nature 1969;222:33–6.
49. Gimbrone MA Jr, Leapman SB, Cotran RS, Folkman J. Tumor dormancy in vivo by prevention of neovascularization. J Exp Med 1972;136:261–76.
50. Hanahan D, Christofori G, Naik P, Arbeit J. Transgenic mouse models of tumour angiogenesis: the angiogenic switch, its molecular controls, and prospects for preclinical therapeutic models. Eur J Cancer 1996;32A:2386–93.
51. Achilles EG, Fernandez A, Allred EN, Kisker O, Udagawa T, Beecken WD, et al. Heterogeneity of angiogenic activity in a human liposarcoma: a proposed mechanism for "no take" of human tumors in mice. J Natl Cancer Inst 2001;93:1075–81.
52. Almog N, Henke V, Flores L, Hlatky L, Kung AL, Wright RD, et al. Prolonged dormancy of human liposarcoma is associated with impaired tumor angiogenesis. Faseb J 2006;20:947–9.
53. Naumov GN, Bender E, Zurakowski D, Kang SY, Sampson D, Flynn E, et al. A model of human tumor dormancy: an angiogenic switch from the nonangiogenic phenotype. J Natl Cancer Inst 2006;98:316–25.
54. Naumov GN, Akslen LA, Folkman J. Role of angiogenesis in human tumor dormancy: animal models of the angiogenic switch. Cell Cycle 2006; 5:1779–87.
55. Aguirre Ghiso JA, Kovalski K, Ossowski L. Tumor dormancy induced by downregulation of urokinase receptor in human carcinoma involves integrin and MAPK signaling. J Cell Biol 1999;147: 89–104.
56. Aguirre-Ghiso JA, Liu D, Mignatti A, Kovalski K, Ossowski L. Urokinase receptor and fibronectin regulate the ERK(MAPK) to p38(MAPK) activity ratios that determine carcinoma cell proliferation or dormancy in vivo. Mol Biol Cell 2001;12:863–79.
57. Aguirre-Ghiso JA, Estrada Y, Liu D, Ossowski L. ERK(MAPK) activity as a determinant of tumor growth and dormancy; regulation by p38(SAPK). Cancer Res 2003;63:1684–95.
58. Aguirre-Ghiso JA. Models, mechanisms and clinical evidence for cancer dormancy. Nat Rev Cancer 2007;7:834–46.
59. Udagawa T, Fernandez A, Achilles EG, Folkman J, D'Amato RJ. Persistence of microscopic human cancers in mice: alterations in the angiogenic balance accompanies loss of tumor dormancy. Faseb J 2002;16:1361–70.
60. Goustin AS, Leof EB, Shipley GD, Moses HL. Growth factors and cancer. Cancer Res 1986;46: 1015–29.
61. Bonni A, Brunet A, West AE, Datta SR, Takasu MA, Greenberg ME. Cell survival promoted by the Ras-MAPK signaling pathway by transcription-dependent and -independent mechanisms. Science 1999;286:1358–62.
62. Rak J, Mitsuhashi Y, Bayko L, Filmus J, Shirasawa S, Sasazuki T, et al. Mutant ras oncogenes upregulate VEGF/VPF expression: implications for induction and inhibition of tumor angiogenesis. Cancer Res 1995;55:4575–80.
63. Good DJ, Polverini PJ, Rastinejad F, Le Beau MM, Lemons RS, Frazier WA, et al. A tumor suppressor-dependent inhibitor of angiogenesis is immunologically and functionally indistinguishable from a fragment of thrombospondin. Proc Natl Acad Sci USA 1990;87:6624–8.
64. Sheibani N, Frazier WA. Repression of thrombospondin-1 expression, a natural inhibitor of angiogenesis, in polyoma middle T transformed NIH3T3 cells. Cancer Lett 1996;107:45–52.
65. Rak J, Yu JL, Klement G, Kerbel RS. Oncogenes and angiogenesis: signaling three-dimensional tumor growth. J Investig Dermatol Symp Proc 2000; 5:24–33.
66. Watnick RS, Cheng YN, Rangarajan A, Ince TA, Weinberg RA. Ras modulates Myc activity to repress thrombospondin-1 expression and increase tumor angiogenesis. Cancer Cell 2003;3: 219–31.

67. Dameron KM, Volpert OV, Tainsky MA, Bouck N. Control of angiogenesis in fibroblasts by p53 regulation of thrombospondin-1. Science 1994; 265:1582–4.
68. Volpert OV, Dameron KM, Bouck N. Sequential development of an angiogenic phenotype by human fibroblasts progressing to tumorigenicity. Oncogene 1997;14:1495–502.
69. Chandrasekaran L, He CZ, Al-Barazi H, Krutzsch HC, Iruela-Arispe ML, Roberts DD. Cell contact-dependent activation of alpha3beta1 integrin modulates endothelial cell responses to thrombospondin-1. Mol Biol Cell 2000;11:2885–900.
70. Lawler J, Sunday M, Thibert V, Duquette M, George EL, Rayburn H, et al. Thrombospondin-1 is required for normal murine pulmonary homeostasis and its absence causes pneumonia. J Clin Invest 1998;101:982–92.
71. Volpert OV. Modulation of endothelial cell survival by an inhibitor of angiogenesis thrombospondin-1: a dynamic balance. Cancer Metastasis Rev 2000;19:87–92.
72. Mettouchi A, Cabon F, Montreau N, Vernier P, Mercier G, Blangy D, et al. SPARC and thrombospondin genes are repressed by the c-jun oncogene in rat embryo fibroblasts. Embo J 1994;13:5668–78.
73. Dejong V, Degeorges A, Filleur S, Ait-Si-Ali S, Mettouchi A, Bornstein P, et al. The Wilms' tumor gene product represses the transcription of thrombospondin 1 in response to overexpression of c-Jun. Oncogene 1999;18:3143–51.
74. Slack JL, Bornstein P. Transformation by v-src causes transient induction followed by repression of mouse thrombospondin-1. Cell Growth Differ 1994;5:1373–80.
75. Tikhonenko AT, Black DJ, Linial ML. Viral Myc oncoproteins in infected fibroblasts down-modulate thrombospondin-1, a possible tumor suppressor gene. J Biol Chem 1996;271:30741–7.
76. Janz A, Sevignani C, Kenyon K, Ngo CV, Thomas-Tikhonenko A. Activation of the myc oncoprotein leads to increased turnover of thrombospondin-1 mRNA. Nucleic Acids Res 2000;28: 2268–75.
77. Van Meir EG, Kikuchi T, Tada M, Li H, Diserens AC, Wojcik BE, et al. Analysis of the p53 gene and its expression in human glioblastoma cells. Cancer Res 1994;54:649–52.
78. Teodoro JG, Parker AE, Zhu X, Green MR. p53-mediated inhibition of angiogenesis through up-regulation of a collagen prolyl hydroxylase. Science 2006;313:968–71.
79. Holmgren L, Jackson G, Arbiser J. p53 induces angiogenesis-restricted dormancy in a mouse fibrosarcoma. Oncogene 1998;17:819–24.
80. Bissell MJ, Radisky D. Putting tumours in context. Nat Rev Cancer 2001;1:46–54.
81. Dolberg DS, Hollingsworth R, Hertle M, Bissell MJ. Wounding and its role in RSV-mediated tumor formation. Science 1985;230:676–8.
82. Sieweke MH, Thompson NL, Sporn MB, Bissell MJ. Mediation of wound-related Rous sarcoma virus tumorigenesis by TGF-beta. Science 1990; 248:1656–60.
83. Morihara K, Takenaka H, Morihara T, Kishimoto S. Primary cutaneous anaplastic large cell lymphoma associated with vascular endothelial growth factor arising from a burn scar. J Am Acad Dermatol 2007;57(5 Suppl):S103–5.
84. Kotzen RM, Swanson RM, Milhorat TH, Boockvar JA. Post-traumatic meningioma: case report and historical perspective. J Neurol Neurosurg Psychiatry 1999;66:796–798.
85. Oosterling SJ, van der Bij GJ, van Egmond M, van der Sijp JR. Surgical trauma and peritoneal recurrence of colorectal carcinoma. Eur J Surg Oncol 2005;31:29–37.
86. Gamatsi IE, McCulloch TA, Bailie FB, Srinivasan JR. Malignant melanoma in a skin graft: burn scar neoplasm or a transferred melanoma? Br J Plast Surg 2000;53:342–4.
87. Flook D, Horgan K, Taylor BA, Hughes LE. Surgery for malignant melanoma: from which limb should the graft be taken? Br J Surg 1986; 73:793–5.
88. Murthy SM, Goldschmidt RA, Rao LN, Ammirati M, Buchmann T, Scanlon EF. The influence of surgical trauma on experimental metastasis. Cancer 1989;64:2035–44.
89. Murthy MS, Summaria LJ, Miller RJ, Wyse TB, Goldschmidt RA, Scanlon EF. Inhibition of tumor implantation at sites of trauma by plasminogen activators. Cancer 1991;68:1724–30.
90. Gill M, Dias S, Hattori K, Rivera ML, Hicklin D, Witte L, et al. Vascular trauma induces rapid but transient mobilization of VEGFR2(+)AC133(+) endothelial precursor cells. Circ Res 2001;88:167–74.
91. Benezra R, Rafii S, Lyden D. The Id proteins and angiogenesis. Oncogene 2001;20:8334–41.
92. Abramovitch R, Marikovsky M, Meir G, Neeman M. Stimulation of tumour growth by wound-derived growth factors. Br J Cancer 1999;79:1392–8.
93. Tomiak E, Piccart M, Mignolet F, Sahmoud T, Paridaens R, Nooy M, et al. Characterisation of complete responders to combination chemotherapy for advanced breast cancer: a retrospective EORTC Breast Group study. Eur J Cancer 1996;32A:1876–87.
94. Withers HR, Lee SP. Modeling growth kinetics and statistical distribution of oligometastases. Semin Radiat Oncol 2006;16:111–9.
95. Swenerton KD, Legha SS, Smith T, Hortobagyi GN, Gehan EA, Yap HY, et al. Prognostic factors in metastatic breast cancer treated with combination chemotherapy. Cancer Res 1979;39:1552–62.

96. Greenberg PA, Hortobagyi GN, Smith TL, Ziegler LD, Frye DK, Buzdar AU. Long-term follow-up of patients with complete remission following combination chemotherapy for metastatic breast cancer. J Clin Oncol 1996;14:2197–205.
97. Indraccolo S, Stievano L, Minuzzo S, Tosello V, Esposito G, Piovan E, et al. Interruption of tumor dormancy by a transient angiogenic burst within the tumor microenvironment. Proc Natl Acad Sci USA 2006;103:4216–21.
98. Kerbel R, Folkman J. Clinical translation of angiogenesis inhibitors. Nat Rev Cancer 2002;2: 727–39.
99. Bouck N. Tumor angiogenesis: the role of oncogenes and tumor suppressor genes. Cancer Cells 1990;2:179–85.
100. O'Reilly M, Rosenthal R, Sage HE, Smith S, Holmgren L, Moses M, et al. The suppression of tumor metastases by a primary tumor. Surg Forum 1993;44:474–6.
101. Holmgren L, O'Reilly MS, Folkman J. Dormancy of micrometastases: balanced proliferation and apoptosis in the presence of angiogenesis suppression. Nat Med 1995;1:149–53.
102. Lay AJ, Jiang XM, Kisker O, Flynn E, Underwood A, Condron R, et al. Phosphoglycerate kinase acts in tumour angiogenesis as a disulphide reductase. Nature 2000;408:869–73.
103. O'Reilly MS, Holmgren L, Shing Y, Chen C, Rosenthal RA, Moses M, et al. Angiostatin: a novel angiogenesis inhibitor that mediates the suppression of metastases by a Lewis lung carcinoma. Cell 1994;79:315–28.
104. Cao Y, O'Reilly MS, Marshall B, Flynn E, Ji RW, Folkman J. Expression of angiostatin cDNA in a murine fibrosarcoma suppresses primary tumor growth and produces long-term dormancy of metastases. J Clin Invest 1998;101:1055–63.
105. O'Reilly MS, Holmgren L, Chen C, Folkman J. Angiostatin induces and sustains dormancy of human primary tumors in mice. Nat Med 1996; 2:689–92.
106. Kerbel RS, Viloria-Petit A, Okada F, Rak J. Establishing a link between oncogenes and tumor angiogenesis. Mol Med 1998;4:286–95.
107. Rak J, Yu JL, Kerbel RS, Coomber BL. What do oncogenic mutations have to do with angiogenesis/vascular dependence of tumors? Cancer Res 2002;62:1931–4.
108. Okada F, Rak JW, Croix BS, Lieubeau B, Kaya M, Roncari L, et al. Impact of oncogenes in tumor angiogenesis: mutant K-ras up-regulation of vascular endothelial growth factor/vascular permeability factor is necessary, but not sufficient for tumorigenicity of human colorectal carcinoma cells. Proc Natl Acad Sci USA 1998;95:3609–14.
109. Petit AM, Rak J, Hung MC, Rockwell P, Goldstein N, Fendly B, et al. Neutralizing antibodies against epidermal growth factor and ErbB-2/neu receptor tyrosine kinases down-regulate vascular endothelial growth factor production by tumor cells in vitro and in vivo: angiogenic implications for signal transduction therapy of solid tumors. Am J Pathol 1997;151: 1523–30.
110. Izumi Y, Xu L, di Tomaso E, Fukumura D, Jain RK. Tumour biology: herceptin acts as an anti-angiogenic cocktail. Nature 2002;416:279–80.
111. Moscow J, Schneider E, Sikic BI, Morrow CS, Cowan KH. Drug resistance and its clinical circumvention. In: Kufe DW, Bast RC, Hite WN, Hong WK, Pollock RE, Weichselbaum RR, Holland JF, Frei E III, editors. Cancer Medicine. Hamilton: BC Decker Inc. 2006:630–47.
112. Boehm T, Folkman J, Browder T, O'Reilly MS. Antiangiogenic therapy of experimental cancer does not induce acquired drug resistance. Nature 1997;390:404–7.
113. Naumov GN, Beaudry P, Bender ER, Zurakowski D, Watnick R, Almog N, et al. Clinical and Experimental Metastasis. International Congress of the Metastasis Research Society; 2004: Springer, 2004:636.
114. Harper J, Naumov GN, Exarhopoulos A, Bender E, Louis G, Folkman J, Moses MA. Predicting the switch to the angiogenic phenotype in a human tumor model. In: Proceedings of the American Association for Cancer Research 2006:837.
115. Klement G, Kikuchi L, Kieran M, Almog N, Yip TT, Folkman J. Early tumor detection using platelet uptake of angiogenesis regulators. Blood 2004;104:239a .
116. Cervi D, Yip TT, Bhattacharya N, Podust VN, Peterson J, Abou-Slaybi, et al. Platelet-associated PF-4 as a biomarker of early tumor growth. Blood 2008;111:1201–7.
117. Schuch G, Heymach JV, Nomi M, Machluf M, Force J, Atala A, et al. Endostatin inhibits the vascular endothelial growth factor-induced mobilization of endothelial progenitor cells. Cancer Res 2003;63:8345–50.
118. Italiano JE Jr, Richardson JL, Patel-Hett S, Battinelli E, Zaslavsky A, Short S, et al. Angiogenesis is regulated by a novel mechanism: pro- and antiangiogenic proteins are organized into separate platelet alpha granules and differentially released. Blood 2008;111:1227–33.
119. Harker LA, Finch CA. Thrombokinetics in man. J Clin Invest 1969;48:963–74.
120. Italiano JE, Hartwig JH. Megakaryocyte development and platelet formation. In: Michelson AD, editor. Platelets. Boston: Academic Press, 2002:21–36.
121. Kaushansky K. Lineage-specific hematopoietic growth factors. N Engl J Med 2006;354:2034–45.
122. Folkman J, Kalluri R. Cancer without disease. Nature 2004;427:787.

blood

2008 111: 1201-1207
Prepublished online Oct 3, 2007;
doi:10.1182/blood-2007-04-084798

Platelet-associated PF-4 as a biomarker of early tumor growth

David Cervi, Tai-Tung Yip, Nandita Bhattacharya, Vladimir N. Podust, Jon Peterson, Abdo Abou-Slaybi, George N. Naumov, Elise Bender, Nava Almog, Joseph E. Italiano, Jr, Judah Folkman and Giannoula L. Klement

Blood (print ISSN 0006-4971, online ISSN 1528-0020), is published semimonthly by the American Society of Hematology, 1900 M St, NW, Suite 200, Washington DC 20036.

Platelet-associated PF-4 as a biomarker of early tumor growth

David Cervi,[1] Tai-Tung Yip,[2] Nandita Bhattacharya,[1] Vladimir N. Podust,[2] Jon Peterson,[1,3] Abdo Abou-Slaybi,[1] George N. Naumov,[1] Elise Bender,[1] Nava Almog,[1] Joseph E. Italiano Jr,[4] Judah Folkman,[1] and Giannoula L. Klement[1,5]

[1]Children's Hospital Boston, Karp Family Research Laboratories, MA; [2]Ciphergen Biosystems, Fremont, CA; [3]Ortho-Clinical Diagnostics, Rochester, NY; [4]Brigham and Women's Hospital, and [5]Dana-Farber Cancer Institute, Boston, MA

Early tumor detection and intervention are important determinants of survival in patients with cancer. We have recently reported that the "platelet angiogenesis proteome" may be used to detect microscopic tumors in mice. We now present evidence that changes in platelet-associated platelet factor-4 (PF-4) detect malignant growth across a spectrum of human cancers in mice. A deregulated expression of an 8206-Da protein was observed by surface-enhanced laser desorption/ionization time-of-flight mass spectrometry (SELDI-ToF MS) proteomic comparison of platelets from normal and tumor-bearing mice. The differentially expressed protein was identified as PF-4 by tandem mass spectrometry and ProteinChip immunoassay using anti–PF-4 antibody. The platelet-associated PF-4 appeared to be up-regulated in early growth of human liposarcoma, mammary adenocarcinoma, and osteosarcoma. A 120-day follow-up study of liposarcoma revealed a sustained 2-fold or higher increase of platelet-associated PF-4 at 19, 30, and 120 days. In contrast, only an insignificant change of PF-4 was observed in the plasma of mice bearing the different human tumor xenografts, and throughout the 120 days of the liposarcoma study. We conclude that platelet-associated PF-4, but not its plasma counterpart, may represent a potential biomarker of early tumor presence. (Blood. 2008;111:1201-1207)

Introduction

The identification of biomarkers of early tumor recurrence, growth, and therapeutic response has been of great interest in oncology. Considerable effort is currently focused on methods for early tumor detection, including those involving detection of specific proteins or proteomic profiles in the serum,[1-4] DNA in stool samples,[5-8] and gene expression profiles in lesional biopsies.[9-12] The realization that angiogenesis is a critical part of tumor progression of solid[13] and liquid[14,15] tumors led, over the past few decades, to numerous attempts to correlate plasma and serum levels of angiogenic proteins with disease progression.[16,17] While helpful in the identification of patients with disseminated disease, the reliability of serum and plasma levels of VEGF, bFGF, or other angiogenesis regulatory proteins in early-stage tumors remains uncertain.[18,19]

Our previous report that platelets may serve as a reservoir of biomarkers[20] introduced the finding that the platelet protein content may reflect the presence of a tumor. Further proteomic analysis of platelets from tumor-bearing and non–tumor-bearing mice revealed that the majority of differentially expressed proteins were angiogenesis regulators, rather than the more abundant proteins such as albumin and fibrinogen. The levels of albumin and fibrinogen contained in the platelets were equal in tumor-bearing and non–tumor-bearing mice. This finding suggests a very selective sequestration of angiogenesis regulating proteins by platelets. We also showed that the enhanced sequestration of angiogenesis regulators in the platelet may enable us to detect tumors as small as 1 mm^3 in mice.

Platelets may sequester these proteins and protect them from plasma proteolytic enzymes. As a result of this sequestration, platelet-associated proteins, and PF-4 in particular, may be more reliable in detecting early cancer growth than their respective plasma or serum counterparts.

Platelet factor-4 (PF-4) is a tetrameric, lysine-rich member of the CXC chemokine family produced almost exclusively by megakaryocytes. Under physiological conditions, only a small amount of platelet factor-4 is taken up by circulating platelets, therefore the bulk of the PF-4 protein originates in megakaryocytes. PF-4 was originally cloned from a human erythroleukemia cell line,[21] and its genetic mapping and polymorphisms were discovered soon thereafter.[22,23] PF-4 is stored within the α-granules of platelets and secreted at high concentrations in the vicinity of injured blood vessels following platelet activation.[24] Platelet factor-4 was discovered to inhibit angiogenesis in 1982.[25] By 1990, it was shown to inhibit tumors in mice.[26] In 1995, platelet factor-4 was reported to bind preferentially to vascular endothelium in vivo[27] and to bind selectively to regions of active angiogenesis in vivo.[28] By 1998, PF-4 was revealed to be a marker of new vessel formation in xenografts of human breast cancer.[29]

In the absence of any known receptor for PF-4, its antiangiogenic effect[30,31] is presumed to be due to its ability to bind stimulatory chemokines such as IL-8[32,33] and to compete with other growth factors for heparin binding.[34,35] The heterodimer of IL-8 and PF-4 enhances the antiproliferative activity of PF-4 and attenuates the stimulatory effects of IL-8.[32] PF-4 also modulates the effect of proangiogenic growth factors. It binds with high affinity to vascular endothelial growth factor ($VEGF_{165}$), preventing the

Submitted April 11, 2007; accepted September 6, 2007. Prepublished online as *Blood* First Edition paper, October 3, 2007; DOI 10.1182/blood-2007-04-084798.

D.C. and T.-T.Y. contributed equally to this work.

An Inside *Blood* analysis of this article appears at the front of this issue.

The online version of this article contains a data supplement.

The publication costs of this article were defrayed in part by page charge payment. Therefore, and solely to indicate this fact, this article is hereby marked "advertisement" in accordance with 18 USC section 1734.

interaction of $VEGF_{165}$ with its receptor (VEGFR-2) thus inhibiting angiogenesis.[34,36] A PF-4 derivative generated by peptide bond cleavage between Thr16 and Ser17 exhibits a 30- to 50-fold greater growth inhibitory activity on endothelial cells than PF-4 itself.[37] The antitumor effect of PF-4 is also revealed by a decrease in the number and size of lung metastases of B16F10 melanoma[38] and a decrease in growth of HCT-116 human colon carcinoma.[39] PF-4 modifies the mitogenic effect of bFGF on fibroblasts,[40] inhibits the proliferation of activated human T cells[41] and tumor-infiltrating lymphocytes, and inhibits cytokine release by tumor stroma.[42]

Here we present new data demonstrating that changes in the platelet concentration of PF-4 may be used as a novel biomarker to detect human tumor xenografts that range from microscopic to macroscopic size. These tumors in mice include human liposarcoma, mammary adenocarcinoma, and osteosarcoma.

Methods

Human-tumor xenografts

All of the cancer cell lines used exhibit either nonangiogenic (microscopic, dormant tumors) or angiogenic (rapidly growing tumors) phenotypes in immunodeficient mice. The nonangiogenic and angiogenic cell lines have been previously described by Folkman and colleagues (Almog et al[43]; Achilles et al[44]; and Naumov et al[45]). For each of the 3 parent cell lines (liposarcoma [SW872], osteosarcoma [KHOS-24OS], and mammary adenocarcinoma [MDA-MB-436]) 2 phenotypes exist, a nonangiogenic tumor and an angiogenic one.

All cell lines were cultured in DMEM containing 10% heat-inactivated fetal bovine serum (HyClone, Logan, UT), 1% antibiotics (penicillin, streptomycin), and 0.29 mg/mL L-glutamine in a humidified 5% CO_2 incubator at 37°C. For injections into mice, 80% to 90% confluent tumor cells were rinsed in phosphate-buffered saline (PBS; Sigma-Aldrich, St Louis, MO), briefly trypsinized and suspended in serum-free DMEM. Five million viable cells from each of the tumor cell lines were suspended in 200 μL serum-free media and implanted subcutaneously (SW872 and KHOS-24OS cell lines) into the flanks of 6- to 8-week-old male severe combined immunodeficient (SCID) mice. For the human breast adenocarcinoma (MDA-MB-436) cell line, 1 million viable cells were suspended in 50 μL serum-free media and implanted in the mammary fat pad through a 0.75- to 1-cm incision. The corresponding sham operation was a 0.75- to 1.0-cm incision. The mice were terminally bled under isoflurane anesthesia at 30 days after implantation to collect the platelets. The mice were obtained from the Massachusetts General Hospital (MGH; Boston, MA). Animals and tumors were monitored daily as per institutional guidelines. Data were analyzed using Student *t* test to determine the *P* values for differences between means; the graphs in Figures 4 and 5 are therefore expressed as means plus or minus SEM.

Platelet and plasma processing for SELDI-ToF mass spectrometry

Blood samples were processed according to standard methods for platelet collection. Briefly, mice were anaesthetized using 2% isofluorane/1 L O_2 flow system. Whole blood (1 mL) was collected by terminal cardiac bleed into 105 mM sodium citrate (pH 5) anticoagulant at a ratio of 1:9 (vol/vol) buffer to blood. The first centrifugation step at 180*g* for 20 minutes at room temperature allowed for the collection of platelet-rich plasma (PRP). A second centrifugation at 900*g* for 30 minutes at room temperature separated the platelets and the upper phase, platelet-poor plasma (PPP). This resulted in 2 separate phases for processing and analysis by surface-enhanced laser desorption/ionization time-of-flight mass spectrometry (SELDI-ToF MS) technology (Ciphergen Biosystems, Fremont, CA), platelet pellets, and PPP. The pellets and 20 μL PPP from each mouse were processed in 25 μL and 40 μL, respectively, U9 buffer (2% CHAPS [3-[(3-cholamidopropyl) dimethylammonio]-1-propansulfonate], 50 mM Tris-HCl, pH 9; Ciphergen Biosystems) for 1 hour at room temperature. Platelet lysates were then centrifuged at 10 000*g* for 1 minute at 4°C. Both platelet extracts and PPP were fractionated by anion-exchange chromatography modified after the expression difference mapping (EDM) serum fractionation protocol (Ciphergen Biosystems). The fractionation was performed in a 96-well format filter plate on a Biomek 2000 Laboratory Work Station (Beckman Coulter, Fullerton, CA) equipped with a Micromix 5 shaker (Siemens Medical Solutions Diagnostics, Deerfield, IL). An aliquot of 20 μL platelet and 60 μL denatured plasma diluted with 100 μL 50 mM Tris-HCl (pH 9) was transferred to a filter-bottom 96-well microplate prefilled with Q Ceramic HyperD F sorbent beads (Pall, East Hills, NY) rehydrated and pre-equilibrated with 50 mM Tris-HCl (pH 9). All liquids were removed from the filtration plate using a multiscreen vacuum manifold (Millipore, Bedford, MA) into respective wells of 96-well microtiter plates with the capture of the initial flow-through as fraction 1. This step was repeated for subsequent incubations with 2 × 100 μL of the following buffers: pH 7.5 (1 M urea, 0.1% CHAPS, 50 mM NaCl, 2.5% acetonitrile, 50 mM Tris-HCl [50 mM HEPES]); pH 5 (1 M urea, 0.1% CHAPS, 50 mM NaCl, 2.5% acetonitrile 50 mM NaAcetate); pH 4 (1 M urea, 0.1% CHAPS, 50 mM NaCl, 2.5% acetonitrile 50 mM NaAcetate); pH 3 (1 M urea, 0.1% CHAPS, 500 mM NaCl, 2.5% acetonitrile 50 mM NaCitrate), which yielded the respective fractions 2, 3, 4, and 5. A final organic wash with 33% isopropanol/16.7% acetonitrile/8% formic acid represents fraction 6.

Expression difference mapping (EDM) on ProteinChip arrays was carried out using weak cationic exchange chromatography protein arrays (WCX2 and CM10 ProteinChip arrays; Ciphergen Biosystems) by loading sample fractions onto a 96-well bioprocessor, and equilibrating with 50 mM sodium acetate 0.1% octyl glucoside (Sigma), pH 5. A further dilution of 40 μL anion exchange chromatography fraction into 100 μL of the same buffer on each array spot was incubated for 1 hour. Array spots were washed for 3 minutes with 100 μL 50 mM sodium acetate 0.1% octyl glucoside (pH 5). After rinsing with water, 1 μL sinapinic acid matrix solution was added twice to each array spot. For protein profiling, all fractions were diluted 1:2.5 in their respective buffers used to pre-equilibrate ProteinChip arrays. This step was followed by readings using the Protein Biology System II (PBSII) and Protein Ciphergen System 4000 (PCS4000) SELDI-ToF mass spectrometer (Ciphergen Biosystems) and processed with the ProteinChip Software Biomarker Edition, Version 3.2.0 (Ciphergen Biosystems). After baseline subtraction, spectra were normalized by a total ion current method. Peak detection was performed using Biomarker Wizard software (Ciphergen Biosystems) using a signal-to-noise ratio of 3.

For immunocapture experiments, anti–PF-4 antibody (rabbit, affinity-purified polyclonal antibody; R&D, Minneapolis, MN) was immobilized on preactivated ProteinChip array (RS100; Ciphergen Biosystems). After blocking and washing of excess antibody, platelet extract diluted in BSA Triton X100 PBS was incubated with the immobilized antibody. After washing with PBS containing urea and CHAPS, the captured proteins were detected by SELDI. To confirm a full capture of the protein, the mobile phase was also incubated on a preactivated spot for a second time to verify immunodepletion. A final confirmation of the protein identity was obtained using murine PF-4 enzyme-linked immunosorbent assay (ELISA; data included as Figure S2).

Protein identification

Candidate protein biomarker was purified by affinity chromatography on beads with immobilized IgG spin columns and by reverse-phase chromatography. The purity of each step was monitored using normal phase (NP) ProteinChip arrays. The enriched fractions were reduced by 5 mM DTT in Tris-HCL buffer (pH 9) and alkylated with 25 mM iodoacetamide. The alkylated preparation was finally purified using 16% tricine sodium dodecyl sulfate–polyacrylamide gel electrophoresis (SDS-PAGE). The gel was stained by Colloidal Blue Staining Kit (Invitrogen, Carlsbad, CA). Selected protein bands were excised, washed with 200 μL 50% methanol/10% acetic acid for 30 minutes, dehydrated with 100 μL acetonitrile (ACN) for 15 minutes, and extracted with 70 μL 50% formic acid, 25% ACN, 15% isopropanol, and 10% water for 2 hours at room temperature with vigorous shaking. The candidate biomarkers in extracts were again verified by

Table 1. Amino acid sequences of identified peptides

m/z	Amino acid sequence	Mowse score*	Significan homology score†	Identity or extensive homology score‡
Peptide I: 1350.75	HCAVPQLIATLK + CAM§	60	>17	>22
Peptide II: 1677.90	HCAVPQLIATLKNGR + CAM	14	>13	>15

*Ion score is −10*Log(P), where P is probability that the match is a random event.
†Individual ion scores higher than a number displayed in the column indicate significant homology.
‡Individual ion scores higher than a number displayed in the column indicate identity or extensive homology ($P < .05$).
§Carbamidomethyl cysteine.

analysis of 2 μL on a normal phase ProteinChip array (NP20). The remaining extract was digested with 20 μL of 10 ng/μL modified trypsin (Roche Applied Science, Indianapolis, IN) in 50 mM ammonium bicarbonate (pH 8) for 3 hours at 37°C. Single MS and MS/MS spectra were acquired on a QSTAR mass spectrometer (Applied Biosystems, Foster City, CA) equipped with a Ciphergen PCI-1000 ProteinChip Interface. A 1-μL aliquot of each protease digest was analyzed on an NP20 ProteinChip array in the presence of CHCA matrix (Ciphergen Biosystems). Spectra were collected from m/z values of 900 to 3000 in single MS mode. After reviewing the spectra, specific ions were selected and subjected to collision-induced dissociation (CID). The CID data were submitted to the database-mining tool Mascot (Matrix Science, Boston, MA) for identification (Table 1; Figure S1, available on the *Blood* website; see the Supplemental Materials link at the top of the online article).

Results

Identification of the differentially expressed PF-4 in tumor-bearing mice

Platelet lysates from healthy non–tumor-bearing mice and those bearing nonangiogenic or angiogenic xenografts of human liposarcoma, mammary adenocarcinoma, and osteosarcoma for a minimum of 30 days were subjected to a standard biomarker discovery protocol. Among the several unknown differentially expressed proteins, elevation was observed in the platelet content of a polypeptide with an apparent molecular weight of 8206 Da (Figures 1,2). This protein was later found to be consistently elevated across 3 repeated experiments, and across several tumor types.

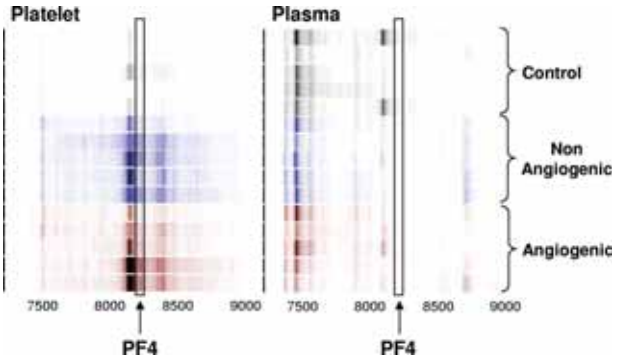

Figure 1. Identification of the platelet- and plasma-derived candidate proteins. Platelets were harvested from mice bearing nonangiogenic or angiogenic xenografts of human liposarcoma at 30 days after tumor implantation and compared with those of their littermate controls using a standard SELDI-ToF biomarker discovery method. A spectral readout from SELDI-ToF MS is presented here in gel view format, and groups are color-coded for clarity. Gray represents protein content of platelets from control animals; blue, from mice bearing the nonangiogenic dormant clone; and red, from mice bearing the angiogenic clone. A differentially expressed protein was observed at 8206 Da. The candidate peptide (↑) was later analyzed and identified as PF-4. Each horizontal strip represents an individual mouse sample (n = 5), and the color intensity corresponds to the height of the protein peak. The experiment was reproduced on 2 independent occasions for a total of 15 mice per group.

A careful analysis was therefore performed to identify the protein of interest. The 8206-Da protein was purified using chromatography and SDS-PAGE. Gel-purified protein was digested with trypsin, and unique tryptic fragments were analyzed by tandem MS (data in Figure S1). The ion with m/z of 1350.75 was identified as Cys-carbamidomethylated peptide HCAVPQLIATLK with Mowse score[46] of 60 (ion score > 17 indicated significant homology; > 22 indicated identity or extensive homology). The ion with m/z of 1677.90 was identified as Cys-carbamidomethylated peptide HCAVPQLIATLKNGR with Mowse score of 14 (ion score > 13 indicated significant homology; > 15 indicated identity or extensive homology). Both peptides corresponded to unique tryptic fragments of mouse PF-4 (SwissProt accession no. Q9Z126) previously identified.[47-49] Theoretic molecular weight of mouse PF-4 is 8210.71 Da, however considering 2 Cys-Cys bridges in the polypeptide molecule, the expected MW is 8206.71 Da. The latter value is very close to the observed experimental molecular weight of the candidate biomarker.

Confirmation of identity of platelet-derived PF-4 by ProteinChip immunoassay using anti–PF-4 antibody

Further validation of this candidate biomarker was obtained by immunoprecipitation using rabbit anti–PF-4 antibody. Figure 2 represents the spectral readout obtained from arrays coated with an immobilized anti–PF-4 antibody prior to incubation with the platelet extracts from mice. The presence of a thick protein peak at 8206 Da (arrow) validates both the presence and theoretic mass of PF-4 (Figure 2). The identity of the differentially expressed protein was further confirmed by immunocapture/immunodepletion of the protein. The protein captured using the PF4-specific antibody has a peak identical to that of the recombinant protein (upper 2 panels of Figure 3), and the peak is absent in the mobile phase of the spotted lysate (Figure 3).

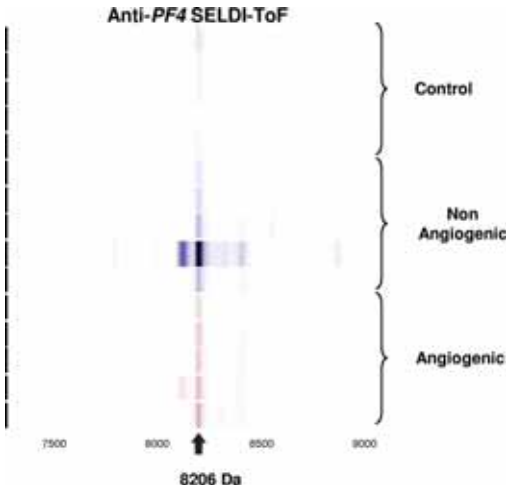

Figure 2. Validation of candidate biomarker by immunoprecipitation. Spectral readout in gel view format obtained from arrays prepared with an anti–PF-4 antibody prior to incubation with platelet extracts from mice within the indicated groups. The labeled arrow indicates both the presence and theoretic mass of PF-4.

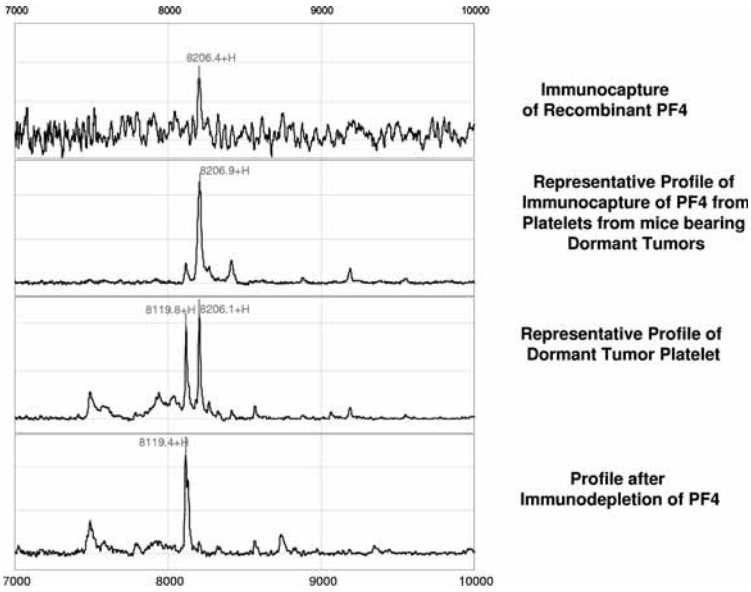

Figure 3. Confirmation of the PF-4 identity by immunocapture and immunodepletion. For immunocapture experiments, anti–PF-4 antibody was immobilized on a preactivated ProteinChip array, followed by incubation with platelet extracts derived from mice bearing the dormant clone of liposarcoma. Comparison of a profile generated by the recombinant PF-4 (first panel) with that generated by platelet lysates of dormant liposarcoma-bearing mice reveals an identical molecular weight and isoelectric point of the protein in question (second panel). Immunodepletion of the PF-4 protein is confirmed by the absence of its respective peak from the mobile phase (fourth panel).

Validation of PF-4 as a surrogate marker of tumor presence

Platelets of nonangiogenic or angiogenic human liposarcoma xenografts, SW872, exhibited a 7-fold elevation of platelet-derived PF-4 compared with non–tumor-bearing controls at 30 days after implantation (Figure 4A) without a corresponding increase of PF-4 in the plasma. In this model, platelets of mice bearing the nonangiogenic xenografts (tumors less than 1 mm) contained PF-4 levels comparable with its angiogenic counterpart. Platelets of mice bearing the angiogenic mammary adenocarcinoma, MDA-MB-436 (Figure 4B), or the angiogenic osteosarcoma, KHOS-24OS (Figure 4C), revealed similar trends at 4- and 2-fold up-regulation, respectively. The nonangiogenic xenografts did not show an elevation of PF-4 in platelets. The platelet-associated PF-4 content was consistently found to be higher than that of the corresponding plasma, even though the degree of elevation varied based on tumor type (Figure 4A-C). Angiogenic tumors were associated with the greatest differences between platelet-derived PF-4 versus that of plasma, even though platelets of mice bearing the nonangiogenic tumors of liposarcoma also showed PF-4 elevation. Liposarcoma xenografts exhibited the greatest platelet content of PF-4, while the increases in PF-4 for mammary adenocarcinoma and osteosarcoma were not as large (Figure 4A-C).

Platelet PF-4 in early tumor detection

To test whether platelet content of angiogenesis regulators can be used in detection of early tumor growth, we explored the ability of PF-4 to predictably detect nonangiogenic (dormant) microscopic tumors in mice over an extended period of time. We conducted a time-course analysis of platelet-associated PF-4 in mice bearing a subcutaneous xenograft of the nonangiogenic (dormant) clone of human liposarcoma (SW872). The malignant progression of liposarcoma has been previously described,[43] and it is known that the nonangiogenic (dormant) clone undergoes a spontaneous switch to the angiogenic phenotype, begins to grow, and becomes detectable by gross examination at a median of approximately 133 days after implantation. We show that PF-4 remains significantly elevated throughout a period of 120 days of observation of the nonangiogenic (dormant) state. Even without a palpable tumor, at 19 days, the median level of PF-4 in platelets is 1.7-fold higher than baseline, without a corresponding increase in plasma level of the protein (Figure 5A,B). The plasma and platelet levels of PF-4 were similar at the time of implantation. However, while platelet PF-4 rose in the first 2 weeks of tumor growth, and remained elevated for the duration of the 120 days of the experiment, plasma PF-4 continued to decline (Figure 5B). The size of the tumor did not exceed 1 mm for the duration of the experiment.

Discussion

Numerous angiogenesis regulatory proteins are present in platelets.[50] While the relative concentrations of these proteins remain stable under physiologic conditions, their levels change significantly in the presence of a tumor. There are other reports documenting angiogenesis regulatory factors in platelets of cancer patients,[51-53] and continuing controversy persists as to whether serum or plasma levels of angiogenesis factors are more accurate for the measurement of angiogenesis-related diseases.[54] In a study of paired serum and plasma samples,[55,56] VEGF levels correlated with platelet count in 116 patients with colorectal cancer, but not in controls. Support can be found for both serum or plasma measurements.[55,57,58]

The diagnostic use of angiogenic proteins such as VEGF, bFGF, or PF-4 in early disease has been hindered in part by the minute levels of the proteins and their short half-lives in the circulation. The finding of platelet sequestration of angiogenesis regulatory proteins suggests a new modality for early detection of human cancer. We propose that angiogenesis regulators are not released from platelets into the circulation. Instead, these proteins are exchanged locally at sites of platelet adhesion and aggregation, where they remain bound to glycosaminoglycans such as heparan sulfate in tissues. As such, the levels of these proteins in plasma or serum increase significantly only in the presence of a large tumor load that generates sufficient angiogenesis regulatory proteins to saturate the mass of circulating platelets. We provide evidence that at least one of these platelet proteins, PF-4, can reliably predict the presence of a microscopic, nonangiogenic (dormant) human tumor in mice and circulates predominantly in platelets early in the disease process. Its relative absence in plasma may explain why the proteomic search for plasma and serum markers of patients with

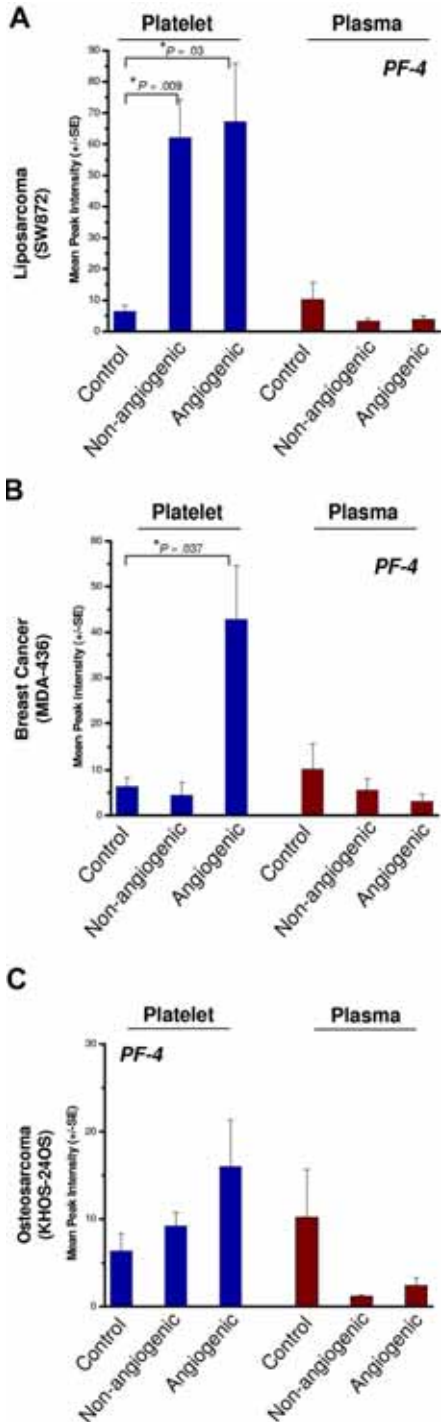

Figure 4. PF-4 in platelets of mice bearing human-tumor xenografts. Platelets of mice bearing xenografts of SW872 liposarcoma (A), MDA-MB-436 mammary adenocarcinoma (B), or KHOS-24 osteosarcoma (C) were analyzed using SELDI-ToF. The blue bars represent whole platelet extracts and brown bars represent plasma. The platelets of non–tumor-bearing control mice served as a reference for the endogenous levels of platelet- and plasma-derived PF-4. The control group is shared by all 3 experiments. Platelets of nonangiogenic or angiogenic human liposarcoma xenografts, SW872, exhibited a 7-fold elevation of platelet-derived PF-4 compared with non–tumor-bearing controls at 30 days after implantation (A) without a corresponding increase of PF-4 in the plasma. Platelets of mice bearing the angiogenic mammary adenocarcinoma, MDA-MB-436 (B), also had significant elevation of platelet but not plasma PF-4. In the case of angiogenic osteosarcoma, KHOS-24OS (C), a similar trend at 4- and 2-fold up-regulation can be observed, but the value did not reach significance. Each bar represents the mean peak intensities corresponding to the level of the protein (± SEM) of 5 to 10 mice per experiment. Student *t* test was used to compare means of the groups. Each experiment was repeated twice.

various cancers[59-61] did not identify this marker. We emphasize that while only PF-4 is being presented here, other angiogenesis regulatory proteins sequestered in platelets may have the same diagnostic capacity and remain to be identified.

We introduce PF-4 as one of the platelet-associated angiogenesis regulators that may serve as an early tumor biomarker. We show that platelet-associated PF-4 can be detected as early as 19 days after implantation, and that a steady elevation of the protein can be observed throughout 120 days (Figure 5). While this paper does not provide sufficient data to support a functional role of PF-4 in tumor angiogenesis, there is sufficient published evidence that PF-4 is an angiogenesis suppressor and a tumor growth suppressor.[25,26,38,39,62-64] PF-4 may modulate tumor growth by modifying VEGF effects[35] or by binding and neutralizing heparin[65] and related sulfated glycosaminoglycans[42] required for the binding of proangiogenic factors.[30,40,66] The binding and neutralization of heparin down-regulates angiogenesis mainly by preventing the binding of other angiogenesis regulators to heparan sulfate in tissues and by interfering with VEGF and bFGF signaling pathways.[67] The high levels of VEGF and bFGF secreted by the nonangiogenic clone of SW872 liposarcoma[43] may be counterbalanced by PF-4 leading to tumor quiescence and dormancy. The increase in platelet-associated PF-4 in dormant (nonangiogenic) tumors may therefore be reflective of the functional inhibition of angiogenesis in liposarcoma, which secretes large amounts of VEGF and bFGF.[43] A feedback loop may exist in animals bearing tumors, such that increased VEGF and bFGF induce megakaryocyte synthesis of PF-4. This is supported by the finding that tumors that do not secrete large amounts of VEGF and bFGF, such as the nonangiogenic clones of MDA-MB-436 mammary adenocarcinoma and the KHOS-24OS osteosarcoma,[45] do not manifest a marked elevation of PF4 (Figure 4). These tumors may use other means of tumor growth suppression. PF-4 appears to be a marker of angiogenesis and was present in the platelets of all of the tested angiogenic tumor models.

The changes in platelet-associated PF4 may have the potential to convey valuable clinical information about the angiogenic potential of the tumor, and a serial measurement of platelet PF-4 levels may provide us with the ability to detect tumor progression in an otherwise healthy subject.

Numerous reports have suggested an active role of platelets in cancer progression[68,69] and in tumor growth and metastasis.[70-72] Most investigators assume that platelets act as a reservoir of angiogenic proteins that are released into the sera.[53,73] However, we show here that platelets actively sequester select proteins in tumor-bearing animals, and that this process is distinct from the nonspecific uptake of proteins such as albumin. One of the main reasons previous proteomic analysis on platelets[74-78] may not have detected the differential expression of angiogenesis-related proteins was because these studies analyzed normal platelets and not platelets of cancer patients. We report for the first time, to our knowledge, the changes in the "platelet angiogenesis proteome" in response to the presence of a tumor in experimental animals.

Platelet-associated PF-4 may be a potential tumor biomarker. Platelet-associated PF-4 should be explored in other mouse models of cancer and in high-risk patient populations predisposed to early tumor progression due to mutations in *APCC*, *p53*, *PTEN*, or *BRCA1*. If validated, it may improve our ability to intervene very early in recurrent cancer, keep cancers in a dormant stage, and possibly convert cancer into a chronic, more manageable disease.[79,80] As biologic modifiers, including angiogenesis inhibitors, which are relatively less toxic, become available for cancer therapy, early treatment may be much more possible than it has been in the past. A long-term goal would be to "treat the biomarker" until it

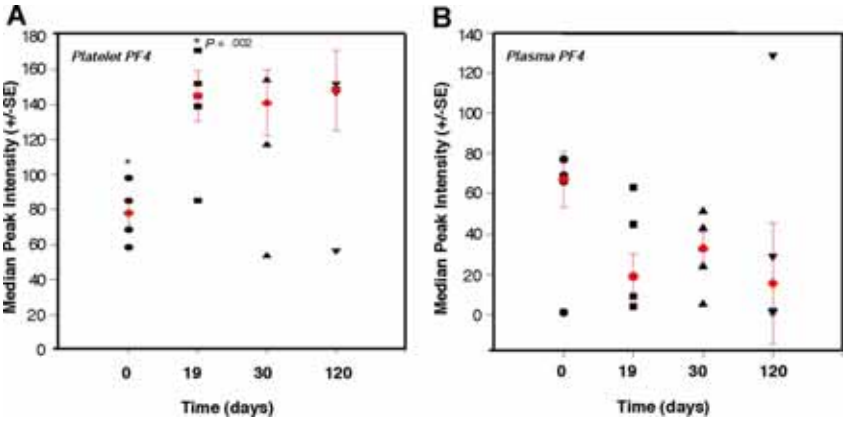

Figure 5. Elevation of platelet-derived PF-4 correlates with the presence of microscopic tumors. Platelets and plasma from mice bearing a nonangiogenic subclone of the human liposarcoma (SW872) were analyzed at the indicated times using SELDI-ToF. The relative levels of PF-4 protein in platelets of non–tumor-bearing mice at time 0 (●; ie, before the implantation of the tumors) were compared with platelet-associated PF-4 on day 19 (■), day 30 (▲), and day 120 (▼). At 19 days, without a palpable tumor, the median level of PF-4 in platelets is 1.7-fold higher than baseline without a corresponding increase in plasma level of the protein. The red symbols within the cluster analysis represent the median peak intensity of 5 to 6 mice plus or minus SEM.

returns to normal, before the onset of symptoms of recurrent tumor and before the tumor can be anatomically located.

Acknowledgments

The authors acknowledge the generosity of Ciphergen Biosystems, for conducting the mass spectrometry assays identification of proteins free of charge, and for sharing much of the available scientific expertise. The authors are grateful for the helpful comments and suggestions provided by Dr Sean Downing.

This work was supported by grants from the Breast Cancer Research Foundation (J.F.), the Department of Defense (DOD grant no. W81XWH-04-1-0316; J.F.), and NASA (grant no. NNH04ZUU002N).

Authorship

Contribution: D.C. wrote the initial draft of the paper and (along with T-T.Y.) executed, analyzed, and evaluated the mass spectrometry data; T-T.Y. performed, analyzed, and evaluated the mass spectrometry data and provided invaluable expertise with the SELDI ToF MS technology; N.B. executed in vitro data and assisted with animal experiments; V.N.P. performed the purification and identification of candidate biomarkers; J.P. and A.A.-S. have been instrumental in the development of a murine PF4 ELISA and quantified the PF-4 protein; G.N.N. provided the breast and osteosarcoma models; E.B. assisted with the animal experiments; N.A. designed and executed the liposarcoma experiment and advised on the dormancy models; J.E.I. contributed to the evaluation of the data and the paper revisions; J.F. provided mentorship for the team and expertise in preparation of the paper; G.L.K. designed and performed the research, provided guidance for the group, analyzed the data, and revised the original paper.

Conflict-of-interest disclosure: The authors declare no competing financial interests.

Correspondence: Giannoula Klement, Children's Hospital Boston, Karp Family Research Laboratories, Rm 11.211, One Blackfan Circle, Boston, MA 02115; e-mail: giannoula.klement@childrens.harvard.edu.

References

1. Krueger KE. The potential of serum proteomics for detection of cancer: promise or only hope? Onkologie. 2006;29:498-499.
2. Huang LJ, Chen SX, Huang Y, et al. Proteomics-based identification of secreted protein dihydrodiol dehydrogenase as a novel serum markers of non-small cell lung cancer. Lung Cancer. 2006;54:87-94.
3. Barker PE, Wagner PD, Stein SE, et al. Standards for plasma and serum proteomics in early cancer detection: a needs assessment report from the national institute of standards and technology: National Cancer Institute Standards, Methods, Assays, Reagents and Technologies Workshop, August 18-19, 2005. Clin Chem. 2006;52:1669-1674.
4. Kawada N. Cancer serum proteomics in gastroenterology. Gastroenterology. 2006;130:1917-1919.
5. Wu GH, Wang YM, Yen AM, et al. Cost-effectiveness analysis of colorectal cancer screening with stool DNA testing in intermediate-incidence countries. BMC Cancer (http://www.biomedcentral-.com). 2006;6:136. Accessed June 1, 2006.
6. Lim SB, Jeong SY, Kim IJ, et al. Analysis of microsatellite instability in stool DNA of patients with colorectal cancer using denaturing high performance liquid chromatography. World J Gastroenterol. 2006;12:6689-6692.
7. Half EE, Lynch PM. Mutated DNA in the stool: does it have a role in colorectal cancer screening? Nat Clin Pract Gastroenterol Hepatol. 2006;3:594-595.
8. Zou H, Harrington JJ, Klatt KK, Ahlquist DA. A sensitive method to quantify human long DNA in stool: relevance to colorectal cancer screening. Cancer Epidemiol Biomarkers Prev. 2006;15:1115-1119.
9. Watanabe T, Kobunai T, Toda E, et al. Distal colorectal cancers with microsatellite instability (MSI) display distinct gene expression profiles that are different from proximal MSI cancers. Cancer Res. 2006;66:9804-9808.
10. Kreike B, Halfwerk H, Kristel P, et al. Gene expression profiles of primary breast carcinomas from patients at high risk for local recurrence after breast-conserving therapy. Clin Cancer Res. 2006;12:5705-5712.
11. Chang Y, Liu B. Difference of gene expression profiles between Barrett's esophagus and cardia intestinal metaplasia by gene chip. J Huazhong Univ Sci Technolog Med Sci. 2006;26:311-313.
12. Asgharzadeh S, Pique-Regi R, Sposto R, et al. Prognostic significance of gene expression profiles of metastatic neuroblastomas lacking MYCN gene amplification. J Natl Cancer Inst. 2006;98:1193-1203.
13. Folkman J. Tumor angiogenesis: therapeutic implications. N Engl J Med. 1971;285:1182-1186.
14. Perez-Atayde AR, Sallan SE, Tedrow U, et al. Spectrum of tumor angiogenesis in the bone marrow of children with acute lymphoblastic leukemia. Am J Pathol. 1997;150:815-821.
15. Ribatti D, Vacca A, Nico B, et al. Bone marrow angiogenesis and mast cell density increase simultaneously with progression of human multiple myeloma. Br J Cancer. 1999;79:451-455.
16. Fuhrmann-Benzakein E, Ma MN, Rubbia-Brandt L, et al. Elevated levels of angiogenic cytokines in the plasma of cancer patients. Int J Cancer. 2000; 85:40-45.
17. Nguyen M. Angiogenic factors as tumor markers. Invest New Drugs. 1997;15:29-37.
18. Dosquet C, Coudert MC, Lepage E, Cabane J, Richard F. Are angiogenic factors, cytokines, and soluble adhesion molecules prognostic factors in patients with renal cell carcinoma? Clin Cancer Res. 1997;3:2451-2458.
19. Abendstein B, Daxenbichler G, Windbichler G, et al. Predictive value of uPA, PAI-1, HER-2 and VEGF in the serum of ovarian cancer patients. Anticancer Res. 2000;20:569-572.
20. Klement G, Yip T-T, Kikuchi L, et al. Early tumor detection using platelet uptake of angiogenesis regulators [abstract]. Blood. 2004;104:239a.
21. Poncz M, Surrey S, LaRocco P, et al. Cloning and characterization of platelet factor 4 cDNA derived from a human erythroleukemic cell line 3. Blood. 1987;69:219-223.
22. Guzzo C, Weiner M, Rappaport E, et al. An Eco R1 polymorphism of a human platelet factor 4 (PF4) gene 1 [abstract]. Nucleic Acids Res. 1987;15:380.
23. Griffin CA, Emanuel BS, LaRocco P, Schwartz E,

Poncz M. Human platelet factor 4 gene is mapped to 4q12-q21.2. Cytogenet Cell Genet. 1987;45:67-69.

24. Stuckey JA, St CR, Edwards BF. A model of the platelet factor 4 complex with heparin. Proteins. 1992;14:277-287.
25. Taylor S, Folkman J. Protamine is an inhibitor of angiogenesis. Nature. 1982;297:307-312.
26. Maione TE, Gray GS, Petro J, et al. Inhibition of angiogenesis by recombinant human platelet factor-4 and related peptides. Science. 1990;247:77-79.
27. Hansell P, Olofsson M, Maione TE, Arfors KE, Borgstrom P. Differences in binding of platelet factor 4 to vascular endothelium in vivo and endothelial cells in vitro. Acta Physiol Scand. 1995;154:449-459.
28. Hansell P, Maione TE, Borgstrom P. Selective binding of platelet factor 4 to regions of active angiogenesis in vivo. Am J Physiol. 1995;269:H829-H836.
29. Borgstrom P, Discipio R, Maione TE. Recombinant platelet factor 4, an angiogenic marker for human breast carcinoma. Anticancer Res. 1998; 18:4035-4041.
30. Bikfalvi A. Recent developments in the inhibition of angiogenesis: examples from studies on platelet factor-4 and the VEGF/VEGFR system. Biochem Pharmacol. 2004;68:1017-1021.
31. Bikfalvi A, Gimenez-Gallego G. The control of angiogenesis and tumor invasion by platelet factor-4 and platelet factor-4-derived molecules. Semin Thromb Hemost. 2004;30:137-144.
32. Dudek AZ, Nesmelova I, Mayo K, et al. Platelet factor 4 promotes adhesion of hematopoietic progenitor cells and binds IL-8: novel mechanisms for modulation of hematopoiesis. Blood. 2003; 101:4687-4694.
33. Nesmelova IV, Sham Y, Dudek AZ, et al. Platelet factor 4 and interleukin-8 CXC chemokine heterodimer formation modulates function at the quaternary structural level. J Biol Chem. 2005;280:4948-4958.
34. Rybak ME, Gimbrone MA Jr, Davies PF, Handin RI. Interaction of platelet factor four with cultured vascular endothelial cells. Blood. 1989;73:1534-1539.
35. Gengrinovitch S, Greenberg SM, Cohen T, et al. Platelet factor-4 inhibits the mitogenic activity of VEGF121 and VEGF165 using several concurrent mechanisms. J Biol Chem. 1995;270:15059-15065.
36. Gengrinovitch S, Berman B, David G, et al. Glypican-1 is a VEGF165 binding proteoglycan that acts as an extracellular chaperone for VEGF165. J Biol Chem. 1999;274:10816-10822.
37. Gupta SK, Hassel T, Singh JP. A potent inhibitor of endothelial cell proliferation is generated by proteolytic cleavage of the chemokine platelet factor 4. Proc Natl Acad Sci U S A. 1995;92:7799-7803.
38. Sharpe RJ, Byers HR, Scott CF, Bauer SI, Maione TE. Growth inhibition of murine melanoma and human colon carcinoma by recombinant human platelet factor 4. J Natl Cancer Inst. 1990;82:848-853.
39. Maione TE, Gray GS, Hunt AJ, Sharpe RJ. Inhibition of tumor growth in mice by an analogue of platelet factor 4 that lacks affinity for heparin and retains potent angiostatic activity. Cancer Res. 1991;51:2077-2083.
40. Watson JB, Getzler SB, Mosher DF. Platelet factor 4 modulates the mitogenic activity of basic fibroblast growth factor. J Clin Invest. 1994;94:261-268.
41. Fleischer J, Grage-Griebenow E, Kasper B, et al. Platelet factor 4 inhibits proliferation and cytokine release of activated human T cells. J Immunol. 2002;169:770-777.
42. Vlodavsky I, Eldor A, Haimovitz-Friedman A, et al. Expression of heparanase by platelets and circulating cells of the immune system: possible involvement in diapedesis and extravasation. Invasion Metastasis. 1992;12:112-127.
43. Almog N, Henke V, Flores L, et al. Prolonged dormancy of human liposarcoma is associated with impaired tumor angiogenesis. FASEB J. 2006;20: 947-949.
44. Achilles EG, Fernandez A, Allred EN, et al. Heterogeneity of angiogenic activity in a human liposarcoma: a proposed mechanism for "no take" of human tumors in mice. J Natl Cancer Inst. 2001; 93:1075-1081.
45. Naumov GN, Bender E, Zurakowski D, et al. A model of human tumor dormancy: an angiogenic switch from the nonangiogenic phenotype. J Natl Cancer Inst. 2006;98:316-325.
46. Pappin DJ, Hojrup P, Bleasby AJ. Rapid identification of proteins by peptide-mass fingerprinting. Curr Biol. 1993;3:327-332.
47. Poncz M, Surrey S, LaRocco P, et al. Cloning and characterization of platelet factor 4 cDNA derived from a human erythroleukemic cell line 3. Blood. 1987;69:219-223.
48. Zhang C, Thornton MA, Kowalska MA, et al. Localization of distal regulatory domains in the megakaryocyte-specific platelet basic protein/platelet factor 4 gene locus. Blood. 2001;98:610-617.
49. Watanabe O, Natori K, Tamari M, et al. Significantly elevated expression of PF4 (platelet factor 4) and eotaxin in the NOA mouse, a model for atopic dermatitis. J Hum Genet. 1999;44:173-176.
50. Folkman J, Browder T, Palmblad J. Angiogenesis research: guidelines for translation to clinical application. Thromb Haemost. 2001;86:23-33.
51. Banks RE, Forbes MA, Kinsey SE, et al. Release of the angiogenic cytokine vascular endothelial growth factor (VEGF) from platelets: significance for VEGF measurements and cancer biology. Br J Cancer. 1998;77:956-964.
52. Gunsilius E, Gastl G. Platelets and VEGF blood levels in cancer patients. Br J Cancer. 1999;81: 185-186.
53. Verheul HM, Hoekman K, Luykx-de Bakker S, et al. Platelet: transporter of vascular endothelial growth factor. Clin Cancer Res. 1997;3:2187-2190.
54. Lee JK, Hong YJ, Han CJ, Hwang DY, Hong SI. Clinical usefulness of serum and plasma vascular endothelial growth factor in cancer patients: which is the optimal specimen? Int J Oncol. 2000;17:149-152.
55. George ML, Eccles SA, Tutton MG, Abulafi AM, Swift RI. Correlation of plasma and serum vascular endothelial growth factor levels with platelet count in colorectal cancer: clinical evidence of platelet scavenging? Clin Cancer Res. 2000;6:3147-3152.
56. Webb NJ, Bottomley MJ, Watson CJ, Brenchley PE. Vascular endothelial growth factor (VEGF) is released from platelets during blood clotting: implications for measurement of circulating VEGF levels in clinical disease. Clin Sci (Lond). 1998;94:395-404.
57. Adams J, Carder PJ, Downey S, et al. Vascular endothelial growth factor (VEGF) in breast cancer: comparison of plasma, serum, and tissue VEGF and microvessel density and effects of tamoxifen. Cancer Res. 2000;60:2898-2905.
58. Wynendaele W, Derua R, Hoylaerts MF, et al. Vascular endothelial growth factor measured in platelet poor plasma allows optimal separation between cancer patients and volunteers: a key to study an angiogenic marker in vivo? Ann Oncol. 1999;10:965-971.
59. Aguayo A, Giles F, Albitar M. Vascularity, angiogenesis and angiogenic factors in leukemias and myelodysplastic syndromes. Leuk Lymphoma. 2003;44:213-222.
60. Molica S, Vacca A, Levato D, Merchionne F, Ribatti D. Angiogenesis in acute and chronic lymphocytic leukemia. Leuk Res. 2004;28:321-324.
61. Ribatti D, Scavelli C, Roccaro AM, et al. Hematopoietic cancer and angiogenesis. Stem Cells Dev. 2004;13:484-495.
62. Hampl M, Tanaka T, Albert PS, et al. Therapeutic effects of viral vector-mediated antiangiogenic gene transfer in malignant ascites. Hum Gene Ther. 2001;12:1713-1729.
63. Giussani C, Carrabba G, Pluderi M, et al. Local intracerebral delivery of endogenous inhibitors by osmotic minipumps effectively suppresses glioma growth in vivo. Cancer Res. 2003;63:2499-2505.
64. Hagedorn M, Zilberberg L, Lozano RM, et al. A short peptide domain of platelet factor 4 blocks angiogenic key events induced by FGF-2. FASEB J. 2001;15:550-552.
65. Folkman J, Shing Y. Control of angiogenesis by heparin and other sulfated polysaccharides. Adv Exp Med Biol. 1992;313:355-364.
66. Perollet C, Han ZC, Savona C, Caen JP, Bikfalvi A. Platelet factor 4 modulates fibroblast growth factor 2 (FGF-2) activity and inhibits FGF-2 dimerization. Blood. 1998;91:3289-3299.
67. Borsig L, Wong R, Feramisco J, et al. Heparin and cancer revisited: mechanistic connections involving platelets, P-selectin, carcinoma mucins, and tumor metastasis. Proc Natl Acad Sci U S A. 2001;98:3352-3357.
68. Verheul HM, Pinedo HM. Tumor growth: a putative role for platelets? [editorial] Oncologist. 1998;3:II.
69. Pinedo HM, Verheul HM, D'Amato RJ, Folkman J. Involvement of platelets in tumour angiogenesis? Lancet. 1998;352:1775-1777.
70. Gasic GJ, Gasic TB, Stewart CC. Antimetastatic effects associated with platelet reduction. Proc Natl Acad Sci U S A. 1968;61:46-52.
71. Camerer E, Qazi AA, Duong DN, et al. Platelets, protease-activated receptors, and fibrinogen in hematogenous metastasis. Blood. 2004;104:397-401.
72. Gasic GJ. Role of plasma, platelets, and endothelial cells in tumor metastasis. Cancer Metastasis Rev. 1984;3:99-114.
73. Benoy I, Salgado R, Colpaert C, et al. Serum interleukin 6, plasma VEGF, serum VEGF, and VEGF platelet load in breast cancer patients. Clin Breast Cancer. 2002;2:311-315.
74. O'Neill EE, Brock CJ, von Kriegsheim AF, et al. Towards complete analysis of the platelet proteome. Proteomics. 2002;2:288-305.
75. Martens L, Van DP, Van DJ, et al. The human platelet proteome mapped by peptide-centric proteomics: a functional protein profile. Proteomics. 2005;5:3193-3204.
76. Garcia A, Prabhakar S, Brock CJ, et al. Extensive analysis of the human platelet proteome by two-dimensional gel electrophoresis and mass spectrometry. Proteomics. 2004;4:656-668.
77. Garcia A, Zitzmann N, Watson SP. Analyzing the platelet proteome. Semin Thromb Hemost. 2004; 30:485-489.
78. Watson SP, Bahou WF, Fitzgerald D, et al. Mapping the platelet proteome: a report of the ISTH Platelet Physiology Subcommittee. J Thromb Haemost. 2005;3:2098-2101.
79. Folkman J, Kalluri R. Cancer without disease [abstract]. Nature. 2004;427:787.
80. Ezzell C. Starving tumors of their lifeblood. Sci Am. 1998;279:33-34.

2008 111: 1227-1233
Prepublished online Oct 25, 2007;
doi:10.1182/blood-2007-09-113837

Angiogenesis is regulated by a novel mechanism: pro- and antiangiogenic proteins are organized into separate platelet {alpha} granules and differentially released

Joseph E. Italiano, Jr, Jennifer L. Richardson, Sunita Patel-Hett, Elisabeth Battinelli, Alexander Zaslavsky, Sarah Short, Sandra Ryeom, Judah Folkman and Giannoula L. Klement

Blood (print ISSN 0006-4971, online ISSN 1528-0020), is published semimonthly by the American Society of Hematology, 1900 M St, NW, Suite 200, Washington DC 20036.

Angiogenesis is regulated by a novel mechanism: pro- and antiangiogenic proteins are organized into separate platelet α granules and differentially released

Joseph E. Italiano Jr,[1,2] Jennifer L. Richardson,[1] Sunita Patel-Hett,[1,2] Elisabeth Battinelli,[1,3] Alexander Zaslavsky,[2] Sarah Short,[2] Sandra Ryeom,[2] Judah Folkman,[2] and Giannoula L. Klement[2,4]

[1]Translational Medicine Division, Brigham and Women's Hospital; [2]Vascular Biology Program, Department of Surgery, Children's Hospital; [3]Department of Hematology and Oncology, Beth Israel Deaconess Medical Center; and [4]Dana-Farber Cancer Institute, Boston, MA

Platelets, in addition to their function in hemostasis, play an important role in wound healing and tumor growth. Because platelets contain angiogenesis stimulators and inhibitors, the mechanisms by which platelets regulate angiogenesis remain unclear. As platelets adhere to activated endothelium, their action can enhance or inhibit local angiogenesis. We therefore suspected a higher organization of angiogenesis regulators in platelets. Using double immunofluorescence and immunoelectron microscopy, we show that pro- and antiangiogenic proteins are separated in distinct subpopulations of α-granules in platelets and megakaryocytes. Double immunofluorescence labeling of vascular endothelial growth factor (VEGF) (an angiogenesis stimulator) and endostatin (an angiogenesis inhibitor), or for thrombospondin-1 and basic fibroblast growth factor, confirms the segregation of stimulators and inhibitors into separate and distinct α-granules. These observations motivated the hypothesis that distinct populations of α-granules could undergo selective release. The treatment of human platelets with a selective PAR4 agonist (AYPGKF-NH_2) resulted in release of endostatin-containing granules, but not VEGF-containing granules, whereas the selective PAR1 agonist (TFLLR-NH_2) liberated VEGF, but not endostatin-containing granules. In conclusion, the separate packaging of angiogenesis regulators into pharmacologically and morphologically distinct populations of α-granules in megakaryocytes and platelets may provide a mechanism by which platelets can locally stimulate or inhibit angiogenesis. (Blood. 2008;111:1227-1233)

Introduction

Angiogenesis, the process of new vessel development, plays an essential role in embryogenesis, but postnatal angiogenesis is limited to sites of abnormal vascular surface. An activated vascular endothelium can be induced by tissue injury or wound healing, by hormonal cycling such as in pregnancy and ovulation, or by tumor-induced vessel growth. In all of these circumstances, platelets act as the initial responder to vascular change and provide a flexible delivery system for angiogenesis-related molecules.[1-4] The process of postnatal angiogenesis is regulated by a continuous interplay of stimulators and inhibitors of angiogenesis, and their imbalance contributes to numerous inflammatory, malignant, ischemic, and immune disorders.[5] There is a revived interest in the overlap between angiogenesis and platelets[6] because several clinical trials have now shown that anticoagulation can improve cancer survival[7,8] beyond the benefit derived from the treatment of deep vein thrombosis alone.

It is known that platelets stimulate endothelial cells in culture and can promote the assembly of capillary-like structures in vitro.[9,10] Platelets may modulate angiogenesis by releasing promoters such as vascular endothelial growth factor (VEGF), basic fibroblast growth factor (bFGF), epidermal growth factor (EGF), platelet derived growth factor (PDGF), and matrix metalloproteinases (MMPs).[1,6,11-18] The repertoire of angiogenesis inhibitors contained within platelets includes endostatin, platelet factor-4, thrombospondin-1, α_2-macroglobulin, plasminogen activator inhibitor-1, and angiostatin.[19,20] Although platelets contain 3 types of secretory granules (α-granules, dense granules, and lysosomes), most angiogenic regulatory proteins have been localized to α-granules. α-Granules are 200 to 500 nm in size and contain proteins that enhance the adhesive process, promote cell-cell interactions, and stimulate vascular repair. By adhering to the endothelium of injured organs and tissues and then secreting the contents of their α-granules, platelets may be capable of depositing high concentrations of angiogenesis regulatory proteins in a localized manner.

A body of experimental data and clinical investigations suggests that platelets are major regulators of angiogenesis.[21] However, because platelets contain both pro- and antiangiogenic regulatory proteins and because it has been assumed that the contents of α-granules are homogeneous, it has been unclear how platelets could either stimulate or inhibit angiogenesis. We provide new details about the organization of angiogenesis regulatory proteins in the α-granules of platelets and address the mechanism of how the selective release of these granules leads to the regulation of angiogenesis. Here we report the novel finding that angiogenic and antiangiogenic proteins are segregated into different sets of α-granules in platelets. We provide a mechanism for the differential release of these α-granules and show that these distinct populations of α-granules may be regulated by differential G-protein–mediated signaling pathways.

Submitted September 20, 2007; accepted October 16, 2007. Prepublished online as *Blood* First Edition paper, October 25, 2007; DOI 10.1182/blood-2007-09-113837.

An inside *Blood* analysis of this article appears at the front of this issue.

The publication costs of this article were defrayed in part by page charge payment. Therefore, and solely to indicate this fact, this article is hereby marked "advertisement" in accordance with 18 USC section 1734.

Methods

Approval was obtained from the Partners Human Research Committee institutional review board, Boston, MA, for these studies. Informed consent was provided in accordance with the Declaration of Helsinki.

Preparation of resting platelets

Human blood from healthy volunteers, drawn into 0.1 volume of Aster-Jandl anticoagulant, was centrifuged at 110*g* for 10 minutes. None of the volunteers had ingested aspirin or other nonsteroidal anti-inflammatory drugs for at least 10 days before blood collection. The platelet-rich plasma was gel-filtered through a Sepharose 2B column equilibrated with a solution containing 145 mM NaCl, 10 mM N-2-hydroxyethylpiperazine-N′-2-ethanesulfonic acid, 10 mM glucose, 0.5 mM Na_2HPO_4, 5 mM KCl, 2 mM $MgCl_2$, and 0.3% bovine serum albumin (BSA), pH 7.4. The number of platelets was counted by fluorescence–activated cell sorting and adjusted to 2×10^8/mL. The isolated platelet suspension was incubated at 37°C for up to 1 hour. The resting state of the platelets was routinely confirmed by PAC1 antibody and antitubulin immunofluorescence staining.

Activation of platelets

Release of α-granules was examined in vitro in response to 10 μm AYPGK-NH2, a selective PAR4-activating peptide, or 8 μm TFLLR-NH2, a PAR1-activating peptide. Peptides were prepared by solid-phase synthesis at the Peptide Synthesis Facility of Synbiocsi (Livermore, CA). Isolated platelets were exposed to PAR activating peptide or vehicle for 10 minutes, fixed with 4% formaldehyde for 20 minutes, attached to polylysine-coated coverslips, and then processed for immunofluorescence microscopy.

Megakaryocyte cultures

Livers were recovered from mouse fetuses, and single-cell suspensions were generated using methods described previously.[22] Between the fourth and sixth days of megakaryocyte culture, cells were placed on a 1.5% to 3% albumin step gradient and sedimented[23] to obtain enriched populations of megakaryocytes.

Immunofluorescence microscopy

Rabbit anti-VEGF antibody (Ab-1) and mouse anti-VEGF (Ab-7) were obtained from Lab Visions (Fremont, CA). Rabbit antiendostatin antibody (Ab-1) was obtained from Lab Visions. Mouse antithrombospondin antibody (Ab-4, 6.1) was obtained from Lab Visions. Rabbit polyclonal antifibroblast growth factor basic was obtained from Abcam (Cambridge, MA). Mouse antifibrinogen was obtained from BD Biosciences (Franklin Lakes, NJ) and rabbit antifibrinogen was obtained from Santa Cruz Biotechnologies. Rabbit anti-von Willebrand factor was obtained from Chemicon (Billerica, MA) and Dako (Carpenteria, CA). Alexa 568 antimouse, Alexa 488 antirabbit, Alexa 568 antirabbit, and Alexa 488 antimouse secondary antibodies were purchased from Jackson Immuno-Research Laboratories (West Grove, PA). Actin filament integrity was assayed by fluorescence microscopy of fixed specimens stained with 1 mM phalloidin-Alexa 488 (Molecular Probes, Eugene, OR) for 30 minutes and washed 4 times with blocking buffer. Resting platelets were fixed for 20 minutes in suspension by the addition of 1 vol of 8% formaldehyde. Solutions of fixed platelets in suspension were placed in wells of a 24-well microliter plate, each containing a polylysine-coated coverslip, and the plate was centrifuged at 250*g* for 5 minutes to attach the cells to the coverslip. Megakaryocytes were fixed with 4% formaldehyde in Hanks' balanced salt solution (GIBCO BRL, Invitrogen, Carlsbad, CA) for 20 minutes, centrifuged at 500*g* for 4 minutes onto coverslips previously coated with poly-L-lysine, and permeabilized with 0.5% Triton X-100 in Hanks' balanced salt solution. Specimens were blocked overnight in phosphate-buffered saline (PBS) with 1% BSA, incubated in primary antibody for 2 to 3 hours, washed, and treated with appropriate secondary antibody for 1 hour, and then washed extensively. Primary antibodies were used at 1 μg/mL in PBS containing 1% BSA and secondary antibodies at 1:500 dilution in the same buffer. Controls were processed identically except for omission of the primary antibody. Controls consisted of either incubating cells with one or both primary antibodies without fluorescently labeled secondary antibodies, or cells incubated with one or both fluorescently labeled secondary antibodies in the absence of primary antibodies. Preparations were mounted in Aqua polymount from Polysciences (Warrington, PA) and analyzed at room temperature on a Nikon TE 2000 Eclipse microscope equipped with a Nikon 100×/1.4 NA objective and a 100-W mercury lamp. Images were acquired with a Hamamatsu (Bridgewater, NJ) Orca IIER CCD camera. Electronic shutters and image acquisition were under the control of Molecular Devices Metamorph software (Downington, PA). Images were acquired by fluorescence microscopy with an image capture time of 200 to 500 ms.

Immunogold-electron microscopy

For preparation of cryosections, isolated human platelets were fixed with 4% paraformaldehyde in 0.1 M Na phosphate buffer, pH 7.4. After 2 hours of fixation at room temperature, the cell pellets were washed with PBS containing 0.2 M glycine to quench free aldehyde groups from the fixative. Before freezing in liquid nitrogen, cell pellets were infiltrated with 2.3 M sucrose in PBS for 15 minutes. Frozen samples were sectioned at −120°C, and the sections were transferred to formvar-carbon coated copper grids and floated on PBS until the immunogold labeling was carried out. The gold labeling was carried out at room temperature on a piece of parafilm. All antibodies and protein A gold were diluted with 1% BSA. The diluted antibody solution was centrifuged for 1 minute at 5000*g* before labeling to avoid possible aggregates. All antibodies were used at a concentration of 1 μg/mL. Grids were floated on drops of 1% BSA for 10 minutes to block for nonspecific labeling, transferred to 5-μL drops of primary antibody, and incubated for 30 minutes. The grids were then washed in 4 drops of PBS for a total of 15 minutes, transferred to 5 μL drops of Protein-A gold for 20 minutes, and washed in 4 drops of PBS for 15 minutes and 6 drops of double distilled water. For double labeling, after the first Protein A gold incubation, grids were washed in 4 drops of PBS for a total of 15 minutes and then transferred to a drop of 1% glutaraldehyde in PBS for 5 minutes and washed in 4 drops of PBS/0.15 M glycine. The second primary antibody was then applied, followed by PBS washing and treatment with different size protein A gold as above. Contrasting/embedding of the labeled grids was carried out on ice in 0.3% uranyl acetate in 2% methyl cellulose for 10 minutes. Grids were picked up with metal loops, leaving a thin coat of methyl cellulose. The grids were examined in a Tecnai G^2 Spirit BioTWIN transmission electron microscope (Hillsboro, OR) at 18 500× magnification at an accelerating voltage of 80 kV. Images were recorded with an AMT 2k CCD camera.

Preparation of photomicrographs

The digital images produced in Metamorph were assembled into composite images using Adobe Photoshop 8.0 (Adobe Systems, San Jose, CA).

Results

The localization of angiogenesis regulatory proteins within the platelet is important for understanding how platelets contribute to new blood vessel formation. The capacity of platelets to regulate angiogenesis could result from segregation of proangiogenic and antiangiogenic regulators into separate granules. To test this possibility, we compared the localization of the most well-characterized proangiogenic protein VEGF and the established antiangiogenic regulator endostatin, in resting platelets by immunofluorescence microscopy. The majority of α-granules stained for either VEGF (labeled green) or endostatin (labeled red), and little evidence of colocalization as would be indicated by yellow in the merged image was observed (Figure 1A-C). Similarly, double

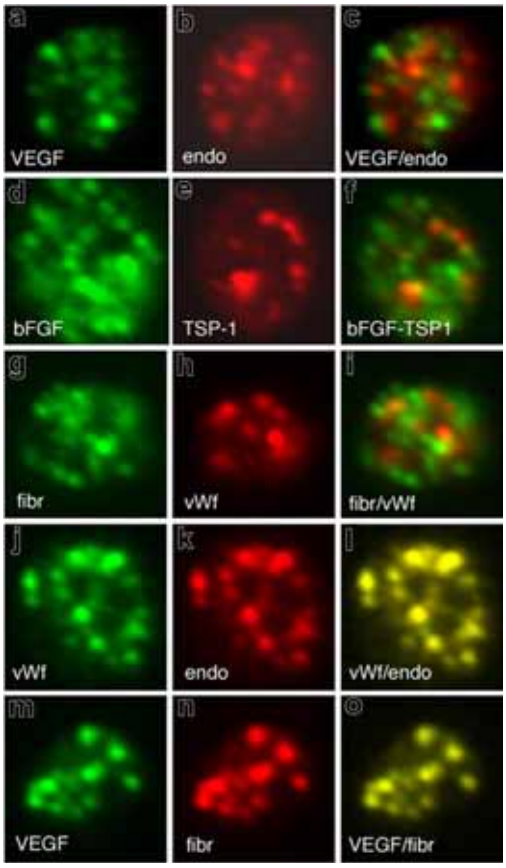

Figure 1. Pro- and antiangiogenic regulators organize into separate, distinct α-granules in resting platelets. Double immunofluorescence microscopy of resting platelets using antibodies against VEGF (A) and endostatin (B) and an overlay (C). Double immunofluorescence microscopy of resting platelets using antibodies against bFGF (D) and TSP-1 (E) and an overlay (F). Double immunofluorescence microscopy of resting platelets using antibodies against fibrinogen (G) and von Willebrand factor (H) and an overlay (I). Double immunofluorescence microscopy of resting platelets using antibodies against von Willebrand factor (J) and endostatin (K) and an overlay (L). Double immunofluorescence microscopy of resting platelets using antibodies against VEGF (M) and fibrinogen (N) and an overlay (O).

immunofluorescence microscopy comparing the localization of the endogenous angiogenesis inhibitor thrombospondin-1 and bFGF, another angiogenesis stimulator, also showed segregation of these proteins into separate, distinct granules (Figure 1D-F). To establish whether the segregation of proteins into distinct α-granules was specific to angiogenesis regulatory proteins, we examined the localization of von Willebrand factor (VWF) and fibrinogen. To evaluate the degree of overlap of proteins, we investigated the combination of fibrinogen and VWF. Surprisingly, fibrinogen and VWF also segregated into separate and distinct α-granules (Figure 1G-I). Immunofluorescence microscopy further revealed that VWF colocalized with endostatin (Figure 1J,K) and fibrinogen predominantly with the VEGF-containing α-granules (Figure 1M-O).

The organization of angiogenesis regulators into distinct α-granules is not exclusive to platelets. Megakaryocytes have been shown to generate platelets by remodeling their cytoplasm into long proplatelet extensions that transport individual α-granules on their microtubule tracks.[24] To address whether inhibitors and stimulators of angiogenesis are packaged into distinct populations of α-granules in the precursor cells of platelets, we analyzed the distribution of angiogenic regulatory proteins in proplatelet-producing mouse megakaryocytes. As observed in platelets, VEGF and endostatin were localized to separate α-granules in the

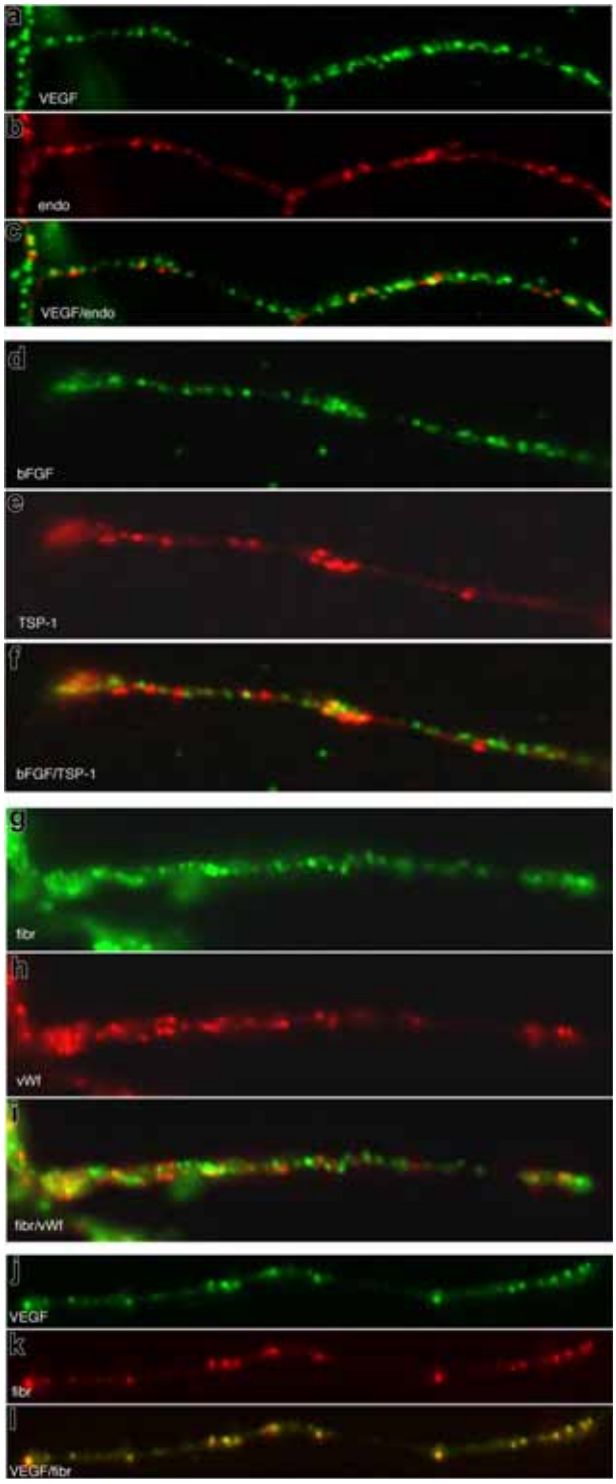

Figure 2. Pro- and antiangiogenic regulatory proteins are segregated into separate, distinct α-granules in megakaryocyte proplatelets. Double immunofluorescence microscopy of proplatelets using antibodies against VEGF (A) and endostatin (B) and an overlay (C). Double immunofluorescence microscopy of proplatelets using antibodies against bFGF (D) and TSP-1 (E) and an overlay (F). Double immunofluorescence microscopy of proplatelets using antibodies against fibrinogen (G) and von Willebrand factor (H) and an overlay (I). Double immunofluorescence microscopy of proplatelets against VEGF (J) and fibrinogen (K) and an overlay (L).

proplatelet extensions (Figure 2A-C). A similar segregated staining pattern was also observed for thrombospondin-1 and basic FGF (Figure 2D-F) as well as fibrinogen and VWF (Figure 2G-I). Most

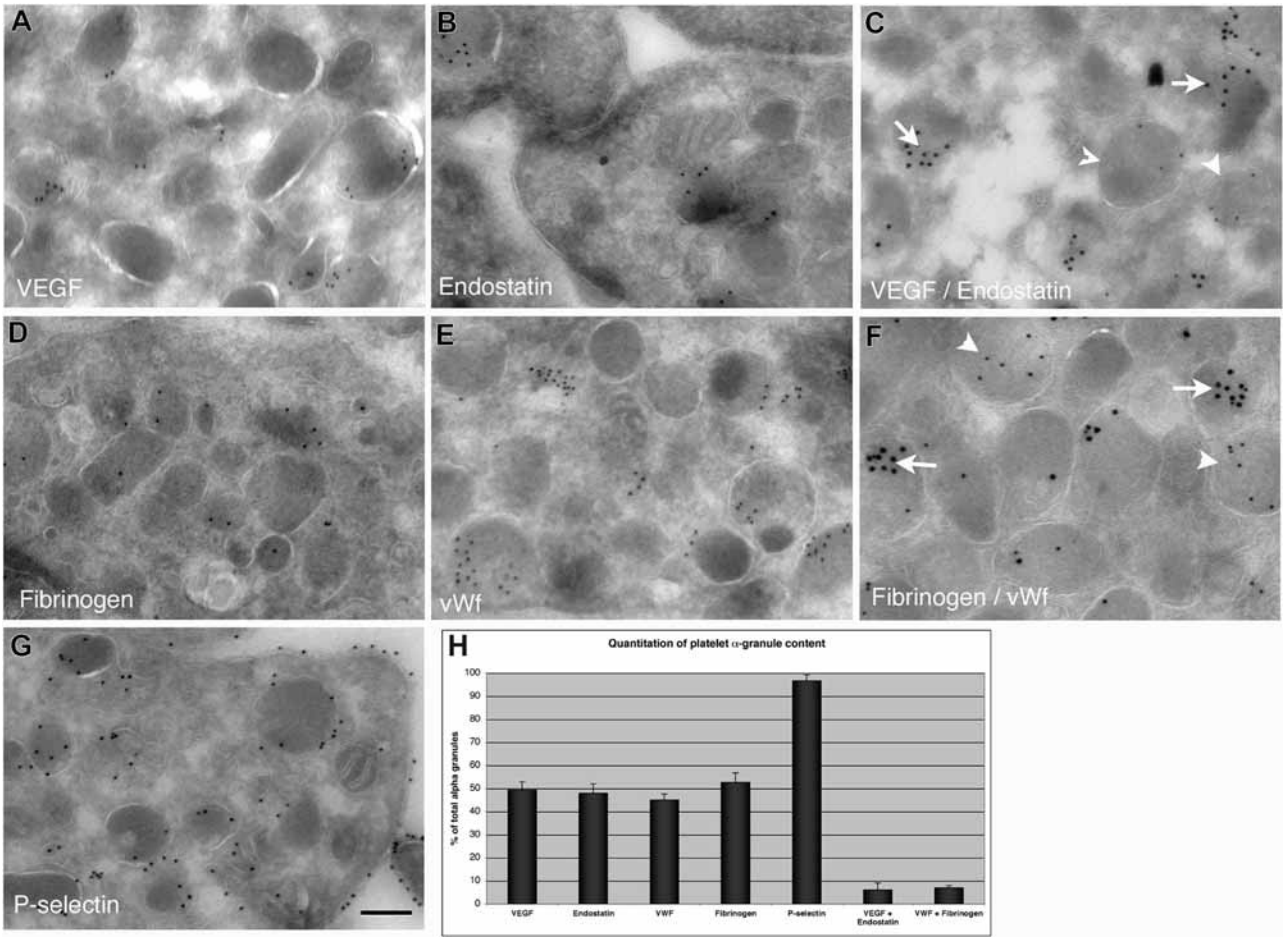

Figure 3. Localization of proteins in resting, human platelets using immunoelectron microscopy of ultrathin cryosections. Single immunogold labeling on ultrathin platelet sections was performed with anti-VEGF (A) and antiendostatin (B) antibodies. Double immunogold labeling on platelet sections was performed with the use of anti-VEGF antibody and antiendostatin antibodies. Large gold particles representing anti-VEGF staining (15 nm, arrows) are evident on one population of α-granules and small gold particles (5 nm) representing endostatin staining are abundantly present on a different population of α-granules (arrowheads) (C). Single immunogold labeling on ultrathin platelet sections was performed with antifibrinogen (D) and anti-VWF (E) antibodies. Double immunogold labeling on platelet sections was performed with the use of antifibrinogen antibody, which was revealed with a 15-nm, gold conjugate (arrows) and then with an antibody to VWF, which was revealed with a 5-nm, gold conjugate (arrowheads) (F). Single immunogold labeling on ultrathin platelet sections was performed with anti–P-selectin antibody (G). Gold particles representing P-selectin staining are abundantly present on the α-granules as well as the cell-surface membrane. Bar represents 300 nm. (H) The bar graph shows the quantitation of the percentage of α-granules positive (via immunogold staining) for specific factors. The data represent 3 separate experiments; error bars represent SD. More than 100 granules were scored for each study.

VWF colocalized with the endostatin-containing α-granules (Figure 2J-L). We confirmed the presence of distinct populations of α-granules in human platelets at the ultra-structural level using immuno-electron microscopy (Figure 3). As expected, anti-VEGF (Figure 3A) and antiendostatin antibodies (Figure 3B) label only a subpopulation of α-granules. Double immunogold microscopy confirmed that the majority of VEGF and endostatin are localized to separate and distinct granules in platelets (Figure 3C). Single immunogold studies revealed that antifibrinogen (Figure 3D) and anti-VWF antibodies (Figure 3E) label only a subpopulation of α-granules. Double immunogold microscopy confirmed that the majority of fibrinogen and VWF are localized to separate and distinct granules in resting platelets (Figure 3G). Anti–P-selectin antibodies specifically labeled almost all α-granules and the plasma membrane of resting platelets (Figure 3G). Quantitative analysis of gold labeling in serial sections revealed that antibodies to VEGF, endostatin, VWF, and fibrinogen each stain approximately 50% of the granule population (Figure 3H). In contrast, anti–P-selectin antibodies label the membrane of all α-granules as well as the surface of the resting platelet. Less than 10% of granules contained gold labeling for both endostatin and VEGF or VWF and fibrinogen together (Figure 3H).

The packaging of VEGF and endostatin into separate α-granules suggested that distinct granule populations may undergo selective release. We tested this hypothesis by stimulating platelets with either PAR4-activating peptide or PAR1-activating peptide. Selective granule release was assessed by immunofluorescence microscopy (Figure 4). Phalloidin staining demonstrated that exposure of platelets to either ligand resulted in aggregation and extension of lamellipodia and filopodia, leading to activation (Figure 4B,D,F,H). Immunofluorescence microscopy revealed that PAR4 treatment resulted in loss of the endostatin labeling, suggesting that most of the endostatin-containing granules were released from the platelets ligated with PAR4-activating peptide (Figure 4C). However, numerous VEGF-containing granules were retained in the cytoplasm of PAR4-treated platelets (Figure 4A). In contrast, immunofluorescence microscopy revealed that ligation of PAR1 resulted in the release of VEGF-containing (green) granules, suggesting that release of VEGF-containing granules was elicited by the PAR1 agonist (Figure 4E). However, a large number of

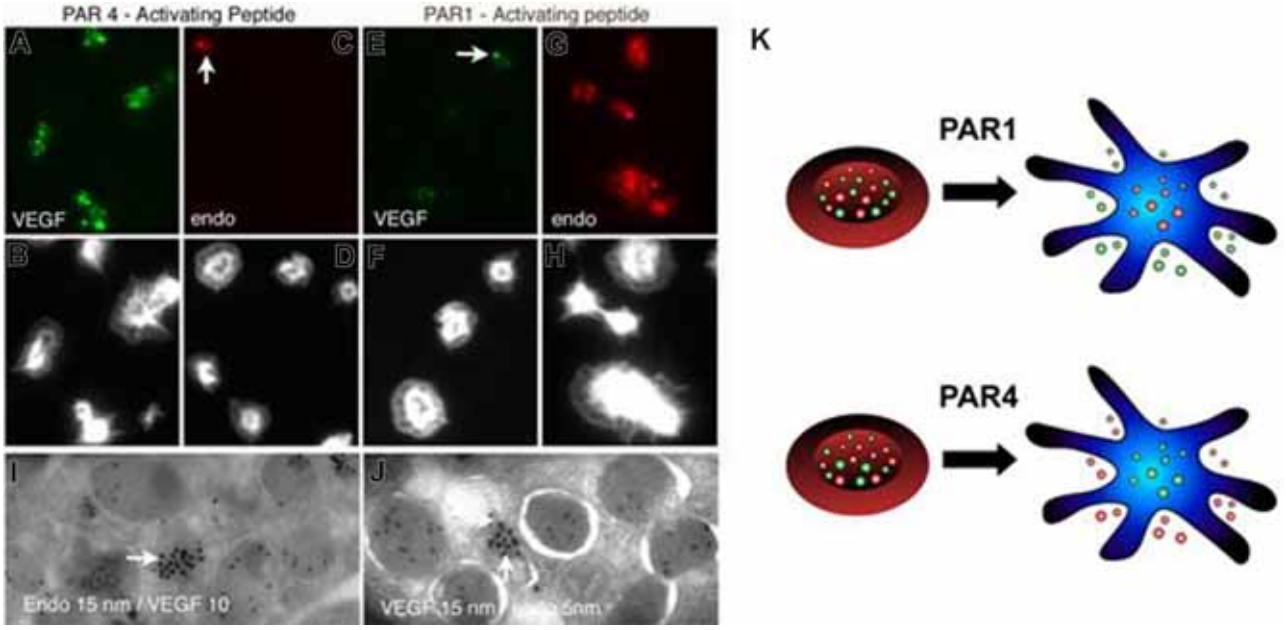

Figure 4. Activation of specific protease activated receptors stimulates the selective release of α-granules containing either endostatin or VEGF. Platelets were treated with platelet buffer in the presence of agonists for 10 minutes with PAR4-activating peptide (A-D), and PAR1-activating peptide (E-H) and then fixed and processed for immunofluorescence microscopy. Cells were stained with either anti-VEGF antibodies (Alexa 488 green labeling; A,E) or antiendostatin antibodies (Alexa 568 red labeling; C,G,) to assay for granule retention or release. All micrographs were taken at the same exposure time. Corresponding staining with Alexa-phalloidin (B,D,F,H) in the bottom panels highlights the morphology of the platelets. Negative controls consisting of incubation with both secondary fluorescently labeled antibodies only or incubation with only primary antibodies failed to show appreciable fluorescence (data not shown). Images are representative of at least 10 high-power fields for each experiment, and each experiment was performed 3 times. Representative images of immunoelectron microscopy of platelets treated with either PAR4-AP (I) or PAR1-AP (J). Double immunogold labeling on platelet sections was performed with the use of anti-VEGF antibody and antiendostatin antibodies. In the PAR4-treated samples (I), large gold particles representing antiendostatin staining (15 nm) are evident on one α-granule (arrow) and small gold particles (5 nm) representing VEGF staining are abundantly present on separate population of multiple α-granules. In the PAR1-treated samples (J), large gold particles representing anti-VEGF staining (15 nm, arrow) are evident on one α-granule (arrow) and small gold particles (5 nm) representing endostatin staining are abundantly present on separate population of multiple α-granules. (K) A model illustrating the mechanism of differential granule release from platelets. A simplified summary of the pathway is shown. Resting platelets contain both proangiogenic (green) and antiangiogenic (red) granules. Selective activation of the PAR1 receptor causes release of granules containing proangiogenic factors, whereas selective activation of the PAR4 receptor causes release of granules containing antiangiogenic factors.

endostatin-containing granules were still retained in the cytoplasm of PAR1-treated platelets. (Figure 4G). To confirm the phenomenon of differential granule release, we analyzed the agonist-mediated release of α-granules at higher resolution using immunoelectron microscopy. Stimulation of platelets with PAR4 agonist resulted in the release of almost all endostatin-containing granules; the majority (84%) of granules remaining in the activated platelets were positive for VEGF (Figure 4I). Treatment of platelets with PAR1 agonist induced the release of the majority of VEGF-containing granules; the majority (88%) of granules remaining in the PAR1-activated platelets were positive for endostatin (Figure 4J).

Discussion

Angiogenesis is a critical element of many physiologic processes such as wound healing, as well as pathologic processes such as tumor growth. In both situations, new blood vessel development is driven locally by the release of proangiogenic factors such as VEGF, bFGF, and PDGF. However, angiogenesis can also be inhibited by local release of antiangiogenic factors such as endostatin and thrombospondin. The proximity to and interaction with the endothelium allow platelets to strongly influence tumor development and wound healing. Platelets have been presumed to contribute to these angiogenesis-dependent processes by providing many pro- and antiangiogenic proteins, but their regulatory role is incompletely understood. In this study, we have shown that platelets contain distinct populations of α-granules that can undergo differential release in vitro. This study suggests that at least 2 populations of α-granules containing endogenous angiogenic regulatory proteins are present in platelets and raises the possibility that platelets contain multiple types of α-granules. Platelets contain a large number of angiogenic regulatory proteins, whose localization will need to be thoroughly established to understand the complexity of α-granule organization within resting platelets. Yet, it can be inferred that this subcellular organization has a physiologic purpose in facilitating the differential release of these proteins in response to tissue stimuli. Our findings of differential granule release also support and provide a mechanistic explanation for earlier studies examining the secretion reaction of platelets. Two independent groups have documented the differential release of α-granule proteins from platelets.[25,26] In addition, morphometric evaluation of the platelet release reaction during thrombogenesis has demonstrated that platelets do not release all of their granules when they are incorporated into a thrombus.[27] The above results showing distinct granules also raise the question of whether other cell types containing secretory granules segregate angiogenic regulatory proteins to regulate differential release. For example, Weibel Palade bodies, the specific secretory organelles of endothelial cells, contain several angiogenesis regulators and have been recently shown to differentially package and release P-selectin and VWF through protease-activated receptors.[28]

What molecular mechanisms regulate the differential packaging of specific proteins into α-granules? α-granules contain a mixture of proteins synthesized by the megakaryocyte as well as proteins

endocytosed from the circulation by both megakaryocytes and the platelets. Although the formation of α-granules is poorly understood,[29,30] it appears that α-granules develop from budding vesicles in the Golgi complex within megakaryocytes, where they transform into multivesicular bodies, which also fuse with endocytic vesicles. Coated pits and vesicles have been observed in platelets and function to take up proteins, such as fibrinogen, by receptor-mediated endocytosis. These endocytic vesicles fuse with the multivesicular bodies. Multivesicular bodies, which are prevalent in early megakaryocytes, are thought to be a common precursor of both α- and dense granules. However, the mechanisms by which α- and dense granules develop into distinct entities are unknown. It is tempting to speculate that a similar process may be used to segregate proteins into distinct subsets of α-granules and that genetic defects that affect the α-granule segregation or differential release may provide an explanation of the wide range of angiogenic responses manifested by different patients.[31] Several angiogenesis-dependent processes may be explained by the sequential release of angiogenesis regulators. For example, in early endothelial injury, an unstable platelet clot is formed and the high-affinity thrombin receptor (PAR1) signals to release by majority pro-angiogenic proteins such as VEGF. In the late stage of tissue reconstruction, a high thrombin state occurs when the majority of the clot is crosslinked by factor XIII, and the low affinity protease-activated receptor (PAR4) is engaged and mainly inhibitors of angiogenesis are released.

Recognizing that activated platelets release growth factors, investigators have begun to enhance tissue regeneration by applying platelets and their derivatives into sites of injuries or surgical intervention. The concept of platelet and tissue interaction and the resulting release of angiogenesis regulators have already been used in the empirical application of platelet preparations to chronic diabetic ulcers,[32,33] chronic cutaneous ulcers,[34] dehiscent wounds,[35-37] and tissue regeneration.[38] Although the majority of evidence indicates that platelets and their derivatives (gels, releasates, and lysates) are promising therapeutic agents for regenerative medicine, little is known about the specific mechanisms underlying platelet-accelerated tissue repair.[39] The ability to generate selective platelet releasates by manipulating protease-activated receptors may provide new opportunities for research and applications of tissue engineering and may aid in therapeutic strategies to promote or inhibit angiogenesis.

Our findings of distinct populations of α-granules that can be differentially released suggest implications and potential for a substantial role in antiangiogenic therapy. It is now well accepted that the growth of a tumor beyond approximately 1 mm is dependent on the development of a neovasculature. One possibility is that tumors also hijack the angiogenic properties of platelets to promote new blood vessel growth by manipulating the protease activated receptors on platelets and triggering the selective release of predominantly proangiogenic factors. The protease-activated receptors on platelets and endothelial cells are likely to play an important role in the sequential and highly selective contribution of angiogenesis regulators to tissues. If confirmed, then it may be possible to develop drugs that instruct platelets, which interact with tumors to release predominantly antiangiogenic proteins.

Acknowledgments

The authors thank Maria Ericsson for assistance with electron microscopy, Dr John Hartwig and Eva Alden for critical reading of the manuscript, and Jenny Grillo for formatting the manuscript.

The work was supported by the National Institutes of Health (grant HL068130, J.E.I.), the Breast Cancer Research Foundation (J.F.), the Department of Defense (grant W81XWH-04-1-0316, J.F.), and NASA (grant NNH04ZUU002N).

Authorship

Contribution: J.E.I. designed and performed experiments and data analysis, interpreted results, provided guidance for the group, and drafted the manuscript; J.L.R., S.P.H., E.B., A.Z., and S.S. performed experiments and data analysis and interpreted results; S.R. and J.F. designed experiments, interpreted results, formulated discussions, and assisted in manuscript preparation and editing; G.L.K. designed experiments, provided guidance for the group, interpreted results, formulated discussions, and assisted in manuscript preparation and editing.

Conflict-of-interest disclosure: The authors declare no competing financial interests.

Correspondence: Joseph E. Italiano Jr, Translational Medicine Division, Brigham and Women's Hospital, One Blackfan Circle, Boston, MA 02115; e-mail: jitaliano@rics.bwh.harvard.edu; or Giannoula Klement, Children's Hospital Boston, Karp Family Research Laboratories, One Blackfan Circle, Boston, MA 02115; e-mail: giannoula.klement@childrens.harvard.edu.

References

1. Browder T, Folkman J, Pirie-Shepherd S. The hemostatic system as a regulator of angiogenesis. J Biol Chem. 2000;275:1521-1524.
2. Folkman J, Browder T, Palmblad J. Angiogenesis research: guidelines for translation to clinical application. Thromb Haemost. 2001;86:23-33.
3. Kisucka J, Butterfield CE, Duda DG, et al. Platelets and platelet adhesion support angiogenesis while preventing excessive hemorrhage. Proc Natl Acad Sci U S A. 2006;103:855-860.
4. Ma L, Perini R, McKnight W, et al. Proteinase-activated receptors 1 and 4 counter-regulate endostatin and VEGF release from human platelets. Proc Natl Acad Sci U S A. 2005;102:216-220.
5. Carmeliet P. Angiogenesis in life, disease and medicine. Nature. 2005;438:932-936.
6. Pinedo HM, Verheul HM, D'Amato RJ, Folkman J. Involvement of platelets in tumour angiogenesis? Lancet. 1998;352:1775-1777.
7. Kakkar AK, Levine MN, Kadziola Z, et al. Low molecular weight heparin, therapy with dalteparin, and survival in advanced cancer: the fragmin advanced malignancy outcome study (FAMOUS). J Clin Oncol. 2004;22:1944-1948.
8. Klerk CP, Smorenburg SM, Otten HM, et al. The effect of low molecular weight heparin on survival in patients with advanced malignancy. J Clin Oncol. 2005;23:2130-2135.
9. D'Amore P, Shepro D. Stimulation of growth and calcium influx in cultured, bovine, aortic endothelial cells by platelets and vasoactive substances. J Cell Physiol. 1977;92:177-183.
10. Pipili-Synetos E, Papadimitriou E, Maragoudakis ME. Evidence that platelets promote tube formation by endothelial cells on matrigel. Br J Pharmacol. 1998;125:1252-1257.
11. Mohle R, Green D, Moore MA, Nachman RL, Rafii S. Constitutive production and thrombin–induced release of vascular endothelial growth factor by human megakaryocytes and platelets. Proc Natl Acad Sci U S A. 1997;94:663-668.
12. Wartiovaara U, Salven P, Mikkola H, et al. Peripheral blood platelets express VEGF-C and VEGF which are released during platelet activation. Thromb Haemost. 1998;80:171-175.
13. Kaplan DR, Chao FC, Stiles CD, Antoniades HN, Scher CD. Platelet alpha granules contain a growth factor for fibroblasts. Blood. 1979;53:1043-1052.
14. Ben-Ezra J, Sheibani K, Hwang DL, Lev-Ran A. Megakaryocyte synthesis is the source of epidermal growth factor in human platelets. Am J Pathol. 1990;137:755-759.
15. Nakamura T, Tomita Y, Hirai R, Yamaoka K, Kaji K, Ichihara A. Inhibitory effect of transforming growth factor-beta on DNA synthesis of adult rat hepatocytes in primary culture. Biochem Biophys Res Commun. 1985;133:1042-1050.
16. Hla T. Physiological and pathological actions of

sphingosine 1-phosphate. Semin Cell Dev Biol. 2004;15:513-520.

17. Galt SW, Lindemann S, Allen L, et al. Outside-in signals delivered by matrix metalloproteinase-1 regulate platelet function. Circ Res. 2002;90: 1093-1099.
18. Daly ME, Makris A, Reed M, Lewis CE. Hemostatic regulators of tumor angiogenesis: a source of antiangiogenic agents for cancer treatment? J Natl Cancer Inst. 2003;95:1660-1673.
19. Iruela-Arispe ML, Bornstein P, Sage H. Thrombospondin exerts an antiangiogenic effect on cord formation by endothelial cells in vitro. Proc Natl Acad Sci U S A. 1991;88:5026-5030.
20. Maione TE, Gray GS, Petro J, et al. Inhibition of angiogenesis by recombinant human platelet factor-4 and related peptides. Science. 1990;247:77-79.
21. Brill A, Varon D. Angiogenesis. In: Michelson AD, ed. Platelets, 2nd edition. San Diego, CA: Academic Press/Elsevier Science; 2007:757-768.
22. Lecine P, Villeval J, Vyas P, Swencki B, Xu Y, Shivdasani R. Mice lacking transcription factor NF-E2 provide in vivo validation of the proplatelet model of thombocytopoiesis and show a platelet production defect that is intrinsic to megakaryocytes. Blood. 1998;92:1608-1616.
23. Drachman JG, Sabath DF, Fox NE, Kaushansky K. Thrombopoietin signal transduction in purified murine megakaryocytes. Blood. 1997;89:483-492.
24. Richardson JL, Shivdasani RA, Boers C, Hartwig JH, Italiano JE Jr. Mechanisms of organelle transport and capture along proplatelets during platelet production. Blood. 2005;106:4066-4075.
25. Zucker M, Brokeman M, Kaplan K. Factor VIII-related antigen in human blood platelets: localization and release by thrombin and collagen. J Lab Clin Med. 1979;94:675-682.
26. Koutts J, Walsh P, Plow E, Fenton JW 2nd, Bouma B, Zimmerman T. Active release of human platelet factor VIII-related antigen by adenosine diphosphate, collagen, and thrombin. J Clin Invest. 1978;62:1255-1263.
27. Baumgartner HR, Muggli R, Tschopp TB, Turitto VT. Platelet adhesion, release and aggregation in flowing blood: effects of surface properties and platelet function. Thromb Haemost. 1976;35:124-138.
28. Cleator JH, Zhu WQ, Vaughan DE, Hamm HE. Differential regulation of endothelial exocytosis of P-selectin and von Willebrand factor by protease-activated receptors and cAMP. Blood. 2006;107: 2736-2744.
29. Lo B, Ling L, Gissen P, et al. Requirement of VPS33B, a member of the Sec1/Munc18 protein family, in megakaryocyte and platelet alpha-granule biogenesis. Blood. 2005;106:4159-4166.
30. Heijnen H, Debili N, Vainchencker W, Breton-Gorius J, Geuze H, Sixma J. Multivesicular bodies are an intermediate stage in the formation of platelet alpha-granules. Blood. 1998;91:2313-2325.
31. Rohan RM, Fernandez A, Udagawa T, Yuan J, D'Amato RJ. Genetic heterogeneity of angiogenesis in mice. FASEB J. 2000;14:871-876.
32. Driver VR, Hanft J, Fylling CP, Beriou JM, Autologel Diabetic Foot Ulcer Study Group. A prospective, randomized, controlled trial of autologous platelet-rich plasma gel for the treatment of diabetic foot ulcers. Ostomy Wound Manage. 2006; 52:68-70, 72, 74.
33. Knighton DR, Fiegel VD. Growth factors and comprehensive surgical care of diabetic wounds. Curr Opin Gen Surg. 1993;32-39.
34. Anitua E, Aguirre JJ, Algorta J, et al. Effectiveness of autologous preparation rich in growth factors for the treatment of chronic cutaneous ulcers. J Biomed Mater Res B Appl Biomater. 2007 [Epub ahead of print].
35. Mazzucco L, Medici D, Serra M, et al. The use of autologous platelet gel to treat difficult-to-heal wounds: a pilot study. Transfusion. 2004;44:1013-1018.
36. Brissett AE, Hom DB. The effects of tissue sealants, platelet gels, and growth factors on wound healing. Curr Opin Otolaryngol Head Neck Surg. 2003;11:245-250.
37. Crovetti G, Martinelli G, Issi M, et al. Platelet gel for healing cutaneous chronic wounds. Transfus Apher Sci. 2004;30:145-151.
38. Anitua E, Andia I, Ardanza B, Nurden P, Nurden AT. Autologous platelets as a source of proteins for healing and tissue regeneration. Thromb Haemost. 2004;91:4-15.
39. Borzini P, Mazzucco L. Platelet gels and releasates. Curr Opin Hematol. 2005;12:473-479.

In Press, Proc Natl Acad Sci USA 2009.

Prosaposin inhibits tumor metastasis via paracrine and endocrine stimulation of stromal p53 and Tsp-1

Soo-Young Kang[1,2], Ole J. Halvorsen[3], Karsten Gravdal[3], Nandita Bhattacharya[1,2], Jung Min Lee[1], Nathan W. Liu[1], Brian T. Johnston[1], Adam B. Johnston[1,4], Svein A. Haukaas[5], Kristie Aamodt[1], Sun Yoo[1], Lars A. Akslen[3], and Randolph S. Watnick[1,2]

[1]Vascular Biology Program, Department of Surgery, Children's Hospital Boston, Boston, MA 02115, [2]Department of Surgery, Harvard Medical School, Boston, MA 02115, [3]The Gade Institute, Section for Pathology, University of Bergen, Haukeland University Hospital, N-5021 Bergen, Norway, [4]Department of Biochemical Sciences, Harvard College, Cambridge, MA 02138, [5]Department of Surgery, Section of Urology, University of Bergen, Haukeland University Hospital, N-5021 Bergen, Norway

RSW contact information: tel. 617-919-2427,
email: randy.watnick@childrens.harvard.edu

Running Title: Prosaposin is a novel inhibitor of tumor metastasis

Abstract

Metastatic tumors can prepare a distant site for colonization via the secretion of factors that act in a systemic manner. We hypothesized that non/weakly metastatic human tumor cells may act in an opposite fashion by creating a microenvironment in distant tissues that is refractory to colonization. By comparing cell lines with different metastatic potential, we have identified a novel tumor-secreted inhibitor of metastasis, prosaposin (Psap), which functions in a paracrine and endocrine fashion by stimulating the expression of thrombospondin-1 (Tsp-1) in fibroblasts present in both primary tumors and distant organs, doing so in a p53-dependent manner. Introduction of Psap in highly metastatic cells significantly reduced the occurrence of metastases, whereas inhibition of Psap production by tumor cells was associated with increased metastatic frequency. In human prostate cancer, decreased Psap expression was significantly associated with metastatic tumors. Our findings suggest that prosaposin, or other agents that stimulate p53 activity in the tumor stroma, may be an effective therapy by inhibition of the metastatic process.

Introduction

The progression of human cancer to the metastatic stage is a major contributing factor to its lethality. In order for a tumor to form lethal metastases it must gain access to the vasculature or lymphatic system (intravasation), survive during transit, exit the vascular or lymphatic channels (extravasation), and proliferate at the metastatic site(1). Upon colonization of a distant tissue, tumor cells must induce neovascularization in order to grow beyond a microscopic size. In this process, heterotypic tumor-stromal signaling can affect tumor growth by regulating the production and secretion of growth-promoting and growth-inhibitory proteins by the surrounding stromal fibroblasts and endothelial cells. Thus, it has been previously demonstrated that tumor cells can stimulate expression of the pro-angiogenic protein VEGF in the surrounding stroma(2, 3), whereas the regulation of thrombospondin-1 (Tsp-1) expression one of the most potent endogenous anti-angiogenic proteins(4) in the tumor-associated stroma, has not been as well studied(5). The expression of thrombospondin-1 is positively regulated by p53 and negatively regulated by Ras and Myc, thereby placing it at a critical nexus of tumor suppressors and oncogenes(6, 7).

We report here a novel mechanism by which tumor cell secretion of Prosaposin (Psap), the precursor form of the lipid hydrolase activators saposin A, B, C, and D (8-11), inhibits the metastatic process. The expression of prosaposin was elevated in non-metastatic prostate and breast cancer cells compared to metastatic cell lines. Our findings indicate that tumor cells at the primary site secrete prosaposin, which acts at distant sites to create a non-permissive, or refractory, environment with respect to colonization by tumor cells.

Results

Tsp-1 expression in tumor cells is inversely related to metastatic potential

The initial step of metastasis is dependent on access to the vasculature or lymphatic system. We hypothesized that metastatic human tumors may differ in the relative expression of pro- and anti-angiogenic proteins compared to non-metastatic tumor cell lines. Thus, we measured the level of VEGF secretion by the weakly metastatic prostate cancer cell line PC3 and a metastatic derivative PC3M-LN4 as well as by the breast cancer cell line MDA-MB-231 and a bone-specific metastatic derivative MDA-MET. PC3M-LN4 cells metastasize to multiple organs, including lymph node, liver, lung and bone, while MDA-MET was derived to metastasize only to bone via intracardiac injection(12, 13). Notably, we determined that the highly metastatic PC3M-LN4 cells and MDA-MET cells secreted lower levels of VEGF than their parental counterparts, even under hypoxic conditions (1% O_2), as measured by ELISA (Fig. 1A). Thus, in these tumor cells VEGF expression is not correlated with increased metastatic ability.

We then turned our attention to the antiangiogenic protein Tsp-1 and observed that its levels were decreased in the metastatic cell lines compared to the parental cell lines (Fig. 1B). The non-metastatic PC3 cells expressed high levels of Tsp-1 while their metastatic PC3M-LN4 derivatives expressed no detectable Tsp-1. Consistent with the expression levels in prostate cancer cells, we observed that the weakly metastatic MDA-MB-231 breast cancer cell line also expressed 20-fold higher levels of Tsp-1 than its bone-specific metastatic derivative MDA-MET (as determined by band volume density) (Fig. 1B). These data indicate an inverse relationship between Tsp-1 expression in tumor cells and metastatic potential.

It has been demonstrated that *c-myc*, a repressor of Tsp-1, is often amplified or overexpressed in several types of human cancer, including prostate and breast cancer (7, 14-

18). Consistent with these observations we observed that levels of c-Myc were significantly lower (8-fold) in non/weakly metastatic prostate and breast cancer cells than in their metastatic derivatives (Fig. 1B). These results indicate that Tsp-1 expression inversely, and c-Myc expression directly, correlates with the metastatic potential of these cells.

Tsp-1 expression in primary tumor stroma is inversely related to metastatic potential

In order to determine whether levels of Tsp-1 observed *in vitro* are indicative of the expression levels *in vivo* and of metastatic frequency, we injected PC3 and PC3M-LN4 cells orthotopically into prostate glands of SCID mice. Strong Tsp-1 staining by immunohistochemistry was observed in the fibrous stroma surrounding invading tumor cells in 14 out of 17 PC3 tumors (Fig. 1C and H) but in only one out of 16 highly metastatic PC3M-LN4 prostate tumors ($p<0.00001$, Fisher's exact test) (Fig. 1C and H). Significantly, the expression of two other antiangiogenic proteins, Thrombospondin-2 (Tsp-2) and Endostatin, revealed no elevation in PC3 primary tumors relative to normal tissue by western blot analysis (Fig. S1).

Consistent with the immunohistochemistry results, 4 of 5 PC3 tumors expressed high levels of Tsp-1 and low/undectectable levels of c-Myc by western blot (Fig. 1D). Conversely, four out of four representative PC3M-LN4 tumors expressed between 5- and 8- fold lower levels of Tsp-1 and between 4- and 7-fold higher levels of c-Myc (Fig. 1D). Strikingly, one of the PC3 tumors that metastasized expressed 10-fold lower levels of Tsp-1 and 8-fold higher levels of c-Myc by western blot (Fig. 1D; P5, 1Cand F).

In keeping with our *in vitro* observations, we observed that 4 out of 5 PC3 tumors sampled contained between 10- and 20-fold higher levels of stromal (murine) VEGF than the 4 sampled tumors formed by the PC3M-LN4 cells, as measured by ELISA (Fig. 1E). Notably, the one metastatic PC3 tumor that expressed levels of VEGF similar to the PC3M-LN4 tumors also expressed low levels of Tsp-1 as determined by immunohistochemistry and western blot (Fig. 1C and E; LN4-1). When taken together these results suggest that tumor cells may acquire metastatic ability by repressing the expression of Tsp-1 without the need for a concomitant increase in VEGF production.

Tsp-1 expression in distal tissues is inversely related to metastases

We then analyzed the lungs from mice injected orthotopically with PC3 or PC3M-LN4 cells. As determined by H&E analyses, 6 weeks post-injection, the PC3M-LN4 cells formed metastases with much greater efficiency than the parental PC3 cells; 10/16 mice injected with PC3M-LN4 cells had detectable micrometastatic colonies in their lungs while only 2/17 mice injected with PC3 cells had detectable micrometastases ($p<0.003$, Fisher's exact test) (Fig. 1F). Large lymph node metastases were detected in 12/16 mice injected with PC3M-LN4 cells, while only the two out of 17 PC3 tumors that metastasized to the lung also metastasized to lymph nodes (Fig. 1H).

By combining all cases with PC3 and PC3M-LN4 tumors, there was a statistically highly significant inverse association between Tsp-1 expression in the tumor stroma and frequency of lung metastases ($p<0.0005$, Fisher's exact test), suggesting that low stromal Tsp-1 expression at the primary site is an indicator of metastatic potential (Fig. 1C, E and H).

By immunohistochemistry we observed that the lung metastases formed by PC3M-LN4 cells, as well as the 2 rare PC3 metastases, contained very low to undetectable levels of Tsp-1 (Fig. 1F; LN4-1, PC3-5 (see inset)). We then examined the lung tissue of mice

harboring PC3 or PC3M-LN4 tumors for Tsp-1 expression by western blot analysis and determined that the mice bearing PC3 tumors had 6-fold greater levels of Tsp-1 in the lung (Fig. 1G). Conversely, the highly metastatic PC3M-LN4 tumors actually repressed the expression of Tsp-1 in the lung by 3-fold. These observations provided the first suggestion that PC3 tumors secrete a protein that not only stimulates Tsp-1 in a paracrine fashion in the stroma of the primary tumor but also stimulates Tsp-1 expression in distal tissues via systemic (endocrine) signaling, a mechanism that is described in more detail below.

Effects of tumor cells on fibroblasts *in vitro*

We sought to determine whether the stimulation of stromal Tsp-1 by human tumor cells could be recapitulated *in vitro*. Treatment of prostate and mammary fibroblasts, in culture, with conditioned media from non-metastatic PC3 prostate or MDA-MB-231 breast cancer cell lines, respectively, stimulated the production of Tsp-1 expression by these fibroblasts 4-fold (Fig. 1Iand J). Conversely, treatment of prostate fibroblasts with conditioned media from the metastastic PC3M-LN4 line resulted in a 3-fold suppression of Tsp-1 protein expression (Fig. 1I).

We noted that conditioned media from the non/weakly metastatic MDA-MB-231 breast cancer cells as well as the “metastatic” derivatives MDA-MET cells stimulated Tsp-1 expression in mammary fibroblasts (Fig. 1J). However, it should be noted that the MDA-MET cells do not metastasize from orthotopic sites of injection (mammary fat pad) but do so only following intracardiac injection. When co-cultured with mammary fibroblasts in a transwell apparatus, the MDA-MET cells no longer stimulated Tsp-1 production in the fibroblasts, while the parental MDA-MB-231 cells continued to do so (Fig. 1J). Thus, the inability to repress Tsp-1 in mammary fibroblasts is consistent with their inability to metastasize from the orthotopic site. When taken together these data indicate that weakly metastatic tumor cell produce a secreted factor that stimulates the expression of Tsp-1 in the surrounding stromal fibroblasts.

Identification of Prosaposin as a Tsp-1 and p53 stimulating protein

In order to determine the mechanism by which weakly metastatic PC3 cells were able to stimulate the expression of Tsp-1 in stromal fibroblasts, we undertook a proteomic analysis of the proteins secreted by PC3 cells *in vitro*. Thus, we treated both prostate and lung fibroblasts with PC3-conditioned media fractionated over a heparin-Cu^{2+} sepharose column and analyzed Tsp-1 expression by western blot analysis(19). We observed that three fractions, eluting between 0.8 and 0.9M NaCl in the presence of 10mM imidazole, contained an activity that stimulated Tsp-1 expression between 3- and 4.5-fold in prostate and lung fibroblasts, respectively (Fig. 2A and B).

Liquid chromatography/mass spectrometry (LC/MS) analysis revealed that only two proteins were common between the active fractions, prosaposin and alpha-2HS-glycoprotein (fetuin A) (Table S1). Western blot analysis of cell lysates and conditioned media from both PC3 and PC3M-LN4 cells revealed that prosaposin (Psap), was expressed at ~10-fold higher levels in the non-metastatic PC3 cells than in their metastatic derivatives PC3M-LN4 cells (Fig. 2C), while there was no significant difference between the two cell populations in fetuin A expression levels (data not shown). Metastatic derivatives of the MDA-MB-231 cell line, derived to metastasize to bone, brain and lung, also expressed between 4- and 10-fold lower levels of Psap (Fig. 2D) than did the parental, weakly metastatic, MDA-MB-231 cells.

Moreover, the relative protein levels of prosaposin secreted into the conditioned media by these cells were similar to the relative levels present in the respective cell lysates, as determined by western blot analysis (Fig 2E).

In order to determine the mechanism by which prosaposin regulates stromal Tsp-1, we turned our attention to the tumor suppressor p53, as it has been demonstrated to be a transcriptional activator of Tsp-1 in human fibroblasts(6). Both PC3 and PC3M-LN4 contain deletion mutations in the p53 gene(20), resulting in the absence of detectable p53 protein in both cell lines(20). Our analyses of PC3 and PC3M-LN4 prostate tumor xenografts revealed that of 7 cases with strong Tsp-1 staining, 6 cases had strong stromal p53 staining. Correspondingly, of 7 cases with weak or negative Tsp-1 staining, 6 cases had negative/weak p53 staining ($p=0.015$, Fisher's exact test, one-sided) (Fig. 2F). Consistent with the immunohistochemical observations, western blot analysis revealed that p53 expression was markedly elevated in the tumor stroma of the PC3 primary tumors but undetectable in the tumors formed by their PC3M-LN4 derivatives (Fig. 2G). We also observed that p53 expression was stimulated in the proximal lumbar lymph nodes from mice bearing PC3 tumors despite the fact that there were no lymph node metastases, as determined by H&E and pan-cytokeratin staining. In contrast, lymph nodes from mice bearing PC3M-LN4 tumors expressed p53 at levels similar to normal lymph nodes (Fig. 2H).

Consistent with the *in vivo* results, PC3-conditioned media stimulated p53 protein levels in prostate fibroblasts by 4-fold, while PC3M-LN4 conditioned media induced a modest repression of p53 in prostate fibroblasts (1.8-fold) (Fig. 2I). Hence, in parallel with earlier analyses of Tsp-1 expression, non-metastatic cells induced p53 levels while metastatic cells caused their repression. In light of the known effects of p53 as a transcriptional activator of Tsp-1 these results suggested that prosaposin acted on stromal fibroblasts via its ability to induce p53 expression and the consequent induction of Tsp-1 expression. Accordingly, we silenced p53 expression in prostate fibroblasts via lentiviral transduction of a short-hairpin RNA (shRNA) *period.* We observed that this shRNA succeeded in suppressing p53 expression by >95%. Notably, conditioned media from PC3 cells completely failed to stimulate Tsp-1 expression in fibroblasts in which p53 had been silenced (Fig. 2J). These results demonstrate that stimulation of Tsp-1 in fibroblasts by PC3 cells is dependent on induction of p53-dependent synthesis in the fibroblasts.

To determine whether Prosaposin production by the PC3 cells was the protein responsible for stimulating p53 synthesis in the stromal fibroblasts and, consequentlyTsp-1 expression by the latter, we transduced PC3 cells with lentiviral constructs specifying three different shRNAs targeted to Psap (Fig. 2K). Western blot analysis revealed that the conditioned media from these cell populations no longer stimulated either p53 or Tsp-1 in prostate and lung fibroblasts, while Tsp-1 levels in the transduced tumor cells remained unchanged (Fig. 2K, L, and M). Hence, Psap production by the cancer cells was necessary for Tsp-1 induction in the stromal fibroblasts,

In order to determine whether prosaposin was necessary and sufficient for the stimulation of Tsp-1, we transduced the metastastic PC3M-LN4 cells with a retroviral construct specifying Psap (Fig. 2N). The resultant cells expressed 15-fold higher levels of prosaposin than the parental PC3M-LN4 cells. Treatment of normal human prostate fibroblasts with conditioned media from these Psap-overexpressing PC3M-LN4 cells reversed their normal ability to repress p53 and Tsp-1 (Fig. 2O); hence, Psap expression by the cancer cells was sufficient to block the induction of p53 and Tsp-1 in stromal fibroblasts. Finally, we

purified a 6x-HN-tagged version of Prosaposin. Treatment of prostate fibroblasts with purified Prosaposin resulted in the stimulation of p53 and Tsp-1 expression (4.6- and 7.9-fold, respectively), further confirming that Prosaposin sufficed, on its own, to elicit the previously observed increase in Tsp-1 expression (Fig. 2P). These data confirmed that Psap stimulates p53 expression and as a result induces the stimulation of Tsp-1 expression.

Prosaposin expression is negatively regulated by Myc

We found that PC3 cells express lower levels of Myc than their metastatic derivative PC3M-LN4. Additionally, a ChIP based mapping study of Myc binding sites identified the Prosaposin promoter as a Myc binding target(21). To examine the possibility that Myc is a negative regulator of Prosaposin, we transduced PC3 cells with a retroviral construct specifying a Myc-Estrogen Receptor (ER) fusion protein, which is activated upon administration of 4-hydroxy-tamoxifen (4-HT)(22). Upon treatment of PC3-MycER cells with 4-HT for 12 hours, and the resulting induction of Myc function, we observed a significant reduction (4-fold) in Psap levels (Fig. 3A). Furthermore, conditioned media from the 4-HT-treated PC3MycER cells failed to stimulate the expression of either p53 or Tsp-1 in prostate or lung fibroblasts, while conditioned media from untreated PC3MycER cells stimulated both p53 and Tsp-1 expression in these two cell types (Fig. 3B).

We further explored the connection between Myc and Psap by silencing Myc expression in PC3M-LN4 cells via lentiviral transduction of an shRNA construct specific for *c-myc*. We identified two shRNA sequences directed against Myc that yielded significant knockdown of Myc protein expression (4- and 8-fold, respectively) (Fig. 3C). Indeed, these two cell lines expressed higher levels (3- and 6-fold, respectively) of Psap than PC3M-LN4 cells, as determined by western blot analysis (Fig. 3D). We also determined that, consistent with Psap overexpression, conditioned media from the PC3M-LN4shMyc cells no longer repressed Tsp-1 expression in lung and prostate fibroblasts (Fig. 3E). Taken together these data indicate that Myc is a negative regulator of Psap expression in these tumor cells.

Prosaposin inhibits tumor metastasis

We speculated that Psap might inhibit the metastatic potential of PC3 cells *in vivo*, given its ability to stimulate p53 and Tsp-1 expression in prostate and lung fibroblasts. To test this hypothesis, we injected $2x10^6$ PC3shPsap cells (Fig. 2J; #3) and independently, PC3pLKO empty vector control cells, into the prostate glands of SCID mice. We observed that 6 of 7 tumors formed by PC3shPsap cells gave rise to large lymph node metastases (as denoted by a "*" in Fig. 5f) whereas zero of 8 tumors generated from PC3pLKO cells gave rise to metastases (p=0.001, Fisher's exact test) (Fig. 4A-E). Significantly, the tumors that arose from PC3shPsap cells formed metastases with a similar frequency to PC3M-LN4 cells (6/7 versus 12/15), albeit with increased latency of ~7-8 weeks as compared to ~5 weeks. Of note, although one of the shPsap tumors grew significantly larger than the PC3pLKO tumors, three of the smaller shPsap tumors (Fig. 4F, #4, 5, and 7), which grew to approximately the same size as the PC3pLKO control tumors, formed visible lymph node metastases (Fig. 4D). Lung metastases were infrequent events, with only 2 out of 7 PC3shpsap tumors displaying detectable metastases by histological examination, compared to 2/17 for PC3 (p=0.006, by Fisher's exact test). These data indicate that reduction of Psap expression, achieved in this instance by use of an shRNA, significantly potentiated the ability of otherwise non-metastatic tumor cells to form lymph node metastases.

Immunohistochemical analysis of p53 and Tsp-1 expression in the primary tumors formed by PC3 and PC3shPsap tumors revealed that p53 expression in the tumor-associated stromal cells of PC3shPsap tumors was completely negative (n=4) (Fig. 4G), in contrast to the stroma of control PC3 tumors in which p53 expression was strongly positive., in contrast to the stong staining in PC3 tumors, most PC3shPsap tumors were weak or negative for Tsp-1 staining within the central parts of the tumors, whereas occasional moderate staining was observed in the periphery, corresponding to the invasive border, but independent of p53 expression (observed in 4 of 10 cases examined) (Fig. 4G). These results were supported by western blot analysis of the tumors formed by PC3shPsap cells, which revealed no stimulation of either p53 or Tsp-1 in the tumor stroma or in the lung or lymph nodes (Fig. 4H-J).

To confirm the ability of prosaposin to inhibit tumor metastasis, we overexpressed the protein in PC3M-LN4 cells (Fig. 2M) and injected $2x10^6$ cells orthotopically in the prostate gland of SCID mice. After 5-6 weeks, the mice were examined visually for the presence of macrometastases as well as histologically and immunohistochemically (by staining for pan-Cytokeratin expression) for the presence of micrometastases. The sizes of the Psap-expressing tumors were similar to those of the PC3M-LN4 tumors (Fig. 4K). We detected lung metastases (denoted by "*" in Fig. 4K) in 2 out of 10 mice injected with PC3M-LN4-psap cells, compared to 10 out of 16 injected with PC3M-LN4 cells (p=0.042, Fisher's exact test).

Immunohistochemical analysis revealed that the PC3M-LN4-psap tumors expressed markedly higher levels of prosaposin than the parental PC3M-LN4 tumors and even higher levels than the PC3 tumors (Fig. 4L). Strikingly the two lung metastases formed by PC3M-LN4-Psap cells also expressed moderate levels of prosaposin (Fig. 5l). As expected, by western blot analysis, the 8 tumors that failed to form metastases expressed between 3- and 6-fold, and 6- and 8-fold higher levels of Tsp-1 in the primary tumors and lung tissue, respectively (Fig. 4M and N). Notably, despite the moderate levels of Psap expression, the 2 tumors that formed metastases expressed similarly low levels of Tsp-1 and p53 in both the primary tumors and lung tissue as the PC3M-LN4 tumors (Fig. 4M and N). These findings suggest that these tumors were able to compensate for the increased expression of Psap, perhaps by increasing the expression of a protein that represses Tsp-1 and p53 in the stroma.

The ability of prosaposin to stimulate the expression of p53 and Tsp-1 in distal tissues indicates that its ability to repress metastasis is a function of both paracrine and endocrine signaling mechanisms.

Tsp-1 expression is required for Prosaposin-mediated suppression of metastasis

We wished to determine whether Tsp-1 expression was required for Prosaposin-mediated suppression of lung metastasis *in vivo* and thus made use of Tsp-$1^{-/-}$ mice(23). We also took advantage of observations that Prosaposin could act systemically to influence the levels of both Tsp-1 and p53 in distant organs (Fig. 4I and J, Fig. S2). Accordingly We injected both wild-type and Tsp-$1^{-/-}$ C57BL/6J mice intraperitoneally with RPMI media or conditioned media from PC3pLKO or PC3shPsap cells daily for 10 days. On the tenth day, we injected $1x10^6$ syngeneic Lewis Lung Carcinoma (LLC) cells via tail vein into wild-type and Tsp-$1^{-/-}$ mice, treated as described above.

The lungs of wild-type mice treated with RPMI alone or PC3shPsap conditioned media contained an average of ~30 metastatic colonies per lung (Fig. 5A and B). Strikingly, we

observed that the lungs of wild-type mice treated with PC3pLKO-conditioned media contained, on average less than 2 metastatic colonies, ~15-fold fewer than control media- or PC3shpsap conditioned media treated mice ($p<0.003$, Wilcoxon unpaired exact test) (Fig. 5A and B). These findings indicate that Prosaposin can actively suppress metastasis formation.

We observed that Psap had no effect on the ability of LLC cells to form metastases in the lungs of *tsp-1*$^{-/-}$ mice (Fig. 5A and B). Hence, in the absence of Tsp-1 production in the lung, Psap failed to suppress metastasis formation by LLC cells. The observed lower numbers of metastases in the Tsp-1 KO mice compared with their wild-type counterparts could be explained by a compensatory 4.5-fold increase in Tsp-2 production induced by LLC cells in these mice, a phenomenon not observed in wild-type mice or human tumors (Fig. S3 and S4).

Reduced expression of Prosaposin is associated with metastases and disease progression in human prostate cancer

We extended these observations by assessing Prosaposin expression in metastatic versus localized human prostate cancer. As such we analyzed a gene expression data set gathered from 55 patients consisting of normal prostate (5), benign prostatic hyperplasia (BPH) (13), localized primary prostate tumors (18) and primary prostate tumors that formed metatastases in the patients (19)(24). Consistent with the xenograft experiments, the relative *psap*, *tsp-1* and *p53* mRNA expression were ~40%, 50% and 30% lower, on average, respectively in the metastatic tumors as compared with localized primary tumors ($p<0.0001$ by ANOVA) (Fig. 5C-E). These data support the results obtained experimentally and demonstrate that in metastatic human prostate cancer, the expression of Prosaposin is reduced compared to non-metastatic tumors.

Discussion

The hypothesis that tumors metastasize to sites that are permissive(25-29), or compatible, was first proposed by Stephen Paget over 100 years ago. We sought to determine whether tumor-secreted factors render distant organs refractory to metastatic colonization, and that a permissive balance between metastatic *seed* and organ *soil* may be influenced by tumor secreted factors in potential metastatic sites. In confirmation of our hypothesis, we observed that tumors formed by a weakly metastatic prostate cancer cell line (PC3) stimulated the expression of Tsp-1 in the stroma of primary tumors as well as in distant organs. In contrast, tumors formed by the highly metastatic PC3M-LN4 cell line expressed low levels of Tsp-1 in the tumor-associated stroma, indicating that high levels of Tsp-1 in the primary tumors and in potential metastatic organs represent a potent barrier to metastasis. Moreover, we find that stromal Tsp-1 expression is regulated by signals released from the tumor cells.

We demonstrate that prosaposin suppresses tumor metastasis by stimulating the expression of p53 and, consequently, Tsp-1 in a paracrine fashion in tumor-associated stromal fibroblasts and in an endocrine fashion in fibroblasts in lymph nodes and lungs. From previous studies, prosaposin (56kDa) is known to be proteolytically cleaved in the lysosome into four Saposins A-D(30), and these proteins function as cofactors for sphingolipid hydrolases(10, 11). Whereas Psap contains a signal sequence that mediates its secretion into the extracellular space(31), its role as an extracellular protein has not been determined. In relation to the prostate, the Psap-encoding gene is amplified in a subset of prostate

cancers, but there have been no studies on the regulation of its expression(32). Also, Saposin C has been found to stimulate the proliferation of prostate fibroblasts and to have neurotrophic activity(33, 34).

We have determined that the expression of Psap is not only reduced in metastatic prostate and breast cancer cell lines, but also in metastatic human prostate tumors (24). Significantly, these data suggest that repression of Psap expression may be a mechanism to enhance tumor metastasis, and may, along with increased Myc expression, comprise a "metastatic switch".

The observation that repression of Psap expression results in the formation of lymph node metastases, accompanied by decreased Tsp-1 expression in the nodes themselves, is somewhat surprising as lymphangiogenesis and lymph node metastases have been demonstrated not to be affected by Tsp-1 in a murine model of skin cancer(35). Thus, it is possible that Tsp-1 inhibits lymphangiogenesis in prostate cancer, but not skin cancer, or that Psap induces the expression of an as yet unidentified inhibitor of lymphangiogenesis. Further studies into the mechanism of Psap stimulation of stromal p53 and Tsp-1 expression may provide novel therapeutic targets that could prevent the metastatic spread of human prostate and breast tumors. Recently, several reports have demonstrated that restoration of p53 activity in murine tumor models leads to rapid tumor regression(36-39). Based on our observations, we propose that activation of stromal p53 may also be a possible strategy to limit and perhaps cause regression of tumor growth and metastasis.

Methods Summary

Tail vein metastasis

Wild-type and Tsp-$1^{-/-}$ C57BL/6J mice were pretreated with 500μL of serum-free conditioned media from PC3 or PC3shPsap cells or serum-free RPMI media for 10 days via intraperitoneal (i.p.) injection. On the 10^{th} day we injected via tail vein mice with $1x10^6$ Lewis Lung Carcinoma cells. Subsequently, i.p. injections of serum-free tumor cell conditioned media or control RPMI were performed for 19 additional days. Following sacrifice, the lungs were photographed and the number of macrometastatic nodules were counted.

Acknowledgements

We thank J. Folkman†, R. Weinberg, B. Zetter, M. Klagsbrun, M. Moses and R. Rodriguez for helpful discussions and insights. The authors also wish to thank Mrs. Gerd Lillian Hallseth and Mr. Bendik Nordanger for excellent technical assistance. We also thank I. Fidler, L. Suva, M. Rosenblatt, K. Polyak and J. Massague for cell lines. We thank Judah Folkman and George Naumov for supplying the Tsp-$1^{-/-}$ mice. We thank Arul Chinnaiyan and the Oncomine website for access to microarray expression data derived from primary human prostate cancer samples. L.A.A. is supported by grants from the Norwegian Research Council, the Norwegian Cancer Society, the Helse Vest Research Fund and the Unger Vetlesen Research Fund. R.S.W is supported by the Gackstatter Foundation, a grant from NASA, and Department of Defense Breast Cancer Innovator Award #W81XWH-04-1-0316.

References

1. Fidler IJ (2003) The pathogenesis of cancer metastasis: the 'seed and soil' hypothesis revisited. *Nat Rev Cancer* 3(6):453-458.
2. Fukumura D*, et al.* (1998) Tumor induction of VEGF promoter activity in stromal cells. *Cell* 94(6):715-725.
3. Dong J*, et al.* (2004) VEGF-null cells require PDGFR alpha signaling-mediated stromal fibroblast recruitment for tumorigenesis. *Embo J* 23(14):2800-2810.
4. Lawler J (2002) Thrombospondin-1 as an endogenous inhibitor of angiogenesis and tumor growth. (Translated from eng) *J Cell Mol Med* 6(1):1-12 (in eng).
5. Kalas W*, et al.* (2005) Oncogenes and Angiogenesis: down-regulation of thrombospondin-1 in normal fibroblasts exposed to factors from cancer cells harboring mutant ras. (Translated from eng) *Cancer Res* 65(19):8878-8886 (in eng).
6. Dameron KM, Volpert OV, Tainsky MA, & Bouck N (1994) Control of angiogenesis in fibroblasts by p53 regulation of thrombospondin-1. *Science* 265(5178):1582-1584.
7. Watnick RS, Cheng YN, Rangarajan A, Ince TA, & Weinberg RA (2003) Ras modulates Myc activity to repress thrombospondin-1 expression and increase tumor angiogenesis. (Translated from eng) *Cancer Cell* 3(3):219-231 (in eng).
8. Sano A*, et al.* (1989) Sphingolipid hydrolase activator proteins and their precursors. (Translated from eng) *Biochem Biophys Res Commun* 165(3):1191-1197 (in eng).
9. Sylvester SR, Morales C, Oko R, & Griswold MD (1989) Sulfated glycoprotein-1 (saposin precursor) in the reproductive tract of the male rat. (Translated from eng) *Biol Reprod* 41(5):941-948 (in eng).
10. Morimoto S*, et al.* (1989) Saposin A: second cerebrosidase activator protein. *Proc Natl Acad Sci U S A* 86(9):3389-3393.
11. Morimoto S, Martin BM, Kishimoto Y, & O'Brien JS (1988) Saposin D: a sphingomyelinase activator. (Translated from eng) *Biochem Biophys Res Commun* 156(1):403-410 (in eng).
12. Pettaway CA*, et al.* (1996) Selection of highly metastatic variants of different human prostatic carcinomas using orthotopic implantation in nude mice. *Clinical Cancer Research : An Official Journal of the American Association For Cancer Research* 2(9):1627-1636.
13. Bendre MS*, et al.* (2002) Expression of interleukin 8 and not parathyroid hormone-related protein by human breast cancer cells correlates with bone metastasis in vivo. *Cancer Res* 62(19):5571-5579.

14. Nag A & Smith RG (1989) Amplification, rearrangement, and elevated expression of c-myc in the human prostatic carcinoma cell line LNCaP. *The Prostate* 15(2):115-122.
15. Escot C*, et al.* (1986) Genetic alteration of the c-myc protooncogene (MYC) in human primary breast carcinomas. *Proceedings of the National Academy of Sciences of the United States of America* 83(13):4834-4838.
16. Janz A, Sevignani C, Kenyon K, Ngo CV, & Thomas_Tikhonenko A (2000) Activation of the myc oncoprotein leads to increased turnover of thrombospondin-1 mRNA. *Nucleic Acids Research (Online)* 28(11):2268-2275.
17. Ngo CV*, et al.* (2000) An in vivo function for the transforming Myc protein: elicitation of the angiogenic phenotype. *Cell Growth & Differentiation : the Molecular Biology Journal of the American Association For Cancer Research* 11(4).
18. Tikhonenko AT, Black DJ, & Linial ML (1996) Viral Myc oncoproteins in infected fibroblasts down-modulate thrombospondin-1, a possible tumor suppressor gene. *Journal of Biological Chemistry* 271(48):30741-30747.
19. Shing Y (1988) Heparin-copper biaffinity chromatography of fibroblast growth factors. *J Biol Chem* 263(18):9059-9062.
20. Isaacs WB, Carter BS, & Ewing CM (1991) Wild-type p53 suppresses growth of human prostate cancer cells containing mutant p53 alleles. *Cancer Res* 51(17):4716-4720.
21. Fernandez PC*, et al.* (2003) Genomic targets of the human c-Myc protein. *Genes Dev* 17(9):1115-1129.
22. Littlewood TD, Hancock DC, Danielian PS, Parker MG, & Evan GI (1995) A modified oestrogen receptor ligand-binding domain as an improved switch for the regulation of heterologous proteins. *Nucleic Acids Research (Online)* 23(10):1686-1690.
23. Lawler J*, et al.* (1998) Thrombospondin-1 is required for normal murine pulmonary homeostasis and its absence causes pneumonia. (Translated from eng) *J Clin Invest* 101(5):982-992 (in eng).
24. Dhanasekaran SM*, et al.* (2001) Delineation of prognostic biomarkers in prostate cancer. *Nature* 412(6849):822-826.
25. Gao D*, et al.* (2008) Endothelial progenitor cells control the angiogenic switch in mouse lung metastasis. *Science* 319(5860):195-198.
26. Gupta GP*, et al.* (2007) Mediators of vascular remodelling co-opted for sequential steps in lung metastasis. *Nature* 446(7137):765-770.
27. Kaplan RN*, et al.* (2005) VEGFR1-positive haematopoietic bone marrow progenitors initiate the pre-metastatic niche. *Nature* 438(7069):820-827.
28. McAllister SS*, et al.* (2008) Systemic endocrine instigation of indolent tumor growth requires osteopontin. *Cell* 133(6):994-1005.

29. Padua D*, et al.* (2008) TGFbeta primes breast tumors for lung metastasis seeding through angiopoietin-like 4. (Translated from eng) *Cell* 133(1):66-77 (in eng).
30. O'Brien JS & Kishimoto Y (1991) Saposin proteins: structure, function, and role in human lysosomal storage disorders. *FASEB J* 5(3):301-308.
31. Hineno T*, et al.* (1991) Secretion of sphingolipid hydrolase activator precursor, prosaposin. *Biochem Biophys Res Commun* 176(2):668-674.
32. Koochekpour S*, et al.* (2005) Amplification and overexpression of prosaposin in prostate cancer. *Genes Chromosomes Cancer* 44(4):351-364.
33. Hiraiwa M, Taylor EM, Campana WM, Darin SJ, & O'Brien JS (1997) Cell death prevention, mitogen-activated protein kinase stimulation, and increased sulfatide concentrations in Schwann cells and oligodendrocytes by prosaposin and prosaptides. *Proc Natl Acad Sci U S A* 94(9):4778-4781.
34. Lee TJ, Sartor O, Luftig RB, & Koochekpour S (2004) Saposin C promotes survival and prevents apoptosis via PI3K/Akt-dependent pathway in prostate cancer cells. *Mol Cancer* 3:31-44.
35. Hawighorst T*, et al.* (2002) Thrombospondin-1 selectively inhibits early-stage carcinogenesis and angiogenesis but not tumor lymphangiogenesis and lymphatic metastasis in transgenic mice. *Oncogene* 21(52):7945-7956.
36. Vassilev LT*, et al.* (2004) In vivo activation of the p53 pathway by small-molecule antagonists of MDM2. *Science* 303(5659):844-848.
37. Martins CP, Brown-Swigart L, & Evan GI (2006) Modeling the therapeutic efficacy of p53 restoration in tumors. *Cell* 127(7):1323-1334.
38. Ventura A*, et al.* (2007) Restoration of p53 function leads to tumour regression in vivo. *Nature* 445(7128):661-665.
39. Xue W*, et al.* (2007) Senescence and tumour clearance is triggered by p53 restoration in murine liver carcinomas. *Nature* 445(7128):656-660.

Figure Legends

Fig. 1.

(A) ELISA of VEGF secretion by PC3 and PC3M-LN4 (LN4) prostate cancer cells and MDA-MB-231 (231) and MDA-MET (MET) breast cancer cells cultured under 20% oxygen (normoxia) or 1% oxygen (hypoxia). Error bars represent SEM (Standard Error of Mean) of 3 independent experiments performed in triplicate);

(B) Western blot analysis of Tsp-1, c-Myc and β–Actin expression by PC3, PC3M-LN4 (LN4), MDA-MB-231 (231) and MDA-MET (MET) cells;

(C) H&E and Tsp-1 immunohistochemistry of PC3 and PC3M-LN4 prostate tumors. Strong and weak stromal Tsp-1 expression (right panel) in non-metastatic (PC3-1, LN4-9) and metastatic (PC3-5, LN4-1) prostate tumors, respectively. Scale bar 100μm;

(D) Western blot analysis of Tsp-1, c-Myc, and β-Actin expression in prostate tumors formed by PC3 (P1-P5) and PC3M-LN4 (L1-L4) cells;

(E) ELISA of VEGF secretion from murine stromal cells present in PC3 (1-5) and PC3M-LN4 (6-9) prostate tumors;

(F) H&E and Tsp-1 immunohistochemical analyses of lung tissue from mice bearing non-metastatic (PC3-1, LN4-9) and metastatic (PC3-5, LN4-1) primary prostate tumors. Micrometastases in the lung tissue are denoted by arrows and magnified in insets. Scale bar 100μm (inset x 265);

(G) Western blot analysis of Tsp-1 and β-Actin expression in lung tissue of normal mice (N), mice bearing PC3 tumors (P1, P2) and mice bearing PC3M-LN4 tumors (L1, L2)

(H) Tabular depiction of Tsp-1 expression (high vs. low) in primary tumors formed by PC3 and PC3M-LN4 cells and the incidence of metastases in mice bearing these tumors.

(I) Western blot analyses of Tsp-1, c-Myc and β–Actin expression in prostate fibroblasts that were untreated (-) or treated with the conditioned media from PC3, or PC3M-LN4 (LN4) cells;

(J) Western blot analyses of Tsp-1 and β–Actin expression in normal human mammary fibroblasts that were untreated (-) or treated with the conditioned media (CM) from MDA-MB-231 (231) and MDA-MET (MET) cells; and,

Fig. 2.

(A) Western blot analyses of Tsp-1 and β-actin expression in prostate fibroblasts treated with fractions of conditioned media from PC3 cells eluted from a Cu^{2+}-heparin column;

(B) Western blot analyses of Tsp-1 and β-actin expression in WI 38 lung fibroblasts treated with fractions of conditioned media from PC3 cells eluted from a Cu^{2+}-heparin column;

(C) Western blot analyses of Psap and β-actin expression in PC3 and PC3M-LN4 (LN4) cells;

(D) Western blot analyses of Psap and β-actin expression in weakly metastatic MDA-MB-231 breast cancer cells (231), and its metastatic derivatives: MDA-Bone (Bone), MDA-Brain (Brain), MDA-MB-LM2-4 (LM), MDA-MET (MET), MDA-MB-231-1833

(bone) (1833) and MDA-MB-LM2-4175 (lung) (4175) cells;

(E) Western blot analyses of Psap expression in the conditioned media of MDA-MB-231 (231), MDA-Bone (Bone), MDA-Brain (Brain), MDA-MB-LM2-4 (LM), MDA-MET (MET), MDA-MB-231-1833 (1833) MDA-MB-LM2-4175 (4175), PC3 and PC3M-LN4 (LN4) cells;

(F) Immunohistochemical analysis of p53 expression in PC3 and PC3M-LN4 (LN4) tumors, where arrows indicate nuclei of stromal fibroblasts that are p53 positive in PC3 tumors and p53 negative in PC3M-LN4 tumors; scale bar 250μM;

(G) Western blot analyses of p53 and β–Actin expression in prostate tissue from non-tumor bearing mice (N), PC3 prostate tumor tissue (P) and PC3M-LN4 prostate tumor tissue (L);

(H) Western blot analyses of p53 and β–Actin expression in normal lymph node tissue (N), lymph node tissue from PC3 tumor bearing mice (P) and lymph node metastases from PC3M-LN4 tumor bearing mice (L);

(I) Western blot analyses of p53 and β–Actin expression in prostate fibroblasts that were untreated (-) or treated with the conditioned media from PC3 or PC3M-LN4 (LN4) cells;

(J) Western blot analyses of Tsp-1, p53 and β–Actin expression in prostate fibroblasts containing empty pLKO vector, (V) or p53 shRNA that were untreated (-) or treated with the conditioned media from PC3 or PC3M-LN4 (LN4) cells;

(K) Western blot analyses of Tsp-1, Psap and β-actin expression in PC3 cells transduced with three shRNA constructs specific for Psap (sh1-3) or an empty pLKO vector (V);

(L) Western blot analyses of Tsp-1, p53 and β-actin expression in prostate fibroblasts treated with conditioned media (CM) from pLKO vector transduced PC3 (V), and PC3 cells transduced with the shRNA sequences specific for *psap* (sh1-sh3);

(M) Western blot analyses of Tsp-1, p53 and β-actin expression in WI 38 lung fibroblasts treated with conditioned media (CM) from pLKO vector transduced PC3 (V), and PC3 cells transduced with the shRNA sequences specific for *psap* (sh1-sh3);

(N) Western blot analyses of Psap and β-actin expression in PC3M-LN4 cells that were transduced with control pLNCX vector (LN4) or pLNCX-Psap (Psap);

(O) Western blot analyses of Tsp-1, p53 and β-actin expression in untreated prostate fibroblasts (-), or treated with conditioned media (CM) from PC3M-LN4 (LN4), PC3M-LN4-pLNCX (V) or PC3M-LN4-Psap (LN4-PS) cells; and,

(P) Western blot analyses of Tsp-1, p53 and β-actin expression in prostate fibroblasts that were untreated (-), or treated with 5μg of purified recombinant human Psap.

Fig. 3.

(A) Western blot analyses of Psap and β-actin expression in pBabepuro vector transduced PC3 (V) or PC3-MycER cells (MycER) that were untreated (-) or treated with 4-HT (+);

(B) Western blot analyses of Tsp-1, p53 and β-actin expression in prostate fibroblasts and WI 38 lung fibroblasts that were untreated (-), treated with 4-HT alone (+) or treated with the conditioned media (CM) from PC3-MycER cells (MycER) in the presence or absence of 4-HT treatment;

(C) Western blot analyses of Myc and β-actin expression in wild-type PC3M-LN4 cells (-), as well as PC3M-LN4 cells lentivirally transduced with empty pLKO vector (V) or

transduced with pLKO specifying two different shRNA sequences for Myc (sh1, sh2);
(D) Western blot analyses of Psap and β-actin expression in PC3M-LN4 cells containing empty pLKO vector (V) or expressing two different shRNA sequences for Myc (sh1, sh2);
(E) Western blot analyses of Tsp-1, p53 and β-actin expression in prostate fibroblasts and WI 38 lung fibroblasts that were untreated (-) or treated with the conditioned media (CM) from PC3M-LN4-shMyc cells (sh1);

Fig. 4.
Photographs of:
(A) SCID mouse bearing primary prostate tumor (xenograft) and distal metastases formed by PC3-shPsap cells (black arrow indicates primary prostate tumor, green arrows indicate lymph node metastases);
(B) SCID mouse bearing primary tumor formed by PC3pLKO cells (arrow indicates primary prostate tumor);
(C) Primary prostate tumor formed by PC3shPsap cells (scale bar=0.5cm);
(D) Lumbar lymph node metastases formed by PC3shPsap cells (scale bar=0.5cm);
(E) Primary prostate tumor formed by PC3pLKO cells (scale bar=0.5cm);
(F) Plot of prostate tumor mass (individual tumors, in milligrams) of PC3shPsap tumors (first 7 lanes) and PC3pLKO tumors (last 4 lanes) from SCID mice. Asterisks refer to tumors that gave rise to metastases;
(G) Immunohistochemistry of p53 (upper panel) and Tsp-1 (lower panel) after Prosaposin knockdown. Reduced expression of p53 and Tsp-1 in the stroma of PC3shPsap prostate tumors (right panel) is observed as compared to PC3 tumors;
(H) Western blot analyses of Tsp-1, Psap, p53 and β-actin expression in normal prostate (N) and primary prostate tumors formed by PC3pLKO (P) and PC3shPsap (sh) cells;
(I) Western blot analyses of Tsp-1, p53 and β-actin expression in normal lymph nodes (N) and lymph nodes from PC3pLKO (P) or PC3shPsap (sh) tumor bearing mice;
(J) Western blot analyses of Tsp-1, p53 and β-actin expression in normal lung tissue (N) and lung tissue from PC3pLKO (P) or PC3shPsap (sh) tumor bearing mice.
(K) Plot of prostate tumor mass (individual tumors, in milligrams) of PC3M-LN4-psap tumors (first 10 lanes) and PC3M-LN4 tumors (last 10 lanes) from SCID mice. Asterisks refer to tumors that gave rise to metastases.
(L) Immunohistochemical staining of Prosaposin (Psap) in prostate tumor xenografts. Upper left panel: Weak Psap expression in highly metastatic PC3M-LN4 tumor (LN4), Upper right panel: Moderate expression in a weakly metastatic PC3 tumor (PC3). Lower left panel: Strong Psap expression in a prostate tumor formed by PC3M-LN4-Psap cells (LN4). Lower right panel: Psap expression in lung micrometastases (right) from a PC3M-LN4-psap tumor (Met).
(M) Western blot analysis of Tsp-1, p53, and β-actin expression in the normal prostate (N), and prostate tumors formed by PC3M-LN4 (L) and PC3M-LN4-psap (L-P) cells;
(N) Western blot analysis of Tsp-1, p53, and β-actin expression in the lung tissue of normal mice (N), and mice bearing prostate tumors formed by PC3M-LN4 (L) and PC3M-LN4-psap (L-P) cells;

Fig. 5.

(A) Photographs of lungs of wild-type (WT, upper panel) C57BL/6J mice and Tsp-$1^{-/-}$ C57BL/6J mice (lower panel) injected with $1x10^6$ Lewis Lung Carcinoma cells and treated with conditioned media from PC3pLKO (PC3) or PC3shPsap cells or serum free RPMI media (control) (arrows indicate lung metastases).
(B) Plot of number of individual metastases in the lungs from mice in six different experimental groups as described in (A);
(C) Relative mRNA expression levels of Psap in localized human prostate cancer (PCA) and metastatic human prostate cancer (Met). Each bar represents the mean of each group. The difference in Psap expression between localized and metastatic prostate tumors is highly significant ($p < 0.0001$ by ANOVA);
(D) Relative mRNA expression levels of Tsp-1 in localized human prostate cancer (PCA) and metastatic human prostate cancer (Met). Each bar represents the mean of each group. The difference in Psap expression between localized and metastatic prostate tumors is highly significant ($p < 0.0001$ by ANOVA);
(E) Relative mRNA expression levels of Psap in localized human prostate cancer (PCA) and metastatic human prostate cancer (Met). Each bar represents the mean of each group. The difference in Psap expression between localized and metastatic prostate tumors is highly significant ($p = 0.0004$ by ANOVA);
(F) Schematic depiction of Prosaposin(Psap)-mediated inhibition of tumor metastasis **(blue hexagons=Prosaposin).**

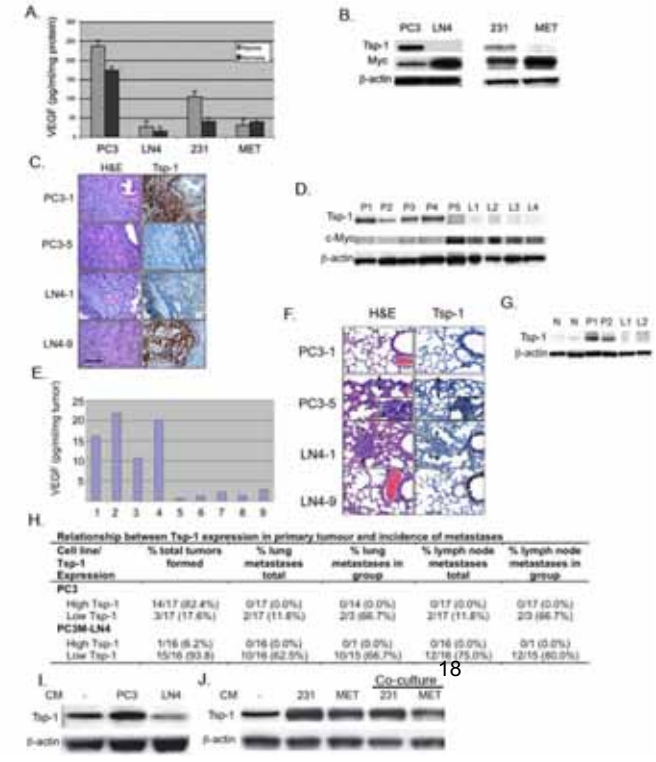

H.

Relationship between Tsp-1 expression in primary tumour and incidence of metastases

Cell line/ Tsp-1 Expression	% total tumors formed	% lung metastases total	% lung metastases in group	% lymph node metastases total	% lymph node metastases in group
PC3					
High Tsp-1	14/17 (82.4%)	0/17 (0.0%)	0/14 (0.0%)	0/17 (0.0%)	0/17 (0.0%)
Low Tsp-1	3/17 (17.6%)	2/17 (11.8%)	2/3 (66.7%)	2/17 (11.8%)	2/3 (66.7%)
PC3M-LN4					
High Tsp-1	1/16 (6.2%)	0/16 (0.0%)	0/1 (0.0%)	0/16 (0.0%)	0/1 (0.0%)
Low Tsp-1	15/16 (93.8)	10/16 (62.5%)	10/15 (66.7%)	12/16 (75.0%)	12/15 (80.0%)

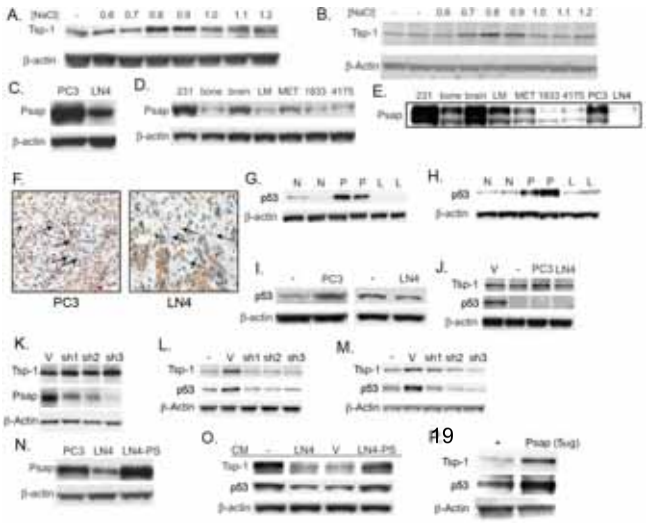
A.
[NaCl]
Tsp-1
β-actin
B.
[NaCl]
Tsp-1
β-Actin
C.
PC3
LN4
Psap
β-actin
D.
231
bone
brain
LM
MET
1833
4175
Psap
β-actin
E.
231
bone
brain
LM
MET
1833
4175
PC3
LN4
Psap
F.
PC3
LN4
G.
N
N
P
P
L
L
p53
β-actin
H.
N
N
P
P
L
L
p53
β-actin
I.
PC3
LN4
p53
β-actin
J.
V
PC3
LN4
Tsp-1
p53
β-actin
K.
V
sh1
sh2
sh3
Tsp-1
Psap
β-Actin
L.
V
sh1
sh2
sh3
Tsp-1
p53
β-Actin
M.
V
sh1
sh2
sh3
Tsp-1
p53
β-Actin
N.
PC3
LN4
LN4-PS
Psap
β-actin
O.
CM
LN4
V
LN4-PS
Tsp-1
p53
β-actin
P.
Psap (5ug)
Tsp-1
p53
β-Actin

19

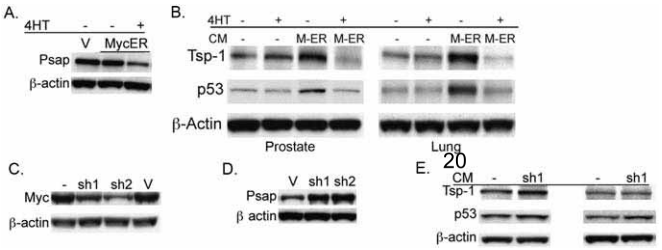
A.
4HT - - +
V MycER
Psap
β-actin
B.
4HT - + - + - + - +
CM - - M-ER M-ER - - M-ER M-ER
Tsp-1
p53
β-Actin
Prostate
Lung
C.
- sh1 sh2 V
Myc
β-actin
D.
V sh1 sh2
Psap
β actin
E.
CM - sh1 - sh1
Tsp-1
p53
β-actin

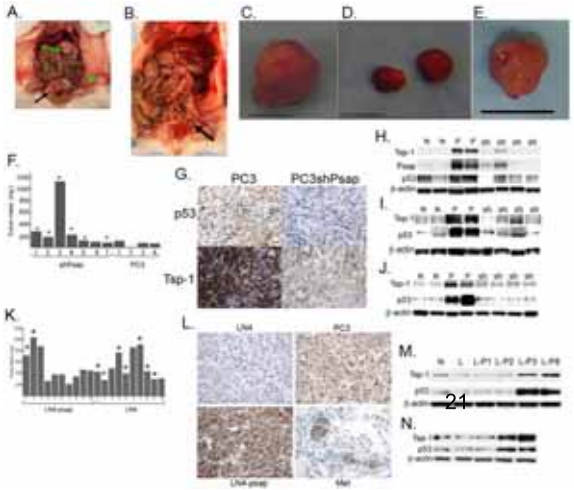
A.
B.
C.
D.
E.
F.
G.
PC3
PC3shPsap
p53
Tsp-1
H.
I.
J.
K.
L.
M.
N.

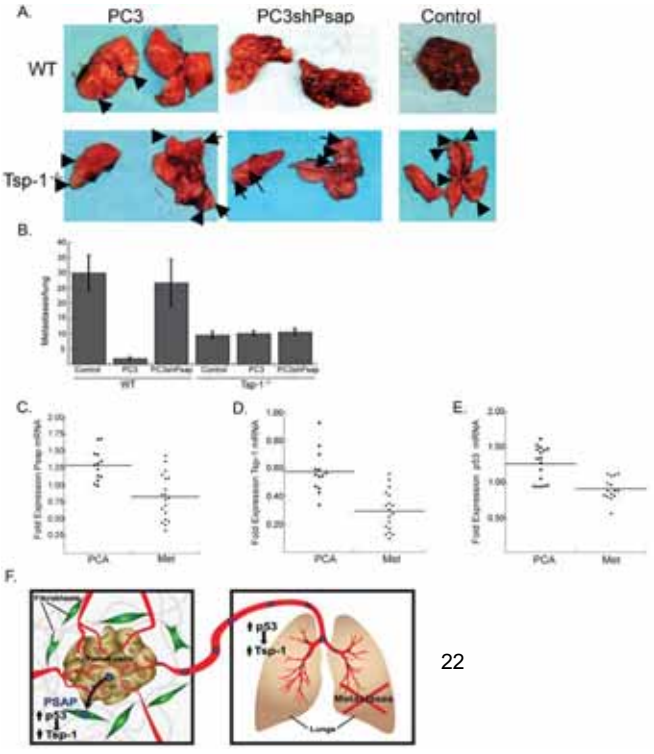
A.
PC3
PC3shPsap
Control
WT
Tsp-1
B.
C.
D.
E.
PCA
Met
F.
PSAP
p53
Tsp-1
Lungs

22

Methods

Cell lines and constructs

The cell lines PC3 and MDA-MB-231 were obtained from the American Type Culture Collection (ATCC, Manassas, VA). PC3M-LN4 was the generous gift of Dr. Isaiah Fidler (MD Anderson Cancer Center, Houston, TX), MDA-MET was the generous gift of Dr. Larry Suva (University of Arkansas for Medical Sciences, Little Rock, AR), MDA-MB-LM2-4175 and 1833 were generously provided by Dr. Joan Massague (Memorial Sloan-Kettering Cancer Center, New York, NY) and have been previously described (8, 9, 38, 39). The bone marrow derived stromal cells were the generous gift of Dr. Michael Rosenblatt (Tufts Medical School, Boston, MA) and were grown in high-glucose DMEM with 10 % heat-inactivated FBS, 250μM L-ascorbic acid and 1 % penicillin/streptomycin. PC3MycER cells were generated by retroviral infection of PC3 cells with pBabepuro-MycER (7, 18). PC3-shProsaposin and PC3M-LN4-shMyc cells were generated by lentiviral infection of PC3 cells with shRNA-Psap and PC3M-LN4 cells with shRNA-Myc respectively (Sigma, St. Louis, MO). Human Prostate Fibroblast (PrF) and lung fibroblasts (MRC5) were also infected with pLKO-shRNAp53 (Sigma, St. Louis, MO) to silence expression of p53 in these fibroblast cells. PC3M-LN4-Psap cells were generated by Cre-recombinase cloning of prosaposin from pDNR-Dual (Harvard Institute of Proteomics, Boston, MA) into pLNCX (Clontech, Moutainview, CA). PC3M-LN4 cells were then transduced with pLNCX-Psap as described previously (40) to generate PC3M-LN4-Psap.

Animal studies

All animal work was done in accordance with a protocol approved by the Institutional Animal Care and Use Committee. Male SCID mice 6-8 weeks old were injected with 2×10^6 viable cells in the prostate gland. The cells were washed and harvested in PBS prior to injection into the prostate glands of anaesthetized mice (2% avertin, 0.5 ml per mouse) in a volume of 0.8 ml. Endpoint assays were conducted at 5 weeks after injection unless significant morbidity required that the mouse be euthanized earlier.

In vitro conditioned media assays and co-culture assays

For the conditioned media assay, 1.5×10^6 tumor cells and fibroblasts cells were grown in the tumor cell media containing 0.1% FBS for 12 hours at which point the conditioned media from the tumor cells was centrifuged to remove any cells or cell debris and transferred to the fibroblasts subsequent to removal of the low serum fibroblast growth media. The fibroblasts and media were harvested 12 hours after addition of the tumor cell conditioned media and lysed for the western blot analysis while the conditioned media was collected for ELISA analysis. For the co-culture assays, 1×10^6 fibroblasts were seeded in the bottom chamber of a transwell tissue culture plates (Corning Inc., Corning, NY) and 1×10^6 tumor cells were seeded on the 0.3μm membrane in the upper chamber. The cells were co-cultured for 24 hours in tumor cell media containing 0.1% FBS before at which point the fibroblasts were harvested and lysed. All assays were performed a minimum of five times and representative samples depicted.

Western blot analyses and ELISA analysis

For Western blotting, cells were harvested as previously described[7]. Conditioned media was concentrated 20-fold using a Centriprep YM-3 (Millipore, Cambridge, MA). Loading was

normalized to total protein present in cell lysates. The membranes were blocked in 5 % nonfat milk and incubated in primary antibody to Tsp-1 (Ab-11, LabVision, Fremont, CA), c-Myc and phospho-Myc (Cell Signaling Technology, Beverly, MA), Prosaposin (Santa Cruz Biotechology, Santa Cruz, CA), β-actin (AbCam, Cambridge, UK). Protein expression, normalized to β-actin, was quantified by band intensity using a Bio-Rad Chemi-Doc XRS system (Bio-Rad, CA).

For ELISA analysis, the conditioned media were centrifuged to remove cell debris and the supernatant retained to measure VEGF levels using an ELISA kit that was specific for human VEGF (R & D, Minneapolis, MN). VEGF levels were normalized against total protein from the cells used in the assay. Xenograft tumors and tissue samples were homogenized and suspended in PBS, or lysis buffer for western blotting, and murine VEGF levels were determined using an ELISA kit that was specific for murine VEGF (R & D, Minneapolis, MN) results were normalized against the mass of the tumors. All error bars included in the graphical depiction of ELISA data represent SEM (Standard Error of Mean).

Fractionation of conditioned media and identification of proteins

For the fractionation of conditioned media from tumor cells we employed a Cu^{2+}-Heparin sepharose column in which heparin sepharose beads were combined in a 1:1 ratio with Cu^{2+}-NTA-agarose beads. We loaded 500mL of serum free conditioned media from PC3 cells onto a 10mL column and then washed with 100mL of wash buffer (10mM $NaPO_4$ PH 7.4), to remove any proteins that bound non-specifically. We then washed the column with 50mL of wash buffer plus 2.0M NaCl to elute any proteins that bound only to heparin but not Cu^{2+}. We then washed again with 100mL wash buffer followed by 50mL of 10mM imidazole to elute any proteins that bound only to Cu^{2+}. After a final wash with 100mL wash buffer we eluted proteins from the column via a linear gradient of NaCl from 0.3M to 2.0M in the presence of 10mM imidazole. We collected ~10mL fractions at 0.05M NaCl intervals. Fractions were dialyzed overnight in 3kd MWCO Slide-A-Lyzer cassettes against sterile PBS to remove excess salt and imidazole. We then treated primary prostate and lung fibroblasts with 1mL of each fraction or control PBS for 14 hours. The cells were then harvested and lysed as described above and Tsp-1 expression was determined. Fractions that elicited a stimulation of Tsp-1 were lyophilized and sent to the proteomics core facility at Children's Hospital for tandem liquid chromatography/mass spectrometry analysis.

Immunohistochemistry

Thin paraffin sections (5 μm) from formalin fixed and paraffin embedded prostate tumors and lung tissue was dewaxed with xylene/ethanol before heat induced microwave epitope retrieval in Tris-HCL (pH 1.0) for 15 minutes. The slides were incubated with a mouse monoclonal thrombospondin-1 antibody (TSP-Ab-4, clone A6.1) (Neomarkers, CA), diluted 1:50 for 60 minutes at room temperature. Sections incubated with isotypic mouse IgG1 (Dako Cytomation, Denmark) served as negative controls. Thrombospondin expression was evaluated subjectively by estimating the staining intensity and percentage positivity. A staining index (values 0-9), obtained as a product of staining intensity (0-3) and proportion of immunopositive tumor cells (≤10%=1, 10-50%=2, >50%=3), was calculated. Cases with a TSP staining index $\leq$ 2 we re defined as weak/negative.

Regarding p53, sections were stained with a mouse monoclonal antibody (p53-PAB1802; cat.# sc-53397) (Santa Cruz Biotechnology, CA, USA), incubated overnight (4^{o}C), dilution 1:10, after heat induced microwave epitope retrieval in TRS (pH 6.0) for 15 minutes. For p53, only nuclear staining was considered, and staining intensity was recorded as either negative/weak or moderate/strong. For both antibodies, immunostaining of tissue sections was performed on the DAKO Autostainer with the DAKO ARK (animal research kit) peroxidase (Dako Cytomation, Copenhagen, Denmark) as detection system. Antigen localization was achieved using the DAB diaminobenzidine peroxidase reaction, counterstained with hematoxylin.

Tissue microarrays and immunohistochemistry. Archival radical prostatectomy specimens were retrieved from the files of Department of Pathology, The Gade Institute, Haukeland University Hospital. Formalin fixed prostatectomy specimens were totally paraffin embedded and studied by whole mount step sections at 5 mm intervals. Tissue microarrays (TMAs) were constructed selecting three tissue cores (0.6 mm in diameter) from the area of highest tumor grade in each case.

Thin paraffin sections (5 mm) from the TMA paraffin block were dewaxed with xylene/ethanol before heat induced microwave epitope retrieval in citrate buffer (pH 6.0) for 20 minutes, and incubated with a polyclonal Prosaposin antibody raised against Saposin C (H-81) (sc-32875, Santa Cruz Biotechnology, CA), diluted 1:2000 for 60 minutes at room temperature. Immunostaining was performed on the DAKO Autostainer with the EnVision chain polymer method (Dako Cytomation, Copenhagen, Denmark) as detection system. Antigen localization was achieved using the DAB diaminobenzidine peroxidase reaction, counterstained with hematoxylin.

Immunostaining was estimated semiquantitatively, and a staining index (SI) obtained as a product of staining intensity (0-3) and proportion of immunopositive tumor cells (<10%=1, 10-50%=2, >50%=3), was calculated. Cases with a staining index $\leq$ 3 were defined as low expressors.

Correlations between variables were assessed by Pearson's chi-square test or Mann-Whitney *U* test. Univariate survival analyses were performed using the product-limit method and log-rank test, and visualized by Kaplan-Meier plots (SPSS statistical package; SPSS, Inc., Chicago, IL).

Supplemental Figure Legends

Table S1. List of proteins identified by tandem LC/MS analysis of the Tsp-1 stimulating fractions of Heparin/Cu^{2+} fractionated PC3 conditioned media. Proteins present in all active fractions are highlighted in yellow.

Figure S1. Western blot analysis of the expression levels of Thrombospondin-2 (Tsp-2), murine endostatin (m-endostatin) and β-actin protein in normal (SCID) mouse prostate (N) tumors formed by PC3 cells (P), and tumor formed by PC3shPsap cells (sh).

Figure S2. Western blot analysis of murine Tsp-2 and β-Actin expression in normal lung tissue (-) and lungs of wild-type and tsp-$1^{-/-}$ C57Bl/6J mice injected with $1x10^6$ Lewis Lung Carcinoma cells and treated with serum free RPMI media (L+M), conditioned media from empty vector containing PC3pLKO (L+P) or PC3shPsap cells (L+S).

Figure S3. Relative mRNA expression levels of Tsp-2 in localized human prostate tumors (PCA) and metastatic human prostate tumors (MET). Each bar represents the mean of each group. The difference in Tsp-2 expression between localized and metastatic prostate tumors has a p-value=0.6797 based on one way ANOVA.

Figure S4. Western blot analysis of Tsp-1, p53 and β-Actin expression in lungs of mice treated with serum free RPMI (C), 200μL, 100μL and 50μL of serum free condition media from PC3pLKO cells (P200, P100, P50), or 200μL and 100μL of serum free conditioned media from PC3shpsap cells for 10 days intraperitoneally.

Supplemental Table 1. **Proteins present in Tsp-1 stimulating Fractions**

PrF 0.7M	PrF 0.8M	WI-38: 0.7M	WI-38: 0.8M
Actin, cytoplasmic 1	Actin, cytoplasmic 1	Ribonucleases P/MRP protein subunit POP1	Actin, cytoplasmic 1
HSP 90-beta	HSP 90-beta	Splice Isoform 1 of 106 kDa O-GlcNAc transferase-interacting protein	Splice Isoform 1 of Fibronectin precursor
Splice Isoform Sap-mu-0 of Proactivator polypeptide precursor	**Splice Isoform Sap-mu-0 of Proactivator polypeptide precursor**	**Splice Isoform Sap-mu-0 of Proactivator polypeptide precursor**	**Splice Isoform Sap-mu-0 of Proactivator polypeptide precursor**
HSP 90-alpha 2	HSP 90-alpha 2	Lumican precursor	Pyruvate kinase 3 isoform 2
Elongation factor 2	Elongation factor 2		Peroxiredoxin 1
Cathepsin D precursor	Cathepsin D precursor		Nucleoside diphosphate kinase B
Alpha-2-HS-glycoprotein precursor	**Alpha-2-HS-glycoprotein precursor**	**Alpha-2-HS-glycoprotein precursor**	**Alpha-2-HS-glycoprotein precursor**
Splice Isoform 1 of Nucleophosmin	Quiescin Q6, isoform a		Quiescin Q6, isoform a
29 kDa protein	58 kDa protein	Serotransferrin precursor	Serotransferrin precursor
Hypothetical protein FLJ45525	Hypothetical protein FLJ45525		Alcadein alpha-1
Importin beta-1 subunit	Fructose-bisphosphate aldolase A	Importin beta-1 subunit	Fructose-bisphosphate aldolase A
Alpha-fetoprotein precursor		Alpha-fetoprotein precursor	Alpha-fetoprotein precursor
DNA-(apurinic or apyrimidinic site) lyase	Complement C3 precursor	Rab proteins geranylgeranyltransferase component A 1	Complement C3 precursor
Annexin A5	Thrombospondin 1 precursor	Heparin cofactor II precursor	Thrombospondin 1 precursor
Transitional endoplasmic reticulum ATPase	Alpha 2 macroglobulin variant	Eukaryotic translation initiation factor 2C, 2	Alpha 2 macroglobulin variant
Metalloproteinase inhibitor 1 precursor	Metalloproteinase inhibitor 1 precursor	Uveal autoantigen	Urokinase-type plasminogen activator precursor
Protein disulfide-isomerase A3 precursor	Splice Isoform APP770 of Amyloid beta A4 protein precursor		Splice Isoform APP770 of Amyloid beta A4 protein precursor
PREDICTED: similar to ATP-dependent DNA helicase II, 70 kDa subunit	EEF1A1 protein		EEF1A1 protein
Hypothetical protein LOC345651	Keratin, type II cytoskeletal 1		Keratin, type II cytoskeletal 1
Splice Isoform 1 of Heat shock cognate 71 kDa protein	ALB protein	ALB protein	ALB protein
Pentraxin-related protein PTX3 precursor	Pentraxin-related protein PTX3 precursor		Lactotransferrin precursor
Tubulin beta-3 chain	Tubulin beta-3 chain		Tubulin beta-3 chain
	Tubulin alpha-6 chain		Tubulin alpha-6 chain
	Alpha enolase		Splice Isoform 1 of Solute carrier family 12 member 7
	Alpha-actinin 1		Alpha-actinin 1
	Peptidyl-prolyl cis-trans isomerase A		Glia derived nexin precursor

Figure S1

Figure S2

Figure S3

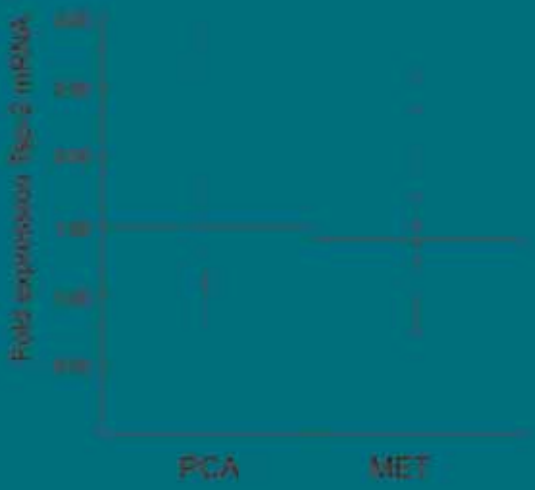

Figure S4